University of Alberta

Exploration of specific carbohydrate epitopes in their native habitat with the Staudinger ligation

by

Ravi Sankar Loka

A thesis submitted to the Faculty of Graduate Studies and Research
in partial fulfillment of the requirements for the degree of

Doctor of Philosophy

Department of Chemistry

Fall 2011
Edmonton, Alberta

Dedicated to my parents, sister, brother in-law and nephew

ABSTRACT

Glycans modulate biological processes and play a vital role in the function of receptors. However, the structure and functions of glycans are often obscured due to the heterogeneity of these structures. We hypothesize that the function of a specific carbohydrate epitope can be elucidated by incorporating an epitope of interest onto an existing glycan and monitoring its interactions within its native habitat. To explore this hypothesis, we have introduced the epitope of interest by adapting the Staudinger ligation strategy. In this strategy a nucleophilic phosphane reagent linked to an epitope reacts bioorthogonally with an electrophilic azide containing molecule and appends the epitope to the desired molecule. An azide can be incorporated into the glycan by the cell's biosynthetic machinery. We synthesized galactose-, lactose- and *N*-acetyl lactosamine (LacNAc)-phosphane reagents and succesfully demonstrated the use of this strategy to make defined glycoproteins. We also demonstrated that this method has utility for immobilization of carbohydrates onto azide derivitized surfaces under mild conditions using very low concentrations of the reagents without altering their binding affinity for lectins. The binding interactions of the carbohydrate epitopes with the lectins, jacalin, and wheat-germ agglutinin (WGA) were examined using surface plasmon resonance. We also designed and synthesized a tri-galactose-phosphane reagent to study multivalent interactions usually observed in biological systems.

ACKNOWLEDGEMENTS

It is a pleasure to thank those people who made this thesis possible. First and foremost, I am grateful to my supervisor Dr. Christopher Cairo for sharing his knowledge and providing guidance and support throughout my Ph.D. program

I would like to thank Chris Sadek, Nikolas Romaniuk and Jonathan Cartmell for their portions of work described in chapters 2 & 4. I would like to thank Dr. Maju Joe, and Dr. Mahendra Sandbhor, Mickey Richards, Dr. Wenji Peng, Dr. Peter Meloncelli and Naresh Tulsi for their advice in synthesis. I would like to thank Jessie Key, Amgad Albohy, Caishun Li and Michael Downey for their help in editing thesis. I would like to thank all the Cairo group members, past and present, for their help during my time here.

Finally, I would like to thank my parents, sister, brother in-law, nephew and friends for their enormous support.

TABLE OF CONTENTS

LIST OF FIGURES

LIST OF SCHEMES

LIST OF TABLES

LIST OF ABBREVIATIONS

Ac_4ManNAz	Peracetylated *N*-azidoacetylmannosamine
AOG	*N*-Amino-N^1-1-OctylGuanidine
Boc	Butyloxycarbonyl
BODIPY	4,4-difluoro-4-bora-3a,4a-diaza-s-indacene, Boron-dipyrromethene
Cbz	Carboxybenzyl
CCD	Charge-Coupled Device
CD45	Cluster of Differentiation 45
CM5	Carboxymethyl-Dextran 5
CMD	Carboxymethyl-Dextran
Con A	Concavalin A
COSY	Correlation spectroscopy
CPMV	Cowpea Mosaic Virus
CuAAC	Copper Catalyzed Azide-Alkyne 1,3-dipolar Cycloaddition
DBU	1,8-Diazabicycloundec-7-ene
DCC	*N*,*N*'-Dicyclohexylcarbodiimide
DCM	Dichloromethane

DFT	Density Functional Theory
DIBAC	Dibenzoazacyclooctyne
DIBO	Dibenzocyclooctyne
DIBoc	Di-t-butyl-dicarbonate
DIFBO	Difluorobenzocyclooctyne
DIFO	Difluorocyclooctyne
DMAP	4-*N*, *N*-Dimethylaminopyridine
DMF	Dimethylformamide
DMSO	Dimethylsulfoxide
DTPM	1,3-Dimethyl-5-[(dimethylamino)methylene]2,4,6(1H, 3H, 5H)-trioxopyrimidine
EDC	1-Ethyl-3-(3-dimethylaminopropyl)-carbodiimide
ESI	Electrospray ionization
Fmoc	Fluorenylmethyloxycarbonyl
FRET	Förster Resonance Energy Transfer
Gal	D-Galactose
GDP	Guanine Diphosphate
HEPES	4-(2-Hydroxyethyl)-1-piperazineethanesulfonic acid

HOMO	Highest Occupied Molecular Orbital
HRP	Horseradish peroxidase
HSQC	Heteronuclear Single Quantum Coherence
IDCP	Iodonium(di-sym-collidine)perchlorate
ITC	Isothermal Titration Calorimetry
K_d	Dissociation Constant
Lac	Lactose, Galβ1,4-Glc
LacNAc	*N*-Acetyllactosamine, Galβ1,4-GlcNAc
LC	Liquid Chromatography
LFA-1	Lymphocyte Function-Associated Antigen-1
LG	Leaving group
LiHMDS	Lithium hexamethyldisilazide
LUMO	Lowest Unoccupied Molecular Orbital
MAL-I	*Maackia amurensis* Lectin-I
ManLev	*N*-Levulinoyl mannosamine
ManNAz	*N*-Azidoacetyl mannosamine
m-CPBA	meta-Chloroperoxybenzoic acid
MeOH	Methanol

MW	Molecular Weight
$NaIO_4$	Sodium periodate
NaOMe	Sodium Methoxide
NHS	*N*-Hydroxysuccinamide
NMR	Nuclear Magnetic Resonance
OPLS	Optimized Potentials for Liquid Simulations
PAMAM	Poly(amidoamine)
PEG	Polyethylene glycol
PG	Protecting Group
PKC	Protein Kinase C
PNGase F	Peptide *N*-glycosidase F
RU	Response Units
SAM	Self-Assembled Monolayer
SDS-PAGE	Sodium Dodecyl Sulfate-Polyacrylamide Gel Electrophoresis
SPR	Surface Plasmon Resonance
TBTA	Tris[(1-benzyl-1*H*-1,2,3-triazol-4-yl)methyl]amine
TCA	Trichloroacetimidate
TBS-T	Tris buffer saline tween

Tf_2O	Trifluoromethanesulfonic Anhydride
THPTA	Tris(hydroxypropyltriazolyl)methylamine
TLC	Thin Layer Chromatography
TMS	Trimethylsilyl
TMSOTf	Trimethylsilyl Ttrifluoromethanesulfonate
TRIS	Tris(hydroxymethyl)aminomethane
WGA	Wheat Germ Agglutinin
UV	Ultraviolet

Chapter 1

Bioorthogonal chemistry: A tool to explore glycans in their native habitat

1.1 Abstract

Glycans on the cell surface are involved in many biological processes. However, the structure and function of glycans are not well understood compared to other biopolymers, such as proteins and nucleic acids due to their heterogeneity. Genetically encoded green fluorescent proteins are extremely useful in understanding the role of proteins in biological systems, but this method is not feasible for the study of glycans, as glycan formation is not genetically controlled. However, a strategy, known as bioorthogonal labeling, has been applied for exploring the role of glycans in biological system. Bioorthogonal reactions, which have been used for this purpose; including their advantages, limitations and applications highlighting glycan modifications are discussed in this chapter. In general, most bioorthogonal reactions have been used to introduce an exogenous epitope, such as a fluorescent molecule or biotin onto the glycan. We propose that incorporation of a native epitope onto the glycan in live cells or living organisms will provide an opportunity to examine the effects of modified glycans thereby providing crucial information about specific epitopes. We propose that the well-known Staudinger ligation can be used for incorporating desired exogenous epitopes.

1.2 Introduction

The biopolymers, ions, and metabolites of living systems play a wide variety of roles in different biological processes. In order to understand cellular processes, there is a need to determine the structure and function of specific biomolecules. The four major types of biopolymers are proteins, lipids, nucleic acids and glycans. The majority of protein biopolymers in mammalian cells are glycosylated, and these glycans, polysaccharides or oligosaccharides are involved in a broad range of biological processes.[1, 2] Carbohydrates are vital for protein folding, stabilization, transport and quality control.[3] Glycans on the cell surface assist in intercellular communication, pathogen recognition and immune responses. Compared to proteins and nucleic acids, the study of glycans is complicated, as their synthesis is not template driven. Additionally glycan structures are often nonlinear, and contain different monosaccharide building blocks with various ring sizes. The complexity of glycosylation sites also results in heterogenous structures.

A number of methods have been developed to explore the structure and function of glycans.[4-6] Mass spectrometry and lectin microarrays are widely used to elucidate the structure of glycans.[7-11] Conventional strategies, like interrupting biosynthetic pathways with small molecules,[12-14] synthesis of defined glycoconjugates,[3] use of exogenous enzymes to alter glycan structures,[15] and glycopolymers which interfere with cellular receptors[16] provide some insight into glycan structure and function. An alternative strategy is the study of glycans in their native habitat by introducing chemical reporters that can be used to track the glycan. The advent of genetically encoded fluorescent proteins has revolutionized the field of proteomics and has been used as a powerful tagging method to introduce reporters onto target proteins.[17] Genetic tagging cannot be applied to glycans as their synthesis is not template driven, unlike proteins and nucleic

acids. Bioorthogonal chemistry is most widely used to tag bioreporters *in vivo* without using genetic encoding.[18-21]

Bioorthogonal chemical reporter strategies are usually a two-step process. In the first step, a bioorthogonal reporter will be introduced onto the target biomolecule by using a native or engineered biosynthetic pathway. Later, an exogenous probe is tagged onto the target by a bioorthogonal reaction, where the reporter and probe are specific to one another and they will not react with any other endogenous functional groups of the biological system (**Figure 1.1**).[21] As

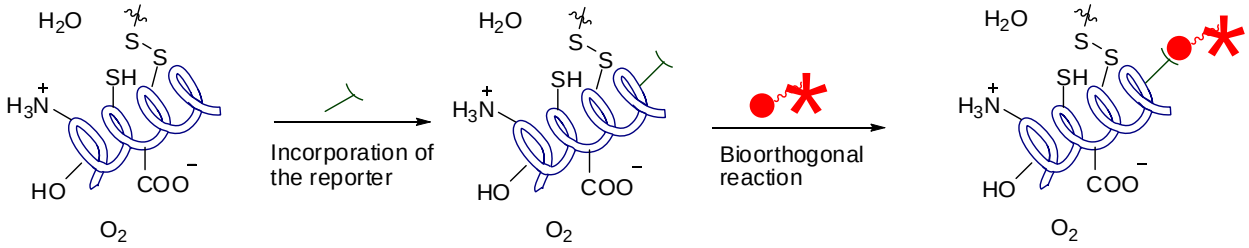

Figure 1.1: General scheme representing a sequential two step bioorthogonal strategy to tag specific biomolecules in a complex biological milieu. A bioorthogonal chemical reporter with nonnative functional group (structure in green) is metabolically incorporated into the target biomolecule (structure in blue) in the presence of different biomolecules with various functionalities such as amines, acids, thiols and alcohols etc. Then a probe (red star) attached to a complementary reactive group (red circle) specific for the reporter is tagged covalently by a bioorthogonal reaction.

the chemical reporter is incorporated using the cell's own machinery by appending to the substrate, it should be smaller in size and compatible such that it will not perturb biological function. The reactants, both reporter and probe, participating in the bioorthogonal reaction must be nontoxic. The bioorthogonal reaction should proceed with faster rates and high yields mostly without any byproduct at neutral pH. The product formed should be stable in the native

environment. With enormous efforts of many research groups several bioorthogonal reactions have been designed that fit these stringent characteristics and implemented to provide insights into the structure, dynamics and function of various biomolecules. This chapter discusses different bioorthogonal reactions developed to date and their specific application in the context of glycan modification.

1.3 Bioorthogonal reactions

1.3.1 Nucleophilic additions onto aldehydes or ketones

Carbonyl functional groups can serve as good bioorthogonal reporters due to the ease of incorporation into various scaffolds and they are inert to endogenous reactive groups usually seen on biopolymers such as proteins and glycans under neutral conditions. Even though endogenous nucleophiles such as amines (lysine), thiols (cysteine) and alcohols (glycans) form reversible Schiff bases with mild carbonyl electrophiles, the equilibrium is shifted towards the carbonyls under physiological conditions. Activated carbonyls under acidic conditions, pH 5-6, react with amine nucleophiles such as aminooxy and hydrazide compounds to form stable imines, oximes **1.1**, and hydrazones **1.2**, (**Scheme 1.1**) respectively due to the α effect.[22]

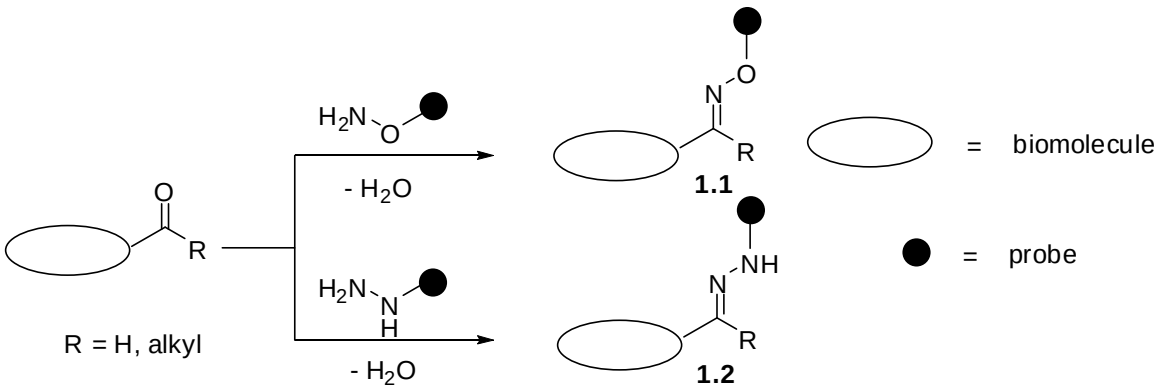

Scheme 1.1: Aldehydes or ketones as bioorthogonal reporters under acidic conditions (pH 5-6). Condensation of alkoxyamines and hydrazides with carbonyl functionality incorporated in target biomolecule to form stable imine derivatives.

Aldehydes were first introduced onto the cell surface by treatment with periodate by Ashwell and co-workers in 1971.[23] Periodate oxidizes terminal vicinal diols (*C*-8 and *C*-9) of sialic acids to give an aldehyde at the *C*-7 position. Gahmberg and coworkers successfully coupled different mono- and oligo-saccharide hydrazines to living red blood O-type cells *in vitro* after periodate treatment to modify their function.[24] Modified O-type cells reacted with anti-A and anti-B sera. Rideout and coworkers in 1986 first demonstrated the use of aldehyde and hydrazine bioorthogonal chemistry for *in vivo* drug assembly in cancer cells.[25] In their self-assembling drug approach, known as covalent modulation, they employed nontoxic precursors, decanal, **1.3**, and *N*-amino-N^1-1-octylguanidine (AOG), **1.4**, to form a cytotoxic hydrazone (**Scheme 1.2**) to kill human erythrocytes by membrane dissolution. Based on the conditions employed, rate constants for this pseudo-first-order reaction of decanal and AOG were found to be in the range of $5.6 \pm 1.6 \times 10^{-4}$ to $9.8 \pm 1.0 \times 10^{-4}$ s^{-1}. This self-assembling hydrazone chemistry was further extended to make antineoplastic drugs based on their properties such as membrane disruption, protein kinase C (PKC) inhibition,[26] metal chelation and DNA intercalation.[27]

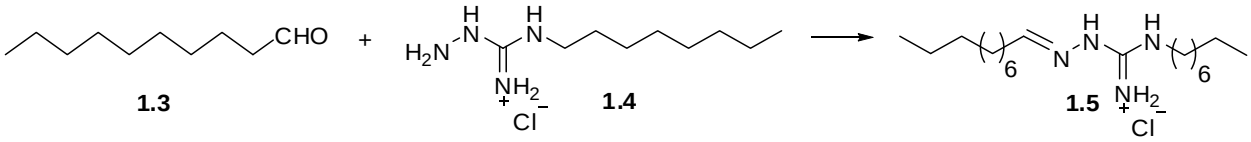

1.3 **1.4** **1.5**

Scheme 1.2: Condensation of aldehyde and hydrazine. Hydrazone derivatives formed after condensation act as biomembrane damaging agent unlike its precursors.

Bertozzi and coworkers[28] used this condensation strategy in cell surface engineering where ketone groups were incorporated onto a sialoglycoconjugate by feeding cells with *N*-levulinoyl mannosamine (ManLev), inspired from the work of Reutter and co-workers.[29, 30] Later ketone was selectively ligated to biotin on treatment with biotinamidocaproyl hydrazide. Based on flow cytometry analysis, they also demonstrated that approximately 1.8 x 10^{-6} ketones per cell were available for chemoselective ligation at saturation. However, this carbonyl condensation strategy has some general disadvantages, including the need for acidic pH (which is a major barrier for *in vivo* experiments), slow reaction rates, high concentration of reactants, and most importantly, ketones and aldehydes are not unique functional groups within cells. These groups are present in cells and biological fluids as sugars, pyruvates and oxaloacetates. Accordingly, this strategy has been used widely for extracellular or cell surface modifications, but may be limiting in applications in the cell or in living organisms. Dawson and co-workers have used aniline as a catalyst, showed the use of both hydrazides[31] and oximes[32] for condensation reaction at neutral pH and reaction rates were increased several fold. Aniline forms a protonated imine, **1.6**, with the carbonyl and readily undergoes transamination with hydrazides or oximes, therefore

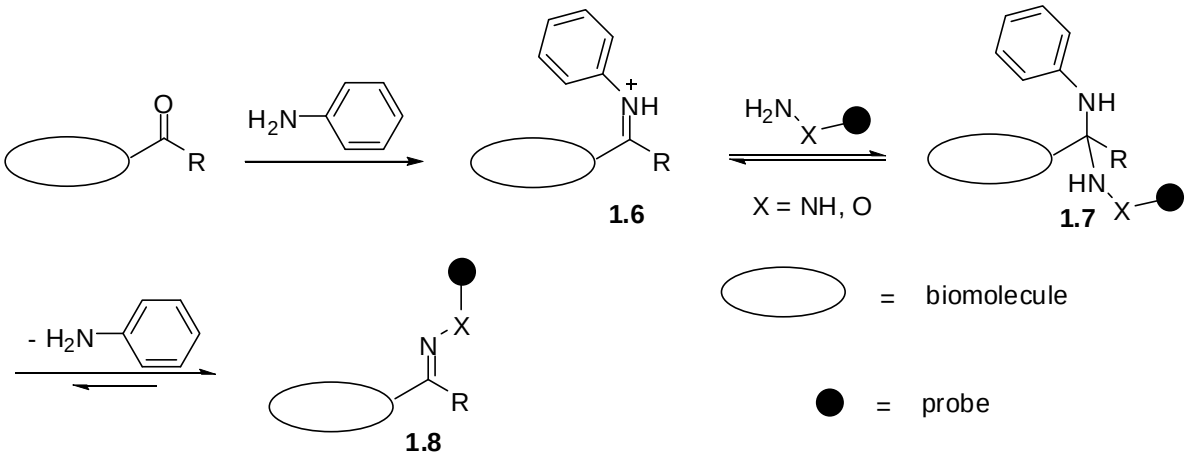

Scheme 1.3: Aldehyde or ketone condensation under neutral pH. Aniline catalyzed transamination accelerates the rate of **1.8** formation.[33]

accelerating the rate of reaction (**Scheme 1.3**).[33] If one has to make a choice between these two strategies, it is worth noting that oximes are more hydrolytically stable than their corresponding hydrazones, as oximes cannot be easily protonated.[34] Paulson and co-workers[35] successfully incorporated biotin tags onto sialic acids by using aniline catalysis (**Scheme 1.4**). They introduced an aldehyde on to the *C*-7 position of sialic acids on BJA-B subclone K88 cells by mild periodate (1 mM $NaIO_4$ at 4 ^oC for 30 min) treatment. Later, in the presence of aniline (10 mM), biotin was attached via a hydroxylamine at pH 6.7. Use of aniline catalysis increased the rate of reaction by eight to ten-fold. Recently, this aninline catalyzed bioorthogonal reaction has been used for imaging qorum sensing receptor of bacteria, *Pseudomonas aeruginosa* by labeling with boron-dipyrromethene (BODIPY),[36] and to quantitate the sialic acid content of cells.[37]

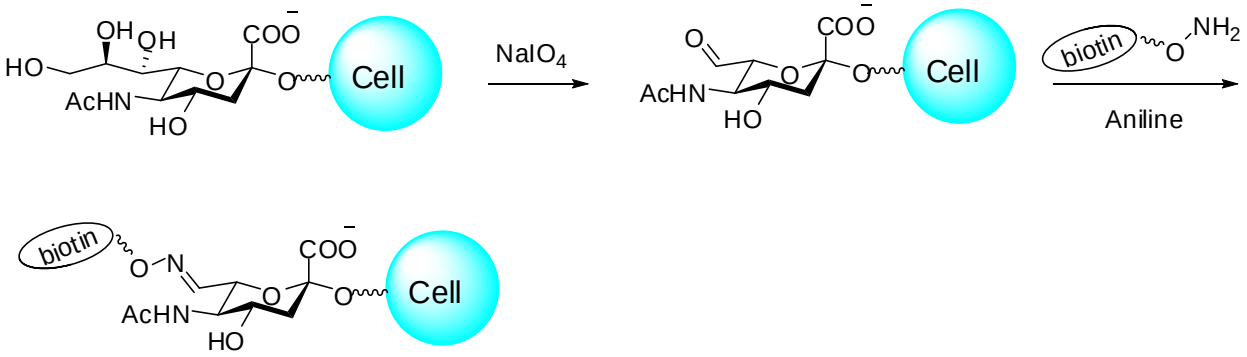

Scheme 1.4: Aniline catalyzed *in vivo* labeling with a biotin-hydroxylamine. Aldehyde was incorporated on the cell surface by periodate treatment. Biotin-hydroxylamine was coupled to the aldehyde in presence of aniline.

1.3.2 Bioorthogonal reactions with azides

Azides are small, nontoxic and completely abiotic[38] functional groups with mild electrophilicity, unlike aldehydes and ketones. Azides are inert to amines and other hard

nucleophiles found in biological systems. As mentioned earlier, azides can be easily incorporated into biomolecules due to their small size. One potential problem with azides is that they are susceptible to reaction with thiols. Thiols can reduce aryl and alkyl azides in basic conditions,[39-41] but their reactivity is reduced in physiological pH. However, reaction of azides with glutathione in cells[42] and their reduction during glycan labeling[43] has been reported. Two bioorthogonal reactions, Staudinger ligation and 1,3-dipolar cycloadditions are used to conjugate desired epitopes with azide.

1.3.2.1 Staudinger ligation

Herman Staudinger (Nobel Laureate, 1953) and Jules Meyer in 1919, reported the reduction of azides into amines with triarylphosphine, popularly known as the Staudinger reaction or Staudinger reduction.[44] This reaction proceeds under mild conditions with high yields. Nucleophilic phosphine attacks the terminal nitrogen of azide followed by loss of a nitrogen molecule to give an aza-ylide, **1.9** (**Scheme 1.5.A**). The iminophosphorane (aza-ylide)

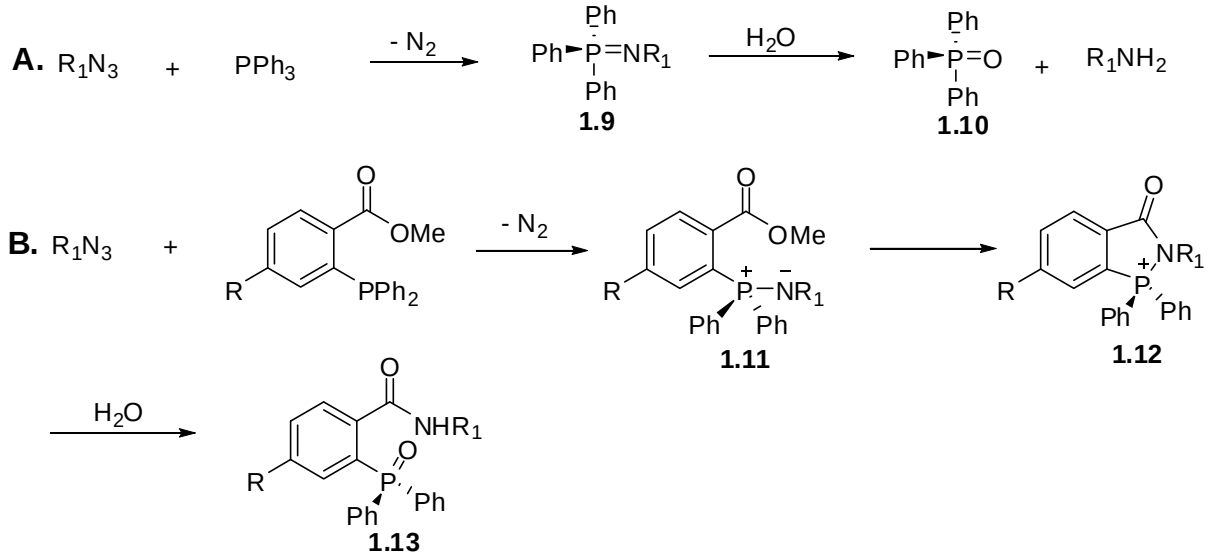

Scheme 1.5: The Staudinger ligation. R and R_1 are moieties to be linked together. By placing an electrophilic trap ortho to phosphorus resulted in an amide bond formation in Staudinger ligation (**B**), whereas free amine in Staudinger reaction (**A**).

intermediate is quite unstable and readily hydrolyzes to give the amine and corresponding phosphine oxide, **1.10**. After almost a century, Bertozzi and coworkers[45] examined the Staudinger reaction as the basis of a potential bioorthogonal reaction. The successful application of the reaction would require a way to stabilize the Aza-ylide intermediate. They installed an intramolecular electrophilic trap, a methyl ester, such that prior to hydrolysis negative charge on the nitrogen of the aza-ylide immediately attacks the carbonyl of the ester to form a five membered ring,[46] **1.12**, with loss of methanol (**Scheme 1.5.B**). Finally, hydrolysis of the five membered ring gives an amide and phosphine oxide, **1.13**. This reaction can be used to ligate two desired moieties, and is therefore referred to as Staudinger ligation.[47]

Raines and co-workers[48] developed another version of the Staudinger ligation, known as the traceless-Staudinger ligation, where the final ligation product loses phosphine oxide. They covalently attached thioesters and azide moieties in presence of phosphine thiol. In the same year, Bertozzi and co-workers[49] also reported a traceless-Staudinger ligation strategy (**Scheme 1.6**). In Bertozzi's formulation a cleavable linker was strategically placed between the acyl group and phosphane. Once the aza-ylide intermediate, **1.14**, formed the nucleophilic nitrogen of the ylide will attack the carbonyl and displace the easily cleavable linkage and phosphorus group. Hydrolysis of this rearranged adduct results in an amide bond, liberating the phosphine oxide (**Scheme 1.6.A**). The traceless-Staudinger ligation strategy has been used to ligate peptides, and doesn't require a terminal cysteine residue in one of the peptides, unlike native chemical ligation.[50] This chemistry has been used for glycopeptide synthesis, where the azide has been incorporated into the *N*-terminus of an unprotected peptide by protease catalysis.[51] Recently Davis and co-workers used this strategy to synthesize well-defined reverse amide *N*-linked glycoproteins.[52] However, they observed undesired side reactions such as reduction of azide and

interaction of phosphane with thio-derivatives. Different traceless-Staudinger ligating reagents have been designed, among them the most widely used reagent is diphenylphosphinomethanethiol, **1.18**.[53] Water soluble reagents such as bis(*p*-*N*,*N*-dimethylaminoethylphenyl)phosphinomethanethiol, **1.19**,[54] bis(*m*-*N*,*N*-dimethylaminomethylphenyl)phosphinomethanethiol, **1.20**,[55] have also been reported. The reagent **1.20** has been found to be better for traceless Staudinger ligation in water due to favorable coulombic effects preventing protonation of the iminophosphorane intermediate. Additionally compound **1.20** can be synthesized efficiently in high yields.[55]

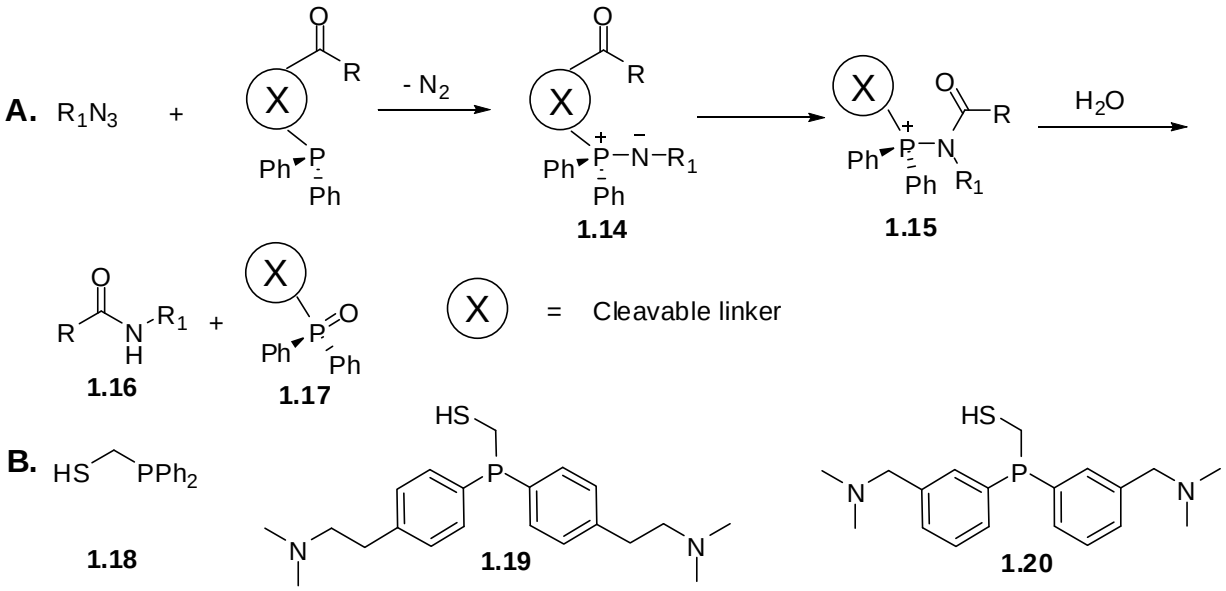

Scheme 1.6: The traceless-Staudinger ligation. R and R_1 are coupling partners. A cleavable linker was placed between the acyl and phosphonium groups such that rearrangement of iminophosphorane followed by hydrolysis results in an amide bond between R and R_1 and liberation of the phosphine oxide (**A**). Compounds **1.18**, **1.19**, and **1.20** are water soluble traceless-Staudinger ligation reagents (**B**).

Bertozzi and co-workers incorporated azides onto the sialic acids of cells by feeding Jurkat cells with peracetylated *N*-azidoacetylmannosamine ($Ac_4ManNAz$) and labeled these azides with biotin using a biotin-attached water soluble phosphine reagent.[45] In 2004, this chemistry was used to tag FLAG-protein in living organisms.[56] Due to its exceptional biocompatibility, Staudinger ligation has been used for glycan imaging *in vivo* and several flurophore-phosphane reagents have been designed for this purpose. Taking advantage of the electronics on phosphorus, a coumarin attached phosphine reagent was made[57] which was fluorescent upon Staudinger ligation due to formation of phosphine oxide. However, it suffered

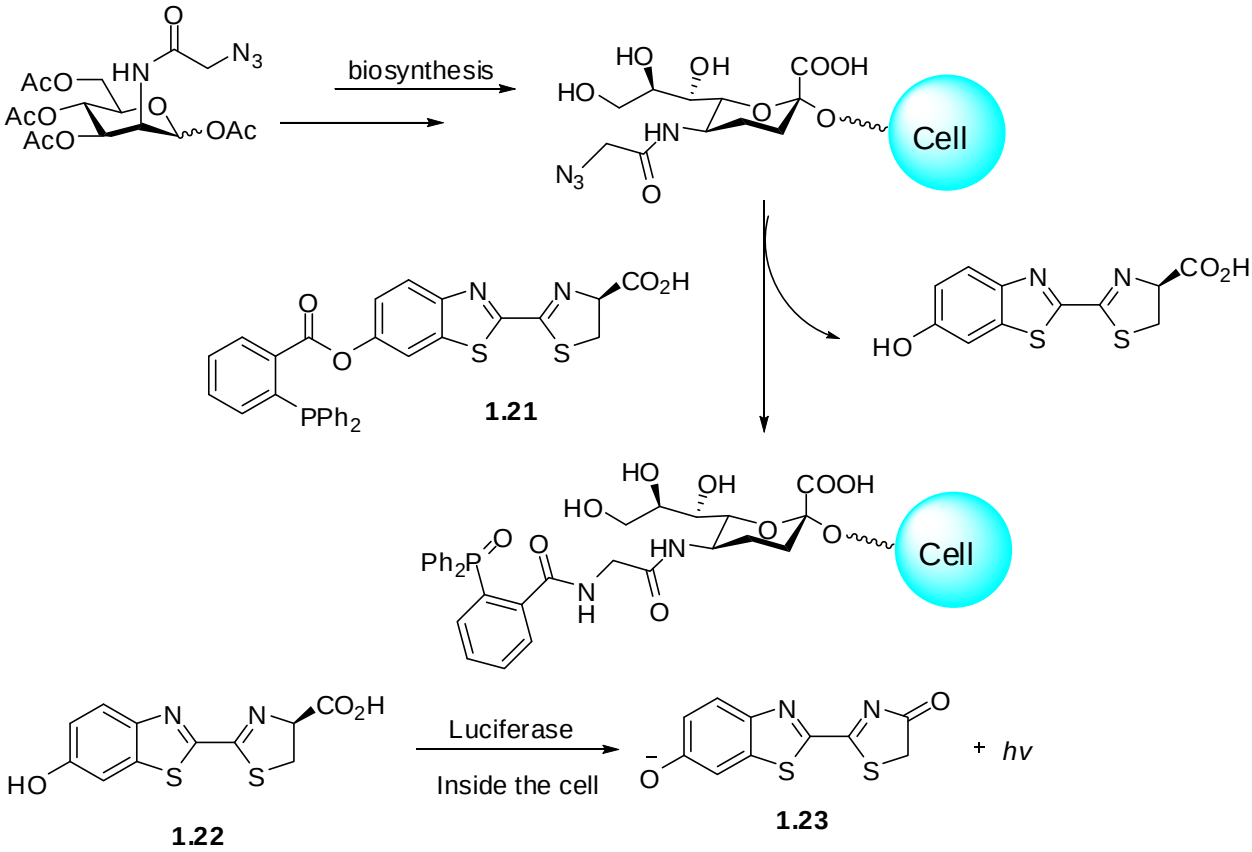

Scheme 1.7: Bioluminiscence for imaging the glycan of live cells using the Staudinger ligation. Luciferine **1.22** released due to Staudinger ligation of phosphine-luciferine compound **1.21** with azide incorporated sialic acids was oxidized by luciferase, resulted in production of light.

from background fluorescence because of phosphane oxidation in air. To address this problem a Förster resonance energy transfer (FRET) based phosphine-fluorophore was designed.[58] The complexity of smart fluorophores[59] and the autofluorescence of tissues to image glycans in mice forced researchers to look for alternative strategies. Recently a bioluminescence based method has been used for imaging the glycan on live cells.[60] This technique is based on release of light during oxidation of luciferin by luciferase. Prostate cancer cells transfected with luciferase were incubated with different concentrations of Ac_4ManNAz (10, 35 or 50 μM) for two days to incorporate azides into sialic acid through biosynthetic pathway and azides were reacted with a hydrophobic phosphane-luciferine conjugate **1.21** (ranging from 3 nM to 100 μM). Luciferase cannot recognize conjugated luciferin, **1.21**, due to the aryl ester bond. Luceferin **1.22**, released after Staudinger ligation diffuses into cells and was converted into oxoluceferin, **1.23**, in the presence of luciferase along with the emission of light (**Scheme 1.7**). Light was detected by a charge-coupled device (CCD) camera. This technique is even sensitive for low concentrations (nM) of phosphine reagent, **1.21**. This technique was adapted for imaging in rats as tissue luminescence is completely absent.[61] Highly sensitive luciferase transgenic mice are readily available. The Staudinger ligation has been used for increasing glycoprotein subtypes from different proteomes,[62, 63] incorporating new functionalities to recombinant proteins,[64] immobilization of proteins with unnatural aminoacids,[65, 66] and fluorescent detection of protein fatty acylation.[67] The slow reaction kinetics[46] of the Staudinger ligation and the need for high concentration of reagent (> 200 μM), coupled with oxidation of phosphine by metabolic enzymes or air are the major drawbacks of this ligation reaction. Another potential problem is reduction of disulfide bonds by phosphanes,[68] however this should not be a significant concern under physiological pH.[45]

1.3.2.2 Click chemistry or 1,3-dipolar cycloadditions

Thermal reaction between the 1,3-dipolar azide and a dipolarophile, such as an alkyne to give 1,2,3-triazole was first reported by Rolf Huisgen in 1961.[69] Azides undergo [3+2] cycloaddition with alkynes to yield two regioisomers of 1,2,3-triazole at elevated temperatures and pressure. Due to the activation barrier of the thermal reaction, attaining these reaction conditions in a biological system is not feasible. Sharpless and co-workers[70] and Meldal and co-workers[71] independently reported Cu(I)-catalyzed 1,3-dipolar cycloaddition between an azide and terminal alkyne to give 1,4-disubstituted-1,2,3 triazoles, **1.24**, with enormous increases in reaction rate (**Scheme 1.8**). The Cu(I)-catalyzed cycloaddition reaction between azides and alkynes (CuAAC) proceeds almost seven times faster than the uncatalyzed azide, alkyne reaction[72] and 25 times faster than Staudinger ligation of azides and triarylphosphines.[73] The key factor responsible for acceleration of the reaction is activation of the terminal alkyne due to formation of copper acetylide intermediate.[74] Copper-catalyzed azide-alkyne 1,3-dipolar cycloaddition is popularly known as an example of 'click chemistry'. Click reactions feature

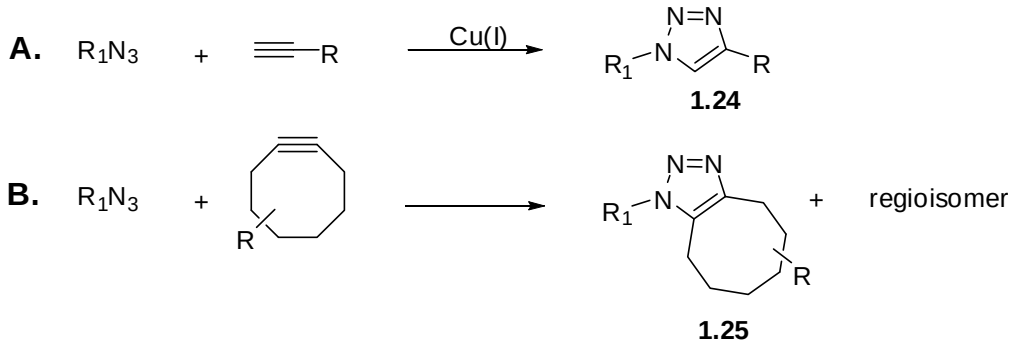

Scheme 1.8: 1,3-Dipolar cycloaddition of azide and alkyne. Copper(I) catalyzed cycloaddition between azide and terminal alkyne yields 1,4-disubstituted 1,2,3 triazole (**A**). Strain promoted cycloadditon between azide and cyclooctyne gives two regio isomers of 1,2,3 triazole (**B**). R and R_1 are different groups to be ligated.

high yields, simple reaction conditions (can proceed in water at room temperature under physiological pH), and selectivity.[75] The first example of labeling a biomolecule using CuAAC was reported by Fin and co-workers in cowpea mosaic virus (CPMV),[76] later this chemistry was used to derivitize CPMV with different multivalent conjugates such as glycans, peptides and polyethylene glycol (PEG)[77, 78] as well as modifying the surface of tobacco mosaic virus.[79] CuAAC has been employed in various fields[80, 81] especially in chemical biology. It has been used for immobilization of nucleic acids,[82, 83] drug development,[84] labeling of nucleotides[85-87] and lipids,[88] selective modification of protein[89] and the activity-based proteome profiling.[90] CuAAC has advantages over the Staudinger ligation in terms of reaction kinetics and requires minimal quantity of azides.[91] The reaction rates of CuAAC can be accelerated further by using Cu(I) stabilizing ligands such as tris[(1-benzyl-1*H*-1,2,3-triazol-4-yl)methyl]amine(TBTA, **Figure 1.2**).[92, 93]

The toxicity of the Cu(I)-catalyst to cells has hampered the application of CuAAC in live cells. Additionally, the low water solubility of the Cu(I) stabilizing ligands, such as TBTA, has led to use of high concentrations of catalyst and Cu(I) ions that are not coordinated, increases the generation of reactive oxygen and nitrogen species thereby damaging the cell.[94] This has been observed in bacterial cells (*Escherichia coli*), mammalian cells and Zebra fish embryos when subjected to the CuAAC reaction.[21, 95] Recently Peng Wu and co-workers[96] and M.G. Finn and co-workers[97]developed water soluble Cu(I) stabilizing ligands to carry out CuAAC in live cells for rapid and efficient labeling. Peng Wu and co-workers discovered that the fucose salvage pathway in zebrafish embryos process modified fucose substrates inefficiently. Microinjection of an alkyne-containing fucose, GDP-FucA1, into zebra fish embryos at the one-cell or two-cell stage and later resulted in metabolically incorporated alkyne as detected with Alexa fluor 488-

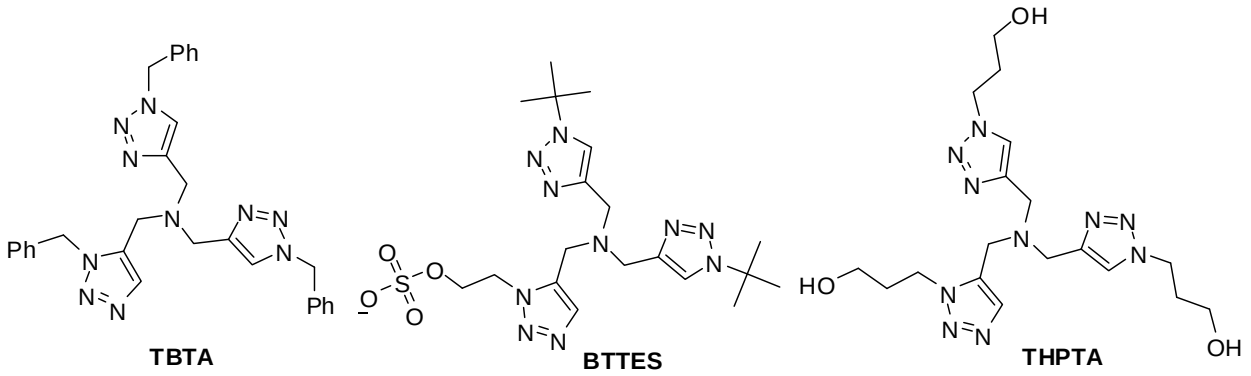

Figure 1.2: Ligands for accelerating the CuAAC reaction. BTTES and THPTA are water soluble ligands designed to decrease the cytotoxicity of Cu(I) ion thereby increasing biocompatibility of CuAAC.

azide using CuAAC in the presence of the water soluble ligand BTTES, a tris(triazolylmethyl) amine-based ligand (**Figure 1.2**). This strategy enabled them to image fucosylated glycans in the envelope layer of the zebra fish embryo. They also labeled azide-incorporated sialic acids in mammalian cells with a biotin probe using this chemistry. M.G. Finn and co-workers labeled azido-sialic acids of mammalian cells with Alexa fluor-alkyne, biotin-alkyne derivatives using water soluble tris(hydroxypropyltriazolyl)methylamine (THPTA) ligand and additive aminoguanidine in CuAAC reaction.[75] THPTA terminates reactive species such as oxygen radicals generated by Cu/ascorbate within the metal-coordination sphere and guanidine takes care of dehydroascorbate and its decomposition products. Peng Wu and co-workers tried the THPTA-Cu(I) catalyst for labeling metabolically-incorporated GDP-FucAl of zebrafish embryos with Alexa fluor 488-azide and they observed less labeling compared to one with BTTES-Cu(I) catalyst.[74]

In order to surmount the toxic effects of copper catalyst in cells, researchers have sought for other alternatives to activate the alkyne in azide-alkyne cycloaddition reactions. Installing

electron withdrawing groups adjacent to the alkyne will activate the dipolarophile and can undergo copper-free cycloaddition with azides at ambient temperatures. However, these alkynes are susceptible to Michael addition with biological nucleophiles. Wittig and Krebs in 1961 reported a reaction of the smallest of the stable cycloalkynes, cyclooctyne and phenyl azide, which exhibited an accelerated rate to form a single triazole product. Destabilization in the ground state due to 18 kcal mol^{-1} of angle strain from the lorge distortion of bond angle, 163^{o} to that of the transition state, enhanced the rate of reaction. Bertozzi and co-workers used this strain promoted cycloaddition reaction (**Scheme 1.8.B**) for both *in vitro* and *in vivo* labeling without apparent cytotoxicity.[98] However, this reaction was slow and the second-order rate constant in aqueous CD_3CN for the cycloaddition reaction between a cyclooctyne derivative and benzyl azide was found to be 0.0012 M^{-1} s^{-1}, lower than that of a Staudinger ligation (0.0025 M^{-1} s^{-1}, 2 fold faster).[46, 73] Assuming that placing an electronegative atom, fluorine, at the propargylic position will decrease the energy gap between lowest unoccupied molecular orbital (LUMO) of the alkyne and the highest molecular orbital (HOMO) of the azide and thereby enhances the rate. Accordingly, installing fluorine next to the triple bond increased the second order reaction constant by 3-fold for the reaction between compound **1.27** and benzylazide in acetonitrile compared to simple cyclooctyne **1.26**.[73] The rate was dramatically increased to 60-fold with difluorocyclooctyne **1.28**, popularly known as DIFO, compared to **1.26**.[99] The rate acceleration was attributed to phase-transfer interactions of fluorine[100] and additional strain imparted due to increase in steric interactions.[101] A second generation of DIFO compounds were produced with improved synthesis.[102] A water soluble DIFO derivative, 6,7-dimethoxyazacyclooct-4-yne, **1.29**, was synthesized from a glucose analogue and showed efficient labeling of azide incorporated

cells in terms of nonspecific binding.[103] The long synthesis of DIFO compounds may limit their applications, however as discussed below a number of groups have expanded on this strategy.

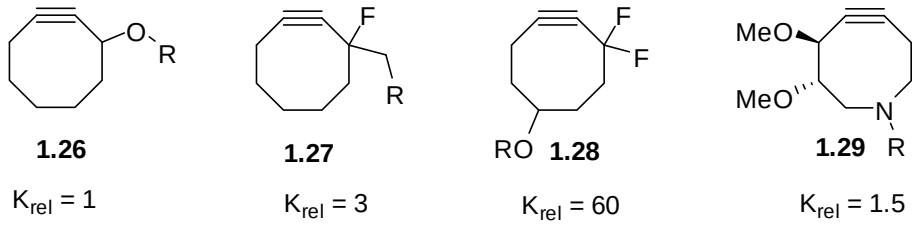

1.26 K_{rel} = 1 **1.27** K_{rel} = 3 **1.28** K_{rel} = 60 **1.29** K_{rel} = 1.5

Figure 1.3: Comparision of second order rate constants of a reaction between various cyclooctynes with benzylazide in acetonitrile. Addition of fluorine atoms at the propargylic position increased the rate by changing the electronics of the alkyne.

Boons and co-workers increased ring strain further by the fusion of benzene rings to cyclooctyne (**1.30**).[104] The rate of cycloaddition reaction with dibenzocyclooctyne (DIBO), **1.30**, was similar to DIFO and it was easily synthesized. One disadvantage is the insolubility of **1.30** in water. Debets et al.[105] have synthesized aza-dibenzocyclooctynes **1.31** (DIBAC) to increase the hydrophilicity of DIBO. Compound **1.31** showed better reaction kinetics than DIBO and DIFO. Taking a cue from the studies of Debets et al. that incorporating an sp^2 center into dibenzocyclooctyne ring can induce additional strain as seen in DIBAC with an exocyclic amide bond, Bertozzi and co-workers installed an amide bond onto a benzo-fused octyne ring (**1.32**).[106] Inserting one more degree of unsaturation into the octyne ring will make the benzocyclooctyne highly unstable. Therefore they opted for an amide bond in the ring which readily creates unsaturation. Biarylazacyclooctynones (BARAC), **1.32**, showed a 12-fold rate increase compared to DIFO. Recently, the same group has reported a hybrid of DIFO and DIBO, called as DIFBO **1.33**[107] based on the speculations of Goddard and co-workers[108] and density functional theory (DFT) methods.[100, 109] DIFBO was found to be highly reactive and immediately

underwent homotrimerization in solution. However, it was stabilized by complexation with β-cyclodextrin. A cyclopropenone derivative **1.34** (**Figure 1.4**) which can generate the corresponding DIBO upon irradiation provides an opportunity for temporal and spatial labeling.[110] A major disadvantage with benzofused derivatives is their lipophilicity, which may lead to nonspecific binding with proteins. Cyclopropane ring-fused derivatives, such as bicyclo[6.1.0]nonyne, **1.35**, have been made to decrease the lipophilicity and showed same kind of reactivity as DIBO compounds.[111] Most of these cyclooctyne derivatives have been employed in labeling of proteins, lipids and imaging of glycans in cells, *Caenorhabditis elegans* and developing zebrafish. Recently, a DIFO derivative was employed to visualize fucosylated glycans in developing zebrafish.[112] In this work, a metabolically incorporated fucosyl azide was reacted with a DIFO-attached imaging probe, whereas a fucosyl-alkyne was used as reporter in biocompatible CuAAC strategy used by Peng Wu and co-workers.[96]

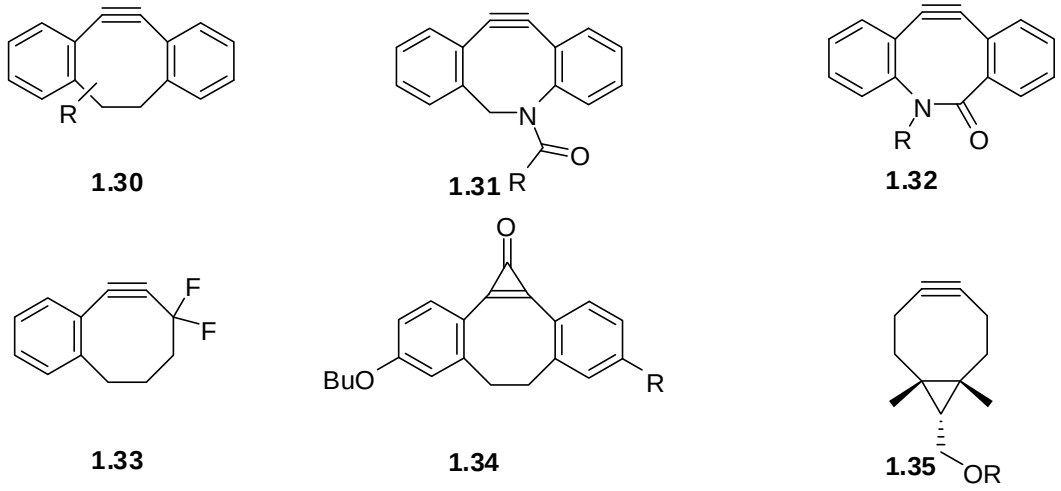

Figure 1.4: Ring fused cyclooctyne. Modification of cyclooctynes for enhancement of the ring strain.

Recently, bioorthogonal cycloaddition reactions with alkenes promoted by ring strain or light have gained interest due to their faster reaction kinetics.[19-21] A [3+2]-cycloaddition followed immediately by a retro-Diels–Alder reaction of oxanorbornadiene with azide,[113] inverse-electron demand Diels–Alder reaction of a trans-cyclooctene[114] or norbornene[115] with tetrazines and photoinducible dipolar cycloaddition of a nitrile imine with an alkene[116, 117] have also been employed for bioconjugation. However, these reactions are not that useful especially for *in vivo* experiments considering incorporation of one of the reporter into the biomolecule or some of them are not truly bioorthogonal.

1.4 Project objectives

Studying the glycan in its native habitat can provide crucial insights about glycan function. Most of the biorthogonal reactions reported have been used to attach external probes such as biotin or fluorescent dyes to the glycan to monitor their function. Thus, many of these studies involve a non-native epitope. Our goal is to introduce an endogenous epitope onto the glycan by using an efficient bioorthogonal method and study the consequences of that modification in the biological system. This strategy will allow us to evaluate the function of specific epitopes in their native environment. Enzymes, such as glycosyl transferases, have been previously employed to introduce native epitopes onto the glycan. For example, Palcic and co-workers[118] have changed the phenotype of O-erythrocytes to B by appending a human blood group B trisaccharide antigen on to the O-erythrocyte with fucosyl transferase. However, this method has some limitations, as few enzymes will tolerate modified substrates and the reactions are low-yielding. An alternative to accomplish this goal is bioorthogonal reactions which provide the ability to attach any desired epitope on to the glycan. As previously mentioned, Gahmberg and co-workers used hydrazine-aldehyde chemistry to modify the function of O-type blood cells

by appending mono or oligosaccharides *in vitro*.[10] We opted to use the Staudinger ligation based on the reports of Bertozzi and co-workers.[73] These studies suggest that Staudinger ligation can be used both in live cells and living organisms, and the required reagents are more synthetically accessible compared to cyclooctyne derivatives.

We developed a methodology to synthesize carbohydrate-phosphane reagents for modification of azide containing proteins by Staudinger ligation (**Chapter 2**).[119] An ethylene glycol linker with the amine at the terminus was attached to the anomeric position of the carbohydrate selectively. Later, a free amine was coupled to an activated ester of the phosphane reagent under mild conditions. The phosphane reagent was introduced at the end of the synthesis to minimize phosphorus oxidation. We successfully used these carbohydrate-phosphane reagents to modify a protein, β-lactoglobulin. Thus, demonstrating this strategy can be used for making defined glycoproteins (**Chapter 2**). These carbohydrate-phosphane reagents were immobilized onto an azide-modified solid surface and their specifity for different lectins were measured using surface plasmon resonance (**Chapter 3**).[120] A trivalent galactose-phosphane reagent was also synthesized (**Chapter 4**) by applying this methodology, in order to study multivalent interactions with lectins.

Cell surface protein receptors are usually glycosylated and these structures can play an integral role in their function. CD45 is a heavily glycosylated protein, known as receptor-like tyrosine phosphatase. CD45 is specifically expressed on leukocytes. It contains both *N*- and *O*-linked glycans in the extracellular domain.[121-123] CD45 isoforms which differ only in glycosylation pattern show differential intracellular signaling due to differential ligand binding.[124, 125] CD45 glycosylation plays a vital role in T- cell development, activation, immune function and apoptosis.[126] Galectin-1, a homodimeric protein, binds preferentially to *N*-acetyl

lactosamine (LacNAc) moieties,[127] and will form clusters and segregate CD45, leading to T-cell death.[128] We propose that conjugation of LacNAc epitopes onto CD45 by Staudinger ligation would allow the examination of apoptosis caused by galectin-1. In order to test our hypothesis, we can make use of different carbohydrate conjugated phosphane reagents (**Chapter 2, 4**). In this thesis, we outline a general methodology for the application of these reagents. We demonstrate the feasibility of this strategy *in vitro* and outline their potential uses *in vivo* (**Chapter 4**).

1.5 References

1. Dwek, R. A., Glycobiology: Toward Understanding the Function of Sugars. *Chem. Rev.* **1996,** *96* (2), 683-720.

2. Varki, A., Biological roles of oligosaccharides: all of the theories are correct. *Glycobiology* **1993,** *3* (2), 97-130.

3. Gamblin, D. P.; Scanlan, E. M.; Davis, B. G., Glycoprotein synthesis: an update. *Chem. Rev.* **2009,** *109* (1), 131-63.

4. Kellam, B.; De Bank, P. A.; Shakesheff, K. M., Chemical modification of mammalian cell surfaces. *Chem. Soc. Rev.* **2003,** *32* (6), 327-37.

5. Saxon, E.; Bertozzi, C. R., Chemical and biological strategies for engineering cell surface glycosylation. *Annu. Rev. Cell Dev. Biol.* **2001,** *17*, 1-23.

6. Agard, N. J.; Bertozzi, C. R., Chemical approaches to perturb, profile, and perceive glycans. *Acc. Chem. Res.* **2009,** *42* (6), 788-97.

7. Hsu, K. L.; Pilobello, K. T.; Mahal, L. K., Analyzing the dynamic bacterial glycome with a lectin microarray approach. *Nat. Chem. Biol.* **2006,** *2* (3), 153-7.

8. Kuno, A.; Uchiyama, N.; Koseki-Kuno, S.; Ebe, Y.; Takashima, S.; Yamada, M.; Hirabayashi, J., Evanescent-field fluorescence-assisted lectin microarray: a new strategy for glycan profiling. *Nat. Methods* **2005,** *2* (11), 851-6.

9. Haslam, S. M.; North, S. J.; Dell, A., Mass spectrometric analysis of N- and O-glycosylation of tissues and cells. *Curr. Opin. Struct. Biol.* **2006,** *16* (5), 584-91.

10. Dell, A.; Morris, H. R., Glycoprotein structure determination by mass spectrometry. *Science* **2001,** *291* (5512), 2351-6.

11. Morelle, W.; Michalski, J. C., Glycomics and mass spectrometry. *Curr. Pharm. Des.* **2005,** *11* (20), 2615-45.

12. Eason, P. D.; Imperiali, B., A potent oligosaccharyl transferase inhibitor that crosses the intracellular endoplasmic reticulum membrane. *Biochemistry* **1999,** *38* (17), 5430-7.

13. Fuster, M. M.; Esko, J. D., The sweet and sour of cancer: glycans as novel therapeutic targets. *Nat. Rev. Cancer* **2005,** *5* (7), 526-42.

14. Laferte, S.; Chan, N. W.; Sujino, K.; Lowary, T. L.; Palcic, M. M., Intracellular inhibition of blood group A glycosyltransferase. *Eur. J. Biochem.* **2000,** *267* (15), 4840-9.

15. Stanley, P.; Ioffe, E., Glycosyltransferase mutants: key to new insights in glycobiology. *FASEB. J.* **1995,** *9* (14), 1436-44.

16. Kiessling, L. L.; Gestwicki, J. E.; Strong, L. E., Synthetic multivalent ligands in the exploration of cell-surface interactions. *Curr. Opin. Chem. Biol.* **2000,** *4* (6), 696-703.

17. Nienhaus, G. U., The green fluorescent protein: a key tool to study chemical processes in living cells. *Angew Chem Int Ed Engl* **2008,** *47* (47), 8992-4.

18. Prescher, J. A.; Bertozzi, C. R., Chemistry in living systems. *Nat Chem Biol* **2005,** *1* (1), 13-21.

19. Lim, R. K.; Lin, Q., Bioorthogonal chemistry: recent progress and future directions. *Chem. Commun. (Cambridge)* **2010,** *46* (10), 1589-600.

20. Jewett, J. C.; Bertozzi, C. R., Cu-free click cycloaddition reactions in chemical biology. *Chem. Soc. Rev.* **2010,** *39* (4), 1272-9.

21. Sletten, E. M.; Bertozzi, C. R., Bioorthogonal chemistry: fishing for selectivity in a sea of functionality. *Angew. Chem. Int. Ed. Engl.* **2009,** *48* (38), 6974-98.

22. St Pierre, T.; Jencks, W. P., Intramolecular catalysis in the reactions of nucleophilic reagents with aspirin. *J. Am. Chem. Soc.* **1968,** *90* (14), 3817-27.

23. Lenten, L. V.; Ashwell, G., Studies on the chemical and enzymatic modification of glycoproteins. A general method for the tritiation of sialic acid-containing glycoproteins. *J. Biol. Chem.* **1971,** *246* (6), 1889-94.

24. Tolvanen, M.; Gahmberg, C. G., In vitro attachment of mono- and oligosaccharides to surface glycoconjugates of intact cells. *J. Biol. Chem.* **1986,** *261* (20), 9546-51.

25. Rideout, D., Self-assembling cytotoxins. *Science* **1986,** *233* (4763), 561-3.

26. Rotenberg, S. A.; Calogeropoulou, T.; Jaworski, J. S.; Weinstein, I. B.; Rideout, D., A self-assembling protein kinase C inhibitor. *Proc. Natl. Acad. Sci. U. S. A.* **1991,** *88* (6), 2490-4.

27. Rideout, D., Self-assembling drugs: a new approach to biochemical modulation in cancer chemotherapy. *Cancer. Invest.* **1994,** *12* (2), 189-202; discussion 268-9.

28. Mahal, L. K.; Yarema, K. J.; Bertozzi, C. R., Engineering chemical reactivity on cell surfaces through oligosaccharide biosynthesis. *Science* **1997,** *276* (5315), 1125-8.

29. Kayser, H.; Zeitler, R.; Kannicht, C.; Grunow, D.; Nuck, R.; Reutter, W., Biosynthesis of a nonphysiological sialic acid in different rat organs, using N-propanoyl-D-hexosamines as precursors. *J. Biol. Chem.* **1992,** *267* (24), 16934-8.

30. Keppler, O. T.; Stehling, P.; Herrmann, M.; Kayser, H.; Grunow, D.; Reutter, W.; Pawlita, M., Biosynthetic modulation of sialic acid-dependent virus-receptor interactions of two primate polyoma viruses. *J. Biol. Chem.* **1995,** *270* (3), 1308-14.

31. Dirksen, A.; Dirksen, S.; Hackeng, T. M.; Dawson, P. E., Nucleophilic catalysis of hydrazone formation and transimination: implications for dynamic covalent chemistry. *J. Am. Chem. Soc.* **2006,** *128* (49), 15602-3.

32. Dirksen, A.; Hackeng, T. M.; Dawson, P. E., Nucleophilic catalysis of oxime ligation. *Angew. Chem. Int. Ed. Engl.* **2006,** *45* (45), 7581-4.

33. Kohler, J. J., Aniline: a catalyst for sialic acid detection. *Chembiochem* **2009,** *10* (13), 2147-50.

34. Kalia, J.; Raines, R. T., Hydrolytic stability of hydrazones and oximes. *Angew. Chem. Int. Ed. Engl.* **2008,** *47* (39), 7523-6.

35. Zeng, Y.; Ramya, T. N.; Dirksen, A.; Dawson, P. E.; Paulson, J. C., High-efficiency labeling of sialylated glycoproteins on living cells. *Nat. Methods* **2009,** *6* (3), 207-9.

36. Rayo, J.; Amara, N.; Krief, P.; Meijler, M. M., Live Cell Labeling of Native Intracellular Bacterial Receptors Using Aniline-Catalyzed Oxime Ligation. *J. Am. Chem. Soc.* **In press**, DOI: 10.1021/ja200455d.

37. Key, J. A.; Li, C.; Cairo, C. W., *Under review*.

38. Griffin, R. J., The medicinal chemistry of the azido group. *Prog. Med. Chem.* **1994,** *31*, 121-232.

39. Cartwright, I. L.; Hutchinson, D. W.; Armstrong, V. W., The reaction between thiols and 8-azidoadenosine derivatives. *Nucleic Acids Res.* **1976,** *3* (9), 2331-9.

40. Staros, J. V.; Bayley, H.; Standring, D. N.; Knowles, J. R., Reduction of aryl azides by thiols: implications for the use of photoaffinity reagents. *Biochem. Biophys. Res. Commun.* **1978,** *80* (3), 568-72.

41. Reardon, J. E.; Crouch, R. C.; St John-Williams, L., Reduction of 3'-azido-3'-deoxythymidine (AZT) and AZT nucleotides by thiols. Kinetics and product identification. *J. Biol. Chem.* **1994,** *269* (23), 15999-6008.

42. Handlon, A. L.; Oppenheimer, N. J., Thiol reduction of 3'-azidothymidine to 3'-aminothymidine: kinetics and biomedical implications. *Pharm. Res.* **1988,** *5* (5), 297-9.

43. Saxon, E.; Luchansky, S. J.; Hang, H. C.; Yu, C.; Lee, S. C.; Bertozzi, C. R., Investigating cellular metabolism of synthetic azidosugars with the Staudinger ligation. *J. Am. Chem. Soc.* **2002,** *124* (50), 14893-902.

44. Staudinger, H.; Meyer, J., Über neue organische Phosphorverbindungen III. Phosphinmethylenderivate und Phosphinimine. *Helv. Chim. Acta* **1919,** *2* (1), 635-46.

45. Saxon, E.; Bertozzi, C. R., Cell surface engineering by a modified Staudinger reaction. *Science* **2000,** *287* (5460), 2007-10.

46. Lin, F. L.; Hoyt, H. M.; van Halbeek, H.; Bergman, R. G.; Bertozzi, C. R., Mechanistic investigation of the staudinger ligation. *J. Am. Chem. Soc.* **2005,** *127* (8), 2686-95.

47. Kohn, M.; Breinbauer, R., The Staudinger ligation-a gift to chemical biology. *Angew. Chem. Int. Ed. Engl.* **2004,** *43* (24), 3106-16.

48. Nilsson, B. L.; Kiessling, L. L.; Raines, R. T., Staudinger ligation: a peptide from a thioester and azide. *Org. Lett.* **2000,** *2* (13), 1939-41.

49. Saxon, E.; Armstrong, J. I.; Bertozzi, C. R., A "traceless" Staudinger ligation for the chemoselective synthesis of amide bonds. *Org. Lett.* **2000,** *2* (14), 2141-3.

50. Tam, A.; Raines, R. T., Protein engineering with the traceless Staudinger ligation. *Methods Enzymol.* **2009,** *462*, 25-44.

51. Liu, L.; Hong, Z. Y.; Wong, C. H., Convergent glycopeptide synthesis by traceless Staudinger ligation and enzymatic coupling. *Chembiochem* **2006,** *7* (3), 429-32.

52. Bernardes, G. J.; Linderoth, L.; Doores, K. J.; Boutureira, O.; Davis, B. G., Site-Selective Traceless Staudinger Ligation for Glycoprotein Synthesis Reveals Scope and Limitations. *Chembiochem* **In press**, DOI: 10.1002/cbic.201100125.

53. Soellner, M. B.; Nilsson, B. L.; Raines, R. T., Reaction mechanism and kinetics of the traceless Staudinger ligation. *J. Am. Chem. Soc.* **2006,** *128* (27), 8820-8.

54. Tam, A.; Soellner, M. B.; Raines, R. T., Water-soluble phosphinothiols for traceless staudinger ligation and integration with expressed protein ligation. *J. Am. Chem. Soc.* **2007,** *129* (37), 11421-30.

55. Tam, A.; Raines, R. T., Coulombic effects on the traceless Staudinger ligation in water. *Bioorg. Med. Chem.* **2009,** *17* (3), 1055-63.

56. Prescher, J. A.; Dube, D. H.; Bertozzi, C. R., Chemical remodelling of cell surfaces in living animals. *Nature* **2004,** *430* (7002), 873-7.

57. Lemieux, G. A.; De Graffenried, C. L.; Bertozzi, C. R., A fluorogenic dye activated by the Staudinger ligation. *J. Am. Chem. Soc.* **2003,** *125* (16), 4708-9.

58. Hangauer, M. J.; Bertozzi, C. R., A FRET-based fluorogenic phosphine for live-cell imaging with the Staudinger ligation. *Angew. Chem. Int. Ed. Engl.* **2008,** *47* (13), 2394-7.

59. Laughlin, S. T.; Bertozzi, C. R., Imaging the glycome. *Proc. Natl. Acad. Sci. U. S. A.* **2009,** *106* (1), 12-7.

60. Cohen, A. S.; Dubikovskaya, E. A.; Rush, J. S.; Bertozzi, C. R., Real-time bioluminescence imaging of glycans on live cells. *J. Am. Chem. Soc.* **2010,** *132* (25), 8563-5.

61. Massoud, T. F.; Gambhir, S. S., Molecular imaging in living subjects: seeing fundamental biological processes in a new light. *Genes Dev.* **2003,** *17* (5), 545-80.

62. Hang, H. C.; Yu, C.; Kato, D. L.; Bertozzi, C. R., A metabolic labeling approach toward proteomic analysis of mucin-type O-linked glycosylation. *Proc. Natl. Acad. Sci. U. S. A.* **2003,** *100* (25), 14846-51.

63. Vocadlo, D. J.; Hang, H. C.; Kim, E. J.; Hanover, J. A.; Bertozzi, C. R., A chemical approach for identifying O-GlcNAc-modified proteins in cells. *Proc. Natl. Acad. Sci. U.S. A.* **2003,** *100* (16), 9116-21.

64. Luchansky, S. J.; Argade, S.; Hayes, B. K.; Bertozzi, C. R., Metabolic functionalization of recombinant glycoproteins. *Biochemistry* **2004,** *43* (38), 12358-66.

65. Watzke, A.; Kohn, M.; Gutierrez-Rodriguez, M.; Wacker, R.; Schroder, H.; Breinbauer, R.; Kuhlmann, J.; Alexandrov, K.; Niemeyer, C. M.; Goody, R. S.; Waldmann, H., Site-selective protein immobilization by Staudinger ligation. *Angew. Chem. Int. Ed. Engl.* **2006,** *45* (9), 1408-12.

66. Gauchet, C.; Labadie, G. R.; Poulter, C. D., Regio- and chemoselective covalent immobilization of proteins through unnatural amino acids. *J. Am. Chem. Soc.* **2006,** *128* (29), 9274-5.

67. Charron, G.; Zhang, M. M.; Yount, J. S.; Wilson, J.; Raghavan, A. S.; Shamir, E.; Hang, H. C., Robust fluorescent detection of protein fatty-acylation with chemical reporters. *J. Am. Chem. Soc.* **2009,** *131* (13), 4967-75.

68. Dmitrenko, O.; Thorpe, C.; Bach, R. D., Mechanism of SN2 disulfide bond cleavage by phosphorus nucleophiles. Implications for biochemical disulfide reducing agents. *J. Org. Chem.* **2007,** *72* (22), 8298-307.

69. Huisgen, R., Centenary Lecture - 1,3-Dipolar Cycloadditions. *Proc. Chem. Soc.* **1961**, 357-96.

70. Rostovtsev, V. V.; Green, L. G.; Fokin, V. V.; Sharpless, K. B., A stepwise huisgen cycloaddition process: copper(I)-catalyzed regioselective "ligation" of azides and terminal alkynes. *Angew. Chem. Int. Ed. Engl.* **2002,** *41* (14), 2596-9.

71. Tornoe, C. W.; Christensen, C.; Meldal, M., Peptidotriazoles on solid phase: [1,2,3]-triazoles by regiospecific copper(i)-catalyzed 1,3-dipolar cycloadditions of terminal alkynes to azides. *J. Org. Chem.* **2002,** *67* (9), 3057-64.

72. Himo, F.; Lovell, T.; Hilgraf, R.; Rostovtsev, V. V.; Noodleman, L.; Sharpless, K. B.; Fokin, V. V., Copper(I)-catalyzed synthesis of azoles. DFT study predicts unprecedented reactivity and intermediates. *J. Am. Chem. Soc.* **2005,** *127* (1), 210-6.

73. Agard, N. J.; Baskin, J. M.; Prescher, J. A.; Lo, A.; Bertozzi, C. R., A comparative study of bioorthogonal reactions with azides. *ACS Chem. Biol.* **2006,** *1* (10), 644-8.

74. Rodionov, V. O.; Fokin, V. V.; Finn, M. G., Mechanism of the ligand-free CuI-catalyzed azide-alkyne cycloaddition reaction. *Angew. Chem. Int. Ed. Engl.* **2005,** *44* (15), 2210-5.

75. Kolb, H. C.; Finn, M. G.; Sharpless, K. B., Click Chemistry: Diverse Chemical Function from a Few Good Reactions. *Angew. Chem. Int. Ed. Engl.* **2001,** *40* (11), 2004-2021.

76. Wang, Q.; Chan, T. R.; Hilgraf, R.; Fokin, V. V.; Sharpless, K. B.; Finn, M. G., Bioconjugation by copper(I)-catalyzed azide-alkyne [3 + 2] cycloaddition. *J. Am. Chem. Soc.* **2003,** *125* (11), 3192-3.

77. Zhou, Z.; Fahrni, C. J., A fluorogenic probe for the copper(I)-catalyzed azide-alkyne ligation reaction: modulation of the fluorescence emission via 3(n,pi)-1(pi,pi) inversion. *J. Am. Chem. Soc.* **2004,** *126* (29), 8862-3.

78. Kaltgrad, E.; O'Reilly, M. K.; Liao, L.; Han, S.; Paulson, J. C.; Finn, M. G., On-virus construction of polyvalent glycan ligands for cell-surface receptors. *J. Am. Chem. Soc.* **2008,** *130* (14), 4578-9.

79. Bruckman, M. A.; Kaur, G.; Lee, L. A.; Xie, F.; Sepulveda, J.; Breitenkamp, R.; Zhang, X.; Joralemon, M.; Russell, T. P.; Emrick, T.; Wang, Q., Surface modification of tobacco mosaic virus with "click" chemistry. *Chembiochem* **2008,** *9* (4), 519-23.

80. Moses, J. E.; Moorhouse, A. D., The growing applications of click chemistry. *Chem. Soc. Rev.* **2007,** *36* (8), 1249-62.

81. Best, M. D., Click chemistry and bioorthogonal reactions: unprecedented selectivity in the labeling of biological molecules. *Biochemistry* **2009,** *48* (28), 6571-84.

82. Seo, T. S.; Bai, X.; Ruparel, H.; Li, Z.; Turro, N. J.; Ju, J., Photocleavable fluorescent nucleotides for DNA sequencing on a chip constructed by site-specific coupling chemistry. *Proc. Natl. Acad. Sci. U. S. A.* **2004,** *101* (15), 5488-93.

83. Yamada, T.; Peng, C. G.; Matsuda, S.; Addepalli, H.; Jayaprakash, K. N.; Alam, M. R.; Mills, K.; Maier, M. A.; Charisse, K.; Sekine, M.; Manoharan, M.; Rajeev, K. G., Versatile site-specific conjugation of small molecules to siRNA using click chemistry. *J. Org. Chem.* **2011,** *76* (5), 1198-211.

84. Kolb, H. C.; Sharpless, K. B., The growing impact of click chemistry on drug discovery. *Drug Discov Today* **2003,** *8* (24), 1128-37.

85. Weisbrod, S. H.; Marx, A., Novel strategies for the site-specific covalent labelling of nucleic acids. *Chem. Commun. (Cambridge)* **2008,** (44), 5675-85.

86. Seo, T. S.; Li, Z.; Ruparel, H.; Ju, J., Click chemistry to construct fluorescent oligonucleotides for DNA sequencing. *J. Org. Chem.* **2003,** *68* (2), 609-12.

87. Gierlich, J.; Burley, G. A.; Gramlich, P. M.; Hammond, D. M.; Carell, T., Click chemistry as a reliable method for the high-density postsynthetic functionalization of alkyne-modified DNA. *Org. Lett.* **2006,** *8* (17), 3639-42.

88. Neef, A. B.; Schultz, C., Selective fluorescence labeling of lipids in living cells. *Angew. Chem. Int. Ed. Engl.* **2009,** *48* (8), 1498-500.

89. Deiters, A.; Cropp, T. A.; Mukherji, M.; Chin, J. W.; Anderson, J. C.; Schultz, P. G., Adding amino acids with novel reactivity to the genetic code of Saccharomyces cerevisiae. *J. Am. Chem. Soc.* **2003,** *125* (39), 11782-3.

90. Speers, A. E.; Adam, G. C.; Cravatt, B. F., Activity-based protein profiling in vivo using a copper(I)-catalyzed azide-alkyne [3 + 2] cycloaddition. *J. Am. Chem. Soc.* **2003,** *125* (16), 4686-7.

91. Speers, A. E.; Cravatt, B. F., Profiling enzyme activities in vivo using click chemistry methods. *Chem. Biol.* **2004,** *11* (4), 535-46.

92. Chan, T. R.; Hilgraf, R.; Sharpless, K. B.; Fokin, V. V., Polytriazoles as copper(I)-stabilizing ligands in catalysis. *Org. Lett.* **2004,** *6* (17), 2853-5.

93. Hong, V.; Presolski, S. I.; Ma, C.; Finn, M. G., Analysis and optimization of copper-catalyzed azide-alkyne cycloaddition for bioconjugation. *Angew. Chem. Int. Ed. Engl.* **2009,** *48* (52), 9879-83.

94. Gaetke, L. M.; Chow, C. K., Copper toxicity, oxidative stress, and antioxidant nutrients. *Toxicology* **2003,** *189* (1-2), 147-63.

95. Link, A. J.; Vink, M. K.; Tirrell, D. A., Presentation and detection of azide functionality in bacterial cell surface proteins. *J. Am. Chem. Soc.* **2004,** *126* (34), 10598-602.

96. Soriano Del Amo, D.; Wang, W.; Jiang, H.; Besanceney, C.; Yan, A. C.; Levy, M.; Liu, Y.; Marlow, F. L.; Wu, P., Biocompatible copper(I) catalysts for in vivo imaging of glycans. *J. Am. Chem. Soc.* **2010,** *132* (47), 16893-9.

97. Hong, V.; Steinmetz, N. F.; Manchester, M.; Finn, M. G., Labeling live cells by copper-catalyzed alkyne--azide click chemistry. *Bioconjug. Chem.* **2010,** *21* (10), 1912-6.

98. Agard, N. J.; Prescher, J. A.; Bertozzi, C. R., A strain-promoted [3 + 2] azide-alkyne cycloaddition for covalent modification of biomolecules in living systems. *J. Am. Chem. Soc.* **2004,** *126* (46), 15046-7.

99. Baskin, J. M.; Prescher, J. A.; Laughlin, S. T.; Agard, N. J.; Chang, P. V.; Miller, I. A.; Lo, A.; Codelli, J. A.; Bertozzi, C. R., Copper-free click chemistry for dynamic in vivo imaging. *Proc. Natl. Acad. Sci. U. S. A.* **2007,** *104* (43), 16793-7.

100. Schoenebeck, F.; Ess, D. H.; Jones, G. O.; Houk, K. N., Reactivity and regioselectivity in 1,3-dipolar cycloadditions of azides to strained alkynes and alkenes: a computational study. *J. Am. Chem. Soc.* **2009,** *131* (23), 8121-33.

101. Bach, R. D., Ring strain energy in the cyclooctyl system. The effect of strain energy on [3 + 2] cycloaddition reactions with azides. *J. Am. Chem. Soc.* **2009,** *131* (14), 5233-43.

102. Codelli, J. A.; Baskin, J. M.; Agard, N. J.; Bertozzi, C. R., Second-generation difluorinated cyclooctynes for copper-free click chemistry. *J. Am. Chem. Soc.* **2008,** *130* (34), 11486-93.

103. Sletten, E. M.; Bertozzi, C. R., A hydrophilic azacyclooctyne for Cu-free click chemistry. *Org. Lett.* **2008,** *10* (14), 3097-9.

104. Ning, X.; Guo, J.; Wolfert, M. A.; Boons, G. J., Visualizing metabolically labeled glycoconjugates of living cells by copper-free and fast huisgen cycloadditions. *Angew. Chem. Int. Ed. Engl.* **2008,** *47* (12), 2253-5.

105. Debets, M. F.; van Berkel, S. S.; Schoffelen, S.; Rutjes, F. P.; van Hest, J. C.; van Delft, F. L., Aza-dibenzocyclooctynes for fast and efficient enzyme PEGylation via copper-free (3+2) cycloaddition. *Chem. Commun. (Cambridge)* **2009,** *46* (1), 97-9.

106. Jewett, J. C.; Sletten, E. M.; Bertozzi, C. R., Rapid Cu-free click chemistry with readily synthesized biarylazacyclooctynones. *J. Am. Chem. Soc.* **2010,** *132* (11), 3688-90.

107. Sletten, E. M.; Nakamura, H.; Jewett, J. C.; Bertozzi, C. R., Difluorobenzocyclooctyne: synthesis, reactivity, and stabilization by beta-cyclodextrin. *J. Am. Chem. Soc.* **2010,** *132* (33), 11799-805.

108. Chenoweth, K.; Chenoweth, D.; Goddard, W. A., 3rd, Cyclooctyne-based reagents for uncatalyzed click chemistry: A computational survey. *Org. Biomol. Chem.* **2009,** *7* (24), 5255-8.

109. Ess, D. H.; Jones, G. O.; Houk, K. N., Transition states of strain-promoted metal-free click chemistry: 1,3-dipolar cycloadditions of phenyl azide and cyclooctynes. *Org. Lett.* **2008,** *10* (8), 1633-6.

110. Poloukhtine, A. A.; Mbua, N. E.; Wolfert, M. A.; Boons, G. J.; Popik, V. V., Selective labeling of living cells by a photo-triggered click reaction. *J. Am. Chem. Soc.* **2009,** *131* (43), 15769-76.

111. Dommerholt, J.; Schmidt, S.; Temming, R.; Hendriks, L. J.; Rutjes, F. P.; van Hest, J. C.; Lefeber, D. J.; Friedl, P.; van Delft, F. L., Readily accessible bicyclononynes for bioorthogonal labeling and three-dimensional imaging of living cells. *Angew. Chem. Int. Ed. Engl.* **2010,** *49* (49), 9422-5.

112. Dehnert, K. W.; Beahm, B. J.; Huynh, T. T.; Baskin, J. M.; Laughlin, S. T.; Wang, W.; Wu, P.; Amacher, S. L.; Bertozzi, C. R., Metabolic Labeling of Fucosylated Glycans in Developing Zebrafish. *ACS Chem. Biol.* **In press**, DOI: 10.1021/cb100284d.

113. van Berkel, S. S.; Dirks, A. T.; Debets, M. F.; van Delft, F. L.; Cornelissen, J. J.; Nolte, R. J.; Rutjes, F. P., Metal-free triazole formation as a tool for bioconjugation. *Chembiochem* **2007,** *8* (13), 1504-8.

114. Blackman, M. L.; Royzen, M.; Fox, J. M., Tetrazine ligation: fast bioconjugation based on inverse-electron-demand Diels-Alder reactivity. *J. Am. Chem. Soc.* **2008,** *130* (41), 13518-9.

115. Devaraj, N. K.; Weissleder, R.; Hilderbrand, S. A., Tetrazine-based cycloadditions: application to pretargeted live cell imaging. *Bioconjug. Chem.* **2008,** *19* (12), 2297-9.

116. Song, W.; Wang, Y.; Qu, J.; Madden, M. M.; Lin, Q., A photoinducible 1,3-dipolar cycloaddition reaction for rapid, selective modification of tetrazole-containing proteins. *Angew. Chem. Int. Ed. Engl.* **2008,** *47* (15), 2832-5.

117. Song, W.; Wang, Y.; Qu, J.; Lin, Q., Selective functionalization of a genetically encoded alkene-containing protein via "photoclick chemistry" in bacterial cells. *J. Am. Chem. Soc.* **2008,** *130* (30), 9654-5.

118. Srivastava, G.; Kaur, K. J.; Hindsgaul, O.; Palcic, M. M., Enzymatic transfer of a preassembled trisaccharide antigen to cell surfaces using a fucosyltransferase. *J. Biol. Chem.* **1992,** *267* (31), 22356-61.

119. Loka, R. S.; Sadek, C. M.; Romaniuk, N. A.; Cairo, C. W., Conjugation of synthetic N-acetyl-lactosamine to azide-containing proteins using the Staudinger ligation. *Bioconjug. Chem.* **2010,** *21* (10), 1842-9.

120. Loka, R. S.; Cairo, C. W., Immobilization of carbohydrate epitopes for surface plasmon resonance using the Staudinger ligation. *Carbohydr. Res.* **2010,** *345* (18), 2641-7.

121. Jackson, D. I.; Barclay, A. N., The extra segments of sequence in rat leucocyte common antigen (L-CA) are derived by alternative splicing of only three exons and show extensive O-linked glycosylation. *Immunogenetics* **1989,** *29* (5), 281-7.

122. Barclay, A. N.; Jackson, D. I.; Willis, A. C.; Williams, A. F., Lymphocyte specific heterogeneity in the rat leucocyte common antigen (T200) is due to differences in polypeptide sequences near the NH_2-terminus. *EMBO. J* **1987,** *6* (5), 1259-64.

123. Cyster, J. G.; Fowell, D.; Barclay, A. N., Antigenic determinants encoded by alternatively spliced exons of CD45 are determined by the polypeptide but influenced by glycosylation. *Int. Immunol.* **1994,** *6* (12), 1875-81.

124. Irles, C.; Symons, A.; Michel, F.; Bakker, T. R.; van der Merwe, P. A.; Acuto, O., CD45 ectodomain controls interaction with GEMs and Lck activity for optimal TCR signaling. *Nat. Immunol.* **2003,** *4* (2), 189-97.

125. Majeti, R.; Bilwes, A. M.; Noel, J. P.; Hunter, T.; Weiss, A., Dimerization-induced inhibition of receptor protein tyrosine phosphatase function through an inhibitory wedge. *Science* **1998,** *279* (5347), 88-91.

126. Earl, L. A.; Baum, L. G., CD45 glycosylation controls T-cell life and death. *Immunol. Cell. Biol.* **2008,** *86* (7), 608-15.

127. Leppanen, A.; Stowell, S.; Blixt, O.; Cummings, R. D., Dimeric galectin-1 binds with high affinity to alpha2,3-sialylated and non-sialylated terminal N-acetyllactosamine units on surface-bound extended glycans. *J. Biol. Chem.* **2005,** *280* (7), 5549-62.

128. Pace, K. E.; Lee, C.; Stewart, P. L.; Baum, L. G., Restricted receptor segregation into membrane microdomains occurs on human T cells during apoptosis induced by galectin-1. *J. Immunol.* **1999,** *163* (7), 3801-11.

Chapter 2

Conjugation of synthetic carbohydrate epitopes to azide-containing proteins using the Staudinger ligation[1, 2, 3]

1. Portions of this work have been published in Loka, R. S.; Sadek, C. M.; Romaniuk, N. A.; Cairo, C. W., *Bioconjug .Chem.* **2010**, *21* (10), 1842-9; Loka, R. S.; Cairo, C. W., Immobilization of carbohydrate epitopes for surface plasmon resonance using the Staudinger ligation. *Carbohydr. Res.* **2010**, *345* (18), 2641-7.

2. Western blot (**Figure 2.2**) and lectin blotting (**Figure 2.5**) were acquired by C. M. Sadek (University of Alberta)

3. Azide modified lactoglobulin was provided by N. A. Romaniuk (University of Alberta)

2.1 Abstract

The generation of defined glycoconjugates is necessary for the study of glycoprotein function, as well as the development of therapeutics. The biosynthesis of glycoproteins produces multiple glycoforms, proteins which differ only in the structure of the attached glycan. This inherent heterogeneity complicates the study of isolated glycans and, in particular, could obscure the role of individual glycan epitopes in biological function. We present a general strategy based on the Staudinger ligation to introduce specific glycan epitopes onto azide-containing proteins. The use of a phosphane-based Staudinger reagent allows for extremely mild reaction conditions which can be applied to aqueous proteins or cells. We demonstrate that multiple carbohydrate epitopes can be incorporated onto a protein backbone, and that the resulting glycans are competent for recognition by lectins. We propose that this general strategy will allow for testing the role of specific glycan epitopes in cellular and biochemical assays and increasing the stability of protein conjugates.

2.2 Introduction

Post-translational modifications can have a dramatic influence on the function and properties of proteins.[1] The most prevalent post-translational modification found in mammalian cells is glycosylation, the covalent attachment of oligosaccharides. These carbohydrates are attached to many cell surface and secreted proteins, by either *O*- (serine or threonine - linked) or *N*-linkages (asparigine – linked). Mammalian glycans are known to affect the function and recognition of proteins with roles in cellular adhesion, antigen recognition, and development.[2] A common difficulty in the study of glycobiology is the heterogeneous nature of glycan structures. Glycoproteins isolated from natural sources are typically a mixture of glycoforms - proteins that differ only in their glycan composition. The presence of multiple glycoforms complicates the interpretation of results from these samples. Therefore, general strategies to produce synthetic glycoconjugates with uniform glycosylation continue to be of interest. The generation of defined glycoconjugates is critical for enabling the study of glycan function and the development of therapeutics. A variety of approaches have been employed for forming protein glycoconjugates, including amine-crosslinking, native chemical ligation, solid-phase peptide synthesis, unnatural amino acid incorporation, chemoenzymatic synthesis, and chemoselective ligation.[3-5] Chemoselective ligation of glycans presents an appealing approach to the bioconjugate chemist, allowing for the combination of a biologically isolated protein with a synthetic glycan.[3, 6, 7] Strategies which employ chemoselective ligation, therefore allow the incorporation of either a known homogeneous glycan en bloc or the introduction of specific glycan epitopes within an existing glycan. Chemoselective modifications of glycoproteins have been demonstrated using both purified glycoproteins, as well as glycoproteins in the membrane of live cells and animals.[7-10] The biosynthesis of glycoproteins produces multiple glycoforms. This inherent heterogeneity

complicates the study of isolated glycans and, in particular, could obscure the role of individual glycan epitopes in biological function. The ability to modify glycoproteins found within the glycocalyx of living cells presents the opportunity to identify the specific roles of glycan epitopes. Chemoselective modification of cell-surface glycans, referred to as *glycoform remodeling*, has been used to target specific cells[11] and to modify the function of glycoproteins.[12] Intriguingly, modifications of cell-surface glycans have been used to alter biological responses, inducing immune-targeting and modifying cellular adhesion.[13, 14]

2.3 Hypothesis

Chemoselective strategies can form the basis of determining the roles of specific changes in glycosylation within complex biological systems. However, the introduction of complex glycan epitopes onto a protein backbone can be challenging, and chemical methods for the synthesis of glycoproteins continues to be an active area of research.[15-17] We chose to employ a popular chemoselective strategy, the Staudinger ligation, which forms a covalent linkage between an azide and a phosphane containing an intramolecular electrophilic trap as shown in **Scheme 2.1**.[8] The azide component may be introduced semi-synthetically[18] or through the metabolic incorporation of azide-containing biosynthetic precursors.[7, 19] The Staudinger ligation has proven to be a robust labeling chemistry and can be carried under extremely mild reaction conditions which can be applied to aqueous proteins or cells. Although there are alternative reactions that exploit the azide functional group which could also be used,[20] Staudinger ligation has its own advantages as described in **Chapter 1**. We assume that this ligation strategy will allow us to incorporate specific epitopes of interest on to the glycan *in vivo* and study its function in native habitat.

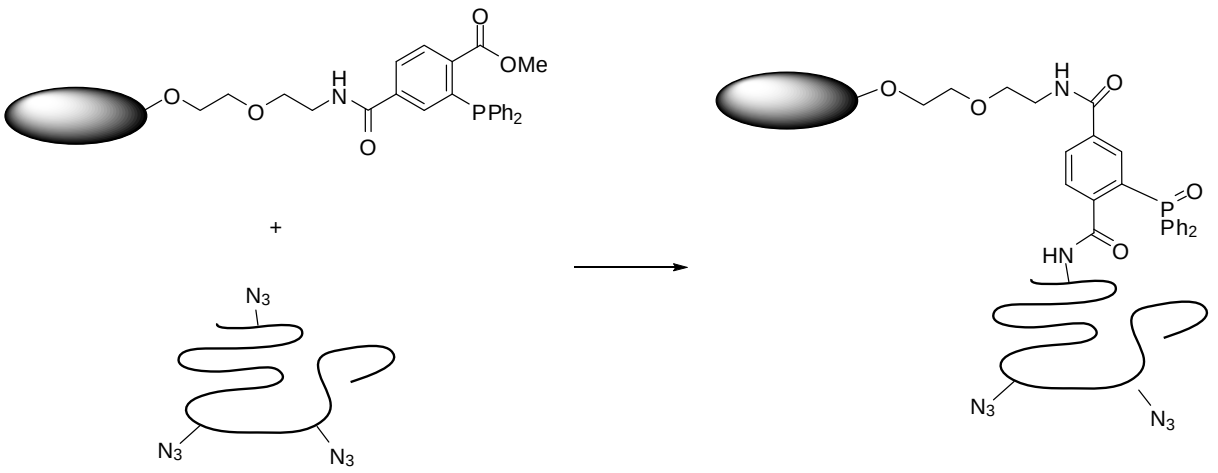

Figure 2.1: Conjugation of specific glycan epitopes onto azide-incorporated proteins. Azide introduced either synthetically or metabolically on to a protein can be used as handle to attach specific carbohydrate epitopes by Staudinger ligation.

We developed an efficient route to reagents able to introduce galactose (Gal), lactose (Lac, Gal-β (1,4)-Glc), and *N*-acetyl-lactosamine (LacNAc, Gal-β(1,4)-GlcNAc) glycans and conjugated them on to synthetically azide incorporated protein(β-lactoglobulin). Our primary target is LacNAc epitopes, as this unit is part of type 2 lactosamine repeats of *N*- and *O*- linked glycans and a component of the Lewis x and y epitopes.[21] We demonstrated that multiple carbohydrate epitopes can be incorporated onto a protein backbone, and that the resulting glycans are competent for recognition by lectins. Thus we propose that this general strategy (**Figure 2.1**) can be useful for testing the role of specific glycan epitopes (ex: LacNAc moieties) in cellular and biochemical assays.

2.4 Biosynthetic labeling of sialic acids

As shown in the general strategy (**Scheme 2.1**), when cells are incubated with peracetylated *N*-azidoacetyl mannosamine (Ac_4ManNAz), the cells own biosynthetic pathway modifies ManNAz into sialic acids with the azide group intact and secretes on to the cell surface.

The azide functionalities on these sialic acids can be then used as handles for conjugation, thus the specific epitope of interest can be introduced by Staudinger Ligation. To test the viability of

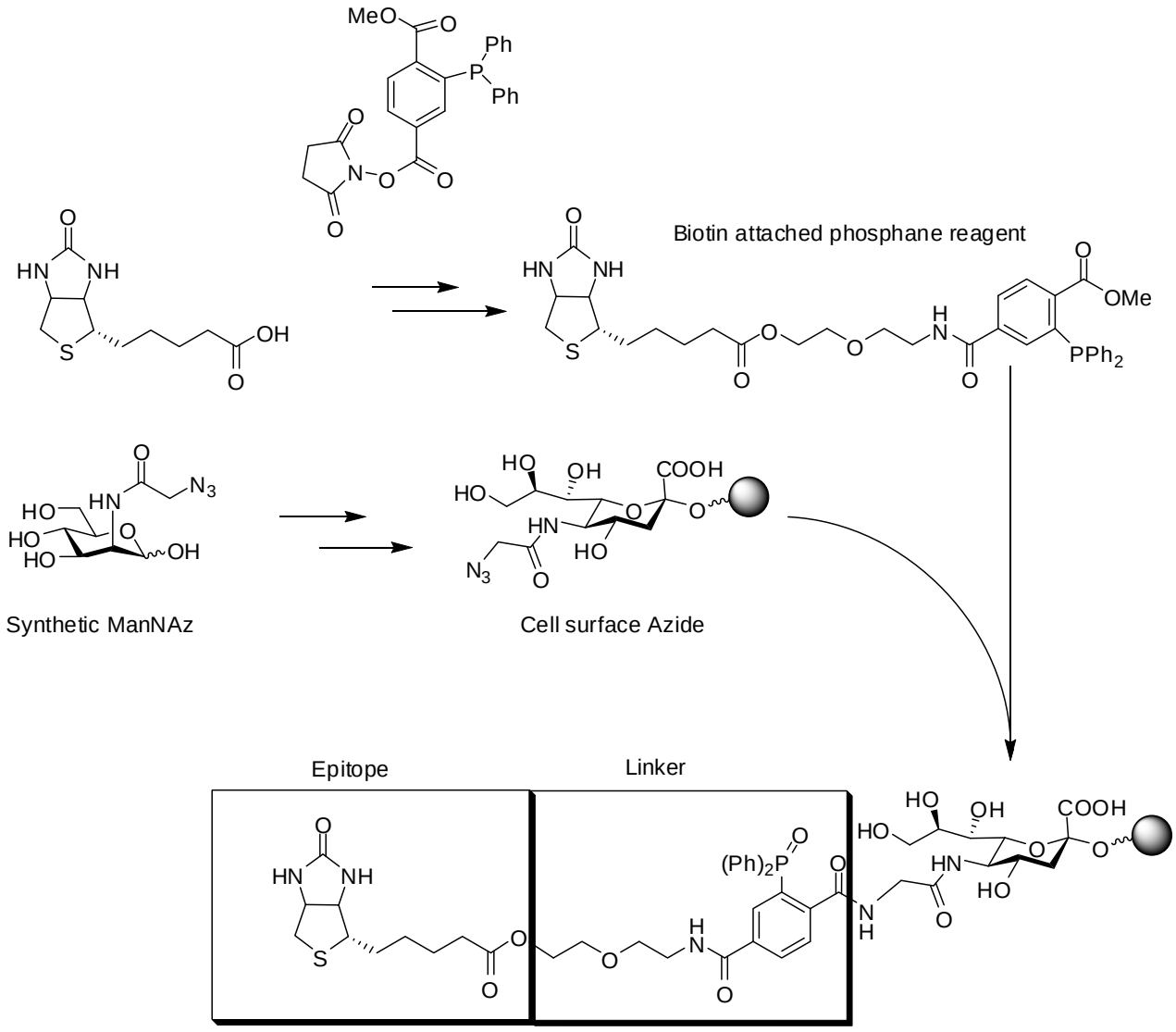

Scheme 2.1: General strategy for labeling azide-containing sialic acids by the Staudinger ligation. Using a biosynthetic labeling strategy, azide groups introduced into glycoproteins can be selectively modified by Staudinger Ligation. By conjugating the phosphane to the reducing end of a synthetic glycan, the biotin can be engineered to interact with streptavidin.

this hypothesis, we first synthesized peracetylated ManNAz and a biotin modified phosphane reagent. These compounds can then be used for the metabolic labeling of cells by following the method established by Bertozzi and co-workers.[22]

2.4.1 Synthesis of peracetylated ManNAz (Ac_4ManNAz)

Bertozzi and co-workers has described a linear synthesis of ManNAz, where azidoacetylation of mannosamine was achieved by treating with iodoacetic anhydride followed by displacement of iodine with sodium azide. This method has several drawbacks, it uses excess expensive reagent iodoacetic anhydride and the displacement subsequently carried on an expensive intermediate (**Scheme 2.2**).[22] To avoid this, we followed the convergent synthesis of

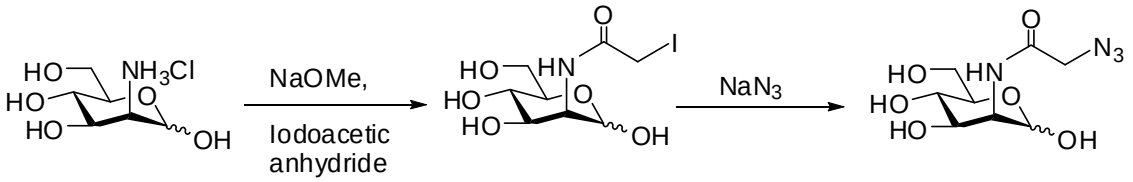

Scheme 2.2: Bertozzi's method for ManNAz synthesis. A linear synthesis of ManNAz from mannosamine.

Chen, X. et al.[23] As shown in scheme **2.3**, the *N*-hydroxysuccinamide (NHS) activated ester of azidoacetic acid was synthesized in two steps from bromoacetic acid, a relatively cheap reagent, by displacing bromine with azide followed by *N*,*N*′-dicyclohexylcarbodiimide (DCC) coupling of NHS to the azidoacetic acid. Mannosamine was treated with the NHS ester, **2.2**, to give azido acylated mannosamine, **2.3**, yields obtained for this step were less than reported. Acylation of **2.3** in presence of acetic anhydride in pyridine with a catalytic amount of DMAP gave Ac_4ManNAz, **2.4**.

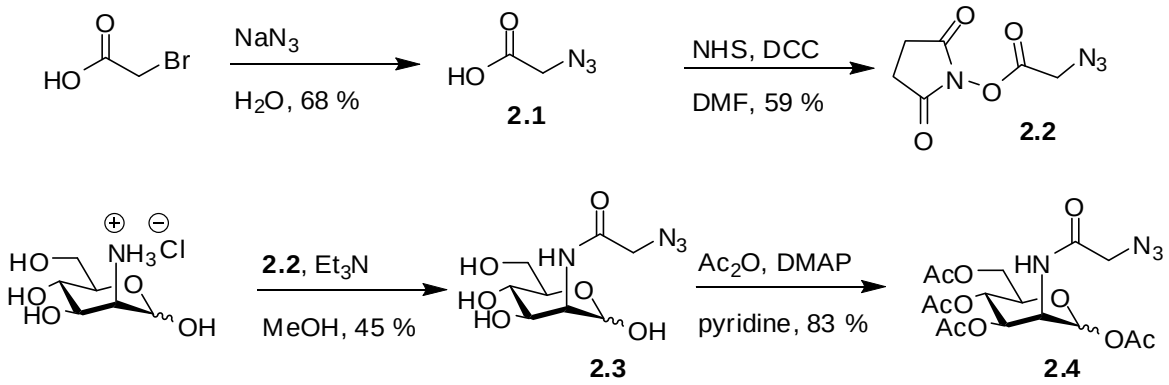

Scheme 2.3: Synthesis of Ac_4ManNAz. A convergent synthesis of ManNAz, where azide was directly incorporated by acylation of amine.

2.4.2 Synthesis of a biotin-phosphane reagent

The Staudinger ligation reagent, **2.6**, consists of a carboxylic acid, para to a methyl ester on phenyl ring and can be used as a handle to introduce an epitope of interest (biotin) through formation of an amide bond. Since this reagent is vulnerable to oxidation,[24] we made an NHS-activated ester that can be used under milder conditions.

2.4.2.1 Synthesis of NHS activated phosphane reagent

The NHS activated phosphane reagent was synthesized from 1-methyl-2-aminoterephthalate in three steps as shown in **Scheme 2.4** by following a well-established protocol[10, 25] with slight modification in workup procedures. The amine of the terephthalate was converted into a diazonium ion by treating with HCl and sodium nitrite, later the diazonium group was displaced with iodide under reflux conditions to afford iodoterephthalate, **2.5**. This iodo derivative was coupled to diphenyl phosphine by palladium catalysis to yield the Staudinger reagent, **2.6a**, along with small amount of its corresponding oxide, **2.6b**, in a 1: 0.09 ratio (based on ^{31}P NMR) respectively. The reagent might have oxidized during coupling or crystallization.

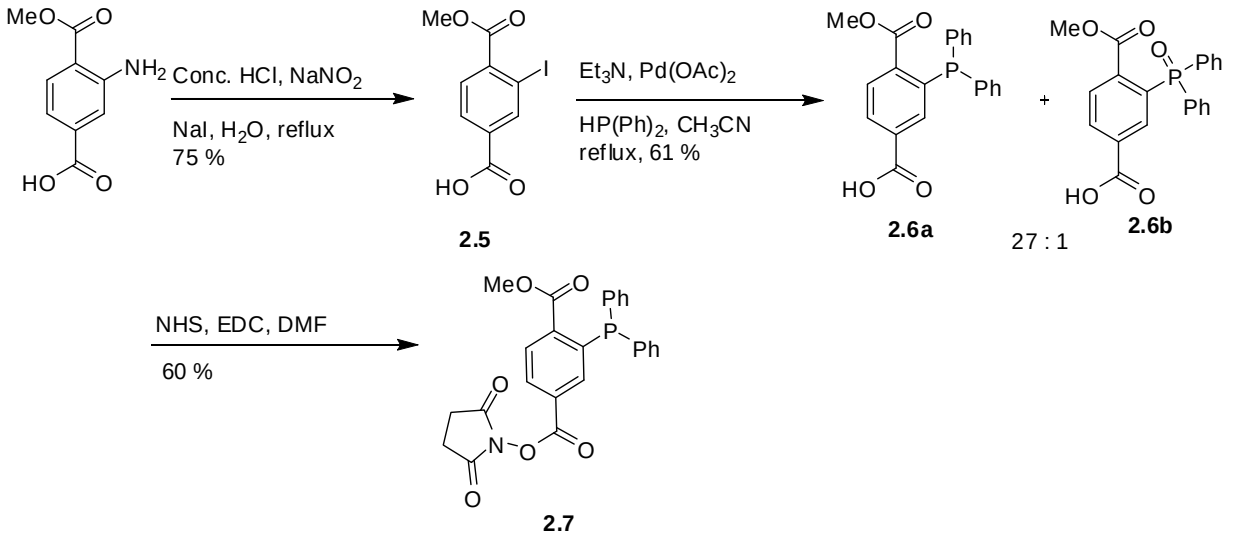

Scheme 2.4: Synthesis of NHS-activated Phosphane reagent, 2.7. As phosphane reagent, **2.6a**, susceptible to oxidation, NHS-actvated ester, **2.7**, was made to avoid coupling reagents.

Without further purification, the mixture was coupled to NHS with 1-ethyl-3-(3-dimethylaminopropyl)- carbodiimide (EDC). After several unsuccessful attempts at crystallization, silica gel column chromatography provided pure activated ester, **2.7**. With **2.7** in hand, we synthesized biotin with a free amine at the terminus of linker for amide bond formation.

2.4.2.2 Synthesis of an amino derivative of biotin and tethering to a phosphane reagent

As we intended to use this reagent for in vivo experiments, it should be soluble in water-miscible solvents such as DMSO. As well, there should be proper space between the glycoprotein and biotin after conjugation to avoid steric issues with the affinity binding proteins, avidin or streptavidin. In light of these requirements, an ethylene glycol linker was used instead of an alkyl chain to increase the solubility in polar solvents. We envisioned protecting the amine with *t*-butyloxycarbonyl (Boc) instead of other masking reagents since deprotection of this group is highly efficient, and doesn't require any further purification. The amine of linker was

selectively protected with Boc by treating with di-*t*-butyl-dicarbonate(DIBOC or Boc anhydride) under solvent free, catalyst free, conditions at room temperature to give carbamate, **2.8**.[26] Esterification of biotin with **2.8** using EDC and 4-*N*,*N*-dimethylaminopyridine (DMAP) gave linker-attached biotin, **2.9**. The reaction didn't proceed well when catalytic amounts of DMAP were used instead of stoichiometric quantities. Boc was deprotected under acidic conditions to obtain free amine, and coupled to activated phosphane reagent, **2.7**, using triethylamine as a base to generate the desired final compound, **2.10**.

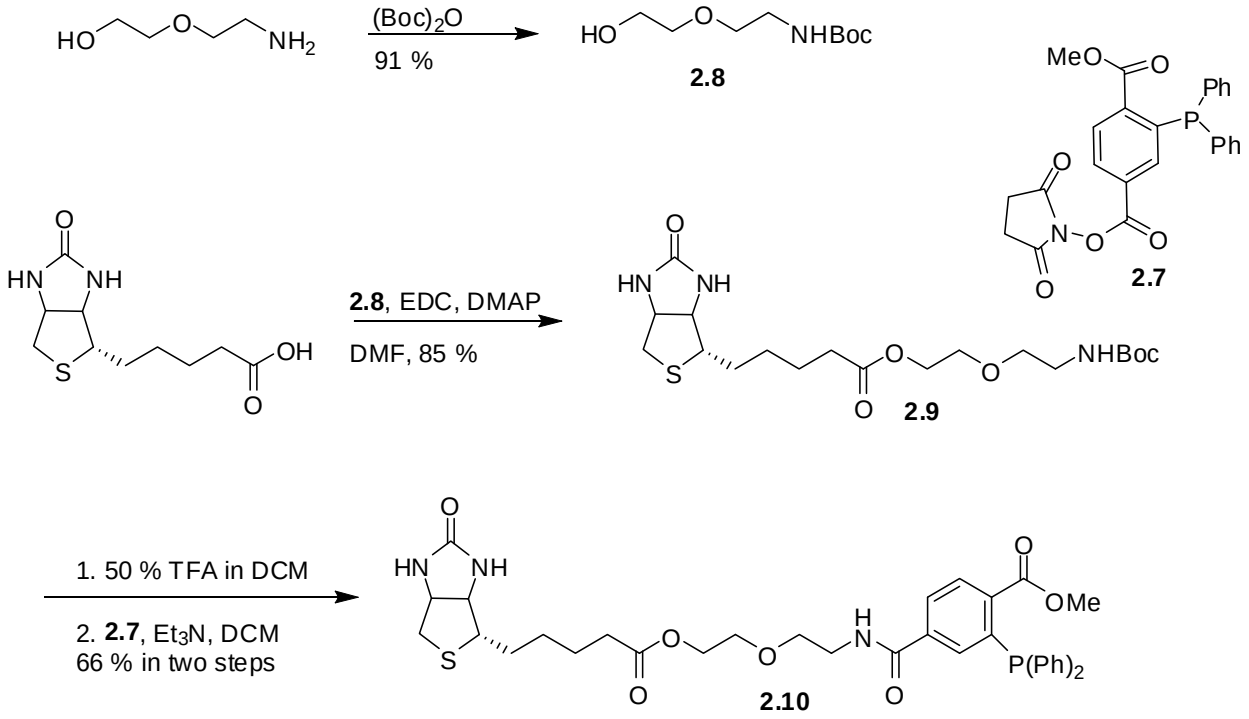

Scheme 2.5: Synthesis of a biotin-phosphane reagent. A Boc-protected amine linker was coupled to biotin, followed by Boc deprotection and resulting free amine was acylated with phosphane reagent, **2.7**.

2.4.3 Biotinylation of metabolically-incorporated azides

To test the utility of the phosphane reagent, **2.10**, we replicated the work of Bertozzi and co-workers.[22] An azide label was incorporated into the glycoprotein, the lymphocyte function associated antigen I (LFA-1) by treating with $Ac_4ManNAz$, **2.4**. The resulting azide containing glycoprotein, **LFA-1**, was reacted with biotin phosphane reagent, **2.10**, and formed biotinylated protein by Staudinger ligation. These proteins were visualized by Westernblotting through binding of strepatavidin. To confirm that the azide labeling was specific for the *N*-glycan, the glycoprotein was treated with Peptide N-glycosidase F (PNGase F) to remove *N*-linked glycans and confirmed by western blot which didn't show any traces of protein as glycans were removed (**Figure 2.2**).

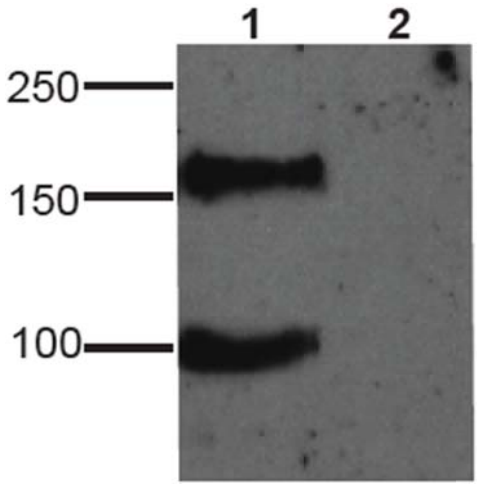

Figure 2.2: Western blot showing biotinylation of azide-incorporated LFA-1. Metabolically incorporated azides on LFA-1 were labeled by Staudinger ligation with the biotinylated phosphine, **2.10**. The biotinylated proteins were separated by SDS-PAGE, blotted to nitrocellulose, and probed with streptavidin-HRP conjugate. Bands were detected by chemiluminescence. PNGase-F treatment was performed overnight at 37 °C on the native heterodimer. Lanes shown: 1-Untreated; 2-PNGase-F-treated.

2.5 Synthesis of glycosyl-phophane reagents

Our ultimate goal was to make defined and stable glycoconjugates with the Staudinger ligation. We therefore first required the development of suitable phosphane derivatives that could install the target carbohydrates onto a model protein. Although our primary interest is the incorporation of a LacNAc disaccharide, we also intended to make related carbohydrate structures to be used as controls in future experiments. We selected a monosaccharide, galactose (Gal), and a disaccharide, lactose (Lac, Gal-β(1,4)-Glc) for this purpose. Based on the synthesis of the biotin phosphane reagent, we decided to use the same linker, and designed the target structures accordingly. The target structures consisted of a carbohydrate epitope, a linker, and a

2.16.

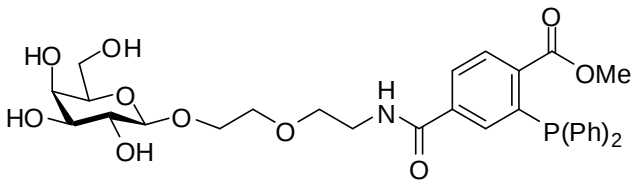

2.21.

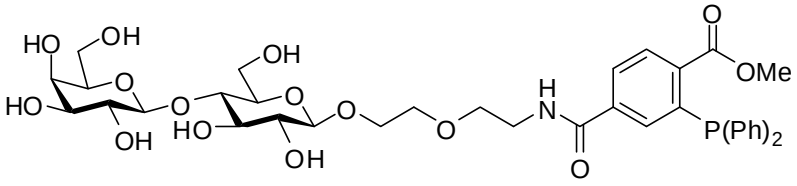

2.40.

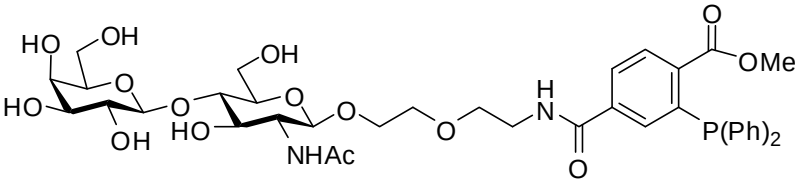

Scheme 2.6: Target structures. Galactose (**2.16**), lactose (**2.21**) and LacNAc (**2.40**) conjugated phosphane reagents were designed on the basis of synthesis of biotin conjugated phosphane reagent, **2.10**.

phosphane group as shown in **Scheme 2.6**. Before designing a synthetic route for these targets, we explored the stability of phosphane reagent, **2.6**, to different acid and base conditions, commonly used for deprotections in carbohydrate chemistry.

2.6 Stability of phosphane reagents to acid/base conditions

As described earlier, phosphane reagents are highly susceptible to oxidation[24] and we monitored the stability of this reagent for a range of acid/base conditions, usually employed for deprotections in carbohydrate chemistry. A fixed amount of compound was taken in an NMR tube and subjected to wide variety of conditions ranging from weak acid to strong base, keeping the final concentrations the same in all the tubes. ^{31}P NMR spectra were recorded at different time points under identical parameters. The reagent, **2.6**, in chloroform (control) showed two ^{31}P peaks (similar to **Figure 2.3**) corresponding to both unoxidized, **2.6a**, (-2.8 ppm) and oxidized, **2.6b**, (30 ppm) in 1:0.09 ratio. We compared these integrations to spectra obtained over time for different conditions and these results were illustrated in **Table 1**. Hydrolysis of methyl ester of the reagent, **2.6**, is inevitable under these conditions. However, hydrolysis of ester should not have considerable effect on the chemical shift of ^{31}P NMR peak, as the reagent, **2.6**, and its NHS-derivative, **2.7**, show similar chemical shift. The phosphane integration of the control slightly changed with time, which may be due to oxidation by air (**Table 1**).

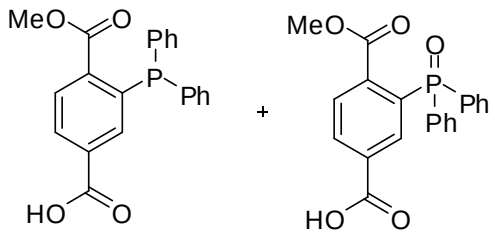

2.6a **2.6b**

Conditions		TFA (95% ,$CDCl_3$)		TFA (5% , $CDCl_3$)		Acetic acid		Piperidine (20% , DMF)		Hydrazine (2% , DMF)		NaOMe (1% , MeOH)		$CDCl_3$ (Control)	
		ppm	Int	ppm	Int	ppm	Int	ppm	Int	ppm	Int	ppm	Int	ppm	Int
Time (in h)	1.5	10.9	-	41.7 10.3	1.0 22.6	36.3 -2.8	1.0 5.8	29.7 -3.0	1.0 9.9	30.1 -3.4	1.0 4.5	NA	NA	32.5 -3.2	1.0 10.7
	12	11.1	-	41.6 10.3	1.0 13.6	36.4 -2.6	1.0 5.4	29.7 -3.0	1.0 5.4	30.2 -3.3	1.0 1.7	NA	NA	32.6 -3.2	1.0 8.8
	24	11.1	-	41.4 10.3	1.0 12.9	36.3 -2.7	1.0 5.3	29.7 -3.0	1.0 3.5	30.1 -3.3	1.0 1.2	-2.6 -6.4	1.9 1.0	32.6 -3.2	1.0 7.7
	48	11.1	-	41.2 10.3	1.0 8.0	NA	NA	29.7 -3.0	1.0 3.9	30.2 -3.3	1.0 0.5	-2.5 -6.3	0.9 1.0	32.7 -3.2	1.0 8.4

Table 2.1: Stability of phosphane reagent 2.6. Chemical shifts are given relative to 80% phosphoric acid as an external chemical shift reference (0 ppm). NA = no data available. Int = integration. The phosphine oxide peak was always integrated as one and appears at more downfield (~ 30 ppm) than phosphine (~ -3 ppm).

There was no change in chemical shifts with weak acid and weak bases even after prolonged time. However changes in integrations over time with weak bases (**Figure 2.3**) suggest that reagent might be degrading. Eventhough integrations are different compared to the control; they remained constant in weak acids throughout the study. The difference might be due

to change in medium (acidic). In the case of strong acids, signals were shifted downfield. This observation likely due to protonation to the phosphonium ion, as spectra taken after the removal of acid after 2 days showed reappearence of the original signal for **2.6a** (-2.9 ppm). In strong base, (NaOMe/MeOH), a new peak appeared (-6.4 ppm) along with phosphane peak (-2.5 ppm) may be due to phosphane oxide reaction with methoxide ion. Based upon these results, we concluded that the phosphane reagent was stable to acids and oxidizes faster in bases.

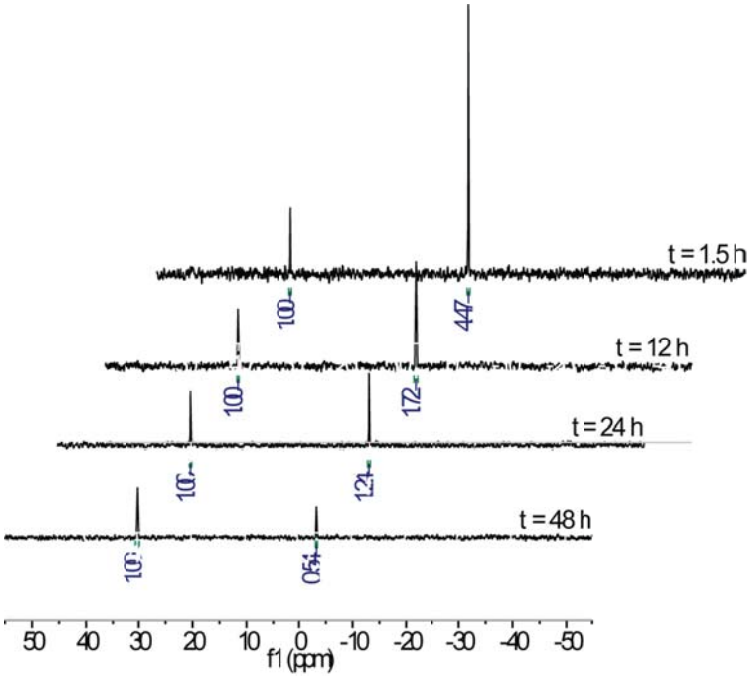

Figure 2.3: ^{31}P NMR of compound 2.6 in a 2% hydrazine-DMF solution. Peaks around 30 ppm, -3 ppm corresponds to phosphane oxide, **2.6b**, and phosphane, **2.6a**, respectively. With increasing time, the integration of the phosphane decreased compared to phosphane oxide peak, indicating its decomposition under these conditions.

2.7 Design and retrosynthetic analysis of target carbohydrates

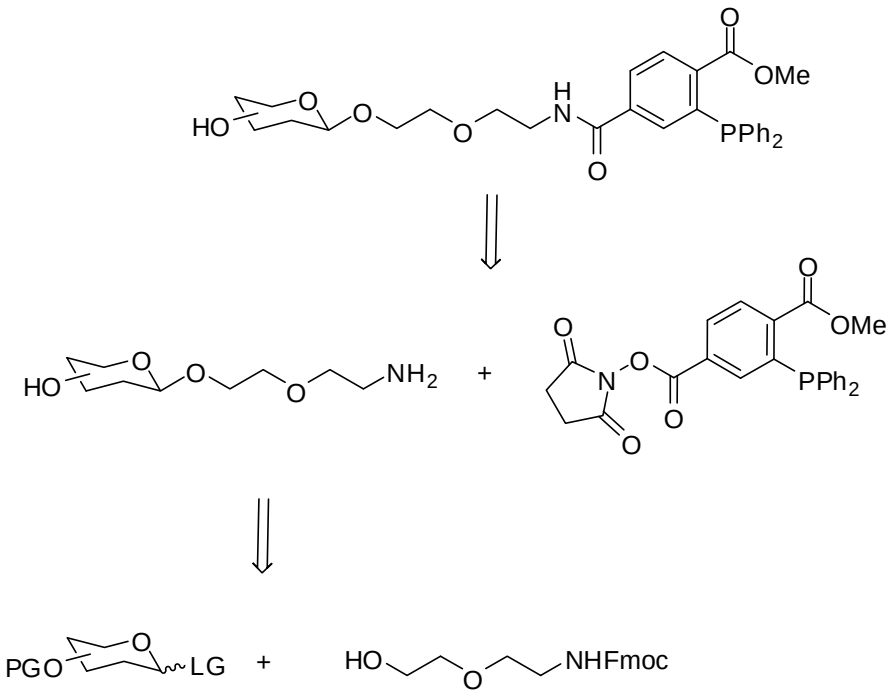

Scheme 2.7: General retrosynthetic plan for target carbohydrates. PG is a protecting group and LG is leaving group. Glycosylation of suitable glucosyl donor with protectected amine containing scaffold followed by global deprotection and acylation with phosphane reagent, **2.7**, will generate desired epitopes.

Due to our concern of phosphane stability we chose to introduce the phosphane late in the synthesis. Therefore, breaking the amide bond at the phosphane will yield the completely deprotected carbohydrate epitope with a free amine as illustrated in **Scheme 2.7**. This amine functionality can be introduced on to the carbohydrate as part of an ethyleneglycol-derived linker by masking the amine with suitable protecting group during glycosylation with a donor of our choice. Since we desired to generate β-linked carbohydrates, the donor should have a participating group next to the point of glycosylation, usually a benzoyl or an acetyl groups. Our

convergent strategy, in brief, involves synthesis of carbohydrate epitopes with a free amine from a suitable donor and ethylene glycol derived linker, and finally coupling this amine to an activated ester of phosphane, **2.7**, under mild conditions**.** This strategy is general and allows for the introduction of alternative amine-containing epitopes as desired.

2.8 Synthesis of a galactose-linked phosphane reagent

To generate a suitable azide reactive galactosyl-phosphane derivative, galactose was protected as the 2,3,4,6-tetrabenzoylated derivative, **2.12**, by perbenzoylation and selective deprotection of the anomeric position was achieved by first converting it into an anomeric bromide on treatment with HBr. The glycosyl bromide was converted to anomeric alcohol with water in presence of silver carbonate as catalyst to provide **2.13** (**Scheme 2.8**).[27] Compound **2.13** was then converted to the trichloroacetimidate derivative (TCA), **2.14**, as a mixture of anomers using trichloroacetonitrile and 1,8-diazabicycloundec-7-ene (DBU). Having access to the TCA donor, we opted for an Fmoc-protected 2-(2-aminoethoxy)-ethanol linker as the acceptor. Even though we had readily available a Boc- protected 2-(2-aminoethoxy)-ethanol linker **2.8**, we have choosen Fmoc-protection keeping in mind that Boc-protection may be unstable under the slightly acidic conditions needed for glycosylation. Fmoc-protection has the added advantage that it can be removed simultaneously with benzoyl groups. The amine of the linker was selectively protected with Fmoc by using Fmoc-O-Suc under basic conditions. Glycosylation of the TCA donor, **2.14**, by an Fmoc-protected linker, **2.11,** in the presence of TMSOTf proceeded in good yield, providing the fully protected compound, **2.15**.[28] Alkaline deprotection conditions[29] simultaneously removed benzoyl and carbamate protecting groups from compound **2.15** to yield the galactosyl-amine derivative. Low yields were observed for this reaction, likely due to benzoylation of the amine. Acylation of the free amine using an *N*-hydroxysuccinimide ester

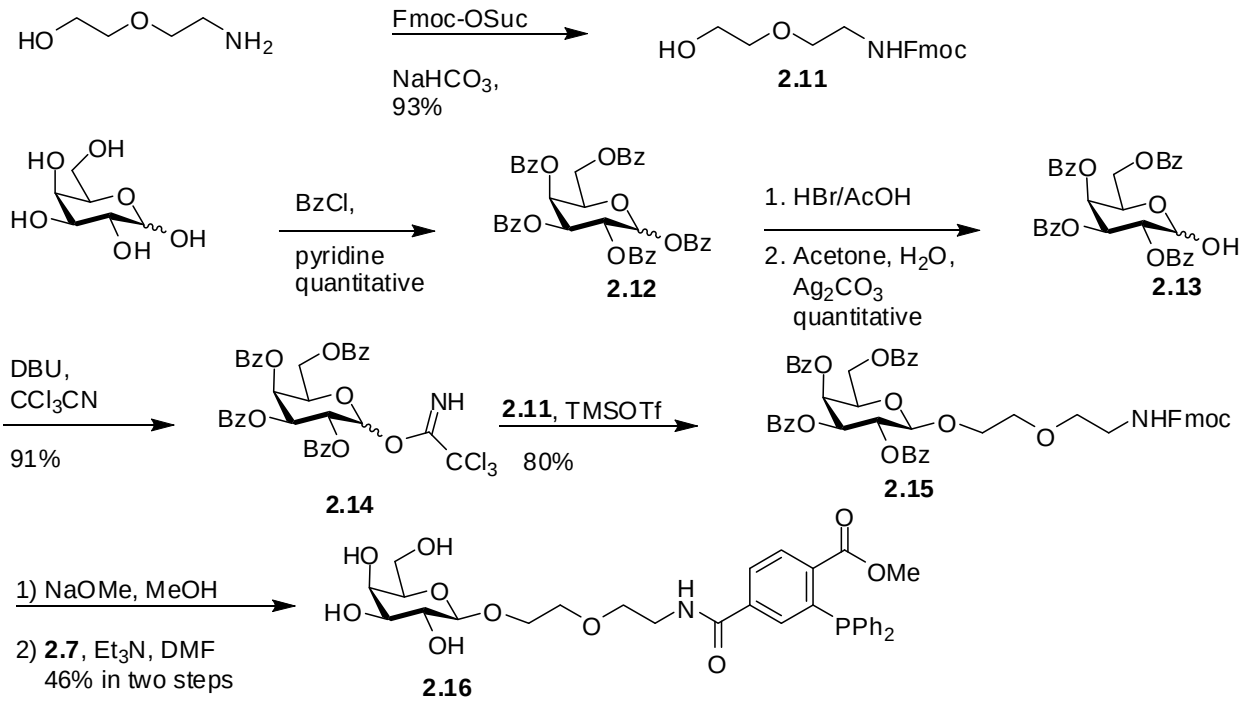

Scheme 2.8: Synthesis of a galactose-phosphane reagent, 2.16. Galactose-phosphane reagent, **2.16**, was generated from galactose with 34% overall yield.

(NHS) derived phosphane, **2.7**, led to the formation of final compound, galactosyl-phosphane reagent, **2.16**, in moderate yield along with small traces of its corresponding oxide. This minor contamination by the phosphine oxide originated from the starting NHS-ester and during purification, but did not appear to be due to the coupling conditions. Based on its ^{31}P NMR spectrum, the amount of oxidized product was found to be around 18%.

2.9 Synthesis of a lactose-linked phosphane reagent

The lactose-containing phosphane was generated using a similar sequence of reactions. Lactose was benzoylated under standard conditions in excellent yields. Perbenzoylated lactose was selectively deprotected at the anomeric position using hydrazine in acetic acid, to give compound **2.18** in good yield.[30] Treatment with DBU and trichloroacetonitrile gave the protected

lactosyl-TCA derivative, **2.19**, as the α-anomer.[28, 30] Glycosylation was carried out using the protected linker (2-(2-aminoethoxy)-ethanol) as before to provide compound **2.20** (**Scheme 2.9**).

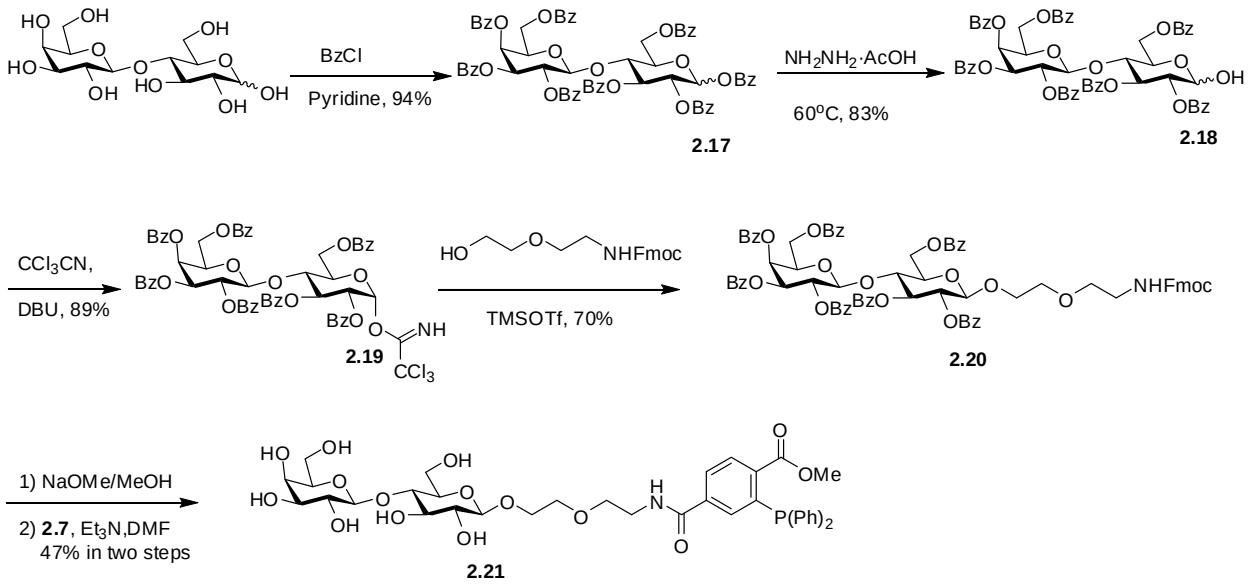

Scheme 2.9: Synthesis of a lactose-phosphane reagent, 2.21. Lactose-phosphane reagent, **2.21**, was generated from lactose with 23% overall yield.

Global deprotection of benzoyl and Fmoc groups was performed by using Zemple´n conditions,[29] resulting in the lactose containing free amine. Finally the amine was coupled to phosphane reagent, **2.**7, to give lactose phosphane reagent **2.21** in two steps. A small portion of oxidized phosphorus compound was observed along with the desired reagent **2.21** and it was found to be around 9% based on its ^{31}P NMR spectrum.

2.10 Synthesis of a LacNAc-linked phosphane reagent

The synthesis of LacNAc derivatives can be more challenging, due in part to the expense of the disaccharide as a starting material. In order to synthesize a LacNAc-phoshane reagent, we needed to generate a suitable lactosamine donor. The conventional method of synthesizing LacNAc donors is from its constituent monosaccharaides, glucosamine and galactose, with

suitable protection.[31] However, this method is cumbersome and time consuming. Enzyme catalyzed methods have been also used to assemble the two monosaccharides to avoid protecting groups.[32, 33] Even though this strategy simplifies the synthesis, it remains expensive and the final compound can only be produced in very small amounts. Disaccharides, such as lactal or lactulose, can be converted into lactosamine donor.[34-36] The advantage of starting with the disaccharide is that the regio- and stereo-chemistry between two monosaccharides is fixed, and the synthesis begins with a cheap advanced intermediate.

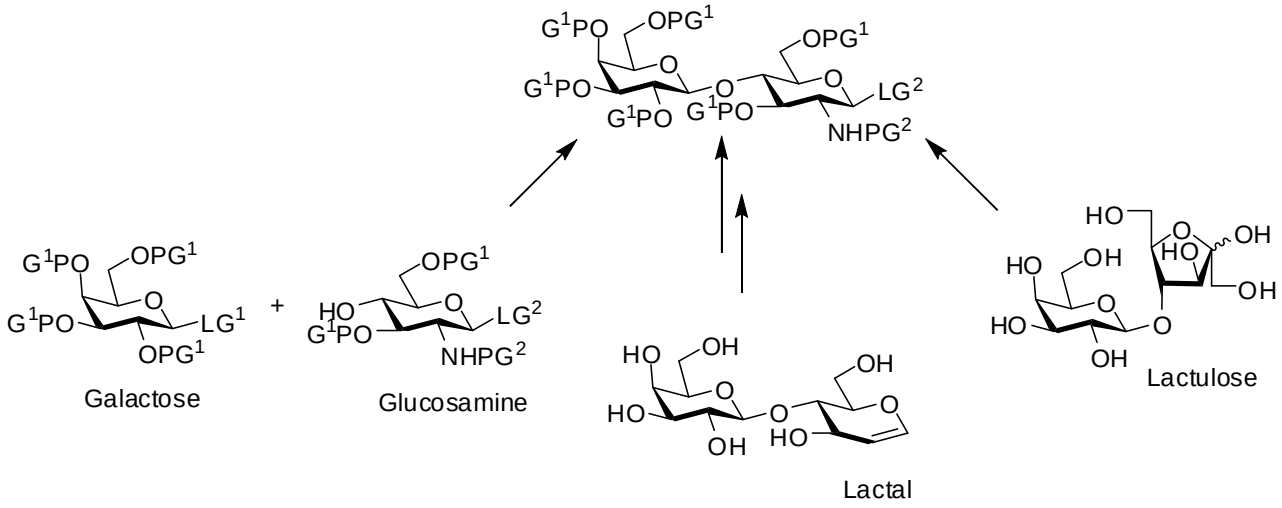

Scheme 2.10: Different strategies to synthesize a lactosamine donor. LG^1 and $LG^2$are orthogonal leaving groups which cannot be activated by using same promoter. PG^1 and PG^2 are protecting groups. PG^2 is participating group to generate 1, 2 trans stereochemistry, usually a phthalamide group.

2.10.1 Synthesis of a lactosamine donor from lactal

There are a number of elegant methods which have been developed to transform glycals into 2-amino-2-deoxy sugars.[34] Schmidt and coworkers reported a method where by nitration

followed by Michael addition of thio-derivatives under strong basic conditions to glycals can generate 2-nitro-1-thioglycosides.[37] Alternatively, glycals can be converted into highly unstable and strained three membered cyclic-aziridine intermediates, and subsequent glycosylation can lead to formation of 2-deoxy-2-amino sugars.[34] These cyclic aziridines can be generated from glycals by 1,3 dipolar-cycloaddition to an azide, and subsequent photochemical conversion of resulting triazoline[38] or by phosphoramidation[39, 40] and sulfonamidoglycosylation.[41, 42] Gin and co-workers[43] have reported the use of *C*-2 amidoglycosylation of glycals to provide direct access to the 2-acetamido-2-deoxy glycosides in a one-pot synthesis.

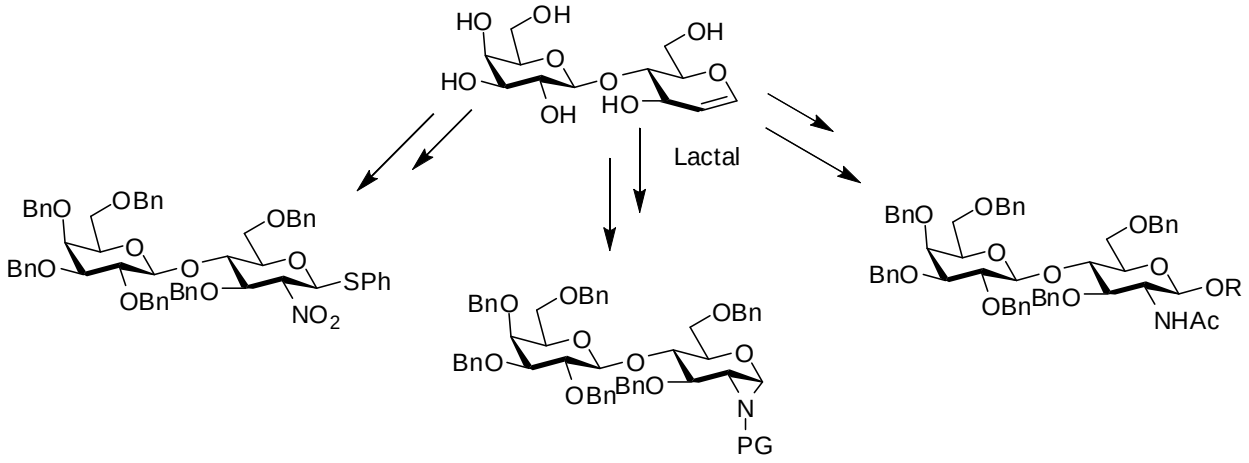

Scheme 2.11: Routes to convert lactal to a lactosamine donor. PG is protecting group. R-OH is an acceptor. Lactal can be converted into an amine derivative by using methods such as cycloaddition with azide, phosphoramidation, and sulfonamidoglycosylation or *C*-2 amidoglycosylation.

Since there are many procedures to modify a lactal into lactosamine donor, we first explored the utility of the most commonly employed strategies. We first decided to use the lactal to form lactosamine derivative following the methods of Danishefsky[42] and Gin.[43] Danishefsky's method has been used widely to synthesize similar intermediates.[34]

2.10.1.1 Synthesis of a lactosamine donor by Danishefsky's strategy[42]

The sulfonamidation of lactal to provide desired lactosamine donor has been previously reported by Danishefsky and co-workers.[42] The starting compound required for this strategy is a benzylated lactal which is prepared from lactose in five steps (**Scheme 2.12**). We converted Lactose to peracylated lactal, **2.22**, by a three step, one-pot procedure.[44] Lactose was peracetylated with acetic anhydride and selectively brominated at the anomeric position upon treatment with hydrogen bromide. A zinc-mediated elimination of bromine resulted in peracetylated lactal in a one-pot preparation. Deprotection of the acetyl groups was achieved under alkaline conditions in good yields.[45] Benzylation of the free lactal, **2.23**, was performed using benzyl bromide in the presence of strong base, sodium hydride, to generate the benzylated lactal, **2.24**.[42]

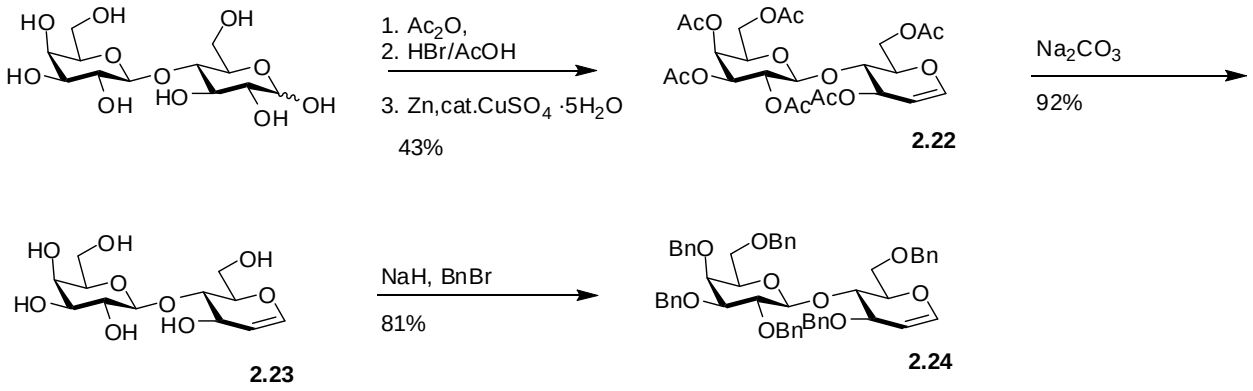

Scheme 2.12: Synthesis of benzylated lactal, 2.24. Peracetylated lactal, **2.22**, was made from lactose by a 3 step-one pot procedure. Acetyl protections were switched with benzyl to make the olefin electron rich.

The reaction of benzylated lactal with a combination of iodonium (di-*sym*-collidine) perchlorate (IDCP) and trimethylsilylethanesulfonamide resulted in *trans*-diaxial

iodosulfonamide, **2.26** in low yield (**Scheme 2.13**). Trimethylsilylethanesulfonamide is an expensive commercial reagent, which can be easily prepared from sodium trimethylsilylethanesulfonate in two steps.[46] In the first step, acid chloride was generated upon treatment with phosphorus pentachloride. Next, reaction with ammonia gave trimethylsilylethanesulfonamide in moderate yield. Glycosidation of iodosulfonamide, **2.26**, was performed with ethanethiol in the presence of excess lithium hexamethyldisilazide (LiHMDS), to

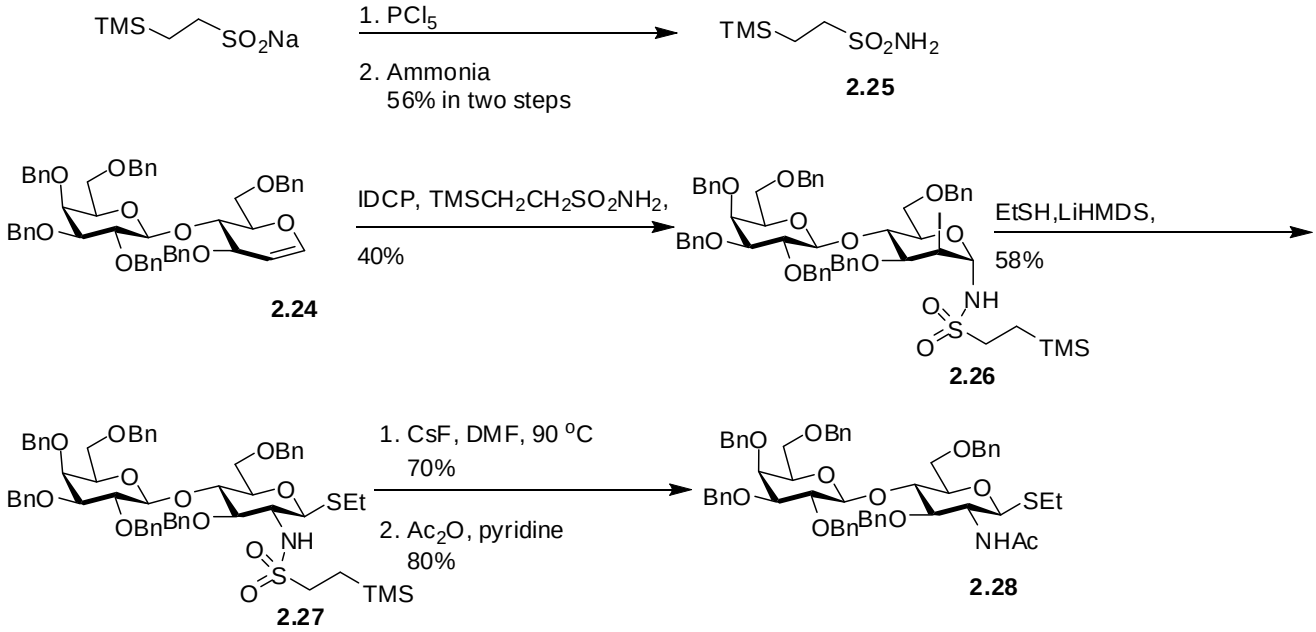

Scheme 2.13: Synthesis of lactosamine thioglycoside from benzylated lactal, 2.24. This strategy is not economical for synthesizing *N*-acetyl lactosamine due to utilization of expensive reagents and poor yields.

afford thioglycoside, **2.27** in 58% yield. The amine was unmasked under higher temperatures (90 ^{o}C) with cesium fluoride. Acylation of the free amine by acetic anhydride gave lactosamino-thioglycoside, **2.28**. Although we succeeded in making the thioglycoside donor, yields obtained for the iodosulfonamidation and glycosylations were low, and further deprotection of the amine, **2.26**, was slow (2 d). We abandoned this route due to its impracticality for large-scale synthesis

and the cost of the reagent, trimethylsilyl ethanesulfonamide. We next explored a one pot C-2 amidoglycosylation introduced by Gin and Co-workers.[43]

2.10.1.2 Synthesis of a lactosamine donor by Gin's strategy[43]

Gin and co-workers demonstrated a one pot procedure of C-2 amidoglycosylation of monosaccharide glycals to produce acetamido glycosides. This protocol involved activation of the glycal by a novel electrophile, thianthrene bis(triflate), **2.30**, followed by treatment with an acetamido nucleophile, and glycosyl acceptor to afford 2-acetamido glycoconjugates. To the best of our knowledge this method has not been applied to a disaccharide glycal. In order to establish this protocol for a lactal, we intended to use methanol as an acceptor.

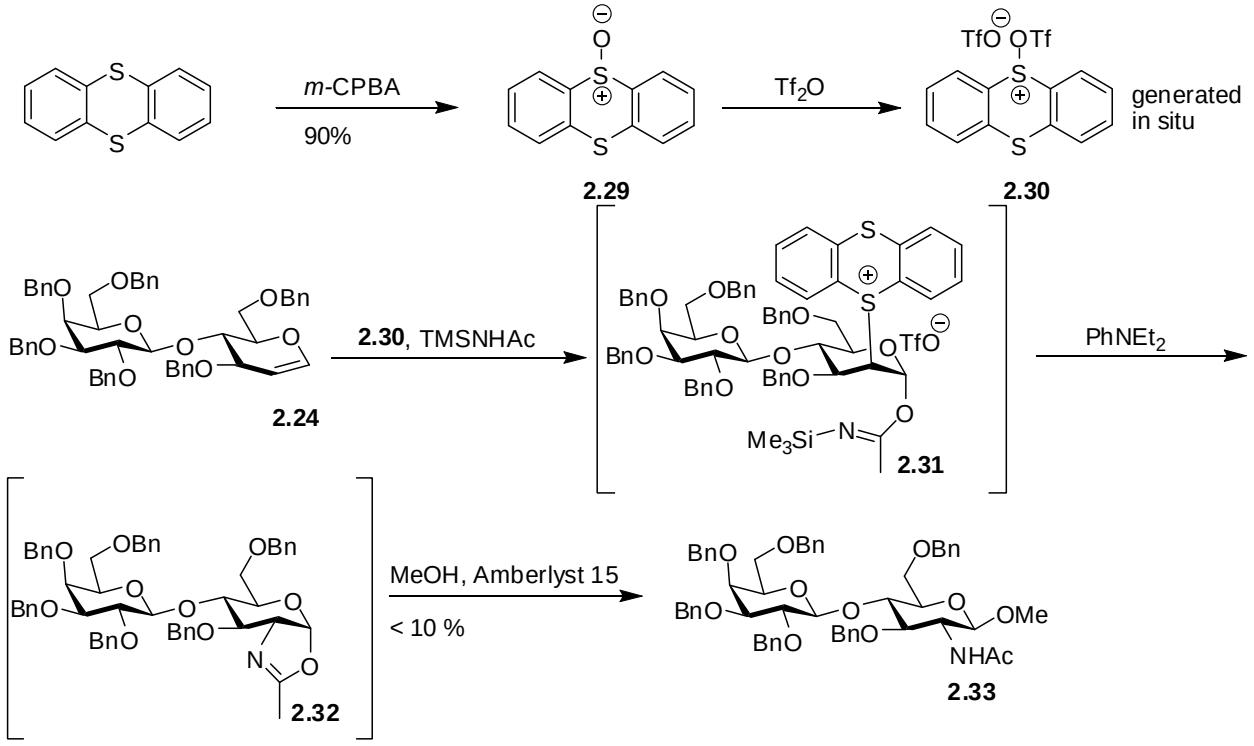

Scheme 2.14: Conversion of lactal to lactosamine by Gin's strategy. Low yields, indicate that this strategy is not feasible for making C-2 acetamido sugars from disaccharides.

The lactal enolether, **2.24**, was activated by thianthrene bis (triflate), generated in situ from thianthrene-5-oxide, **2.29**, and Tf_2O. Thianthrene-5-oxide was in turn derived from thianthrene, by oxidation with *m*-CPBA (meta-chloroperoxybenzoic acid) in good yield.[47] Activated lactal was attacked with an acetamido nucleophile at the anomeric position to give glycosyl imidate, **2.31**. Intramolecular displacement of thianthrene by imine and *N*-desilylation under mild basic conditions, subsequent rearrangement afforded oxazoline, **2.32**, which could be opened under strong acidic conditions generated by amberlyst-15 resin. In the presence of an alcohol acceptor, methanol, 2-acetamido methyllactoside, **2.33**, was formed in low yield (ca > 10%, including contaminants, confirmed by mass spectrometry). Our attempts to purify this compound further were unsuccessful. We attempted to improve this reaction by using excess amount, of thianthrene bis(triflate) or *N*-(TMS)acetamide, however these conditions did not provide significant improvement in the yield.

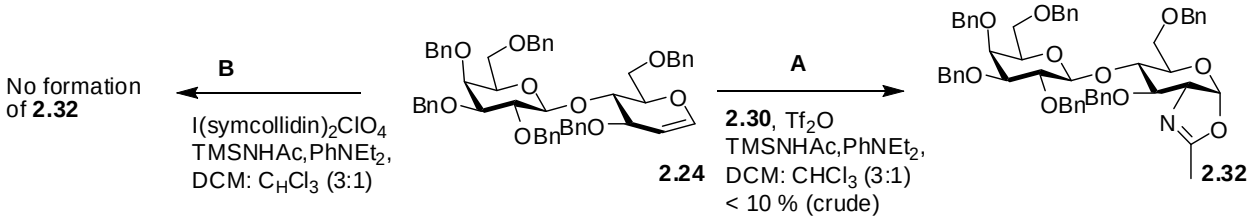

Scheme 2.15: Synthesis of benzyl oxazoline, 2.32. Gin's strategy (A) to make oxazoline gave low yields (crude). Lactal activation by iodinum (B) instead of thianthrene bis(triflate) to generate oxazoline as final product was not successful.

Attempts to isolate oxazoline intermediate, **2.32**, before glycosylation with methanol were unsuccessful (**Scheme 2.15, A**). We also investigated the use of iodonium ions, (Danishefsky's strategy) as the lactal activator and *N*-(TMS)acetamide (Gin's strategy) for amination followed by rearrangement to generate oxazoline, **2.32** (**Scheme 2.15, B**). Neither of

these approaches showed product formation. Although Gin's method is a simple way to access monosaccharide amines in one pot, the low yields we obtained for a disaccharide limited its utility for our strategy.

2.10.2 Synthesis of a lactosamine donor from lactulose by the Heyns rearrangement

We found that the method reported by Wrodnigg and Stutz [35, 36] based on the Heyns rearrangement of lactulose can provide excellent yields of the peracetylated lactosamine in one pot (**Scheme 2.16**). Reductive amination of lactulose with benzylamine, followed by Heyns rearrangement under acidic conditions afforded benzyllactosamine, **2.34**. Debenzylation of the amine by hydrogenation with Pd/C catalyst in acidic medium gave the chloride salt of lactosamine. Acylation of lactosamine under basic conditions yielded peracetylated lactosamine. Though we succeeded in obtaining the peracetylated lactosamine, **2.37**, we were unable to purify it. We explored acylation of the amine followed by benzoyl protection or phthalamide protection of the amine to obtain the pure lactosamine derivative. Unfortunately our efforts at this were unsuccessful. Instead, we followed the protocol of Stutz et al., by protecting lactosamine as the DTPM derivative (1,3-dimethyl-5-[(dimethylamino)methylene]2,4,6(1H,3H,5H)-trioxopyrimidine), which could then be purified by precipitation.[36] DTPM, **2.35** was made from *N*,*N*-dimethylformamide dimethyl acetal and 1,3-dimethylbarbituric acid in good yield.[48]

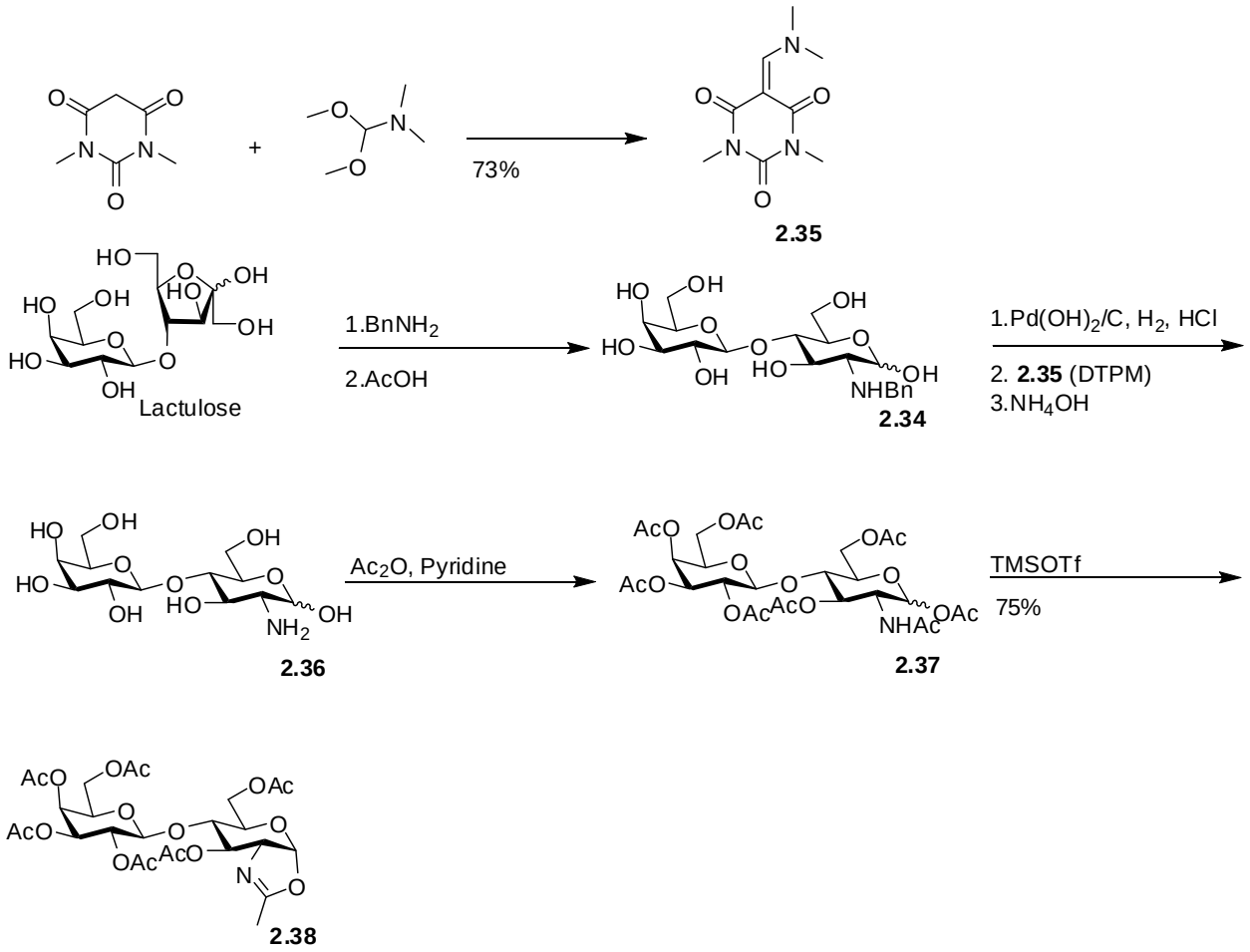

Scheme 2.16: Conversion of lactulose to oxazoline, 2.38. After debenzylation of **2.34**, amine was protected with DTPM. DTPM protected compound precipitates out and makes purification easier.

Subsequent removal of DTPM[48] and acetylation provides compound **2.37** as a relatively economical starting material. The acetyl-protected LacNAc (**2.37**) was converted to oxazoline, **2.39**, by following a standard protocol (**Scheme 2.16**).[49]

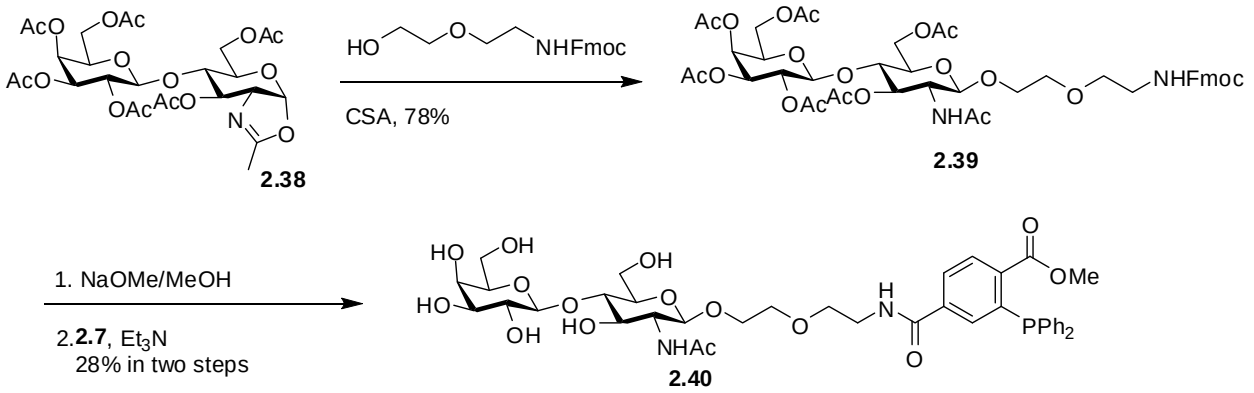

Scheme 2.16: Synthesis of LacNAc-phosphane, 2.40, from oxazoline. LacNAc-phosphane reagent, **2.40**, was obtained in 3 steps from oxazolidine with 22% yield.

The oxazolidine donor, **2.38**, was then modified to incorporate a linker, to provide the fully-protected compound **2.39**. Removal of Fmoc and acetyl groups was achieved under basic conditions.[29] Free amine was acylated with phosphane reagent, **2.7**, to generate LacNAc-phosphane, **2.40**. The purity and oxidation state of the resulting phosphane compounds was confirmed using ^{31}P and ^{1}H NMR spectroscopy. Typically, we observed minor oxidation of the phosphane (ca. ~ 17%) based on NMR.

2.11 Conjugation of carbohydrates to a model protein

The carbohydrate-phosphane reagents (**2.16, 2.21** and **2.40**) contained small amounts of oxidized phosphorus (ca. ~ 15%). The phosphine oxide is expected to be unreactive for the Staudinger ligation, and should not interfere with the use of these reagents for conjugation. With these carbohydrate-phosphane derivatives in hand, we turned our attention to the formation of glycoprotein conjugates. We sought to determine the reactivity of the reagents on a model azide-containing protein, and to confirm the availability of the incorporated glycans as recognition elements within a glycoconjugate. We selected β-lactoglobulin as a model protein, due to its

small size and lack of glycosylation. The protein has 178 amino acids and a molecular weight of 18 kDa.[50] We modified lactoglobulin by acylation with an NHS-activated azido-acetic acid derivative (succinimidyl 2-azidoacetate, **2.2**) [51] to generate a model azide-containing protein. The sequence contains 16 lysine residues, which in addition to the *N*-terminus of the protein, provides 17 possible sites for acylation.

To confirm the reactivity of phosphane reagents **2.16**, **2.21**, and **2.40**, each was incubated with the azide-modified lactoglobulin. The isolated protein was then analyzed by mass spectrometry (MS) to observe the formation of the desired glycoconjugates (**Figure 2.4**). For the galactose labeling reagent, **2.16**, we observed clear evidence of the incorporation of between 1 – 13 saccharides. The most intense peaks observed were for 8 – 11 sites of incorporation. Conjugation reactions performed with the lactose reagent, **2.21**, gave similar results, with incorporation of between 1 – 16 disaccharides. The most intense peaks were seen for 8 – 12 sites of incorporation. Similar results were found with the LacNAc reagent, **2.40**, with 2-13 disacharides incorporation and most intense peaks for 8 – 12 sites of incorporation. Complete analyses of the observed peaks for all glycoconjugates were provided in the experimental section (**Table 2.2, 2.3** and **2.4**). We concluded that the Staudinger ligation reagents were efficiently incorporating the desired carbohydrate residues into the proteins. We then turned our attention to testing the availability of the glycan residues as recognition elements as part of the glycoconjugate.

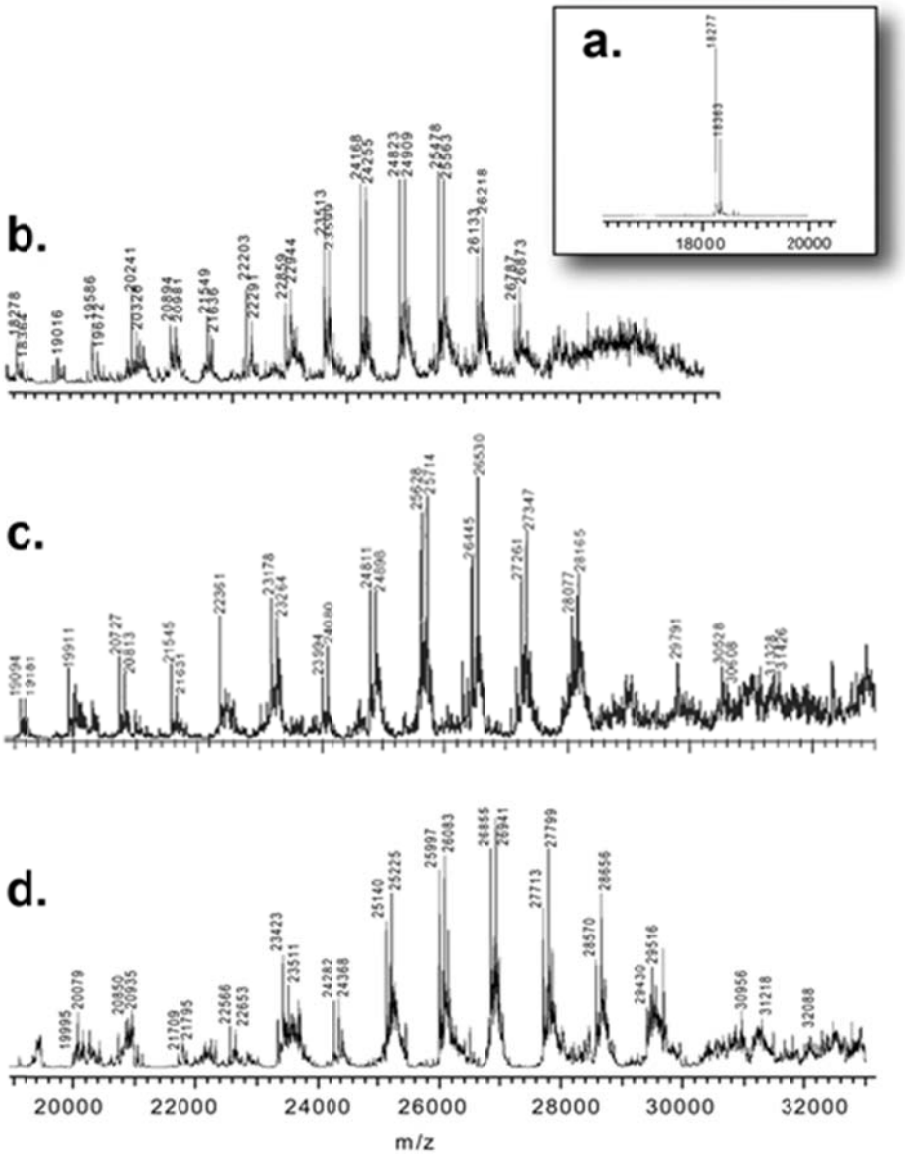

Figure 2.4: Mass spectral characterization of glycoconjugates. Glycoconjugates were analyzed using LC-MS to confirm the attachment of glycans. Lactoglobulin consists of A- and B-isoforms. Labeled protein samples were analyzed by LC-MS. Proteins analyzed were: (**a.**) unlabelled protein, (**b.**) azide-labeled protein reacted with compound **2.16**, (**c.**) the azide-labeled protein reacted with compound **2.21**, and (**d**.) azide-labeled protein reacted with compound **2.40**, All the conjugate samples showed incorporation of as many as 13 glycans.

Samples of Gal-, Lac-, and LacNAc-conjugated lactoglobulin were used in a lectin-blotting experiment.[52] The proteins were blotted onto nitrocellulose then probed with the *Maackia amurensis* lectin-I (MAL-I), which binds LacNAc and sialyl-LacNAc glycans[53] (**Figure 2.5**). Among the glycoconjugates studied, the lectin demonstrated a strong preference for labeling lactoglobulin which had been modified with the LacNAc reagent, **2.41**. Reduced staining was observed for the Lac conjugate, while neither the Gal conjugate nor the unreacted azido-lactoglobulin conjugates showed any reactivity to the lectin. These results confirm that the carbohydrate residues of the glycoconjugates are intact and capable of recognition by lectins.

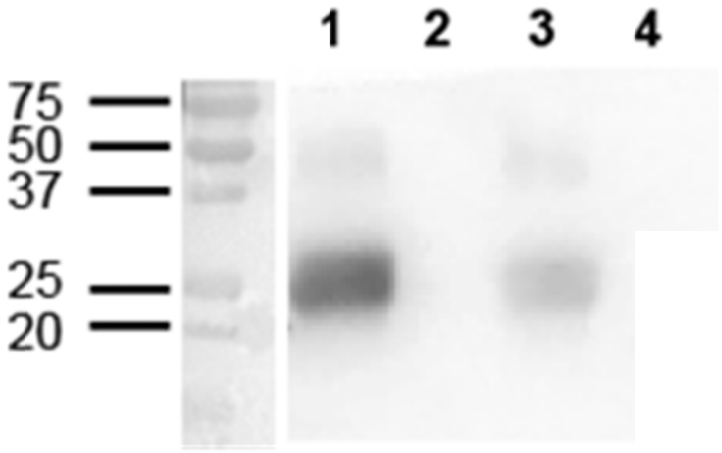

Figure 2.5: Lectin blotting characterization of glycoconjugates. Lactoglobulin glycoconjugates were probed with biotinylated MAL-I lectin to confirm the attachment of the desired glycans. Proteins were loaded on an SDS-PAGE gel (5%-15%), transferred to nitrocellulose and probed with MAL-I. The blot was developed with streptavidin-HRP. Lanes shown are: **1**. lactoglobulin-LacNAc, **2**. lactoglobulin-Gal, **3**. lactoglobulin-Lac, **4**. azido-acetic acid labeled lactoglobulin. The expected MW for the azido-acetic acid modified lactoglobulin is 18 kDa. MW markers are shown from a separate exposure of the same gel using visible light (ponceau stain): 75, 50, 37, 25, and 20 kDa.

2.12 Conclusions & future work

In this chapter, we have demonstrated a general route to glycoconjugates which incorporate synthetic glycans using the Staudinger ligation. The chemistry is based on the generation of a carbohydrate epitope with a free amine, which is then acylated to incorporate a phosphane label. In synthesis of galactose and lactose phosphane derivatives, we used trichloroacetimidate as donors for glycosylation. Synthesizing the donor for lactosamine was challenging. We explored the sulfonamidation strategy of Danishefsky[42] and C-2 amido glycosylation of Gin[43] to make these derivatives from benzylated lactal. However, we found that neither of these methods was feasible for large scale synthesis. We synthesized peracetylated lactosamine from lactulose in one-pot by following the method developed by Wrodnigg and Stutz. [35, 36] Lactulose was converted into lactosamine by Heyns rearrangement. DTPM was used to protect the amine and results in precipitation of pure compound. Then it is transformed into peracetylated lactosamine. This one-pot procedure provided peracetylated lactosamine from lactulose in excellent yields. The oxazoline donor was made from peracetylated lactosamine. These donors (trichloroacetimidate or oxazoline) were glycosylated with a suitable linker, deprotected and then the amine was coupled to activated ester of phosphane reagent. These carbohydrate- phosphane reagents will react with azide-containing proteins to generate a new glycoconjugates. We show that a model protein, lactoglobulin, can incorporate as many as 13 synthetic glycans, and that the resulting glycoconjugates are specifically recognized by lectins. This strategy provides a simple method for generating multi-site modified glycoconjugates under extremely mild conditions which are compatible with proteins and live cells.

Although we have only explored the use of three carbohydrate epitopes, we expect the chemistry employed here will be general, and could be easily adapted for the incorporation of

other glycan epitopes. Additionally, this modular strategy allows for only minimal development of new chemistry to generate different glycoconjugates. More complex glycans could be generated through the use of reductive amination of purified or chemoenzymatically prepared glycans.[54] Our studies here have used purified proteins which have been acylated to incorporate azide groups. However, this approach could be adapted for the development of other protein or lipid glycoconjugates.[55-57] An alternative strategy would be to isolate proteins or glycoproteins which have metabolically-incorporated azides.[58] This strategy could allow for selective modification of glycoproteins to test the role of specific glycan structures in biological activity. Although alternative chemistries could be employed for labeling azide-containing proteins, the Staudinger ligation strategy allows for mild conditions that are compatible with live cells.

Our group is interested in developing chemoselective strategies for increasing the proportion of specific glycan epitopes in cell-surface glycoproteins. We chose to develop chemistry for lactosamine derivatives since lactosamine repeats are commonly found in complex *N*-linked glycans and core-2 *O*-linked glycans.[59] Importantly, these structures can modulate the function of immunoreceptors, and the relative proportions of LacNAc incorporation can vary due to cell maturity or activation. The LacNAc epitope is essential for the recruitment of endogenous galectins to immunoreceptors, which induce cellular signals such as apoptosis and leukocyte stimulation.[59, 60] Thus, bioconjugate methods that can modify the content of LacNAc epitopes found within glycoproteins could be used to probe the role of a single glycan epitope in biological function. Finally, the strategy described here could be used as a method to increase the biological half-life of therapeutic proteins through attachment of defined glycans.[61-63]

2.13 Experimental procedures

2.13.1 General experimental methods

Dry solvents (CH_2Cl_2, MeOH, CH_3CN, and DMF) were purchased from Sigma Aldrich in capped DriSolv™ bottles and used without purification and stored under argon. Toluene and pyridine were dried on molecular sieves and stored under desiccated atmosphere. Reactions were conducted under a stream of argon at ambient temperature, unless otherwise noted, and monitored by TLC on silica gel G-25 UV254 (0.25 mm). Developed TLC plates were visualized under UV lamp and charred by heating plates that were dipped in cerium molybdate stain or phosphomolybdic acid stain. NMR experiments were conducted on Varian 300, 400 or 500 MHz instruments. Chemical shifts are reported relative to the deuterated solvent peak and are in parts per million (ppm). Phosphoric acid was used as an external standard for ^{31}P NMR. ^{1}H NMR and ^{13}C peak assignments were made on the basis of 2D-NMR such as COSY and HSQC experiments. ESI-MS spectra were carried out on samples suspended in solvent with added NaCl. β-Lactoglobulin was obtained as a mixture of bovine A- and B- isoforms (Sigma-Aldrich) and used without further purification.

2.13.2 Synthetic methods

Synthesis of azidoaceticacid (2.1):

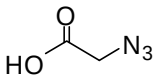

2.1

Sodium azide (4.182g, 39.3 mmol) was dissolved in 12 mL of deionized water and cooled to 0° C. Bromoacetic acid (4.456g, 32.1 mmol) was then added to the reaction, and the solution was slowly warmed to room temperature and stirred for 24 h. The mixture was acidified to pH 1 with

the addition of 4 mL of HCl (1:1, HCl:H_2O). The solution was extracted with diethyl ether (3 x 30 mL). The organic layers were combined and dried over Na_2SO_4 and concentrated to give a colorless liquid (2.211 g, 68.2 % yield). ^{1}H NMR (300 MHz, $CDCl_3$) : δ 3.98 (s, 2H), 10.72 (s,1H); HRMS calculated for $C_2H_3O_2N_3$ $(M)^+$, 101.0225, found 101.0223.

Synthesis of Succinimidyl 2-azidoacetate (2.2):

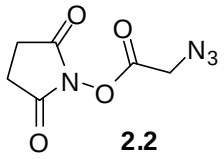

2.2

To a solution of azidoacetic acid, **2.1** (1.918 g, 18.98 mmol) and NHS (2.184 g, 18.98 mmol) in anhydrous DMF (26.6 mL) under argon was added DCC (3.916 g, 18.98 mmol) at 0 °C. The solution was stirred overnight at room temperature. The reaction was filtered to remove DCU. The filtrate was concentrated, and the product was crystallized from DCM/hexanes to give a white solid (2.230 g, 59.3% yield). ^{1}H NMR (300 MHz, $CDCl_3$) δ 4.24 (s, 2H), 2.87 (s, 4H); mp 113.9-116.1 ºC.

Synthesis of *N*-azidoacetyl-α/β-D-mannosamine (2.3):

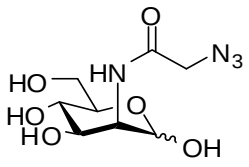

2.3

D-Mannosamine hydrochloride salt (1.80 g, 8.35 mmol) was dissolved in 36 mL of dry MeOH under argon. Triethylamine (4.7 mL) was then added followed by Succinimidyl 2-azidoacetate **2.2** (2.16 g, 10.9 mmol). The reaction mixture was stirred overnight at room temperature and concentrated. The residue was purified by a flash chromatography on eluting with $CHCl_3$: MeOH (10:1) and dissolved in 2 mL water, lyophilization afforded 1.053 g (44.8%) of white solid. ^{1}H

NMR (300 MHz, D_2O) : (1:0.79 α:β anomeric mixture) δ 5.17 (d, *J* = 2 Hz,1H), 5.08 (d, *J* = 2 Hz, 0.79H), 4.52 (dd, *J* = 2.2, 6.2 Hz, 0.75H), 4.39 (dd, *J* = 2.2, 6.2 Hz, 1H), 4.14 (t, *J* = 7.2 Hz, 2H), 4.09 (t, *J* = 6.6 Hz, 3H), 3.94-3.79 (m, 6H), 3.68-3.42 (m, 3H); HRMS calculated for $C_8H_{14}N_4O_6Na$ 285.08056, found 285.08039.

Synthesis of 1,3,4,6-Tetra-*O*-acetyl-*N*-azidoacetyl-α/β –D-mannosamine (2.4):

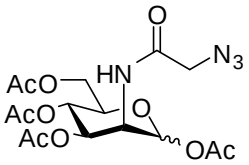

2.4

N-azidoacetyl-D-mannosamine **2.3** (580 mg, 2.2 mmol) was dissolved in 46.5 ml of pyridine and cooled to 0 °C. To this was added Ac_2O (23.2 mL, 255.2 mmol) and catalytic amount of DMAP (27 mg, 0.2 mmol). The reaction mixture was stirred overnight, while warming to RT. The resulting light orange solution was diluted with DCM (200 mL) and washed successively with 1 N HCl (3 x 65 mL), aq sat. $NaHCO_3$ (1 x65 mL), H_2O (1 x 65 mL), and Brine (1 x 65 mL).The combined aqueous layers were back extracted with DCM (100 mL). The combined organic layers were dried over Na_2SO_4 and concentrated. Traces of pyridine were further removed by co-evaporating with toluene (3 x 60 ml) under reduced pressure. The crude product was purified by a flash column chromatography eluting with gradient of 1:10 to 1:2 EtOAC/ Hexanes to obtain 700 mg of yellow oil (75.9% yield). ^{1}H NMR (400 MHz, $CDCl_3$): (1:0.6 α:β anomeric mixture) , δ 6.65 (d, *J* = 8.8 Hz, 0.6 H), 6.58 (d, *J* = 9.6 Hz, 1H), 6.05 (d, *J* = 1.6 Hz, 1H), 5.89 (d, *J* = 1.6 Hz, 0.6H), 5.35 (dd, *J* = 4.2,10.2 Hz, 1H), 5.22 (t, *J* = 10.0 Hz, 1H), 5.17 (t, *J* = 9.8 Hz, 0.6H), 5.07(dd, *J* = 3.8, 9.8 Hz, 0.6H), 4.74(ddd, *J* = 1.6, 3.6, 9.2 Hz, 0.58H), 4.62 (ddd, *J* = 2, 4.3, 9.32 Hz, 1H), 4.28-4.22 (m,1.68H), 4.17-4.02 (m, 6H), 3.85-3.80 (m, 0.6 H), 2.19-1.99 (4s, 22H). ^{13}C NMR (100 MHz, $CDCl_3$): δ 20.5, 20.51, 20.6, 20.62, 20.7, 49.2, 49.6, 52.3, 52.5, 61.6, 61.7,

64.9, 65.0, 68.7, 70.2, 71.3,73.3, 90.2, 91.2,165.9, 166.6, 167.2, 168.0, 168.2, 169.4, 169.95, 170.0, 170.4; HRMS calcd for $C_{16}H_{22}N_4O_{10}Na$ 453.12281, found 453.12307.

Synthesis of 2-Iodo-terephthalic acid 1-methyl ester (2.5):

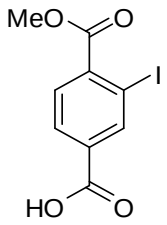

2.5

To a solution of 1-methyl-2-aminoterephthalate (2.5 g, 12.81 mmol) in deionized water (4 mL) at 0 °C was added Con HCl (17.5 mL, 211.75 mmol). To this was added $NaNO_2$ (937.3 mg, 13.58 mmol) in deionized water (5 ml) and stirred for 5 min. followed by the addition of NaI (2.034 g, 13.57 mmol) in deionized water (5 mL) and stirred for 5 more minutes at 0 °C. The reaction mixture was refluxed at 90 °C for 10 min. Solution of 1-methyl-2-aminoterephthalate, in acid was milky yellow, addition of $NaNO_2$ and NaI solutions results in the formation of brown precipitate. The reaction mixture was cooled to room temperature and precipitate was collected by filtration and washed with water (3x20 mL). The resulting solid was dried under vacuum overnight to obtain pure yellow compound **2.5** (2.95 g, 75% yield). ^{1}H NMR (400 MHz, $CDCl_3$) δ 8.68 (d, J = 1.6 Hz, 1H), 8.11 (dd, J = 8.1, 1.6 Hz, 1H), 7.83 (d, J = 8.1 Hz, 1H), 3.97 (s, 3H); HRMS calculated for $C_9H_7IO_4$ $(M)^+$, 305.9389, found 305.9389.

Synthesis of 2-(Diphenyl-phosphanyl)-terephthalic acid 1-methyl ester (2.6):

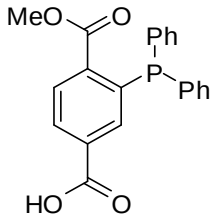

2.6a

To a solution of 2-iodo-terephthalicacid1-methyl ester (1.6 g, 5.23 mmol) in acetonitrile (10 ml) with 4A° molecular sieves, triethyl amine (782 µl, 5.75 mmol) and $Pd(OAc)_2$ (117.8 mg, 0.52 mmol) were added under argon and stirred for 5 minutes. To this diphenyl phosphine (924 µl) was added. The reaction mixture was refluxed at 85 °C for 5 hrs. The 2-iodo-terephthalic acid 1-methyl ester in acetonitrile is cloudy until addition of triethylamine, which yields a clear solution. Upon addition of $Pd(OAc)_2$, the mixture turns deep red. The molecular sieves were removed by filtration and the filtrate was concentrated. The resulting solid was purified by crystallization with DCM/MeOH to obtain **22.6** as yellow solid (1.303 g, 69% yield). ^{1}H NMR (400 MHz, $CDCl_3$) δ 8.27 (dd, *J* = 19.2, 10.8 Hz, 0.2H), 8.12 – 8.04 (m, 2H), 7.93 (dd, *J* = 7.9, 3.5 Hz, 0.1H), 7.68 (d, *J* = 2.8 Hz, 1.4H), 7.61 – 7.44 (m, 0.7H), 7.42 – 7.27 (m, 10H), 3.76 (s, 3H), 3.51 (s, 0.3H).^{13}C NMR (101 MHz, $CDCl_3$) δ 170.26, 166.60, 141.25 (d, *J* = 29.3 Hz), 138.80 (d, *J* = 20.2 Hz), 136.83 (d, *J* = 10.1 Hz), 135.47, 133.75(d, *J* = 7.1 Hz), 131.85, 130.46, 129.61, 128.92, 128.56 (d, *J* = 10.1 Hz), 52.25. ^{31}P NMR (162 MHz, $CDCl_3$) δ 33.04 (s, 0.09P), -3.21(s, 1.00P); HRMS calculated for $C_{21}H_{17}O_4P$ $(M)^+$, 364.0865, found 364.0862.

Synthesis of Succinimidyl 3-diphenylphosphino-4-methoxy-carbonylbenzoate (2.7):

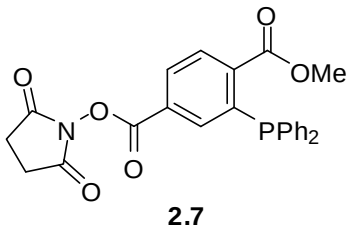

2.7

To a mixture of 2-(diphenyl-phosphanyl)-terephthalic acid 1-methyl ester **2.6** (1.978g, 1 mmol) and EDCI (1.244 g, 1.2 mmol) in DMF (10 mL), NHS (0.684 G, 1.1 mmol) was added and stirred for one day. The reaction mixture was concentrated under reduced pressure then extracted with mixture of DCM and H_2O (50 mL). The organic layer was dried over anhydrous Na_2SO_4, concentrated under vacuum. The residue was purified by flash column chromatography (1:1 hexane/EtOAc) to afford a yellow solid (1.29 g, 52%). ^{1}H NMR (400 MHz,$CDCl_3$) δ 8.13 (s, 2H), 7.67 (d, *J* = 3.6 Hz, 1H), 7.40 – 7.26 (m, 10H), 3.76 (s, 3H), 2.84 (s, 4H).^{13}C NMR (100 MHz, $CDCl_3$) δ 168.8, 166.2 (d, *J* = 3.0 Hz), 161.0, 142.3 (d, *J* = 31.3 Hz), 139.6 (d, *J* = 19.2 Hz), 136.4 (d, *J* = 10.1 Hz), 136.0, 133.8 (d, *J* = 21.2 Hz), 130.7, 129.6, 129.1, 128.6(d, *J* = 8.1 Hz) , 127.7, 52.4, 25.5. ^{31}P NMR (162 MHz, $CDCl_3$) δ -2.9; HR-ESIMS calculated for $C_{25}H_{20}NO_6PNa(M+Na)^+$, 484.0921, found 484.0919; mp 151.2-153.6 ºC.

Synthesis of *tert*-Butyl[2-(2-hydroxyethoxy)ethyl]carbamate (2.8):

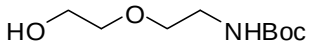

2.8

A solution of 2-(2-aminoethoxy)-ethanol (99.7 μL, 1 mmol) and Boc_2O (218.3 mg, 1 mmol) was stirred at room temperature for one hour. The reaction mixture was then concentrated and dried on under vacuum, to give compound 1 as colorless oil. ^{1}H NMR (400 MHz, $CDCl_3$) δ 5.42 (s, 1H), 3.65 – 3.53 (m, 2H), 3.47 – 3.35 (m, 5H), 3.23 – 3.12 (m, 2H), 1.30 (s, 9H); ^{13}C NMR (101

MHz, $CDCl_3$) δ 156.2, 79.0, 72.2, 70.1, 61.3, 40.2, 28.3; HR-ESIMS calculated for $C_9H_{19}NO_4Na$ $(M+Na)^+$ 228.1206, found 228.1205.

Synthesis of 2-(2-(*tert*-Butoxycarbonylamino)ethoxy)ethyl 5-((3aS,4S,6aR)-2-oxohexahydro-1H-thieno[3,4-d]imidazol-4-yl)pentanoate (2.9):

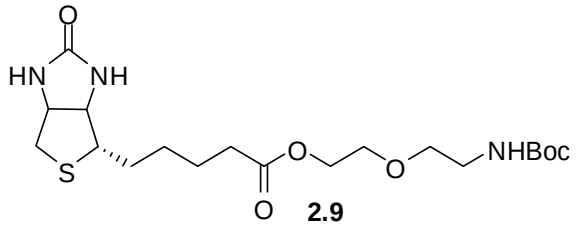

2.9

To a stirred solution of biotin (100 mg, 0.40 mmol) was added EDC (92 mg, 0.48 mmol) and DMAP (58.6 mg, 0.48 mmol) in DMF (3 mL). The carbamate (*tert*-Butyl [2-(2-Hydroxy ethoxy) ethyl] carbamate, **2.8**; 90.2 mg, 0.44 mmol) in DMF (2 mL) was then added to the solution, and the reaction mixture was stirred at room temperature for 24 h. The solution was concentrated and purified by column chromatography (DCM/MeOH, 10:1) to yield compound **1** (145 mg, 82%) as a white solid. ^{1}H NMR (400 MHz, $CDCl_3$) δ 5.90 (s, 1H), 5.04 (s, 1H), 4.50 (dd, J = 7.7, 4.9 Hz, 1H), 4.30 (dd, J = 7.7, 4.6 Hz, 1H), 4.27 – 4.16 (m, 2H), 3.65 (t, J = 4.7 Hz, 2H), 3.61 – 3.47 (m, 3H), 3.31 (s, 2H), 3.15 (dd, J = 12.0, 7.2 Hz, 1H), 2.91 (dd, J = 12.8, 4.9 Hz, 1H), 2.73 (d, J = 12.8 Hz, 1H), 2.37 (t, J = 7.5 Hz, 2H), 1.81 – 1.58 (m, 4H), 1.44 (s, 11H).

Synthesis of Methyl 2-(diphenylphosphino)-4-(2-(2-(5-((3aS,4S,6aR)-2-oxohexahydro-1H-thieno[3,4-d]imidazol-4-yl)pentanoyloxy)ethoxy)ethylcarbamoyl)benzoate (2.10):

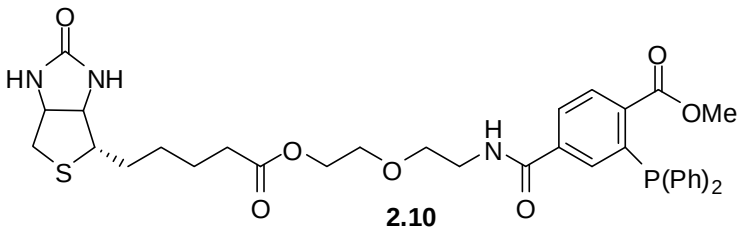

2.10

Compound **2.9** (145 mg, 0.34 mmol) was stirred in a 3 mL solution of TFA in DCM (1:1) for 3 h, then concentrated to give free amine. The resulting amine was added to a solution of DCM (3.5 mL) containing triethylamine (56.8 µL, 0.41 mmol) and succinimidyl-3-diphenylphosphino-4-methoxy-carbonylbenzoate **2.7** (189.1 mg, 0.41 mmol), and stirred overnight. The solution was concentrated and purified by column chromatography (EtOAc/MeOH, 9:1) to yield compound **2.10** (153 mg, 67%) as a yellow solid with minor amounts of the corresponding phosphine oxide (ca. ~4%). ^{1}H NMR (400 MHz, $CDCl_3$) δ 8.06 (dd, *J* = 8.0, 3.6 Hz, 1H), 7.90 (dd, *J* = 7.9, 3.3 Hz, 0.1H), 7.81 (dd, *J* = 8.1, 1.4 Hz, 1H), 7.38 (dd, *J* = 3.7, 1.5 Hz, 1H), 7.36 – 7.26 (m, 10H), 6.91 (s, 1H), 5.85 (s, 1H), 5.27 (s, 1H), 4.63 – 4.38 (m, 1H), 4.33 – 4.11 (m, 3H), 3.72 (s, 3H), 3.69 – 3.43 (m, 6.7H), 3.12 – 3.07 (m, 1H), 2.87 (dd, *J* = 12.8, 4.8 Hz, 1H), 2.69 (d, *J* = 12.8 Hz, 1H), 2.42 – 2.20 (m, 2H), 1.64 – 1.61 (m, 4H), 1.47 – 1.33 (m, 2H); phospine oxide: δ 8.36 (d, *J* = 13.7 Hz, 0.1H), 8.15 (d, *J* = 7.9 Hz, 0.1H), 7.68 (m, 0.5H), 7.52 (m, 0.3H), 7.45 (m, 0.5H), 3.40 (s, 0.3H); ^{13}C NMR (101 MHz, $CDCl_3$) δ 173.5, 166.8, 166.76, 166.6, 141.3 (d, J_{C-P} = 29.0 Hz), 137.3, 137.2 (d, J_{C-P} = 11.0 Hz), 136.7 (d, J_{C-P} = 19.0 Hz), 133.9 (d, J_{C-P} = 21.0 Hz), 132.9, 131.9, 130.8, 128.9, 128.6 (d, J_{C-P} = 7.0 Hz), 126.7, 69.3, 68.9, 62.8, 61.9, 60.1, 55.5, 52.2, 40.5, 39.8, 33.8, 28.2, 28.15, 24.7; ^{31}P NMR (162 MHz, $CDCl_3$) δ 32.90 (s, 0.04P), -2.39(s, 1.00P); HR-ESIMS calculated for $C_{35}H_{40}N_3O_7PSNa$ $(M+Na)^+$ 700.2217, found 700.2214.

Synthesis of 9*H*-fluoren-9-ylmethyl [2-(2-hydroxyethoxy)ethyl]carbamate (2.11):

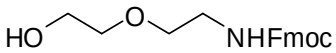

2.11

In a round bottom flask, 23 mL of 10% $NaHCO_3$ was added to 2-(2-aminoethoxy)-ethanol (700 µL, 7 mmol) in 20 mL of dioxane. The mixture was stirred for 15 min, then 9-fluorenylmethyl-*N*-succinimidyl carbonate (2.833 g, 8.4 mmol) was added. The reaction mixture was stirred

overnight then extracted with DCM (60 mL). The DCM layer was washed with water (2 x 50 mL) and dried over anhydrous Na_2SO_4. The solvent was evaporated under vacuum and the residue was purified by column chromatography using EtOAc/Hexane (2:1) to yield 2.203 g (92.4%) of **2.11** as an off-white solid. ^{1}H NMR (400 MHz, $CDCl_3$) δ 7.76 (d, *J* = 7.5 Hz, 2H), 7.59 (d, *J* = 7.4 Hz, 2H), 7.39 (t, *J* = 7.4 Hz, 2H), 7.31 (td, *J* = 7.5, 1.2 Hz, 2H), 5.37 (s, 1H), 4.43 (d, *J* = 6.7 Hz, 2H), 4.21 (t, *J* = 6.7 Hz, 1H), 3.71 (dd, *J* = 9.3, 5.5 Hz, 2H), 3.54 (d, *J* = 4.5 Hz, 4H), 3.38 (d, *J* = 5.0 Hz, 2H), 2.44 (t, *J* = 5.8 Hz, 1H). ^{13}C NMR (100 MHz, $CDCl_3$) δ 156.6, 143.9, 141.3, 127.7, 127.0, 125.0, 120.0, 72.3, 70.1, 66.6, 61.7, 47.3, 40.9. ESIMS calculated for $C_{19}H_{21}NO_4Na$ $[M+Na]^+$ 350.1363, found: 350.1357; mp 64.3-66.9 ºC.

Synthesis of 1, 2, 3, 4, 6-Penta-*O*-benzoyl-α/β-D-galactopyranoside (2.12):

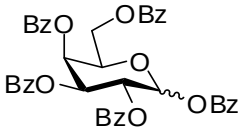

2.12

Benzoyl chloride (12.6 mL, 100 mmol) was added slowly to a suspension of galactose (3 g, 16.7 mmol) in 40 mL of pyridine and stirred at room temperature for 24 h under argon. Excess benzoyl chloride was quenched by adding 30 mL MeOH with cooling. The reaction mixture was concentrated under vacuum. The crude product was dissolved in DCM (25 mL) and washed with water (3 x 30 mL). The organic layer was dried over anhydrous Na_2SO_4. The solvent was evaporated under vacuum and the crude residue was purified by column chromatography using EtOAc/Hexane (1:2) to yield 10.5 g (90%) of **2.12** as a white solid. ^{1}H NMR (500 MHz, $CDCl_3$) δ 8.13 (t, *J* = 6.4 Hz, 4H), 7.97 (d, *J* = 7.3 Hz, 2H), 7.88 (d, J = 7.3 Hz, 2H), 7.83 (d, *J* = 7.3 Hz, 2H), 7.65 (td, *J* = 7.4, 1.1 Hz, 2H), 7.52 (dd, *J* = 11.9, 7.6 Hz, 5H), 7.46 (t, *J* = 7.4 Hz, 2H), 7.39 (t, *J* = 7.7 Hz, 2H), 7.29 (dd, *J* = 9.7, 8.0 Hz, 4H), 6.97 (d, *J* = 3.6 Hz, 1H), 6.21 (d, *J* = 2.2 Hz,

1H), 6.14 (dd, *J* = 10.7, 3.2 Hz, 1H), 6.05 (dd, *J* = 10.7, 3.6 Hz, 1H), 4.85 (t, *J* = 6.6 Hz, 1H), 4.65 (dd, *J* = 11.3, 6.4 Hz, 1H), 4.44 (dd, *J* = 11.3, 6.9 Hz, 1H); ^{13}C NMR (125 MHz, $CDCl_3$) δ 165.9, 165.7, 165.5, 165.4, 164.5, 133.9, 133.7, 133.4, 133.3, 133.2, 130.0, 129.95, 129.8, 129.76, 129.3, 129.0, 128.98, 128.9, 128.8, 128.74, 128.7, 128.42, 128.41, 128.4, 90.7, 69.5, 68.6, 68.5, 67.7, 61.9; ESIMS calculated for $C_{41}H_{32}O_{11}Na$ $[M+Na]^+$ 723.1837, found: 723.1834.

Synthesis of 2, 3, 4, 6-Tetra-*O*-benzoyl-α/β-D-galactopyranoside (2.13):

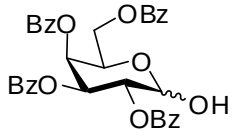

2.13

Penta-*O*-benzoyl galactoside, **2.12** (3 g, 4.3 mmol), was treated with 1.6 mL of HBr/AcOH (33%) in 10 mL of DCM for 1 h. The solution was washed twice with 10 mL of saturated $NaHCO_3$, NaCl, and 8 mL DI water. The DCM was evaporated and the solid was dried under vacuum. The resulting white solid was dissolved in 15 mL acetone and 0.7 mL DI water with Ag_2CO_3 (602 mg, 2.2 mmol) and stirred for 2.3 h. The solution was filtered through a pad of celite and dried under vacuum to yield a quantitative amount of **2.13** as a white solid. ^{1}H NMR (500 MHz, $CDCl_3$) δ 8.15 – 8.08 (m, 3H), 8.06 – 7.96 (m, 5H), 7.86 – 7.79 (m, 2H), 7.67 – 7.54 (m, 1H), 7.54 – 7.43 (m, 5H), 7.43 – 7.31 (m, 6H), 7.23 (t, *J* = 7.9 Hz, 3H), 6.16 - 6.11 (m,1H), 6.06 (s, 0.3H), 5.90 (s,1H), 5.77 (d, *J* = 3.5 Hz, 0.5H), 5.75 (d, *J* = 3.7 Hz, 1H),5.14 (t, *J* = 7.4 Hz, 0.3H), 4.89 (t, *J* = 6.8 Hz, 1H), 4.77 (d, *J* = 7.8 Hz, 0.3H), 4.71 (dd, *J* = 11.2, 6.3 Hz, 0.3H), 4.63 (dd, *J* = 11.3, 6.3 Hz, 1H), 4.47 (m, 0.3H), 4.40 (m, 2H); ^{13}C NMR (125 MHz, $CDCl_3$) δ 164.2, 163.8, 163.76, 163.7, 163.3, 163.2, 163.16, 131.2, 131.1, 131.05, 130.9, 130.89, 130.86, 130.8, 130.7, 127.5, 127.45, 127.4, 127.36, 127.34, 127.3, 127.26, 127.2, 126.9, 126.8, 126.75, 126.6, 126.5, 126.47, 126.2, 126.18, 126.16, 126.0, 125.95, 125.9, 125.8, 125.78, 93.7, 88.6,

69.6, 69.0, 68.8, 67.2, 66.9, 65.8, 65.7, 64.2, 59.9, 59.7; ESIMS calculated for $C_{34}H_{28}O_{10}Na$ $[M+Na]^+$ 619.1575, found: 619.1576.

Synthesis of 2, 3, 4, 6-Tetra-*O*-benzoyl-α/β-D-galactopyranosyl trichloroacetamidate (2.14):

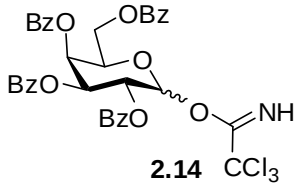

2.14

Compound **2.13** (1.10 g, 1.8 mmol), DBU (60 µL) and trichloroacetonitrile (2.2 mL, 4.8 mmol) were dissolved in DCM (25 mL) and stirred for 4 h at room temperature. DCM was evaporated and the residue was purified by column chromatography with EtOAc/Hexane (1:2) to yield 1.214 g (91.3%) of **2.14** as a white solid. ^{1}H NMR (500 MHz, $CDCl_3$) δ 8.77 (s, 0.3H), 8.67 (s, 1H), 8.12 (dd, *J* = 8.2, 1.1 Hz, 3H), 8.08 (dd, *J* = 8.2, 1.2 Hz, 0.7H), 8.00 (ddd, *J* = 11.6, 8.3, 1.2 Hz, 4H), 7.94 (ddd, *J* = 20.6, 8.3, 1.2 Hz, 1.4H), 7.83 (dd, *J* = 8.3, 1.2 Hz, 2H), 7.69 – 7.63 (m, 1H), 7.63 – 7.58 (m, 1H), 7.58 – 7.49 (m, 6H), 7.48 – 7.27 (m, 11H), 6.96 (d, *J* = 3.7 Hz, 1H), 6.74 (s, 0.3H), 6.22 – 6.19 (m, 1H), 6.17 (dt, *J* = 7.0, 4.3 Hz, 0.4H), 6.12 (dd, *J* = 10.7, 3.3 Hz, 1H), 6.01 (dd, *J* = 10.7, 3.7 Hz, 1H), 5.82 (d, *J* = 4.2 Hz, 0.3H), 5.80 (s, 0.3H), 4.91 (dd, *J* = 8.8, 4.7 Hz, 1.3H), 4.85 – 4.73 (m, 1H), 4.65 (dd, *J* = 11.5, 6.9 Hz, 1H), 4.48 (dd, *J* = 11.5, 6.0 Hz, 1H); ^{13}C NMR (125 MHz, $CDCl_3$) δ 166.0, 165.9, 165.7, 165.6, 165.52, 165.51, 165.5, 165.2, 160.6, 160.3, 133.8, 133.7, 133.6, 133.4, 133.3, 133.26, 133.1, 130.05, 130.0, 129.97, 129.9, 129.86, 129.8, 129.75, 129.7, 129.5, 129.4, 129.3, 129.0, 128.9, 128.8, 128.74, 128.7, 128.5, 128.46, 128.4, 128.35, 102.9, 93.8, 91.0, 90.8, 84.6, 80.8, 77.2, 70.1, 69.8, 68.6, 68.4, 67.9, 63.4, 62.2; ESIMS calculated for $C_{36}H_{28}Cl_3NO_{10}Na$ $[M+Na]^+$ 762.0671, found: 762.0671.

Synthesis of 9H-fluoren-9ylmethyl {2-[2-*O*-(2, 3, 4, 6-tetra-*O*-benzoyl-β-D-galactopyranosyl)-2-hydroxyethoxy]ethyl}carbamate (2.15):

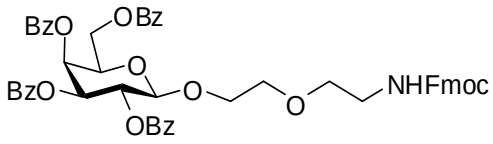

2.15

Compound **2.14** (977 mg, 1.32 mmol) was dissolved in 15 mL of DCM and stirred overnight at room temperature with TMSOTf (2.34 mL, 1% in DCM, 0.13 mmol) and 9H-fluoren-9-yl[2-(2-hydroxy ethoxy)-ethyl]carbamate **2.11** (654 mg, 1.98 mmol). The solvent was removed and the product was purified by column chromatography with EtOAc/hexane (1:2) to yield 957 mg (80.1%) of **2.15** as a white solid. ^{1}H NMR (500 MHz, $CDCl_3$) δ 8.09 (d, *J* = 7.5 Hz, 2H), 8.05 – 8.01 (m, 2H), 7.98 (dd, *J* = 8.2, 1.1 Hz, 2H), 7.80 (dd, *J* = 8.3, 1.2 Hz, 2H), 7.77 (d, *J* = 7.6 Hz, 2H), 7.68 – 7.53 (m, 4H), 7.52 – 7.34 (m, 10H), 7.30 (t, *J* = 7.4 Hz, 2H), 7.27 – 7.21 (m, 2H), 6.01 (d, *J* = 3.4 Hz, 1H), 5.83 (dd, *J* = 10.4, 7.9 Hz, 1H), 5.65 (dd, *J* = 10.4, 3.5 Hz, 1H), 5.16 (s, 1H), 4.90 (d, *J* = 7.9 Hz, 1H), 4.70 (dd, *J* = 11.3, 6.5 Hz, 1H), 4.52 – 4.36 (m, 3H), 4.32 (t, *J* = 6.4 Hz, 1H), 4.23 (t, *J* = 6.9 Hz, 1H), 4.06 (dt, *J* = 11.1, 4.1 Hz, 1H), 3.87 – 3.67 (m, 1H), 3.61 (t, *J* = 4.1 Hz, 2H), 3.38 (t, *J* = 4.7 Hz, 2H), 3.29 – 2.96 (m, 2H); ^{13}C NMR (125 MHz, $CDCl_3$) δ 166.1, 165.6, 165.3, 156.4, 144.0, 141.3, 133.6, 133.4, 133.3, 133.29, 130.0, 129.8, 129.78, 129.7, 129.4, 129.38, 129.0, 128.8, 128.6, 128.5, 128.45, 128.3, 127.7, 127.1, 125.1, 119.9, 101.8, 71.6, 71.4, 70.2, 70.1, 69.8, 69.4, 68.1, 66.6, 62.0, 47.3, 40.8; ESIMS calculated for $C_{53}H_{47}NO_{13}Na$ $[M+Na]^+$ 928.2940, found: 928.2935.

Synthesis of Methyl 2-(diphenylphosphino)-4-[2(2-*O*-β-D-galactopyranosyl-2-hydroxyethoxy)ethylcarbamoyl]benzoate (2.16):

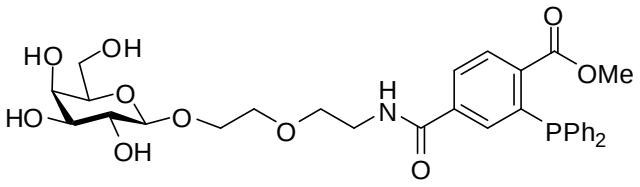

2.16

Deprotection of compound **2.15** (453 mg, 0.5 mmol) was achieved under Zémplen conditions by stirring in a solution of MeOH (8 mL) with 1% NaOMe/MeOH (5.6 mL) for 4 h. The solvent was removed and a solution of DCM/H_2O (20 mL, 1:1) was added. The water layer was washed with DCM (2 × 10 mL) and lyophilized to yield 111 mg of white solid. The solid (50 mg, 0.19 mmol) was then stirred with succinimidyl-3-diphenylphosphino-4-methoxy-carbonylbenzoate **2.7**, (106 mg, 0.23 mmol) and two drops of triethylamine in 5 mL of DMF for 2.3 h at room temperature. The DMF was removed under vacuum and the crude product was purified by column chromatography (Iatrobeads, Mitsubishi Kagaku Iatron, Inc.) with EtOAc/MeOH (8:2) to yield 76 mg (65%) of **2.16** as a yellow solid containing a small amount of the corresponding phosphine oxide. ^{1}H NMR (500 MHz, CD_3OD) 8.04 (dd, J = 8.0, 3.6 Hz, 1H), 7.81 (dd, J = 8.0, 1.7 Hz, 1H), 7.44 (dd, J = 3.9, 1.7 Hz, 1H), 7.39 – 7.31 (m, 6H), 7.26 (m, 4H), 4.24 (d, J = 7.6 Hz, 1H), 3.98 (dt, J = 10.8, 4.2 Hz, 1H), 3.81 (t, J = 3.2 Hz, 1H), 3.78 – 3.68 (m, 4H), 3.67 (s, 3H), 3.66 – 3.61 (m, 3H), 3.59 (t, J = 5.5 Hz, 2H), 3.54 – 3.40 (m, 7H); phosphine oxide: δ 8.13 (dt, J = 8.0, 1.5 Hz, 0.2H), 7.97 (m, 0.8H), 7.70 – 7.59 (m, 1.3H), 7.58 – 7.50 (m, 0.9H); ^{13}C NMR (125 MHz, CD_3OD) δ 169.5, 168.4 (d, $J_{C\text{-}P}$ = 2.5 Hz), 142.3 (d, $J_{C\text{-}P}$ = 27.5 Hz), 138.9, 138.6 (d, $J_{C\text{-}P}$ = 11.3 Hz), 138.3 (d, $J_{C\text{-}P}$ = 20.0 Hz), 135.1 (d, $J_{C\text{-}P}$ = 21.3 Hz), 134.5, 131.6 (d, $J_{C\text{-}P}$ = 2.5 Hz), 130.1, 129.7 (d, $J_{C\text{-}P}$ = 7.5 Hz), 127.9, 105.1, 76.8, 75.0, 72.6, 71.3, 70.4, 70.3, 69.8, 62.6, 52.6, 41.0; phosphine oxide: δ 138.3 (d, $J_{C\text{-}P}$ = 11.3 Hz), 133.6 (d, $J_{C\text{-}P}$ = 3.8 Hz), 133.5 (d,

$J_{C\text{-}P}$ = 7.5 Hz), 132.9 (d, $J_{C\text{-}P}$ = 10.0 Hz), 132.7, 132.2, 131.8 (d, $J_{C\text{-}P}$ = 7.5 Hz), 129.9 (d, $J_{C\text{-}P}$ = 12.5 Hz), 52.9; ^{31}P NMR (202 MHz, CD_3OD) δ 35.0 (s, 0.22P), -2.8 (s, 1.00P); ESIMS calculated for $C_{31}H_{36}PNO_{10}Na$ $[M+Na]^+$ 636.1969, found: 636.1951.

Synthesis of 2,3,4,6-Tetra-*O*-benzoyl-β-D-galactopyranosyl-(1→4)-1,2,3,6-tetra-*O*-benzoyl-α/β-D-glucopyranose (2.17):

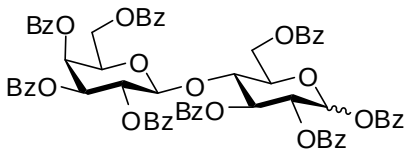

2.17

Benzoyl chloride was added slowly to a suspension of D-lactose (514 mg, 1.5 mmol) in 10 mL of pyridine and stirred at room temperature for 24 h under argon. Excess benzoyl chloride was quenched by adding MeOH with cooling. The reaction mixture was concentrated under high vacuum. The crude product was dissolved in DCM (25 mL) and washed with water (3 x 30 mL). The organic layer was dried over anhydrous Na_2SO_4. The solvent was evaporated under vacuum. The product was purified by column chromatography using EtOAc/Hexane (1:2) to yield 1.66 g (93.9%) of **2.17** as a white solid. ^{1}H NMR (500 MHz, $CDCl_3$) δ 8.13 (dd, *J* = 8.2, 1.2 Hz, 1H), 8.08 – 7.97 (m, 13H), 7.96 – 7.85 (m, 5H), 7.77 – 7.71 (m, 3H), 7.69 – 7.25 (m, 28H), 7.20 (ddd, *J* = 11.4, 10.0, 5.6 Hz, 6H), 6.76 (d, *J* = 3.8 Hz, 0.3H), 6.21 (dd, *J* = 10.1, 9.3 Hz, 0.3H), 6.15 (d, *J* = 8.1 Hz, 1H), 5.95 (t, *J* = 9.3 Hz, 1H), 5.82 – 5.77 (m, 1.3H), 5.77 – 5.71 (m, 2.4H), 5.62 (dd, *J* = 10.3, 3.8 Hz, 0.3H), 5.39 (dd, *J* = 10.4, 3.4 Hz, 1H), 4.96 (d, *J* = 7.9 Hz, 0.3H), 4.91 (d, *J* = 7.9 Hz, 1H), 4.64 – 4.50 (m, 3H), 4.40 (td, *J* = 9.5, 3.0 Hz, 1.3H), 4.31 (dt, *J* = 10.2, 2.5 Hz, 0.3H), 4.08 (ddd, *J* = 9.9, 3.7, 1.9 Hz, 1H), 3.90 (t, *J* = 6.6 Hz, 1.4H), 3.85 – 3.76 (m, 1.5H), 3.76 – 3.68 (m, 1.3H); ^{13}C NMR (125 MHz, $CDCl_3$) δ 165.8, 165.77, 165.6, 165.5, 165.45,

165.43, 165.4, 165.3, 165.24, 165.2, 165.19, 164.9, 164.8, 164.5, 164.48, 133.9, 133.7, 133.5, 133.45, 133.4, 133.39, 133.37, 133.3, 133.26, 130.1, 130.07, 130.0, 129.8, 129.78, 129.76, 129.71, 129.7, 129.66, 129.65, 129.6, 129.57, 129.5, 129.43, 129.42, 129.4, 128.9, 128.86, 128.8, 128.7, 128.63, 128.6, 128.59, 128.56, 128.55, 128.5, 128.47, 128.4, 128.34, 128.3, 128.25, 101.3, 101.2, 92.6, 89.9, 75.7, 75.6, 73.9, 72.9, 72.0, 71.8, 71.4, 71.2, 70.7, 70.4, 70.1, 69.9, 69.8, 67.5, 62.1, 61.8, 61.0; ESIMS calculated for $C_{68}H_{54}O_{19}Na$ $[M+Na]^+$ 1197.3152, found: 1197.3142.

Synthesis of 2,3,4,6-Tetra-*O*-benzoyl-β-D-galactopyranosyl-(1→4)-2,3,6-tri-*O*-benzoyl-α/β-D-glucopyranose (2.18):

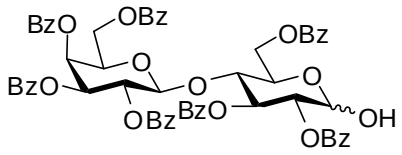

2.18

Hydrazine acetic acid (220 µL) was added to a solution of **2.17** (600 mg, 0.51 mmol) in DMF (10 mL) and the mixture was stirred at 60 ^oC for 6 h. A white solid crashed out after addition of water (20 mL) and was filtered. The solid was dissolved in DCM (10 mL) and washed with water (2 x 15 mL). The organic layer was dried over anhydrous Na_2SO_4 and evaporated under vacuum. The crude residue was purified by column chromatography using EtOAc/Hexane (1:1) to yield 455 mg (83.3%) of **2.18** as a white solid. ^1H NMR (500 MHz, $CDCl_3$) δ 8.07 – 7.93 (m, 15H), 7.89 (dd, *J* = 8.3, 1.2 Hz, 3H), 7.73 (dd, *J* = 8.3, 1.2 Hz, 3H), 7.66 – 7.25 (m, 28H), 7.25 – 7.13 (m, 6H), 6.15 (dd, *J* = 9.9, 9.5 Hz, 1H), 5.87 (t, *J* = 7.47, 0.3H), 5.78 – 5.69 (m, 3H), 5.63 (d, *J* = 3.6 Hz, 1H), 5.47 – 5.36 (m, 1.5H), 5.32 – 5.28 (m, 0.3H), 5.25 (dd, *J* = 10.3, 3.7 Hz, 1H), 4.95 (d, *J* = 7.8 Hz, 1.23H), 4.93 – 4.87 (m, 0.6H), 4.58 (dd, *J* = 12.3, 1.9 Hz, 1.5H), 4.53 – 4.45 (m, *J* = 12.3, 4.1 Hz, 1.6H), 4.37 (ddd, *J* = 10.1, 3.1, 2.0 Hz, 1H), 4.31 – 4.22 (m, *J* = 9.7,

4.2 Hz, 1.5H), 3.92 (q, *J* = 6.4 Hz, 1.6H), 3.89 – 3.83 (m, 1.5H), 3.83 – 3.69 (m, *J* = 29.7, 11.3, 7.0 Hz, 2H); ^{13}C NMR (125 MHz, $CDCl_3$) δ 166.6, 166.2, 166.1, 166.0, 165.7, 165.6, 165.5, 165.47,165.45, 165.4, 165.3, 164.9, 133.6, 133.44, 133.4, 133.37, 133.3, 133.1, 130.0, 129.95, 129.8, 129.7, 129.6, 129.5, 129.43, 129.4, 129.38, 129.1, 129.0, 128.8, 128.7, 128.6, 128.59, 128.5, 128.4, 128.3, 101.1, 95.8, 90.3, 76.1, 76.0, 74.0, 73.3, 72.6, 72.2, 72.0, 71.8, 71.4, 70.3, 70.1, 70.0, 68.4, 67.6, 67.58, 62.5, 62.45, 61.2, 61.1; ESIMS calculated for $C_{61}H_{50}O_{18}Na$ $[M+Na]^+$ 1093.2889, found: 1093.2886.

Synthesis of 1-*O*-[2,3,4,6-Tetra-*O*-benzoyl-β-D-galactopyranosyl-(1→4)-2,3,6-tri-*O*-benzoyl-α-D-glucopyranosyl] trichloroacetimidate (2.19):

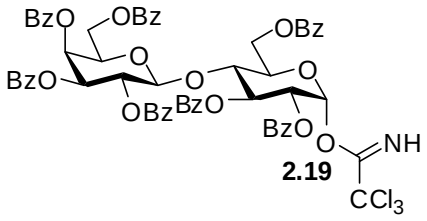

2.19

Compound **2.18** (430 mg, 0.4 mmol), DBU (6 μL) and trichloroacetonitrile (481 μL, 4.8 mmol) were dissolved in DCM (10 mL) and stirred for 4 h at room temperature. DCM was evaporated and the residue was purified by column chromatography with EtOAc/Hexane (1:1) to yield 434 mg (89.0%) of **2.19** as a white solid. ^{1}H NMR (500 MHz, $CDCl_3$) δ 8.57 (s, 1H), 7.99 (dddd, *J* = 15.9, 12.8, 8.4, 1.3 Hz, 12H), 7.90 (dd, *J* = 8.3, 1.2 Hz, 2H), 7.73 (dd, *J* = 8.4, 1.3 Hz, 2H), 7.70 – 7.54 (m, 4H), 7.54 – 7.26 (m, 17H), 7.26 – 7.15 (m, 5H), 6.72 (d, *J* = 3.8 Hz, 1H), 6.20 – 6.12 (m, 1H), 5.79 – 5.71 (m, 2H), 5.55 (dd, *J* = 10.2, 3.8 Hz, 1H), 5.40 (dd, *J* = 10.3, 3.4 Hz, 1H), 4.95 (d, *J* = 7.9 Hz, 1H), 4.62 – 4.47 (m, 2H), 4.39 – 4.30 (m, 2H), 3.91 (t, *J* = 7.1 Hz, 1H), 3.83 (dd, *J* = 11.3, 6.3 Hz, 1H), 3.74 (dd, *J* = 11.3, 7.3 Hz, 1H); ^{13}C NMR (175 MHz, $CDCl_3$) δ 165.7, 165.52, 165.5, 165.4, 165.2, 165.17, 164.8, 160.7, 133.5, 133.4, 133.3, 130.0, 129.9, 129.8, 129.7, 129.65, 129.6, 129.57, 129.5, 129.4, 128.9, 128.7, 128.6, 128.57, 128.54, 128.5,

128.4, 128.3, 128.2, 101.3, 93.1, 90.7, 75.6, 71.9, 71.4, 71.35, 70.5, 70.3, 70.0, 67.5, 61.9, 61.0; ESIMS calculated for $C_{63}H_{50}Cl_3NO_{18}Na$ $[M+Na]^+$ 1236.1986, found: 1236.1997.

Synthesis of 9H-fluoren-9ylmethyl {2-[2-*O*-(2, 3, 4, 6-tetra-*O*-benzoyl-β-D-galactopyranosyl-(1→4)-2,3,6-tri-*O*-benzoyl-β-D-glucopyranosyl)-2-hydroxyethoxy]ethyl}carbamate (2.20):

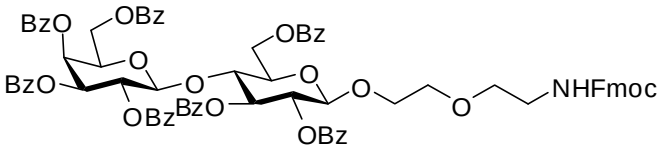

2.20

Compound **2.19** (403 mg, 0.33 mmol) was dissolved in 10 mL of DCM and stirred overnight at room temperature with TMSOTf (65 µL, 1% in DCM) and 9*H*-fluoren-9-yl[2-(2-hydroxyethoxy)-ethyl]carbamate **2.11** (131 mg, 0.4 mmol). The solvent was removed and the resulting solid was purified by column chromatography with EtOAc/hexane (1:1) to yield 325 mg (70.3%) of **2.20** as a white solid. ^{1}H NMR (500 MHz, $CDCl_3$) δ 7.99 (dt, *J* = 11.8, 7.0 Hz, 11H), 7.91 (d, *J* = 7.3 Hz, 2H), 7.83 – 7.72 (m, 4H), 7.72 – 7.53 (m, 6H), 7.48 (t, *J* = 7.7 Hz, 6H), 7.45 – 7.27 (m, 15H), 7.22 (t, *J* = 7.8 Hz, 2H), 7.14 (t, *J* = 7.7 Hz, 2H), 5.83 (t, *J* = 9.5 Hz, 1H), 5.74 (m, 2H), 5.50 (dd, *J* = 9.6, 8.1 Hz, 1H), 5.39 (dd, *J* = 10.3, 3.3 Hz, 1H), 5.19 (s, 1H), 4.86 (d, *J* = 7.8 Hz, 1H), 4.76 (d, *J* = 7.8 Hz, 1H), 4.62 (d, *J* = 11.4 Hz, 1H), 4.53 (dd, *J* = 12.1, 4.4 Hz, 1H), 4.47 – 4.31 (m, 2H), 4.31 – 4.13 (m, 2H), 4.01 – 3.78 (m, 3H), 3.78 – 3.58 (m, 3H), 3.51 (s, 2H), 3.34 (t, *J* = 4.6 Hz, 2H), 3.12 (t, *J* = 5.0 Hz, 2H). ^{13}C NMR (125 MHz, $CDCl_3$) δ 165.8, 165.5, 165.4, 165.38, 165.2, 164.8, 156.4, 144.0, 141.3, 133.5, 133.4, 133.3, 133.27, 133.2, 130.0, 129.8, 129.7, 129.6, 129.5, 129.4, 129.35, 128.9, 128.7, 128.6, 128.58, 128.5, 128.4, 128.3, 127.7, 127.1, 125.2, 125.1, 120.0, 101.3, 101.1, 76.1, 73.2, 72.8, 71.83, 71.8, 71.4, 70.2, 69.9, 69.88, 69.4, 67.5, 66.6, 62.4, 61.1, 47.3, 40.8; ESIMS calculated for $C_{80}H_{69}NO_{21}Na$ $[M+Na]^+$ 1402.4254, found: 1402.4256.

Synthesis of Methyl 2-(diphenylphosphino)-4-{2[2-*O*-β-D-galactopyranosyl-(1→4)-β-D-glucopyranosyl-2-hydroxyethoxy]ethylcarbamoyl]}benzoate (2.21):

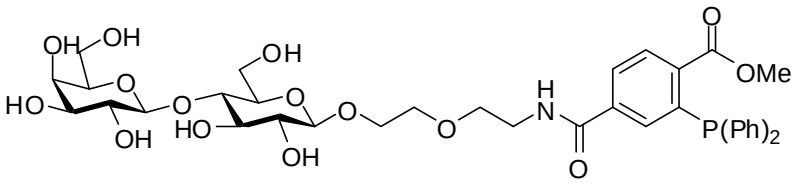

2.21

Deprotection of compound **2.20** (325 mg, 0.24 mmol) was achieved under Zémplen conditions by stirring in a solution of MeOH (6 mL) with 1% NaOMe/MeOH (6 mL) overnight. The solvent was removed and a solution of DCM/H_2O (10 mL, 1:1) was added. The water layer was washed with DCM (2 × 5 mL) and the aqueous layer was lyophilized to yield 85 mg of a white solid. A portion of the solid (32 mg, 0.08 mmol) was stirred with succinimidyl-3-diphenylphosphino-4-methoxy-carbonylbenzoate 11 (42 mg, 0.09 mmol), and two drops of triethylamine for 3 h at room temperature in DMF (5 mL). The solvent was removed under vacuum and the product was purified by column chromatography (Iatrobeads) with EtOAc/MeOH (8:2) to yield 36 mg (62%) of 13 as a yellow solid containing a small amount of the corresponding phosphine oxide. ^{1}H NMR (500 MHz, CD_3OD) 8.04 (dd, J = 8.0, 3.6 Hz, 1H), 7.80 (dd, J = 8.0, 1.7 Hz, 1H), 7.43 (dd, J = 3.9, 1.7 Hz, 1H), 7.40 – 7.30 (m, 6H), 7.26 (m,4H), 4.35 (d, J = 7.6 Hz, 1H), 4.32 (d, J = 7.8 Hz, 1H), 3.96 (ddd, J = 22.3, 13.3, 8.9 Hz, 1H), 3.88 (dd, J = 12.1, 2.5 Hz, 1H), 3.84 – 3.75 (m, 4H), 3.74 – 3.68 (m, 2H), 3.68 (s, 3H), 3.67 – 3.62 (m, 2H), 3.61 – 3.57 (m, 3H), 3.56 – 3.41 (m, 7H), 3.38 (ddd, J = 9.2, 4.2, 2.5 Hz, 1H), 3.26 – 3.19 (m, 1H); phospine oxide: δ 8.13 (dt, J = 8.0, 1.6 Hz, 0.1H), 7.99 (dd, J = 8.0, 3.7 Hz, 0.1H), 7.95 (dd, J = 13.8, 1.7 Hz, 0.1H), 7.72 – 7.59 (m, 0.7H), 7.55 (m, 0.4H); ^{13}C NMR (125 MHz, CD_3OD) δ 169.5, 168.4 (d, $J_{C\text{-}P}$ = 2.5 Hz), 142.3 (d, $J_{C\text{-}P}$ = 27.5 Hz), 138.9, 138.6 (d, $J_{C\text{-}P}$ = 10.0 Hz), 138.3 (d, $J_{C\text{-}P}$ = 20.0 Hz), 135.1 (d, $J_{C\text{-}P}$ = 20.0 Hz), 134.5, 131.6 (d, $J_{C\text{-}P}$ = 2.5 Hz), 130.1, 129.7 (d, $J_{C\text{-}P}$ = 7.5 Hz), 127.9,

105.1, 104.4, 80.7, 77.1, 76.5, 76.4, 74.9, 74.8, 72.6, 71.2, 70.4, 70.3, 69.9, 62.5, 62.0, 52.6, 41.0; ^{31}P NMR (202 MHz, CD_3OD) δ 35.0 (s, 0.10P), -2.8 (s, 1.00P); ESIMS calculated for $C_{37}H_{46}PNO_{15}Na$ $[M+Na]^+$ 798.2497, found: 798.2489.

Synthesis of 2,3,4,6-Tetra-*O*-acetyl-β-D-galactopyranosyl-(1→4)-3,6-di-*O*-acetyl-glucal (2.22):

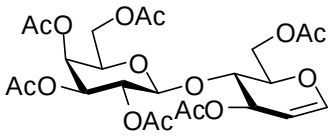

2.22

3.6 mL of 33% HBr/acetic acid was added to a suspension of D-lactose (6.0 g, 16.7 mmol) in acetic anhydride (15.0 mL, 158.7mmol) and the mixture was stirred overnight at room temperature. The reaction was stopped when the solution became clear and then poured onto a suspension of a pulverized mixture of $CuSO_4.H_2O$ (1.1 g) and Zinc (43.7 g) in a solution of water (60 mL) and acetic acid (90 mL) containing sodium acetate (33.0 g). The resultant mixture was stirred for 1.5 h in a water bath and filtered. The solid was collected and washed with ethylacetate (200 mL) followed by water (200 mL). The organic layer of the filtrate was washed successively with saturated $NaHCO_3$ (200 mL), brine (200 mL) and dried over anhydrous Na_2SO_4. The solvent was removed under reduced pressure and the residue was purified by column chromatography with EtOAc: Hexanes (1:1) to afford 4.2 g of **2.22** as white solid (43%). ^{1}H NMR (498 MHz, $CDCl_3$) δ 6.38 (d, *J* = 6.6 Hz, 1H), 5.37 (t, *J* = 5.0 Hz, 1H), 5.33 (d, *J* = 2.6 Hz, 1H), 5.15 (dd, *J* = 10.5, 8.0 Hz, 1H), 4.97 (dd, *J* = 10.5, 3.4 Hz, 1H), 4.80 (dd, *J* = 6.1, 3.4 Hz, 1H), 4.63 (d, *J* = 8.0 Hz, 1H), 4.40 (dd, *J* = 11.7, 2.6 Hz, 1H), 4.18 – 4.03 (m, 4H), 3.96 (dd, *J* = 7.4, 5.5 Hz, 1H), 3.88 (t, *J* = 6.8 Hz, 1H), 2.40 – 1.85 (6s, 18H).

Synthesis of β-D-galactopyranosyl-(1→4)-glucal (2.23):

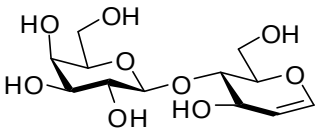

2.23

To compound **2.22** (1.12 g, 2.0 mmol) in 20 mL of MeOH, was added Na_2CO_3 (1.39 g, 13.1 mmol) and stirred for 2 h. The suspension was filtered to remove Na_2CO_3 and the filtrate was concentrated to give 566.7 mg of **2.23** (92%) as a white solid. ^{1}H NMR (500 MHz, D_2O) δ 6.44 (dd, *J* = 6.1, 1.5 Hz, 1H), 4.81 (dd, *J* = 6.1, 2.6 Hz, 1H), 4.52 (d, *J* = 7.8 Hz, 1H), 4.40 – 4.34 (m, 1H), 4.01 (dt, *J* = 9.2, 3.7 Hz, 1H), 3.92 (t, *J* = 3.1 Hz, 3H), 3.84 (dd, *J* = 9.3, 6.6 Hz, 1H), 3.80 – 3.70 (m, 3H), 3.66 (dd, *J* = 9.9, 3.4 Hz, 1H), 3.55 (dd, *J* = 9.9, 7.8 Hz, 1H).

Synthesis of 2,3,4,6-Tetra-*O*-benzyl-β-D-galactopyranosyl-(1→4)-3,6-di-*O*-benzyl-glucal (2.24):

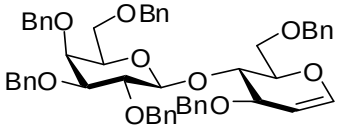

2.24

NaH (960 mg, 24.0 mmol) was added to a solution of lactal **2.23** (607 mg, 2.0 mmol) in 20 mL of DMF at 0 ^{o}C and stirred for 30 m at the same temperature. Benzyl bromide (2.9 mL, 24.0 mmol) was then added dropwise and stirred for 18 h by slowly warming to room temperature. Reaction mixture was neutralized by drop wise addition of acetic acid at 0 ^{o}C and concentrated. The crude was dissolved in ethylacetate (50 mL) and washed with saturated $NaHCO_3$ (50 mL). The organic layer was back extracted with ethylacetate (2 x 50 mL). The combined organic layers were dried over anhydrous Na_2SO_4 and concentrated. The residue was purified by a

column chromatography with EtOAc:Hexanes (1:6), to yield an oily compound **2.24** (1.4 g, 81%). ^{1}H NMR (500 MHz, $CDCl_3$) δ 7.47 – 7.27 (m, 30H), 6.50 (dd, *J* = 6.2, 0.9 Hz, 1H), 5.29 (s, 1H), 5.01 (d, *J* = 11.6 Hz, 1H), 4.94 (dd, *J* = 6.1, 3.5 Hz, 1H), 4.91 (d, *J* = 10.8 Hz, 1H), 4.83 – 4.74 (m, 3H), 4.67 (s, 2H), 4.66 – 4.61 (m, 1H), 4.54 (s, 2H), 4.42 (q, *J* = 11.7 Hz, 2H), 4.33 (dd, *J* = 9.3, 5.4 Hz, 1H), 4.27 – 4.09 (m, 2H), 3.95 (d, *J* = 2.6 Hz, 1H), 3.91 (dd, *J* = 10.7, 6.3 Hz, 1H), 3.86 (dd, *J* = 9.7, 7.7 Hz, 1H), 3.75 (dd, *J* = 10.7, 3.5 Hz, 1H), 3.63 (dd, *J* = 8.9, 7.5 Hz, 1H), 3.58 – 3.49 (m, 3H). ^{13}C NMR (126 MHz, $CDCl_3$) δ 144.5, 138.9, 138.8, 138.76, 138.6, 138.2, 138.0, 128.5, 128.4, 128.37, 128.3, 128.28, 128.24, 128.2, 128.0, 127.8, 127.7, 127.62, 127.6, 127.57, 127.4, 102.9, 99.9, 82.4, 79.5, 76.0, 75.2, 74.7, 73.6, 73.55, 73.4, 73.2, 73.0, 72.4, 70.4, 68.7, 68.1. ; ESIMS calculated for $C_{54}H_{56}O_9Na$ $[M+Na]^+$ 871.3817, found: 871.3820.

Synthesis of 2-(Trimethylsilyl)ethanesulfonamide (2.25):

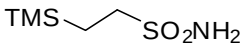

2.25

Phosphoruspentachloride (1.54 g, 7.5 mmol) was added in portions to a suspension of sodium 2-(trimethylsilyl)ethanesulfonate (1.02 g, 5.0 mmol) in 20 mL DCM and stirred at room temperature for 1 h. The organic layer was washed with saturated $NaHCO_3$ (3 x 15 mL), dried over Na_2SO_4 and evaporated to give white solid. The white solid was dissolved in 20 mL DCM, and NH_3 gas was passed in to the solution through NaOH plug for 45 m at -10 ^{o}C. The mixture was stirred overnight at room temperature and filtered over celite, and concentrated. The residue was dissolved in EtOAc, and then washed with water followed by brine. The organic layer was dried over Na_2SO_4 and concentrated to yield 508 mg (56%) of white solid, **2.25**. ^{1}H NMR (300 MHz, $CDCl_3$) δ 4.86 (s, 2H), 3.26 – 2.69 (m, 2H), 1.46 – 0.80 (m, 2H), 0.06 (s, 9H).

Synthesis of *N*-(2,3,4,6-Tetra-*O*-benzyl-β-D-galactopyranosyl-(1→4)-3,6-di-*O*-benzyl-1,2-dideoxy-2-iodo-α-D-mannopyranosyl)-2-(trimethylsilyl)ethanesulfonamide (2.26):

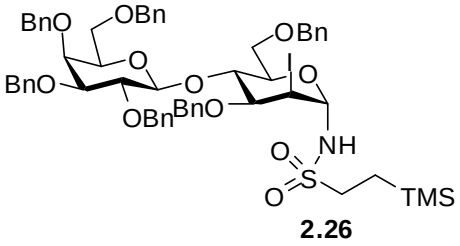

2.26

Benzyllactal **2.24** (237 mg, 0.28 mmol) followed by 2-(Trimethylsilyl)ethaneslfonamide **2.25** (203 mg, 1.12 mmol) were added to a 6 mL of DCM with 120 mg of 4 A^{o} powdered molecular sieves (freshly flame dried). The reaction mixture was stirred for 35 m at room temperature. The mixture was cooled to 0 ^{o}C, and I(symcollidine)$_2$ClO$_4$, generated from Ag(symcollidine)$_2$ClO$_4$ (378 mg, 0.84 mmol) and I_2 (206 mg, 0.87 mol) in a 6 mL of DCM with 120 mg of 4 A^{o} powdered molecular sieves (freshly flame dried), added via cannula and stirred for 2 h (Ag(symcollidine)$_2$ClO$_4$ was prepared by adding 2 mL of symcollidine to a solution of silver nitrate (0.9 g) and NaClO$_4$ (1.1 g) in 15 mL of water and stirred for 1 h. White precipitate formed is filtered and dried). The reaction mixture was diluted with 40 mL of DCM and filtered. The filtrate was washed with saturated aq $Na_2S_2O_3$ (2 x 60 mL), saturated aq $CuSO_4$ (3 x 60 mL) and brine (1 x 60 mL). The organic layer was dried over Na_2SO_4 and concentrated. The residue was purified by column chromatography with EtOAc:Hexanes (1:5 to 1:4) to afford 114 mg (35%) of **2.26** as an oily colorless liquid. ^{1}H NMR (498 MHz, $CDCl_3$) δ 7.57 – 6.82 (m, 30H), 5.20 (t, *J* = 10.1 Hz, 1H), 4.94 (d, *J* = 11.6 Hz, 1H), 4.86 (dd, *J* = 10.4, 9.1 Hz, 2H), 4.75 (dd, *J* = 20.0, 8.7 Hz, 3H), 4.65 (dd, *J* = 17.0, 11.5 Hz, 2H), 4.53 (d, *J* = 11.3 Hz, 1H), 4.43 (tdd, *J* = 12.9, 8.8, 4.0 Hz, 5H), 4.22 (d, *J* = 7.7 Hz, 2H), 4.10 (s, 1H), 3.87 (q, *J* = 7.9 Hz, 2H), 3.80 (dd, *J* = 9.7, 7.8 Hz, 1H), 3.68 (dd, *J* = 3.3, 1.8 Hz, 1H), 3.62 – 3.39 (m, 5H), 3.05 (dtd, *J* = 19.5, 13.8, 4.6 Hz,

2H), 1.11 – 0.90 (m, 2H), -0.05 (s, 9H). ^{13}C NMR (125 MHz, $CDCl_3$) δ 138.6, 138.5, 138.4, 138.0, 137.8, 137.3, 128.6, 128.6, 128.5, 128.5, 128.4, 128.2, 128.1, 128.0, 127.97, 127.9, 127.83, 127.8, 127.7, 103.9, 82.2, 79.8, 79.3, 78.4, 77.1, 75.4, 74.8, 74.5, 74.1, 73.8, 73.6, 73.5, 73.3, 69.0, 67.6, 51.2, 30.0, 10.6, -1.9; ESIMS calculated for $C_{59}H_{70}NO_{11}SiSINa$ $[M+Na]^+$ 1178.3376, found: 1178.3380.

Synthesis of Ethyl 2,3,4,6-tetra-*O*-benzyl-β-D-galactopyranosyl-(1→4)-2-deoxy-3,6-di-*O*-benzyl-2-[2-(trimethylsilyl)ethanesulfonamido]-1-thio-β-D-glucopyranoside (2.27):

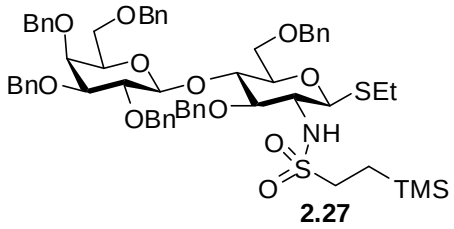

2.27

A solution of iodosulfonamide **2.26** (130 mg, 0.11 mmol) in 1 mL of DMF was added drop wise to a solution of ethane thiol (41.8 μL, 0.57 mmol) and LiHMDS (1M in THF, 340 μL, 0.34 mmol) in 3 mL DMF at -40 ^{o}C. The reaction mixture was slowly warmed to room temperature and stirred overnight. Most of the DMF was removed by concentrating under reduced pressure, and the residue was dissolved in EtOAc (15 mL), then washed with saturated $NaHCO_3$ (3 x 15 mL), dried over Na_2SO_4, and concentrated. The residue was purified by column chromatography with hexanes: EtOAc (3:1) to yield 70 mg (58%) of oily compound **2.27**. ^{1}H NMR (498 MHz, $CDCl_3$) δ 7.48 – 7.08 (m, 30H), 4.92 (d, *J* = 11.2 Hz, 2H), 4.79 (s, 2H), 4.73 (d, *J* = 10.8 Hz, 1H), 4.69 (d, *J* = 2.9 Hz, 2H), 4.59 (d, *J* = 7.5 Hz, 1H), 4.55 (dd, *J* = 10.7, 3.8 Hz, 2H), 4.52 (d, *J* = 12.1 Hz, 1H), 4.46 – 4.35 (m, 3H), 4.29 (d, *J* = 11.7 Hz, 1H), 3.99 (t, *J* = 7.2 Hz, 1H), 3.90 (d, *J* = 2.8 Hz, 1H), 3.83 – 3.74 (m, 3H), 3.67 (dd, *J* = 10.6, 3.6 Hz, 1H), 3.62 – 3.56 (m, 1H), 3.56 – 3.47 (m, 2H), 3.47 – 3.40 (m, 2H), 3.37 (dd, *J* = 7.8, 5.6 Hz, 1H), 3.24 – 3.05 (m, 2H), 2.78 –

2.65 (m, 2H), 1.28 (t, J = 7.4 Hz, 3H), 1.10 – 1.01 (m, 2H), -0.02 (s, 9H). ^{13}C NMR (125 MHz, $CDCl_3$) δ 138.9, 138.6, 138.5, 138.3, 138.2, 138.0, 128.4, 128.38, 128.35, 128.3, 128.27, 128.2, 128.1, 128.0, 127.9, 127.8, 127.7, 127.6, 127.55, 127.53, 127.5, 127.4, 127.38, 103.2, 83.6, 82.3, 81.3, 79.9, 76.7, 75.4, 74.7, 73.5, 73.4, 73.38, 73.3, 73.2, 72.6, 68.9, 68.1, 57.8, 51.3, 24.2, 14.9, 10.4, -1.9; ESIMS calculated for $C_{61}H_{75}NO_{11}SiS_2Na$ $[M+Na]^+$ 1112.4443, found: 1112.4435.

Synthesis of Ethyl 2,3,4,6-tetra-*O*-benzyl-β-D-galactopyranosyl-(1→4)-2-acetamido-2-deoxy -3,6-di-*O*-benzyl-1-thio-β-D-glucopyranoside (2.28):

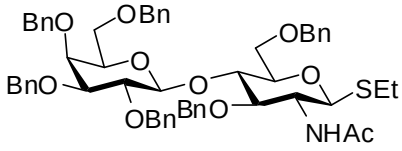

2.28

Powdered CsF (46 mg, 0.3 mmol) was added to a solution of compound **2.27** in 4ml of DMF and refluxed for 2 d. DMF was removed by concentrating under high vacuum. Saturated $NaHCO_3$ (6 mL) was added to the residue and washed with ether (3 x 5 mL). The Combined organic layers were dried over Na_2SO_4 and concentrated under reduced pressure. ^{1}H NMR (498 MHz, $CDCl_3$) δ 7.70 – 6.79 (m, 30H), 5.21 (d, J = 10.6 Hz, 1H), 4.97 (d, J = 11.5 Hz, 1H), 4.82 (s, 2H), 4.72 (s, 2H), 4.59 – 4.51 (m, 3H), 4.46 (d, J = 7.7 Hz, 1H), 4.39 (dd, J = 18.1, 11.9 Hz, 2H), 4.28 (dd, J = 10.8, 7.1 Hz, 2H), 4.01 (t, J = 9.4 Hz, 1H), 3.92 (d, J = 2.9 Hz, 1H), 3.84 (dd, J = 11.0, 4.2 Hz, 1H), 3.79 (dd, J = 9.7, 7.8 Hz, 1H), 3.73 (d, J = 11.0 Hz, 1H), 3.53 (dd, J = 12.7, 5.8 Hz, 1H), 3.47 – 3.30 (m, 4H), 2.89 (t, J = 9.6 Hz, 1H), 2.80 – 2.62 (m, 2H), 1.66 (s, 2H), 1.30 (t, J = 7.4 Hz, 3H); ESIMS calculated for $C_{56}H_{64}NO_9S$ $[M+H]^+$ 926.4296, found: 926.4294.

The free amine was dissolved in 3 mL of pyridine and 0.3 mL of Ac_2O was added. The reaction mixture was stirred at room temperature for overnight. Excess Ac_2O was quenched with MeOH

and concentrated. The residue was purified by silica gel chromatography to yield yellow oily liquid. ^{1}H NMR (500 MHz, $CDCl_3$) δ 7.67 – 6.78 (m, 30H), 5.54 (d, *J* = 8.2 Hz, 1H), 4.97 (dd, *J* = 15.3, 11.4 Hz, 2H), 4.87 (d, *J* = 9.8 Hz, 1H), 4.84 (s, 2H), 4.74 (s, 2H), 4.61 (d, *J* = 11.3 Hz, 1H), 4.57 (dd, *J* = 11.8, 3.8 Hz, 2H), 4.50 – 4.35 (m, 3H), 4.30 (d, *J* = 11.8 Hz, 1H), 4.00 (dd, *J* = 20.0, 11.4 Hz, 1H), 3.93 (d, *J* = 2.9 Hz, 1H), 3.88 – 3.71 (m, 3H), 3.67 – 3.50 (m, 3H), 3.45 (dd, *J* = 9.7, 2.9 Hz, 1H), 3.43 – 3.36 (m, 2H), 2.82 – 2.51 (m, 2H), 1.90 (s, 3H), 1.28 (t, *J* = 7.4 Hz, 3H). ^{13}C NMR (126 MHz, $CDCl_3$) δ 170.1, 139.0, 138.9, 138.7, 138.5, 138.45, 138.0, 128.4, 128.38, 128.3, 128.26, 128.2, 127.9, 127.88, 127.8, 127.7, 127.6, 127.5, 127.47, 127.4, 127.37, 103.0, 83.2, 82.4, 80.0, 79.8, 79.6, 75.4, 74.7, 74.1, 73.7, 73.5, 73.1, 73.05, 72.7, 68.6, 68.2, 55.4, 24.3, 23.6, 15.1; ESIMS calculated for $C_{58}H_{66}NO_{10}S$ $[M+H]^+$ 968.4402, found: 968.4414.

Synthesis of Thianthrene-5-oxide (2.29):

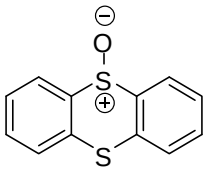

2.29

A solution of *meta*-chloroperbenzoic acid, *m*-CPBA (986.1 mg, 4.4 mmol) in 5 mL DCM was added to an ice cold solution of thianthrene (865.3 mg, 4 mmol) in 2 mL DCM and stirred for about 2.5 h. The reaction mixture was washed with saturated $NaHCO_3$ (8 mL), water (8 mL) and dried over Na_2SO_4. The organic layer was concentrated and purified by silica gel chromatography with EtOAc:Hexanes (1:3) to yield 836 mg (90%) of compound **2.29**. ^{1}H NMR (400 MHz, $CDCl_3$) δ 7.93 (ddd, *J* = 7.8, 1.4, 0.4 Hz, 2H), 7.62 (ddd, *J* = 7.7, 1.2, 0.5 Hz, 2H), 7.55 (td, *J* = 7.6, 1.2 Hz, 2H), 7.44 (td, *J* = 7.6, 1.2 Hz, 2H); HRMS calculated for $C_{12}H_8OS_2$ $(M)^+$ 232.0017, found 232.0013.

Synthesis of Methyl 2,3,4,6-tetra-*O*-benzyl-β-D-galactopyranosyl-(1→4)-2-acetamido-2-deoxy-3,6-di-*O*-benzyl-β-D-glucopyranoside (2.33):

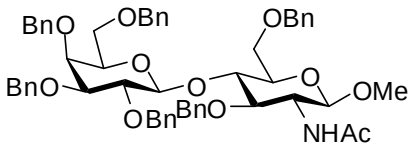

2.33

Trifluoromethanesulfonic anhydride (58.4 μL, 0.17 mmol) was added to a solution of benzyl lactal (146 mg, 0.17 mmol) and thianthrene-5-oxide (82.1 mg, 0.35 mmol) in 8 mL of chloroform and dichloromethane (3:1 v/v) mixture at -78 °C. The entire reaction mixture was stirred 11 m, then *N*,*N*-diethylaniline (110 μL, 0.69 mmol) was added, followed by *N*-(TMS)acetamide (68.2 mg, 0.51 mmol).The mixture was immediately brought to room temperature and stirred for 30 min. Dry MeOH (22 μL, 0.51 mmol) was added to the mixture followed by 137.3 mg of Amberlyst-15 acidic resin (washed with acetone and dried at 65^{o}C under reduced pressure). The reaction was stirred for 38 h, filtered, concentrated under vacuum, and purified by silica gel flash column chromatography (2:1 hexane/ethyl acetate), to obtain a 21 mg of compound (1:2 hexane/ethyl acetate, R_f = 0.4), MS showed $(M+Na)^+$of title compound **2.33**. Compound **2.32** was isolated with impurities (4:1 ethyl acetate/hexanes, R_f = 0.6).

Synthesis of 1, 3-dimethyl-5-[(dimethylamino)methylene]2, 4, 6 (1H, 3H, 5H)-trioxopyrimidine (2.35):

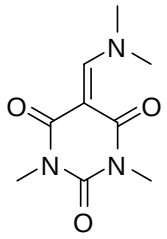

2.35

A solution of 1,3-dimethylbarbituric acid (3.0 g, 19.2mmol) in 20 mL $CHCl_3$ was added drop wise to a solution of *N*,*N*-dimethylformamide dimethyl acetal (2.82 mL, 21.0 mmol) in 30 mL $CHCl_3$ at 0 ^oC over 2 h under constant stirring. The reaction mixture was washed with water (3 x 40 mL) and brine (40 mL). The organic layer was dried over Na_2SO_4, filtered and evaporated. The crude solid was washed with diethyl ether (3 x 10 mL) to yield compound **2.35** as yellow solid (2.97 g, 73%).^{1}H NMR (300 MHz, $CDCl_3$) δ 8.12 (s, 1H), 3.41 (s, 3H), 3.37 (s, 3H), 3.29 (s, 6H).

Synthesis of β-D-galactopyranosyl-(1→4)-2-acetamido-2-deoxy-α/β-D-glucopyranose (2.36):

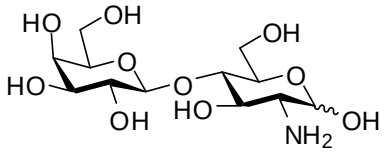

2.36

Benzylamine (25 mL, 228.9 mmol) was added to lactulose (10 g, 29.2 mmol) at 0 ^oC and warmed to ambient temperature and stirred at 43 ^oC for 5 d, until TLC ($MeOH/CHCl_3/NH_4OH$ 2:1:1) showed lactulosylamine as major product. A solution of MeOH (25 mL) was added, after cooling the reaction mixture to room temperature. This methanolic solution was added in portions to 1500 mL of diethyl ether under constant stirring for 1 h and kept at -20 ^oC overnight. A yellow precipitate was formed and collected by filtration, followed by drying under reduced pressure. Glacial aceticacid (7 mL) was added to the yellow solid (13.8 g, crude) in 56 mL of MeOH and stirred at room temperature for 3 h. The mixture was poured into 1500 mL of diethyl ether and kept at -20 ^oC overnight. The precipitate was collected by filtration, and dried under reduced pressure to give the crude product as yellow solid (14.3 g), containing *N*-benzyllactosamine **2.34**. The crude benzyllactosamine **2.34**, was dissolved in 18 mL of deionized

water and pH was adjusted to 1 by drop wise addition of 1.0 mL HCl. 850 mg of 20% $Pd(OH)_2/C$ (5% by weight), Pearlman's catalyst, was added and kept on a par shaker at 60 psi for 3 d. The catalyst was filtered off and solution was concentrated, followed by co-evaporation with benzene/ether (1:1) under reduced pressure gave 12 g of crude lactosaminehydrochloride as yellow solid. Triethylamine (3.6 mL, 26.0 mmol) and DTPM reagent (4.6 g, 21.8 mmol) were added to crude lactosaminehydrochloride (6.4 g) dissolved in 80 mL of MeOH and stirred for 2 h at room temperature. The white precipitate formed was collected by filtration, washed with MeOH several times and dried under reduced pressure to give 3.7 g (60%) of pure compound. ESIMS calculated for $C_{19}H_{29}N_3O_{13}Na$ $[M+Na]^+$ 530.1593, found: 530.1574.

To DTPM protected lactosamine (4 g, 7.5 mmol) from previous reaction, NH_4OH (30 mL) was added and stirred for 40 m at ambient temperature. The white precipitate (unreacted DTPM-lactosamine,side products of deprotection) was filterd off and washed with water. Entire filtrate, aqueous and NH_4OH solution, washed with $CHCl_3$ (3x30 mL). Aqueous layer was concentrated under reduced pressure to yield 2.4 g (90%) of lactosamine **2.36**, as light yellow solid. ESIMS calculated for $C_{12}H_{24}NO_{10}$ $[M+H]^+$ 342.1395, found: 342.1397.

Synthesis of 2, 3, 4, 6-Tetra-*O*-acetyl-β-D-galactopyranosyl-(1→4)-2-acetamido-1,3,6-tri-*O*-acetyl-2-deoxy-α/β-D-glucopyranose (2.37):

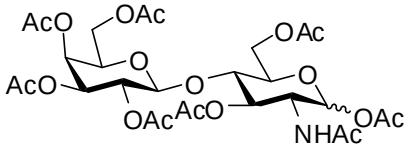

2.37

Acetic anhydride (5 mL) and DMAP (20 mg) were added to a solution of **2.36** in 10 mL of pyridine and the mixture was stirred at room temperature for 18 h. Excess acetic anhydride was

quenched by adding MeOH at 0 ^{o}C and concentrated and co-evaporated with toluene (3 x 10 mL) under reduced pressure. The residue was purified by silica gel chromatography using Hexanes:EtOAc (3:1) to 100% EtOAc to afford 923 mg (93%) of peracetylated lactosamine, **2.37**, as slight yellow solid. ^{1}H NMR (498 MHz, $CDCl_3$) δ 6.08 (d, *J* = 3.6 Hz, 1H), 5.86 (d, *J* = 9.7 Hz, 0.3H), 5.66 (d, *J* = 9.1 Hz, 1H), 5.62 (d, *J* = 7.7 Hz, 0.3H), 5.34 (d, *J* = 3.2 Hz, 2H), 5.22 (dd, *J* = 11.0, 8.3 Hz, 1H), 5.10 (dd, *J* = 10.4, 7.9 Hz, 1.3H), 5.07 – 5.03 (m, 0.3H), 4.95 (dd, *J* = 10.4, 3.5 Hz, 1.4H), 4.52 (d, *J* = 7.9 Hz, 1H), 4.48 (d, *J* = 7.9 Hz, 0.4H), 4.43 (dd, *J* = 12.0, 3.0 Hz, 0.3H), 4.41 – 4.33 (m, 2H), 4.26 (dd, *J* = 17.2, 9.4 Hz, 0.3H), 4.17 – 4.04 (m, 4.1H), 3.92 – 3.80 (m, 3.6H), 3.79 – 3.73 (m, 0.3H), 3.28 (d, *J* = 7.0 Hz, 0.4H), 2.16 (s, 3H), 2.13 (s, 3.8H), 2.10 (s, 3.7H), 2.08 (s, 3H), 2.07 (s, 0.6H), 2.07 (s, 0.9H), 2.05 (s, 3.4H), 2.04 (s, 4.5H), 1.95 (s, 3.7H), 1.94 (s, 0.8H), 1.91 (s, 3H). ESIMS calculated for $C_{28}H_{39}NO_{18}Na$ $[M+Na]^{+}$ 700.2059, found: 700.205

Synthesis of 2-Methyl-{3,6-di-*O*-acetyl-1,2-dideoxy-4-*O*-(2,3,4,6-tetra-*O*-acetyl-β-D-galactopyranosyl)-α-D-gluco-pyrano}-[2,1-d]-oxazoline (2.38):

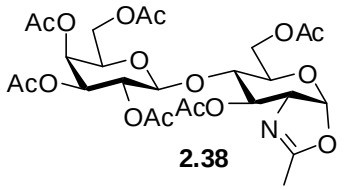

2.38

Peracetylated LacNAc **2.37** (567 mg, 0.84 mmol) was dissolved in 10 mL of 1,2-dichloro ethane and stirred with TMSOTf (167 µL, 1.05 mmol) at 50 ^{o}C for 12 h. The reaction mixture was then warmed to room temperature. Triethylamine (0.6 mL) was added and the reaction mixture was stirred for 30 min. The solvent was removed under vacuum and the crude mixture was purified by column chromatography with toluene/EtOAc/Et_3N (100:200:1) to yield 400 mg (75%) of **2.38**

as a yellow solid. ^{1}H NMR (498 MHz, $CDCl_3$) δ 5.90 (d, *J* = 7.3 Hz, 1H), 5.63 (s, 1H), 5.36 (d, *J* = 3.4 Hz, 1H), 5.16 (dd, *J* = 10.0, 8.3 Hz, 1H), 4.99 (dd, *J* = 10.3, 3.5 Hz, 1H), 4.64 (d, *J* = 8.0 Hz, 1H), 4.24 – 4.02 (m, 5H), 3.94 (t, *J* = 6.7 Hz, 1H), 3.64 (d, *J* = 9.5 Hz, 1H), 3.53 – 3.45 (m, 1H), 2.15 (s, 3H), 2.10 (s, 3H), 2.10 (s, 3H), 2.09 (s, 3H), 2.04 (s, 3H), 2.02 (s, 3H), 1.96 (s, 3H); ^{13}C NMR (125 MHz, $CDCl_3$) δ 170.6, 170.32, 170.3, 170.1, 169.4, 169.2, 166.8, 102.4, 99.1, 78.0, 71.0, 70.9, 70.5, 68.8, 67.5, 66.9, 65.0, 63.5, 61.1, 21.0, 20.8, 20.7, 20.66, 20.6, 20.5, 13.9; ESIMS calculated for $C_{26}H_{35}NO_{16}Na$ $[M+Na]^+$ 640.1848, found: 640.1846.

Synthesis of 9H-fluoren-9ylmethyl {2-[2-*O*-(2, 3, 4, 6-tetra-*O*-acetyl-β-D-galactopyranosyl-(1→4)-2-acetamido-3,6-di-*O*-acetyl-2-deoxy-β-D-glucopyranosyl)-2-hydroxyethoxy]ethyl}carbamate (2.39):

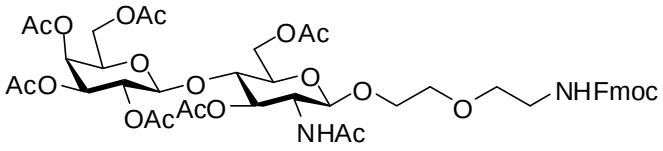

2.39

Oxazoline **2.38** (355 mg, 0.58 mmol) and 9*H*-fluoren-9-yl[2-(2-hydroxyethoxy)-ethyl]carbamate **2.11** (569 mg, 1.74 mmol) were stirred with a catalytic amount of camphor sulfonic acid (CSA) (12 mg) in 12 mL of 1,2-dichloroethane under refluxing conditions (90 °C) for 2.3 h. The reaction mixture was cooled and poured over ice water and then washed successively with aqueous saturated $NaHCO_3$, water, and dried over anhydrous Na_2SO_4. The solvent was evaporated under vacuum and the residue was purified by column chromatography using EtOAc to yield 427 mg (78.0%) of **2.39** as a yellow solid. ^{1}H NMR (500 MHz, $CDCl_3$) δ 7.77 (d, *J* = 7.5 Hz, 2H), 7.63 (d, *J* = 7.3 Hz, 2H), 7.40 (t, *J* = 7.5 Hz, 2H), 7.31 (tt, *J* = 7.5, 1.2 Hz, 2H), 5.89 (d, *J* = 9.0 Hz, 1H), 5.60 (s, 1H), 5.34 (d, *J* = 2.7 Hz, 1H), 5.11 (dd, *J* = 10.5, 7.9 Hz, 2H), 4.97 (dd,

J = 10.5, 3.5 Hz, 1H), 4.55 – 4.45 (m, 3H), 4.43 (d, *J* = 6.9 Hz, 2H), 4.24 (t, *J* = 6.8 Hz, 1H), 4.13 (dd, *J* = 11.8, 5.4 Hz, 1H), 4.11 – 4.00 (m, 3H), 3.94 – 3.81 (m, 2H), 3.77 (t, *J* = 8.3 Hz, 1H), 3.69 – 3.56 (m, 4H), 3.53 (s, 2H), 3.44 – 3.23 (m, 2H), 2.14 (s, 3H), 2.10 (s, 3H), 2.05 (s, 6H), 2.03 (s, 3H), 1.97 (s, 3H), 1.94 (s, 3H); ^{13}C NMR (126 MHz, $CDCl_3$) δ 170.4, 170.3, 170.1, 170.0, 169.4, 156.8, 144.0, 141.3, 127.7, 127.1, 125.1, 120.0, 100.9, 75.6, 72.7, 72.0, 70.8, 70.7, 70.3, 70.2, 69.1, 68.5, 66.6, 66.57, 62.5, 60.8, 53.0, 50.8, 47.3, 41.1, 23.2, 20.87, 20.8, 20.7, 20.62, 20.6, 20.5; ESIMS calculated for $C_{45}H_{56}N_2O_{20}Na$ $[M+Na]^+$ 967.3319, found: 967.3307.

Synthesis of Methyl 2-(diphenylphosphino)-4-{2[2-*O*-(β-D-galactopyranosyl-(1→4)-2-acetamido-2-deoxy-β-D-glucopyranosyl)-2hydroxyethoxy]ethylcarbamoyl]}benzoate (2.40):

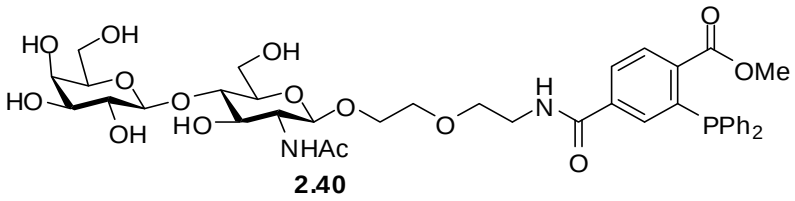

2.40

Deprotection of compound **2.39** (183 mg, 0.19 mmol) was achieved under Zémplen conditions by stirring in a solution of MeOH (4 mL) with 1% NaOMe/MeOH (2.3 mL) for 2.3 h. The reaction mixture was neutralized with Amberlite resin 120. The resin was washed with MeOH, stirred with 10 mL of ammonia for 30 m and filtered. The ammonia was removed by evaporation and dried overnight under vacuum to give 52 mg of a white solid. The solid (36 mg, 0.08 mmol) was dissolved in 5 mL of DMF and stirred with succinimidyl-3-diphenylphosphino-4-methoxy-carbonylbenzoate **2.7** (106 mg, 0.23 mmol), and two drops of triethylamine for 4 h at room temperature. The solvent was removed under vacuum and the material was purified by column chromatography (Iatrobeads) with DCM/MeOH (3:1) to yield 43 mg (50%) of **2.40** as a yellow solid containing a small amount of the corresponding phospine oxide. ^{1}H NMR (500 MHz, CD_3OD) 8.05 (dd, *J* = 8.0, 3.6 Hz, 1H), 7.82 (dd, *J* = 8.0, 1.7 Hz, 1H), 7.44 (dd, *J* = 3.9, 1.7 Hz,

1H), 7.39 – 7.30 (m, 6H), 7.30 – 7.22 (m, 4H), 4.43 (d, J = 8.4 Hz, 1H), 4.37 (d, J = 7.6 Hz, 1H), 3.96 – 3.89 (m, 1H), 3.88 (d, J = 2.4 Hz, 1H), 3.85 – 3.78 (m, 2H), 3.78 – 3.68 (m, 3H), 3.67 (s, 3H), 3.67 – 3.44 (m, 13H), 3.43 – 3.38 (m, 1H), 3.36 (ddd, J = 9.4, 4.4, 2.5 Hz, 1H), 1.92 (s, 3H); phospine oxide: δ 8.15 (dt, J = 8.0, 1.6 Hz, 0.2H), 8.00 (dd, J = 8.0, 3.6 Hz, 0.25H), 7.95 (dd, J = 13.8, 1.7 Hz, 0.25H), 7.68 – 7.58 (m, 1.4H), 7.54 (m,1H); ^{13}C NMR (125 MHz, CD_3OD) δ 173.5, 169.5, 168.5 (d, J_{C-P} = 2.5 Hz), 142.3 (d, J_{C-P} = 28.8 Hz), 138.9, 138.6 (d, J_{C-P} = 10.0 Hz), 138.26 (d, J_{C-P} = 18.7 Hz), 135.1 (d, J_{C-P} = 20.0 Hz), 134.5, 131.7 (d, J_{C-P} = 2.5 Hz), 130.1, 129.7 (d, J_{C-P} = 6.3 Hz), 127.9, 105.2, 102.8, 81.1, 77.2, 76.6, 74.9, 74.2, 72.6, 71.2, 70.4, 70.3, 70.0, 62.5, 62.0, 56.7, 52.6, 41.0, 23.1; phosphine oxide: δ 139.8 (d, J_{C-P} = 7.5 Hz), 138.3 (d, J_{C-P} = 11.3 Hz), 133.6, 132.9 (d, J_{C-P} = 12.5 Hz), 129.9 (d, J_{C-P} = 12.5 Hz), 53.0; ^{31}P NMR (202 MHz, CD_3OD) δ 35.00 (s, 0.21P), -2.80 (s, 1.00P); ESIMS calculated for $C_{39}H_{49}PN_2O_{15}Na$ $[M+Na]^+$ 839.2763, found: 839.2756.

Synthesis of azidoacetic acid labeled β-lactoglobulin:

Protein samples of β-lactoglobulin (5 mg, 0.3 mmol) were dissolved in borate buffer (50 mM, pH 9, 1 mL). A solution of succinimidyl 2-azidoacetate **2.2**, in dioxane was added (27 mg/mL, 70 µl, 35 equiv) and was left at room temperature for 1 h after vortexing. The labeled protein was purified using ultracentifugation (10 kDa MW cutoff). The sample was lyophilized and stored at –20 °C.

Staudinger ligation of azide-labeled protein:

Samples of azide-labeled protein (200 µg) were dissolved in 100 µL of buffer (10 mM, ammonium acetate, pH 8.9). Staudinger reagents in DMSO/H_2O (1:15, 1 mg/mL; 300 µL) were added to the protein solution and allowed to react for 12 h at room temperature. The mixture was lyophilized and dissolved in 100 µL of buffer (10 mM, ammonium acetate, pH 8.9).

2.13.3 Stability studies of 2-(diphenyl-phosphanyl)-terephthalic acid 1-methyl ester (2.6)

The compound, **2.6,** (2 mg in each) was dissolved in 600 µL of different solvents, $CDCl_3$ (control), 5% TFA in $CDCl_3$, 95% TFA in CDCl3, aceticacid, 20% piperidine in DMF, 2% hydrazine in DMF , 1% NaOMe in MeOH and transfered to seven different NMR tubes. Then ^{31}PNMR was recorded at 1.5 h, 12 h,24 h and 48 h under constant parameters (nt = 256, d_1 = 0.1, gain = 60).

2.13.4 Western blotting of biotinylated LFA-1

Jurkat cells cultured in growth media supplemented with 14 mM Ac $_4$ManNAz (**2.4**) for variable time periods, depending on the assay. LFA-1 bearing azide-labeled sialic (LFA-1-Az) was immunoprecipitated with TS2/4 mAb sepharose (method by Springer et al.).[64, 65] However, before elution from the beads, azide-tagged sialic acids were biotinylated by Staudinger ligation by adding compound **2.10** (50 mg/mL) and mixing overnight at 4 °C. Detection of biotinylated LFA-1 was achieved by Western blot. Proteins were eluted by boiling at 95 °C in Laemmli buffer, and separated by 4/7% SDS-PAGE. Proteins were transferred to nitrocellulose, then the membranes were blocked with 5% milk in TBS-T. Membranes were probed with streptavidin-HRP (Bio Rad) in 2.5% milk TBS-T. Bands were visualized by chemiluminescence (Pierce). Removal of biotinylated sialic acids through removal of *N*-glycans, was achieved by treating immunoaffinity purified LFA-1-Az with PNGase F (New England Biolabs, Ipswich, MA) according to the supplier's directions. Proteins were denatured by boiling with SDS, followed by incubation with PNGase F overnight at 37°C.

2.13.5 Lectin blotting of glycoconjugates

Labeled glycoprotein samples were separated by SDS-PAGE (5%/15%) and transferred to nitrocellulose. The membrane was blocked for 2 h with CarboFree Blocking Solution (Vector

Labs), and incubated with biotinylated MAL-I lectin (Vector Labs) diluted in blocking solution (1 μg/mL) for 1 h. The membrane was washed with TBS-T (Tris-buffered saline, 0.1% Tween 20), and incubated with streptavidin-HRP (Bio-Rad) in blocking solution for 1 h. The membrane was washed again with TBS-T, and positive signals were then detected by enhanced chemiluminescence (Amersham). All incubations after protein transfer were performed at room temperature.

2.13.6 LC-MS of glycoconjugates

The LC-MS experiments were carried out on an Agilent 6220 Accurate-Mass TOF LC/MS system (Agilent Technologies, Santa Clara, California, USA). Samples were injected on a 75 × 0.5 mm Poroshell *C*-8 column with a particle size of 5 μm (Agilent Technologies, Santa Clara, California, USA) with an Opti-pak trap cartridge kit, 5μL bed, C8 (Optimize Technologies, Oregon City, USA). After loading of the sample, the column was flushed for 3 min at a 0.15 mL min^{-1} flow rate with 95% mobile phase A (0.1% formic acid in water) and 5% mobile phase B (0.1% FA in acetonitrile) in order to effectively remove the salts and reagents. Elution of the protein was performed by gradually increasing the concentration of phase B in the mobile phase to 95% over a period of 11 m. The column was maintained at 70 °C. Protein molecular weight information was generated using the maximum entropy deconvolution algorithm in the Agilent Mass Hunter BioConfirm software.

Table 2.2: Observed mass of galactose conjugates in mass spectrum

*Gal-SR (compound **2.16**)*		
assignment (isoform + n)	*calculated* [a]	*observed*
B	18278	18278
A	18364	18364
A + 1	19018	19016
A + 2	19672	19672
B + 2	19586	19586
A + 3	20327	20326
B + 3	20241	20241
A + 4	20981	20981
B + 4	20895	20894
A + 5	21635	21636
B + 5	21549	21549
A + 6	22289	22291
B + 6	22203	22203
A + 7	22943	22944
B + 7	22857	22859
A + 8	23598	23599
B + 8	23512	23513
A + 9	24252	24255
B + 9	24166	24168
A + 10	24906	24909
B + 10	24820	24823
A + 11	25560	25563
B + 11	25474	25478
A + 12	26215	26218
B + 12	26129	26133
A + 13	26869	26873
B + 13	26783	26787

a. Expected masses were calculated based on the formula $M_{lac} + n*M_{linker}$, where the M_{lac} that of either β-lactoglobulin (A isoform, 18364 Da) or β-lactoglobulin (B isoform, 18278 Da), *n* is the number of sites, and M_{linker} = 654.2 Da.

Table 2.3: Observed mass of lactose conjugates in mass spectrum

*Lactose-SR (compound **2.21**)*		
assignment (isoform + n)	*calculated*[a]	*observed*
A + 1	19180	19181
B + 1	19094	19094
B + 2	19911	19911
A + 3	20813	20813
B + 3	20727	20727
A + 4	21629	21631
B + 4	21543	21545
B + 5	22359	22361
A + 6	23262	23264
B + 6	23176	23178
A + 7	24078	24080
B + 7	23992	23994
A + 8	24894	24898
B + 8	24808	24811
A + 9	25710	25714
B + 9	25624	25628
A + 10	26527	26530
B + 10	26441	26445
A + 11	27343	27347
B + 11	27257	27261
A + 12	28159	28165
B + 12	28073	28077
A + 14	29792	29791
A + 15	30608	30608
B + 15	30522	30528
A + 16	31424	31426

a. Expected masses were calculated based on the formula $M_{lac} + n*M_{linker}$, where the M_{lac} that of either β-lactoglobulin (A isoform, 18364 Da) or β-lactoglobulin (B isoform, 18278 Da), *n* is the number of sites, and M_{linker} = 816.3 Da.

Table 2.4: Observed mass of LacNAc conjugates in mass spectrum

*LacNAc-SR (compound **2.40**)*		
assignment (isoform + n)	*calculated*[a]	*observed*
A + 2	20079	20079
B + 2	19993	19995
A + 3	20936	20935
B + 3	20850	20850
A + 4	21793	21795
B + 4	21707	21709
A + 5	22650	22653
B + 5	22564	22566
A + 6	23508	23511
B + 6	23422	23423
A + 7	24365	24368
B + 7	24279	24282
A + 8	25222	25225
B + 8	25136	25140
A + 9	26080	26083
B + 9	25994	25997
A + 10	26937	26941
B + 10	26851	26855
A + 11	27794	27799
B + 11	27708	27713
A + 12	28651	28656
B + 12	28565	28570
A + 13	29509	29516
B + 13	29423	29430

a. Expected masses were calculated based on the formula $M_{lac} + n*M_{linker}$, where the M_{lac} that of either β-lactoglobulin (A isoform, 18364 Da) or β-lactoglobulin (B isoform, 18278 Da), *n* is the number of sites, and M_{linker} = 857.3 Da.

2.14 References

1. Imperiali, B.; O'Connor, S. E., Effect of N-linked glycosylation on glycopeptide and glycoprotein structure. *Curr. Opin. Chem. Biol.* **1999,** *3* (6), 643-9.

2. Dwek, R. A., Glycobiology: Toward Understanding the Function of Sugars. *Chem. Rev.* **1996,** *96* (2), 683-720.

3. Hang, H. C.; Bertozzi, C. R., Chemoselective approaches to glycoprotein assembly. *Acc. Chem. Res.* **2001,** *34* (9), 727-36.

4. Peri, F.; Nicotra, F., Chemoselective ligation in glycochemistry. *Chem. Commun. (Cambridge)* **2004,** (6), 623-7.

5. Hecht, M. L.; Stallforth, P.; Silva, D. V.; Adibekian, A.; Seeberger, P. H., Recent advances in carbohydrate-based vaccines. *Curr. Opin. Chem. Biol.* **2009,** *13* (3), 354-9.

6. Carrico, I. S., Chemoselective modification of proteins: hitting the target. *Chem. Soc. Rev.* **2008,** *37* (7), 1423-31.

7. Luchansky, S. J.; Argade, S.; Hayes, B. K.; Bertozzi, C. R., Metabolic functionalization of recombinant glycoproteins. *Biochemistry* **2004,** *43* (38), 12358-66.

8. Saxon, E.; Bertozzi, C. R., Cell surface engineering by a modified Staudinger reaction. *Science* **2000,** *287* (5460), 2007-10.

9. Chang, P. V.; Chen, X.; Smyrniotis, C.; Xenakis, A.; Hu, T.; Bertozzi, C. R.; Wu, P., Metabolic labeling of sialic acids in living animals with alkynyl sugars. *Angew. Chem. Int. Ed. Engl.* **2009,** *48* (22), 4030-3.

10. Kiick, K. L.; Saxon, E.; Tirrell, D. A.; Bertozzi, C. R., Incorporation of azides into recombinant proteins for chemoselective modification by the Staudinger ligation. *Proc. Natl. Acad. Sci. U. S. A.* **2002,** *99* (1), 19-24.

11. Mahal, L. K.; Yarema, K. J.; Bertozzi, C. R., Engineering chemical reactivity on cell surfaces through oligosaccharide biosynthesis. *Science* **1997,** *276* (5315), 1125-8.

12. Yarema, K. J.; Mahal, L. K.; Bruehl, R. E.; Rodriguez, E. C.; Bertozzi, C. R., Metabolic delivery of ketone groups to sialic acid residues. Application To cell surface glycoform engineering. *J. Biol. Chem.* **1998,** *273* (47), 31168-79.

13. Lemieux, G. A.; Bertozzi, C. R., Modulating cell surface immunoreactivity by metabolic induction of unnatural carbohydrate antigens. *Chem. Biol.* **2001,** *8* (3), 265-75.

14. Sampathkumar, S. G.; Li, A. V.; Jones, M. B.; Sun, Z.; Yarema, K. J., Metabolic installation of thiols into sialic acid modulates adhesion and stem cell biology. *Nat. Chem. Biol.* **2006,** *2* (3), 149-52.

15. Grogan, M. J.; Pratt, M. R.; Marcaurelle, L. A.; Bertozzi, C. R., Homogeneous glycopeptides and glycoproteins for biological investigation. *Annu. Rev. Biochem.* **2002,** *71*, 593-634.

16. Bernardes, G. J.; Castagner, B.; Seeberger, P. H., Combined approaches to the synthesis and study of glycoproteins. *ACS Chem. Biol.* **2009,** *4* (9), 703-13.

17. Gamblin, D. P.; Scanlan, E. M.; Davis, B. G., Glycoprotein synthesis: an update. *Chem. Rev.* **2009,** *109* (1), 131-63.

18. Ochiai, H.; Huang, W.; Wang, L. X., Expeditious chemoenzymatic synthesis of homogeneous N-glycoproteins carrying defined oligosaccharide ligands. *J. Am. Chem. Soc.* **2008,** *130* (41), 13790-803.

19. Vocadlo, D. J.; Hang, H. C.; Kim, E. J.; Hanover, J. A.; Bertozzi, C. R., A chemical approach for identifying O-GlcNAc-modified proteins in cells. *Proc. Natl. Acad. Sci. U. S. A.* **2003,** *100* (16), 9116-21.

20. Sletten, E. M.; Bertozzi, C. R., Bioorthogonal chemistry: fishing for selectivity in a sea of functionality. *Angew. Chem. Int. Ed. Engl.* **2009,** *48* (38), 6974-98.

21. Varki, A.; Cummings, R. D.; Esko, J.; Freeze, H. H.; Hart, G.; Marth, J., (1999) *Essentials of glycobiology*, Cold Spring Harbor Laboratory Press, Cold Spring Harbor, NY.

22. Saxon, E.; Luchansky, S. J.; Hang, H. C.; Yu, C.; Lee, S. C.; Bertozzi, C. R., Investigating cellular metabolism of synthetic azidosugars with the Staudinger ligation. *J. Am. Chem. Soc.* **2002,** *124* (50), 14893-902.

23. Yu, H.; Chen, X., Carbohydrate post-glycosylational modifications. *Org. Biomol. Chem.* **2007,** *5* (6), 865-72.

24. Zhang, H.; Ma, Y.; Sun, X. L., Chemically-selective surface glyco-functionalization of liposomes through Staudinger ligation. *Chem. Commun. (Cambridge)* **2009,** (21), 3032-4.

25. Wang, C. C.; Seo, T. S.; Li, Z.; Ruparel, H.; Ju, J., Site-specific fluorescent labeling of DNA using Staudinger ligation. *Bioconjug. Chem.* **2003,** *14* (3), 697-701.

26. Jia, X.; Huang, Q.; Li, J.; Li, S.; Yang, Q., Environmentally Benign N-Boc Protection under Solvent- and Catalyst-Free Conditions. *Synlett.* **2007,** (5), 806-8.

27. Mbadugha, B. N.; Menger, F. M., Sugar/steroid/sugar conjugates: sensitivity of lipid binding to sugar structure. *Org. Lett.* **2003,** *5* (22), 4041-4.

28. Stadelmaier, A.; Figueroa-Perez, I.; Deininger, S.; von Aulock, S.; Hartung, T.; Schmidt, R. R., A Staphylococcus aureus lipoteichoic acid (LTA) derived structural variant with two diacylglycerol residues. *Bioorg. Med. Chem.* **2006,** *14* (18), 6239-54.

29. Zemple´n, G.; Pacsu, E., Über die Verseifung acetylierter Zucker und verwandter Substanzen. *Ber. Dtsch. Chem. Ges. Ber. Deutsch. Chem. Ges.* **1929,** *62*, 1613-4

30. Biswas, G.; Jeon, O. Y.; Lee, W. S.; Kim, D. C.; Kim, K. T.; Lee, S.; Chang, S.; Chung, S. K., Novel guanidine-containing molecular transporters based on lactose scaffolds: lipophilicity effect on the intracellular organellar selectivity. *Chemistry* **2008,** *14* (30), 9161-8.

31. Buskas, T.; Konradsson, P.; Oscarson, S., Synthesis of polylactosamine structures through regio-selective glycosylations. *J. Carbohydr. Chem.* **2001,** *20*, 569-83.

32. Wong, C.-H.; Halcomb, R. L.; Ichikawa, Y.; Tetsuya, K., Enzymes in organic synthesis: application to the problems of carbohydrate recognition (part 2). *Angew. Chem.* **1995,** *107*, 569-93.

33. Wong, C.-H.; Halcomb, R. L.; Ichikawa, Y.; Tetsuya, K., Enzymes in organic synthesis: application to the problems of carbohydrate recognition (part 2). *Angew. Chem., Int. Ed. Engl.* **1995,** *34* (5), 521-46.

34. Bongat, A. F.; Demchenko, A. V., Recent trends in the synthesis of O-glycosides of 2-amino-2-deoxysugars. *Carbohydr. Res.* **2007,** *342* (3-4), 374-406.

35. Wrodnigg, T. M.; Stutz, A. E., The Heyns rearrangement revisited: An exceptionally simple two-step chemical synthesis of D-lactosamine from lactulose. *Angew. Chem., Int. Ed. Engl.* **1999,** *38* (6), 827-828.

36. Stutz, A. E.; Dekany, G.; Eder, B.; Illaszewicz, C.; Wrodnigg, T. M., An exceptionally simple chemical synthesis of O-glycosylated D-glucosamine derivatives by Heyns rearrangement of the corresponding O-glycosyl fructoses. *J. Carbohydr. Chem.* **2003,** *22* (5), 253-265.

37. Barroca, N.; Schmidt, R. R., 2-nitro thioglycoside donors: versatile precursors of beta-D-glycosides of aminosugars. *Org. Lett.* **2004,** *6* (10), 1551-4.

38. Dahl, R. S.; Finney, N. S., A surprising dipolar cycloaddition provides ready access to aminoglycosides. *J. Am. Chem. Soc.* **2004,** *126* (27), 8356-7.

39. Lafont, D.; Descotes, G., Synthèse de phosphoramidates de 2-désoxy-2-iodoglycosyles *Carbohydr. Res.* **1987,** *166*, 195-209.

40. Lafont, D.; Descotes, G., Nouvelle voie d'accès aux 1,2-trans-2-amino-2-désoxyglycopyranosides par l'intermédiaire des phosphoramidates de 1,2-trans-2-désoxy-2-iodoglycopyranosyles *Carbohydr. Res.* **1988,** *175*, 35-48.

41. Griffith, D. A.; Danishefsky, S. J., Sulfonamidoglycosylation of Glycals. A Route to Oligosaccharides with 2-Aminohexose Subunits. *J. Am. Chem. Soc.* **1990,** *114*, 8329-31.

42. Wang, Z.-G.; Warren, J. D.; Dudkin, V. Y.; Zhang, X.; Iserloh, U.; Visser, M.; Eckhardt, M.; Seeberger, P. H.; Danishefsky, S. J., A highly convergent synthesis of an N-linked glycopeptide presenting the H-type 2 human blood group determinant. *Tetrahedron* **2006,** *62* (20), 4954-78.

43. Liu, J.; Gin, D. Y., C2-amidoglycosylation. Scope and mechanism of nitrogen transfer. *J. Am. Chem. Soc.* **2002,** *124* (33), 9789-97.

44. Shull, B. K.; Wu, Z.; Koreeda, M., A Convenient, Highly Efficient One-Pot Preparation of Peracetylated Glycals From Reducing Sugars. *J. Carbohydr. Chem.* **1996,** *15* (8), 955-64.

45. Upreti, M.; Ruhela, D.; Vishwakarma, R. A., Synthesis of the Tetrasaccharide Cap Domain of the Antigenic Lipophosphoglycan of Leishmania donovani Parasite. *Tetrahedron* **2000,** *56* (35), 6577-84.

46. Declerck, V.; Ribiere, P.; Martinez, J.; Lamaty, F., Sequential aza-Baylis-Hillman/ring closing metathesis/aromatization as a novel route for the synthesis of substituted pyrroles. *J. Org. Chem.* **2004,** *69* (24), 8372-81.

47. Fujita, T.; Kamiyama, H.; Osawa, Y.; Kawaguchi, H.; Bung, J. K.; Tatami, A.; Kawashima, W.; Maeda, T.; Nakanishi, A.; Morita, H., Photo SN-bond cleavage and related reactions of thianthrene sulfilimine derivatives. *Tetrahedron* **2007,** *63* (32), 7708-16.

48. Dekany, G.; Bornaghi, L.; Papageorgiou, J.; Taylor, S., A novel amino protecting group: DTPM. *Tetrahedron Lett.* **2001,** *42* (17), 3129-3132.

49. Nishimura, S. I.; Matsuoka, K.; Furuike, T.; Ishii, S.; Kurita, K.; Nishimura, K. M., Synthetic Glycoconjugates .2. Normal-Pentenyl Glycosides as Convenient Mediators for the Syntheses of New Types of Glycoprotein Models. *Macromolecules* **1991,** *24* (15), 4236-4241.

50. Piez, K. A.; Davie, E. W.; Folk, J. E.; Gladner, J. A., β-Lactoglobulins A and B. *J. Biol. Chem.* **1961,** *236* (11), 2912-2916.

51. Yu, H.; Yu, H.; Karpel, R.; Chen, X., Chemoenzymatic synthesis of CMP-sialic acid derivatives by a one-pot two-enzyme system: comparison of substrate flexibility of three microbial CMP-sialic acid synthetases. *Bioorg. Med. Chem.* **2004,** *12* (24), 6427-6435.

52. Freeze, H. H., Lectin analysis of proteins blotted onto filters. *Curr Protoc Mol Biol* **2001,** *Chapter 17*, Unit17 7.

53. Yamamoto, K.; Konami, Y.; Irimura, T., Sialic Acid-Binding Motif of Maackia amurensis Lectins. *J Biochem* **1997,** *121* (4), 756-761.

54. Chen, R.; Tolbert, T. J., Study of On-Resin Convergent Synthesis of N-Linked Glycopeptides Containing a Large High Mannose N-Linked Oligosaccharide. *J. Am. Chem. Soc.* **2010,** *132* (9), 3211-3216.

55. Gamblin, D. P.; Scanlan, E. M.; Davis, B. G., Glycoprotein Synthesis: An Update. *Chem. Rev.* **2009,** *109* (1), 131-163.

56. Bennett, C. S.; Wong, C. H., Chemoenzymatic approaches to glycoprotein synthesis. *Chem. Soc. Rev.* **2007,** *36* (8), 1227-1238.

57. Smith, M. D.; Gong, D.; Sudhahar, C. G.; Reno, J. C.; Stahelin, R. V.; Best, M. D., Synthesis and convenient functionalization of azide-labeled diacylglycerol analogues for modular access to biologically active lipid probes. *Bioconjugate Chem.* **2008,** *19* (9), 1855-1863.

58. Luchansky, S. J.; Argade, S.; Hayes, B. K.; Bertozzi, C. R., Metabolic functionalization of recombinant glycoproteins. *Biochemistry* **2004,** *43* (38), 12358-12366.

59. Earl, L. A.; Baum, L. G., CD45 Glycosylation controls T-cell life and death. *Immunol. Cell Biol.* **2008,** *86* (7), 608-615.

60. Suzuki, O.; Nozawa, Y.; Abe, M., The regulatory roles of cell surface sialylation and N-glycans in human B cell lymphoma cell adhesion to galectin-1. *Int. J. Oncol.* **2006,** *28* (1), 155-160.

61. Jacobs, P. P.; Callewaert, N., N-glycosylation Engineering of Biopharmaceutical Expression Systems. *Curr. Mol. Med.* **2009,** *9* (7), 774-800.

62. Sola, R. J.; Griebenow, K., Glycosylation of Therapeutic Proteins An Effective Strategy to Optimize Efficacy. *BioDrugs* **2010,** *24* (1), 9-21.

63. Sinclair, A. M.; Elliott, S., Glycoengineering: The effect of glycosylation on the properties of therapeutic proteins. *J. Pharm. Sci.* **2005,** *94* (8), 1626-1635.

64. Kurzinger, K.; Springer, T. A., Purification and structural characterization of LFA-1, a lymphocyte function-associated antigen, and Mac-1, a related macrophage differentiation antigen associated with the type three complement receptor. *J. Biol. Chem.* **1982,** *257* (20), 12412-8.

65. Dustin, M. L.; Carpen, O.; Springer, T. A., Regulation of locomotion and cell-cell contact area by the LFA-1 and ICAM-1 adhesion receptors. *J. Immunol.* **1992,** *148* (9), 2654-63.

Chapter 3

Immobilization of carbohydrate epitopes for surface plasmon resonance using the Staudinger ligation[1]

1. Portions of this work have been previously published in Loka, R. S.; Cairo, C. W., Immobilization of carbohydrate epitopes for surface plasmon resonance using the Staudinger ligation. *Carbohydr. Res.* **2010**, *345* (18), 2641-7.

3.1 Abstract

The detection of carbohydrate-protein interactions is often performed using techniques which require surface immobilization of the lectin or the glycan. A commonly used assay for lectin binding is surface plasmon resonance (SPR). We describe an implementation of Staudinger ligation chemistry as a method to immobilize carbohydrate epitopes to the biosensor surface. This was accomplished by first introducing an azide functionality to a carboxymethyldextran surface, followed by reaction with a phosphane-modified carbohydrate ligand. The chemistry employed was extremely mild and was easily adapted to a commercial biosensor system. Using this approach, we investigated the binding of jacalin and wheat germ agglutinin (WGA) to galactose, lactose, and *N*-acetyl-lactosamine. We observed that WGA binding shows evidence of multivalent interaction with the surface. Additionally, we found that jacalin binding was influenced by the presence of a flexible and hydrophobic galactosyl aglycone.

3.2. Introduction

Lectin-carbohydrate interactions are critical to a variety of biological recognition events. Among many known processes in humans, native lectins take part in inflammation, cancer, antigen recognition, and fertilization.[1-3] The measurement of lectin-carbohydrate interactions can be challenging, and a variety of methods have been employed including fluorescence spectroscopy,[4] isothermal titration calorimetry (ITC),[5] surface plasmon resonance (SPR),[6] and microarrays.[7-9] Solid-phase methods, including SPR and microarrays, are commonly employed due to their sensitivity and small sample requirements. For lectin-carbohydrate interactions, surface methods have the added advantage that surface density can be controlled to mimic multivalent presentations found in nature.[10] However, the application of solid-phase methods requires suitable surface chemistry which preserves the lectin-carbohydrate interaction under study. The development of improved, orthogonal, or more facile immobilization strategies is therefore of continued interest for assay development.

SPR has been an important technique for the analysis of lectin-carbohydrate interactions. In this technique the carbohydrate (biomolecule) is immobilized on to the surface, then lectin (ligand) is introduced on to the surface through flowing solution and vice versa. The interactions between lectin and carbohydrate are measured by changes in surface plasmon resonance and represented as a sensorgram. Typical immobilization strategies exploit amine-carboxylate crosslinking of the lectin to the surface.[11] Alternative approaches have used biotin,[12] amine,[13] thiol,[14] or lipid-tags[15] to generate carbohydrate surfaces. There has been a rapid expansion of bioorthogonal chemistry in recent years,[16] with a large number of groups developing selective strategies for protein or ligand immobilization.[17] An important subset of bioorthogonal reactions, those with excellent yields and substrate tolerance, are known as ‘click’ reactions.[18] These

reactions can provide useful alternatives to traditional immobilization strategies. The Staudinger ligation has been used to detect glycosyltransferase activity on microarrays[19] and to immobilize azide-labeled carbohydrates or proteins to a phosphane-derived surface.[20, 21] A modification of this strategy, which used a traceless Staudinger ligation, has also been reported for generating a self-assembled monolayer (SAM) and microarray surfaces.[22, 23] Native chemical ligation of proteins to an SPR surface has also been described.[24] Microarrays used for lectin-binding studies have been generated using alkyne-modified carbohydrates and a sulfonyl-azide surface.[25] Carbohydrate surfaces suitable for SPR lectin binding studies have been generated using azide-modified glycans and a SAM containing an alkyne.[26, 27]

3.3. Hypothesis

Although the Staudinger ligation has been applied for surface immobilization on SAM and microarray surfaces, there are no reports of adapting this chemistry to commercial SPR systems. Commercial SPR biosensors often use carboxymethyldextran (CMD) surfaces, and require relatively mild reaction conditions which avoid organic solvents. Application of the Staudinger ligation should be compatible with these requirements. One potential limitation of this strategy is the sensitivity of the phosphane reagents to oxidation.[28] We hypothesize that an azide-modified surface could be more robust than an immobilized phosphane, and would reduce complications due to oxidation by only capturing intact groups. In previous work (**Chapter 2**), we employed a synthetic strategy for generating phosphane-labeled carbohdyrate ligands which could be used to generate glycoprotein conjugates.[29] We chose to adapt this strategy as a method to immobilize carbohydrate ligands on an SPR biosensor. It can be accomplished by first introducing an azide functionality to a carboxymethyldextran surface, followed by reaction with a phosphane-modified carbohydrate ligand (**Figure 3.1**). We found the Staudinger ligation to an

azide surface provided an active and stable biosensor. Using this method we investigated the binding of wheat germ aggluttinin and jacalin binding to Galβ, Galβ1,4-Glcβ(Lac), and Galβ1,4-GlcNAcβ(LacNAc) linked compounds described in **Chapter 2**.

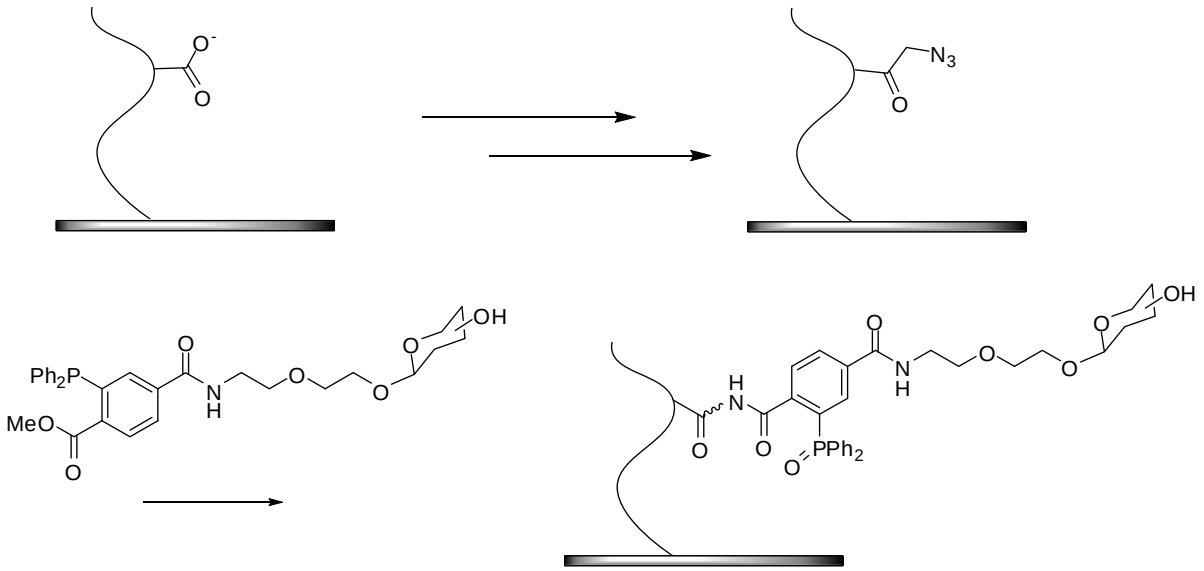

Figure 3.1: Surface modification of the CM5 chip by Staudinger ligation. Azide modification is cheaper and the surface will be robust compared to phosphane reagent on the surface.

3.4. Preparation of the biosensor surface

We developed a surface immobilization protocol suitable for immobilization of Staudinger-Bertozzi reagents.[30] We first functionalized the CMD surface with ethylenediamine (EDA) by activating the acids on the surface with *N*-hydroxysuccinamide (NHS) in presence of *N*-ethyl-*N'*-(3-diethylaminopropyl)-carbodiimide (EDC) and coupling with EDA under continuous flow of HEPES buffer of pH 7.4.[31] The amines on the surface could then be easily acetylated with an NHS-ester of azidoacetic acid, **3.5** (**Figure 3.2**).[29] We found that compound **3.5** required elevated concentrations of DMSO to keep the compound soluble, and that the compound was subject to hydrolysis if the solutions were not used rapidly.

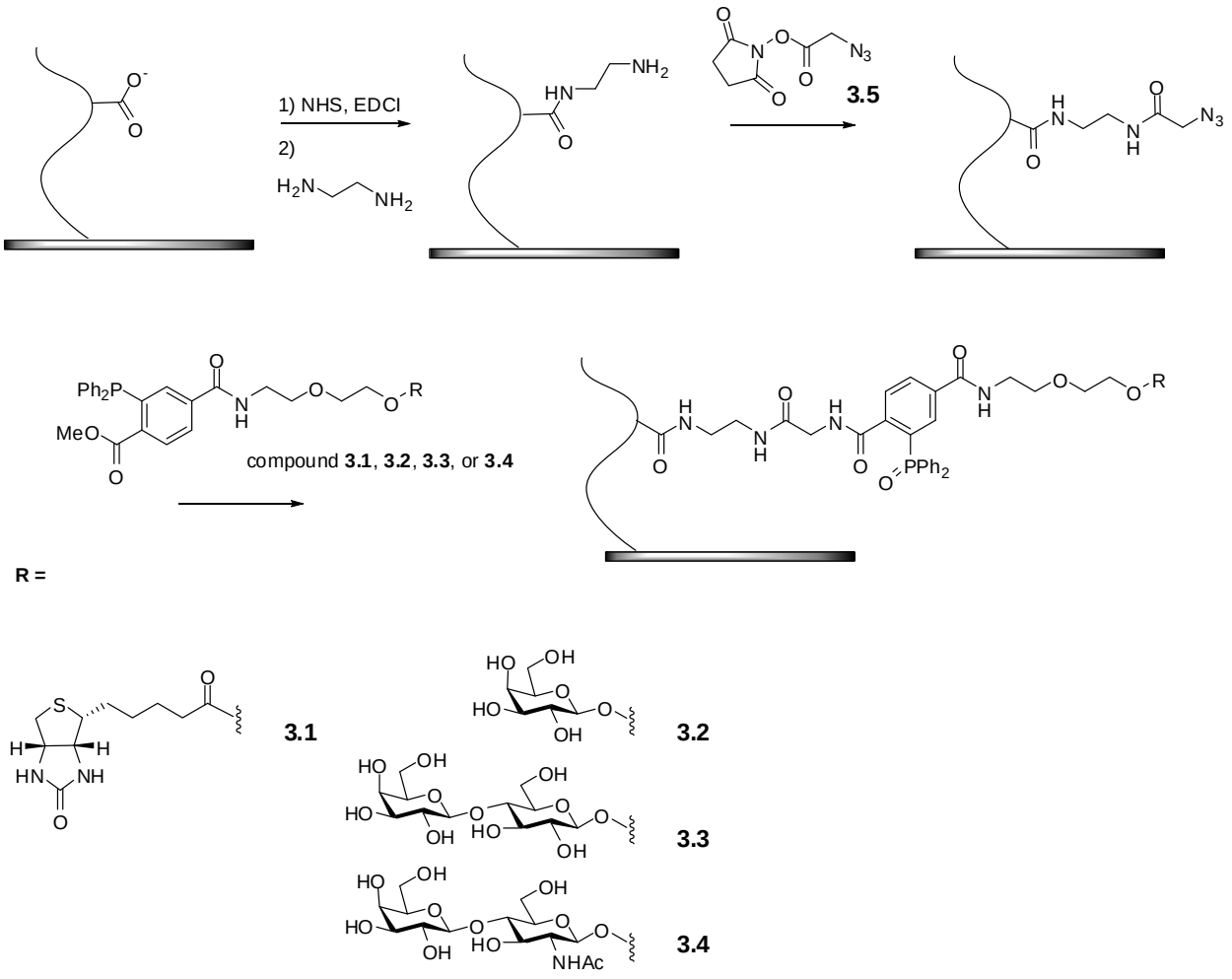

Figure 3.2: Conjugation of carbohydrate epitopes to a CMD surface.The preparation of compounds **3.1**, **3.2**, **3.3**, and **3.4** were as described in **Chapter 2**.[29] Control surfaces were generated with a biotin-labeled phosphane, **3.1**.

Once the azide was immobilized, the surface was stable and could be reacted with an appropriate Staudinger-Bertozzi reagent as desired. We previously reported the synthesis of Staudinger-Bertozzi reagents which contained galactose (**3.2**, Galβ), lactose (**3.3**, Lac), and *N*-acetyl-lactosamine (**3.4**, LacNAc) moieties.[29] These compounds were used to derivatize the CM5

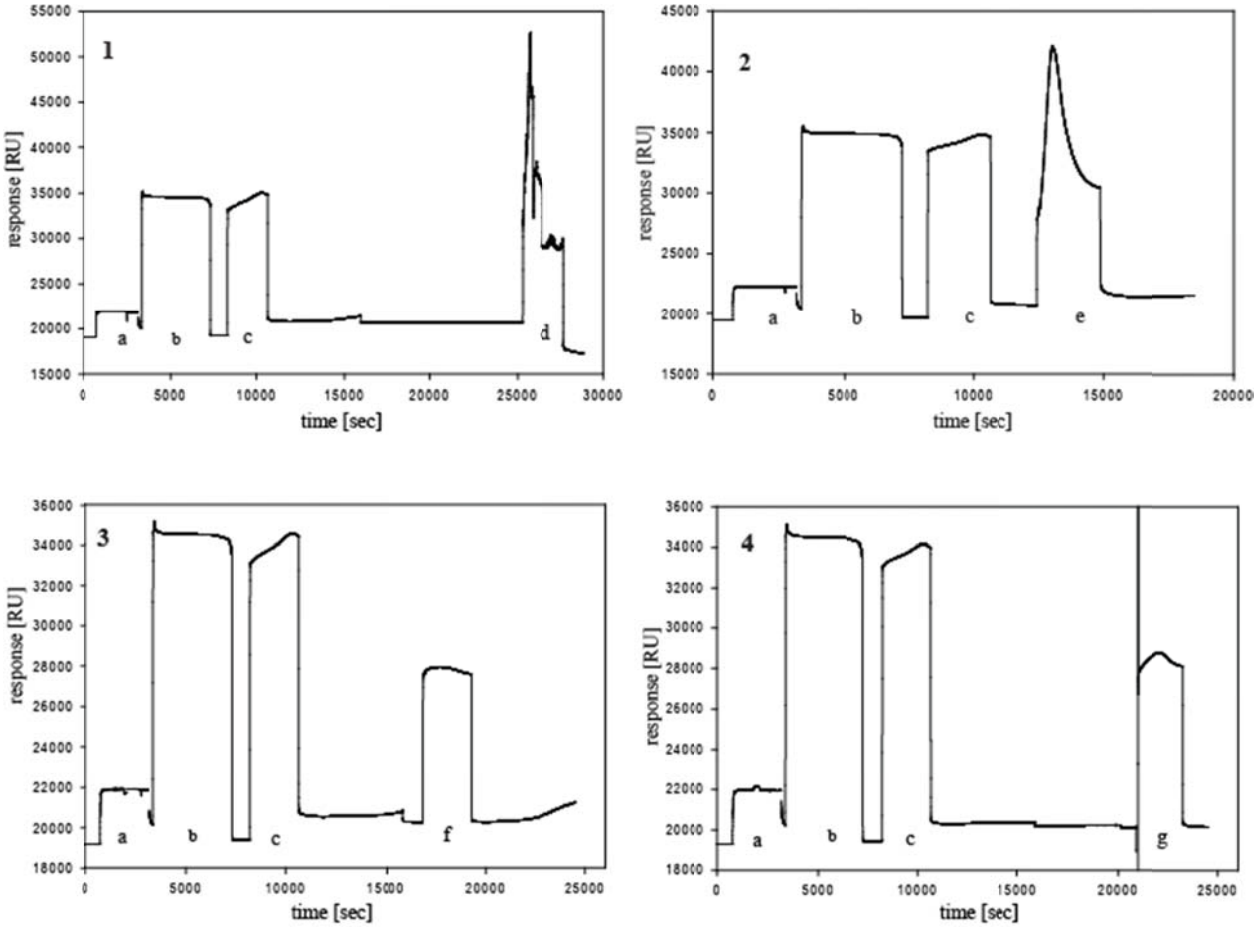

Figure 3.3: Modification of a biosensor surface with a carbohydrate ligand, the sensorgrams are shown for chemical modification of the sensor surface as described in Figure 3.2. The carboxymethyl dextran is first activated with (a) EDCI/NHS (200 µL, 0.1 M), and then modified with (b) ethylenediamine (325 µL, 1 M, pH 8.5). The amine surface was then labed with (c) NHS-azido-acetic acid, 5 (200 µL, 50 mM, 10% DMSO/H_2O). The azides on the surface were then allowed to react with the phosphane-modified (d) biotin, **3.1** (e) galactose, **3.2** (f) lactose, **3.3**, and (g) LacNAc, **3.4** reagents (each 200 µL, 1.25 mM, 6% DMSO/ running buffer). The changes in base line RU were; **3.1**, -1760; **3.2**, 1970; **3.3**, 1120; and **3.4**, 860 RU.

surface after the treatment as described above to incorporate azide functionality. Separate lanes of a single CM5 chip were then exposed to compounds **3.1**, **3.2**, **3.3**, and **3.4** to generate the desired surfaces (**Figure 3.3**). The biotin-modified surface (compound **3.1**) was used for background subtraction of the other lanes as a negative control. The biotin modified surface showed negative response units (RU) compared to carbohydrate derivitized lanes which is most likely due to differences between the refractive indices. For example proteins, sugars and aliphatic polyethylene (similar to biotin) have significantly different refractive indices.[32, 33]

To the best of our knowledge, this is the first report of an azide-modified surface used for SPR detection. Although, it is important to note that work from the laboratories of Bertozzi,[19] Waldmann,[20] and Raines[23] have previously used variations of the Staudinger ligation as a surface immobilization strategy. In our formulation of the Staudinger ligation, we chose to use an azide surface to avoid any issues with oxidation of the phosphane component.[28] In this arrangement, oxidized phosphane would fail to react with the surface. By reversing this configuration to have the phosphane on the surface, any oxidation would reduce the number of available surface sites. Therefore, the azide-surface may be advantageous if the surface requires storage or preparation separate from the immobilization step. Additionally, in this configuration the protocol requires less of the costly phosphane reagent.

3.5. Detection of lectin specificity for carbohydrate surfaces.

To test the binding of lectins to the carbohydrate-modified surfaces, we injected solutions of jacalin (*Artocarpus integrifolia* agglutinin)[34] and wheat germ agglutinin (WGA)[35] over all lanes of the biosensor (**Figure 3.4**). We observed that jacalin bound specifically to the galactose-containing compound **3.2**, and WGA bound only the GlcNAc-containing compound **3.4**. Neither

lectin recognized the Lac-modified surface (compound **3.3**), and only bulk-response was observed for the control lane (compound **3.1**).

Before further investigating the binding of these lectins, we scrutinized different regenerating conditions, ranging from strong acids to strong base. One of the lanes on CM5 surface was derivitized with LacNAc and examined regeneration of this surface with glycine (pH 1.5 and 2.5) and sodium hydroxide (50 mM) after binding with WGA. We ran six consecutive cycles on the same lane for each regenerating solution. In the first cycle, running buffer (blank) followed by regenerating solution and for rest of the five cycles WGA (10.6 μM) followed by regenerating solution were injected. Response units (RU) at the beginning of a cycle were compared with RU after regeneration, in the case of glycine (pH 1.5), they were same for all six cycles but with sodium hydroxide (50 mM), showed large differences for the first two cycles (**Figure 3.5**). Glycine (pH 2.5) was examined after the sodium hydroxide on the same lane, however no information was provided about its regeneration efficacy, as the surface was already degraded. Therefore our findings suggested that sodium hydroxide solution (50 mM) degraded the surface (**Figure 3.5**) and cannot be used as a regenerating solution. Whereas, glycine (pH 1.5) is a suitable regenerating reagent (**Figure 3.6**) and we used these conditions throughout our experiments.

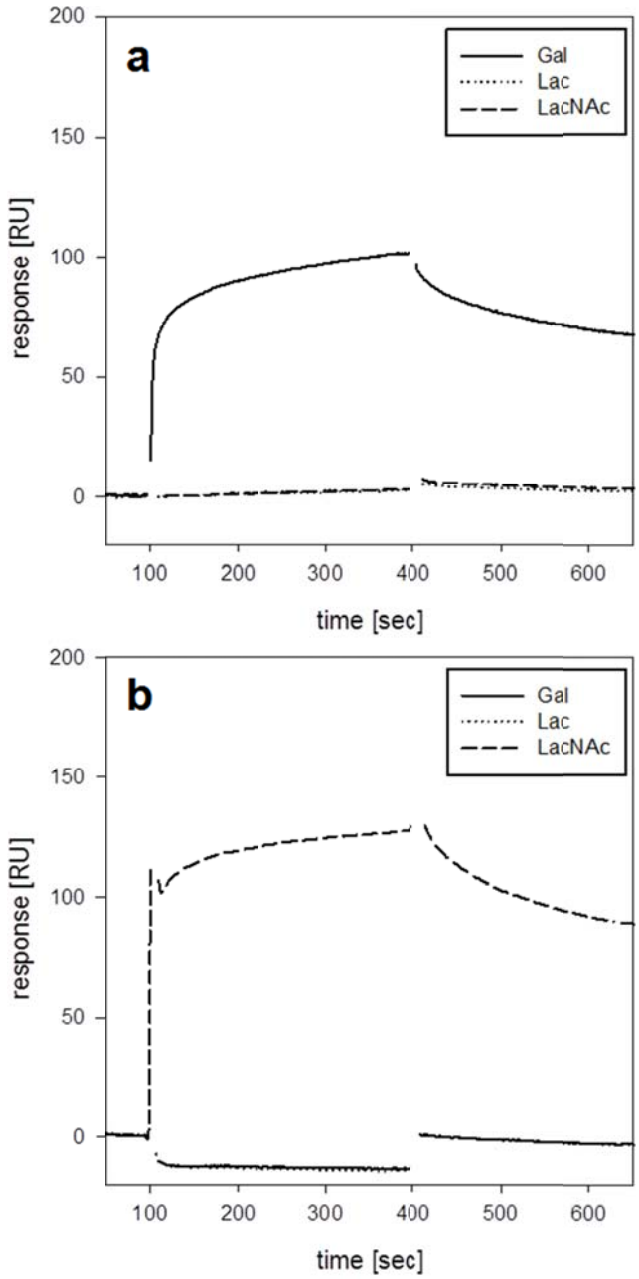

Figure 3.4: Specific binding of lectins to a carbohydrate-modified surface. (**a**) Jacalin (9.45 μM, 10 μL min^{-1}) and (**b**) WGA (21.1 μM, 10 μL min^{-1}) were injected over a sensor chip modified with compound **3.2**, **3.3**, and **3.4**. Jacalin binds specifically to the galactose-containing compound **3.2**, and WGA binds specifically to *N*-acetyl-lactosamine compound **3.4**. Sensorgrams shown were reference subtracted using a surface modified with compound **3.1**. Spikes due to subtraction or injection artifacts have been removed for clarity.

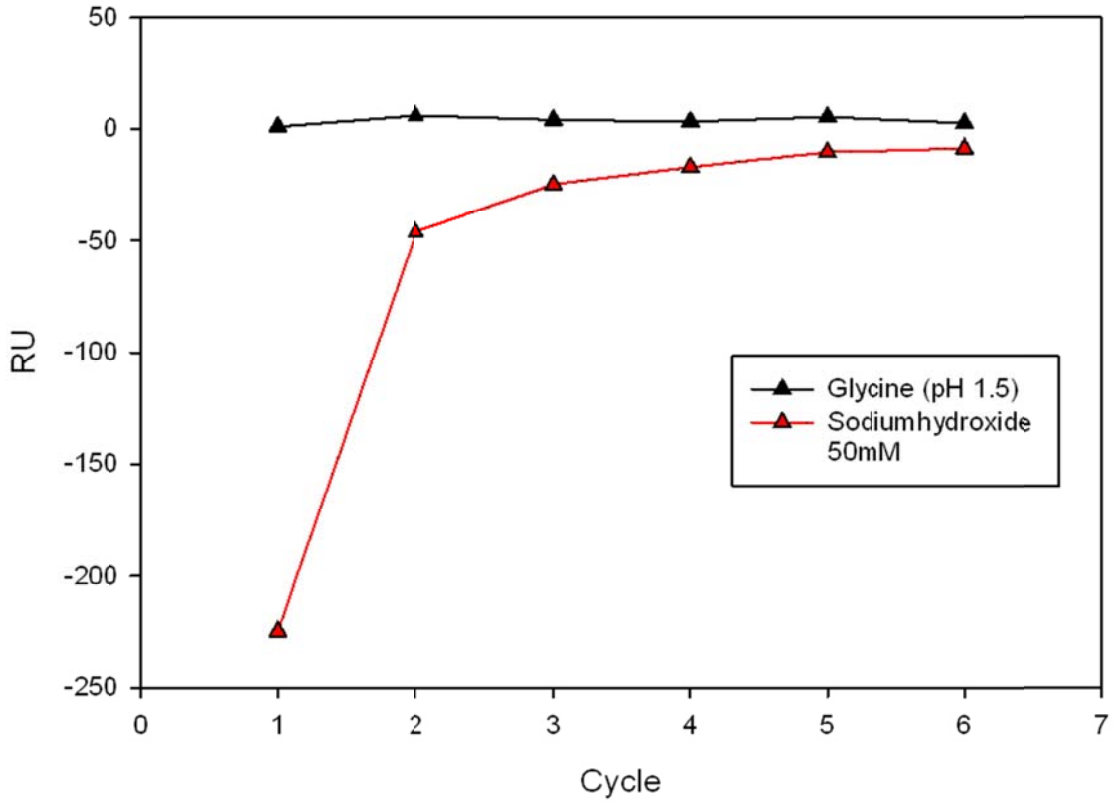

Figure 3.5: Comparision of regeneration of LacNAc-phosphane surface after binding with WGA (10.6 µM, 10 µL min^{-1}) by glycine (pH 1.5), NaOH (50 mM). Difference in RU at the starting of a cycle and after regeneration was almost zero with glycine (pH 1.5) in all six cycles, whereas with sodium hydroxide (50 mM) there was big difference in RU for first two cycles.

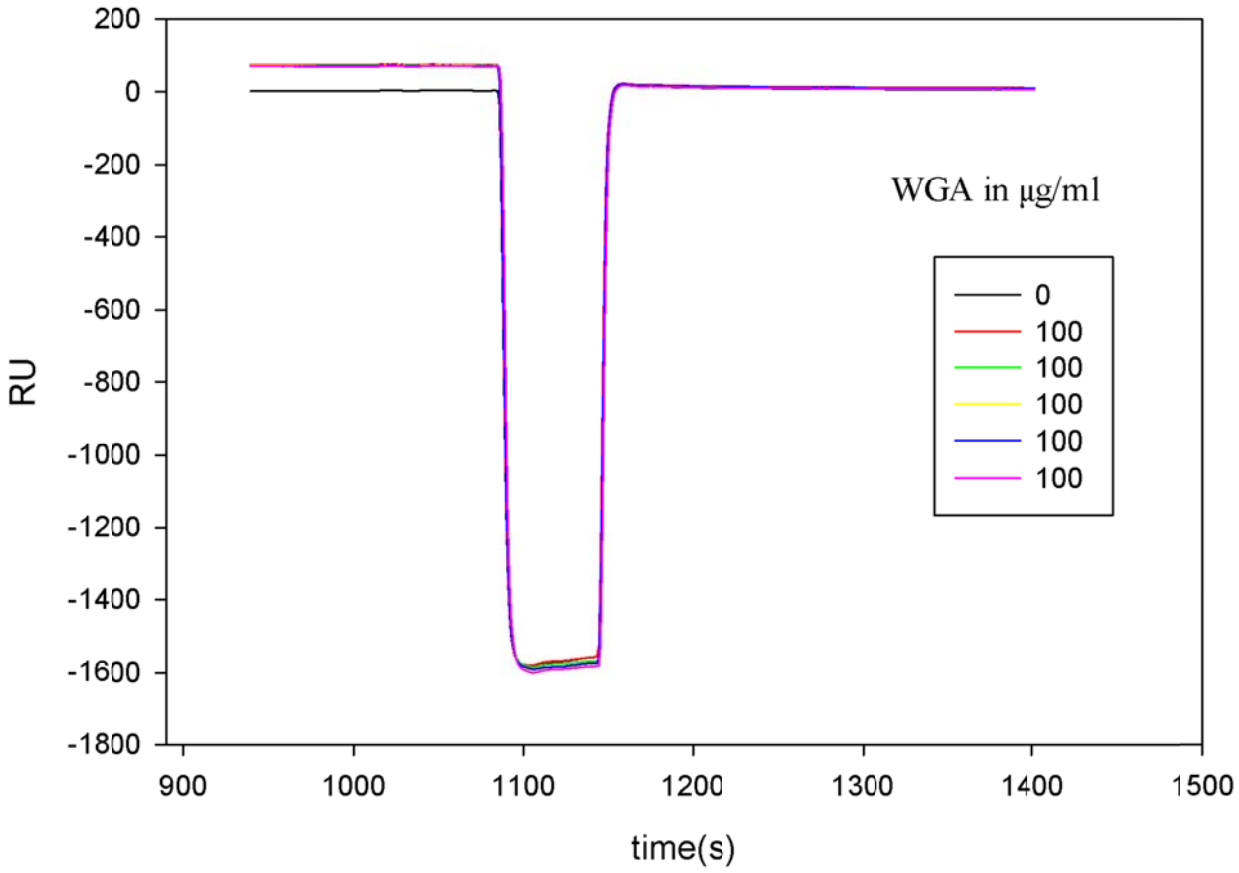

Figure 3.6: Regeneration of surfaces using glycine (pH 1.5). WGA (100 µg/mL, 10 µL min^{-1}) was injected five times into a lane modified with LacNAc-phosphane **3.4**, and surface was regenerated by using the glycine (pH 1.5) each time. There was no change in the RU, on comparison with blank run, after regeneration.

WGA is known to bind specifically to GlcNAc mono- and oligosaccharides.[35] Jacalin is known to bind in preference to α-Gal; however, only weak binding to β-Gal would be expected (**Table 1**).[36] To explore the binding of each lectin in more detail, we proceeded to determine the affinity of each lectin using SPR.

entry	*Lectin, (ligand)*	*model or reference*		*[μM]*			*[RU]*	
1	*Jacalin, (Galα-OMe)*	*[36]*		*29*			*na*	
2	*Jacalin, (Galβ-OMe)*	*[36]*		*6250*			*na*	
3	*Jacalin, (Galβ1,3-GlcNAc)*	*[37]*		*25000*			*na*	
4	*Jacalin, (**3.2**)*	*one-site*	K_d	*800*	*± 70*	B_{max}	*55*	*± 1*
5		*two-site*	K_{d1}	*200*	*± 600*	B_{max1}	*19*	*± 4*
6			K_{d2}	*1800*	*± 2600*	B_{max2}	*40*	*± 36*
7	*WGA, (GlcNAc)*	*[35]*		*1300*			*na*	
8	*WGA, (GlcNAcβ1,4–GlcNAc)*	*[35]*		*200*			*na*	
9	*WGA, (Galβ1,6–GlcNAc)*	*[38]*		*1700*			*na*	
10	*WGA, (**3.4**)*	*one-site*	K_d	*190*	*± 40*	B_{max}	*111*	*± 4*
11		*two-site*	K_{d1}	*40*	*± 80*	B_{max1}	*70*	*± 40*
12			K_{d2}	*1300*	*± 1800*	B_{max2}	*60*	*± 30*

Table 3.1: Lectin affinities determined for Jacalin and WGA. Standard deviations derived from semi-log plot (**Figure 3.14**)

3.6. Determination of Jacalin and WGA affinity

One of the advantages of a sensitive SPR assay is that it can be used to determine the affinity of biomolecular interactions by direct observation of association and dissociation kinetics. However, kinetic determinations are inherently more challenging as a variety of artifacts may obscure an accurate measurement.[6]

3.6.1 WGA affinity to LacNAc

We injected a series of six concentrations of WGA lectin over the surface, and analyzed the binding of WGA to **3.4** (**Figure 3.7**). Attempts to fit these data to a typical 1:1 binding model failed. More complex models, including bivalent binding and conformational change models, were unsuccessful, with all tested models giving poor fits (data not shown).[39] These observations suggest that lectin binding to the surface follows complex kinetics. Therefore, we used equilibrium binding to determine the affinity of the lectin. A series of lectin concentrations, six different concentrations in first run and 18 different concentrations in second run were injected over the biosensor surface and the response at steady-state binding was recorded. The resulting values were plotted versus the lectin concentrations to provide binding isotherms (**Figures 3.8** & **3.9**).

The equilibrium binding data were fit to a single or two-site binding model to obtain the affinity of each interaction (**Table 3.1**). The first run was fit to single-site binding model (**Figure 3.8**). The K_d obtained from this data was 600 ± 42 μM with r^2 = 0.983. The binding data obtained for the affinity of WGA for compound **3.4** in second run was partly described by the single-site model (190 ± 40 μM, r^2 = 0.824). The two runs showed different K_d values and the r^2 value for the second run was less compared to the first run. This difference may be due to having more concentrations taken for the second run compared to the first. A Scatchard plot of second run gave a concave-up curve, suggesting heterogeneity in the binding data (**Figure 3.13**).[40, 41] Consistent with this finding, a fit of the data to the two-site model showed improvement over the single-site model (r^2 = 0.868), and gave values of 40 ± 80 μM and 1300 ± 1800 μM for the two affinity constants. The WGA lectin is known to be specific for GlcNAc containing saccharides; however, its affinity for LacNAc has has not been previously determined. Measurement of WGA

affinity for GlcNAc using isothermal titration calorimetry (ITC) found a value of 1.3 mM.[35] Larger oligosaccharides of β1,4-linked GlcNAc gave tighter binding, for example the dimer gave an affinity of 200 μM. The affinity of an isomeric disaccharide of LacNAc, Galβ1,6-GlcNAc, for WGA has been determined to be 1.7 mM.[38]

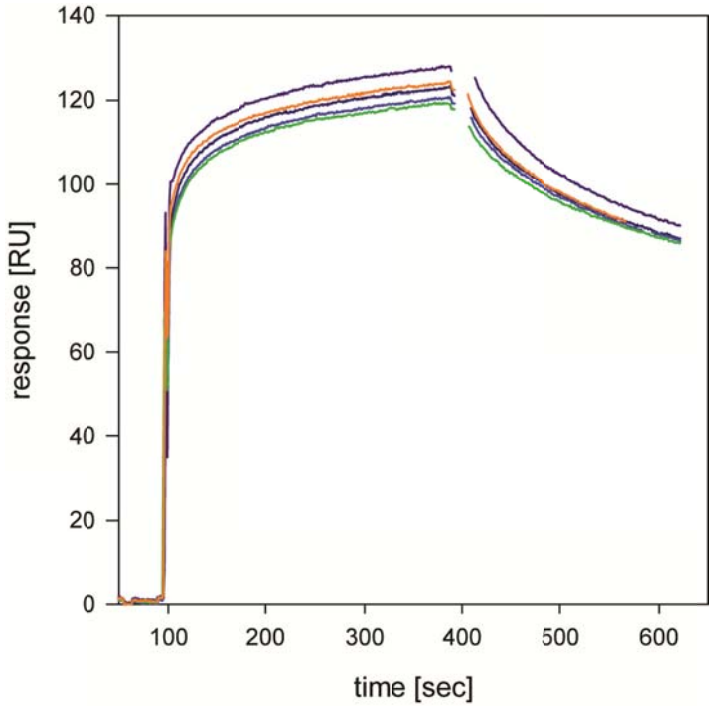

Figure 3.7: Binding of WGA to an *N*-acetyl-lactosamine surface. WGA was injected over the *N*-acetyl-lactosamine surface (21.2, 12.7, 10.6, 7.9, 6.4, 5.3 μM, 10 μL min^{-1}). Sensorgram shown was reference subtracted using a surface modified with compound **3.1**. Spikes due to subtraction or injection artifacts have been removed for clarity.

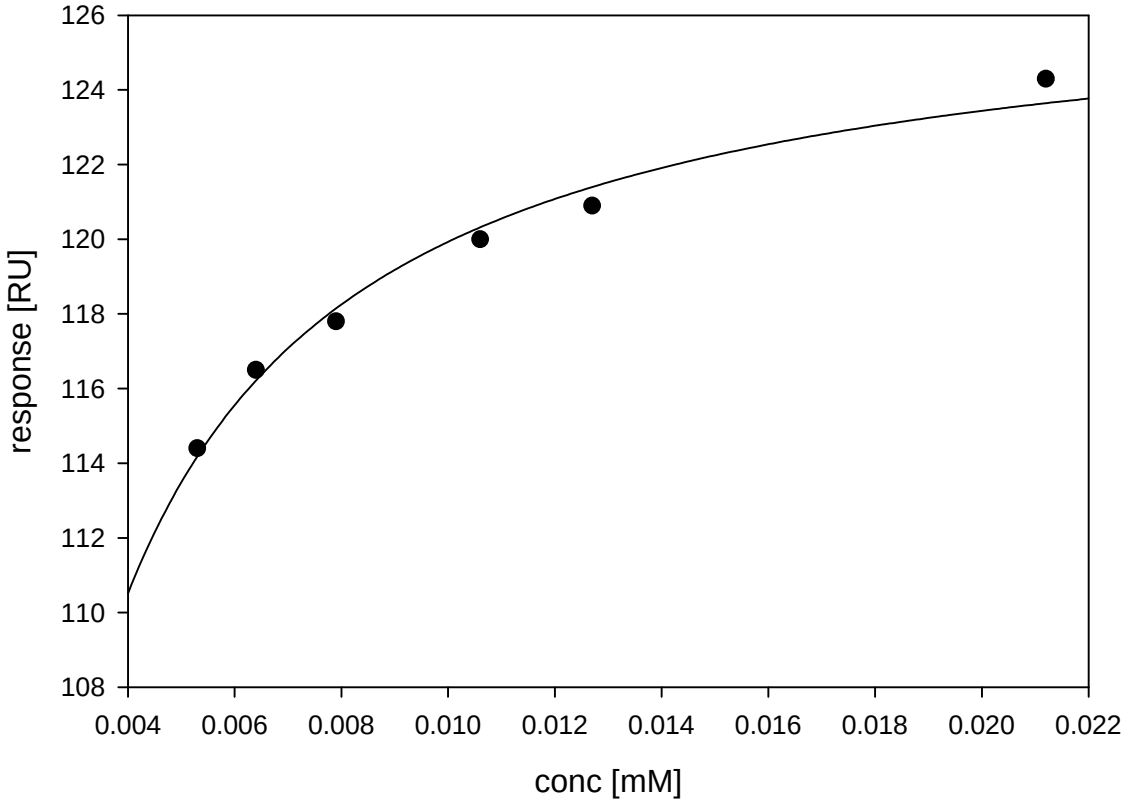

Figure 3.8: Binding isotherm of WGA for the first run. The binding of WGA to the *N*-acetyl-lactosamine surface (21.2, 12.7, 10.6, 7.9, 6.4, 5.3 μM) is shown in single-site model. Each point is a steady-state RU value at the end of association phase.

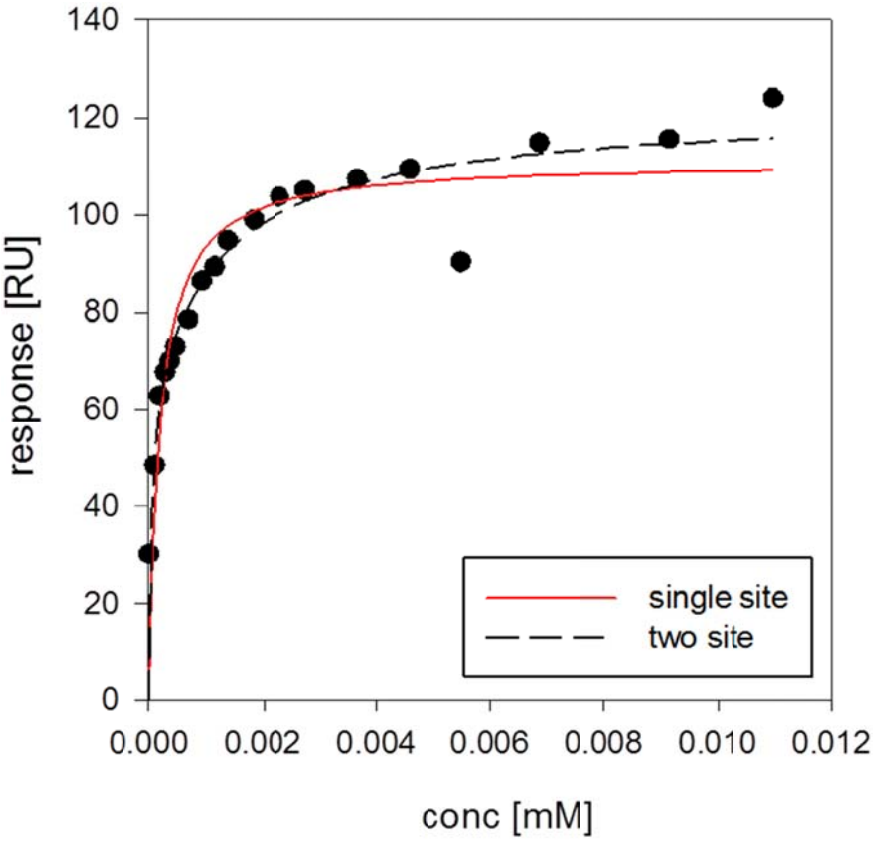

Figure 3.9: Binding isotherm of WGA for the second run. The binding of WGA to the *N*-acetyl-lactosamine surface (11, 9.1, 6.9, 5.5, 4.6, 3.7, 2.7, 2.3, 1.8, 1.4, 1.1, 0.92, 0.69, 0.46, 0.37, 0.27, 0.19, 0.09 μM) is shown. Each point is a steady-state RU value at the end of association phase. For semi-log and Scatchard analysis see experimental section, **Figure 3.14**.

The binding of WGA to **3.4** is, therefore, of unusually high affinity. When the data were analyzed using the single-site binding model, the observed affinity of **3.4** is similar to the GlcNAc dimer. However, when the non-linearity of the Scatchard plot is taken into account a more complex model is required. We interpret the non-ideal Scatchard plot as an indication of

heterogeneous binding sites on the surface. This heterogeneity is likely the result of high affinity sites which arise from carbohydrate epitopes on the surface which are close enough to bridge multiple sites of a single WGA tetramer. In support of this model, the lower affinity site should yield the expected solution affinity of GlcNAc for WGA. This is indeed the case when the data are fit to the two-site model. This interpretation suggests an approximately 30-fold enhancement of affinity at sites which can engage the lectin in a chelated binding mode.[42] Non-ideal effects due to surface density or multivalent binding are well known in SPR measurements, and these results allow us to quantify one mechanism of the enhancement of lectin affinity.[10, 41, 43]

3.6.2 Jacalin affinity to galactose

A series of six different concentrations of jacalin were injected over the surfaces and analyzed its binding to **3.2** (**Figure 3.10**). All the tested models, 1:1 binding model, bivalent binding or conformational change models gave poor fits. These unsuccessful models indicated that jacalin binding followed complex kinetics. We switched to equilibrium binding to determine the affinity of jacalin. The response at steady state binding was recorded for a two different series of jacalin concentrations injected over biosensor surface and binding isotherms were derived by plotting the resulting values versus the lectin concentration for these two different runs (**Figures 3.11** & **3.12**).

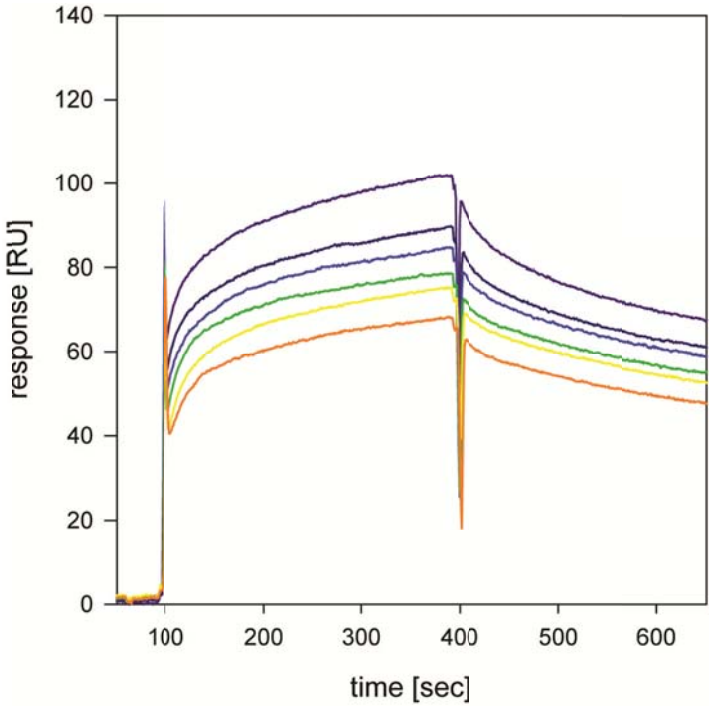

Figure 3.10: Binding of Jacalin to galactose. Jacalin was injected over the galactose surface (9.5, 5.7, 4.7, 3.5, 2.8, 2.4 μM, 10 μL min^{-1}). Sensorgrams shown were reference subtracted using surface modified with compound **3**.**1**. Spikes due to subtraction or injection artifacts have been removed for clarity.

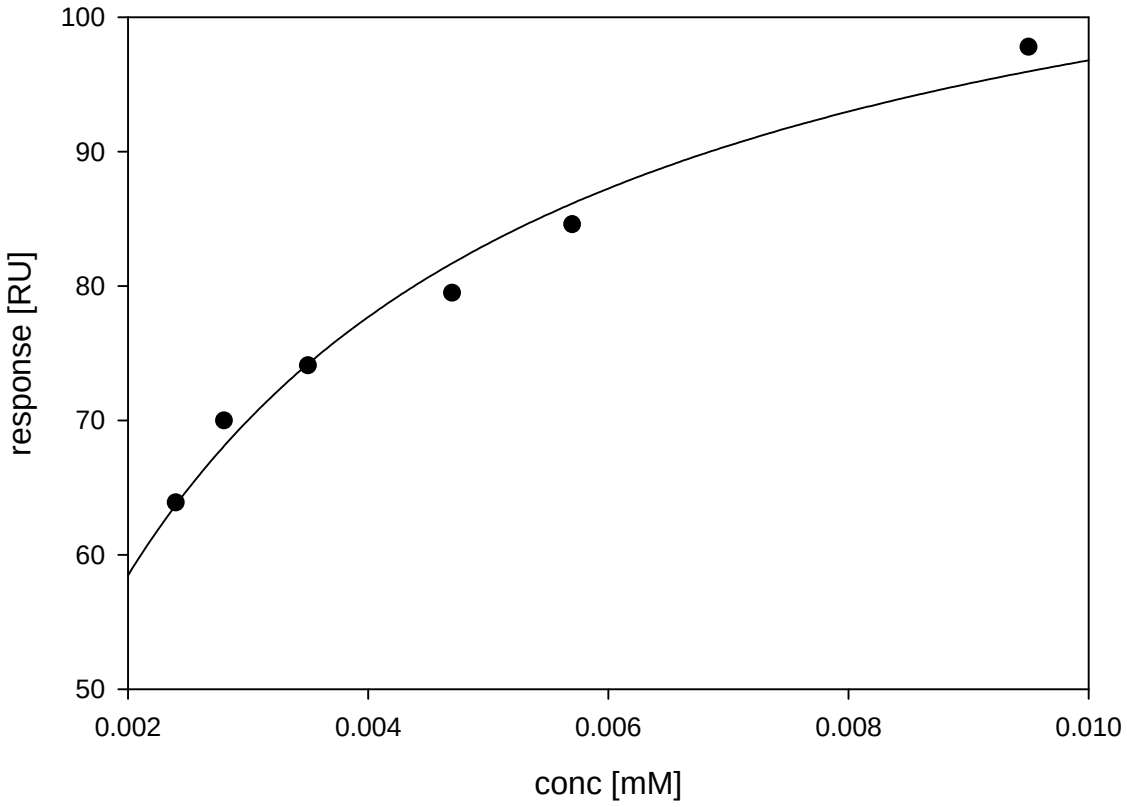

Figure 3.11: Binding isotherm of Jacalin for the first run. The binding of jacalin to the galactose-modified surface (9.5, 5.7, 4.7, 3.5, 2.8, 2.4 μM) is shown by a single-site model. Each point is a steady-state RU value at the end of the association phase.

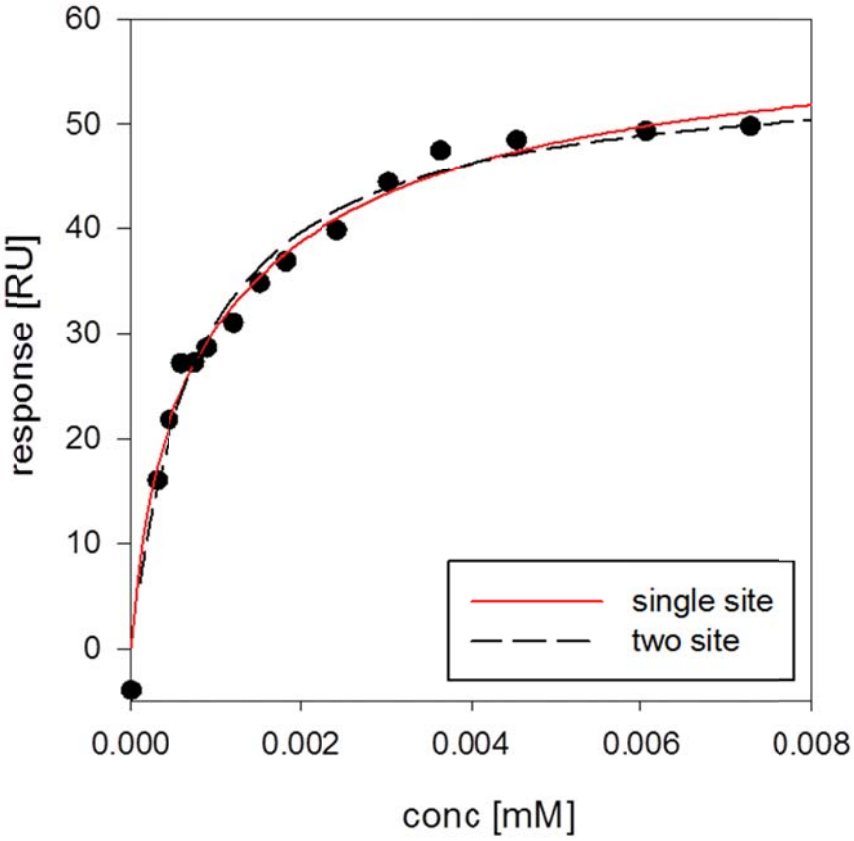

Figure 3.12: Binding isotherm of Jacalin for the second run. The binding of jacalin to the galactose-modified surface (7.3, 6.1, 4.5, 3.6, 3.0, 2.4, 1.8, 1.5, 1.2, 0.91, 0.76, 0.61, 0.46, 0.30 μM) is shown. Each point is a steady-state RU value at the end of the association phase. See experimental section for semi-log and Scatchard analysis (**Figure 3.14**).

A single (eq. 1) or two-site (eq. 2) binding model were used to fit the equilibrium binding data to get the affinity of each interaction (**Table 3.1**). A single-site model for the first run (**Figure 3.11**) gave a dissociation constant of 2000 ± 20 (r^2 = 0.98) and 800 ± 70 μM (r^2 = 0.98) for the second run (**Figure 3.12**). The dissociation constants for these two different runs were likely different due to a different number of concentrations used in the two runs. When the second run data were plotted in semi-log form or as a Scatchard plot (**Figure 3.14**), it could be seen that jacalin binding was well described by a single-site model. Fitting the same data to a

two-site model gave an affinity for **3.2** of 200 ± 600 μM at the first site, and 1800 ± 2600 μM for the second site (r^2 = 0.99). Although this model provides a slightly improved fit, the lack of a concave Scatchard plot suggests that the two-site model should not be used. Based on the single-site affinity, the binding of a βGal derivative appears to be remarkably high. Previous reports have determined the affinity of βGal to jacalin is close to 5 mM, while the αGal anomer has much higher affinity.[36] Hagiwara et al. have found that Galβ-*p*-nitrophenyl has greater affinity to jacalin than GalNAc, suggesting an ability for the lectin to accommodate a hydrophobic β-linked aglycone.[34] Additionally, Smith et al. have reported that αGal derivatives with a hydrophobic aglycone have slightly improved affinity to jacalin.[14] Comparison of the single-site affinity measured here for a βGal derivative falls between the expected affinity of a GalαOMe and GalβOMe, suggesting that **3.2** has higher than expected affinity for the lectin (*vide infra*).

3.7. A Structural model of Jacalin binding

Our determination of the affinity of jacalin for compound **3.2** gave an unexpectedly high value for a β-galactoside. Previous work with ITC has found that Galβ-OMe has significantly weaker binding than the Galα-OMe derivative. Structural determinations of galactoside binding to jacalin have concluded that the key H-bond interactions between the protein and the glycoside are at *O*-4, *O*-6, and *O*-3. The methyl aglycone of the α-galactoside has been shown to project over the face of Y122, while the aglycone of the β-galactoside results in unfavorable steric interactions with the same tyrosine residue. This steric interaction resulted in a decrease in affinity of approximately 100-fold.[44] Previous observations by Smith et al. and Hagiwara et al. - suggest that α- and β-galactosides with a hydrophobic aglycone retain tight affinity to jacalin.[14, 34] In light of these structural data, we were intrigued at our result. We considered that a possible

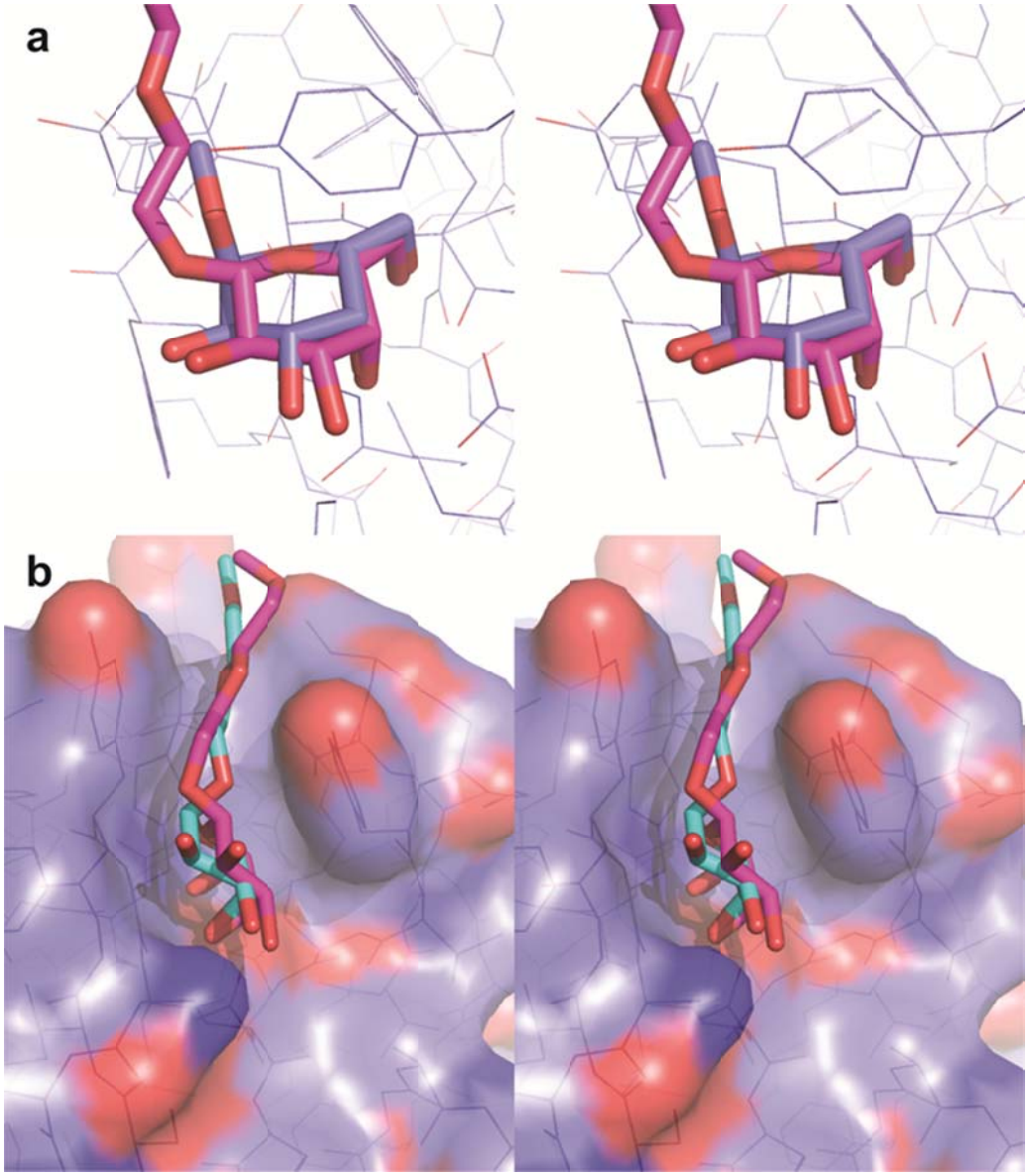

Figure 3.13: Molecular modeling of Jacalin binding. (**a**) Models of a β-galactoside with a PEG aglycone (magenta) were generated, and then minimized (see Experimental procedure **3.9.5**). The critical H-bond contacts at *O*-4 and *O*-6 are maintained, although the orientation of the ring was slightly twisted from that of the α-galactoside (blue). (**b**) The aglycone may occupy secondary site A, which is a relatively hydrophobic channel formed by Y78 and Y122. Both the α- and β-anomers with a flexible aglycon are able to take advantage of contacts in secondary site A; however, an additional carbohydrate residue would be too bulky to be accommodated.

explanation for these findings was that a flexible and hydrophobic linker could impart additional specificity to the glycoside. To examine this hypothesis in more detail, we used molecular modeling to examine the binding of α- and β-galactosides with a short flexible linker (**Figure 3.13**).

We found that a modified α-galactoside could maintain an almost identical orientation of the saccharide in the binding site as compared to the orientation of the free saccharide. The flexible linker of the aglycone could insert into a short hydrophobic channel formed by Y78 and Y122 on the protein. This region of the binding site was referred to as 'secondary site A' by Jeyaprakash et al.[37] In the case of the β-galactoside, we found that in order to accommodate the β-linked aglycone, the orientation of the ring in the active site was slightly altered. Importantly, the position of the major H-bond contacts at *O*-3, *O*-4, and *O*-6 were maintained. We also confirmed that the aglycone of the β-galactoside was able to gain favorable interactions at secondary site A. Thus, our model suggests that additional hydrophobic interactions at secondary site A can explain previous results with synthetic galactosides.[14, 34] Additionally, the model suggests that tighter binding ligands for jacalin could be developed by exploiting these contacts.

3.8. Conclusions & future work

In this chapter we described a useful implementation of Staudinger reagents for the immobilization of carbohydrates to a biosensor surface. To avoid issues of phosporous oxidation, we have used an azide-derivitized surface, which is then reacted with a soluble phosphane. Using this method, we are able to detect the specificity of lectins for carbohydrate modified surfaces. We confirmed that expected lectin-carbohydrate interactions, such as WGA binding to GlcNAc, could be observed and quantified. We are also able to quantify an enhancement of WGA binding due to multivalent binding of the lectin with a high-density GlcNAc surface.[42] Additionally, we

observed an unexpected interaction of a β-galactoside with jacalin. We proposed a structural model for the interaction of the galactosyl aglycone with secondary subsite A of the protein. Our model helps to rationalize our binding results, as well as previous reports of jacalin binding to synthetic substrates.

Most of the simple mono- and oligosaccharides show less affinity for the lectins, whereas myriad of carbohydrates and glycoconjugates in nature show large binding affinity to the lectins due to their multivalency. Therefore to explore the multivalency effect on lectin binding, we planned to synthesize clustered carbohydrate-phosphane reagents. The design and synthesis of these reagents will be discussed in **Chapter 4**. The Bertozzi-Staudinger ligation used here for immobilization introduces a set of aromatic group on to the surface along with epitope of interest. These aromatic groups may alter the avidity of lectins. Future work may address use of a trace-less Staudiger ligation to avoid this problem.[45]

3.9. Experimental procedures

3.9.1 Syntheis of phosphane compounds 3.1, 3.2, 3.3, and 3.4.

The synthesis of compounds **3.1**, **3.2**, **3.3**, and **3.4** were as previously described.[29] Briefly, carbohydrate epitopes were generated with an amine terminated ethylene glycol linker. The amine was then reacted with an *N*-hydroxy-succinimidyl-phosphane reagent, to provide the desired compounds.[29, 46]

3.9.2. Biosensor surface preparation

Surfaces were prepared using a BIAcore 3000 and CM5 (carboxymethyldextran) sensor chip. Reactions were performed at a flow rate of 5 μL min^{-1} in order to maximize contact time. The chip was equilibrated, and then reacted, with the following solutions to generate an azide-modified surface: 1) 200 μL of a 1:1 solution of *N*-ethyl-*N'*-(3-diethylaminopropyl)-carbodiimide (EDCI) (0.1 M in water) and *N*-hydroxy-succinimide (NHS) (0.1 M in water); 2) 325 μL of ethylenediamine (EDA) (1 M in water, pH 8.5); 3) 200 μL of azidoacetic acid-NHS ester 5 (50 mM in 10% DMSO, 90% 25 mM $NaHCO_3$, pH 8.5).[29, 47] Carbohydrate or control surfaces were then generated by injection of the appropriate phosphane compound (3.1, 3.2, 3.3, or 3.4) (200 μL in 6% DMSO/water). The change in RU of each surface after treatment with the phosphane compounds were: 3.1, -1760; 3.2, 1970; 3.3, 1120; and 3.4, 860 RU.

3.9.3. Lectin binding

All binding experiments were conducted on a BIAcore 3000 SPR system in HEPES running buffer (10 mM HEPES, 150 mM NaCl, 1 mM $CaCl_2$, 0.005% surfactant P20, pH 7.4). Experiments were performed at a flow rate of 10 μL min^{-1} (kinject). Data obtained from carbohydrate-modified surfaces were corrected by subtraction of the response in a control lane modified with compound **3.1** which was run in parallel for all injections. Jacalin and WGA were

obtained from US Biological (Swampscott, MA) and Sigma-Aldrich (St Louis, MO), respectively. Stock solutions of each protein were made in running buffer, and concentrations were determined by A_{280}. Equilibrium binding data were fit to either a single site,

$$RU = \frac{B_{\max} F}{K_d + F}, \qquad \text{(eq. 1)}$$

or two site model,

$$RU = \frac{B_{\max 1} F}{K_{d1} + F} + \frac{B_{\max 2} F}{K_{d2} + F}. \qquad \text{(eq. 2)}$$

[48]

3.9.4 Regeneration conditions

A blank (HEPES buffer) and five times, WGA (10.6 μM) were injected on to all the lanes of CM5 modified surface under lectin binding conditions described above and each time surface is regenerated by glycine 1.5. Repeated the same with NaOH(50 mM) solution.

3.9.5. Molecular modeling

Models of the interaction between jacalin and galactosyl residues containing a 3,5-dioxaheptyl aglycone were generated using a reported crystal structure (PDB ID: 1UH1).[37, 49] The structure was modified using Macromodel (Schrodinger, Inc.) to incorporate either an α- or β-linked aglycone. The carbohydrate and protein residues within 10 Å of the ligand were then minimized and subjected to molecular dynamics for 10 ps, followed by an additional minimization (OPLS force field;[50] water solvent was modeled by a continuous dielectric).

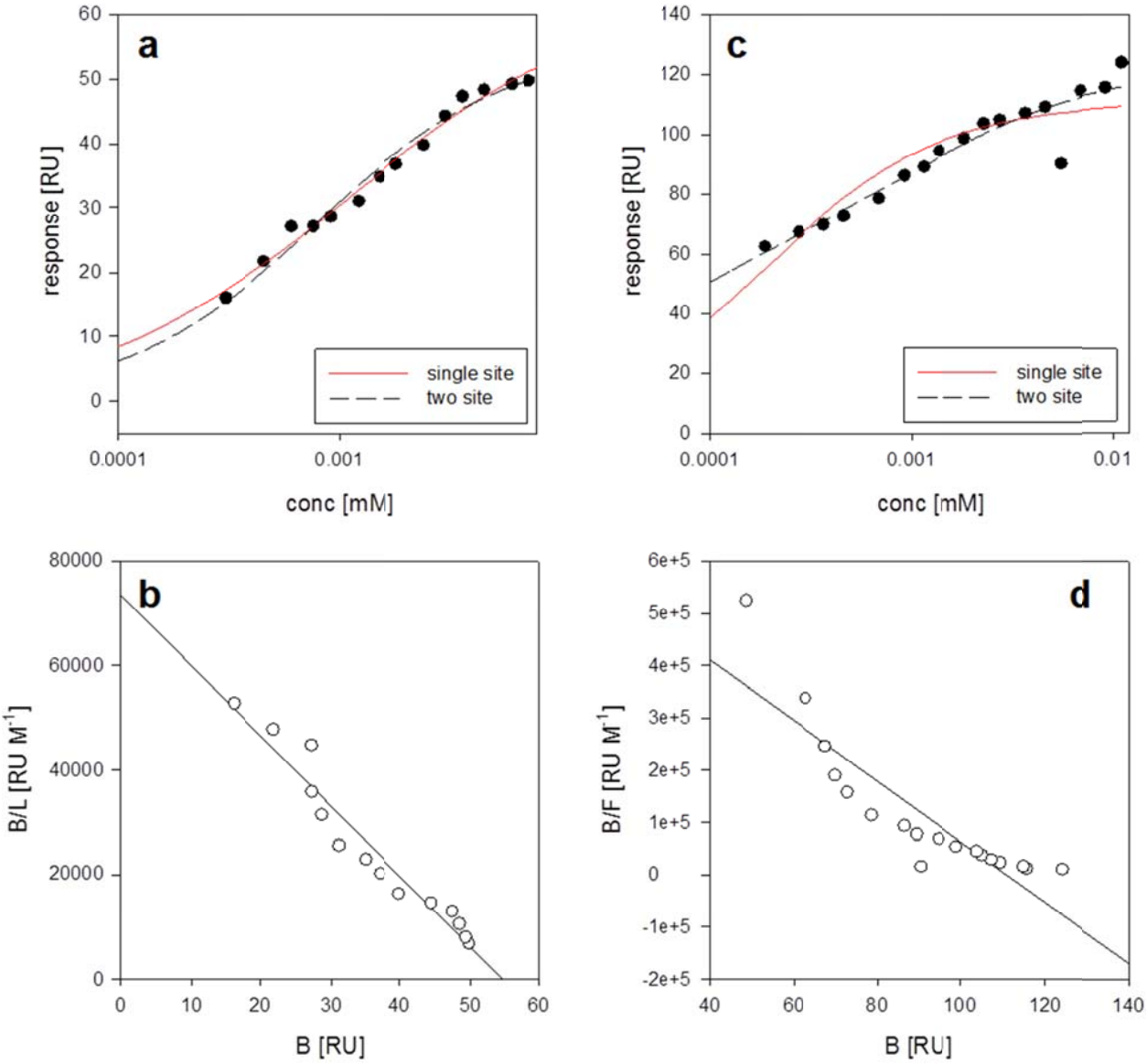

Figure 3.14: Semi-log and Scatchard plots of lectin binding. The binding data for Jacalin interacting with a galactose-modified surface for second run is shown as a (a) semi-log plot, and (b) as a Scatchard plot. The binding data for WGA interacting with an *N*-acetyl-lactosamine-modified surface for second run is shown as a (c) semi-log plot, and (d) as a Scatchard plot. All data are identical to those shown in **Figures 3.9 & 3.12**.

3.10. References

1. Dwek, R. A., Glycobiology: Toward Understanding the Function of Sugars. *Chem. Rev.* **1996,** *96* (2), 683-720.

2. Dube, D. H.; Bertozzi, C. R., Glycans in cancer and inflammation--potential for therapeutics and diagnostics. *Nat. Rev. Drug Discov.* **2005,** *4* (6), 477-88.

3. Hernandez, J. D.; Baum, L. G., Ah, sweet mystery of death! Galectins and control of cell fate. *Glycobiology* **2002,** *12* (10), 127R-36R.

4. Lee, Y. C., Fluorescence spectrometry in studies of carbohydrate-protein interactions. *J. Biochem.* **1997,** *121* (5), 818-25.

5. Dam, T. K.; Brewer, C. F., Thermodynamic studies of lectin-carbohydrate interactions by isothermal titration calorimetry. *Chem. Rev.* **2002,** *102* (2), 387-429.

6. Rich, R. L.; Myszka, D. G., Advances in surface plasmon resonance biosensor analysis. *Curr. Opin. Biotechnol.* **2000,** *11* (1), 54-61.

7. Krishnamoorthy, L.; Mahal, L. K., Glycomic analysis: an array of technologies. *ACS Chem. Biol.* **2009,** *4* (9), 715-32.

8. Manimala, J. C.; Roach, T. A.; Li, Z.; Gildersleeve, J. C., High-throughput carbohydrate microarray profiling of 27 antibodies demonstrates widespread specificity problems. *Glycobiology* **2007,** *17* (8), 17C-23C.

9. Kiessling, L. L.; Cairo, C. W., Hitting the sweet spot. *Nat. Biotechnol.* **2002,** *20* (3), 234-5.

10. Bamdad, C., The use of variable density self-assembled monolayers to probe the structure of a target molecule. *Biophys. J.* **1998,** *75* (4), 1989-96.

11. Hutchinson, A. M., Characterization of glycoprotein oligosaccharides using surface plasmon resonance. *Anal. Biochem.* **1994,** *220* (2), 303-7.

12. Linman, M. J.; Taylor, J. D.; Yu, H.; Chen, X.; Cheng, Q., Surface plasmon resonance study of protein-carbohydrate interactions using biotinylated sialosides. *Anal. Chem.* **2008,** *80* (11), 4007-13.

13. Gestwicki, J. E.; Cairo, C. W.; Mann, D. A.; Owen, R. M.; Kiessling, L. L., Selective immobilization of multivalent ligands for surface plasmon resonance and fluorescence microscopy. *Anal. Biochem.* **2002,** *305* (2), 149-55.

14. Smith, E. A.; Thomas, W. D.; Kiessling, L. L.; Corn, R. M., Surface plasmon resonance imaging studies of protein-carbohydrate interactions. *J. Am. Chem. Soc.* **2003,** *125* (20), 6140-8.

15. Mann, D. A.; Kanai, M.; Maly, D. J.; Kiessling, L. L., Probing low affinity and multivalent interactions with surface plasmon resonance: Ligands for concanavalin A. *J. Am. Chem. Soc.* **1998,** *121* (41), 10575-82.

16. Sletten, E. M.; Bertozzi, C. R., Bioorthogonal chemistry: fishing for selectivity in a sea of functionality. *Angew. Chem. Int. Ed. Engl.* **2009,** *48* (38), 6974-98.

17. Camarero, J. A., Recent developments in the site-specific immobilization of proteins onto solid supports. *Biopolymers* **2008,** *90* (3), 450-8.

18. Kolb, H. C.; Finn, M. G.; Sharpless, K. B., Click Chemistry: Diverse Chemical Function from a Few Good Reactions. *Angew. Chem. Int. Ed. Engl.* **2001,** *40* (11), 2004-2021.

19. Hang, H. C.; Yu, C.; Pratt, M. R.; Bertozzi, C. R., Probing glycosyltransferase activities with the Staudinger ligation. *J. Am. Chem. Soc.* **2004,** *126* (1), 6-7.

20. Kohn, M.; Wacker, R.; Peters, C.; Schroder, H.; Soulere, L.; Breinbauer, R.; Niemeyer, C. M.; Waldmann, H., Staudinger ligation: a new immobilization strategy for the preparation of small-molecule arrays. *Angew. Chem. Int. Ed. Engl.* **2003,** *42* (47), 5830-4.

21. Watzke, A.; Kohn, M.; Gutierrez-Rodriguez, M.; Wacker, R.; Schroder, H.; Breinbauer, R.; Kuhlmann, J.; Alexandrov, K.; Niemeyer, C. M.; Goody, R. S.; Waldmann, H., Site-selective protein immobilization by Staudinger ligation. *Angew. Chem. Int. Ed. Engl.* **2006,** *45* (9), 1408-12.

22. Grandjean, C.; Boutonnier, A.; Guerreiro, C.; Fournier, J. M.; Mulard, L. A., On the preparation of carbohydrate-protein conjugates using the traceless Staudinger ligation. *J. Org. Chem.* **2005,** *70* (18), 7123-32.

23. Kalia, J.; Abbott, N. L.; Raines, R. T., General method for site-specific protein immobilization by Staudinger ligation. *Bioconjug Chem.* **2007,** *18* (4), 1064-9.

24. Helms, B.; van Baal, I.; Merkx, M.; Meijer, E. W., Site-specific protein and peptide immobilization on a biosensor surface by pulsed native chemical ligation. *Chembiochem* **2007,** *8* (15), 1790-4.

25. Govindaraju, T.; Jonkheijm, P.; Gogolin, L.; Schroeder, H.; Becker, C. F.; Niemeyer, C. M.; Waldmann, H., Surface immobilization of biomolecules by click sulfonamide reaction. *Chem. Commun. (Cambridge)* **2008,** (32), 3723-5.

26. Grabosch, C.; Kleinert, M.; Lindhorst, T. K., Glyco-SAMs by 'Dual Click': Thiourea-Bridged Glyco-OEG Azides for Cycloaddition on Surfaces. *Synthesis-Stuttgart* **2010,** (5), 828-36.

27. Kleinert, M.; Winkler, T.; Terfort, A.; Lindhorst, T. K., A modular approach for the construction and modification of glyco-SAMs utilizing 1,3-dipolar cycloaddition. *Org. Biomol. Chem.* **2008,** *6* (12), 2118-32.

28. Zhang, H.; Ma, Y.; Sun, X. L., Chemically-selective surface glyco-functionalization of liposomes through Staudinger ligation. *Chem. Commun. (Cambridge)* **2009,** (21), 3032-4.

29. Loka, R. S.; Sadek, C. M.; Romaniuk, N. A.; Cairo, C. W., Conjugation of synthetic N-acetyl-lactosamine to azide-containing proteins using the Staudinger ligation. *Bioconjug Chem.* **2010,** *21* (10), 1842-9.

30. Saxon, E.; Bertozzi, C. R., Cell surface engineering by a modified Staudinger reaction. *Science* **2000,** *287* (5460), 2007-10.

31. O'Shannessy, D. J.; Brigham-Burke, M.; Peck, K., Immobilization chemistries suitable for use in the BIAcore surface plasmon resonance detector. *Anal. Biochem.* **1992,** *205* (1), 132-6.

32. Stenberg, E.; Persson, B.; Roos, H.; Urbaniczky, H., Quantitative determination of surface concentration of protein with surface plasmon resonance using radiolabeled proteins *Journal of Colloid and Interface Science* **1991,** *143* (2), 513-26

33. Mehan, N.; Gupta, V.; Sreenivas, K.; Mansingh, A., Surface plasmon resonance based refractive index sensor for liquids. *Indian J. of pure and appl. physics* **2005,** *43*, 854-58.

34. Hagiwara, K.; Collet-Cassart, D.; Kobayashi, K.; Vaerman, J. P., Jacalin: isolation, characterization, and influence of various factors on its interaction with human IgA1, as assessed by precipitation and latex agglutination. *Mol. Immunol.* **1988,** *25* (1), 69-83.

35. Bains, G.; Lee, R. T.; Lee, Y. C.; Freire, E., Microcalorimetric study of wheat germ agglutinin binding to N-acetylglucosamine and its oligomers. *Biochemistry* **1992,** *31* (50), 12624-8.

36. Mahanta, S. K.; Sastry, M. V.; Surolia, A., Topography of the combining region of a Thomsen-Friedenreich-antigen-specific lectin jacalin (Artocarpus integrifolia agglutinin). A thermodynamic and circular-dichroism spectroscopic study. *Biochem. J.* **1990,** *265* (3), 831-40.

37. Jeyaprakash, A. A.; Katiyar, S.; Swaminathan, C. P.; Sekar, K.; Surolia, A.; Vijayan, M., Structural basis of the carbohydrate specificities of jacalin: an X-ray and modeling study. *J. Mol. Biol.* **2003,** *332* (1), 217-28.

38. Muraki, M.; Ishimura, M.; Harata, K., Interactions of wheat-germ agglutinin with GlcNAc beta 1,6Gal sequence. *Biochim. Biophys. Acta.* **2002,** *1569* (1-3), 10-20.

39. Lienemann, M.; Paananen, A.; Boer, H.; de la Fuente, J. M.; Garcia, I.; Penades, S.; Koivula, A., Characterization of the wheat germ agglutinin binding to self-assembled monolayers of neoglycoconjugates by AFM and SPR. *Glycobiology* **2009,** *19* (6), 633-43.

40. Klotz, I. M., Numbers of receptor sites from Scatchard graphs: facts and fantasies. *Science* **1982,** *217* (4566), 1247-9.

41. Shinohara, Y.; Hasegawa, Y.; Kaku, H.; Shibuya, N., Elucidation of the mechanism enhancing the avidity of lectin with oligosaccharides on the solid phase surface. *Glycobiology* **1997,** *7* (8), 1201-8.

42. Kiessling, L. L.; Pohl, N. L., Strength in numbers: non-natural polyvalent carbohydrate derivatives. *Chem. Biol.* **1996,** *3* (2), 71-7.

43. Tassa, C.; Duffner, J. L.; Lewis, T. A.; Weissleder, R.; Schreiber, S. L.; Koehler, A. N.; Shaw, S. Y., Binding affinity and kinetic analysis of targeted small molecule-modified nanoparticles. *Bioconjug. Chem.* **2010,** *21* (1), 14-9.

44. Sastry, M. V.; Banarjee, P.; Patanjali, S. R.; Swamy, M. J.; Swarnalatha, G. V.; Surolia, A., Analysis of saccharide binding to Artocarpus integrifolia lectin reveals specific recognition of T-antigen (beta-D-Gal(1----3)D-GalNAc). *J. Biol. Chem.* **1986,** *261* (25), 11726-33.

45. Saxon, E.; Armstrong, J. I.; Bertozzi, C. R., A "traceless" Staudinger ligation for the chemoselective synthesis of amide bonds. *Org. Lett.* **2000,** *2* (14), 2141-3.

46. Wang, C. C.; Seo, T. S.; Li, Z.; Ruparel, H.; Ju, J., Site-specific fluorescent labeling of DNA using Staudinger ligation. *Bioconjug Chem.* **2003,** *14* (3), 697-701.

47. Yu, H.; Huang, S.; Chokhawala, H.; Sun, M.; Zheng, H.; Chen, X., Highly efficient chemoenzymatic synthesis of naturally occurring and non-natural alpha-2,6-linked sialosides: a P. damsela alpha-2,6-sialyltransferase with extremely flexible donor-substrate specificity. *Angew. Chem. Int. Ed. Engl.* **2006,** *45* (24), 3938-44.

48. Attie, A. D.; Raines, R. T., Analysis of Receptor-Ligand Interactions. *J. Chem. Educ.* **1995,** *72* (2), 119.

49. Arockia Jeyaprakash, A.; Jayashree, G.; Mahanta, S. K.; Swaminathan, C. P.; Sekar, K.; Surolia, A.; Vijayan, M., Structural basis for the energetics of jacalin-sugar interactions: promiscuity versus specificity. *J. Mol. Biol.* **2005,** *347* (1), 181-8.

50. Damm, W.; Frontera, A.; TiradoRives, J.; Jorgensen, W. L., OPLS all-atom force field for carbohydrates. *J. Comput. Chem.* **1997,** *18* (16), 1955-70.

Chapter 4

Design and synthesis of multivalent glycoconjugates for the Staudinger ligation[1]

1. Compound, 3-oxo-1-phenyl-2,7,10,13-tetraoxa-4-azahexadecan-16-oic acid, **4.27**, was provided by J. Cartmell (University of Alberta).

4.1 Abstract

Glycans on the cell surface play vital roles in biological processes. The function of a specific carbohydrate epitope may not be well understood due to the heterogeneity of the glycocalyx. We previously reported a method to generate defined glycoproteins, both *in vivo* and *in vitro*, using the Staudinger ligation. This strategy provides elucidation of the function of specific carbohydrate epitopes in a complex glycoconjugate. The synthesis of glycoproteins was achieved using mono and disaccharide phosphane reagents. However, many naturally occurring glycans of glycoproteins are multivalent; therefore, to mimic a multivalent presentations, we designed a strategy for making multivalent Staudinger ligation reagents. To demonstrate the method, we synthesized a trivalent galactose phosphane reagent. Our synthetic approach involves tri-galactosylation of Tris(hydroxymethyl)aminomethane (TRIS) modified acceptor and generation of free amine followed by acylation with succinimidyl 3-diphenylphosphino-4-methoxy-carbonylbenzoate. TRIS was elongated to circumvent steric hindrance at the amine during acylation. This synthetic strategy can be used to generate different trivalent-glycosyl phosphane reagents.

4.2 Introduction

In **Chapter 2**, we discussed the importance of glycan structures on proteins within different cellular processes. Heterogeneity of these glycans has complicated the study of their role in biological processes. To unravel the function of glycans there is a need to develop homogenous and defined glycoconjugates. We have generated mono and disaccharide-phosphane reagents and successfully demonstrated Staudinger ligation as a method to synthesize defined glycoconjugates (**Chapter 2**).[1] This chemistry maintains the binding specificity of the carbohydrate epitope, as immobilization of specific carbohydrate epitopes to surfaces allows detection of specific binding (**Chapter 3**).[2] In these studies we confirmed that lectins typically have low affinity for monosaccharides (The dissociation constant, K_d, to the lectins are in the range of 10^3 to 10^6 M^{-1}).

Many naturally occurring glycoconjugates found on the cell surface, including glycoproteins, and glycolipids are multivalent, and which can be critical for their biological function.[3-5] Multivalent carbohydrates show enhanced avidity and specificity for lectins as a consequence of the cluster glycoside effect,[6] this has prompted the synthesis of many glycoconjugate clusters to promote interactions with lectins.[7-10] The mechanism and basic structural requirements for multivalent interactions between carbohydrate and protein (lectin) are not well understood.[11] The lectin, concavalin A (Con A), a homotetramer at neutral pH and each monomer has a binding site for α-mannopyranoside, has been an extensively examined model system to understand carbohydrate-protein interactions.[12] For example, Kiessling and co-workers have synthesized a series of polymer-mannosides of similar length but with different numbers of mannosides based on ring opening metathesis polymerization to study the influence of binding epitope density on multivalent interaction with Con A and found that the factors such as

stoichiometry of the complex, rate of cluster formation, and receptor proximity depends on the density of binding sites.[13] They also demonstrated that the size, shape and valency of the multivalent ligands will influence their interactions with receptors.[14] Proximity binding effects have been explored with monomeric and dimeric Con A using isothermal titration microcalorimetry (ITC) with mannose-functionalized poly(amidoamine) (PAMAM) dendrimers[12] and different generations of these dendrimers were also used in the study of their activity with Con A.[15] All these studies indicate the importance of generating different multivalent ligands in order to understand carbohydrate-protein interactions.

Based on our work described in **(Chapter 2)**[1] to mimic complex carbohydrate structures, we chose to synthesize trimers of β-galactoside, α-mannoside and β-glucoside attached Staudinger reagents. To conjugate these reagents we could again use azide modified proteins to study their multivalent interactions with the lectins. To develop the synthetic strategy we planned trimers of β-galactoside and α-mannoside. These compounds could interact with Jacalin (*Artocarpus integrifolia* agglutinin) and Con A lectins, respectively. A trimer of glucoside would serve as a control. In this chapter, we describe the design and synthesis of a trimeric glycoside attached Staudinger ligating reagent, and establish this methodology for introducing other desired carbohydrate epitopes.

4.3 Design and retrosynthetic analysis of trimer-glycoside-linked Staudinger reagents

With the knowledge of our previous work described in **Chapter 2** for the synthesis of mono (gal) and linear disaccharide (lactose, LacNAc)-Staudinger ligation reagents, we expected that the essential requisites for the synthesis of the target reagents were suitable glycosyl donor, acceptor or linker and an *N*-hydroxy succinamide (NHS) activated phosphane reagent, such as **4.1** (synthesis described in **Chapter 2**).[2] The synthesis, in brief, should involve glycosylation of

an orthogonally protected amine linker, followed by deprotection and coupling of the free

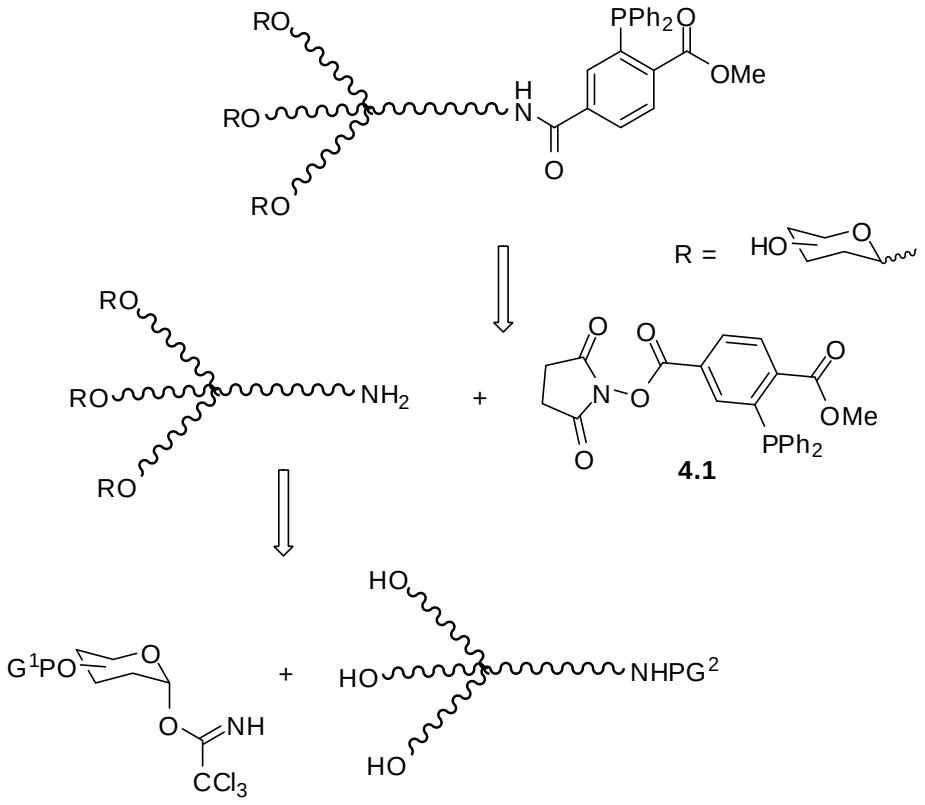

Scheme 4.1: General retrosynthetic plan for trimer-glycoside phosphane reagents. Glycosylation on to triol linker with amine proetection, removal of protecting groups and finally coupling to **4.1** should generate the desired structures. PG^1 and PG^2 are orthogonal protecting groups, PG^1 could be acetyl or benzoyl to generate the required stereochemistry at the anomeric position.

amine to the phosphane reagent, **4.1**. Therefore, we can generate trimer-glycoside-Staudinger ligating reagents by following a similar sequence of reactions. The target structure has three glycosides (**Scheme 4.1**) and can be introduced in one step by glycosylation onto a triol linker with a protected amine. Subsequent deprotection of the amine, followed by amide bond formation with the phosphane reagent, **4.1**, should afford the target structures. We intended to

generate trivalent β-galactoside, α-mannoside and β-glucosides and to achieve required stereochemistry at the anomeric position, the donor should have a participating group at the *C*-2 position; therefore benzoyl or acetyl protecting groups were selected. Our retrosynthetic analysis suggests that to generate target compounds, the required building blocks are benzoyl/acetyl protected donor, protected triol-linker, and a phosphane reagent, **4.1**.

4.4 Synthesis of the protected-triol linker

Several different scaffolds such as cyclodextrins, polymers[16], dendrimers[17, 18], calix[4]-allenes, crown ethers, oligosilsesquioxanes[19] and peptides[20] have been used to generate

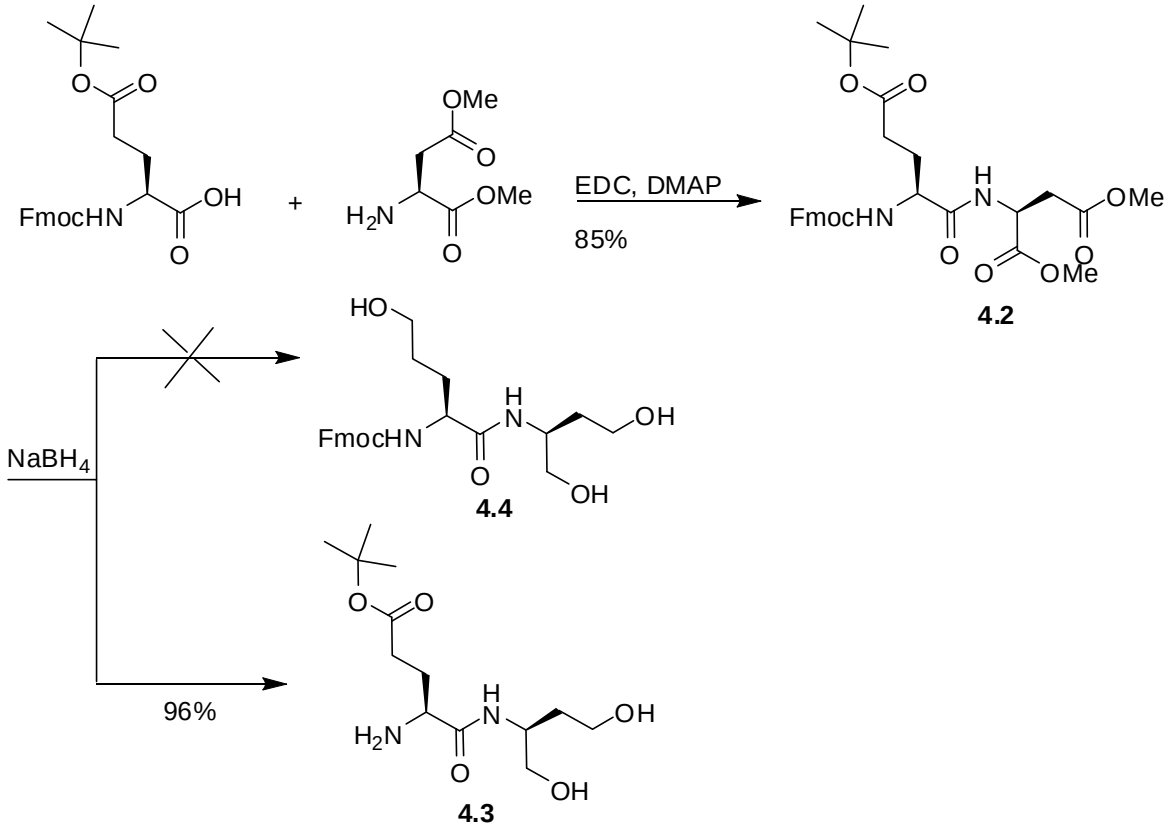

Scheme 4.2: Synthesis of an *N*-α-Fmoc-protected triol linker from glutamic acid and aspartic acid. Reduction of compound, **4.2**, with sodium borohydride gave undesired compound, **4.3**, instead desired triol, **4.4**.

glycoclusters. We first envisioned that the triol linker could be generated from a combination of selectively protected glutamic acid and aspartic acid. Synthesis of triol-linker started with coupling of Fmoc-L-glutamic acid 5-*tert*-butyl ester to aspartic acid hydrochloride dimethyl ester in the presence of 1-ethyl-3-(3-dimethylaminopropyl)carbodiimide (EDC) and 4-*N*,*N*-dimethylaminopyridine (DMAP) to give **4.2** in good yield (**Scheme 4.2**).[21] Later, our attempts to reduce the triester of **4.2** with sodium borohydride to generate triol linker, **4.4**,[22] were unsuccessful. We instead found that, although the methyl esters were reduced, the *t*-butyl ester remained intact and Fmoc was lost to give the undesired product, **4.3**. Based on this finding, we chose to replace Fmoc-L-glutamic acid 5-*tert*-butyl ester with the *N*-Cbz-L-glutamic acid 5-methyl ester (**Scheme 4.3**).

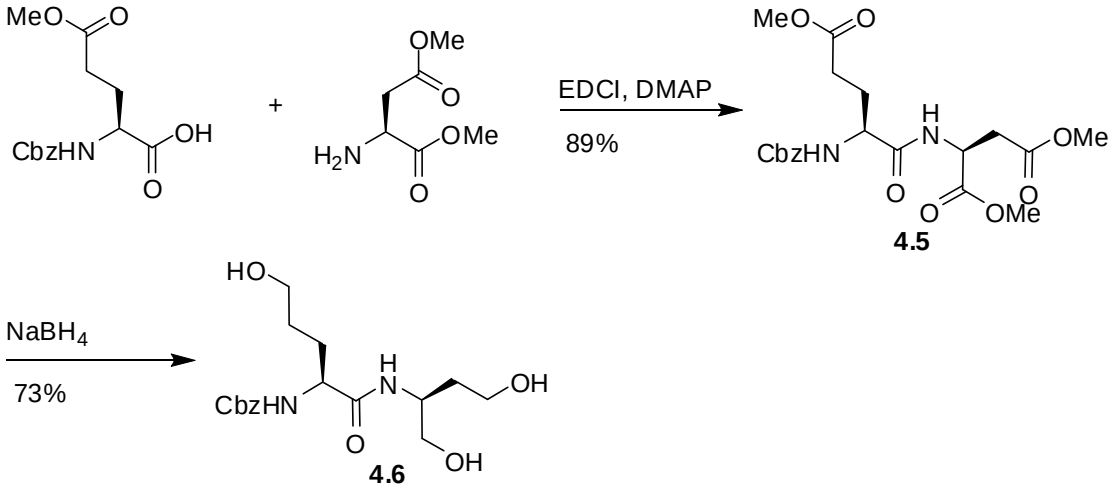

Scheme 4.3: Synthesis of a triol linker from Cbz protected glutamic acid and aspartic acid.

Cbz-protected amine with triol, **4.6**, was generated in two steps from selectively protected glutamic and aspartic acids.

Compound **4.5**, was generated by coupling of *N*-Cbz-L-glutamic acid-5-methyl ester to aspartic acid dimethyl ester using EDC and DMAP in 89% yield.[21] The trimethyl esters of **4.5** were reduced to alcohols with sodium borohydride to give the desired triol linker, **4.6**, in 73 % yield.[22] During work up of this reaction, water was added to the reaction mixture to remove salts formed from quenching of excess sodium borohydride by HCl. Although we used excess amounts of dichloromethane (DCM) to extract compound **4.6**, from the aqueous layer, the low solubility of the compound **4.6**, in DCM reduced the isolated yield.

4.5 Synthesis of glycosyl donors

With triol linker, **4.6**, in hand, we turned our attention to generating suitable donors for glycosylation. We chose to use the Schmidt glycosylation protocol.[23] Synthesis of the mannose trichloroacetimidate (TCA) donor (**Scheme 4.4**) started with the benzoylation of D-mannose to give penta-benzoylated mannose **4.7**, which was converted to the anomeric alcohol, **4.8**, in a two-step one pot procedure. Treatment of **4.7** with HBr/AcOH gave the mannosyl bromide. Displacement of the bromide with water was achieved in presence of silver carbonate. The lower yield of **4.8** was attributed to the formation of mannose orthoesters. In the presence of trichloroacetonitrile and 1,8-diazabicycloundec-7-ene (DBU), compound **4.8** was transformed into the mannose TCA donor, **4.9**.

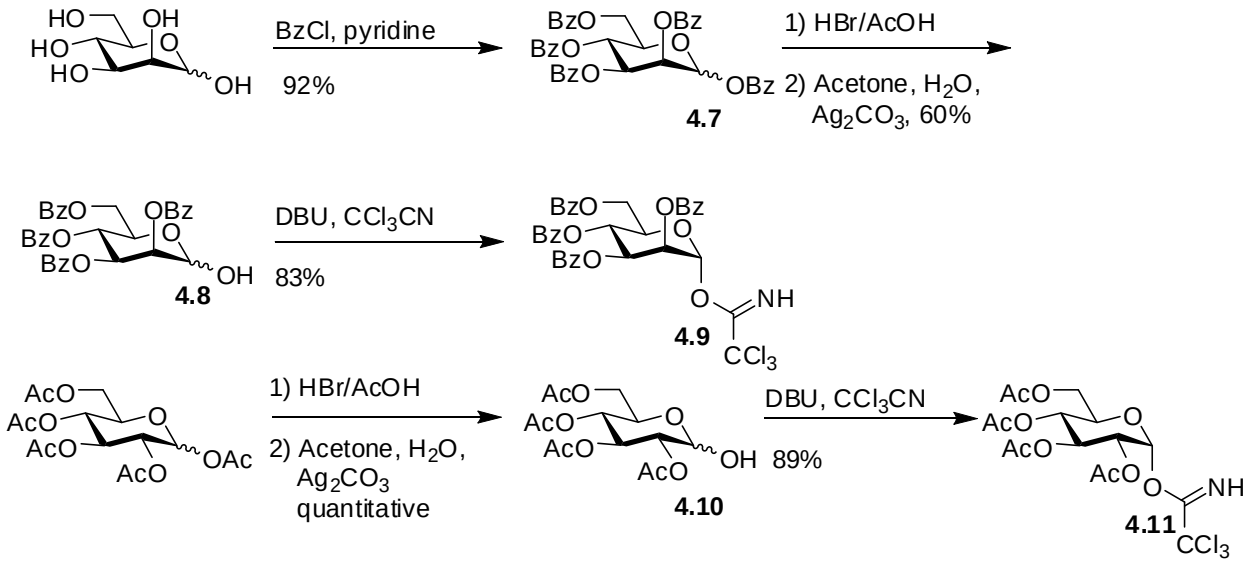

Scheme 4.4: Synthesis of mannose and glucose TCA, 4.9, and 4.11 donors. Trichloroacetimidate donors of mannose and glucose were generated in similar fashion as galactose trichloroacetimidate donor.[1]

Glucose TCA donor **4.11** was generated from a penta-acetyl glucose (**Scheme 4.4**) following a similar route with better yields than the mannose donor, **4.9**, and synthesis of galactose donor **4.12** discussed in **Chapter 2**.

4.6 Glycosylation of the triol-dipeptide linker, 4.6.

Triol-dipeptide linker **4.6** was sparingly soluble in DCM; therefore, we used an excess amount of solvent (DCM) and prolonged times (up to 2 d) for glycosylation. When we examined the glycosylation (**Scheme 4.5**) of linker **4.6** with the trichloroacetimidate donors **4.9**, **4.11** and **4.12** in presence of catalytic amount of trimethylsilyloxytriflate (TMSOTf), product formation was seen only in the case of the galactose derivative (confirmed by HRMS).

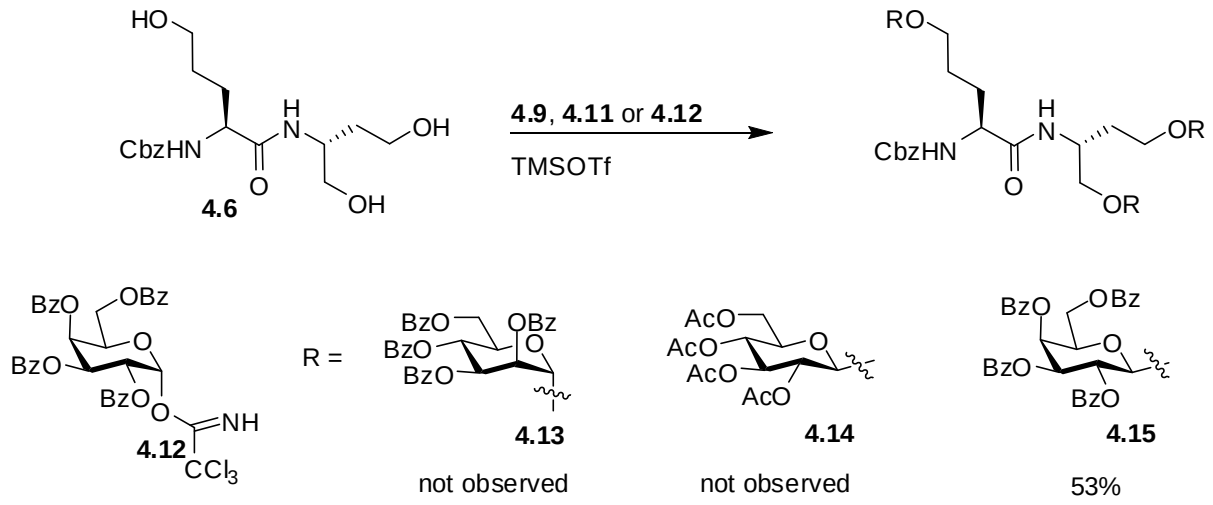

Scheme 4.5: Glycosylation of the triol-dipeptide linker, 4.6, with TCA donors. Donors of mannose, **4.13**, and glucose, **4.11**, did not react with acceptor, **4.6.** However, tri-gal cluster, **4.15**, was isolated with moderate yield.

The formation of product, **4.13**, was not observed possibly due to the resulting orthoester of mannose formed because of the reduced reactivity of acceptor, **4.6**. This issue has been encountered in multi-mannosylation reactions.[24] In the case of glucosylation, the acetyl donor, **4.11**, is highly reactive compared to the benzoyl donor, resulting in decomposition under these reaction conditions. As a result, formation of **4.14** was not observed. Although we succeeded in obtaining the galactose derivative **4.15**, our attempts to obtain pure compound were unsuccessful. Our results suggested that the solubility of the triol-linker, **4.6**, was the major issue with glycosylation of **4.6**. Our observations were donor-dependent, and the reactivity of the donors could be partly responsible for the low yield observed.

4.7 Glycosylation of *N*-Cbz-tris(hydroxymethyl)aminomethane linker 4.19

The synthesis of trivalent manno- and glucoclusters have been reported using TRIS (tris(hydroxymethyl)aminomethane) in Cbz-protected form.[25] We thought that the strategy

reported by H. A. Shaikh et al[25] could be adopted to generate trivalent glycocluster-linked phosphane reagents. In their strategy they used benzoyl-protected TCA donors. Therefore, we synthesized benzoyl-protected glucosyl TCA donor, **4.18** (**Scheme 4.6**), from the D-glucose by following the strategy used for generating mannose and galactose donors **4.9** and **4.12**.

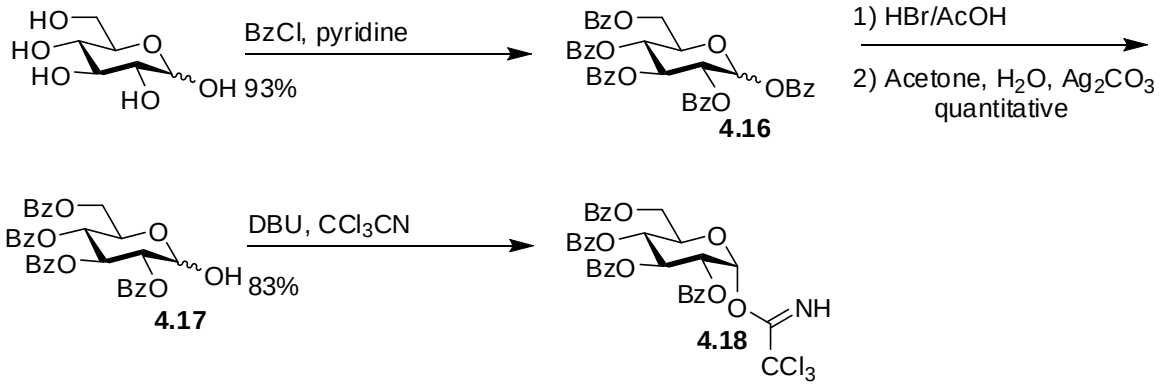

Scheme 4.6: Synthesis of the glucose TCA donor, 4.18. A less reactive benzoyl-protected glucose trichloroacetimidate donor was synthesized as an alternate to acetyl-protected donor, **4.11**, to prevent decomposition under glycosylation condition.

The amine of TRIS was protected selectively as a O-benzylcarbamate (**Scheme 4.7**) by treating with benzyl chloroformate and sodium bicarbonate.[26] Glycosylation of TRIS derivative, **4.19**, was performed in the presence of a catalytic amount of boron trifluoride etherate ($BF_3{\cdot}Et_2O$) with the TCA donors, **4.9**, **4.12** and **4.18**. This reaction proceeded well, with good yields, to generate the trivalent protected glycol-cluster compounds **4.20**, **4.21** and **4.22** (**Scheme 4.7**). Although we used fewer equivalents of the TCA donors compared to Shaikh's strategy, our yields were similar or better for compound **4.20**.

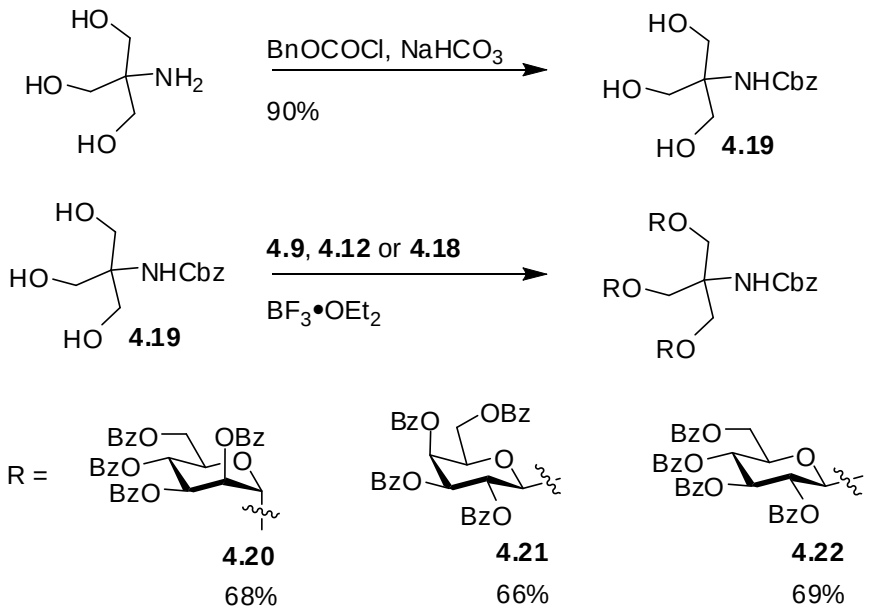

Scheme 4.7: Glycosylation of the TRIS-linker, 4.19, with TCAdonors, 4.9, 4.12, and 4.18. The tri-glycosylation of triol, **4.19**, succeeded with good yields (~ 67%) compared to the dipeptide- linker, **4.6**.

4.8 Generation of TRIS glyco-clusters with a free amine

Debenzoylation of glycoclusters **4.20** and **4.21** was accomplished under Zemple´n conditions[27] to give **4.23** and **4.24** in excellent yields (**Scheme 4.8**). Deprotection of Cbz-protected amines **4.23** and **4.24** was achieved by palladium-catalyzed hydrogenation to generate compounds **4.25** and **4.26**.[25] With a series of glyco-cluster amino derivatives in hand, we proceeded to test their utility for acylation by **4.1**. Unfortunately acylation of free amines **4.25** and **4.26** to generate the final cluster-Staudinger ligating reagents in the presence of triethylamine with the phosphane reagent, **4.1**, were unsuccessful. Prolonged reaction times (3 d) did not improve yields. We propose that the crowded steric repulsions might have hindered the

acylation reaction; therefore, we decided to modify the TRIS-linker with an ethylene glycol linker to provide additional space between the glycocluster and the amine nucleophile.

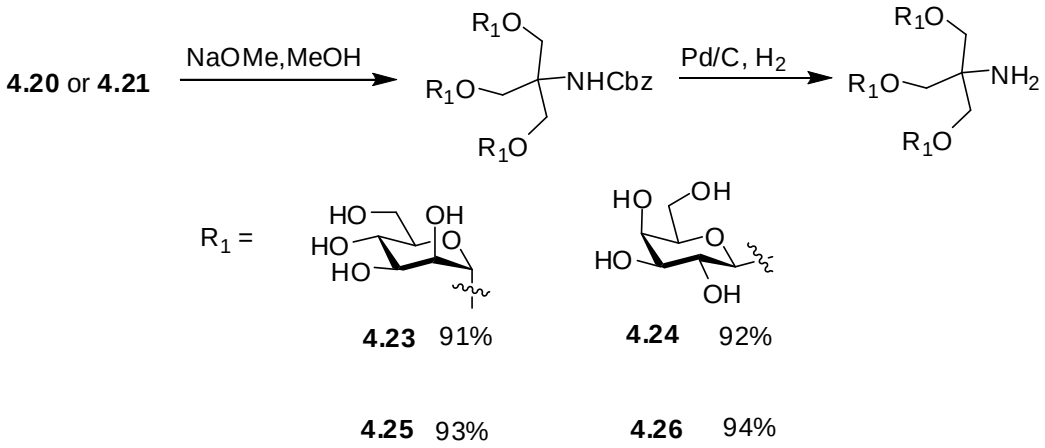

Scheme 4.8: Deprotection of glycoclusters 4.20 and 4.21. Generation of the free amine precursors for acylation with phosphane reagent **4.1**.

4.9 Elongation of the TRIS-linker

We employed a polyethyleneglycol (PEG)-based spacer, **4.27**, to increase the polarity of molecule to provide additional space between the glycocluster and the amine. An additional advantage of using a lengthy spacer is that the glycosyl cluster will be far away from the set of aromatic groups introduced as part of the ligation strategy on the modified protein. Therefore, the spacer should reduce interference of the aromatic groups with their binding to lectins. The amine of the spacer was protected with Cbz, which can be easily removed by hydrogenation, typically without purification in almost quantitative yields. The acid of the ethylene glycol spacer, **4.27**, was activated with the *N*-hydroxysuccinamide (NHS) in presence of EDC and DMAP to give 3-oxo-1-phenyl-2,7,10,13-tetraoxa-4-azahexadecan-16-succinimidate, **4.28**. The NHS-activated acid, **4.28**, was coupled to the amine of the TRIS to provide an elongated TRIS scaffold, **4.29**, in 75% yield (**Scheme 4.9**).

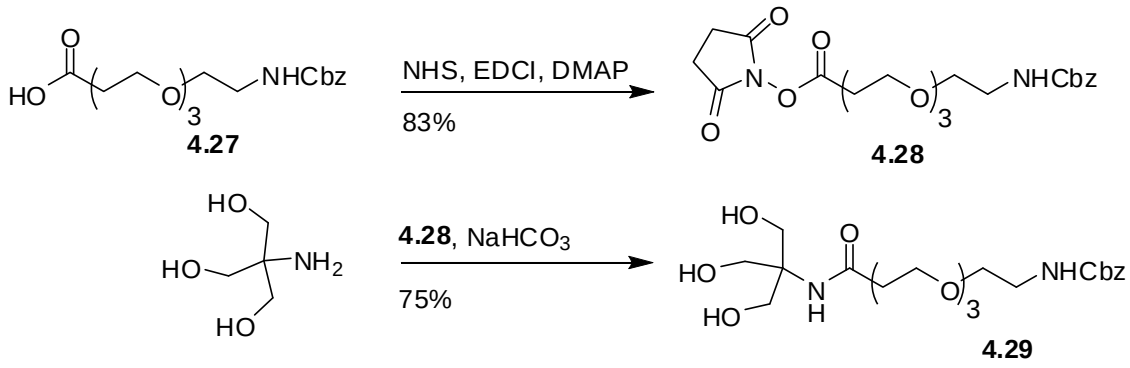

Scheme 4.9: Elongation of the TRIS-linker with a tetraethyleneglycol spacer. TRIS was elongated in order to circumvent steric hindrance at the amine during coupling with phosphane reagent, **4.1**.

4.10 Galactosylation of the improved TRIS-linker

With our improved linker, we sought to test the reactivity with a TCA donor. Galactosylation of the improved TRIS-linker, **4.29**, with galactosyl TCA donor, **4.12**, in presence of a catalytic amount of $BF_3{\cdot}Et_2O$ gave trivalent galactosyl cluster, **4.30**, in good yields (**Scheme 4.10**). Debenzoylation of galactosyl cluster, **4.30**, with sodium methoxide in methanol (Zemple´n conditions)[27] gave compound **4.31** and deprotection of Cbz-protected amine of **4.31** by hydrogenation with catalytic amount of palladium, yielded free amine galactosyl cluster, **4.32**. Completely deprotected galactosyl cluster, **4.32**, was obtained in moderate yield (51%) from elongated-TRIS linker, **4.29**, in three steps.

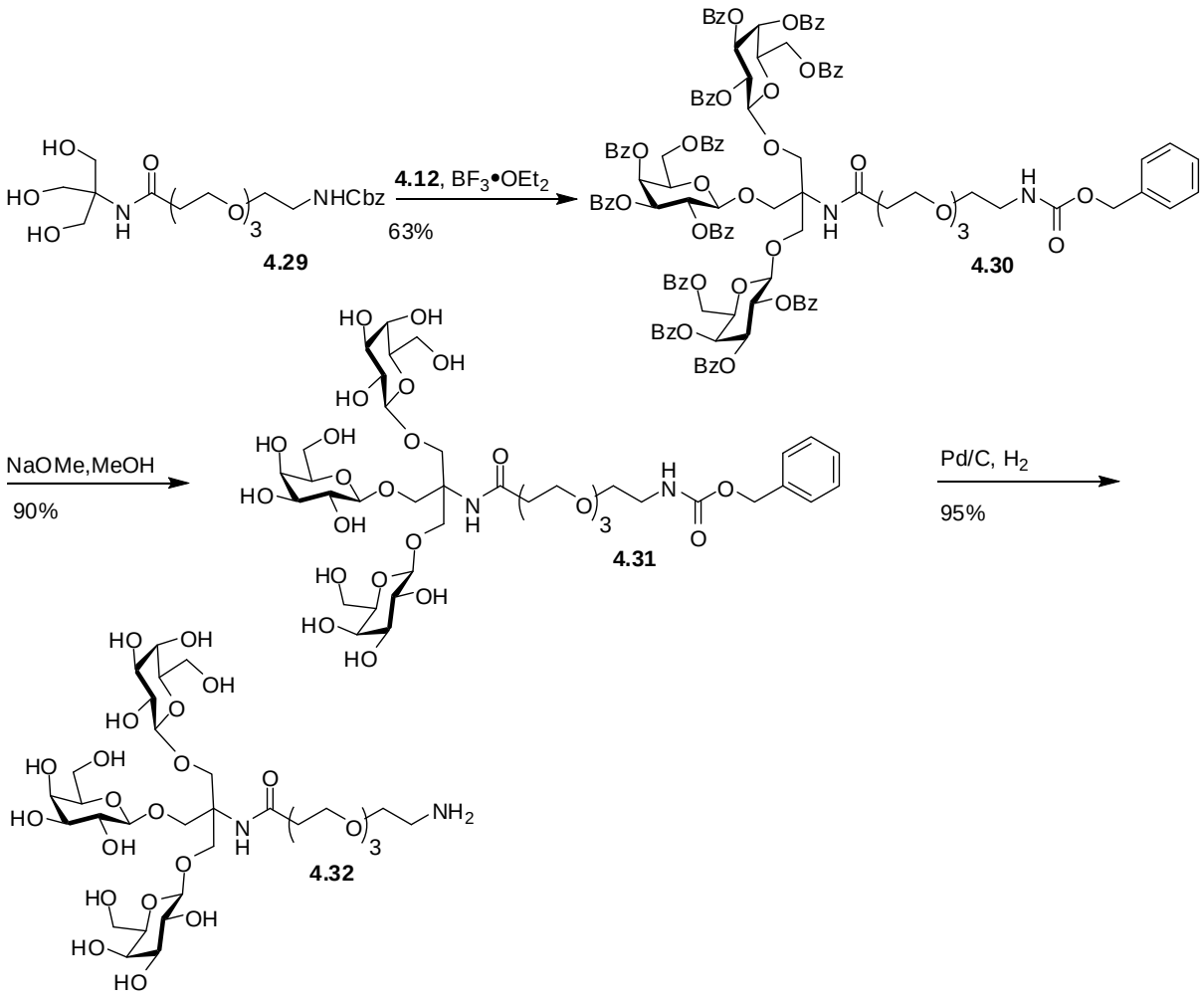

Scheme 4.10: Synthesis of galactosyl-cluster 4.32 with improved TRIS-linker. Debenzoylation and Cbz deprotection of galactosyl cluster, **4.31**, provided a free amine, **4.32**.

4.11 Synthesis of a galactosyl cluster-Staudinger ligation reagent

Acylation of the free amine of **4.32** with the phosphane reagent, **4.1**, and triethylamine as base provided the desired galatosylcluster-Staudinger reagent **4.33** (**Scheme 4.11**) in 51% yield.

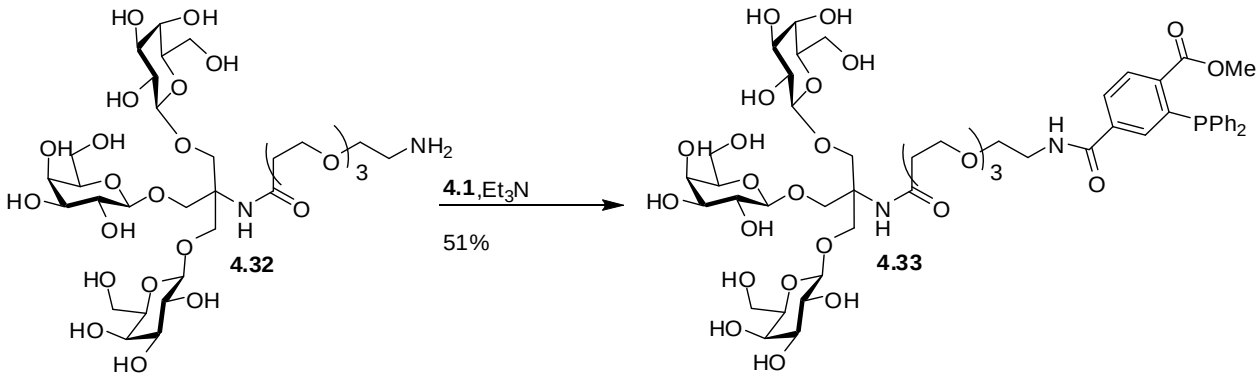

Scheme 4.11: Acylation of compound 4.32 with phosohane reagent 4.1. Free amine **4.32** was coupled to activated acid of phosphane reagent in dimethylformamide (DMF).

Byproducts and excess reagents were removed by washing with DCM and the residue was further purified by reverse phase column chromatography to afford pure **4.33**, with only minor of oxidized phosphane (~ 13%).

4.12 Conclusions & future work

In this chapter, we described the synthesis of a tri-gal-Staudinger ligation reagent by following a similar chemical strategy used for making mono and disaccharide-Staudinger ligation reagents in **Chapter 2**.[1] The most effective strategy used was galactosylation of an improved TRIS-linker with suitable amine protection and generation of free amine followed by coupling to a phosphane reagent. The key element of the synthesis was the selection of a suitable triol-linker with an amine. We explored three linkers, a triol-linker generated from glutamic and aspartic acids, **4.6**, a TRIS-linker and an improved TRIS-linker. Linker, **4.6**, was only slightly soluble in solvent, as a result glycosylation reactions were slow or trichloroacetimidate donors were decomposed before the desired glycosylation could occur. Although glycosylation of the TRIS-linker with trichloroacetimidate donors proceeded smoothly, acylation of the amine of the

later with phosphane reagent, **4.1**, was not successful due to steric hindrance at the amine. Therefore, to avoid steric problems, the TRIS-linker was elongated with an ethylene glycol spacer. The elongated TRIS-scaffold, **4.29**, was greatly improved and showed greater solubility in dichloromethane (DCM). The increased space between tri-glycosyl, amine part of the reagent improved yields of the acylation reaction.

Based on our results, the tri-mannose- and tri-glucose-phosphane reagents can also be generated using the strategy reported for the synthesis of tri-gal-phosphane reagent **4.33**. In general, the tri-glycosyl cluster phosphane reagents of this kind can be made by using the improved TRIS-scaffold, **4.29**. The space between carbohydrate moieties plays a vital role in their multivalent interaction with lectins, however carbohydrate moieties of tri-cluster, **4.33**, or tri-clusters to be synthesized by using TRIS-scaffold, **4.29**, seems to be crowded and this may hinder/reduce the binding of these moieties with lectins. Multivalent interactions of these tri-clusters with different lectins can be studied by immobilizing them onto an azide modified biosensor surface using surface plasmon resonance as described in **Chapter 3**.[2] This study may give an idea about their interactions and effect of steric crowding on binding with lectins, accordingly TRIS scaffold can be further modified to provide enough space between carbohydrate moieties thereby enhancing their affinity for lectins. As discussed earlier, the major problem one can foresee in synthesizing multi-glycosyl clusters is the decreased solubility of the scaffold in solvents like DCM, due to the increased polarity of these compounds. With the knowledge of synthesis of tri-cluster phosphane reagents, this strategy can be used to generate multi-glycosyl cluster-phosphane reagents provided if one has access to the suiltable scaffold.

.

4.13 Experimental procedures

4.13.1 General experimental methods

Dry solvents (CH_2Cl_2, MeOH, CH_3CN, and DMF) were purchased from Sigma Aldrich in capped DriSolv™ bottles and used without purification and stored under argon. Toluene and pyridine were dried on molecular sieves and stored under desiccated atmosphere. Reactions were conducted under a stream of argon at ambient temperature, unless otherwise noted, and monitored by TLC on silica gel G-25 UV254 (0.25 mm). Developed TLC plates were visualized under UV lamp and charred by heating plates that were dipped in cerium molybdate stain or phosphomolybdic acid stain. NMR experiments were conducted on Varian 300, 400 or 500 MHz instruments. Chemical shifts are reported relative to the deuterated solvent peak and are in parts per million (ppm). Phosphoric acid was used as an external standard for ^{31}P NMR. ^{1}H NMR and ^{13}C peak assignments were made on the basis of 2D-NMR such as COSY and HSQC experiments. ESI-MS spectra were carried out on samples suspended in solvent with added NaCl.

4.13.2 Synthetic methods

Synthesis of (*S*)-Dimethyl 2-((*S*)-2-(((9H-fluoren-9-yl)methoxy)carbonylamino)-5-tert-butoxy-5-oxopentanamido)succinate (4.2):

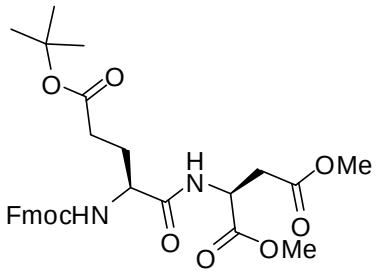

4.2

To a solution of Fmoc-L-glutamic acid 5-*tert*-butyl ester (1.064 g, 2.5 mmol) in 20 mL DCM aspartic acid hydrochloride dimethyl ester (0.593 g, 3.0 mmol), DMAP (0.575, 3 mmol) were

added and stirred for 15 min, then EDC (0.367 g, 3.0 mmol) was added and entire reaction mixture stirred overnight. The reaction mixture was diluted to 60 mL with DCM and washed successively with hydrochloric acid (1N, 30 mL), saturated sodium bicarbonate (30 mL), and brine (30 mL) then dried over sodium sulfate, filtered and concentrated. The residue was purified by flash column chromatography with EtOAc:Hexanes (1:2) to afford a white solid (1.205 g, 85%). ^{1}H NMR (400 MHz, $CDCl_3$) δ 7.76 (d, *J* = 7.5 Hz, 2H), 7.60 (d, *J* = 7.4 Hz, 2H), 7.40 (t, *J* = 7.5 Hz, 2H), 7.31 (td, *J* = 7.4, 0.9 Hz, 2H), 7.18 (d, *J* = 8.1 Hz, 1H), 5.73 (d, *J* = 7.6 Hz, 1H),4.94 – 4.84 (m, 1H), 4.49 – 4.26 (m, 3H), 4.22 (t, *J* = 7.1 Hz, 1H), 3.75 (s, 3H), 3.67 (s, 3H), 3.05 (dd, *J* = 17.2, 4.5 Hz, 1H), 2.83 (dd, *J* = 17.2, 4.6 Hz, 1H), 2.52 – 2.33 (m, 2H), 2.22 – 2.06 (m, 1H), 2.03 – 1.92 (m, 1H), 1.47 (s, 9H). ^{13}C NMR (101 MHz, $CDCl_3$) δ 172.7, 171.2, 171.15, 170.7, 156.1, 143.8, 141.3, 127.7, 127.1, 125.1, 120.0, 81.0, 67.2, 54.2, 52.8, 52.1, 48.5, 47.1, 36.0, 31.5, 28.3, 28.1. HR-ESIMS calculated for $C_{30}H_{36}N_2O_9Na$ $(M+Na)^+$ 591.2313, found 591.2312.

Synthesis (*S*)-tert-butyl 4-amino-5-((*S*)-1,4-dihydroxybutan-2-ylamino)-5-oxopentanoate (4.3):

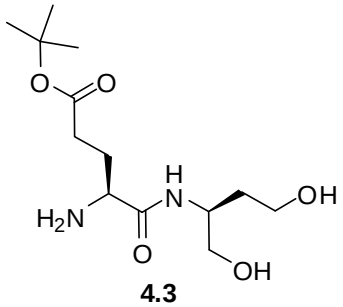

4.3

To a freshly prepared solution of $NaBH_4$ (0.681 g, 18 mmol) in aq MeOH (17 mL, 80%), a solution of **4.2** (0.583 g, 1.0 mmol) in MeOH (10 mL) and THF (10 mL) was added drop wise at 0 ^{o}C and stirred overnight at room temperature. Reaction mixture was neutralized with HCl (2N, 3 mL) and salts were removed by filtration. The filtrate was concentrated, dissolved in 10 mL of

water and extracted with DCM (3 X 10 mL). Aqueous layer was concentrated under reduced pressure to give white solid (0.279 g, 96%).[1]H NMR (498 MHz, CD_3OD) δ 4.05 (qd, *J* = 9.6, 4.9 Hz, 1H), 3.93 (t, *J* = 6.4 Hz, 1H), 3.67 – 3.56 (m, 3H), 3.53 (dd, *J* = 11.1, 6.1 Hz, 1H), 2.51 – 2.39 (m, 2H), 2.15 – 2.05 (m, 2H), 1.89 – 1.82 (m, 1H), 1.72 – 1.63 (m, 1H), 1.45 (s, 9H). ^{13}C NMR (125 MHz, CD_3OD) δ 173.4, 170.0, 82.3, 64.8, 59.7, 53.9, 50.5, 34.9, 31.6, 28.4, 27.9. HR-ESIMS calculated for $C_{13}H_{26}N_2O_5Na$ $(M+Na)^+$ 313.1734, found 313.1736.

Synthesis of (*S*)-Dimethyl 2-((*S*)-2-(benzyloxycarbonylamino)-5-methoxy-5-oxopentanamido)succinate (4.5):

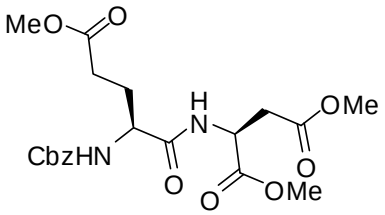

4.5

To a solution of *N*-Carbobenzyloxy-D-glutamic acid 5-methyl ester (0.295 g, 1.0 mmol) in 10 mL DCM, aspartic acid hydrochloride dimethyl ester (0.237 g, 1.2 mmol), DMAP (0.147, 1.2 mmol) were added at 0 ^oC and stirred for 20 m, then EDC (0.367 g, 1.2 mmol) was added and the entire reaction mixture was stirred overnight at room temperature. The reaction mixture was diluted to 20 mL with DCM and washed successively with hydrochloric acid (1N, 15 mL), saturated sodium bicarbonate (15 mL), and brine (15 mL) then dried over sodium sulfate, filtered and concentrated. The residue was purified on short pad of silica with EtOAc:Hexanes (1:1) to afford a white solid (0.390 g, 89%).[1]H NMR (400 MHz, $CDCl_3$) δ 7.40 – 7.28 (m, 5H), 7.13 (d, *J* = 7.8 Hz, 1H), 5.62 (d, *J* = 7.4 Hz, 1H), 5.10 (s, 2H), 4.91 – 4.79 (m, 1H), 4.37 – 4.23 (m, 1H), 3.74 (s, 3H), 3.69 (s, 3H), 3.68 (s, 3H), 3.04 (dd, *J* = 17.2, 4.5 Hz, 1H), 2.81 (dd, *J* = 17.2, 4.3 Hz, 1H), 2.60 – 2.41 (m, 2H), 2.25 – 2.11 (m, 1H), 2.05 – 1.90 (m, 1H). ^{13}C NMR (101 MHz,

$CDCl_3$) δ 173.7, 171.3, 171.0, 170.7, 156.0, 136.2, 128.5,128.2, 128.0, 67.0, 54.0, 52.9, 52.1, 51.9, 48.5, 35.9, 30.0, 28.4. HR-ESIMS calculated for $C_{20}H_{26}N_2O_9Na$ $(M+Na)^+$ 461.1531, found 461.1532.

Synthesis of Benzyl (*S*)-1-((*S*)-1,4-dihydroxybutan-2-ylamino)-5-hydroxy-1-oxopentan-2-ylcarbamate (4.6):

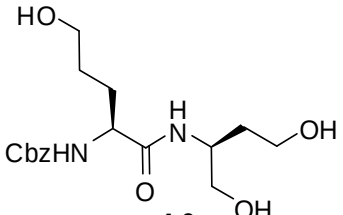

4.6

A solution of **4.5** (2.629 g, 6.0 mmol) in MeOH (18 ml) and THF (18 mL) was added drop wise to a freshly prepared solution of $NaBH_4$ (3.872 g, 108 mmol) in aq MeOH (30 mL, 80%) at 0 ^oC and stirred overnight at room temperature. The reaction mixture was neutralized with 2N aq HCl and salts were removed by filtration. The filtrate was concentrated and the residue was suspended in 50 mL water, and then extracted with chloroform (3 x 150 mL). The combined organic layers were dried over sodium sulfate, filtered and concentrated to afford a white solid (1.551 g, 73%). ^1H NMR (400 MHz, CD_3OD) δ 7.38 – 7.24 (m, 5H), 5.08 (s, 2H), 4.08 (dd, *J* = 8.4, 5.5 Hz, 1H), 3.99 (td, *J* = 9.7, 5.0 Hz, 1H), 3.56 (m, 6H), 1.90 – 1.75 (m, 2H), 1.73 – 1.50 (m, 4H). ^{13}C NMR (101 MHz, CD_3OD) δ 174.7, 158.1, 137.8, 129.1, 128.7, 128.5, 67.3, 64.6, 62.0, 59.4, 56.1, 49.7, 34.6, 29.5. HR-ESIMS calculated for $C_{17}H_{26}N_2O_6Na$ $(M+Na)^+$ 377.1683, found 377.1685.

Synthesis of 1, 2, 3, 4, 6-Penta-*O*-benzoyl-α/β-D-mannopyranoside (4.7):

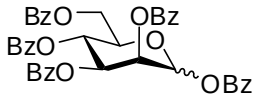

4.7

Benzoyl chloride (12.6 mL, 100 mmol) was added slowly to a suspension of mannose (3 g, 16.7 mmol) in 40 mL of pyridine and stirred at room temperature for 24 h under argon. Excess benzoyl chloride was quenched by adding 30 mL MeOH with cooling. The reaction mixture was concentrated under vacuum. The crude product was dissolved in DCM (25 mL) and washed with water (3 x 30 mL). The organic layer was dried over anhydrous Na_2SO_4. The solvent was evaporated under vacuum and the crude residue was purified by column chromatography using EtOAc/Hexane (1:2) to yield 10.8 g (92%) of **4.7** as a white solid. ^{1}H NMR (498 MHz, $CDCl_3$) δ 8.23 – 7.27 (Bz, 36H), 6.64 (d, *J* = 2.0 Hz, 1H), 6.44 (d, *J* = 1.1 Hz, 0.4H), 6.29 (t, *J* = 10.2 Hz, 1H), 6.18 (t, *J* = 9.8 Hz, 0.4H), 6.12 (dd, *J* = 3.2, 1.1 Hz, 0.4H), 6.08 (dd, *J* = 10.2, 3.3 Hz, 1H), 5.92 (dd, *J* = 3.3, 2.0 Hz, 1H), 5.81 (dd, *J* = 9.9, 3.2 Hz, 0.4H), 4.77 (dd, *J* = 12.3, 2.8 Hz, 0.4H), 4.71 (dd, *J* = 12.3, 2.6 Hz, 1H), 4.61 – 4.55 (m, 1.4H), 4.52 (dd, *J* = 12.3, 3.7 Hz, 1H), 4.41 – 4.34 (m, 0.4H). ^{13}C NMR (125 MHz, $CDCl_3$) δ 166.9, 166.88, 166.5, 166.4, 166.3, 166.1, 166.12, 166.0, 165.0, 164.7, 134.9, 134.6, 134.5, 134.4, 134.38, 134.2, 133.9, 131.0, 130.9, 130.8, 130.7, 130.66, 130.6, 130.62, 130.2, 129.9, 129.7, 129.66, 129.6, 129.57, 129.5, 129.50, 129.4, 129.3, 129.31, 129.29, 129.27, 129.26, 129.2, 129.21, 92.2, 92.1, 74.2, 72.4, 72.1, 70.8, 70.3, 70.26, 67.3, 67.1, 63.5, 63.2. HR-ESIMS calculated for $C_{41}H_{32}O_{11}Na$ $(M+Na)^+$ 723.1837, found 723.1833.

Synthesis of 2, 3, 4, 6-Tetra-*O*-benzoyl-α/ β-D-mannopyranoside (4.8):

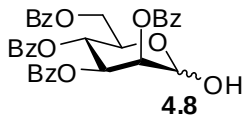

4.8

Penta-*O*-benzoyl mannoside, **4.7** (10.6 g, 15.2 mmol), was treated with 5.6 mL of HBr/AcOH (33%) in 30 mL of DCM for 1.3 h. The solution was washed twice with 25 mL of saturated $NaHCO_3$, NaCl, and 20 mL DI water. The DCM was evaporated and the solid was dried under

vacuum. The resulting white solid was dissolved in 30 mL acetone and 2.5 mL water with Ag_2CO_3 (2.1 g, 7.8 mmol) and stirred for 3 h. The solution was filtered through a pad of celite and dried under vacuum. The residue was purified by a column chromatography using EtOAc/Hexane (1:2) to afford 5.4 g (60%) of **4.8** as a white solid.^{1}H NMR (498 MHz, $CDCl_3$) δ 8.18 – 7.22 (m, 20H), 6.18 (t, *J* = 10.1 Hz, 1H), 6.01 (dd, *J* = 10.2, 3.3 Hz, 1H), 5.75 (dd, *J* = 3.2, 1.9 Hz, 1H), 5.54 (s, 1H), 4.77 (dd, *J* = 12.2, 2.7 Hz, 1H), 4.67 (dt, *J* = 10.1, 3.1 Hz, 1H), 4.45 (dd, *J* = 12.2, 3.7 Hz, 1H), 3.73 (s, 1H). ^{13}C NMR (125 MHz, $CDCl_3$) δ 166.4, 165.6, 165.5, 133.4, 133.41, 133.2, 133.1, 129.83, 129.81, 129.8, 129.75, 129.3, 129.1, 129.0, 128.6, 128.4, 128.3, 92.4, 70.9, 69.8, 68.9, 66.9, 62.8. HR-ESIMS calculated for $C_{34}H_{28}O_{10}Na$ $(M+Na)^+$ 619.1575, found 619.1577.

Synthesis of 2, 3, 4, 6-Tetra-*O*-benzoyl-D-mannopyranosyl trichloroacetamidate (4.9):

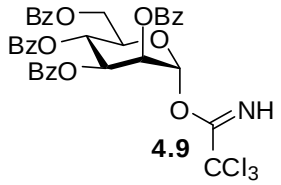

Compound **4.8** (5.0 g, 8.4 mmol), DBU (280 µL) and trichloroacetonitrile (10.3 mL, 22.4 mmol) were dissolved in DCM (40 mL) and stirred for 4 h at room temperature. DCM was evaporated and the residue was purified by column chromatography with EtOAc/Hexane (1:2) to yield 5.17 g (83.3%) of **4.9** as a white solid.^{1}H NMR (500 MHz, $CDCl_3$) δ 8.87 (s, 1H), 8.12 – 7.24 (Bz, 20H*), 6.58 (d, *J* = 1.9 Hz, 1H), 6.24 (t, *J* = 10.2 Hz, 1H), 5.98 (dd, *J* = 10.1, 3.3 Hz, 1H), 5.95 (dd, *J* = 3.3, 2.0 Hz, 1H), 4.73 (dd, *J* = 12.3, 2.5 Hz, 1H), 4.64 (ddd, *J* = 10.2, 4.0, 2.5 Hz, 1H), 4.51 (dd, *J* = 12.3, 4.2 Hz, 1H). HR-ESIMS calculated for $C_{36}H_{28}Cl_3NO_{10}Na$ $(M+Na)^+$ 762.0671, found 762.0659.

*Integrated upto 25 in H NMR due to insufficient relaxation time

Synthesis of 2, 3, 4, 6-Tetra-*O*-acetyl-α/ β-D-glucopyranoside (4.10):

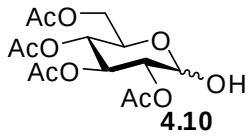

4.10

Penta-*O*-acetyl glucoside (2.9 g, 7.5 mmol), was treated with 3.5 mL of HBr/AcOH (33%) in 10 mL of DCM for 3 h and diluted to 30 mL with DCM. The solution was washed twice with 10 mL of saturated $NaHCO_3$, NaCl, and 6 mL DI water. The DCM was evaporated and the solid was dried under vacuum. The resulting white solid was dissolved in 10 mL acetone and 1.0 mL water with Ag_2CO_3 (1 g, 3.7 mmol) and stirred for 3 h. The solution was filtered through a pad of celite and dried under vacuum to give quantitative amount of **4.10** as a white solid.^{1}H NMR (498 MHz, $CDCl_3$) δ 5.52 (t, *J* = 10.0 Hz, 0.3H), 5.45 (t, *J* = 3.5 Hz, 0.3H), 5.24 (t, *J* = 9.6 Hz, 1H), 5.07 (t, *J* = 10.0 Hz, 1.3H), 4.88 (dd, *J* = 9.7, 8.1 Hz, 1.3H), 4.73 (t, *J* = 8.3 Hz, 1H), 4.28 – 4.20 (m, 1.7H), 4.17 – 4.10 (m, 1.3H), 3.83 (d, *J* = 8.7 Hz, 1H), 3.74 (ddd, *J* = 10.1, 4.8, 2.4 Hz, 1H), 3.54 (d, *J* = 3.3 Hz, 0.3H), 2.09 – 1.99 (CH_3, 15.5H). ^{13}C NMR (125 MHz, $CDCl_3$) δ 170.84, 170.8, 170.76, 170.2, 170.15, 170.1, 169.6, 169.5, 95.5, 90.1, 73.2, 72.2, 72.1, 71.08, 69.9, 68.5, 68.4, 67.2, 62.0, 61.95, 20.73, 20.71, 20.7, 20.66, 20.6, 20.57, 20.56. HR-ESIMS calculated for $C_1H_{20}O_{10}Na$ $(M+Na)^+$ 371.0949, found 371.0954.

Synthesis of 2, 3, 4, 6-Tetra-*O*-acetyl-D-glucopyranosyl trichloroacetamidate (4.11):

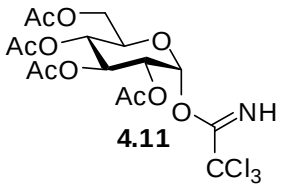

4.11

Compound **4.10** (1.6 g, 4.6 mmol), DBU (180 µL) and trichloroacetonitrile (2.8 mL, 27.6 mmol) were dissolved in DCM (15 mL) and stirred for 4 h at room temperature. DCM was evaporated and the residue was purified by column chromatography with EtOAc/Hexane (1:2) to yield 2.0 g

(89%) of **4.11** as a white solid.^{1}H NMR (498 MHz, $CDCl_3$) δ 8.69 (s, 1H), 6.56 (d, *J* = 3.7 Hz, 1H), 5.56 (t, *J* = 9.9 Hz, 1H), 5.18 (t, *J* = 10.0 Hz, 1H), 5.13 (dd, *J* = 10.2, 3.7 Hz, 1H), 4.27 (dd, *J* = 12.4, 4.2 Hz, 1H), 4.21 (ddd, *J* = 10.3, 4.1, 2.1 Hz, 1H), 4.13 (dd, *J* = 12.4, 2.2 Hz, 1H), 2.08 – 2.00 (4 CH_3 s, 12H).^{13}C NMR (125 MHz, $CDCl_3$) δ 170.5, 170.0, 169.8, 169.5, 160.8, 92.9, 90.7, 70.0, 69.9, 69.7, 67.8, 61.4, 20.7, 20.6, 20.4. HR-ESIMS calculated for $C_{16}H_{20}Cl_3NO_{10}Na$ $(M+Na)^+$ 514.0045, found 514.0032.

Synthesis of Benzyl (*S*)-1-[(*S*)-1,4-di(2, 3, 4, 6-tetra-*O*-benzoyl-β-D-galactopyranosyloxy) butan-2-ylamino]-5-(2, 3, 4, 6-tetra-*O*-benzoyl-β-D-galactopyranosyloxy)-1-oxopentan-2-ylcarbamate (4.15):

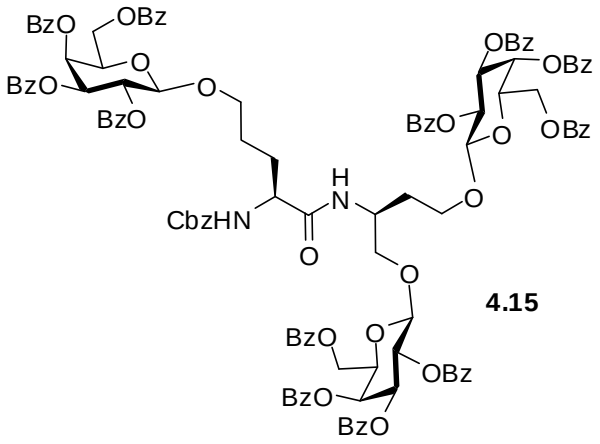

A solution of DCM (50 mL) was charged with compound **4.5** (35.4 mg, 0.1 mmol) and stirred for 1 h. Galactosyl-trichloroacetimidate donor **4.12** (266.7 mg, 0.36 mmol), TMSOTf (0.72 mL, 1% in DCM) were added and entire reaction mixture stirred for 2 d. The reaction mixture was concentrated and purified by column chromatography with EtOAc/Hexanes (1:1) to yield **4.15** as white solid (53%). HR-ESIMS calculated for $C_{119}H_{104}N_2O_{33}Na$ $(M+Na)^+$ 2111.6414, found 2111.6386.

Synthesis of 1, 2, 3, 4, 6-Penta-*O*-benzoyl-α/β-D-glucopyranoside (4.16):

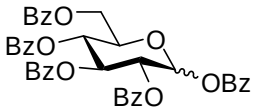

4.16

Benzoyl chloride (12.6 mL, 100 mmol) was added slowly to a suspension of mannose (3 g, 16.7 mmol) in 40 mL of pyridine and stirred at room temperature for 24 h under argon. Excess benzoyl chloride was quenched by adding 30 mL MeOH with cooling. The reaction mixture was concentrated under vacuum. The crude product was dissolved in DCM (25 mL) and washed with water (3 x 30 mL). The organic layer was dried over anhydrous Na_2SO_4. The solvent was evaporated under vacuum and the crude residue was purified by column chromatography using EtOAc/Hexane (1:2) to yield 10.8 g (92%) of **4.16** as a white solid. ^{1}H NMR (500 MHz, $CDCl_3$) δ 8.20 – 7.28 (Ar, 25H), 6.86 (d, *J* = 3.7 Hz, 1H), 6.33 (t, *J* = 10.0 Hz, 1H), 5.87 (t, *J* = 9.8 Hz, 1H), 5.69 (dd, *J* = 10.3, 3.8 Hz, 1H), 4.68 – 4.58 (m, 2H), 4.54 – 4.46 (m, 1H). ^{13}C NMR (126 MHz, $CDCl_3$) δ 166.1, 165.9, 165.4, 165.1, 164.4, 133.9, 133.5, 133.51, 133.4, 133.2, 130.1, 129.9, 129.9, 129.8, 129.76, 129.6, 129.1, 128.9, 128.8, 128.7, 128.6, 128.5, 128.43, 128.4, 90.1, 70.53, 70.5, 70.46, 68.9, 62.5.

Synthesis of 2, 3, 4, 6-Tetra-*O*-benzoyl-α/ β-D-glucopyranoside (4.17):

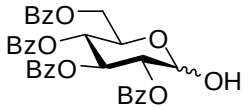

4.17

Penta-*O*-benzoyl glucoside, **4.16** (4.7 g, 6.7 mmol), was treated with 2.5 mL of HBr/AcOH (33%) in 20 mL of DCM for 1.4 h. The solution was washed twice with 20 mL of saturated $NaHCO_3$, NaCl, and 10 mL DI water. The DCM was evaporated and the solid was dried under vacuum. The resulting white solid was dissolved in 20 mL acetone and 1.1 mL water with

Ag_2CO_3 (0.93 g, 3.4 mmol) and stirred for 3.3 h. The solution was filtered through a pad of celite and dried under vacuum to afford quantitative amount of **4.17** as a white solid.

Synthesis of 2, 3, 4, 6-Tetra-*O*-benzoyl-D-glucopyranosyl trichloroacetamidate (4.18):

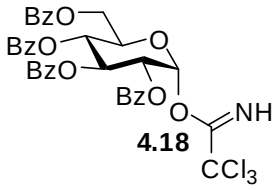

4.18

Compound **4.17** (3.9 g, 6.5 mmol), DBU (220 µL) and trichloroacetonitrile (8 mL, 17.4 mmol) were dissolved in DCM (40 mL) and stirred for 4 h at room temperature. DCM was evaporated and the residue was purified by column chromatography with EtOAc/Hexane (1:2) to yield 4.030 g (83%) of **4.18** as a white solid.

Synthesis of *N*-Cbz-Tris(hydroxymethyl)aminomethane (4.19):

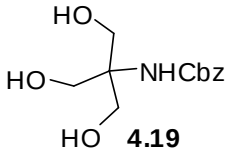

4.19

Benzylchloroformate (1.2 g, 7 mmol, 1.4 mL) was added drop wise into a stirred suspension of $NaHCO_3$ (0.88 g, 6.6 mmol) and tris(hydroxymethyl)aminomethane (1.0 g, 8.4 mmol) in H_2O (10 mL) and EtOAc (20 mL) at 0 ^oC and stirred for 5 h at room temperature. The solid was filtered off and the layers separated. The aqueous layer was extracted with EtOAc (3 X 20 mL) and the combined organic layers were washed with H_2O (20 mL) and concentrated. The residue was dissolved in diisopropyl ether (3.5 mL), cooled in an ice-bath and then filtered to give **4.19** as a white solid (1.92 g, 90%). ^1H NMR (400 MHz, CD_3OD) δ 7.43 – 7.22 (m, 5H), 5.04 (s, 2H), 3.73 (s, 6H).^{13}C NMR (101 MHz, CD_3OD) δ 157.8, 137.8, 129.1, 128.7, 128.6, 67.1, 62.2, 61.5. HR-ESIMS calculated for $C_{12}H_{17}NO_5Na$ $(M+Na)^+$ 278.0999, found 278.1002.

Synthesis of *N*-Cbz-Tris(2, 3, 4, 6-Tetra-*O*-benzoyl-α-D-mannopyranosyloxymethyl)-methylamine (4.20):

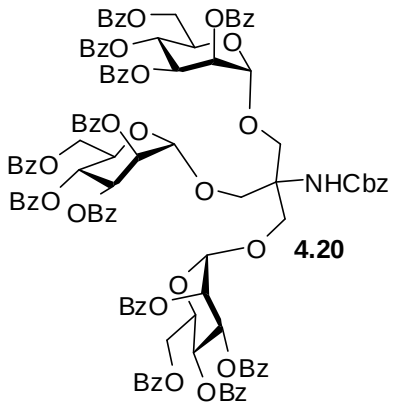

Compound **4.19** (255.1 mg, 1 mmol) and mannosyl trichloroacetimidate **4.9** (3.3 g, 4.5 mmol) were dissolved in 50 mL of DCM and cooled to 0 ^{o}C. Then $BF_3{\cdot}Et_2O$ (890 µL, 8.1 mmol) was added drop wise and entire reaction mixture was stirred at room temperature overnight. A saturated aq.solution of $NaHCO_3$ was added and organic layer was separated. The aqueous phase was extracted with DCM (3 X 100 mL) and combined organic layers were washed with brine (60 mL), dried over Na_2SO_4 and filtered. The filtrate was concentrated and purified by flash chromatography (EtOAc/Hexanes, 1:1) to yield **4.20** as a white solid (1.343 g, 68%). ^{1}H NMR (500 MHz, $CDCl_3$) δ 8.30 – 7.00 (Ar, 65H), 6.24 (t, *J* = 10.1 Hz, 3H), 5.96 (dd, *J* = 10.2, 3.3 Hz, 3H), 5.82 (dd, *J* = 3.2, 1.7 Hz, 3H), 5.37 (s, 1H), 5.33 (d, *J* = 1.6 Hz, 3H), 5.21 (s, 2H), 4.87 – 4.78 (m, 3H), 4.66 – 4.57 (m, 6H), 4.50 (d, *J* = 10.3 Hz, 3H), 4.11 (d, *J* = 10.4 Hz, 3H). ^{13}C NMR (126 MHz, $CDCl_3$) δ 166.2, 165.5, 165.4, 165.2, 155.2, 136.0, 133.3, 133.2, 133.1, 132.9, 130.1, 129.9, 129.8, 129.8, 129.7, 129.4, 129.1, 128.9, 128.6, 128.5, 128.4, 128.3, 128.2, 98.8, 70.3, 70.2, 69.6, 67.5, 67.2, 66.5, 62.6, 58.8.

Synthesis of *N*-Cbz-Tris(2, 3, 4, 6-Tetra-*O*-benzoyl-β-D-galactopyranosyloxymethyl)-methylamine (4.21):

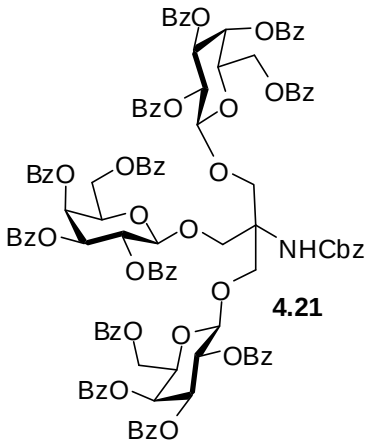

Compound **4.19** (255.1 mg, 1 mmol) and galactosyl trichloroacetimidate **4.12** (3.3 g, 4.5 mmol) were dissolved in 50 mL of DCM and cooled to 0 ^{o}C. Then $BF_3{\cdot}Et_2O$ (890 µL, 8.1 mmol) was added drop-wise and entire reaction mixture was stirred at room temperature overnight. A saturated aq solution of $NaHCO_3$ was added and organic layer was separated. Aqueous phase was extracted with DCM (3 X 100 mL) and combined organic layers were washed with brine (60 mL), dried over Na_2SO_4, filtered. The filtrate was concentrated and purified by flash chromatography (EtOAc/Hexanes, 1:1) to yield **4.21** as a white solid (1.319 g, 66%).^{1}H NMR (498 MHz, $CDCl_3$) δ 8.17 – 7.17 (Ar, 65H), 5.84 (d, *J* = 3.6 Hz, 3H), 5.66 (dd, *J* = 10.4, 8.0 Hz, 4H), 5.34 (dd, *J* = 10.4, 3.6 Hz, 3H), 4.79 (d, *J* = 12.0 Hz, 1H), 4.69 (d, *J* = 11.7 Hz, 1H), 4.48 (dd, *J* = 11.3, 6.6 Hz, 3H), 4.38 (dd, *J* = 11.3, 6.7 Hz, 3H), 4.33 (d, *J* = 10.7 Hz, 3H), 4.05 (d, *J* = 8.0 Hz, 3H), 3.71 (t, *J* = 6.8 Hz, 3H), 3.60 (d, *J* = 10.8 Hz, 3H). ^{13}C NMR (125 MHz, $CDCl_3$) δ 165.9, 165.6, 165.4, 164.8, 154.8, 136.4, 129.5, 129.45, 129.0, 128.8, 114.7, 101.9, 71.2, 71.16, 69.9, 68.5, 67.9, 61.8, 58.8. HR-ESIMS calculated for $C_{114}H_{95}NO_{32}Na$ $(M+Na)^+$ 2012.5729, found 2012.5708.

Synthesis of *N*-Cbz-Tris(2, 3, 4, 6-Tetra-*O*-benzoyl-β-D-glucopyranosyloxymethyl)-methylamine (4.22):

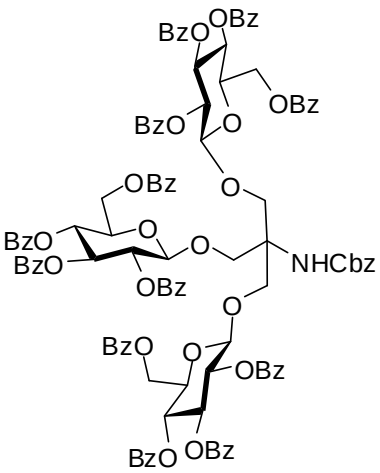

Compound **4.19** (306.2 mg, 1.2 mmol) and glucosyl trichloroacetimidate **4.18** (4 g, 5.4 mmol) were dissolved in 50 mL of DCM and cooled to 0 ^{o}C. Then $BF_3{\cdot}Et_2O$ (1.1 mL, 9.7 mmol) was added drop wise and entire reaction mixture was stirred at room temperature overnight. A saturated aq.solution of $NaHCO_3$ was added and organic layer was separated. The aqueous phase was extracted with DCM (3 x 100 mL) and combined organic layers were washed with brine (60 mL), dried over Na_2SO_4, filtered. The filtrate was concentrated and purified by flash chromatography (EtOAc/Hexanes, 1:1) to yield **4.22** as a white solid (1.643 g, 69%).^{1}H NMR (498 MHz, $CDCl_3$) δ 8.22 – 7.19 (Ar, 65H), 5.59 (t, *J* = 9.7 Hz, 4H), 5.45 (t, *J* = 9.7 Hz, 3H), 5.30 (dd, *J* = 9.8, 8.0 Hz, 3H), 4.82 (d, *J* = 12.1 Hz, 1H), 4.77 (d, *J* = 11.9 Hz, 1H), 4.50 (dd, *J* = 12.1, 2.9 Hz, 3H), 4.32 (dd, *J* = 12.1, 5.8 Hz, 3H), 4.24 (d, *J* = 10.7 Hz, 3H), 3.99 (d, *J* = 7.9 Hz, 3H), 3.60 – 3.44 (m, 6H). ^{13}C NMR (125 MHz, $CDCl_3$) δ 166.1, 165.7, 165.1, 164.6, 154.9, 136.5, 133.7, 133.5, 133.3, 133.2, 130.0, 129.8, 129.8, 129.7, 129.6, 129.4, 129.0, 128.9, 128.86, 128.6, 128.57, 128.5, 128.47, 128.4, 101.5, 72.5, 71.9, 71.8, 69.5, 68.5, 66.2, 63.1, 58.9. HR-ESIMS calculated for $C_{114}H_{95}NO_{32}Na$ $(M+Na)^+$ 2012.5729, found 2012.5721.

Synthesis of *N*-Cbz-Tris(α-D-mannopyranosyloxymethyl)-methylamine (4.23):

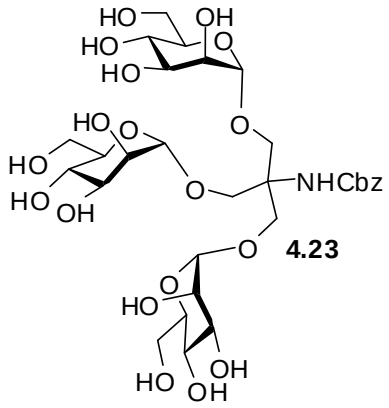

To a suspension of **4.20** (900 mg, 0.45 mmol) in 10 mL MeOH, 18 mL of 1% NaOMe/MeOH was added and stirred at room temperature for 6 h. The reaction mixture was neutralized with Amberlite IR-120 (H^+ form) ion exchange resin and filtered. Then the solvents were removed under reduced pressure and the residue was dissolved in 10 mL H_2O, washed with Et_2O (3 x 6 mL). The aqueous layer was concentrated and dried on vacuum to afford **4.23** as white solid (304 mg, 91%).^{1}H NMR (498 MHz, D_2O) δ 7.54 – 7.26 (m, 5H), 5.08 (s, 2H), 3.91 – 3.86 (m, 6H), 3.82 (dd, *J* = 12.2, 2.2 Hz, 3H), 3.76 (dd, *J* = 9.5, 3.4 Hz, 3H), 3.71 (dd, *J* = 12.2, 5.8 Hz, 3H), 3.66 (d, *J* = 10.0 Hz, 3H), 3.62 (t, *J* = 9.7 Hz, 4H), 3.59 – 3.53 (m, 3H). ^{13}C NMR (125 MHz, D_2O) δ 162.4, 137.3, 129.7, 129.3, 128.5, 101.2, 73.9, 71.5, 70.8, 67.5, 66.7, 66.67, 61.8, 61.6, 59.3. HR-ESIMS calculated for $C_{30}H_{47}NO_{20}Na$ $(M+Na)^+$ 764.2584, found 764.2583.

Synthesis of *N*-Cbz-Tris(β -D-galactopyranosyloxymethyl)-methylamine (4.24):

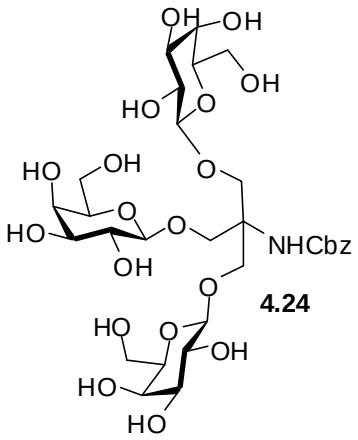

To a suspension of **4.20** (1.3 g, 0.65 mmol) in 10 mL MeOH, 26 mL of 1% NaOMe/MeOH was added and stirred at room temperature for 6 h. The reaction mixture was neutralized with Amberlite IR-120 (H^+ form) ion exchange resin and filtered. The solvent was removed under reduced pressure and the residue was dissolved in 10 mL H_2O, washed with Et_2O (3 x 6 mL). The aqueous layer was concentrated and dried on vacuum to afford **4.24** as white solid (445 mg, 92%).^{1}H NMR (498 MHz, D_2O) δ 7.47 – 7.37 (Ar, 5H), 5.10 (d, *J* = 12.3 Hz, 1H), 5.05 (d, *J* = 12.7 Hz, 1H), 4.31 (d, *J* = 7.7 Hz, 3H), 4.16 (d, *J* = 10.7 Hz, 3H), 3.92 – 3.85 (m, 6H), 3.74 (dd, *J* = 11.7, 7.7 Hz, 3H), 3.69 (dd, *J* = 11.7, 4.6 Hz, 3H), 3.59 – 3.54 (m, 6H), 3.50 (dd, *J* = 9.9, 7.7 Hz, 3H). ^{13}C NMR (125 MHz, D_2O) δ 137.3, 129.7, 129.3, 129.0, 104.5, 76.0, 73.4, 71.6, 69.0, 63.8, 61.8, 59.7.

Synthesis of Tris(α-D-mannopyranosyloxymethyl)-methylamine (4.25):

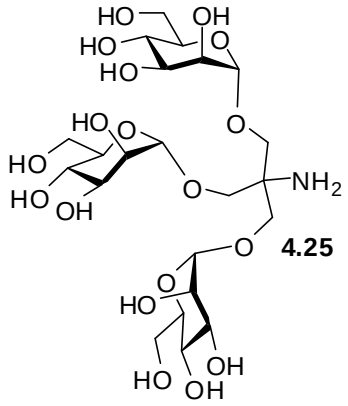

A catalytic amount of Pd on activated charcoal was added to the Cbz-protected trimannosyl cluster **4.23** (280 mg, 0.38 mmol), dissolved in 10 mL MeOH. The reaction mixture was stirred at room temperature under H_2 balloon for 20 h, then filtered through celite and concentrated to yield **4.25** as white solid (215 mg, 93%).^{1}H NMR (498 MHz, D_2O) δ 4.91 – 4.76 (m, 3H), 3.99 – 3.96 (m, 3H), 3.87 (d, *J* = 11.4 Hz, 3H), 3.80 (dd, *J* = 8.5, 3.4 Hz, 3H), 3.77 – 3.69 (m, 6H), 3.67 – 3.53 (m, 6H), 3.43 (d, *J* = 9.9 Hz, 3H). ^{13}C NMR (125 MHz, D_2O) δ 101.2, 82.6, 73.8, 71.5, 70.8, 69.6, 67.7, 61.8. HR-ESIMS calculated for $C_{22}H_{41}NO_{18}Na$ $(M+Na)^+$ 630.2216, found 630.2216.

Synthesis of Tris(β -D-galactopyranosyloxymethyl)-methylamine (4.26):

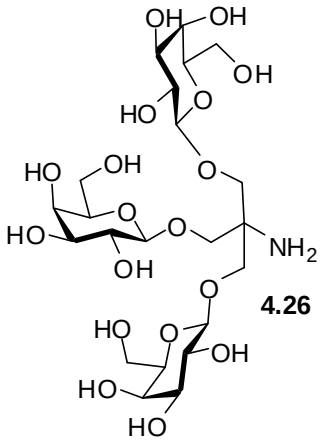

A catalytic amount of Pd on activated charcoal was added to the Cbz-protected trigalactosyl cluster **4.24** (403 mg, 0.54 mmol), dissolved in 10 mL MeOH. The reaction mixture was stirred at room temperature under H_2 balloon for 1 d, then filtered through celite and concentrated to yield **4.25** as a white solid (310 mg, 94%).^{1}H NMR (498 MHz, D_2O) δ 4.38 (d, *J* = 7.8 Hz, 3H), 3.93 (d, *J* = 10.5 Hz, 3H), 3.90 (dd, *J* = 3.4, 0.6 Hz, 3H), 3.77 (dd, *J* = 11.7, 7.9 Hz, 3H), 3.72 (dd, *J* = 11.7, 4.4 Hz, 3H), 3.70 – 3.65 (m, 6H), 3.63 (dd, *J* = 10.0, 3.5 Hz, 3H), 3.53 (dd, *J* = 10.0, 7.8 Hz, 3H). ^{13}C NMR (125 MHz, $CDCl_3$) δ 106.1, 77.6, 75.1, 73.3, 73.0, 71.2, 63.5, 58.6. HR-ESIMS calculated for $C_{22}H_{41}NO_{18}Na$ $(M+Na)^+$ 630.2216, found 630.2224.

Synthesis of 3-oxo-1-phenyl-2,7,10,13-tetraoxa-4-azahexadecan-16-succinimidate (4.28):

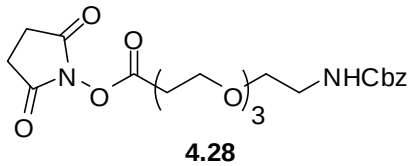

4.28

To a solution of 3-oxo-1-phenyl-2,7,10,13-tetraoxa-4-azahexadecan-16-oic acid, **4.27**, (391 mg, 1.1 mmol) and EDCI (1.368 g, 1.3 mmol) in DCM (10 mL), NHS (753 mg, 1.2 mmol) was added and stirred for one day. The reaction mixture was concentrated under reduced pressure then extracted with mixture of DCM and H_2O (50 mL). The organic layer was dried over anhydrous Na_2SO_4, concentrated under vacuum. The residue was purified by flash column chromatography (2:1 hexane/EtOAc) to afford **4.28** as a colorless oily liquid (389 mg, 82%).^{1}H NMR (500 MHz, $CDCl_3$) δ 7.37 – 7.27 (m, 5H), 5.37 (s, 1H), 5.08 (s, 2H), 3.79 (t, *J* = 6.3 Hz, 2H), 3.65 – 3.57 (m, 8H), 3.55 (t, *J* = 5.0 Hz, 2H), 3.41 – 3.31 (m, 2H), 2.84 (t, *J* = 6.3 Hz, 2H), 2.77 (s, 4H). ^{13}C NMR (126 MHz, $CDCl_3$) δ 169.0, 166.8, 156.5, 136.7, 128.5, 128.2, 128.1, 70.7, 70.6, 70.5, 70.3, 70.0, 66.6, 65.7, 40.9, 32.2, 25.6.

Synthesis of benzyl 15-hydroxy-14,14-bis(hydroxymethyl)-12-oxo-3,6,9-trioxa-13-azapentadecylcarbamate (4.29):

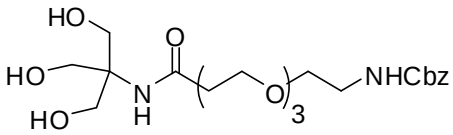

4.29

To a solution of trizma base (121 mg, 1 mmol) in dioxane:water (15 mL, 3:2) was added compound **4.28** (382 mg, 0.85 mmol), two drops of aq.saturated $NaHCO_3$ (pH of the reaction mixture around 8) and stirred for 1 d. The reaction mixture was concentrated and the residue was purified by flash chromatography using EtOAc/MeOH (9:1) to afford **4.29** as a colorless oily liquid (303 mg, 78%).^{1}H NMR (500 MHz, $CDCl_3$) δ 7.38 – 7.26 (m, 5H), 5.86 (s, 1H), 5.09 (s, 2H), 4.34 (s, 3H), 3.79 – 3.46 (m, 18H), 3.45 – 3.28 (m, 2H), 2.48 (t, J = 5.4 Hz, 2H). ^{13}C NMR (126 MHz, $CDCl_3$) δ 173.4, 156.7, 136.6, 128.5, 128.2, 128.1, 70.5, 70.2, 70.0, 67.2, 66.7, 63.5, 61.5, 40.8, 37.5. HR-ESIMS calculated for $C_{21}H_{34}N_2O_9Na$ $(M+Na)^+$ 481.2157, found 481.2151.

Synthesis of Benzyl 15-(2, 3, 4, 6-Tetra-*O*-benzoyl-β-D-galactopyranosyloxy)-14,14-bis(2, 3, 4, 6-Tetra-*O*-benzoyl-β-D-galactopyranosyloxymethyl)-12-oxo-3,6,9-trioxa-13-azapentadecylcarbamate (4.30):

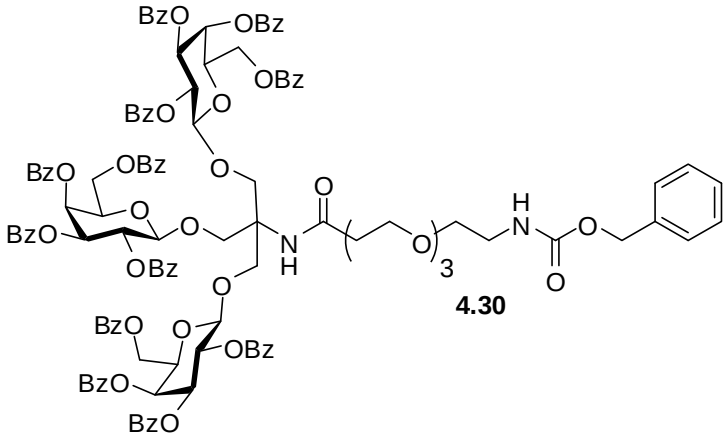

4.30

Compound **4.29** (76.3 mg, 0.17 mmol) and galactosyl trichloroacetimidate **4.12** (561 mg, 0.77 mmol) were dissolved in 20 mL of DCM and cooled to 0 ^{o}C. Then $BF_3{\cdot}Et_2O$ (151 µL, 1.37 mmol) was added drop-wise and entire reaction mixture was stirred at room temperature overnight. A saturated aq solution of $NaHCO_3$ was added and organic layer was separated. The aqueous phase was extracted with DCM (3 X 25 mL) and combined organic layers were washed with brine (10 mL), dried over Na_2SO_4, filtered. The filtrate was concentrated and purified by flash chromatography (EtOAc/Hexanes, 2:1) to yield **4.30** as a white solid (230 mg, 63%).^{1}H NMR (500 MHz, $CDCl_3$) δ 8.28 – 7.16 (Ar, 65H), 6.23 (s, 1H), 5.85 (d, *J* = 3.4 Hz, 3H), 5.65 (dd, *J* = 10.4, 8.0 Hz, 3H), 5.49 – 5.34 (m, 4H), 5.09 (s, 2H), 4.52 (dd, *J* = 11.2, 6.2 Hz, 3H), 4.42 (d, *J* = 10.2 Hz, 2H), 4.36 (dd, *J* = 11.2, 7.3 Hz, 3H), 4.15 (d, *J* = 8.0 Hz, 3H), 3.73 (t, *J* = 6.8 Hz, 2H), 3.70 – 3.45 (m, 17H), 3.43 – 3.29 (m, 3H), 2.20 (qd, *J* = 15.1, 7.3 Hz, 2H). ^{13}C NMR (126 MHz, $CDCl_3$) δ 171.4, 165.9, 165.6, 165.43, 164.9, 156.5, 136.7, 133.7, 133.6, 133.4, 133.3, 130.0, 129.9, 129.7, 129.5, 129.4, 129.04, 129.0, 128.8, 128.7, 128.6, 128.5, 128.3, 128.1, 128.0, 101.8, 71.2, 71.1, 70.5, 70.3, 70.0, 69.96, 68.1, 67.9, 67.0, 66.6, 61.5, 59.5, 40.9, 37.4.

Synthesis of Benzyl 15-(β-D-galactopyranosyloxy)-14,14-bis(β-D-galactopyranosyloxymethyl)-12-oxo-3,6,9-trioxa-13-azapentadecylcarbamate (4.31):

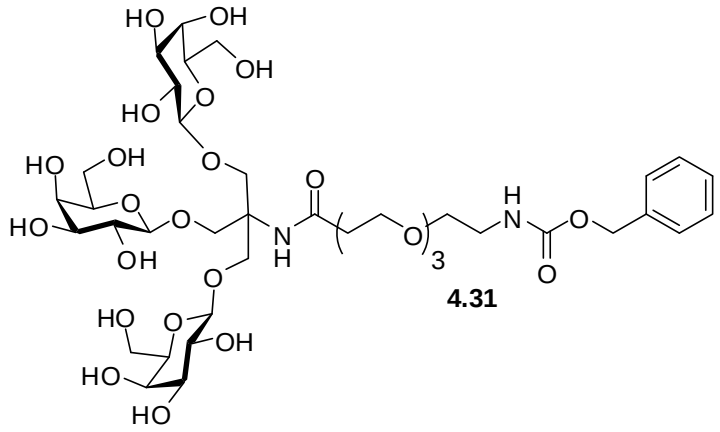

4.31

To a suspension of **4.30** (217 mg, 0.099 mmol) in 6 mL MeOH, 4 mL of 1% NaOMe/MeOH was added and stirred at room temperature for 6 h. The reaction mixture was neutralized with Amberlite IR-120 (H^+ form) ion exchange resin and filtered. Then the solvents were removed under reduced pressure and the residue was dissolved in 10 mL H_2O, washed with Et_2O (3 x 6 mL). Aqueous layer was concentrated and dried on vacuum to afford **4.31** as a white solid (84 mg, 90%). ^{1}H NMR (498 MHz, CD3OD) δ 7.54 – 7.12 (m, 5H), 5.06 (s, 2H), 4.27 (dd, *J* = 13.7, 9.0 Hz, 5H), 3.92 (d, *J* = 10.3 Hz, 3H), 3.80 (d, *J* = 2.8 Hz, 3H), 3.75 (dd, *J* = 11.3, 6.9 Hz, 3H), 3.72 – 3.66 (m, 6H), 3.65 – 3.55 (m, 10H), 3.55 – 3.47 (m, 8H), 3.44 (dd, *J* = 9.7, 3.3 Hz, 3H), 2.56 – 2.30 (m, 2H). ^{13}C NMR (125 MHz, CD_3OD) δ 174.2, 138.4, 129.5, 129.0, 128.9, 105.5, 76.7, 75.0, 72.6, 71.5, 71.5, 71.3, 71.25, 71.0, 70.3, 69.5, 68.3, 67.5, 62.6, 61.3, 41.8, 38.4.

Synthesis of 15-(β-D-galactopyranosyloxy)-14,14-bis(β-D-galactopyranosyloxymethyl)-12-oxo-3,6,9-trioxa-13-azapentadecylamine (4.32):

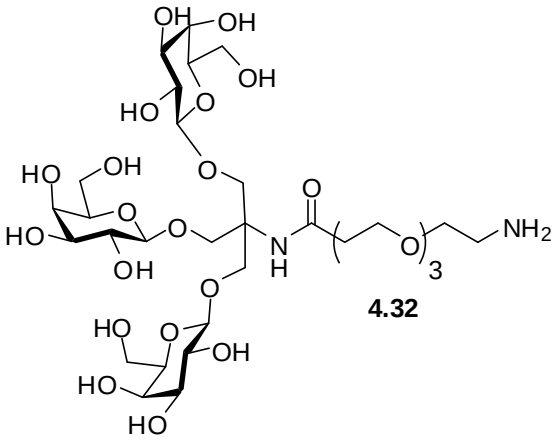

4.32

A catalytic amount of Pd on activated charcoal was added to the Cbz-protected trigalactosyl cluster **4.31** (73.8 mg, 0.078 mmol), dissolved in 6 mL MeOH. The reaction mixture was stirred at room temperature under a H_2 balloon for 1 d, then filtered through celite and concentrated to yield **4.32** as a white solid (63.3 mg, 95%).^{13}C NMR (125 MHz, D_2O) δ 174.9, 104.4, 82.6, 76.0,

73.4, 71.61, 70.5, 70.4, 70.3, 69.5, 68.6, 67.5, 61.8, 60.8, 48.0, 40.3, 37.3. HR-ESIMS calculated for $C_{31}H_{58}N_2O_{22}Na$ $(M+Na)^+$ 833.3373, found 833.3371.

Synthesis of methyl 2-(diphenylphosphino)-4-[15-(β-D-galactopyranosyloxymethyl)-14,14-bis(β-D-galactopyranosyloxymethyl)-12-oxo-3,6,9-trioxa-13-azapentadecylcarbamoyl]benzoate (4.33):

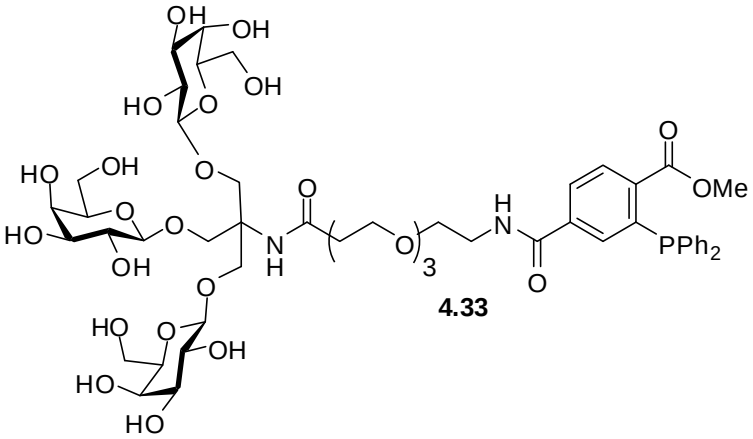

4.33

Compound **4.32** (27.1 mg, 0.03 mmol) was stirred with succinimidyl-3-diphenylphosphino-4-methoxy-carbonylbenzoate **4.1** (28 mg, 0.08 mmol), and two drops of triethylamine for 4 h at room temperature in DMF (5 mL). The solvent was removed under vacuum and the product was washed with dichloromethane to give 40 mg of crude residue. 5 mg of crude was purified by reverse phase column (*C*-18) chromatography with a gradient of H_2O and MeOH to yield 2.5 mg (51%) of **4.33** as a light yellow solid containing a small amount of the corresponding phosphine oxide. ^{1}H NMR (500 MHz, CD_3OD) δ 8.05 (dd, *J* = 8.0, 3.5 Hz, 1H), 7.81 (dd, *J* = 8.1, 1.6 Hz, 1H), 7.69 – 7.50 (m, 2H), 7.44 (dd, *J* = 3.9, 1.7 Hz, 1H), 7.41 – 7.31 (m, 8H), 7.30 – 7.21 (m, 5H), 4.28 (dd, *J* = 15.4, 9.0 Hz, 5H), 3.93 (d, *J* = 10.3 Hz, 3H), 3.81 (d, *J* = 3.2 Hz, 3H), 3.75 (dd, *J* = 11.3, 6.9 Hz, 4H), 3.72 – 3.64 (m, 10H), 3.64 – 3.42 (m, 23H), 2.57 – 2.31 (m, 2H). ^{13}C NMR (126 MHz, CD_3OD) δ 174.2, 169.4, 168.5, 142.3 (d, *J* = 28.8 Hz), 138.9, 138.6 (d, *J* = 10.0 Hz), 138.3 (d, *J* = 18.8 Hz), 135.1 (d, *J* = 21.3 Hz), 134.5, 131.6, 130.1, 129.7 (d, *J* = 7.5

Hz), 127.88, 105.52, 76.74, 74.97, 72.57, 71.54, 71.49, 71.32, 71.26, 70.36, 69.46, 68.30, 62.57, 61.33, 52.63, 41.01, 38.30, 30.76. ^{31}P NMR (161 MHz, CD_3OD) δ 34.90 (s, 0.15P), -3.24 (s, 1.00P)

4.14 References

1. Loka, R. S.; Sadek, C. M.; Romaniuk, N. A.; Cairo, C. W., Conjugation of synthetic N-acetyl-lactosamine to azide-containing proteins using the Staudinger ligation. *Bioconjug Chem.* **2010,** *21* (10), 1842-9.

2. Loka, R. S.; Cairo, C. W., Immobilization of carbohydrate epitopes for surface plasmon resonance using the Staudinger ligation. *Carbohydr. Res.* **2010,** *345* (18), 2641-7.

3. Courtney, A. H.; Puffer, E. B.; Pontrello, J. K.; Yang, Z. Q.; Kiessling, L. L., Sialylated multivalent antigens engage CD22 in trans and inhibit B cell activation. *Proc. Natl. Acad. Sci. U S A.* **2009,** *106* (8), 2500-5.

4. Kitov, P. I.; Mulvey, G. L.; Griener, T. P.; Lipinski, T.; Solomon, D.; Paszkiewicz, E.; Jacobson, J. M.; Sadowska, J. M.; Suzuki, M.; Yamamura, K.; Armstrong, G. D.; Bundle, D. R., In vivo supramolecular templating enhances the activity of multivalent ligands: a potential therapeutic against the Escherichia coli O157 AB5 toxins. *Proc. Natl. Acad. Sci. U S A.* **2008,** *105* (44), 16837-42.

5. Bertozzi, C. R.; Kiessling, L. L., Chemical glycobiology. *Science* **2001,** *291* (5512), 2357-64.

6. Lee, R. T.; Lee, Y. C., Affinity enhancement by multivalent lectin-carbohydrate interaction. *Glycoconj. J.* **2000,** *17* (7-9), 543-51.

7. Pieters, R. J., Maximising multivalency effects in protein-carbohydrate interactions. *Org. Biomol. Chem.* **2009,** *7* (10), 2013-25.

8. Pieters, R. J., Intervention with bacterial adhesion by multivalent carbohydrates. *Med. Res. Rev.* **2007,** *27* (6), 796-816.

9. Imberty, A.; Chabre, Y. M.; Roy, R., Glycomimetics and glycodendrimers as high affinity microbial anti-adhesins. *Chemistry* **2008,** *14* (25), 7490-9.

10. Chabre, Y. M.; Roy, R., Recent trends in glycodendrimer syntheses and applications. *Curr. Top. Med. Chem.* **2008,** *8* (14), 1237-85.

11. Mammen, M.; Choi, S. K.; Whitesides, G. M., Polyvalent Interactions in Biological Systems: Implications for Design and Use of Multivalent Ligands and Inhibitors. *Angew. Chem., Int. Ed. Engl.* **1998,** *37*, 2754-94.

12. Mangold, S. L.; Cloninger, M. J., Binding of monomeric and dimeric Concanavalin A to mannose-functionalized dendrimers. *Org. Biomol. Chem.* **2006,** *4* (12), 2458-65.

13. Cairo, C. W.; Gestwicki, J. E.; Kanai, M.; Kiessling, L. L., Control of multivalent interactions by binding epitope density. *J. Am. Chem. Soc.* **2002,** *124* (8), 1615-9.

14. Gestwicki, J. E.; Cairo, C. W.; Strong, L. E.; Oetjen, K. A.; Kiessling, L. L., Influencing receptor-ligand binding mechanisms with multivalent ligand architecture. *J. Am. Chem. Soc.* **2002,** *124* (50), 14922-33.

15. Woller, E. K.; Cloninger, M. J., The lectin-binding properties of six generations of mannose-functionalized dendrimers. *Org. Lett.* **2002,** *4* (1), 7-10.

16. Choi, S. K.; Mammen, M.; Whitesides, G. M., Monomeric inhibitors of influenza neuraminidase enhance the hemagglutination inhibition activities of polyacrylamides presenting multiple C-sialoside groups. *Chem. Biol.* **1996,** *3* (2), 97-104.

17. Page, D.; Zanini, D.; Roy, R., Macromolecular recognition: effect of multivalency in the inhibition of binding of yeast mannan to concanavalin A and pea lectins by mannosylated dendrimers. *Bioorg. Med. Chem.* **1996,** *4* (11), 1949-61.

18. Zanini, D.; Roy, R., Chemoenzymatic synthesis and lectin binding properties of dendritic N-acetyllactosamine. *Bioconjug Chem.* **1997,** *8* (2), 187-92.

19. Gao, Y.; Eguchi, A.; Kakehi, K.; Lee, Y. C., Efficient preparation of glycoclusters from silsesquioxanes. *Org. Lett.* **2004,** *6* (20), 3457-60.

20. Lee, R. T.; Lee, Y. C., Facile synthesis of a high-affinity ligand for mammalian hepatic lectin containing three terminal N-acetylgalactosamine residues. *Bioconjug Chem.* **1997,** *8* (5), 762-5.

21. Wilson, A. J.; Hong, J.; Fletcher, S.; Hamilton, A. D., Recognition of solvent exposed protein surfaces using anthracene derived receptors. *Org. Biomol. Chem.* **2007,** *5* (2), 276-85.

22. Heidelberg, T.; Martin, O. R., Synthesis of the glycopeptidolipid of Mycobacterium avium Serovar 4: first example of a fully synthetic C-mycoside GPL. *J. Org. Chem.* **2004,** *69* (7), 2290-301.

23. Schmidt, R. R.; Kinzy, W., Anomeric-oxygen activation for glycoside synthesis: the trichloroacetimidate method. *Adv. Carbohydr. Chem. Biochem.* **1994,** *50*, 21-123.

24. Dubber, M.; Sperling, O.; Lindhorst, T. K., Oligomannoside mimetics by glycosylation of 'octopus glycosides' and their investigation as inhibitors of type 1 fimbriae-mediated adhesion of Escherichia coli. *Org. Biomol. Chem.* **2006,** *4* (21), 3901-12.

25. Shaikh, H. A.; Sonnichsen, F. D.; Lindhorst, T. K., Synthesis of glycocluster peptides. *Carbohydr. Res.* **2008,** *343* (10-11), 1665-74.

26. Baldoli, C.; Rigamonti, C.; Maiorana, S.; Licandro, E.; Falciola, L.; Mussini, P. R., A new triferrocenyl-tris(hydroxymethyl)aminomethane derivative as a highly sensitive electrochemical marker of biomolecules: application to the labelling of PNA monomers and their electrochemical characterization. *Chemistry* **2006,** *12* (15), 4091-100.

27. Zemple´n, G.; Pacsu, E., Über die Verseifung acetylierter Zucker und verwandter Substanzen. *Ber. Dtsch. Chem. Ges.* **1929,** *62*, 1613-4.

Chapter 5

Conclusions and future work

5.1 Conclusions

Our methodology developed for generating carbohydrate-phosphane reagents was general and involves three important steps; Glycosylation of a suitable carbohydrate donor with an amine-linker followed by removal of all the protecting groups, and finally amine coupling to an activated ester of phosphane reagent, **4.1**. Introducing the phosphane reagent in activated ester form not only minimizes oxidation of phosphane, but also makes purification easier. We successfully synthesized galactose, lactose, LacNAc (**Chapter 2**)[1] and trigalactosyl-phosphane reagents (**Chapter 4**). An Fmoc-protected amine containing polyethyleneglycol (PEG) linker was used for the glycosylation in the synthesis of galactose, lactose, LacNAc phosphane reagents and Fmoc group was deprotected along with benzoyl or acetyl groups in a single step under Zemple´n conditions. However, the yields for the deprotection step were low. This may be due to acylation or benzoylation of the free amine. To overcome this, in the synthesis of trigalactosyl-phosphane reagent, we opted for a Cbz-protected amine scaffold. Removal of benzoyls or acetyls in the first step and Cbz-protection in the next step provided the desired compound in good yields.

These carbohydrate-phosphane reagents can be incorporated on any azide-modified surface or molecules by Staudinger ligation under mild conditions. An azide incorporated protein, β-lactoglobulin, was converted in to glycoprotein by using this ligation chemistry. Galactose-, lactose- and LacNac-phosphane reagents (**Chapter 2**) were immobilized on an azide-derivatized surface and found their binding specificity for different lectins using surface plasmon resonance (**Chapter 3**).[2] This strategy requires small amounts (in μM) of carbohydrate-phosphane reagents and preserves their binding specificity. One problem, we encountered during making an azide-derivitized surface was the solubility of succinimidyl 2-azidoacetate used for

acylating amine groups on the surface. However, solubility can be increased by using a PEG-derivatized azide containing succinimidyl-esters.

Synthesis of a suitable scaffold for multivalent display of carbohydrates was important step in making a triglycosyl-phosphane reagent. The amines of the triglycosyl-TRIS, **4.25** and **4.26** were difficult to acylate with the phosphane reagent, likely due to steric hindrance. In order to overcome this problem, a PEG linker was attached to the amine. This linker provides enough space between amine of the TRIS and phosphane reagent in final compound. The trimannosyl-, triglucosyl-phosphane reagents can be generated from trichloroacetamidate (TCA) donors of respective carbohydrates and an elongated TRIS (Tris(hydroxymethyl)aminomethane) scaffold, **4.29** by following similar sequence of reactions used in synthesis of trigalactosyl-phosphane reagent, **4.33**. In generating all the carbohydrate-phosphane reagents we observed minor oxidation of phosphorus. However phosphorus oxide compounds can be reduced to the phosphane with reducing agents such as trichlorosilane.[3]

5.2 Future directions

5.2.1 Synthesis of other derivatives of phosphane reagents

As mentioned earlier our synthetic strategy for making carbohydrate-phosphane reagents is simple and can be adopted for generating various derivatives. Any epitope of interest should be attached to a linker with amine which can be later acylatead with a phosphane reagent, **4.1**. We are planning to synthesize a polyLacNAc-phosphane reagent and charged-phosphane reagents.

5.2.1.1 Synthesis of polyLacNAc-phosphane reagent

We synthesized the LacNAc-phosphane reagent, as it is part of repeats of lactosamine units in N-linked and O-linked glycans.[4] However to mimic the exactly polyLacNAc units of

these glycans one could synthesize a triLacNAc-phosphane reagent such as **5.7**. This target can be generated from an oxazoline donor of lactosamine, **2.38**. The compound **2.38** can be converted into different donors and acceptors (**Scheme 5.1**).

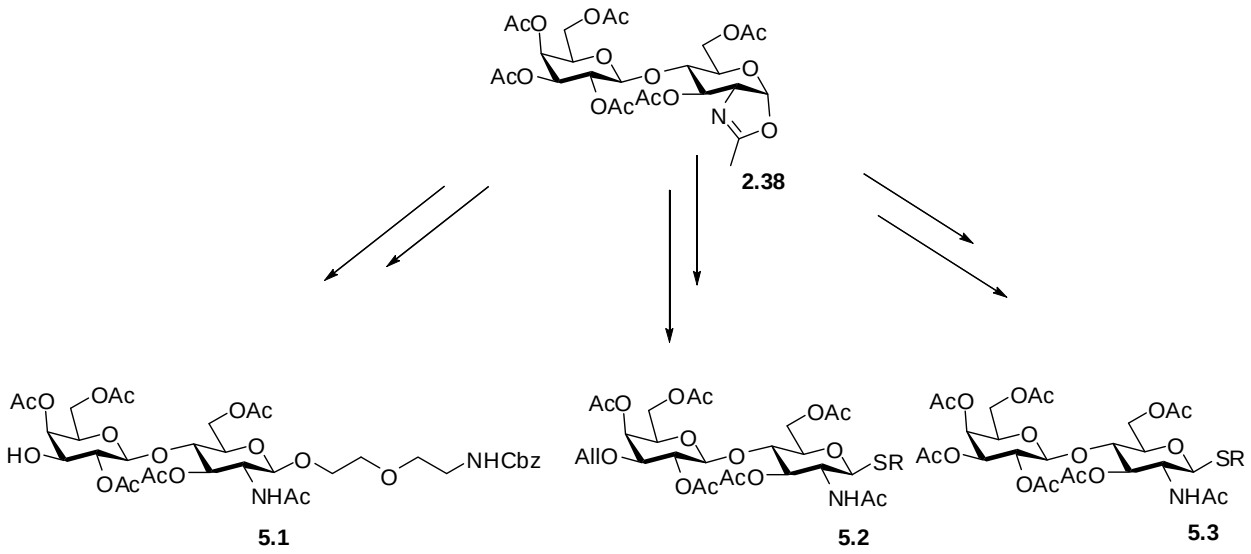

Scheme 5.1: Synthesis of different donors and acceptors from oxazoline, 2.38. Compound **2.38** can be modified into a thioldonors **5.2**, **5.3** and an acceptor **5.1**.

A linker attached acceptor such as **5.1** can be produced from **2.38** in five steps (**Scheme 5.2**). First glycosylation of **2.38** with Cbz protected linker followed by deprotection of acetyl groups under Zemplen conditions will provide **5.4**. Later selectively protecting 3-OH of galactose of deprotected compound **5.4** with allyl using dibutyltinether[5] followed by acylation will yield **5.5**. Selective deprotection of the allyl should give acceptor **5.1**.[5] Glycosylation of **2.38** with aromatic thiol should give donor **5.3**. Compound **5.3** can be converted into **5.2** by following similar route used to generate **5.5** from oxazoline **2.38**.

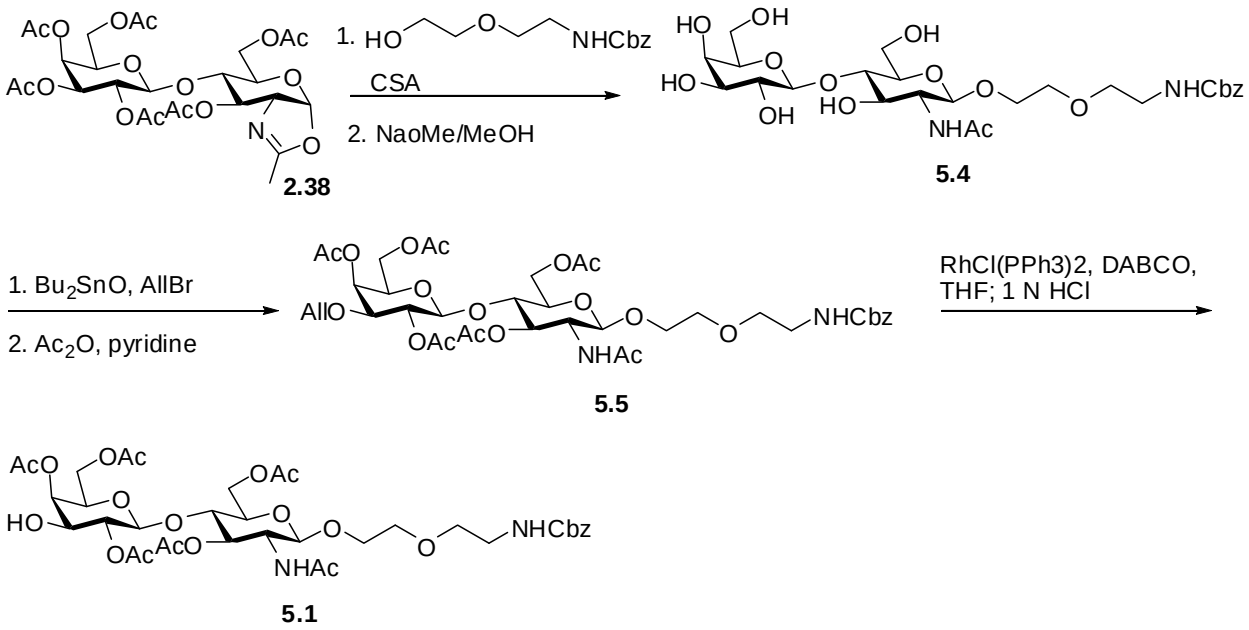

Scheme 5.2: Synthesis of acceptor from oxazoline 2.38. A selectively deprotectd 3-OH of galactose of lactosamine can be prepared from peracetylated oxazoline derivative **2.38**.

Glycosylation of the thio donor **5.2** with acceptor **5.1** by activating sulfur will give a tetra- saccharide. Deprotection of the allyl group of tetra-saccharide followed by glycosylation with donor **5.3** should give hexa-saccharide **5.6**. This can be converted into final compound **5.7** by deprotection of the acetyl and the Cbz group and coupling free amine to the phosphane reagent **4.1**. (**Scheme 5.3**).

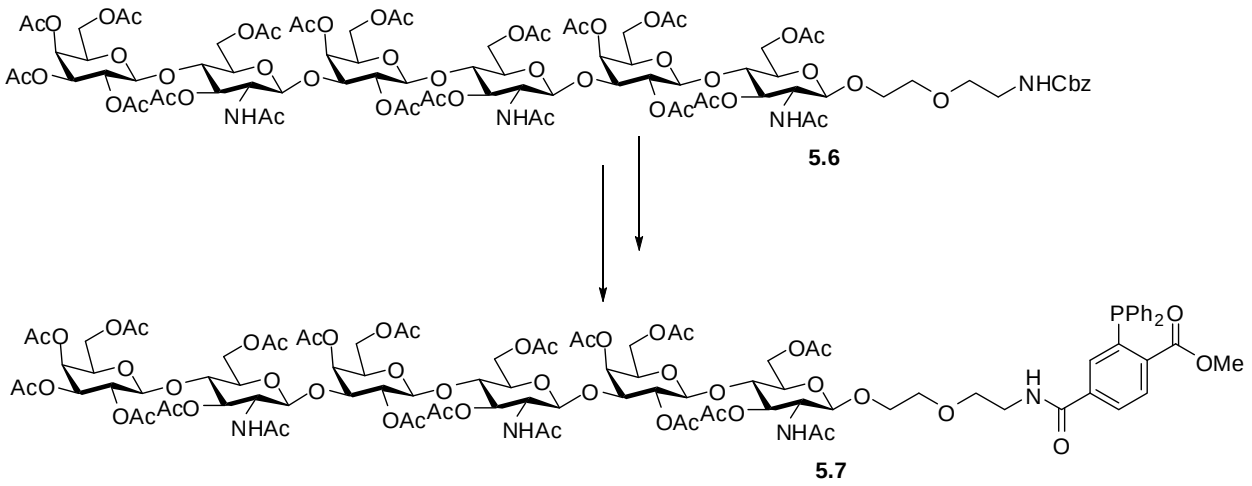

Scheme 5.3: Synthesis of triLacNAc-phosphane reagent 5.7 from linker attached hexasaccharide 5.6. Global deprotection of acetyl followed by Cbz and acylation of free amine with compound **4.1** will generate **5.7**.

5.2.1.2 Synthesis of charged-phosphane reagents

Introducing a cationic or anionic species on to the cell surface could change the properties of the cell surface. To test this hypothesis, desired charge attached phosphane reagents can be synthesized and can be incorporated onto an azide-containing sialic acid on the cell surface. A tri-anionic or cationic species can be generated from aminotriester **5.8**.[6] Coupling of **5.8** to phosphane reagent **4.1** followed by deprotection of ester groups under acidic conditions will give trianionic-phosphane reagent **5.9**. Aminotriester **5.8** can be modified into an Fmoc protected derivative **5.10** by known procedures.[6] A mono-Boc protected ethylene diamine can be coupled to triacid to give **5.11**. Deprotection of Fmoc, coupling of resulting free amine with phosphane reagent 4.1 follwed by deprotection of Boc will give tricationic-phosphane reagent **5.12** (**Scheme 5.4**).

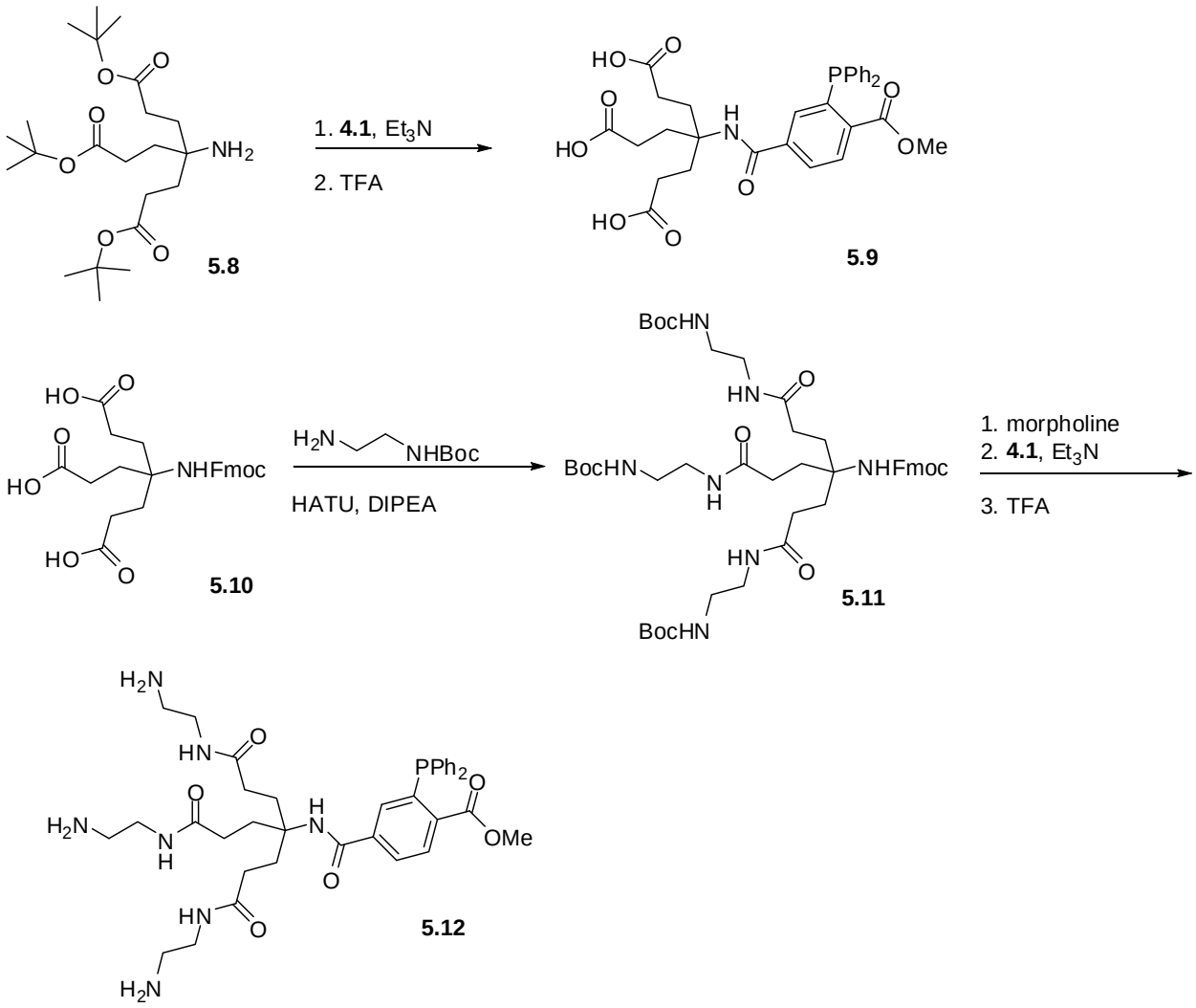

Scheme 5.4: Synthesis of anionic-, cationic-phosphane reagents. Boc deprotections are efficient, this strategy should not require further purification and the phosphane moiety is stable under these conditions.

5.2.2 Other bioorthogonal reactions

The Bertozzi-Staudinger ligation strategy employed for introducing carbohydrate epitopes on azide containing molecules will also introduce phenyl groups along with carbohydrates. Even though we didn't see any effect of the phenyl groups on binding of carbohydrates to the lectins (**Chapter 3**),[2] they might cause some steric hindrance and usually

they are not found in native habitats. In order to mimic nature, future work could synthesize carbohydrate-phosphane reagents based on the traceless Staudinger ligation, where the desired epitopes could be introduced without phenyl groups as discussed in **Chapter 1**.[7, 8] Recently Davis and co-workers[9] synthesized sugar-phosphane reagents for traceless Staudinger ligation and conjugated them onto azide containing proteins. However, this strategy has some limitations such as competing reduction of azide and sulfur interaction with phosphane. Low solubility of the reagent might have also increased azide reduction compared to amide bond formation. Sugar-phosphane reagents (**Figure 5.1**) with greater solubility in water for traceless Staudinger ligation could be accessed using a modification of our strategy in **Chapter 2**. Another reason for slow reaction might be thiol triphenyl which is not better leaving group and can be converted into a better leaving group by adding an electron withdrawing group para to thiol on aromatic ring.

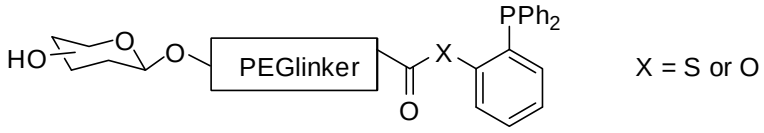

Figure 5.1: Carbohydrate-phosphane reagents for traceless-Staudinger ligation. These reagents will allow ligation of the desired carbohydrate epitopes without incorporating phenyl groups.

5.2.3 Modifying cell surface with phosphane reagents

As discussed in **Chapter 1**, our objective was to use this chemistry to introduce specific native carbohydrate epitopes onto a protein receptor in live cells and study their effects in a native environment. CD45 is a transmembrane protein tyrosine phosphatase, heavily

glycosylated and expressed exclusively on lymphocytes. Glycans, both N- and O-linked, on this receptor play integral part in its function.[10-12] Therefore altering the glycan will change its function, and the large number of CD45 molecules on the cell surface. It is known that galectin-1 binds to LacNAc epitopes[13] on CD45 leading to agglutination causing T-cell death.[14] LacNAc-

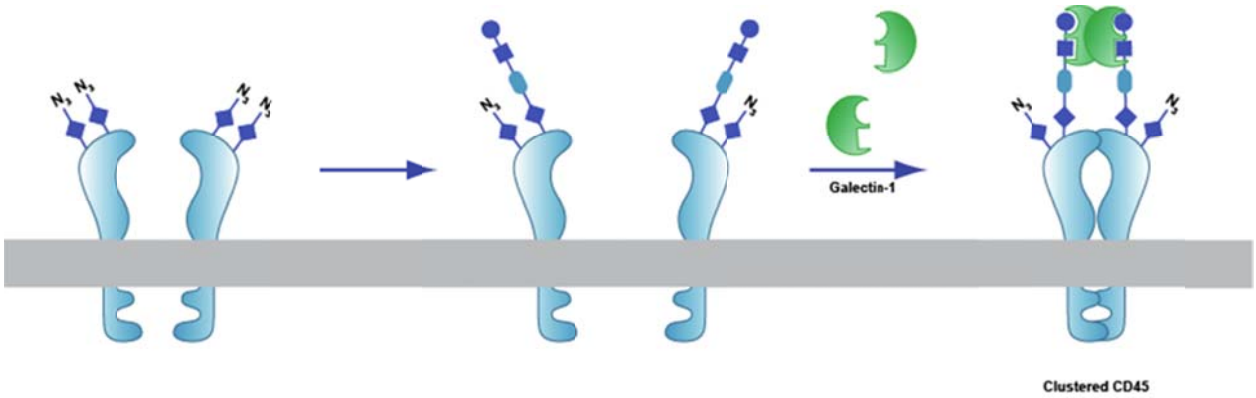

Figure 5.2: CD45 clustering hypothesis due to LacNAc epitope incorporation. LacNAc can be conjugated to metabolically azide incorporated CD45 by Staudinger ligation and it will interact with galectin-1 causing clustering of CD45.

phosphane reagent (**Chapter 2**) can be used to incorporate these moieties onto azide labeled CD45 by Staudinger ligation and study their binding interaction with galectin-1 (**Figure 5.2**). As mentioned earlier, due to heterogeneity of the glycan, it is difficult to know the function of a specific carbohydrate unit. However appending the epitope of interest to the existing glycan by Staudinger ligation should provide an opportunity to explore function by examining their interaction with native lectins. Multivalent carbohydrate-phosphane reagents designed here will enhance their interactions with the lectins thereby enhancing the effect of the modified glycan. We hope that this strategy of introducing specific native epitope onto the receptor in their native environment will serve as a potential tool for unraveling the function of the epitope of interest and designing new therapeutics

5.3 References

1. Loka, R. S.; Sadek, C. M.; Romaniuk, N. A.; Cairo, C. W., Conjugation of synthetic N-acetyl-lactosamine to azide-containing proteins using the Staudinger ligation. *Bioconjug Chem.* **2010,** *21* (10), 1842-9.

2. Loka, R. S.; Cairo, C. W., Immobilization of carbohydrate epitopes for surface plasmon resonance using the Staudinger ligation. *Carbohydr. Res.* **2010,** *345* (18), 2641-7.

3. Zhang, H.; Ma, Y.; Sun, X. L., Chemically-selective surface glyco-functionalization of liposomes through Staudinger ligation. *Chem. Commun. (Cambridge)* **2009,** (21), 3032-4.

4. Varki, A.; Cummings, R. D.; Esko, J.; Freeze, H. H.; Hart, G.; Marth, J., Essentials of Glycobiology. *Cold spring harbor laboratory press, Cold spring harbor, NY.* **1999**.

5. Wang, Z.-G.; Warren, J. D.; Dudkin, V. Y.; Zhang, X.; Iserloh, U.; Visser, M.; Eckhardt, M.; Seeberger, P. H.; Danishefsky, S. J., A highly convergent synthesis of an N-linked glycopeptide presenting the H-type 2 human blood group determinant. *Tetrahedron* **2006,** *62* (20), 4954-78.

6. Kleinert, M.; Röckendorf, N.; Lindhorst, T. K., Glyco-SAMs as glycocalyx mimetics: synthesis of L-fucose- and D-mannose-
terminated building blocks. *Eur. J. Org. Chem.* **2004**, 3931-40.

7. Saxon, E.; Armstrong, J. I.; Bertozzi, C. R., A "traceless" Staudinger ligation for the chemoselective synthesis of amide bonds. *Org. Lett.* **2000,** *2* (14), 2141-3.

8. Nilsson, B. L.; Kiessling, L. L.; Raines, R. T., Staudinger ligation: a peptide from a thioester and azide. *Org. Lett.* **2000,** *2* (13), 1939-41.

9. Bernardes, G. J.; Linderoth, L.; Doores, K. J.; Boutureira, O.; Davis, B. G., Site-Selective Traceless Staudinger Ligation for Glycoprotein Synthesis Reveals Scope and Limitations. *Chembiochem* **In press**.

10. Majeti, R.; Bilwes, A. M.; Noel, J. P.; Hunter, T.; Weiss, A., Dimerization-induced inhibition of receptor protein tyrosine phosphatase function through an inhibitory wedge. *Science* **1998,** *279* (5347), 88-91.

11. Irles, C.; Symons, A.; Michel, F.; Bakker, T. R.; van der Merwe, P. A.; Acuto, O., CD45 ectodomain controls interaction with GEMs and Lck activity for optimal TCR signaling. *Nat. Immunol.* **2003,** *4* (2), 189-97.

12. Earl, L. A.; Baum, L. G., CD45 glycosylation controls T-cell life and death. *Immunol. Cell Biol.* **2008,** *86* (7), 608-15.

13. Leppanen, A.; Stowell, S.; Blixt, O.; Cummings, R. D., Dimeric galectin-1 binds with high affinity to alpha2,3-sialylated and non-sialylated terminal N-acetyllactosamine units on surface-bound extended glycans. *J. Biol. Chem.* **2005,** *280* (7), 5549-62.

14. Pace, K. E.; Lee, C.; Stewart, P. L.; Baum, L. G., Restricted receptor segregation into membrane microdomains occurs on human T cells during apoptosis induced by galectin-1. *J. Immunol.* **1999,** *163* (7), 3801-11.

Appendix: Spectral data

^{1}H NMR (300 MHz, $CDCl_3$)

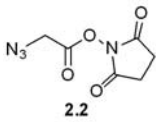

2.2

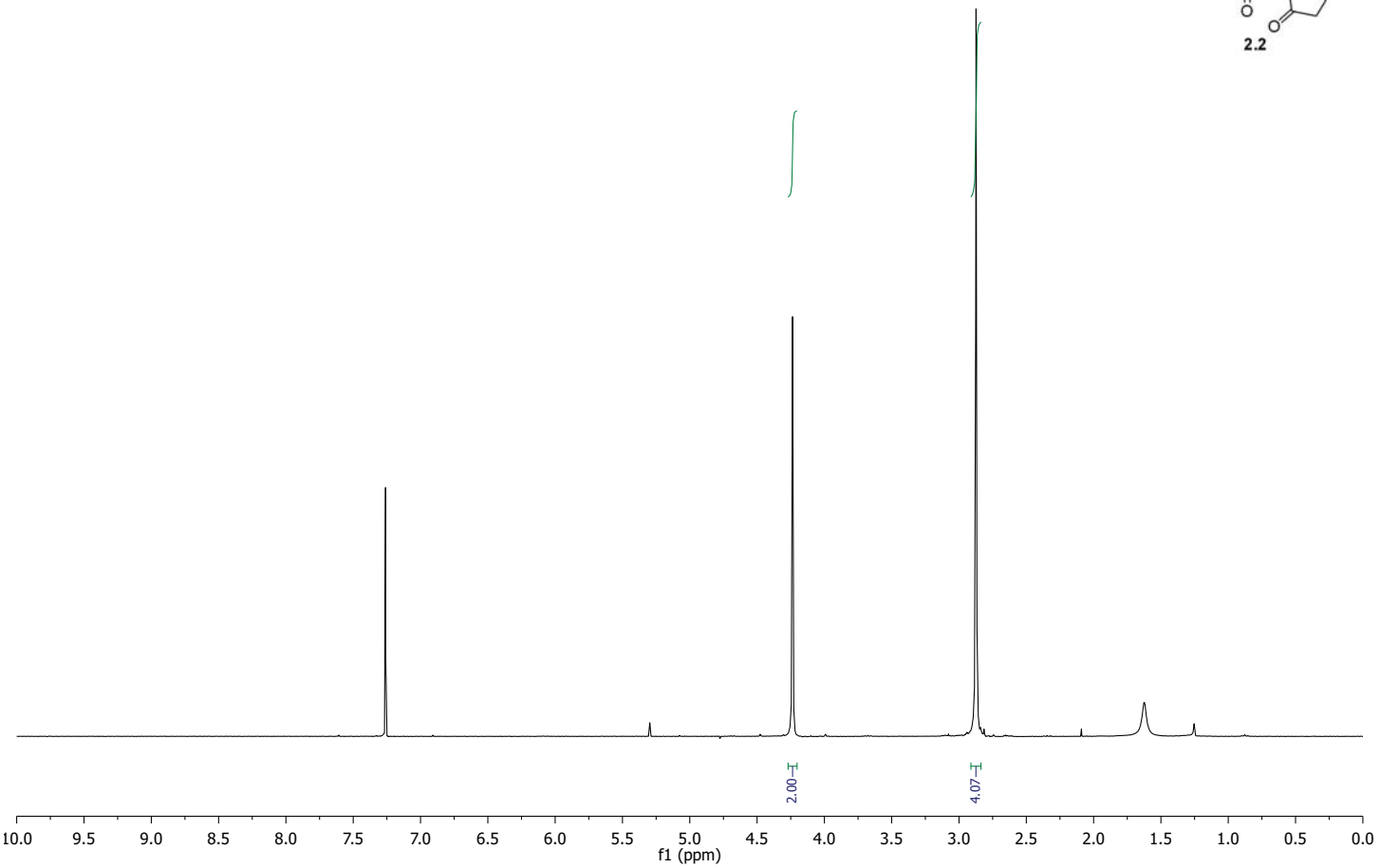

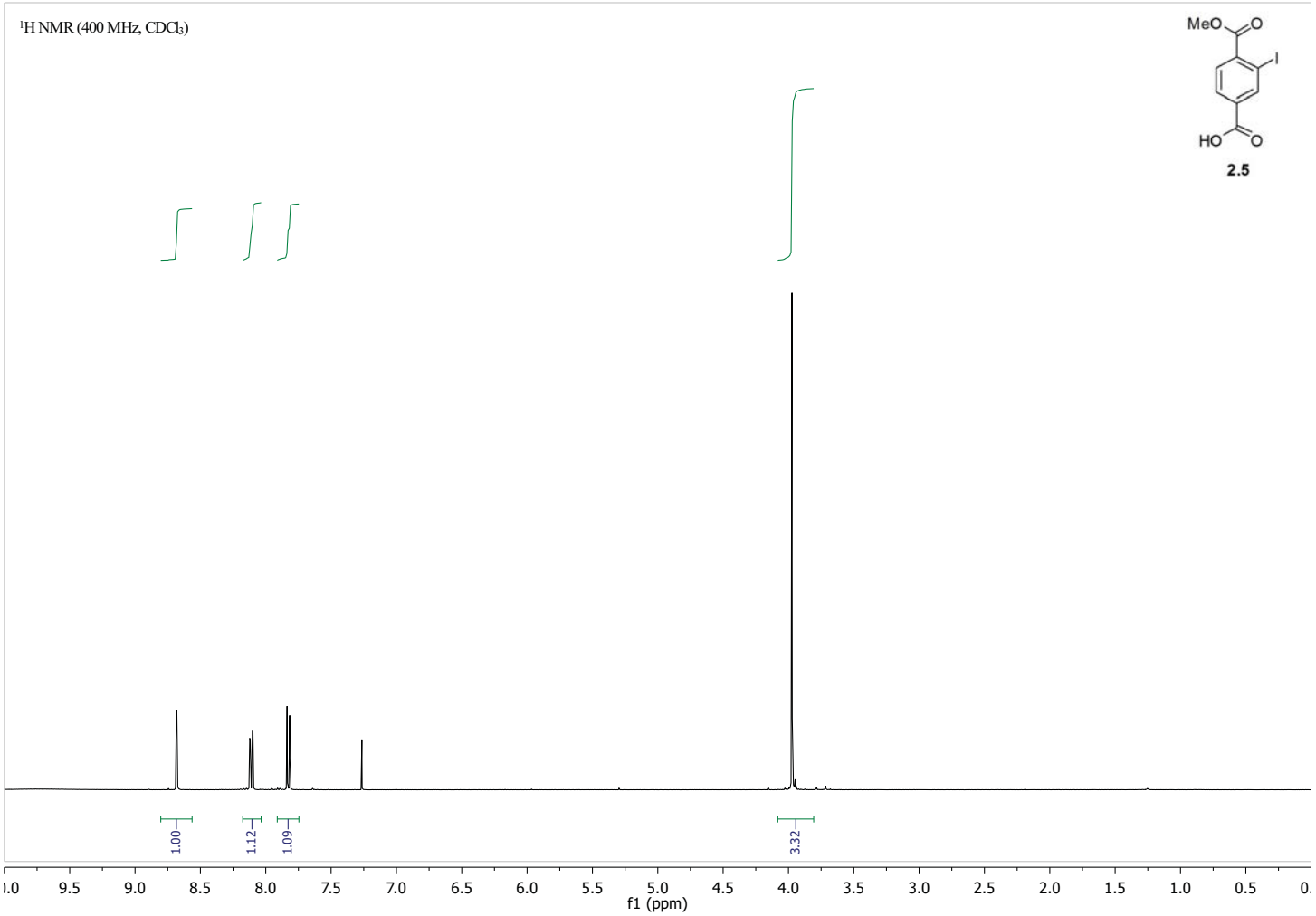
^{1}H NMR (400 MHz, $CDCl_3$)
MeO
O
I
HO
O
2.5
1.00
1.12
1.09
3.32
9.5
9.0
8.5
8.0
7.5
7.0
6.5
6.0
5.5
5.0
4.5
4.0
3.5
3.0
2.5
2.0
1.5
1.0
0.5
f1 (ppm)

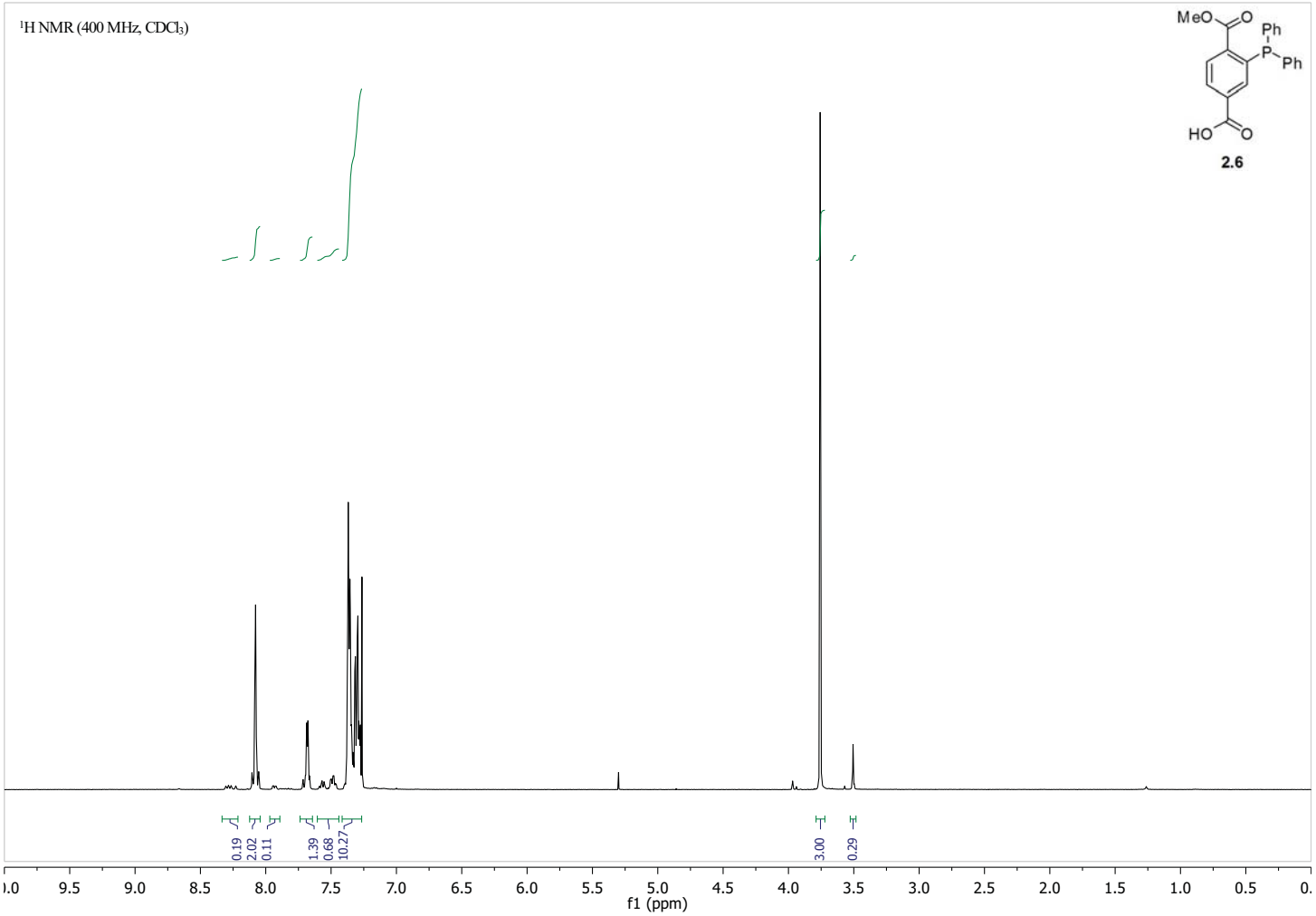
^{1}H NMR (400 MHz, $CDCl_3$)
MeO
O
Ph
P
Ph
HO
O
2.6
0.19
2.02
0.11
1.39
0.68
10.27
3.00
0.29
f1 (ppm)

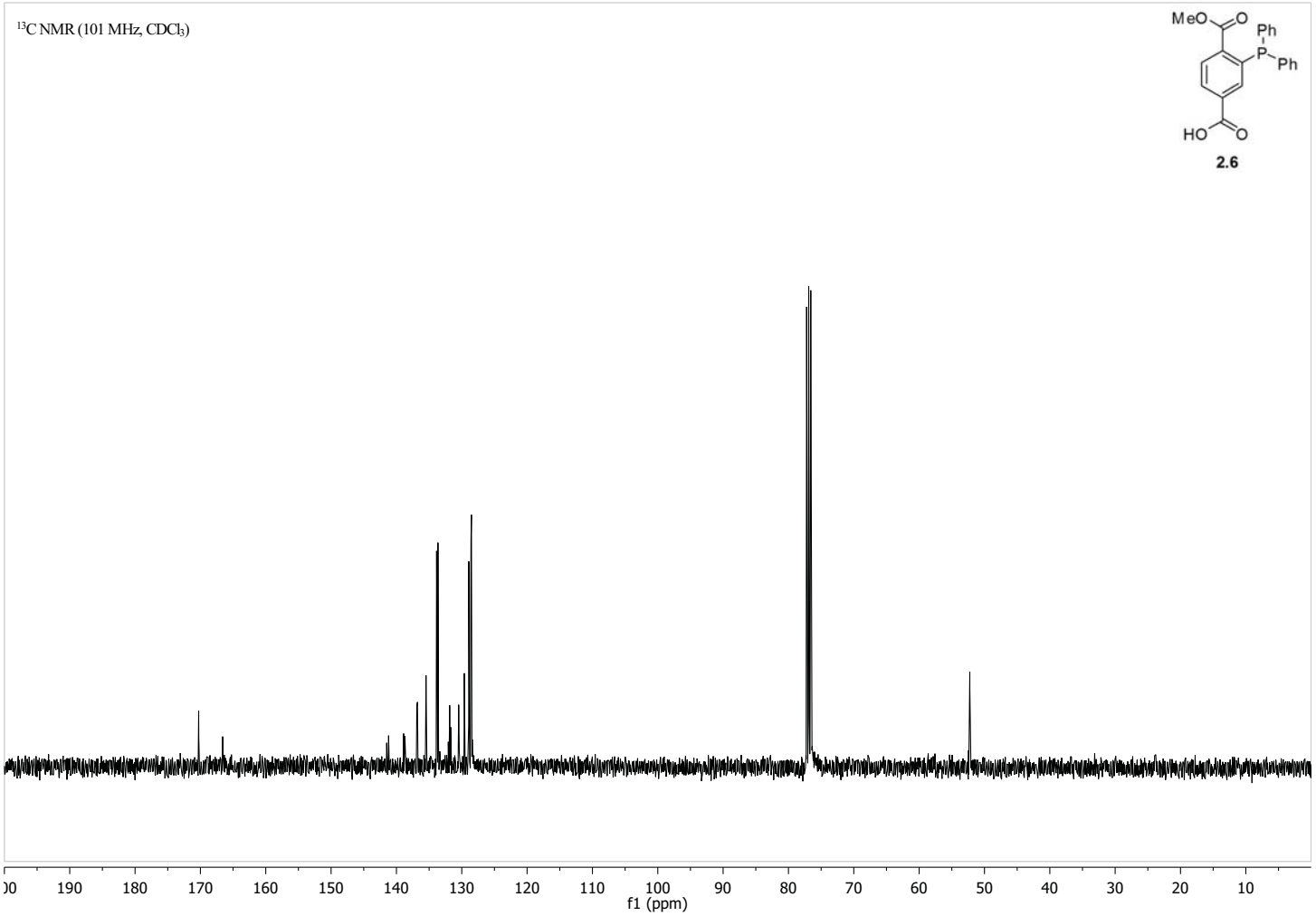
^{13}C NMR (101 MHz, $CDCl_3$)
MeO
O
Ph
P
Ph
HO
O
2.6
190
180
170
160
150
140
130
120
110
100
90
80
70
60
50
40
30
20
10
f1 (ppm)

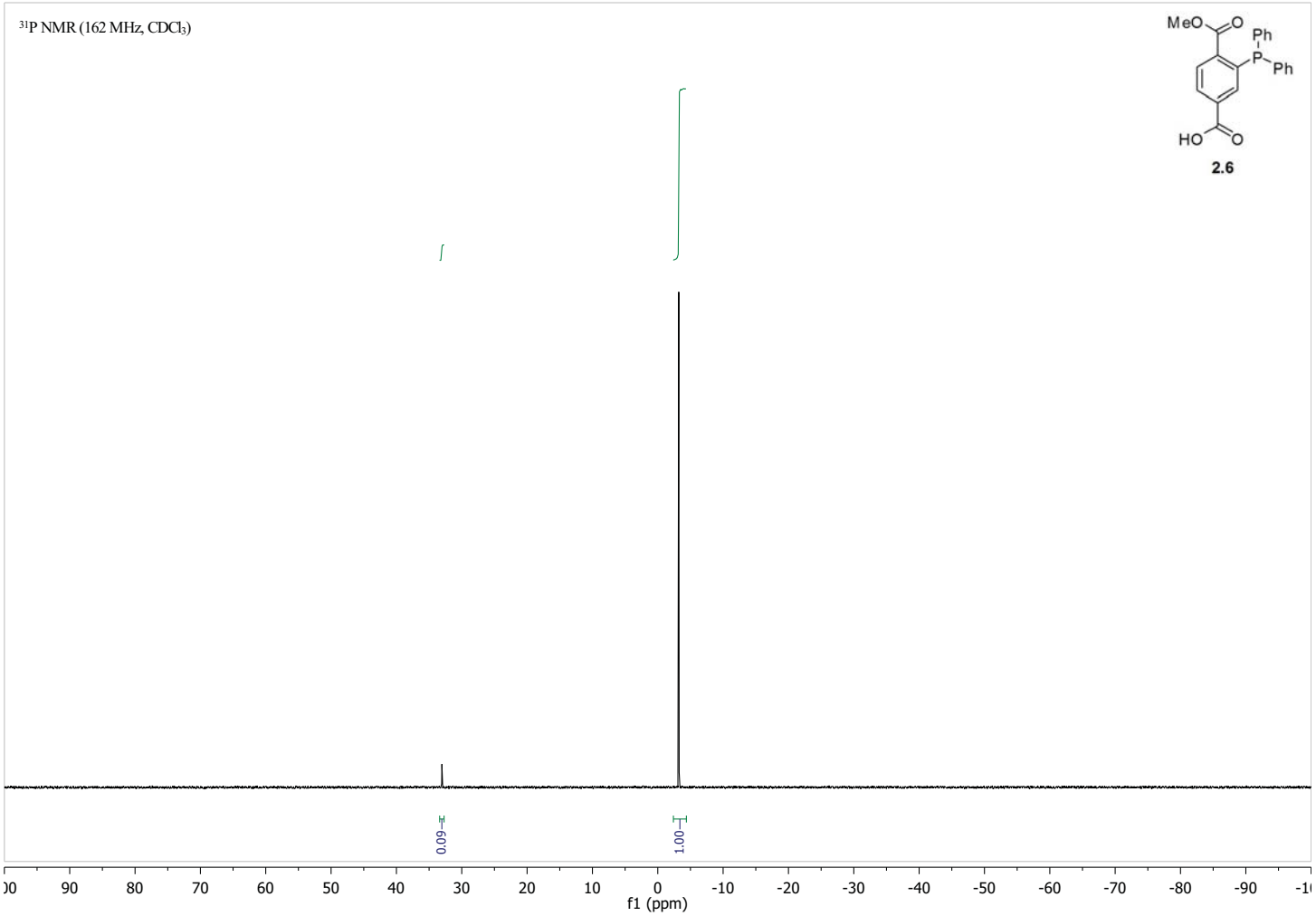
31P NMR (162 MHz, CDCl3)
MeO
O
Ph
P
Ph
HO
O
2.6
0.09
1.00
90
80
70
60
50
40
30
20
10
0
-10
-20
-30
-40
-50
-60
-70
-80
-90
f1 (ppm)

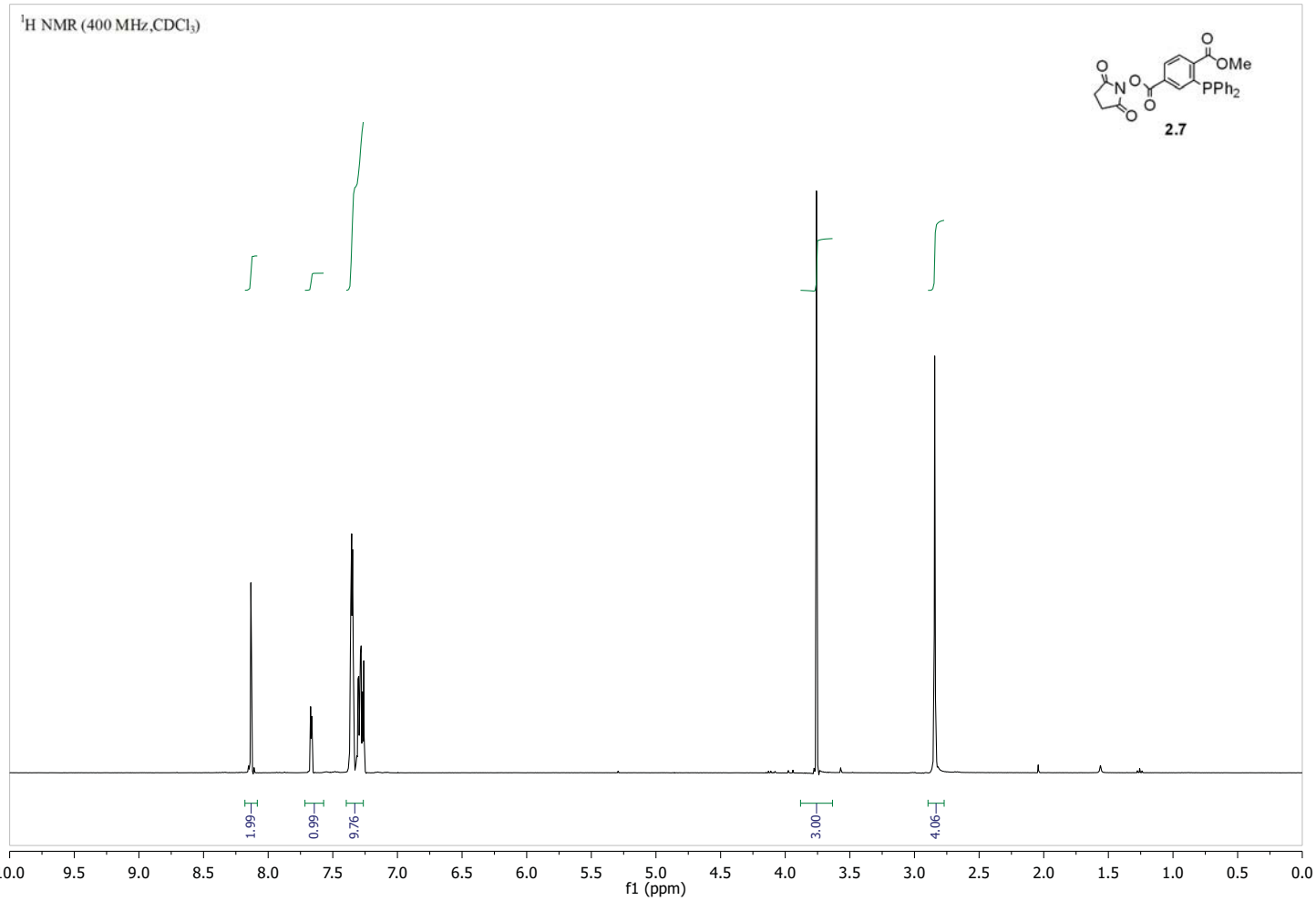
^{1}H NMR (400 MHz,$CDCl_3$)
OMe
PPh_2
2.7
1.99
0.99
9.76
3.00
4.06
10.0 9.5 9.0 8.5 8.0 7.5 7.0 6.5 6.0 5.5 5.0 4.5 4.0 3.5 3.0 2.5 2.0 1.5 1.0 0.5 0.0
f1 (ppm)

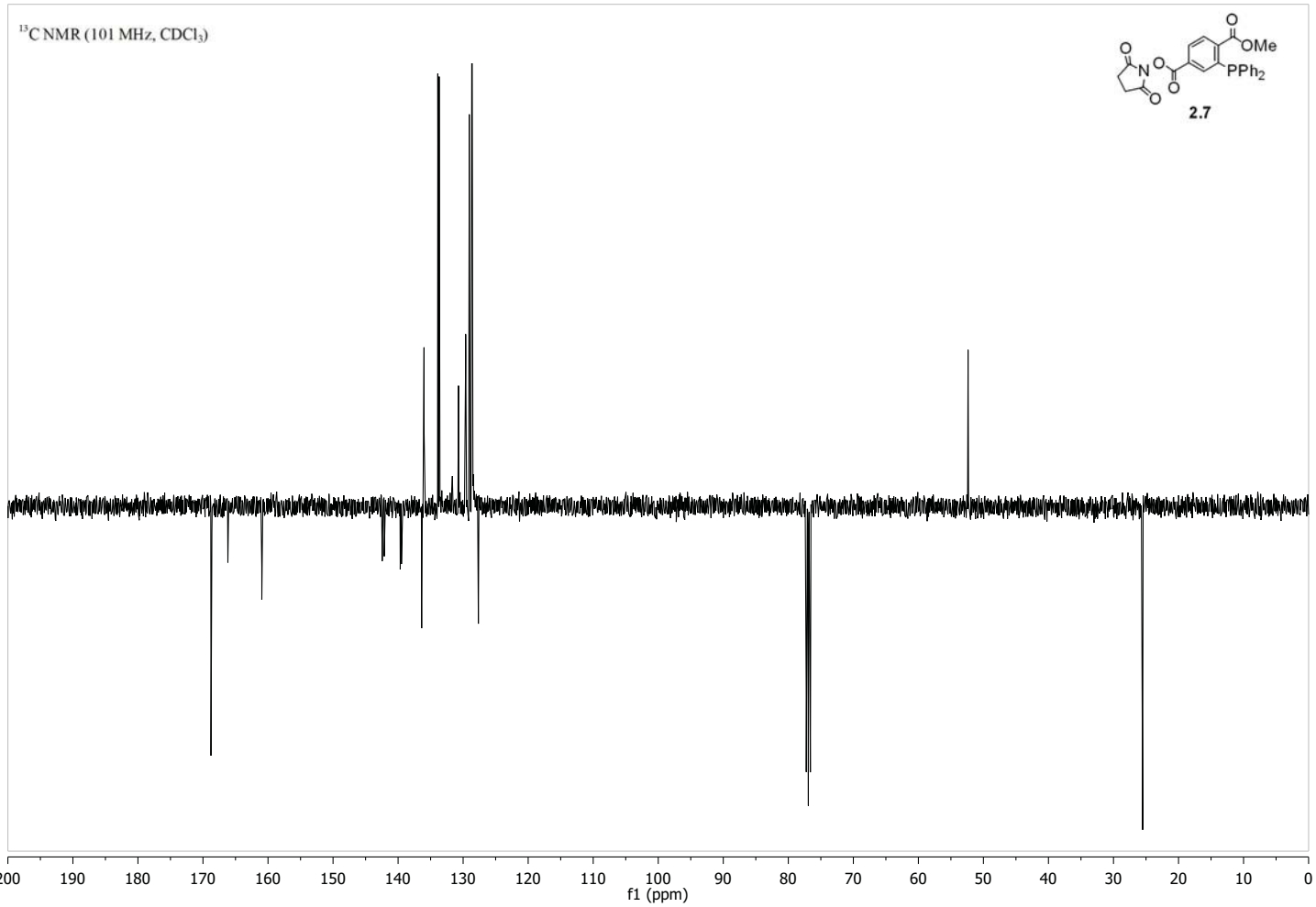
^{13}C NMR (101 MHz, $CDCl_3$)
OMe
PPh2
2.7
200 190 180 170 160 150 140 130 120 110 100 90 80 70 60 50 40 30 20 10 0
f1 (ppm)

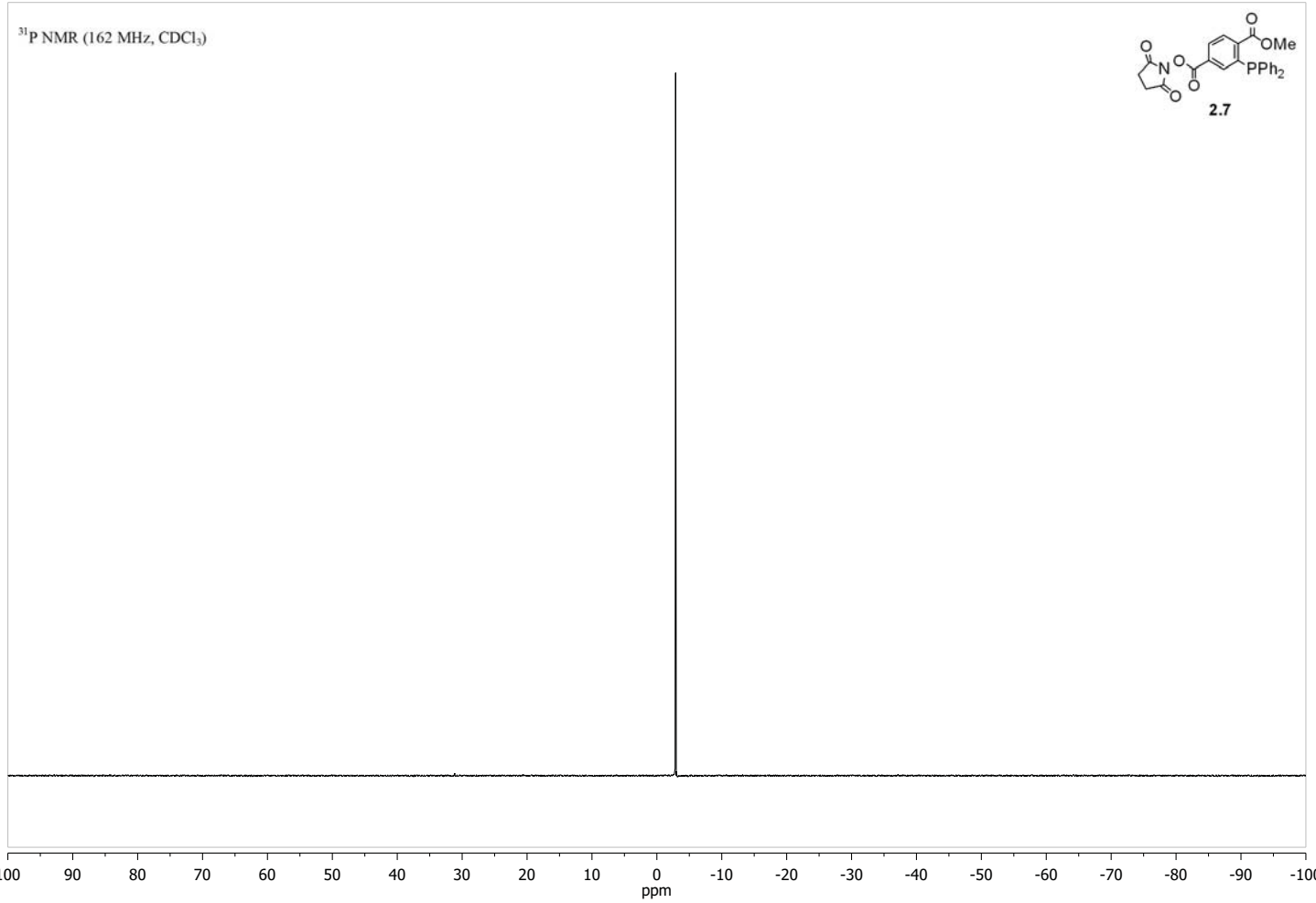
31P NMR (162 MHz, CDCl3)
OMe
PPh2
2.7
100
90
80
70
60
50
40
30
20
10
0
-10
-20
-30
-40
-50
-60
-70
-80
-90
-100
ppm

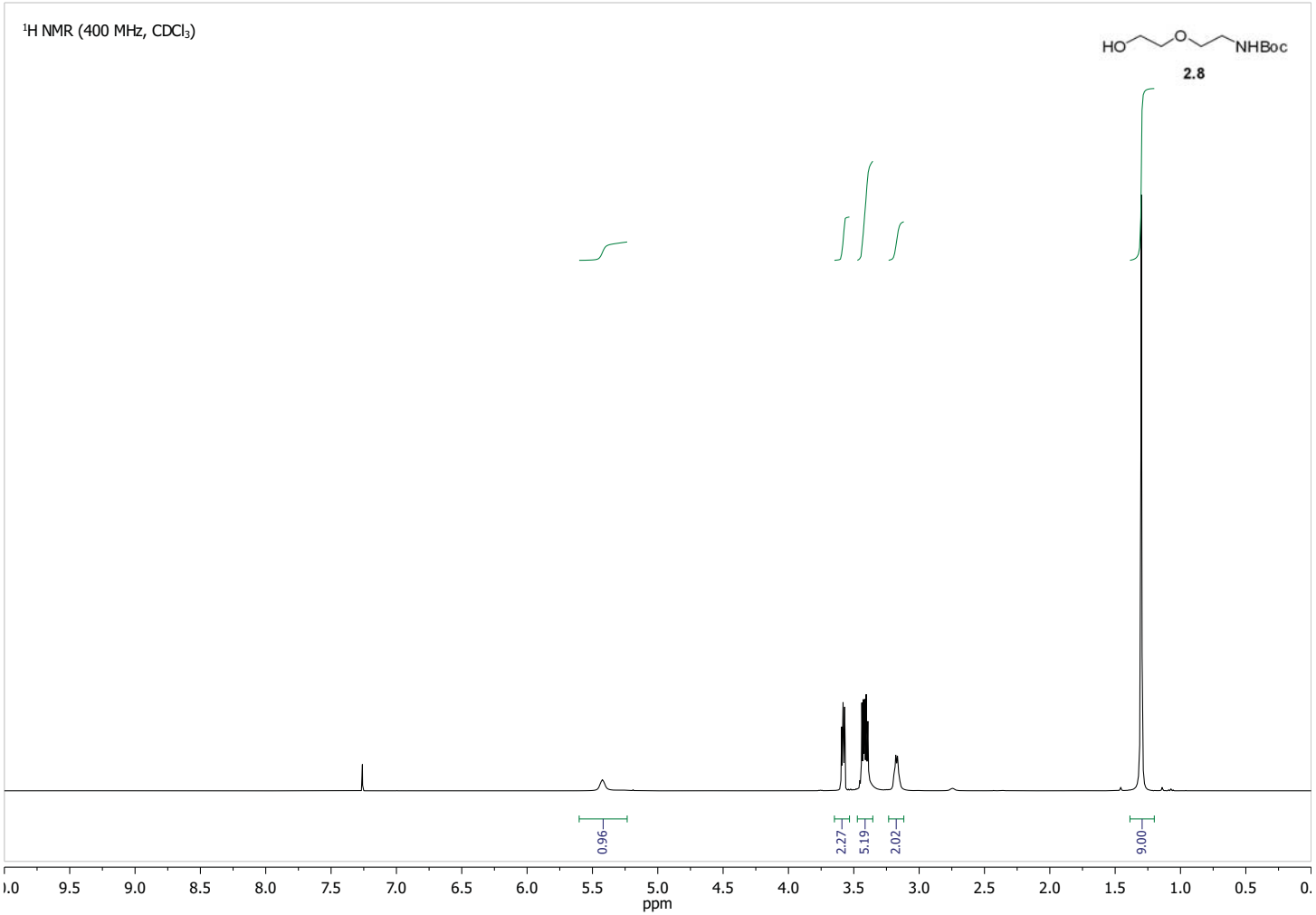
^{1}H NMR (400 MHz, $CDCl_3$)
HO
O
NHBoc
2.8
0.96
2.27
5.19
2.02
9.00
9.5
9.0
8.5
8.0
7.5
7.0
6.5
6.0
5.5
5.0
4.5
4.0
3.5
3.0
2.5
2.0
1.5
1.0
0.5
ppm

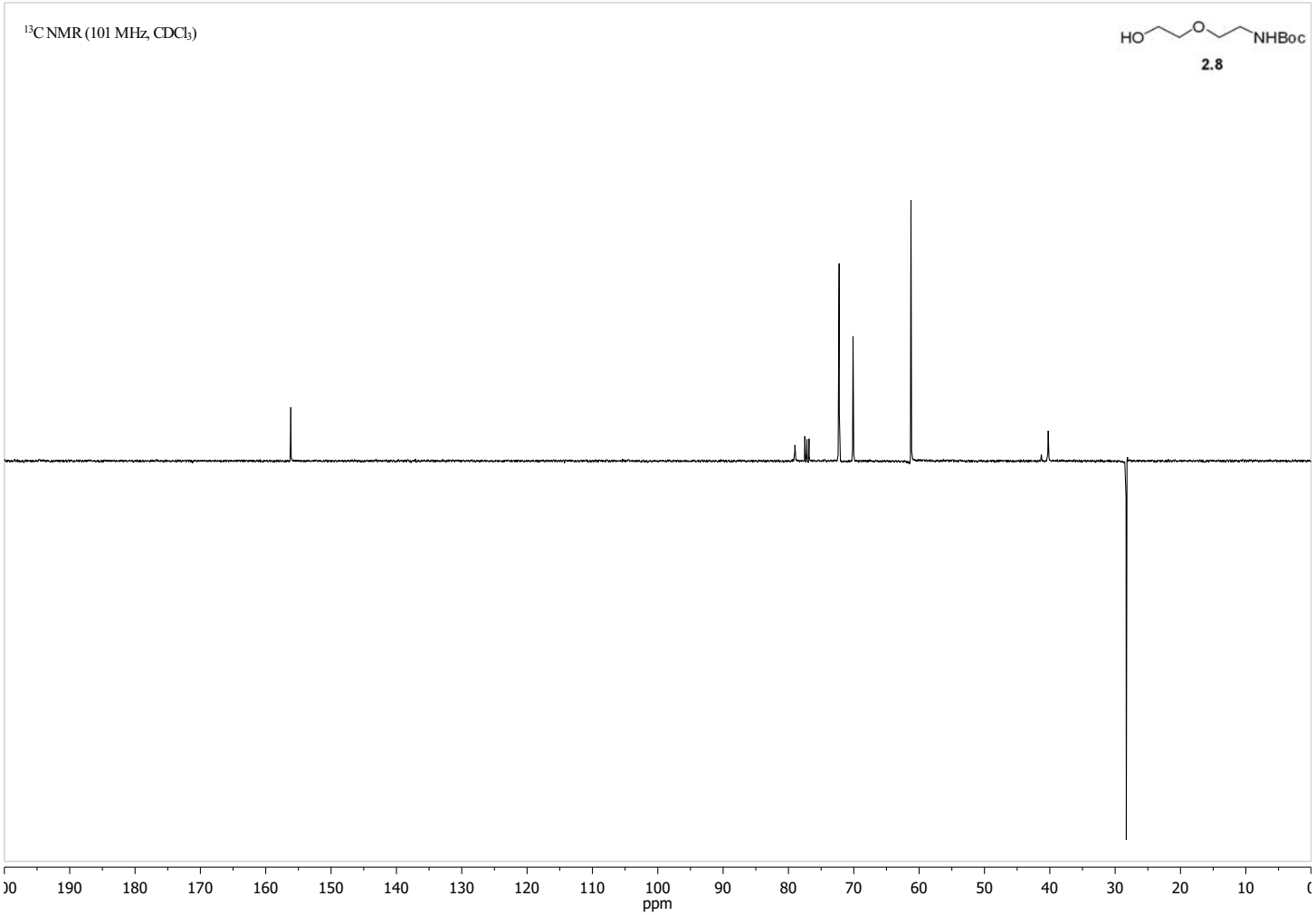
^{13}C NMR (101 MHz, $CDCl_3$)
HO
O
NHBoc
2.8
190
180
170
160
150
140
130
120
110
100
90
80
70
60
50
40
30
20
10
ppm

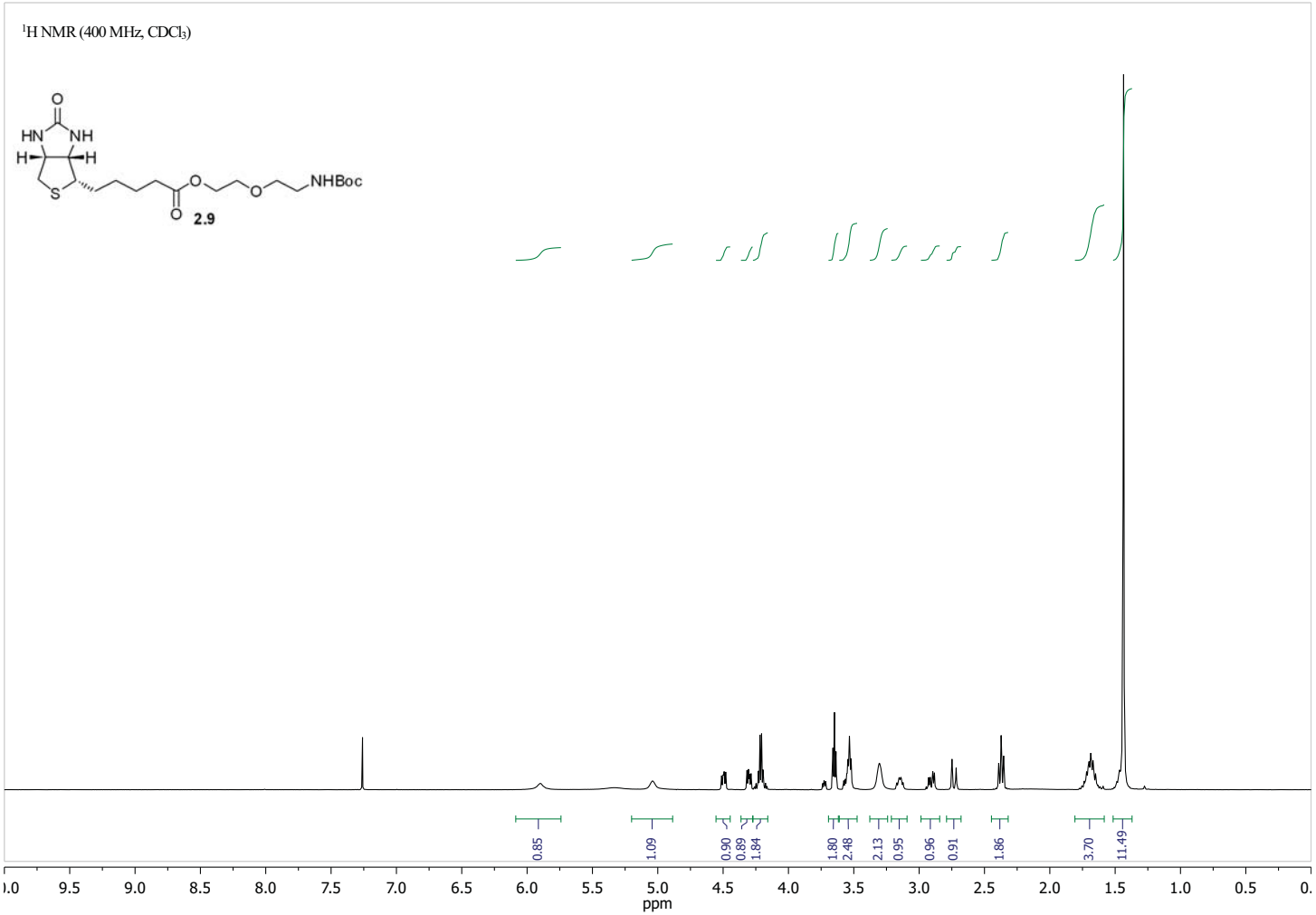
^{1}H NMR (400 MHz, $CDCl_3$)
HN
NH
H
H
S
O
O
O
O
NHBoc
2.9
0.85
1.09
0.90
0.89
1.84
1.80
2.48
2.13
0.95
0.96
0.91
1.86
3.70
11.49
9.5
9.0
8.5
8.0
7.5
7.0
6.5
6.0
5.5
5.0
4.5
4.0
3.5
3.0
2.5
2.0
1.5
1.0
0.5
ppm

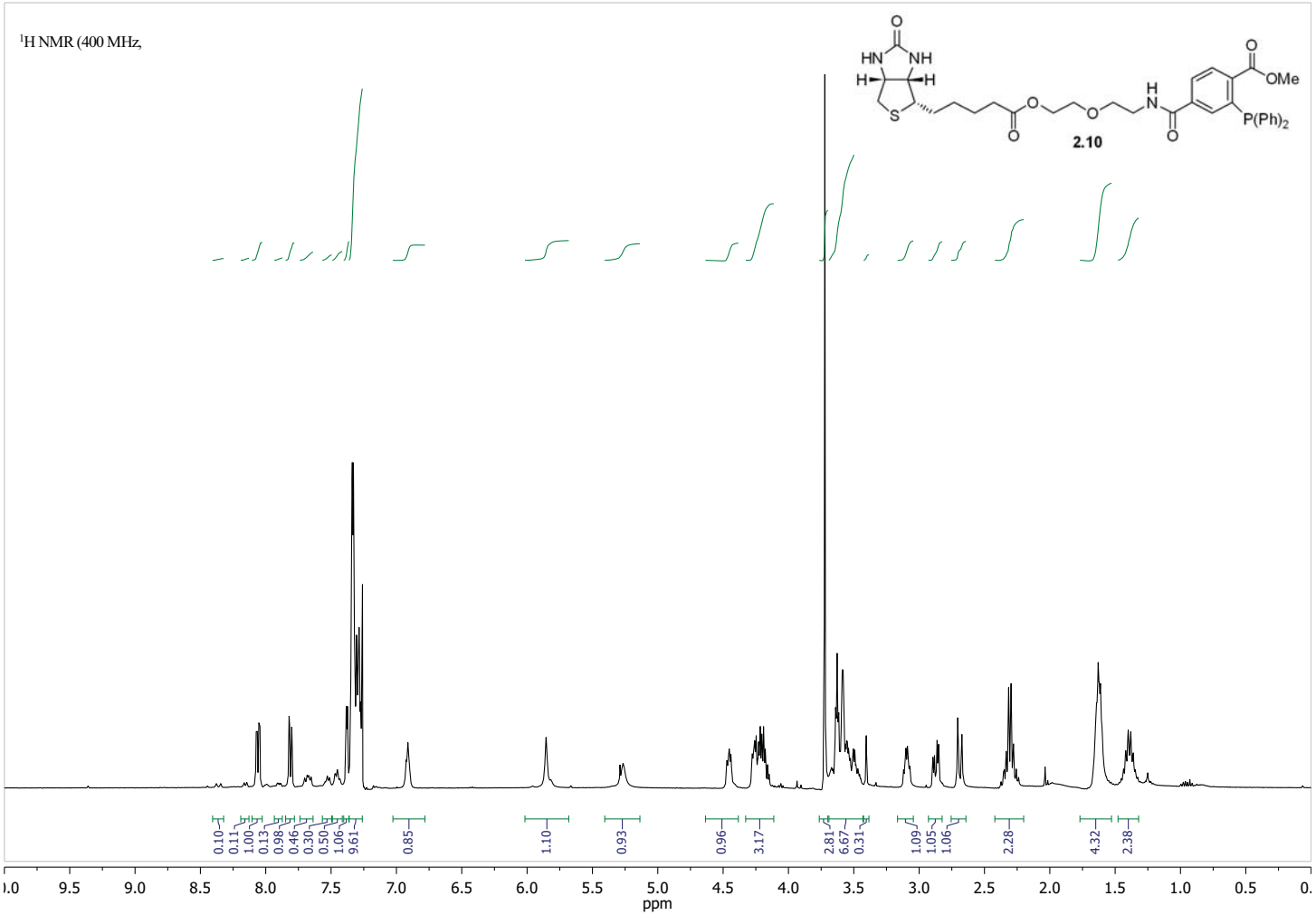
^{1}H NMR (400 MHz,
2.10
0.10
0.11
1.00
0.13
0.98
0.46
0.30
0.50
1.06
9.61
0.85
1.10
0.93
0.96
3.17
2.81
6.67
0.31
1.09
1.05
1.06
2.28
4.32
2.38
9.5
9.0
8.5
8.0
7.5
7.0
6.5
6.0
5.5
5.0
4.5
4.0
3.5
3.0
2.5
2.0
1.5
1.0
0.5
ppm

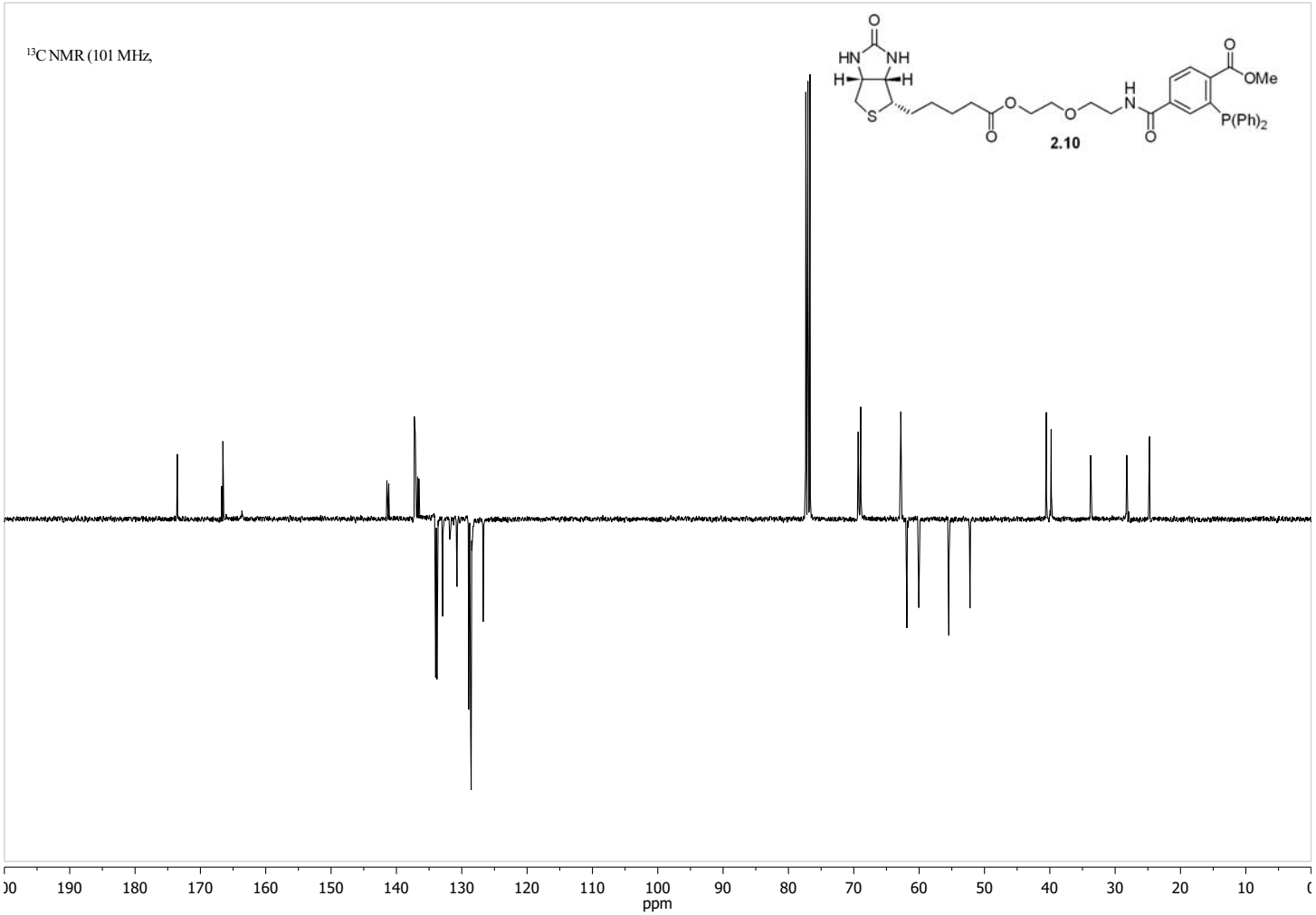
^{13}C NMR (101 MHz,
2.10
ppm

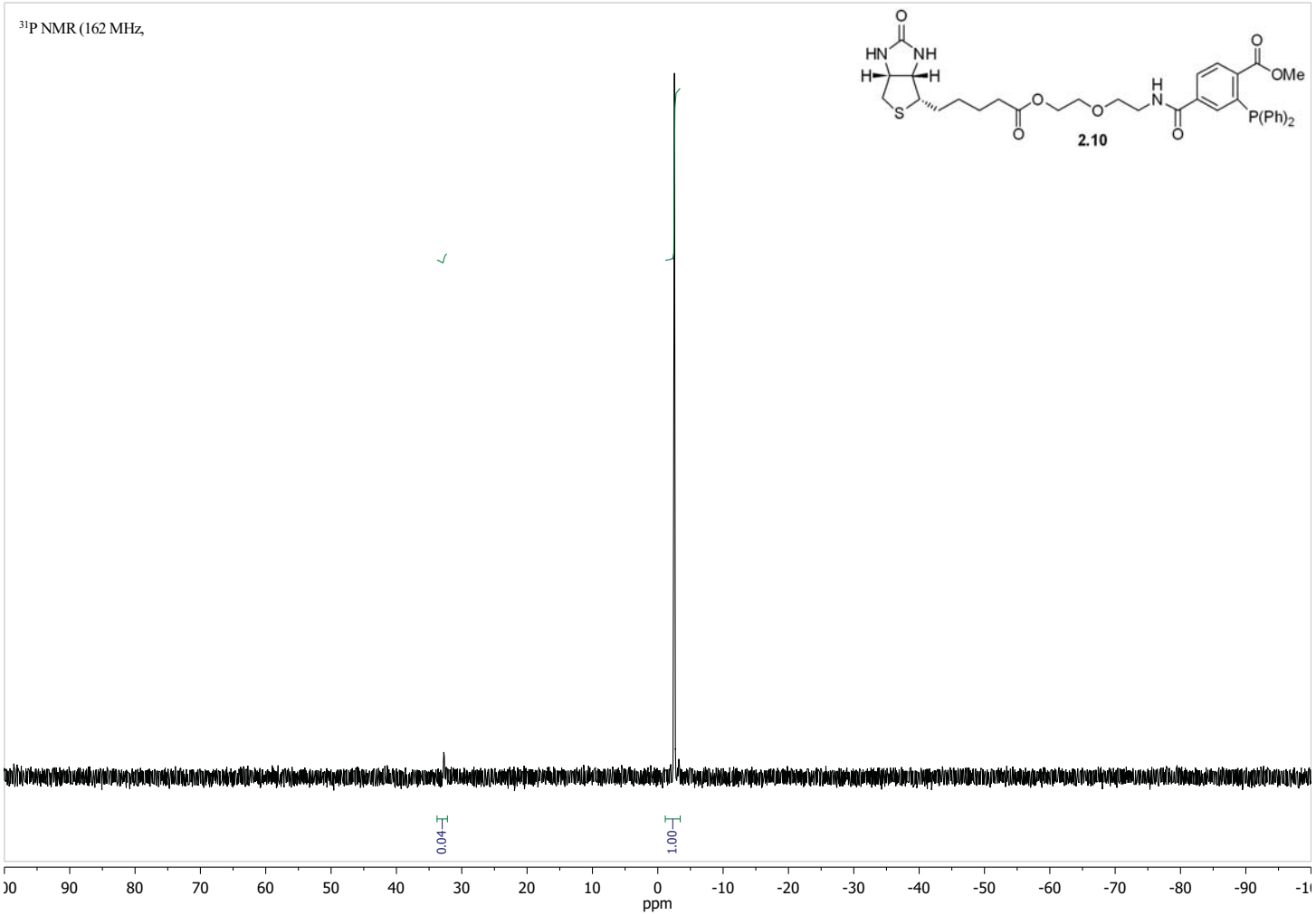
31P NMR (162 MHz,
2.10
0.04
1.00
90
80
70
60
50
40
30
20
10
0
-10
-20
-30
-40
-50
-60
-70
-80
-90
ppm

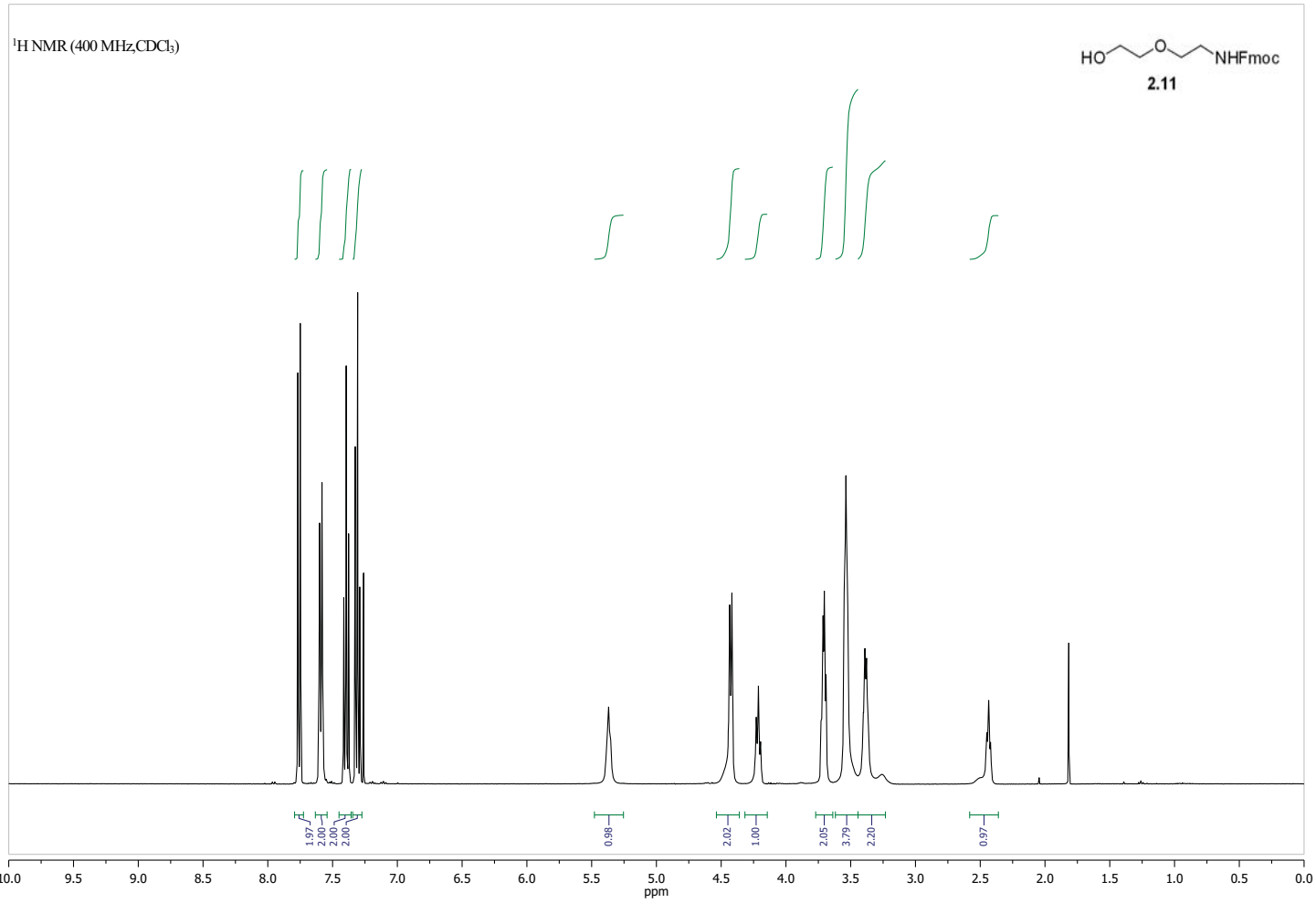
1H NMR (400 MHz,CDCl3)
HO
O
NHFmoc
2.11
1.97
2.00
2.00
2.00
0.98
2.02
1.00
2.05
3.79
2.20
0.97
10.0
9.5
9.0
8.5
8.0
7.5
7.0
6.5
6.0
5.5
5.0
4.5
4.0
3.5
3.0
2.5
2.0
1.5
1.0
0.5
0.0
ppm

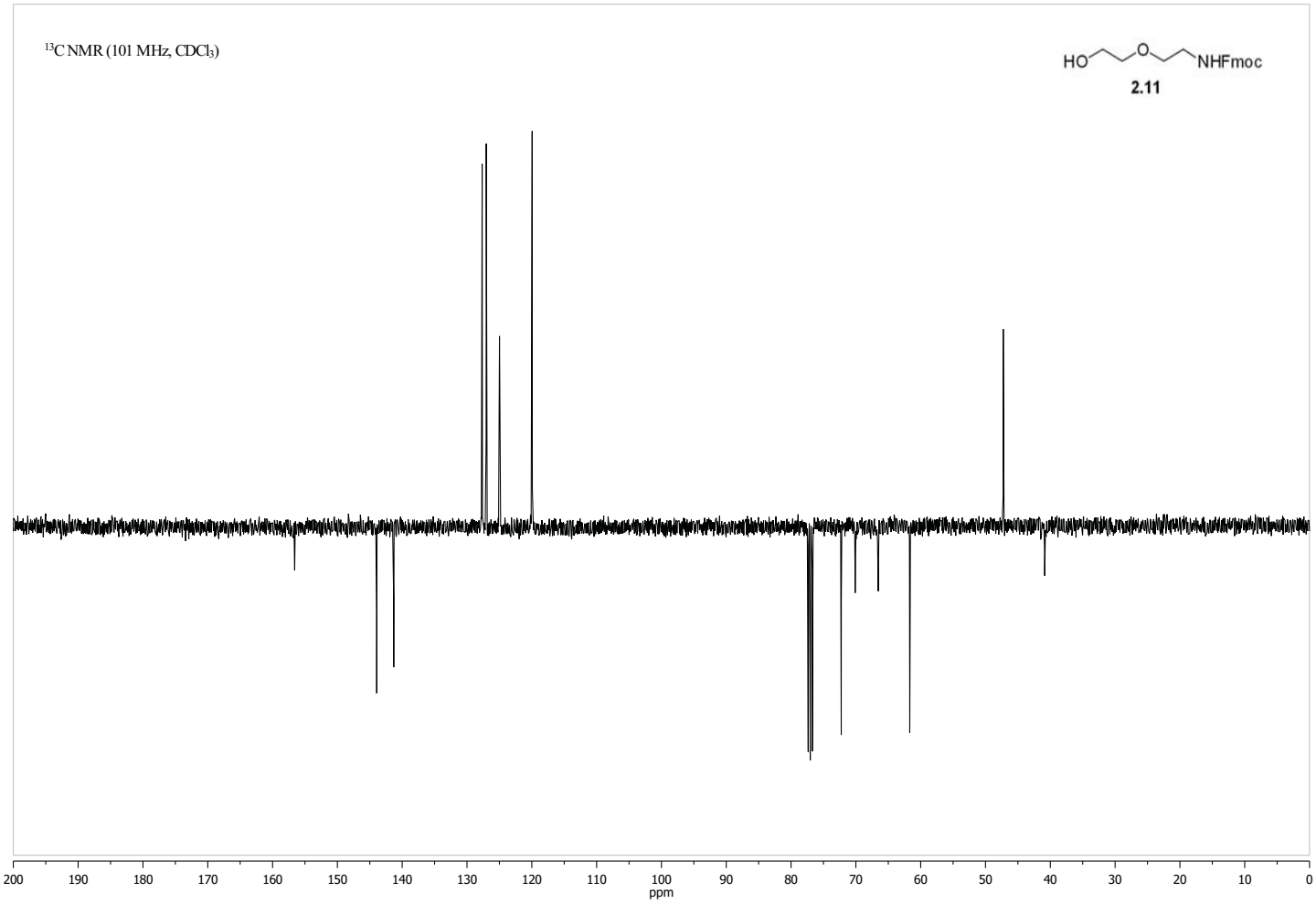
^{13}C NMR (101 MHz, $CDCl_3$)
HO
O
NHFmoc
2.11
200
190
180
170
160
150
140
130
120
110
100
90
80
70
60
50
40
30
20
10
0
ppm

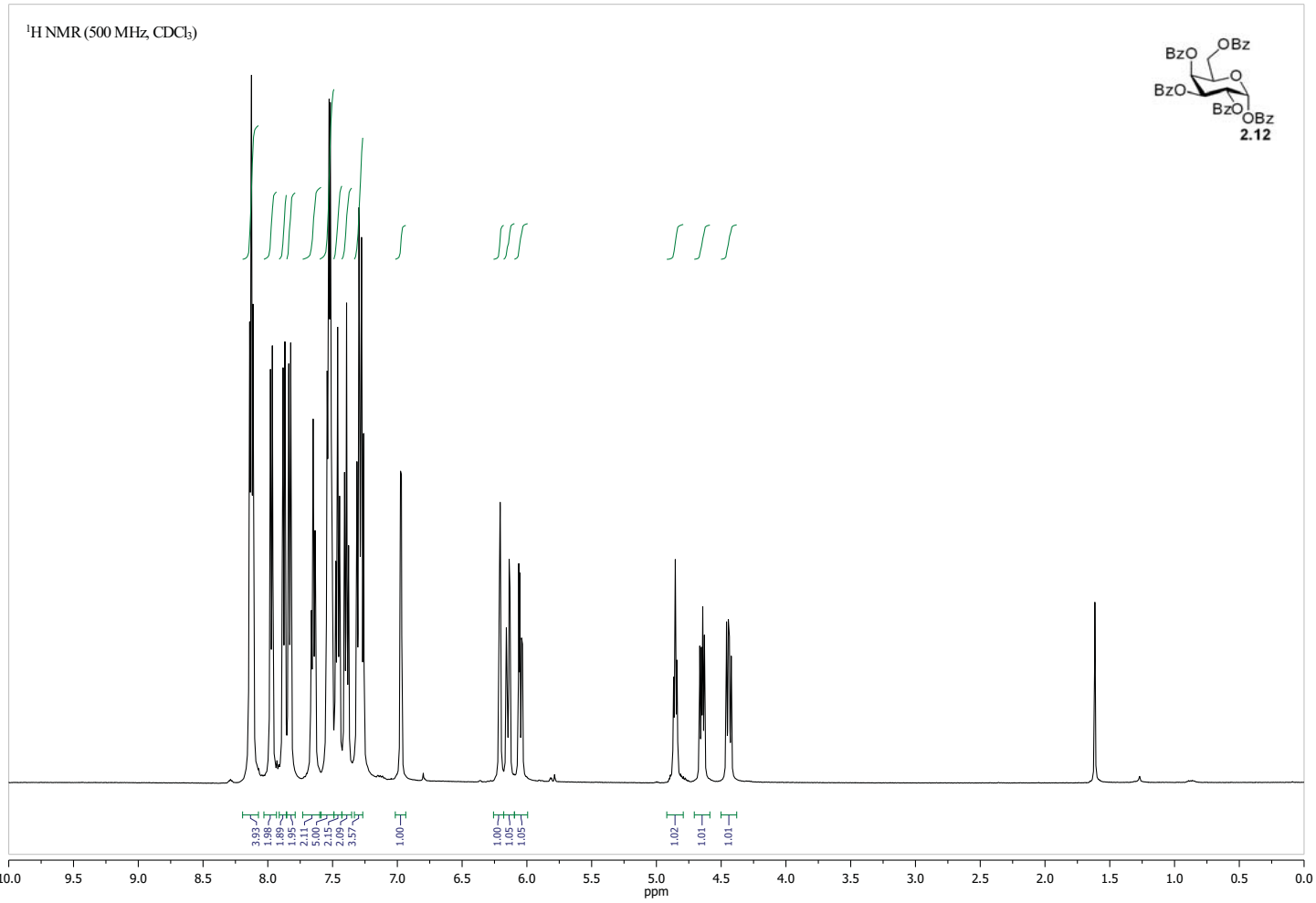
^{1}H NMR (500 MHz, $CDCl_3$)
BzO
OBz
O
BzO
BzO
OBz
2.12
3.93
1.98
1.98
1.95
2.11
5.00
2.15
2.09
3.57
1.00
1.00
1.05
1.05
1.02
1.01
1.01
10.0
9.5
9.0
8.5
8.0
7.5
7.0
6.5
6.0
5.5
5.0
4.5
4.0
3.5
3.0
2.5
2.0
1.5
1.0
0.5
0.0
ppm

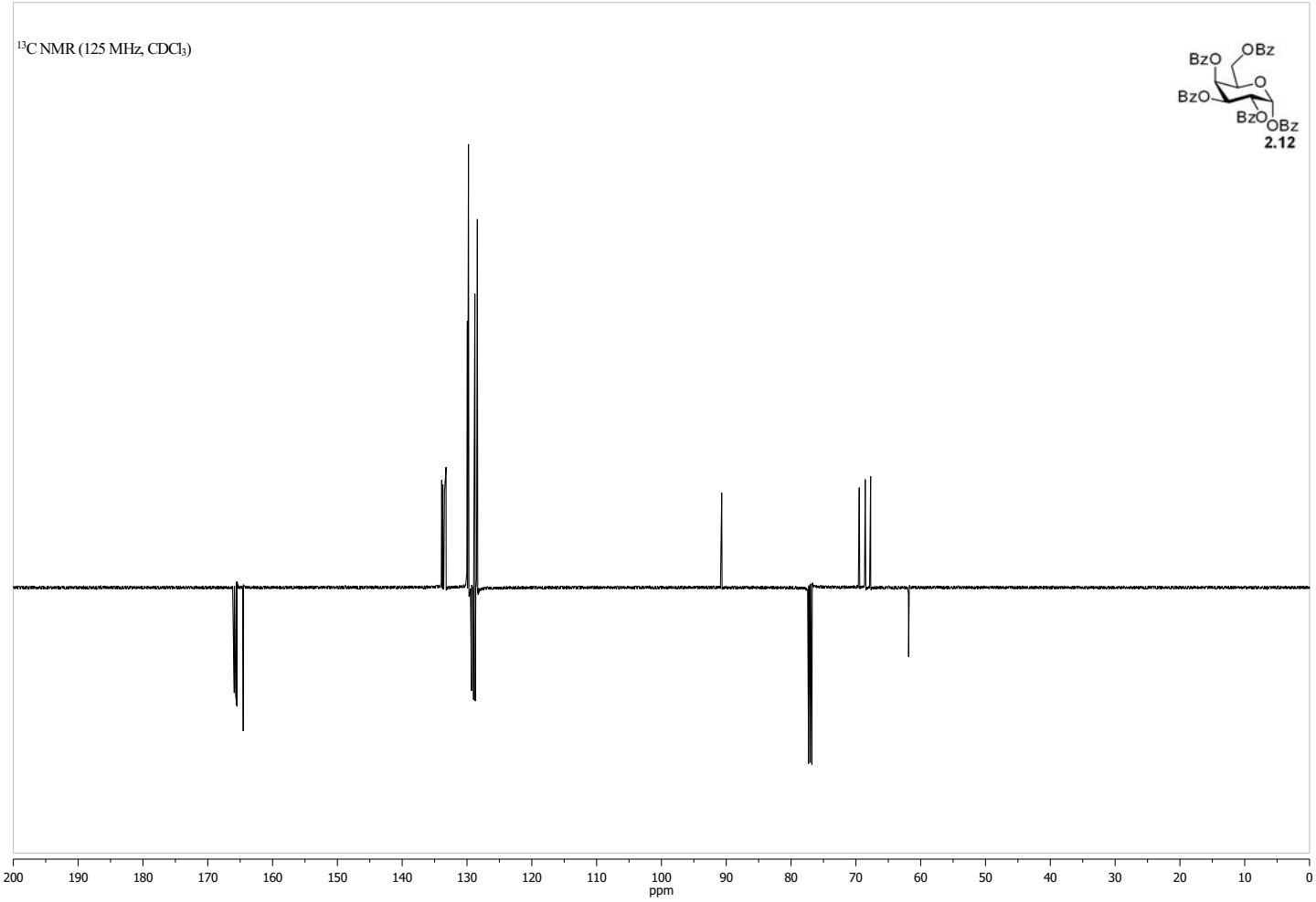
^{13}C NMR (125 MHz, $CDCl_3$)
BzO
OBz
BzO
O
BzO
OBz
2.12
200
190
180
170
160
150
140
130
120
110
100
90
80
70
60
50
40
30
20
10
0
ppm

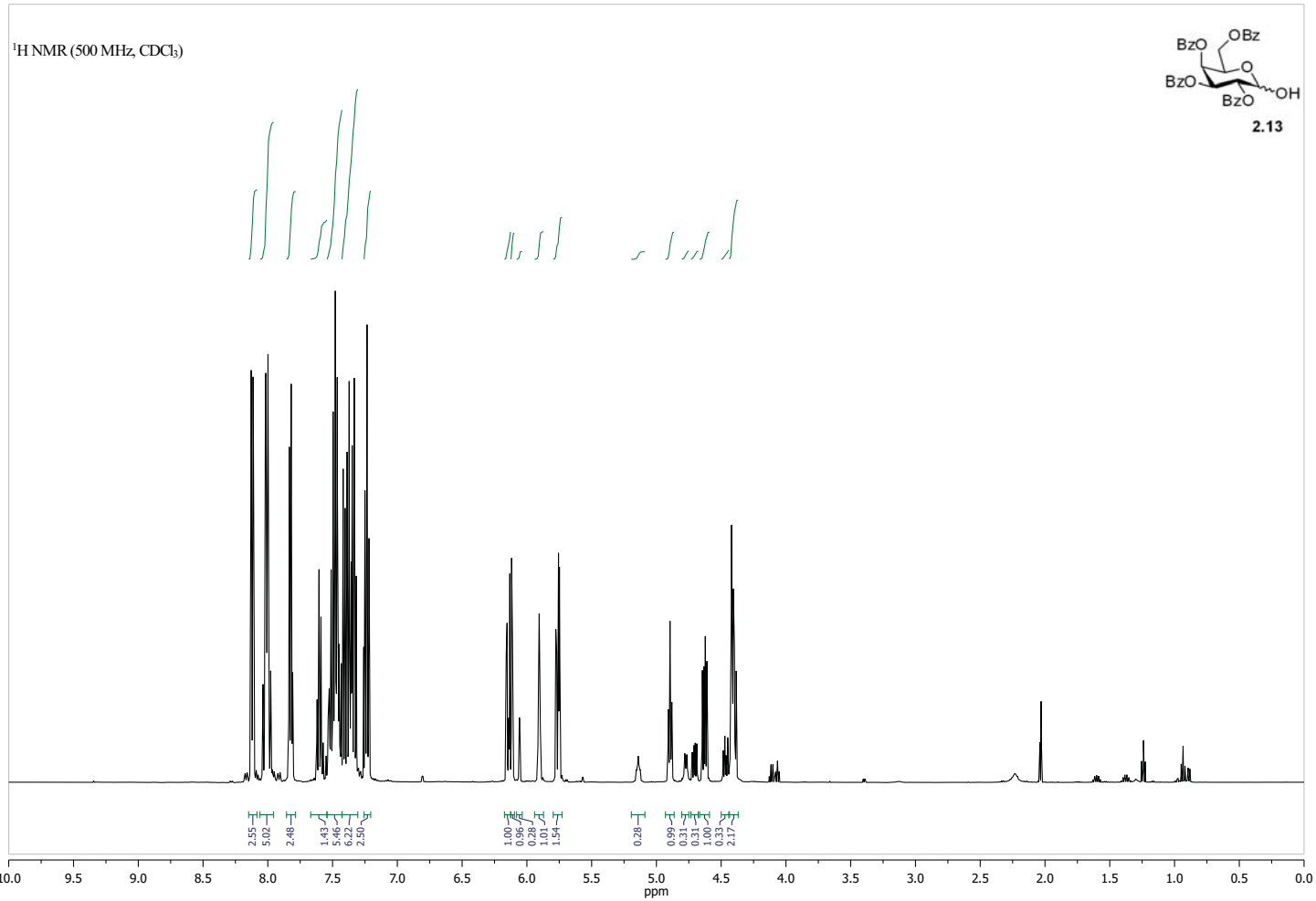
^{1}H NMR (500 MHz, $CDCl_3$)
BzO
OBz
O
BzO
BzO
OH
2.13
2.55
5.02
2.48
1.43
5.46
6.22
2.50
1.00
0.96
0.28
1.01
1.54
0.28
0.99
0.31
0.31
1.00
0.33
2.17
10.0
9.5
9.0
8.5
8.0
7.5
7.0
6.5
6.0
5.5
5.0
4.5
4.0
3.5
3.0
2.5
2.0
1.5
1.0
0.5
0.0
ppm

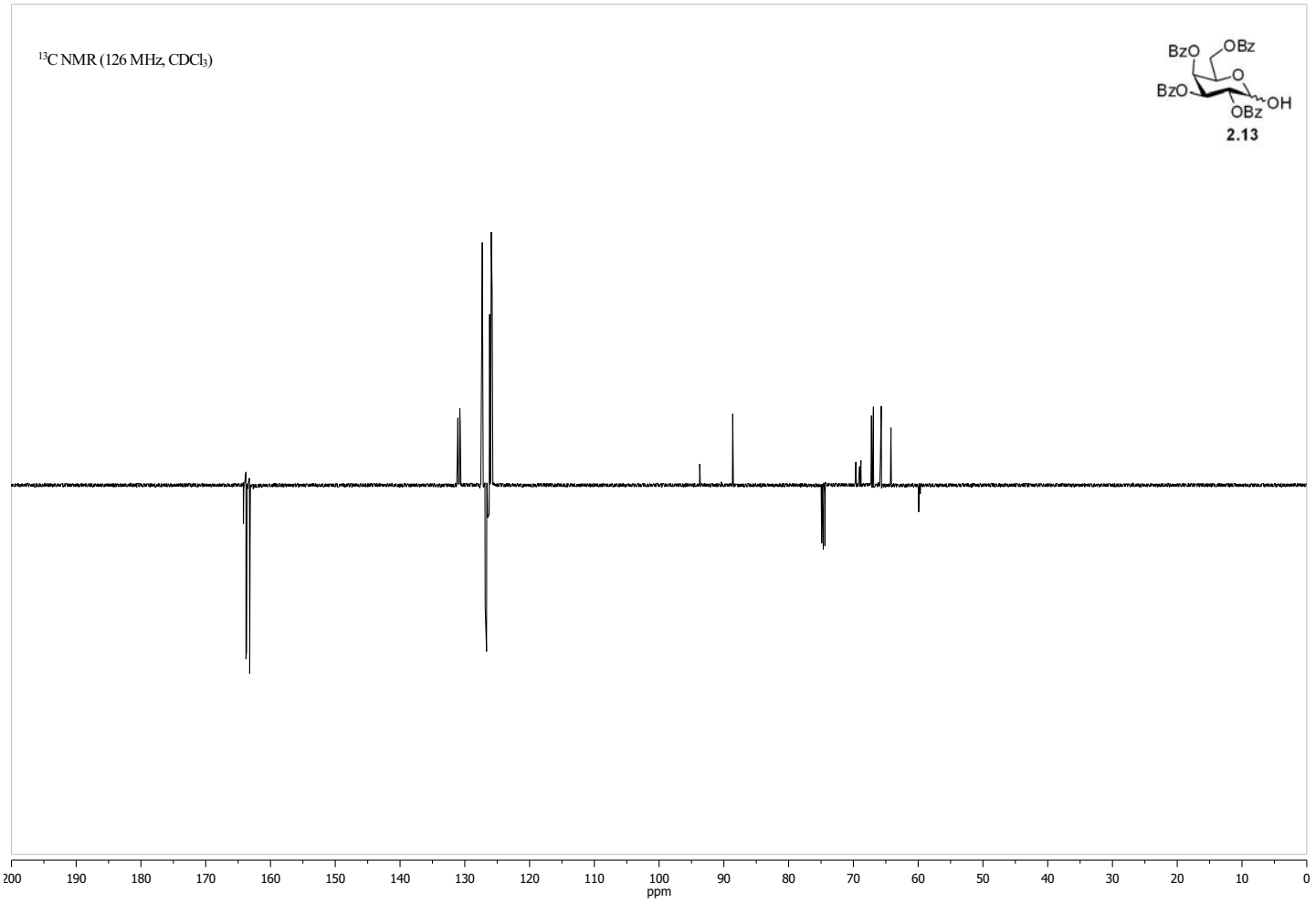
^{13}C NMR (126 MHz, $CDCl_3$)
BzO
OBz
O
BzO
OH
OBz
2.13
200
190
180
170
160
150
140
130
120
110
100
90
80
70
60
50
40
30
20
10
0
ppm

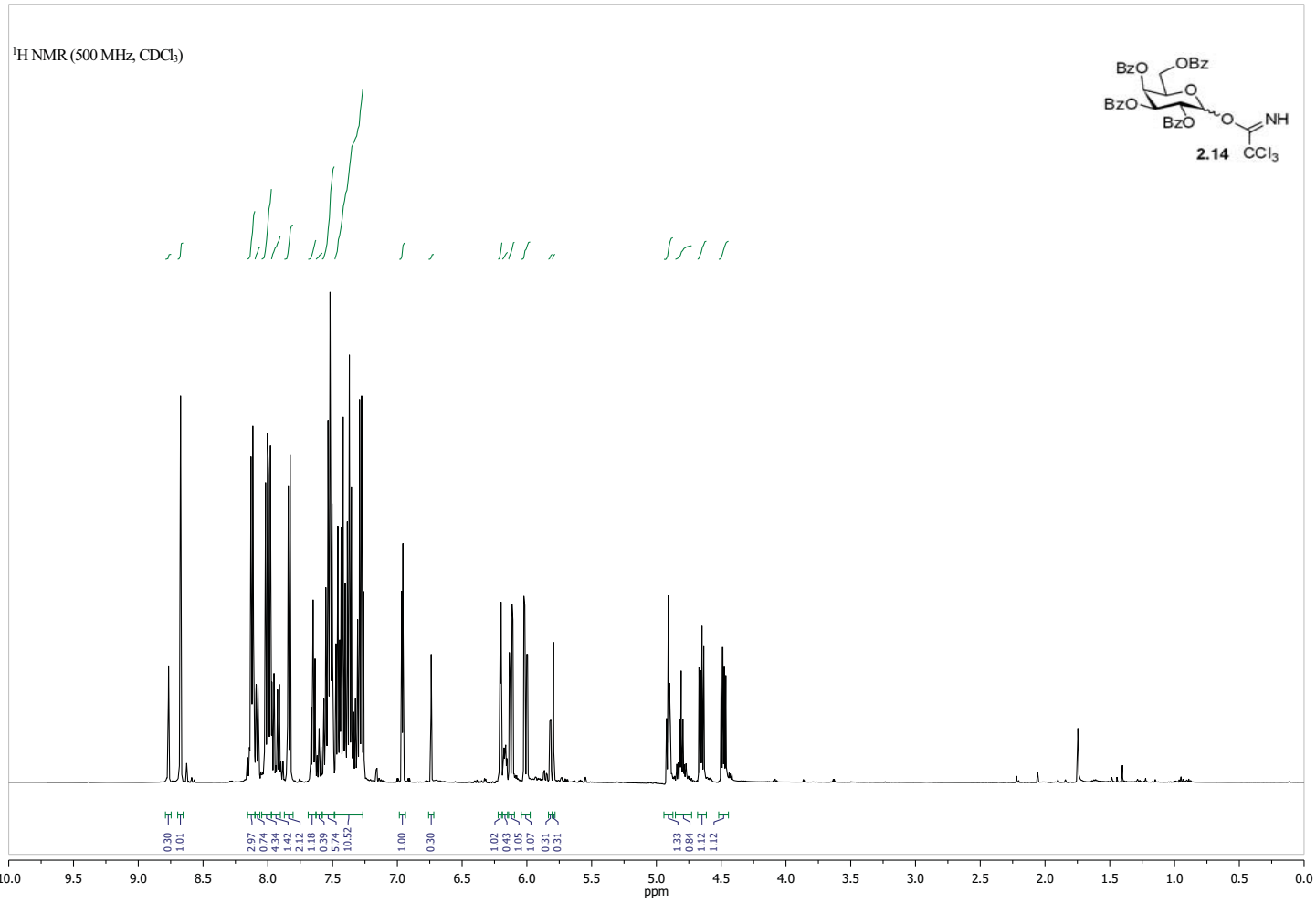
1H NMR (500 MHz, CDCl3)
BzO
OBz
BzO
BzO
O
O
NH
CCl3
2.14
0.30
1.01
2.97
0.74
4.34
1.42
2.12
1.18
0.39
5.74
10.52
1.00
0.30
1.02
0.43
1.05
1.07
0.31
0.31
1.33
0.84
1.12
1.12
10.0
9.5
9.0
8.5
8.0
7.5
7.0
6.5
6.0
5.5
5.0
4.5
4.0
3.5
3.0
2.5
2.0
1.5
1.0
0.5
0.0
ppm

^{13}C NMR (126 MHz, $CDCl_3$)

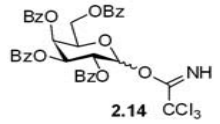

2.14

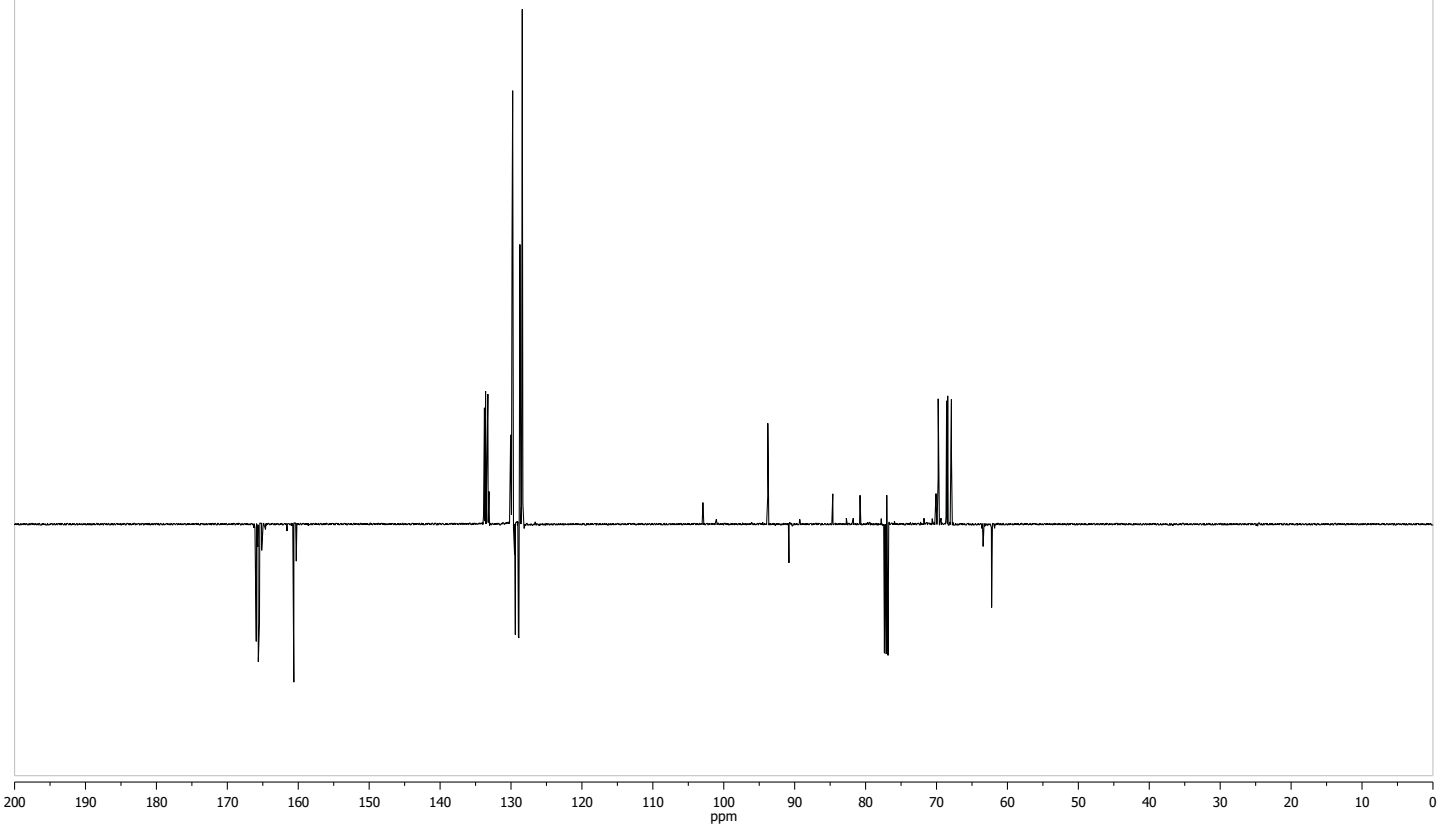

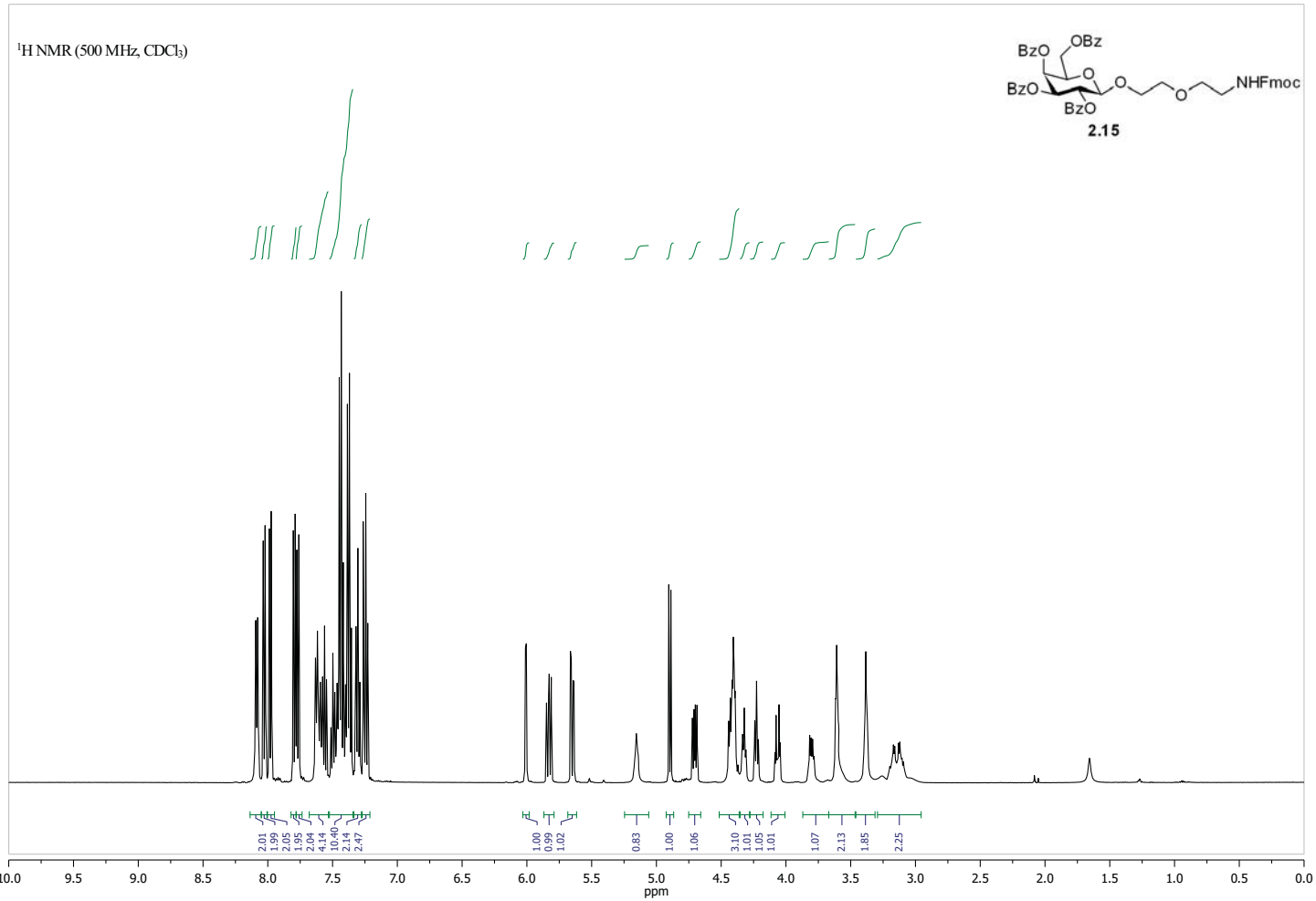
^{1}H NMR (500 MHz, $CDCl_3$)
BzO
OBz
BzO
BzO
O
O
O
NHFmoc
2.15
2.01
1.99
2.05
1.95
2.04
4.14
10.40
2.14
2.47
1.00
0.99
1.02
0.83
1.00
1.06
3.10
1.01
1.05
1.01
1.07
2.13
1.85
2.25
10.0
9.5
9.0
8.5
8.0
7.5
7.0
6.5
6.0
5.5
5.0
4.5
4.0
3.5
3.0
2.5
2.0
1.5
1.0
0.5
0.0
ppm

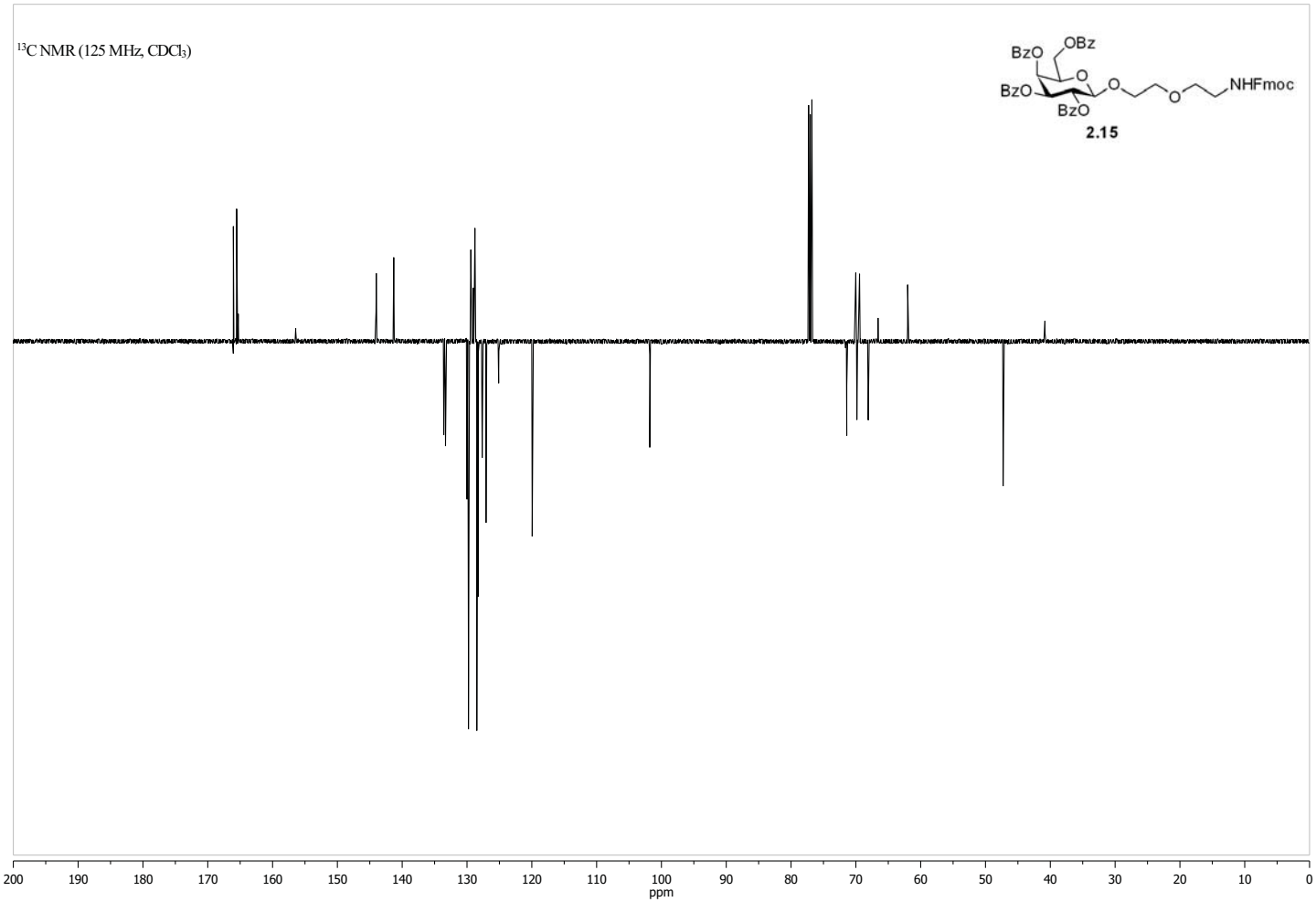
^{13}C NMR (125 MHz, $CDCl_3$)
BzO
OBz
BzO
BzO
O
O
O
NHFmoc
2.15
200
190
180
170
160
150
140
130
120
110
100
90
80
70
60
50
40
30
20
10
0
ppm

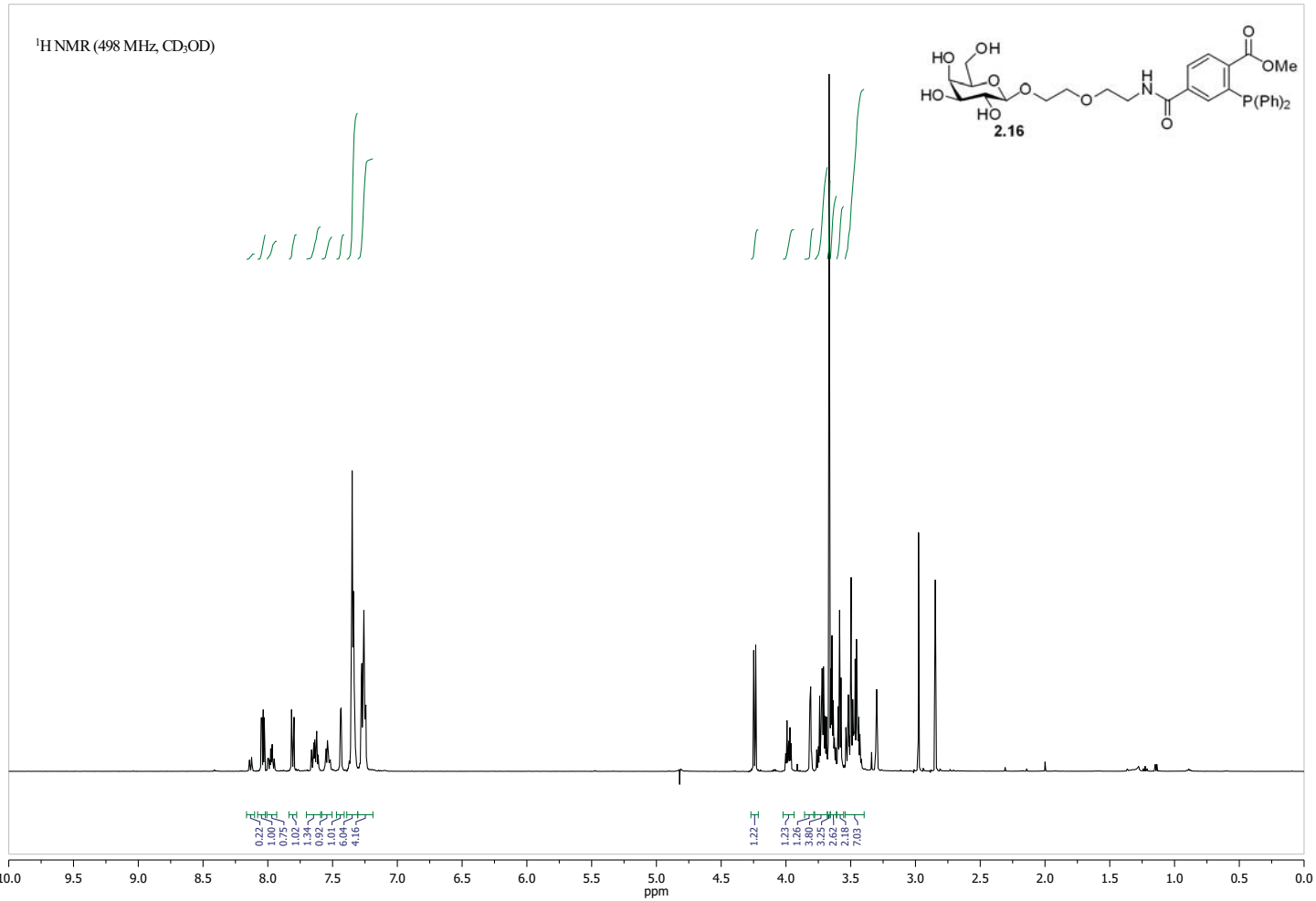
^{1}H NMR (498 MHz, CD_3OD)
HO
OH
HO
O
HO
O
O
H
N
O
OMe
P(Ph)2
2.16
0.22
1.00
0.75
1.02
1.34
0.92
1.01
6.04
4.16
1.22
1.23
1.26
3.80
3.25
2.62
2.18
7.03
10.0
9.5
9.0
8.5
8.0
7.5
7.0
6.5
6.0
5.5
5.0
4.5
4.0
3.5
3.0
2.5
2.0
1.5
1.0
0.5
0.0
ppm

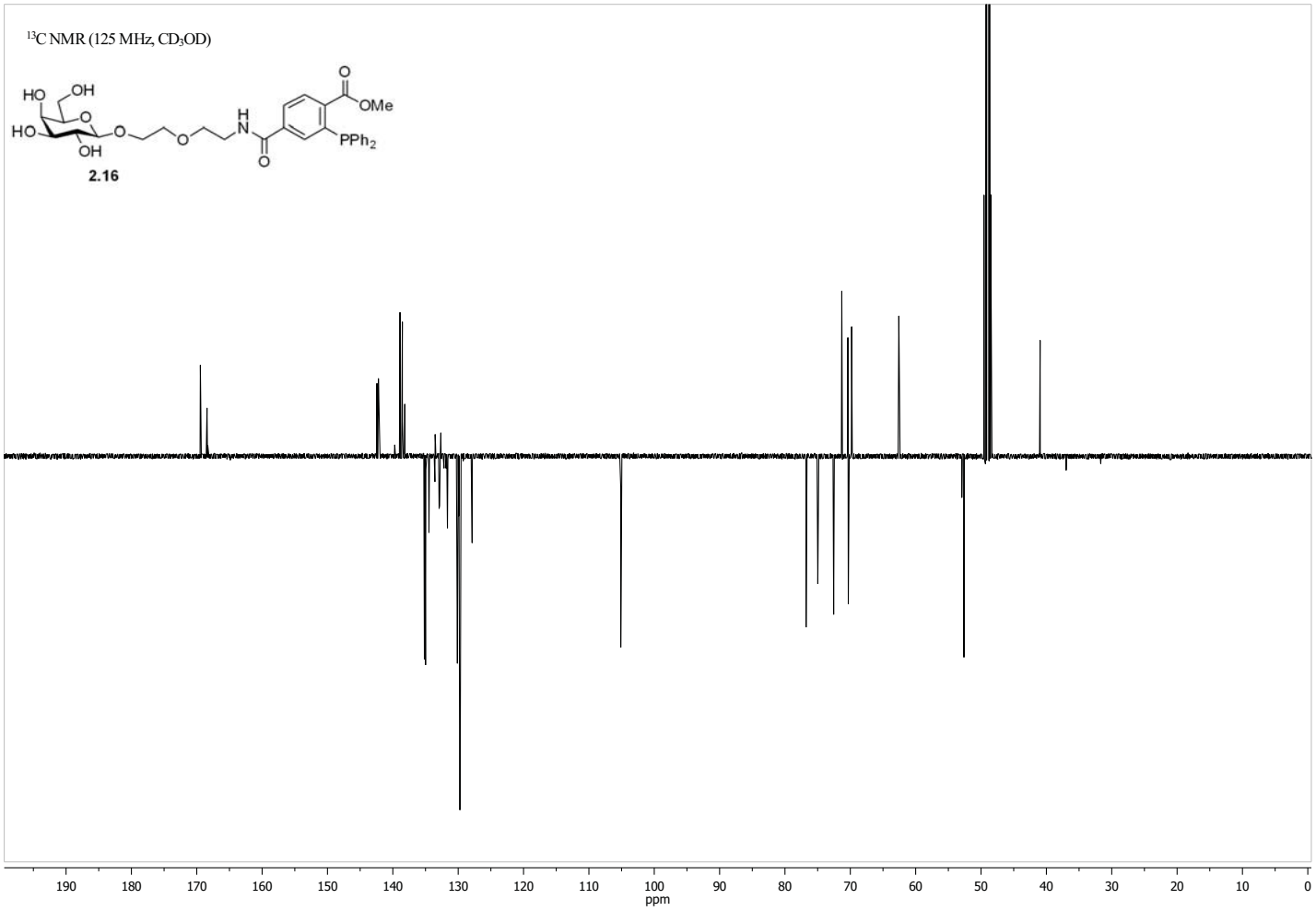
^{13}C NMR (125 MHz, CD_3OD)
HO
OH
O
HO
OH
O
O
N
H
O
O
OMe
PPh_2
2.16
190
180
170
160
150
140
130
120
110
100
90
80
70
60
50
40
30
20
10
0
ppm

^{31}P NMR (202 MHz, CD_3OD)

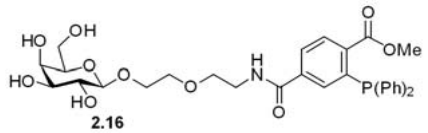

2.16

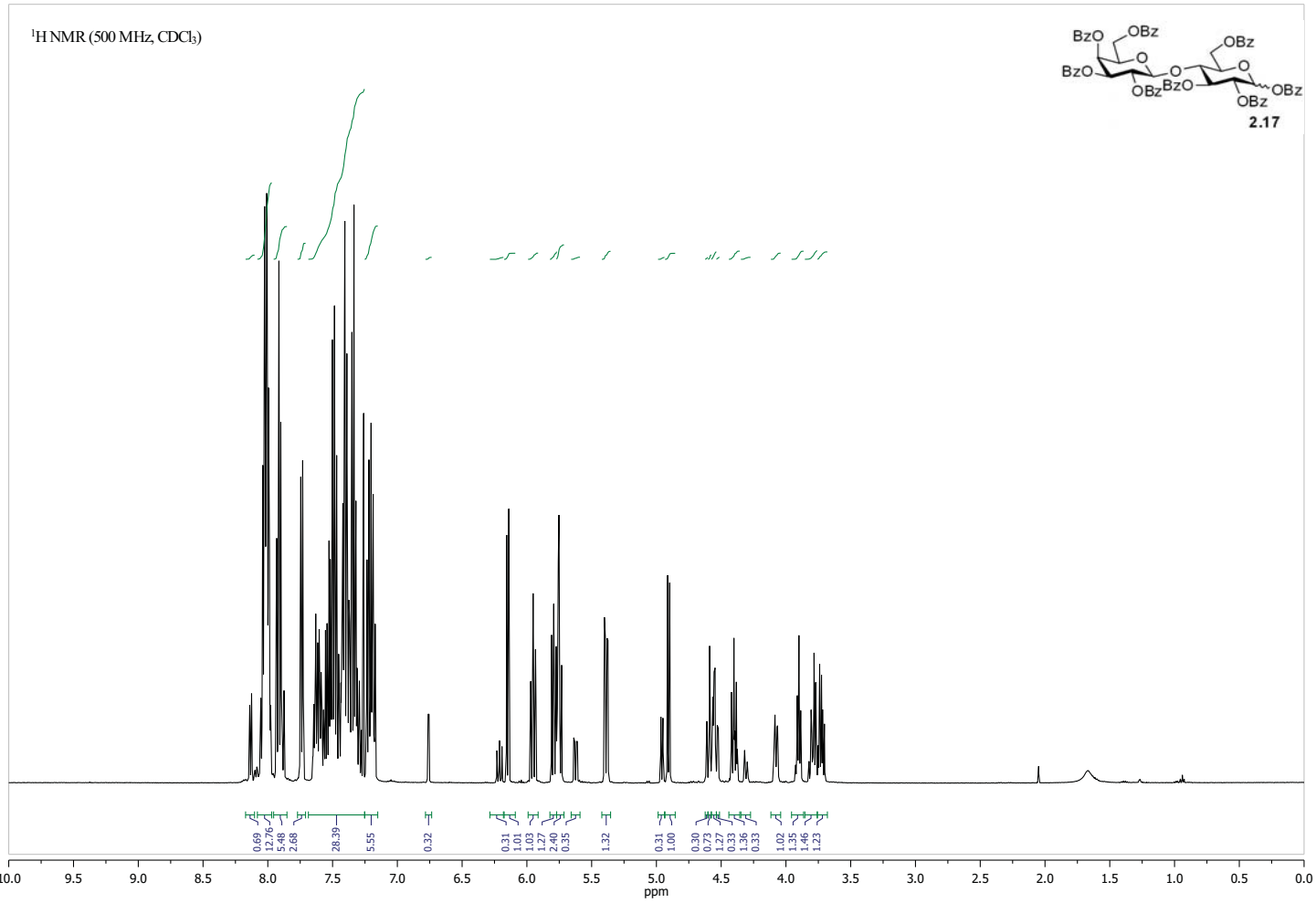
^{1}H NMR (500 MHz, $CDCl_3$)
BzO
OBz
OBz
BzO
OBz
BzO
OBz
OBz
2.17
0.69
12.76
5.48
2.68
28.39
5.55
0.32
0.31
1.01
1.03
1.27
2.40
0.35
1.32
0.31
1.00
0.30
0.73
1.27
0.33
1.36
0.33
1.02
1.35
1.46
1.23
10.0
9.5
9.0
8.5
8.0
7.5
7.0
6.5
6.0
5.5
5.0
4.5
4.0
3.5
3.0
2.5
2.0
1.5
1.0
0.5
0.0
ppm

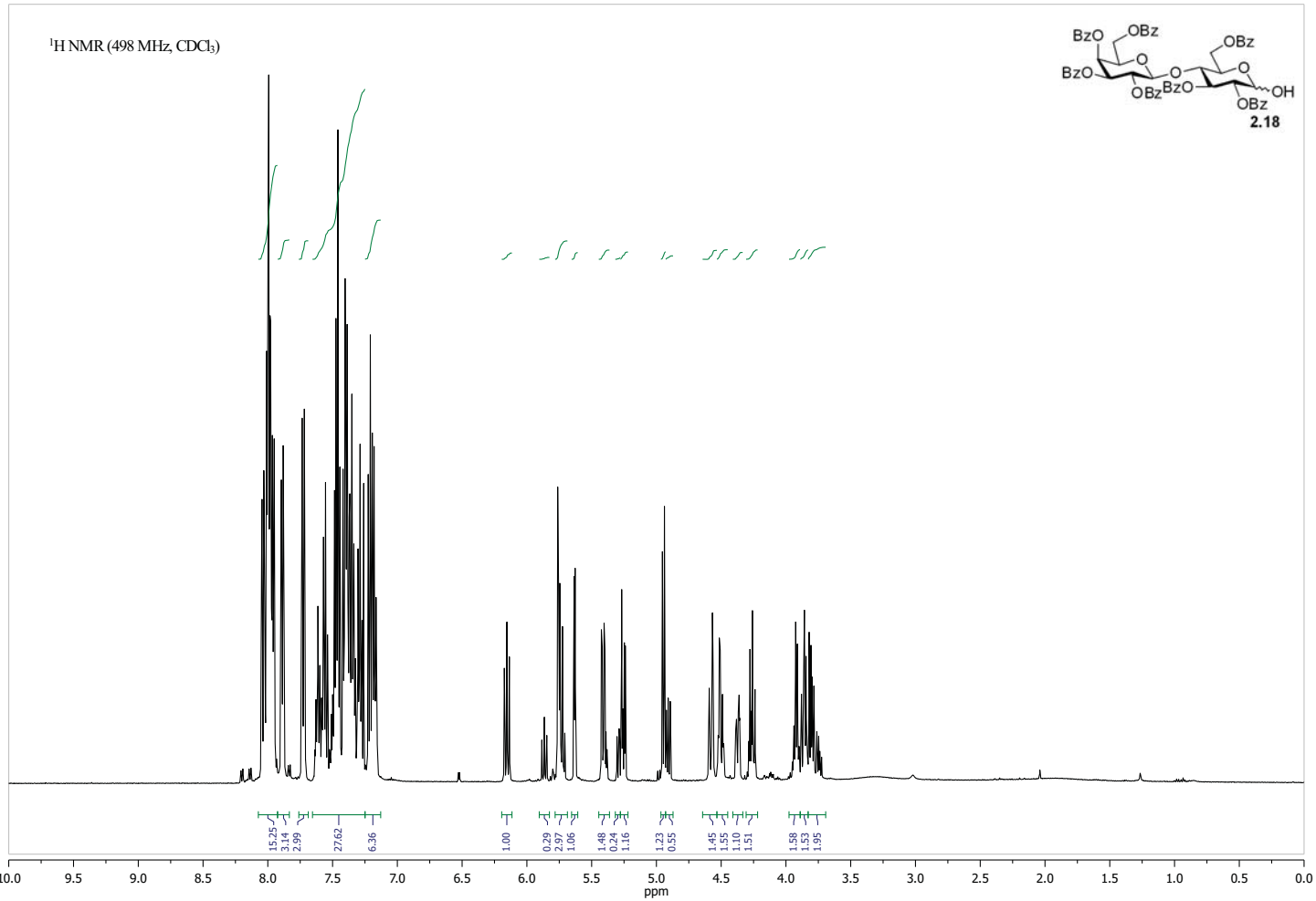
^{1}H NMR (498 MHz, $CDCl_3$)
BzO
OBz
OBz
BzO
OBz
BzO
OBz
OH
2.18
15.25
3.14
2.99
27.62
6.36
1.00
0.29
2.97
1.06
1.48
0.24
1.16
1.23
0.55
1.45
1.55
1.10
1.51
1.58
1.53
1.95
10.0
9.5
9.0
8.5
8.0
7.5
7.0
6.5
6.0
5.5
5.0
4.5
4.0
3.5
3.0
2.5
2.0
1.5
1.0
0.5
0.0
ppm

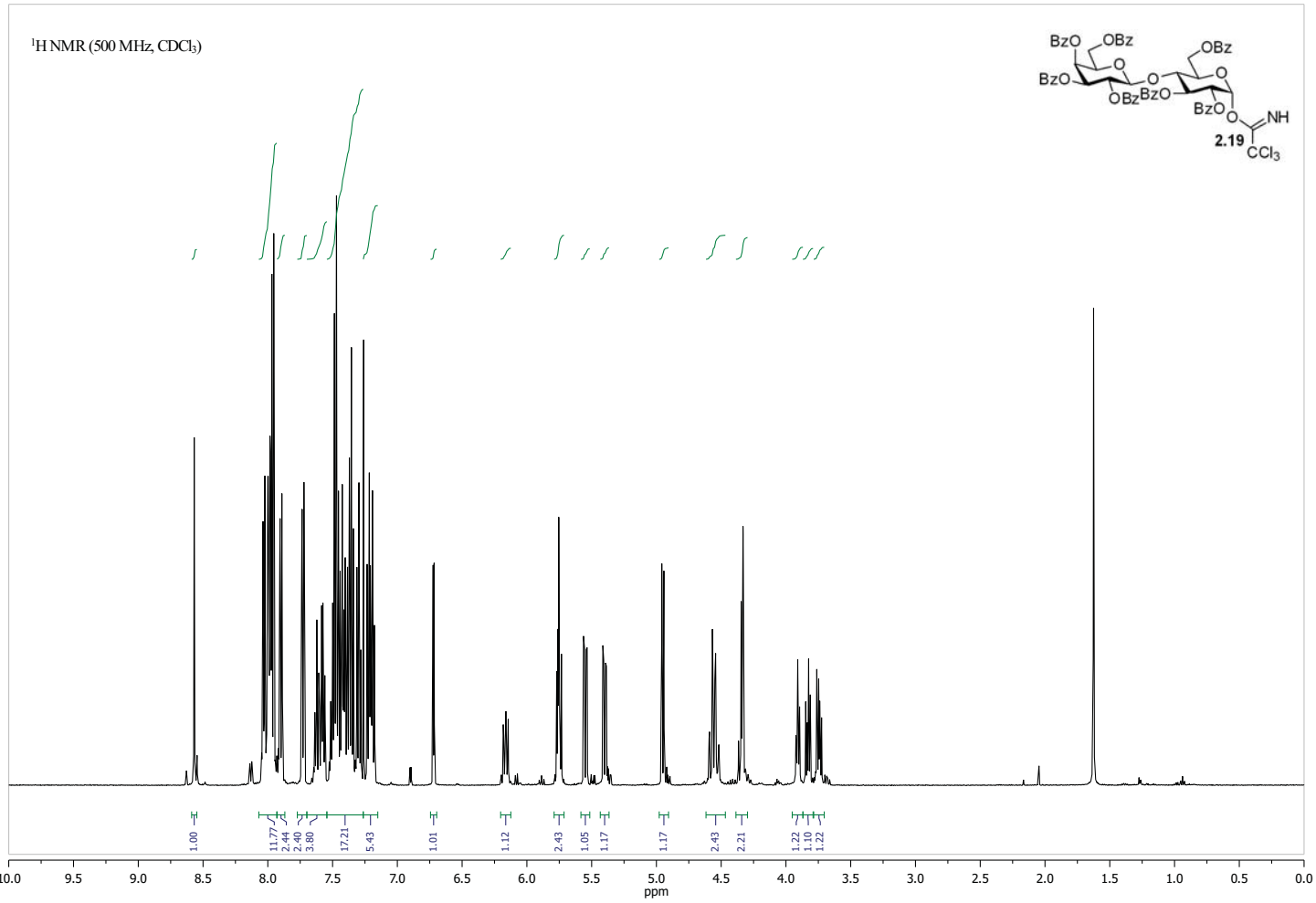
^{1}H NMR (500 MHz, $CDCl_3$)
BzO
OBz
OBz
BzO
O
O
OBz
BzO
O
BzO
O
NH
2.19
CCl_3
1.00
11.77
2.44
2.40
3.80
17.21
5.43
1.01
1.12
2.43
1.05
1.17
1.17
2.43
2.21
1.22
1.10
1.22
10.0
9.5
9.0
8.5
8.0
7.5
7.0
6.5
6.0
5.5
5.0
4.5
4.0
3.5
3.0
2.5
2.0
1.5
1.0
0.5
0.0
ppm

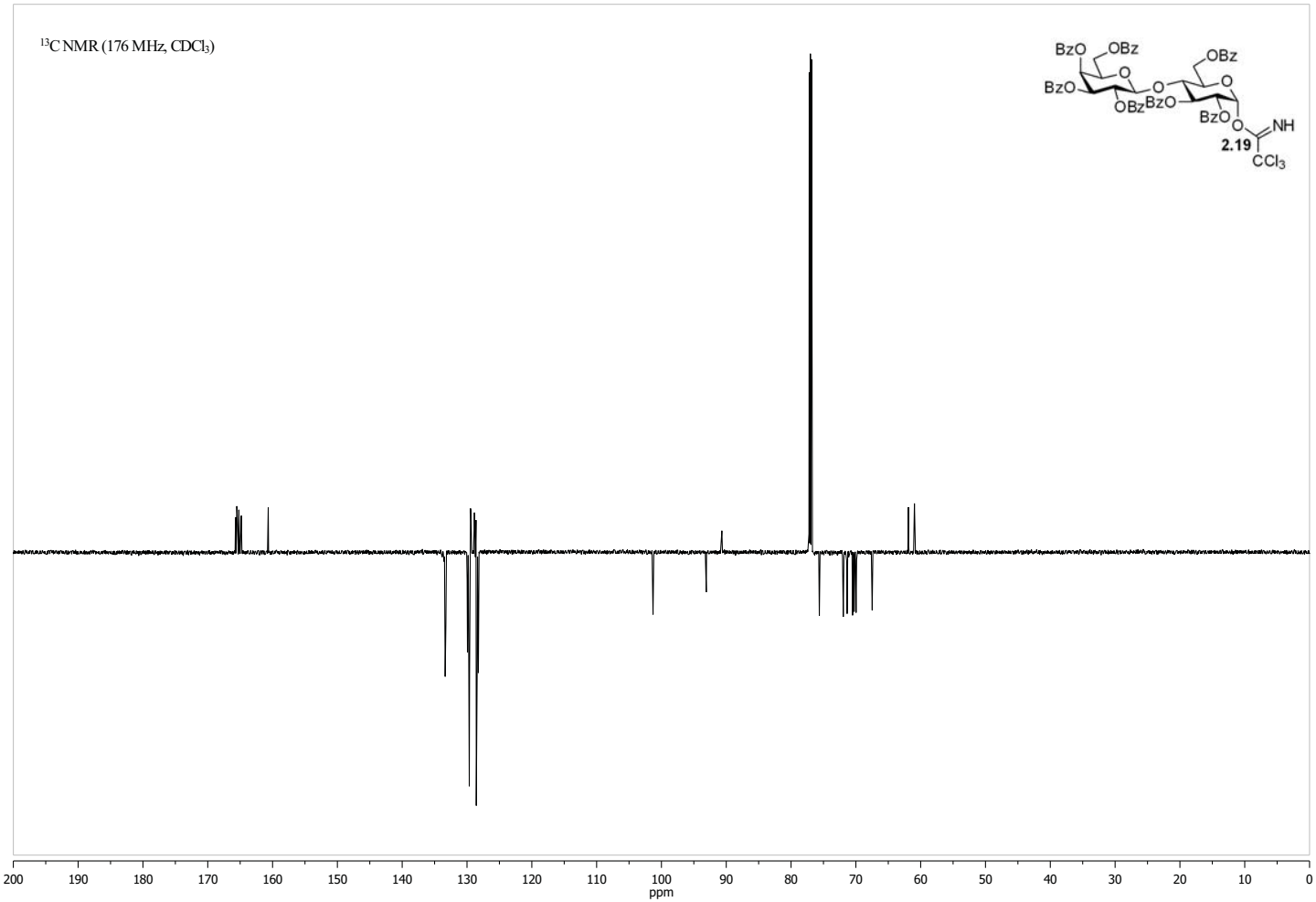
^{13}C NMR (176 MHz, $CDCl_3$)
BzO
OBz
OBz
BzO
O
O
O
OBz
BzO
BzO
O
NH
2.19
CCl_3
200
190
180
170
160
150
140
130
120
110
100
90
80
70
60
50
40
30
20
10
0
ppm

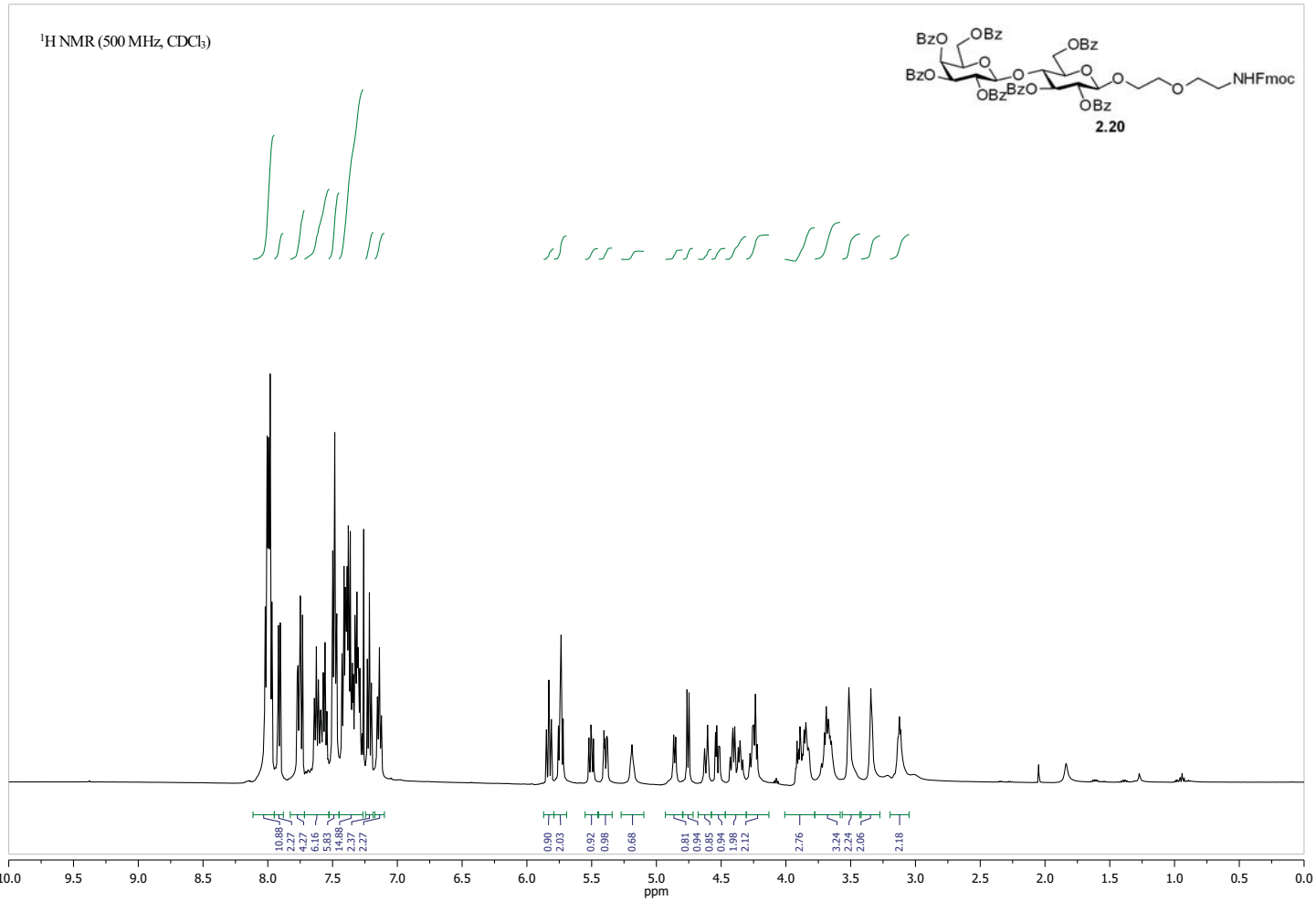
^{1}H NMR (500 MHz, CDCl$_3$)
BzO
OBz
BzO
OBz
BzO
OBz
OBz
O
O
O
O
O
NHFmoc
2.20
10.88
2.27
4.27
6.16
5.83
14.88
2.37
2.27
0.90
2.03
0.92
0.98
0.68
0.81
0.94
0.85
0.94
1.98
2.12
2.76
3.24
2.24
2.06
2.18
10.0
9.5
9.0
8.5
8.0
7.5
7.0
6.5
6.0
5.5
5.0
4.5
4.0
3.5
3.0
2.5
2.0
1.5
1.0
0.5
0.0
ppm

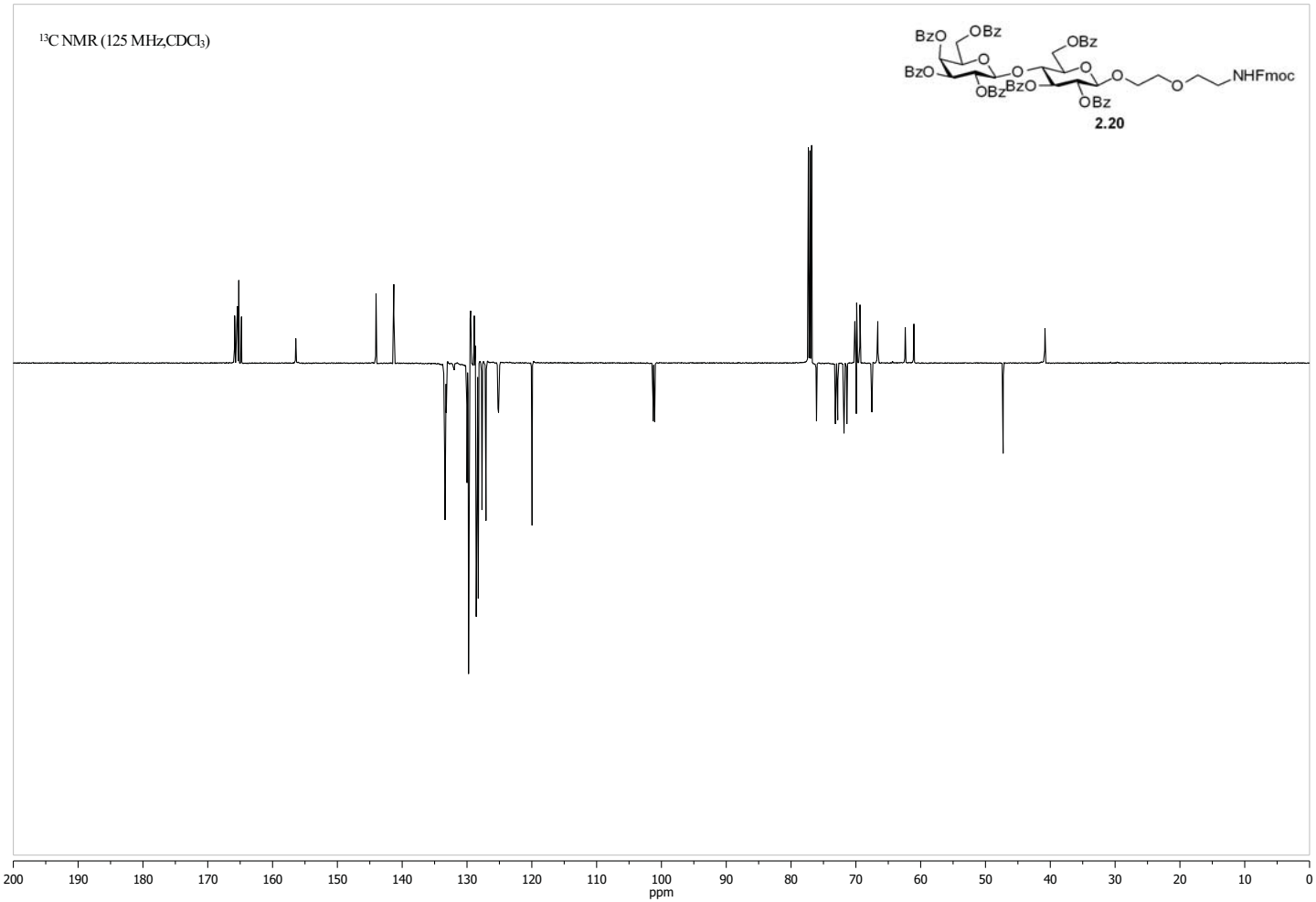
13C NMR (125 MHz,CDCl3)
BzO
OBz
BzO
OBz
BzO
OBz
OBz
O
NHFmoc
2.20
200
190
180
170
160
150
140
130
120
110
100
90
80
70
60
50
40
30
20
10
0
ppm

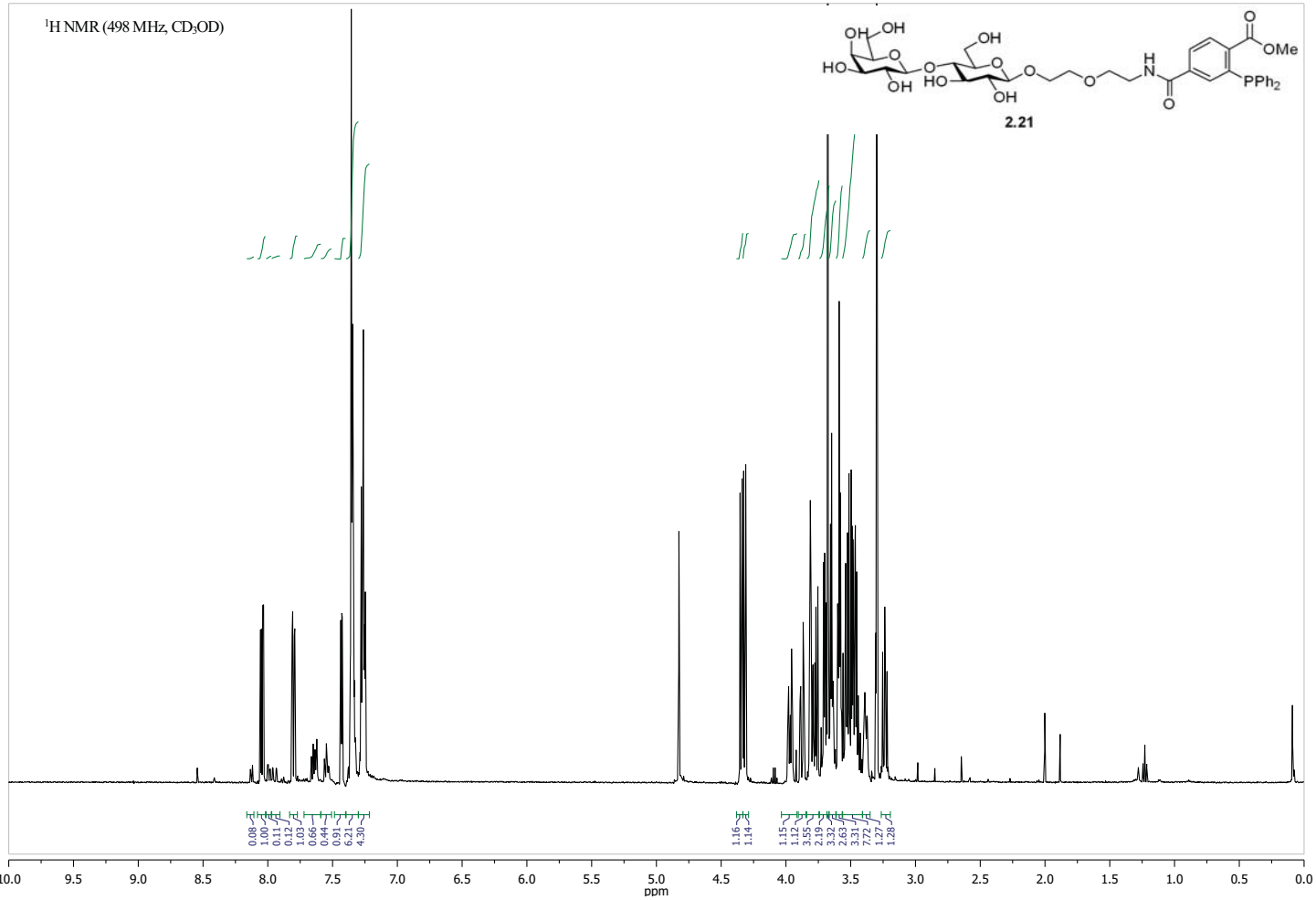
^{1}H NMR (498 MHz, CD_3OD)
2.21
ppm

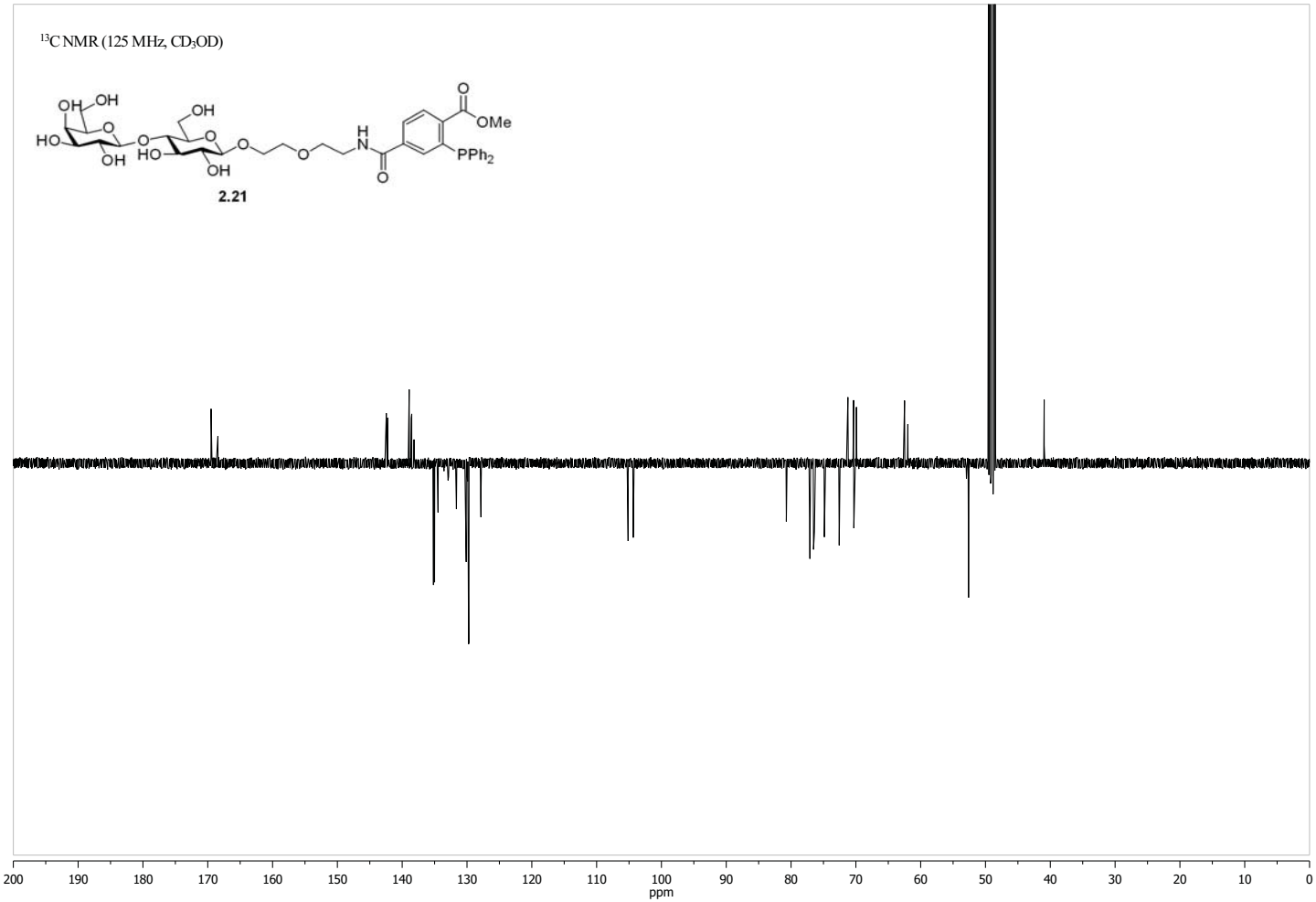
13C NMR (125 MHz, CD3OD)
2.21
200
190
180
170
160
150
140
130
120
110
100
90
80
70
60
50
40
30
20
10
0
ppm

^{31}P NMR (202 MHz, CD_3OD)

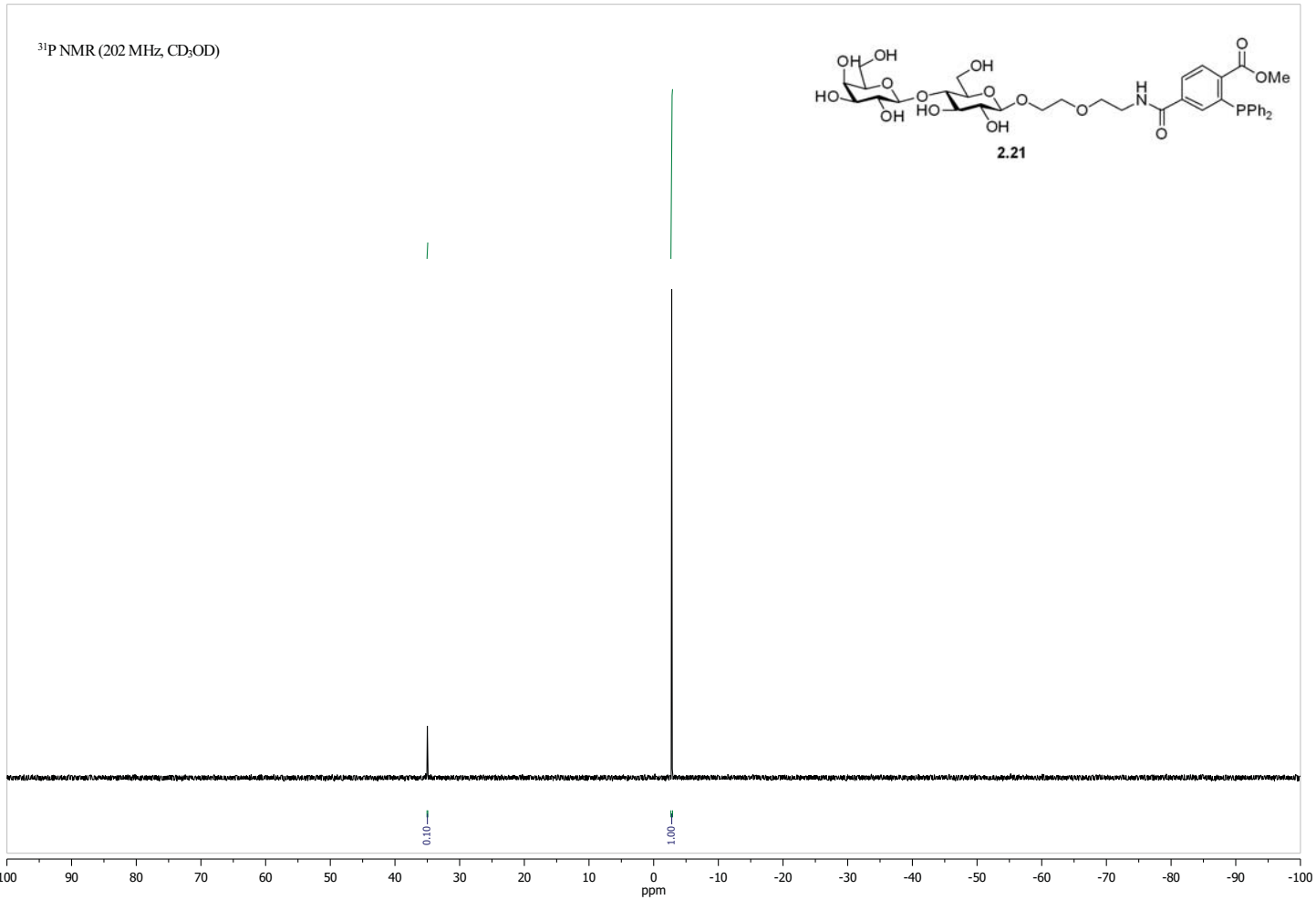

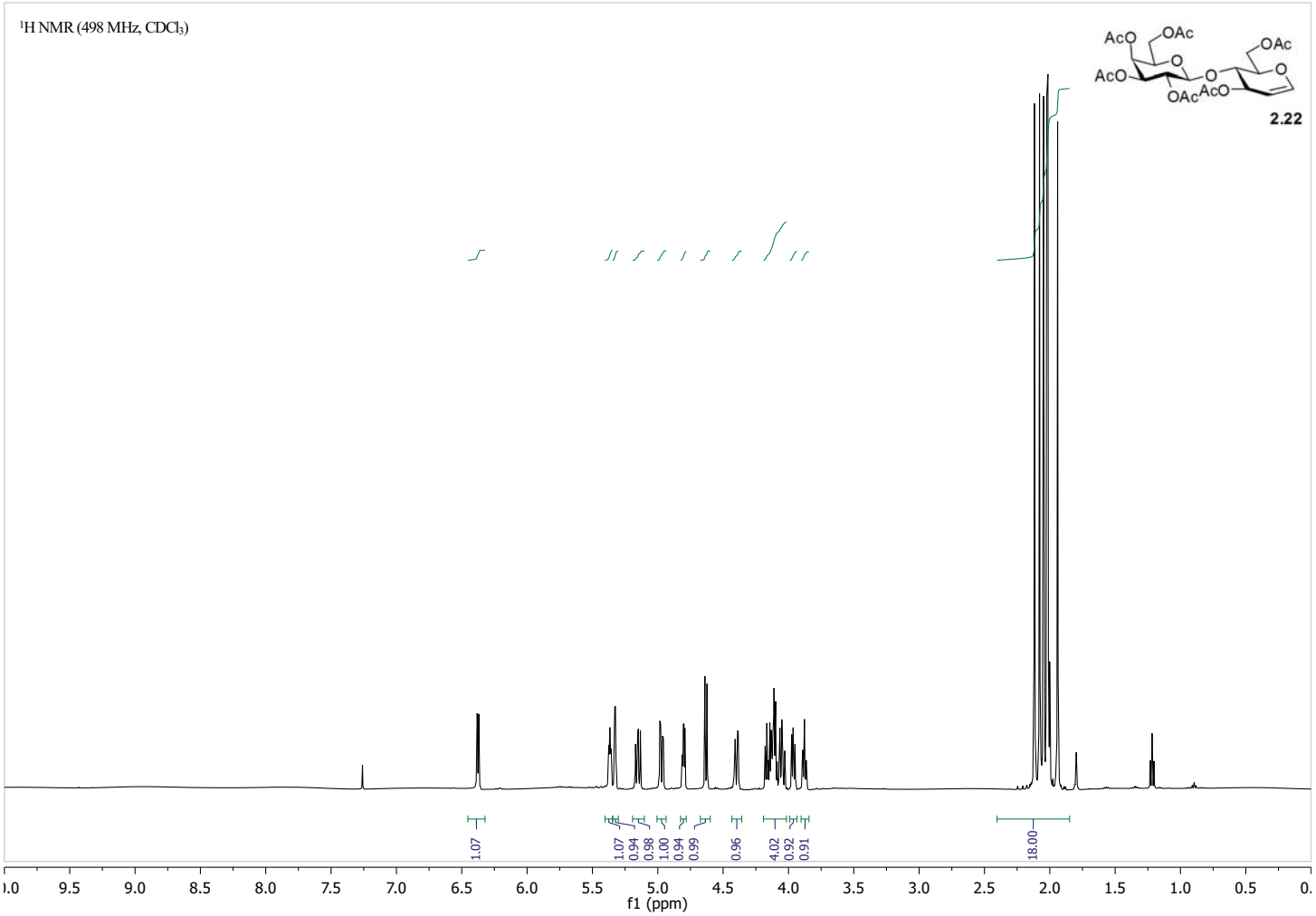
^{1}H NMR (498 MHz, CDCl$_3$)
AcO
OAc
AcO
OAc
AcO
OAc
OAc
2.22
1.07
1.07
0.94
0.98
1.00
0.94
0.99
0.96
4.02
0.92
0.91
18.00
f1 (ppm)

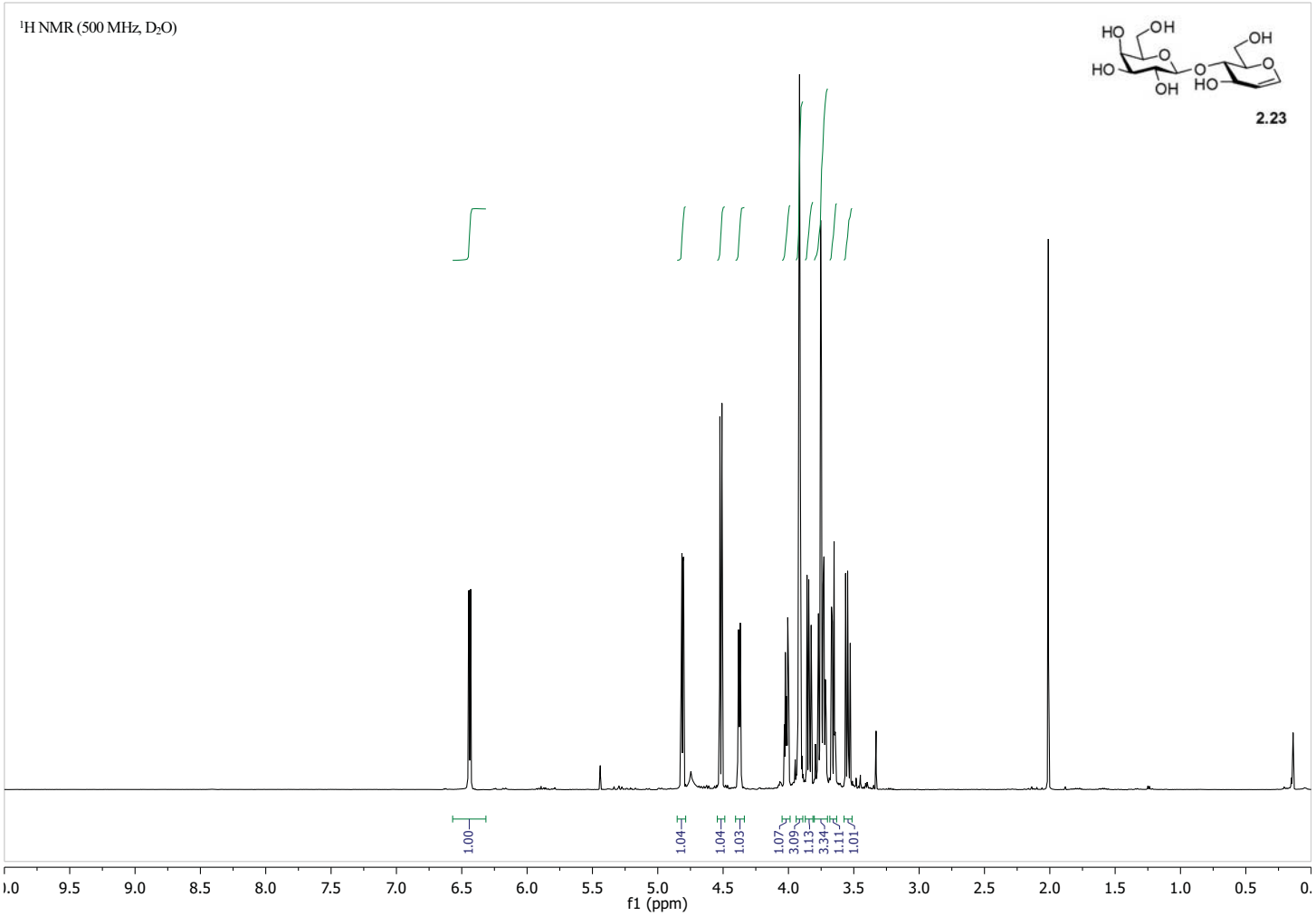
^{1}H NMR (500 MHz, D_2O)
HO
OH
O
HO
OH
O
OH
O
HO
2.23
1.00
1.04
1.04
1.03
1.07
3.09
1.13
3.34
1.11
1.01
9.5
9.0
8.5
8.0
7.5
7.0
6.5
6.0
5.5
5.0
4.5
4.0
3.5
3.0
2.5
2.0
1.5
1.0
0.5
f1 (ppm)

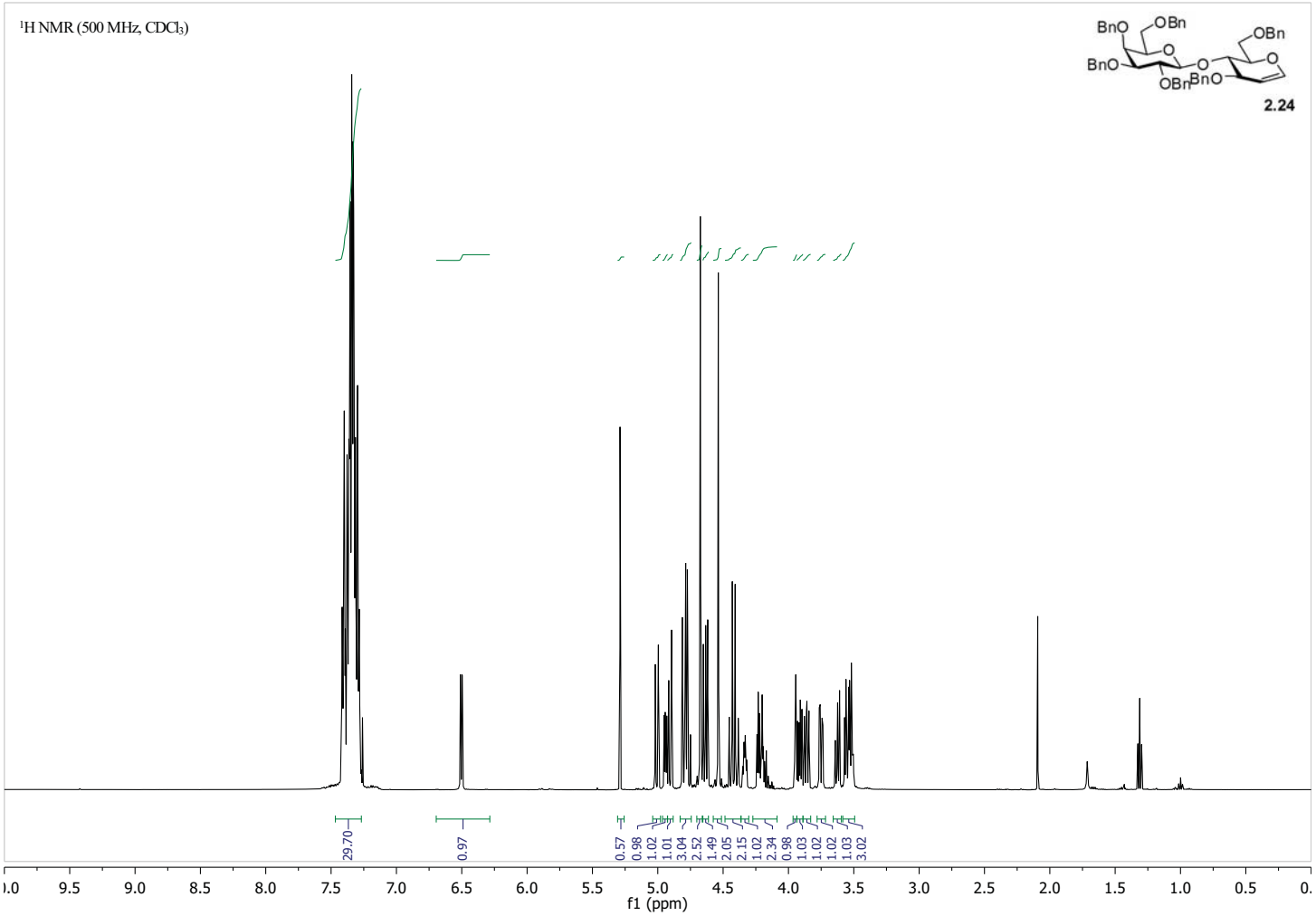
^{1}H NMR (500 MHz, $CDCl_3$)
BnO
OBn
OBn
BnO
OBn
BnO
2.24
29.70
0.97
0.57
0.98
1.02
1.01
3.04
2.52
1.49
2.05
2.15
1.02
2.34
0.98
1.03
1.02
1.02
1.03
3.02
9.5
9.0
8.5
8.0
7.5
7.0
6.5
6.0
5.5
5.0
4.5
4.0
3.5
3.0
2.5
2.0
1.5
1.0
0.5
f1 (ppm)

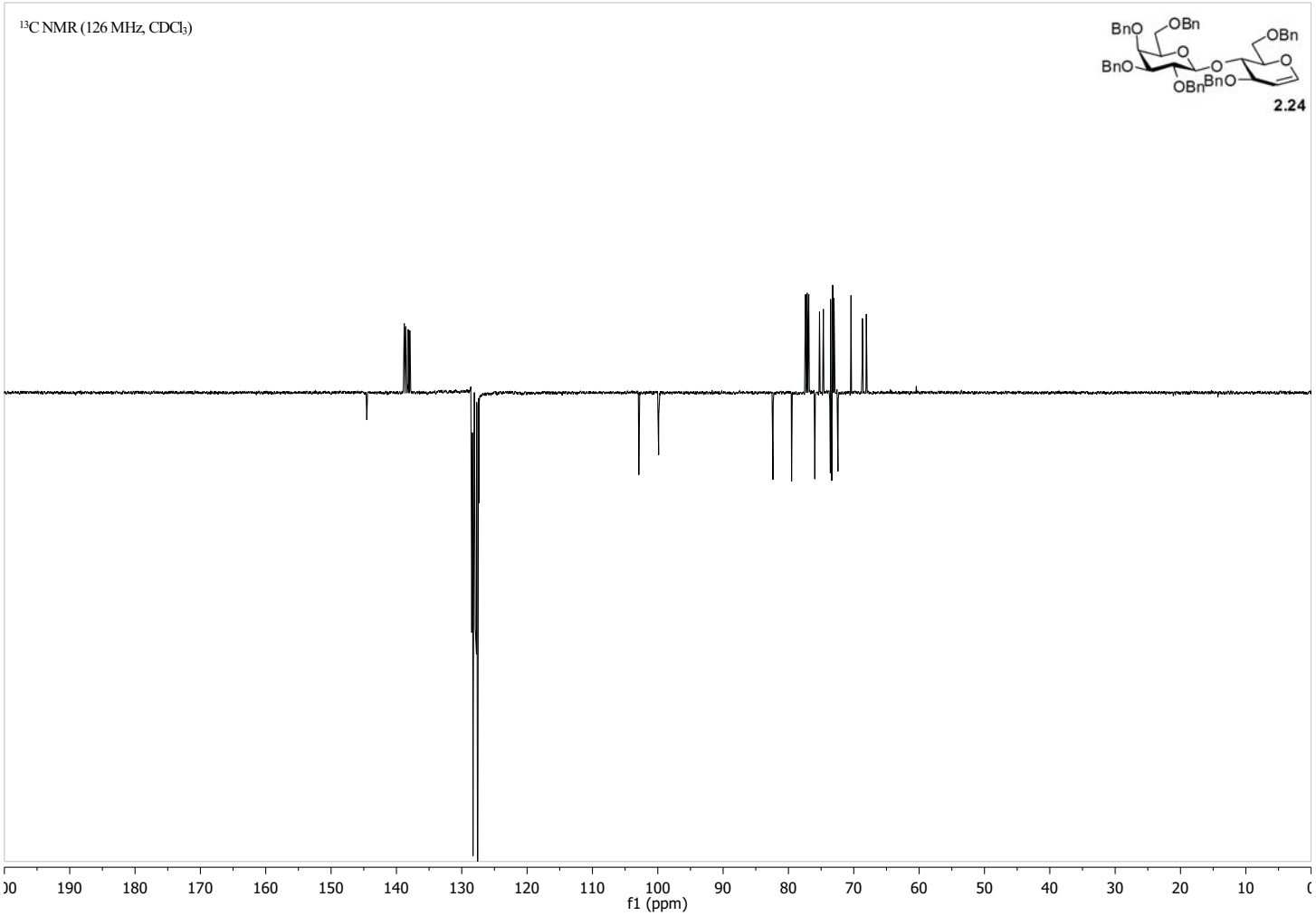
13C NMR (126 MHz, CDCl3)
BnO
OBn
BnO
OBn
BnO
OBn
O
O
O
O
2.24
190
180
170
160
150
140
130
120
110
100
90
80
70
60
50
40
30
20
10
f1 (ppm)

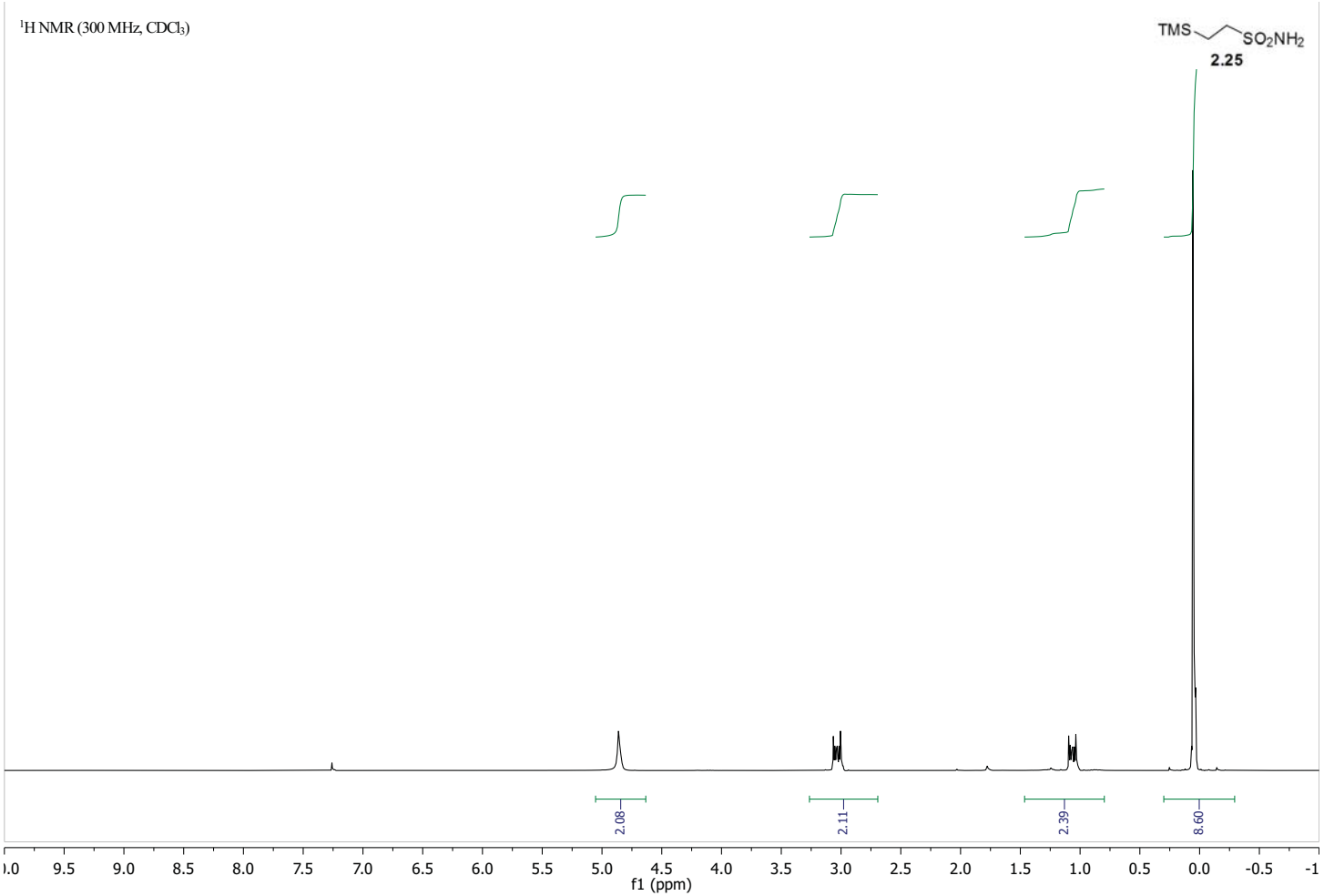
^{1}H NMR (300 MHz, $CDCl_3$)
TMS
SO_2NH_2
2.25
2.08
2.11
2.39
8.60
f1 (ppm)

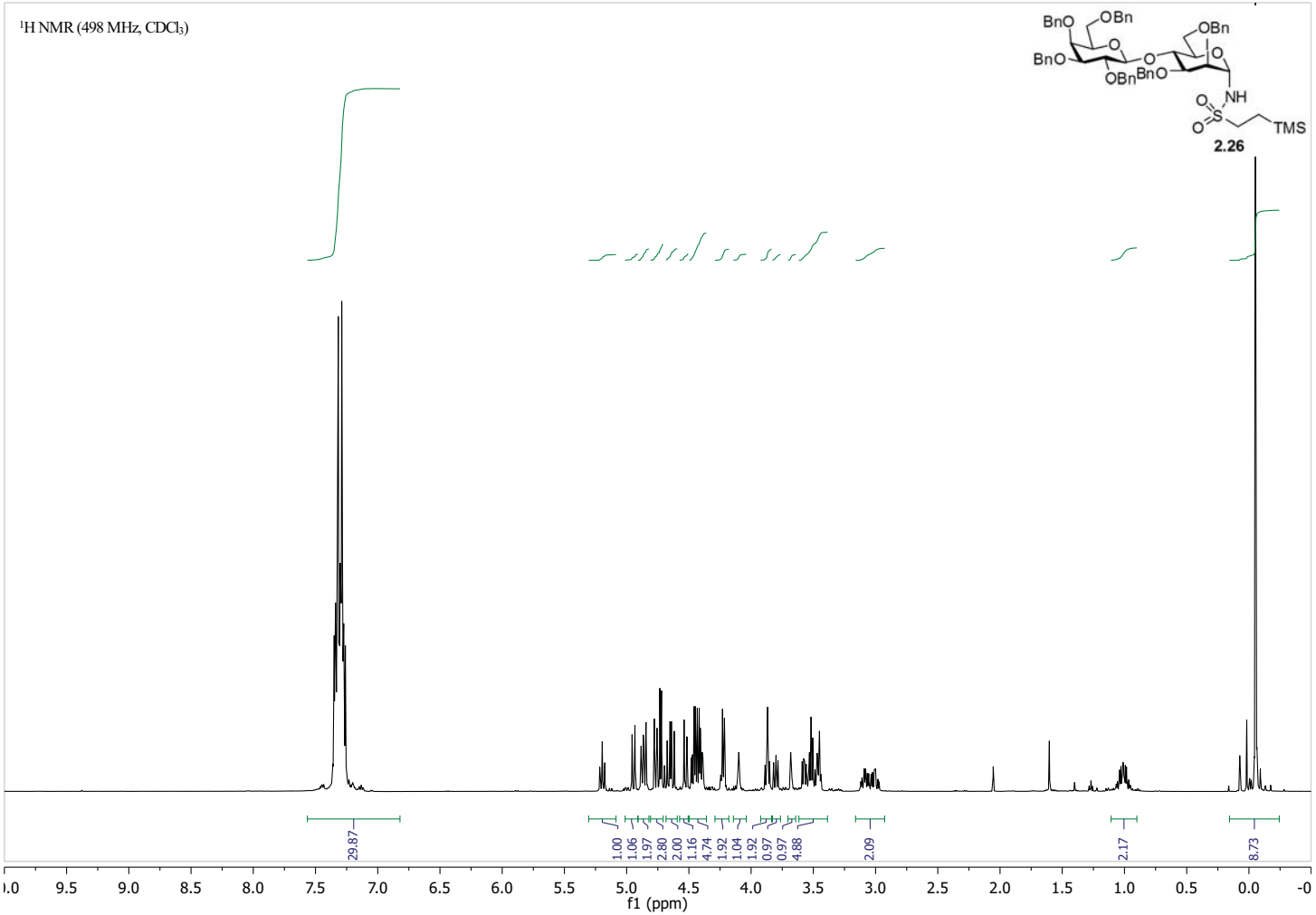
^{1}H NMR (498 MHz, CDCl$_3$)
BnO
OBn
OBn
BnO
OBn
BnO
O
O
O
NH
S
TMS
2.26
29.87
1.00
1.06
1.97
2.80
2.00
1.16
4.74
1.92
1.04
1.92
0.97
0.97
4.88
2.09
2.17
8.73
f1 (ppm)

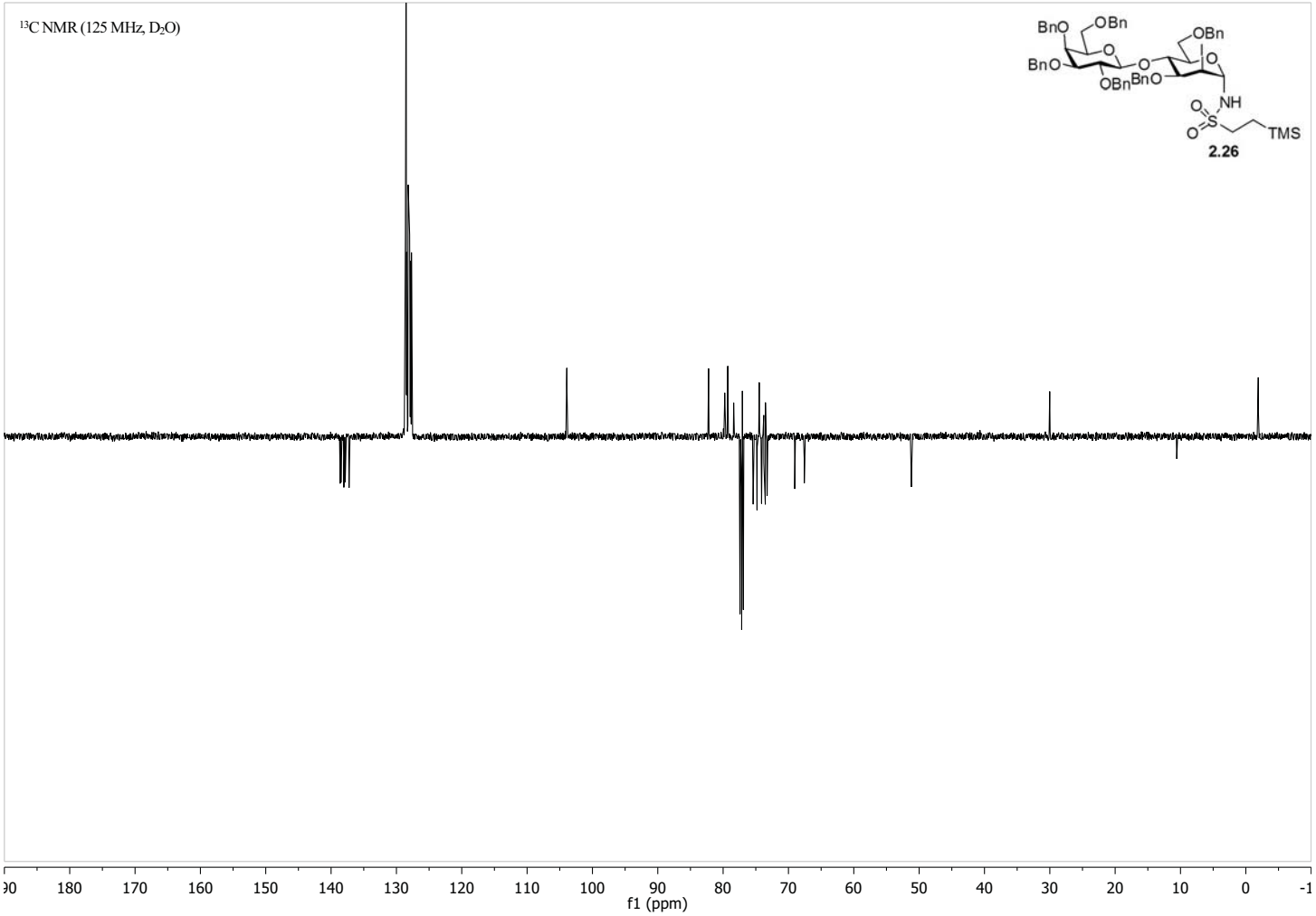
^{13}C NMR (125 MHz, D_2O)
BnO
OBn
OBn
BnO
OBn
BnO
O
O
O
NH
S
O
O
TMS
2.26
180
170
160
150
140
130
120
110
100
90
80
70
60
50
40
30
20
10
0
f1 (ppm)

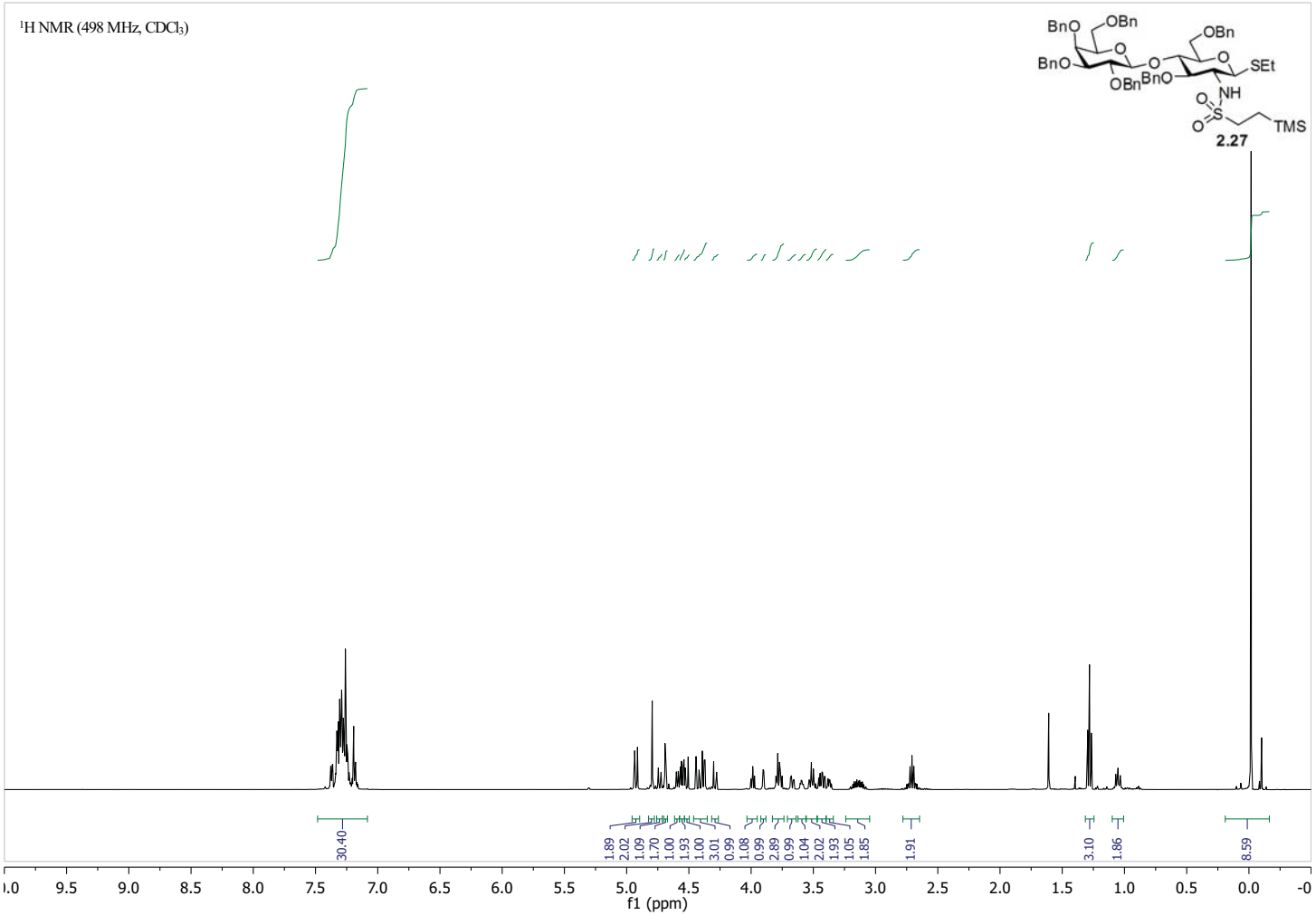
^{1}H NMR (498 MHz, CDCl$_3$)
BnO
OBn
OBn
BnO
O
O
SEt
OBn
BnO
NH
O
S
O
TMS
2.27
30.40
1.89
2.02
1.09
1.70
1.00
1.93
1.00
3.01
0.99
1.08
0.99
2.89
0.99
1.04
2.02
1.93
1.05
1.85
1.91
3.10
1.86
8.59
9.5
9.0
8.5
8.0
7.5
7.0
6.5
6.0
5.5
5.0
4.5
4.0
3.5
3.0
2.5
2.0
1.5
1.0
0.5
0.0
f1 (ppm)

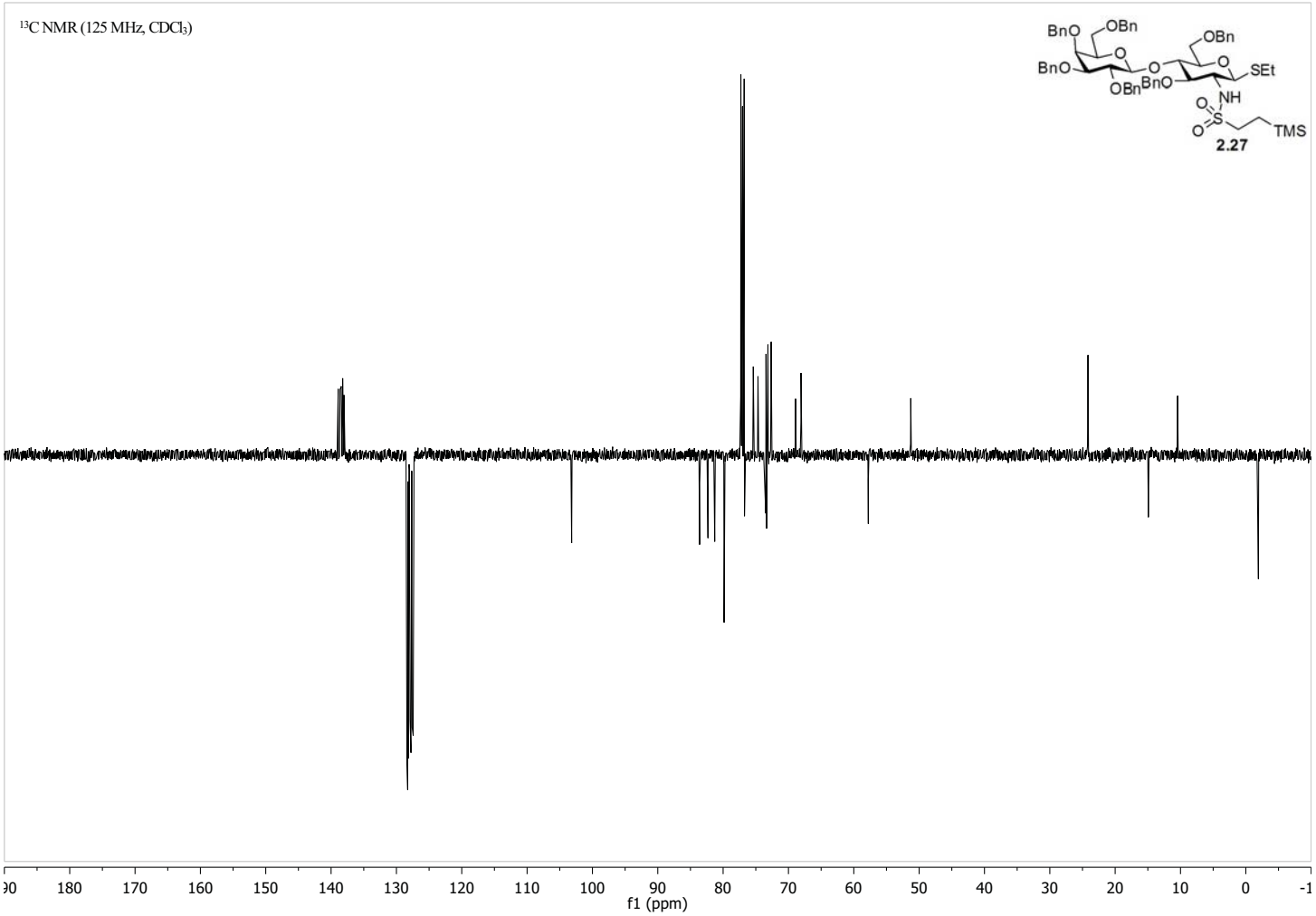
13C NMR (125 MHz, CDCl3)
BnO
OBn
OBn
BnO
O
O
O
SEt
OBn
BnO
NH
O
S
O
TMS
2.27
180
170
160
150
140
130
120
110
100
90
80
70
60
50
40
30
20
10
0
f1 (ppm)

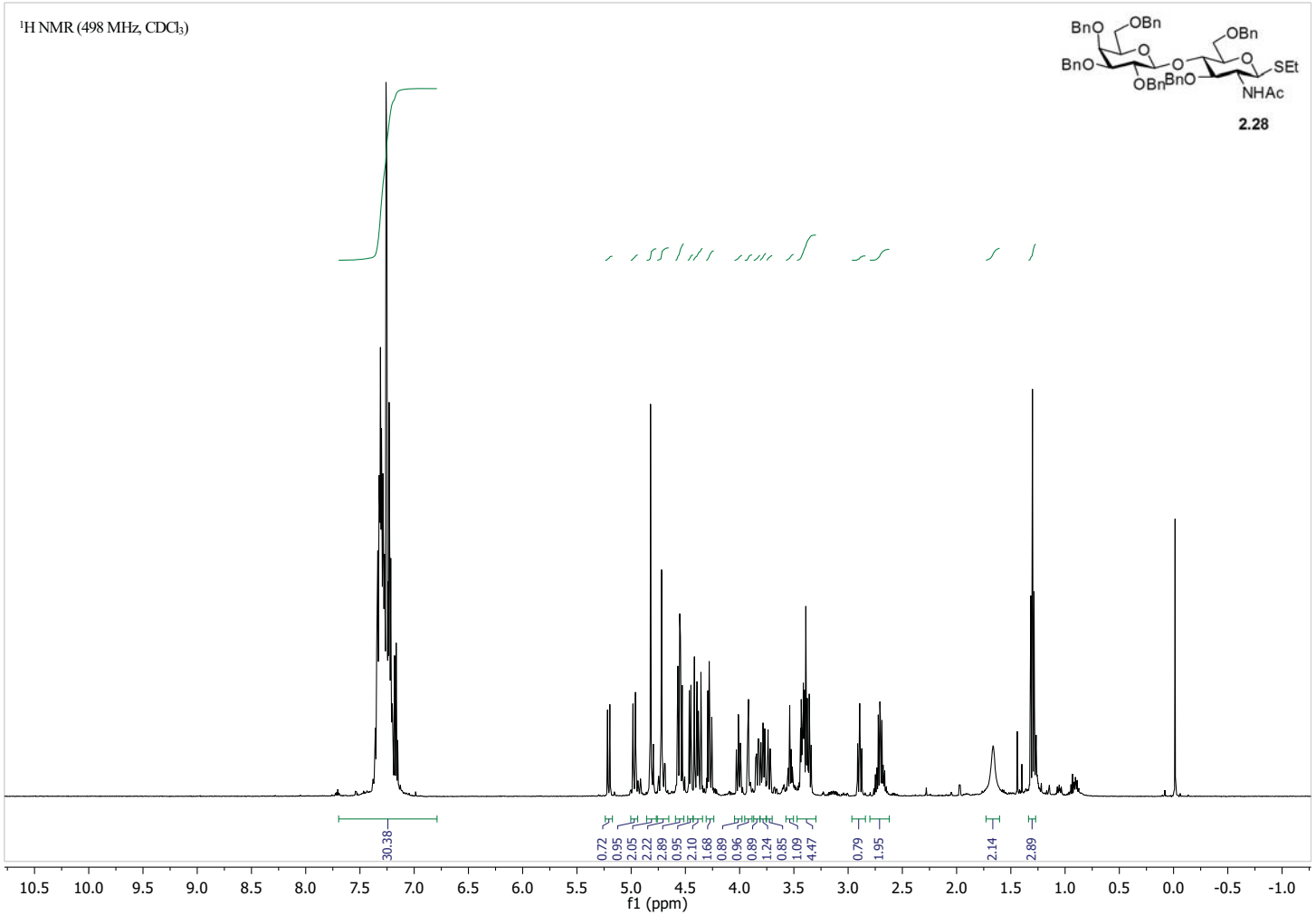
^{1}H NMR (498 MHz, $CDCl_3$)
BnO
OBn
OBn
BnO
O
O
SEt
OBn
BnO
NHAc
2.28
30.38
0.72
0.95
2.05
2.22
2.89
0.95
2.10
1.68
0.89
0.96
0.89
1.24
0.85
1.09
4.47
0.79
1.95
2.14
2.89
10.5 10.0 9.5 9.0 8.5 8.0 7.5 7.0 6.5 6.0 5.5 5.0 4.5 4.0 3.5 3.0 2.5 2.0 1.5 1.0 0.5 0.0 -0.5 -1.0
f1 (ppm)

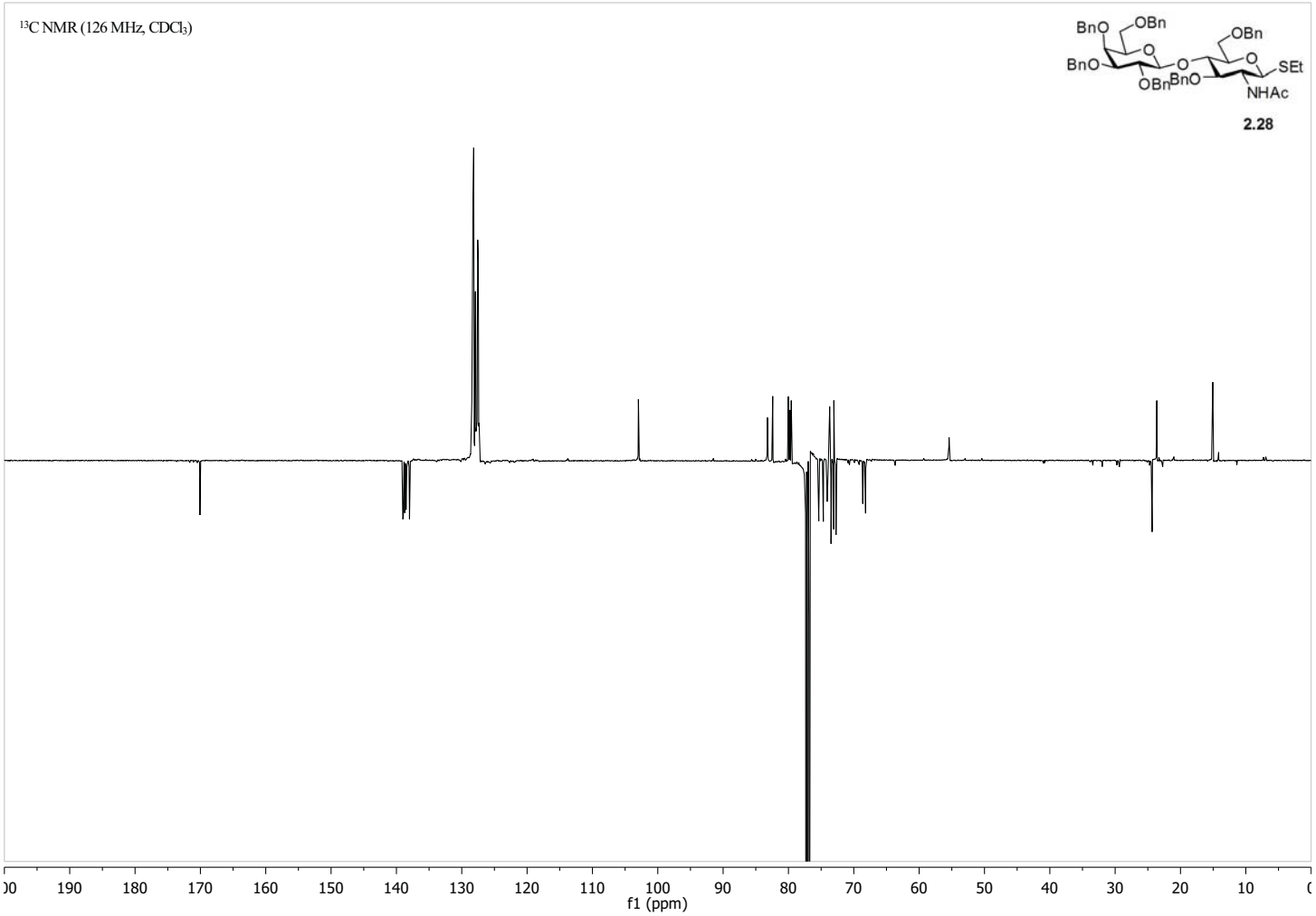
13C NMR (126 MHz, CDCl3)
BnO
OBn
BnO
OBn
O
O
BnO
OBn
O
SEt
NHAc
2.28
190
180
170
160
150
140
130
120
110
100
90
80
70
60
50
40
30
20
10
f1 (ppm)

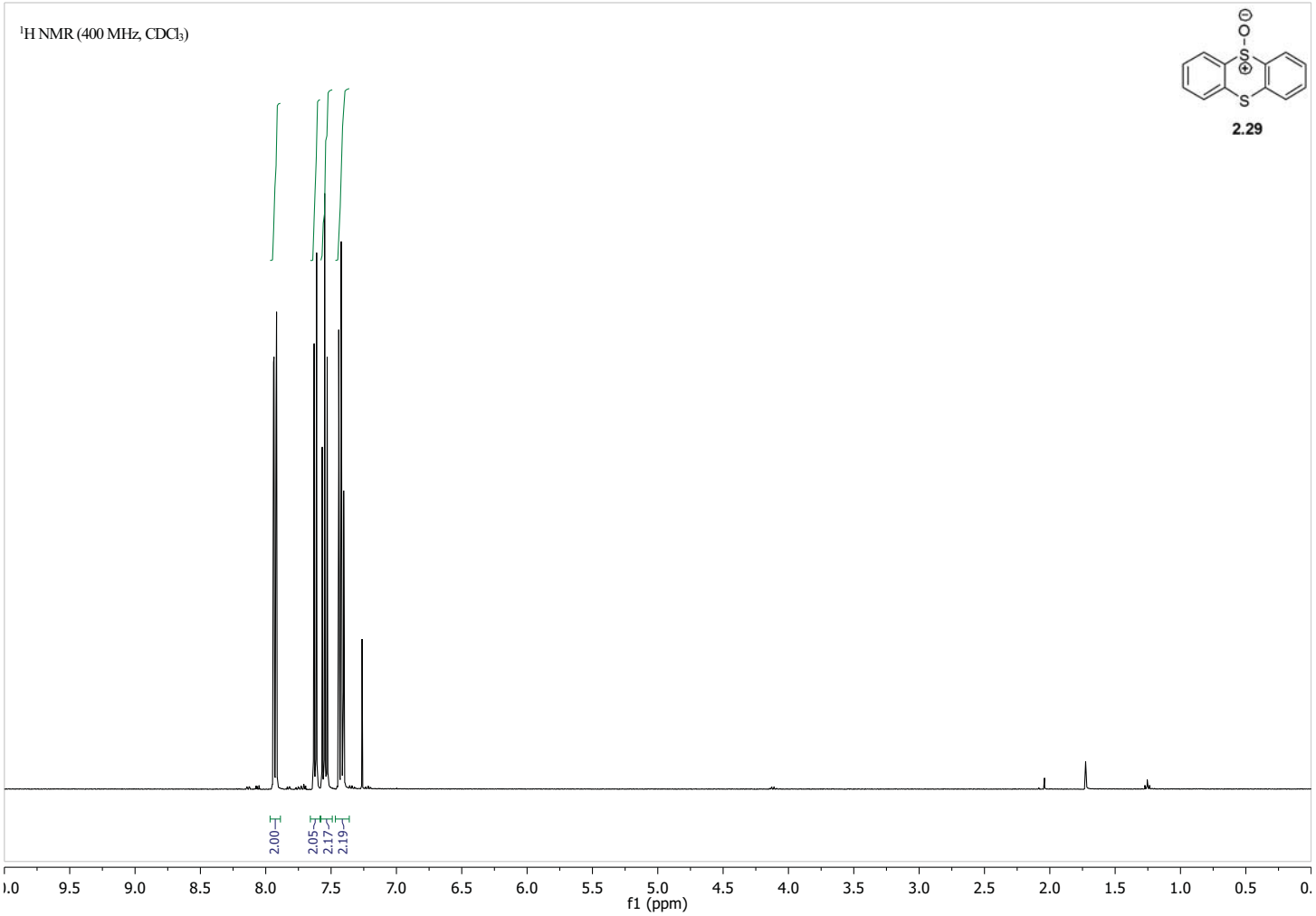
^{1}H NMR (400 MHz, CDCl$_3$)
2.29
2.00
2.05
2.17
2.19
9.5
9.0
8.5
8.0
7.5
7.0
6.5
6.0
5.5
5.0
4.5
4.0
3.5
3.0
2.5
2.0
1.5
1.0
0.5
f1 (ppm)

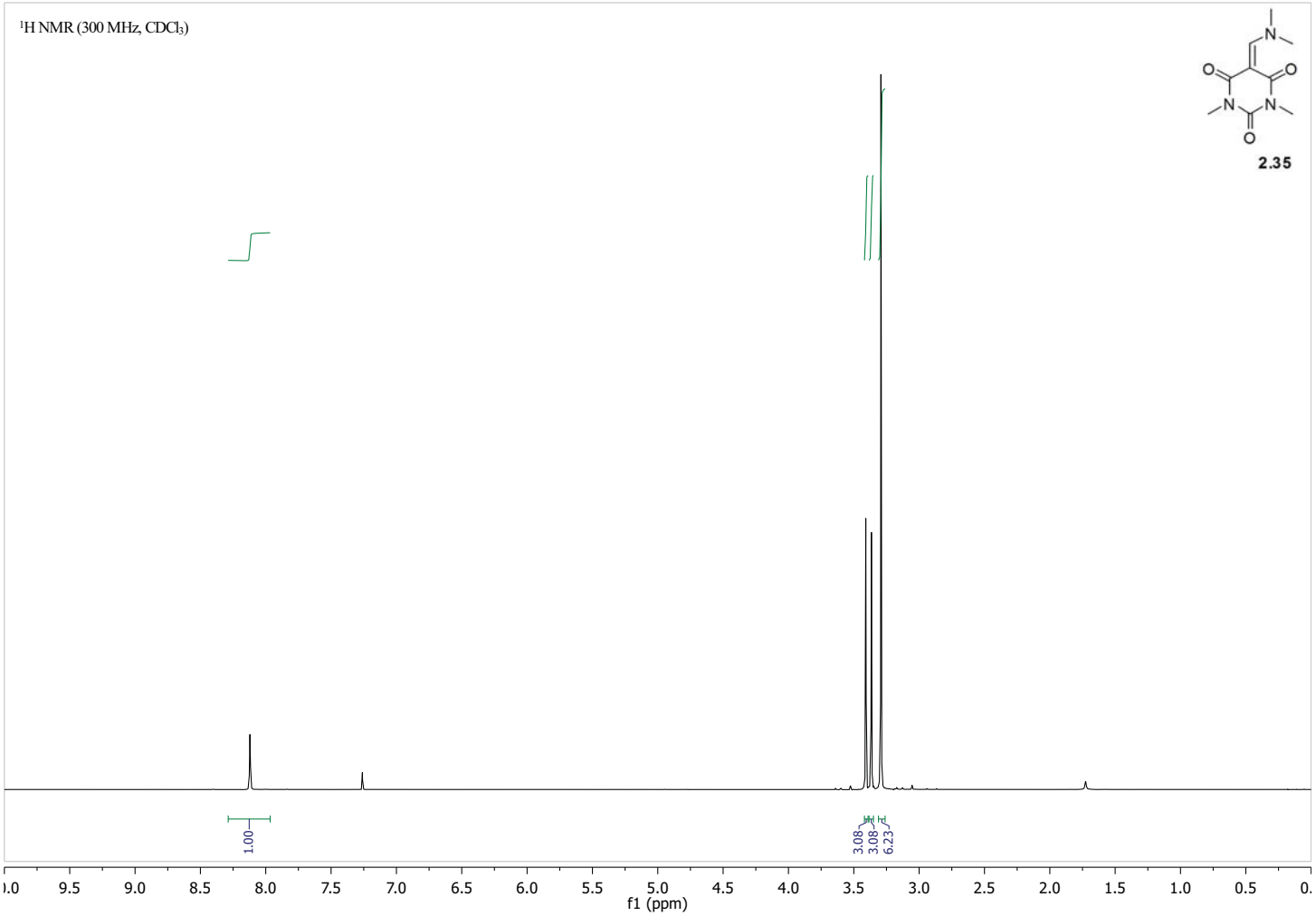
^{1}H NMR (300 MHz, $CDCl_3$)
2.35
1.00
3.08
3.08
6.23
f1 (ppm)

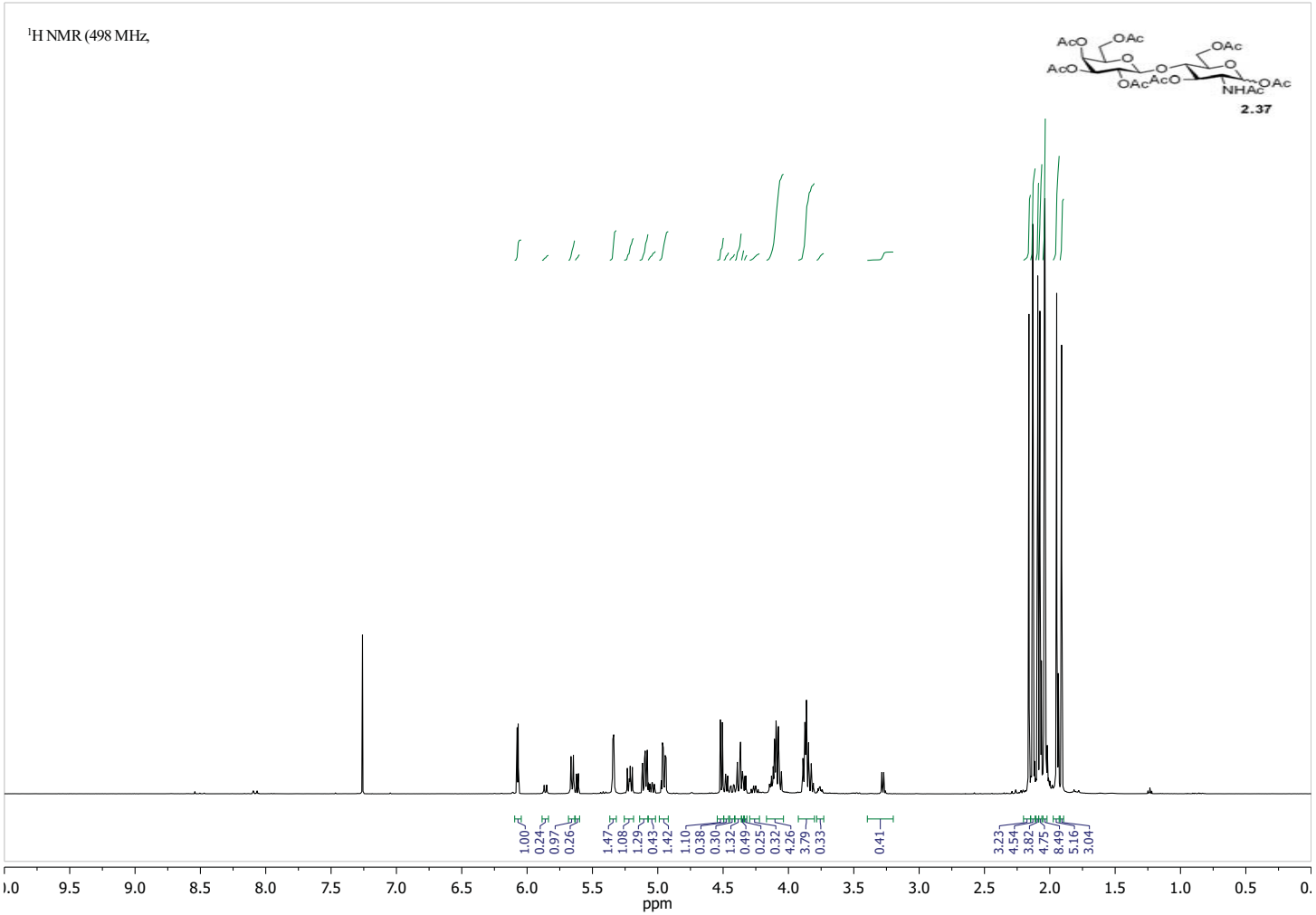
^{1}H NMR (498 MHz,
2.37
1.00
0.24
0.97
0.26
1.47
1.08
1.29
0.43
1.42
1.10
0.38
0.30
1.32
0.49
0.25
0.32
4.26
3.79
0.33
0.41
3.23
4.54
3.82
4.75
8.49
5.16
3.04
ppm

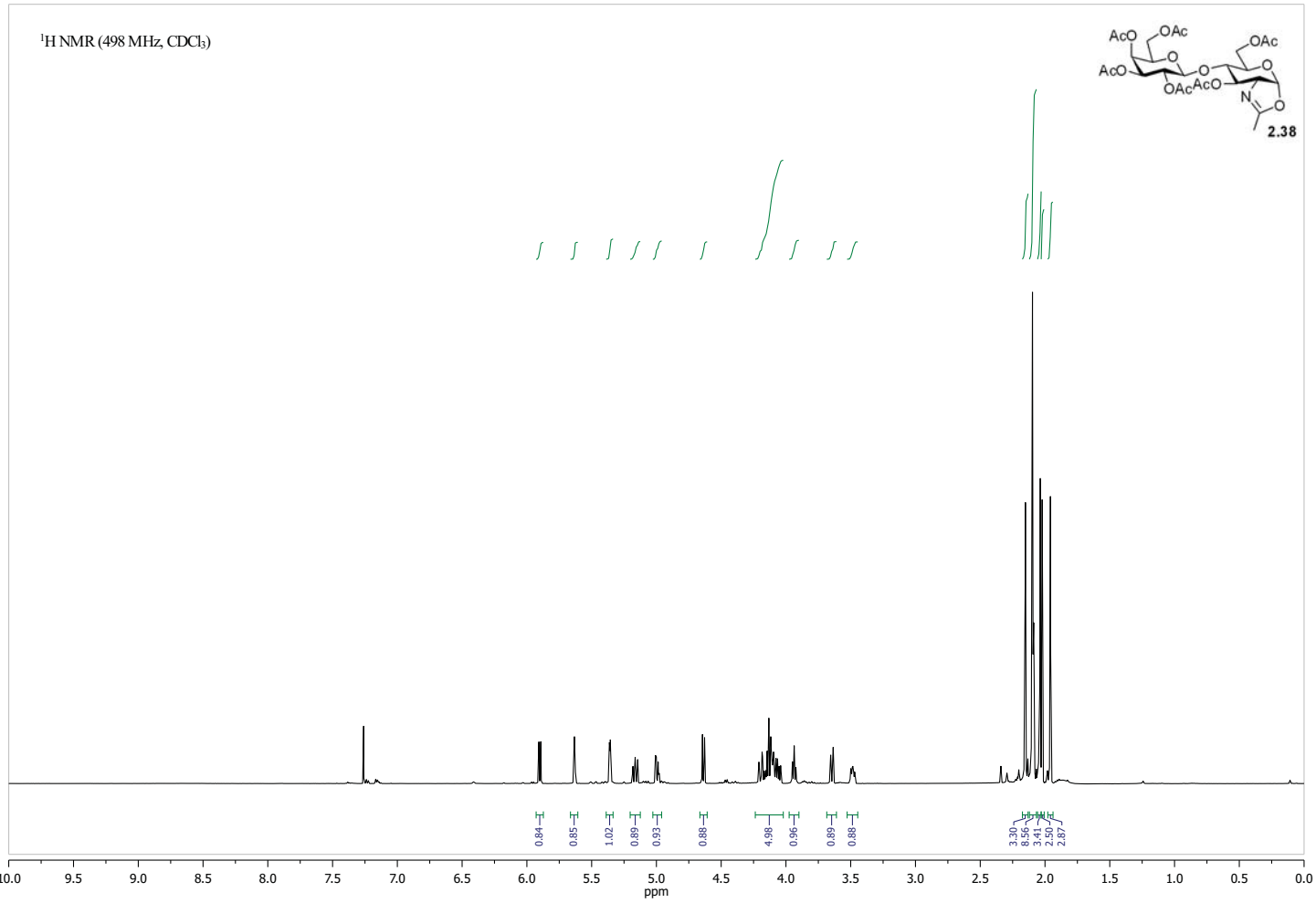
^{1}H NMR (498 MHz, $CDCl_3$)
2.38
0.84
0.85
1.02
0.89
0.93
0.88
4.98
0.96
0.89
0.88
3.30
8.56
3.41
2.50
2.87
10.0
9.5
9.0
8.5
8.0
7.5
7.0
6.5
6.0
5.5
5.0
4.5
4.0
3.5
3.0
2.5
2.0
1.5
1.0
0.5
0.0
ppm

^{13}C NMR (125 MHz, $CDCl_3$)

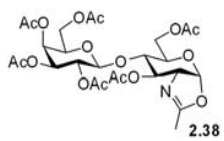

2.38

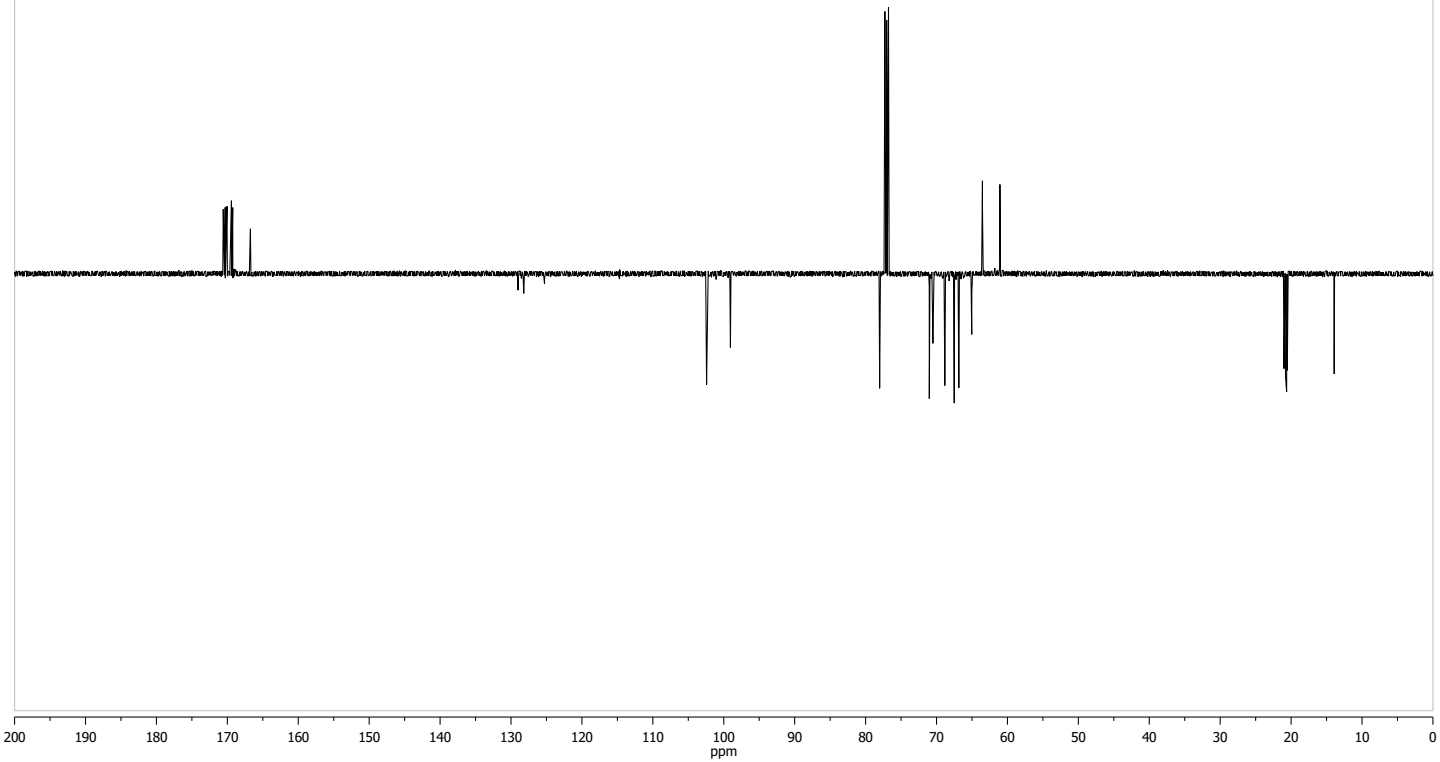

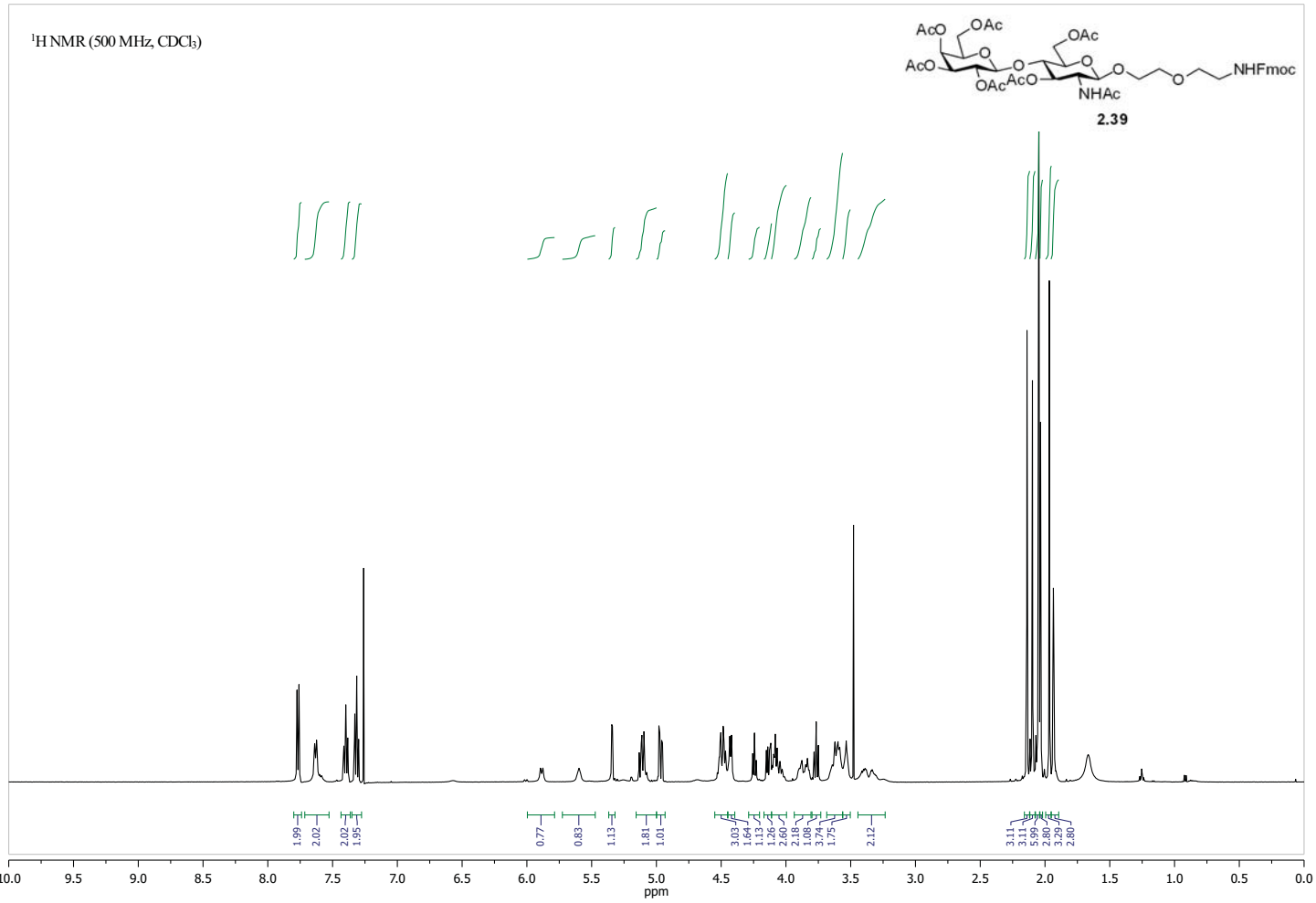
^{1}H NMR (500 MHz, $CDCl_3$)
AcO
OAc
AcO
OAc
OAc
AcO
NHAc
NHFmoc
2.39
1.99
2.02
2.02
1.95
0.77
0.83
1.13
1.81
1.01
3.03
1.64
1.13
1.26
2.60
2.18
1.08
3.74
1.75
2.12
3.11
3.11
5.93
2.80
3.29
2.80
10.0
9.5
9.0
8.5
8.0
7.5
7.0
6.5
6.0
5.5
5.0
4.5
4.0
3.5
3.0
2.5
2.0
1.5
1.0
0.5
0.0
ppm

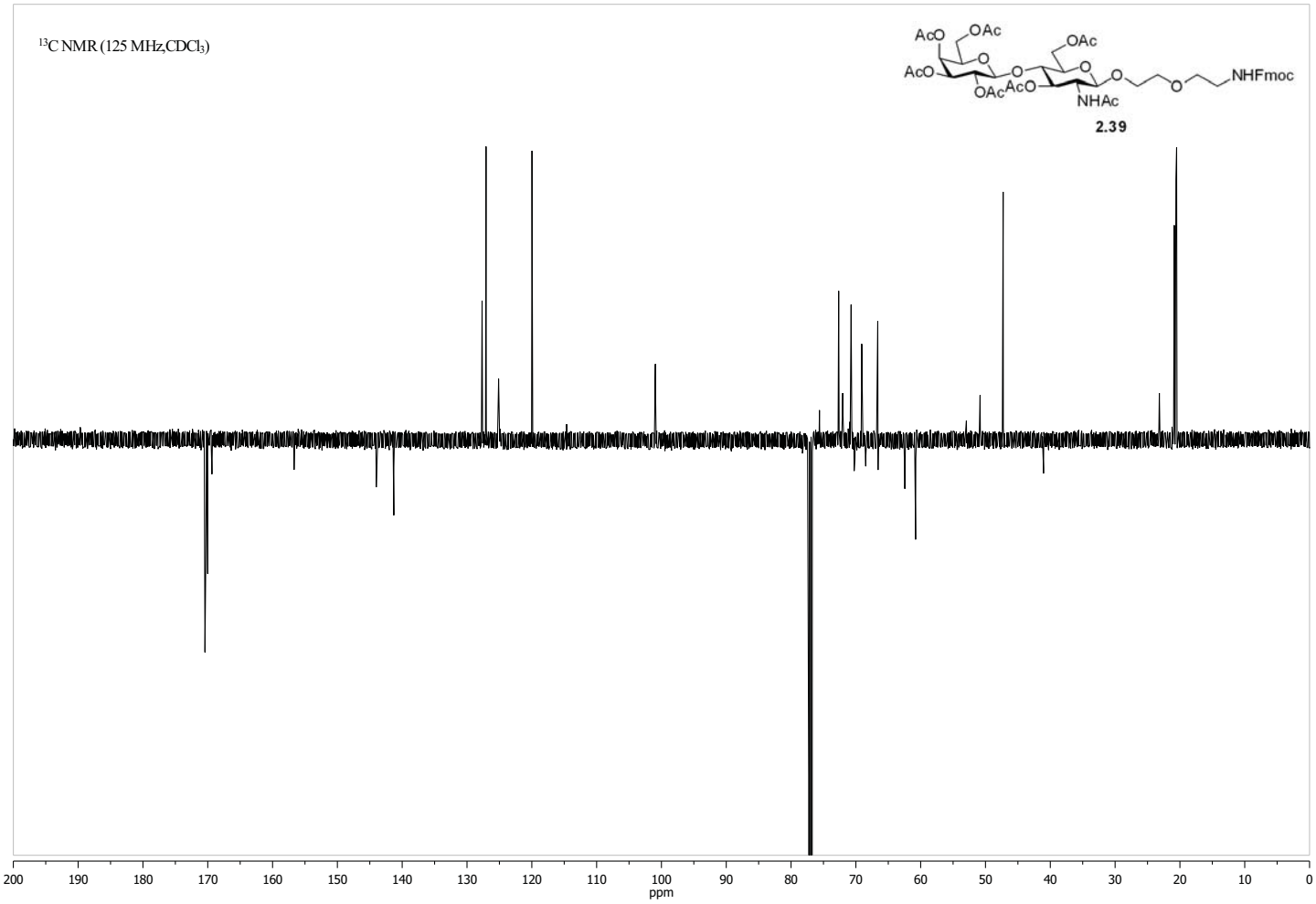
^{13}C NMR (125 MHz,$CDCl_3$)
AcO
OAc
AcO
OAc
AcO
OAc
NHAc
NHFmoc
2.39
200
190
180
170
160
150
140
130
120
110
100
90
80
70
60
50
40
30
20
10
0
ppm

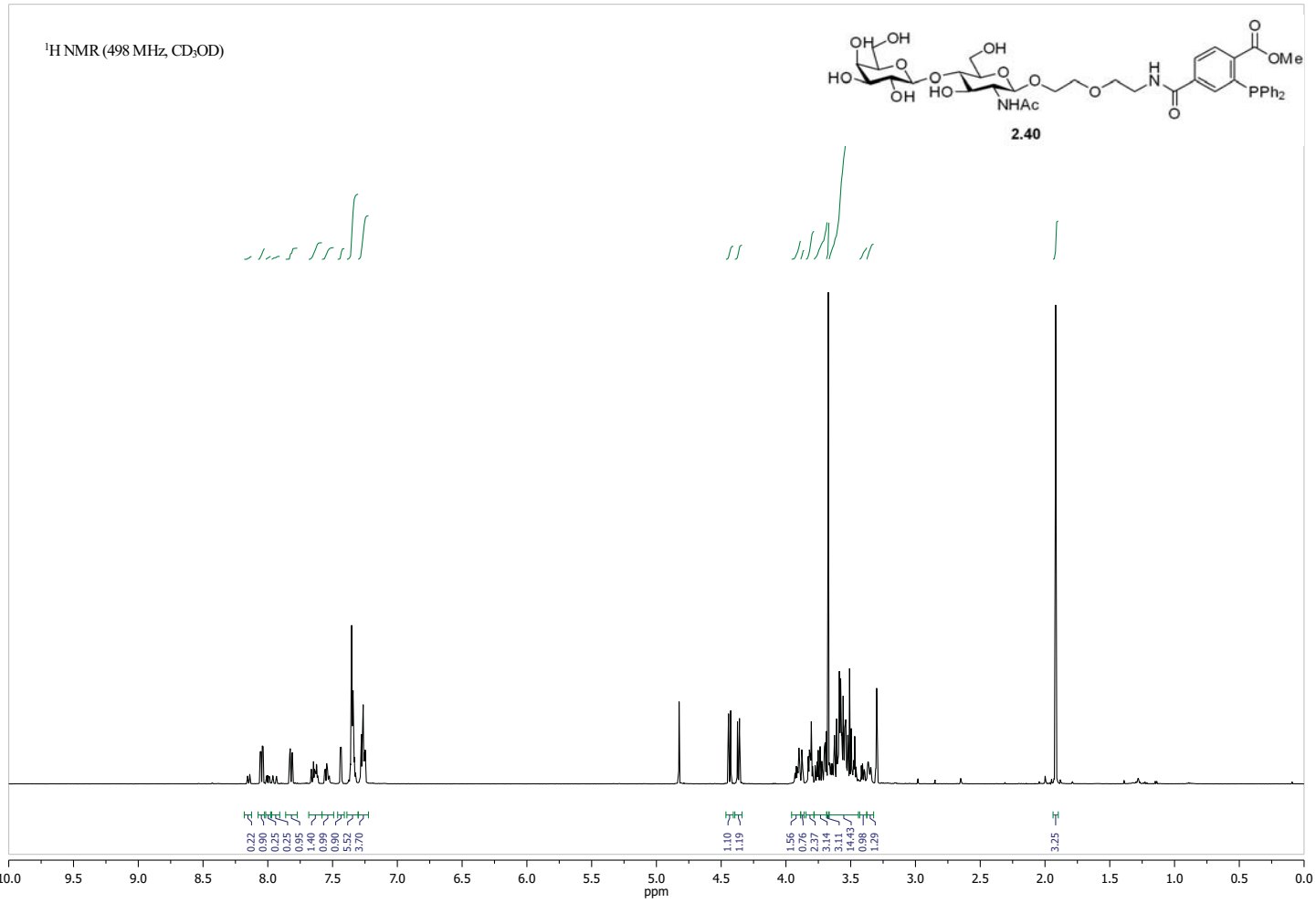
^{1}H NMR (498 MHz, CD_3OD)
2.40
10.0
9.5
9.0
8.5
8.0
7.5
7.0
6.5
6.0
5.5
5.0
4.5
4.0
3.5
3.0
2.5
2.0
1.5
1.0
0.5
0.0
ppm

^{13}C NMR (125 MHz, CD_3OD)

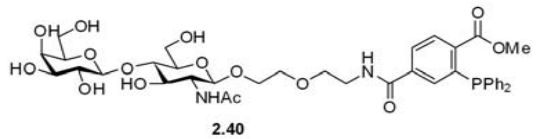

2.40

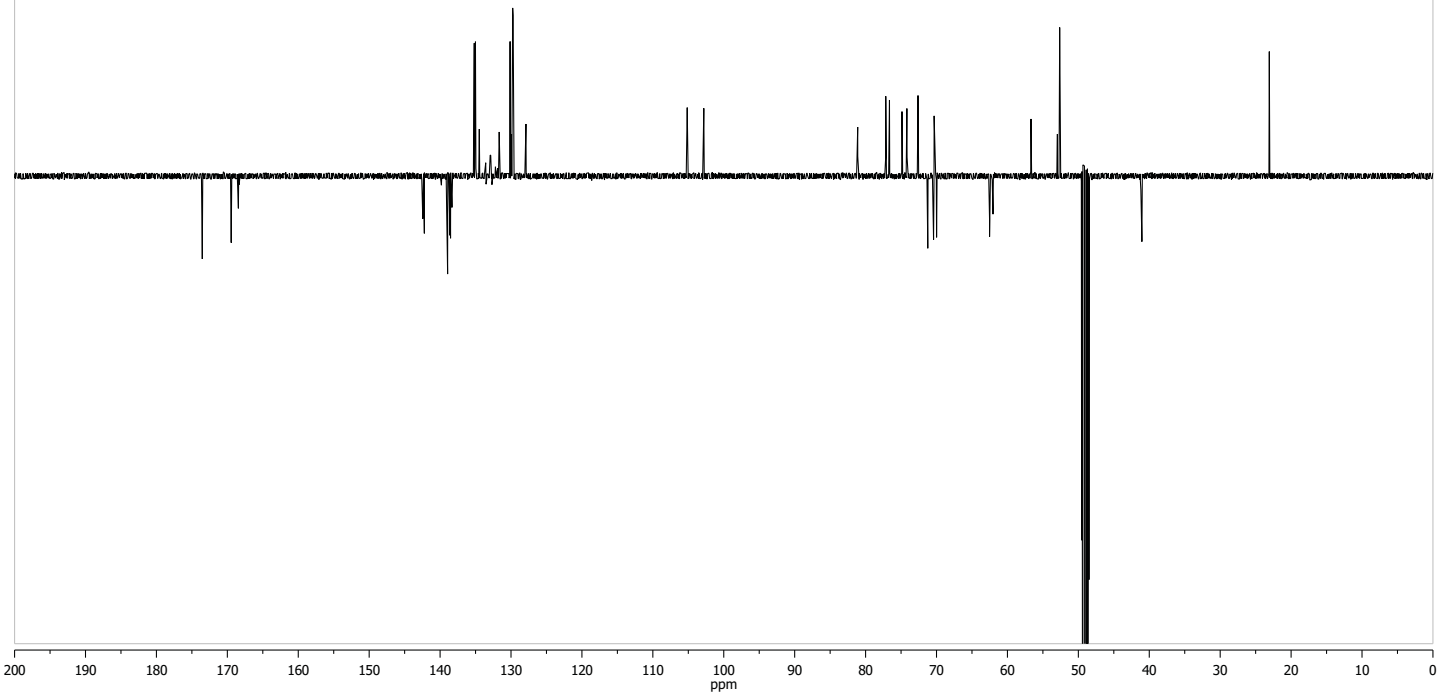

^{31}P NMR (202 MHz, CD_3OD)

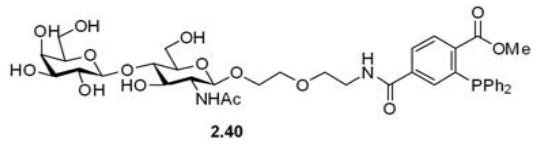

2.40

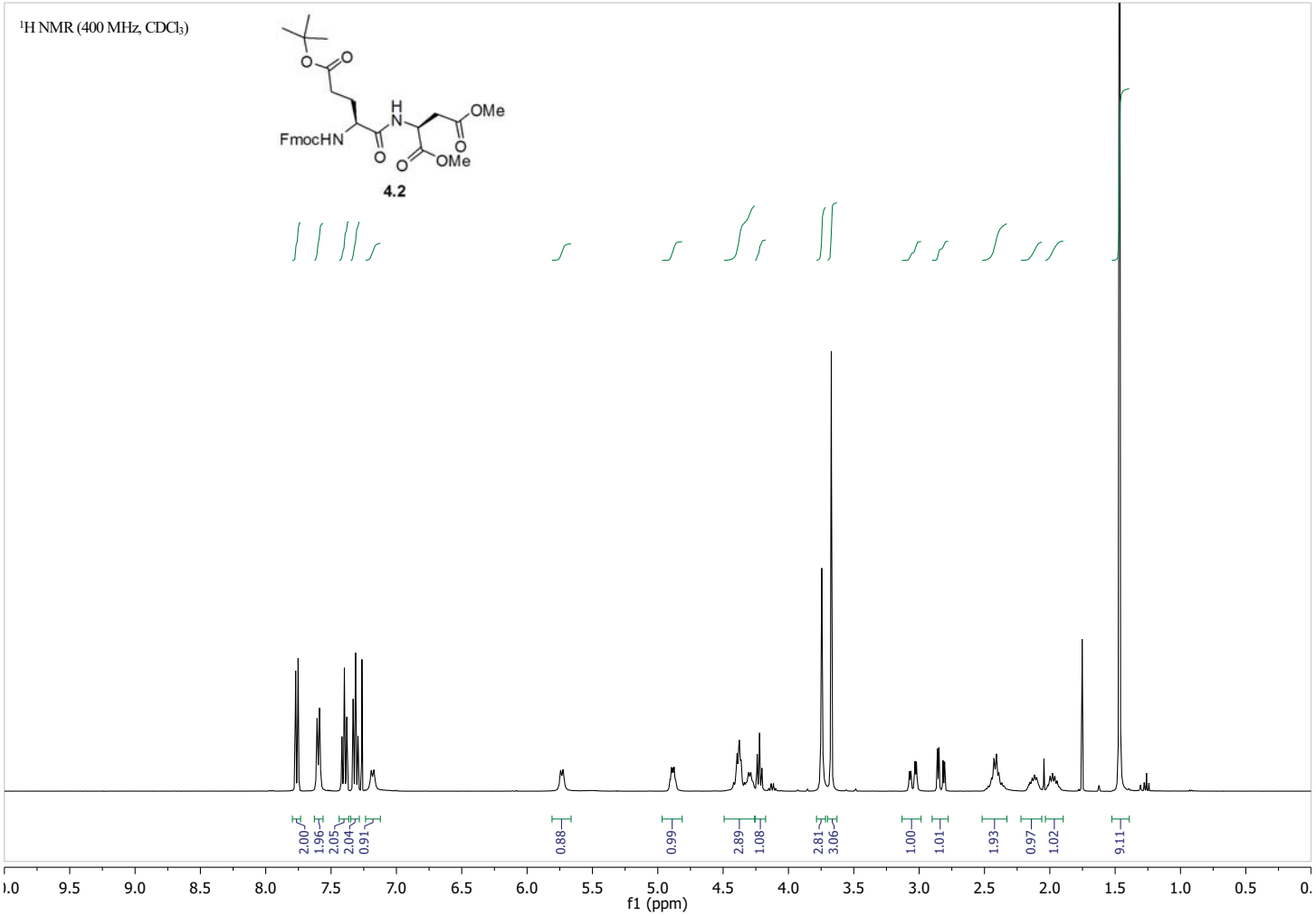
^{1}H NMR (400 MHz, CDCl$_3$)
FmocHN
OMe
OMe
4.2
2.00
1.96
2.05
2.04
0.91
0.88
0.99
2.89
1.08
2.81
3.06
1.00
1.01
1.93
0.97
1.02
9.11
f1 (ppm)

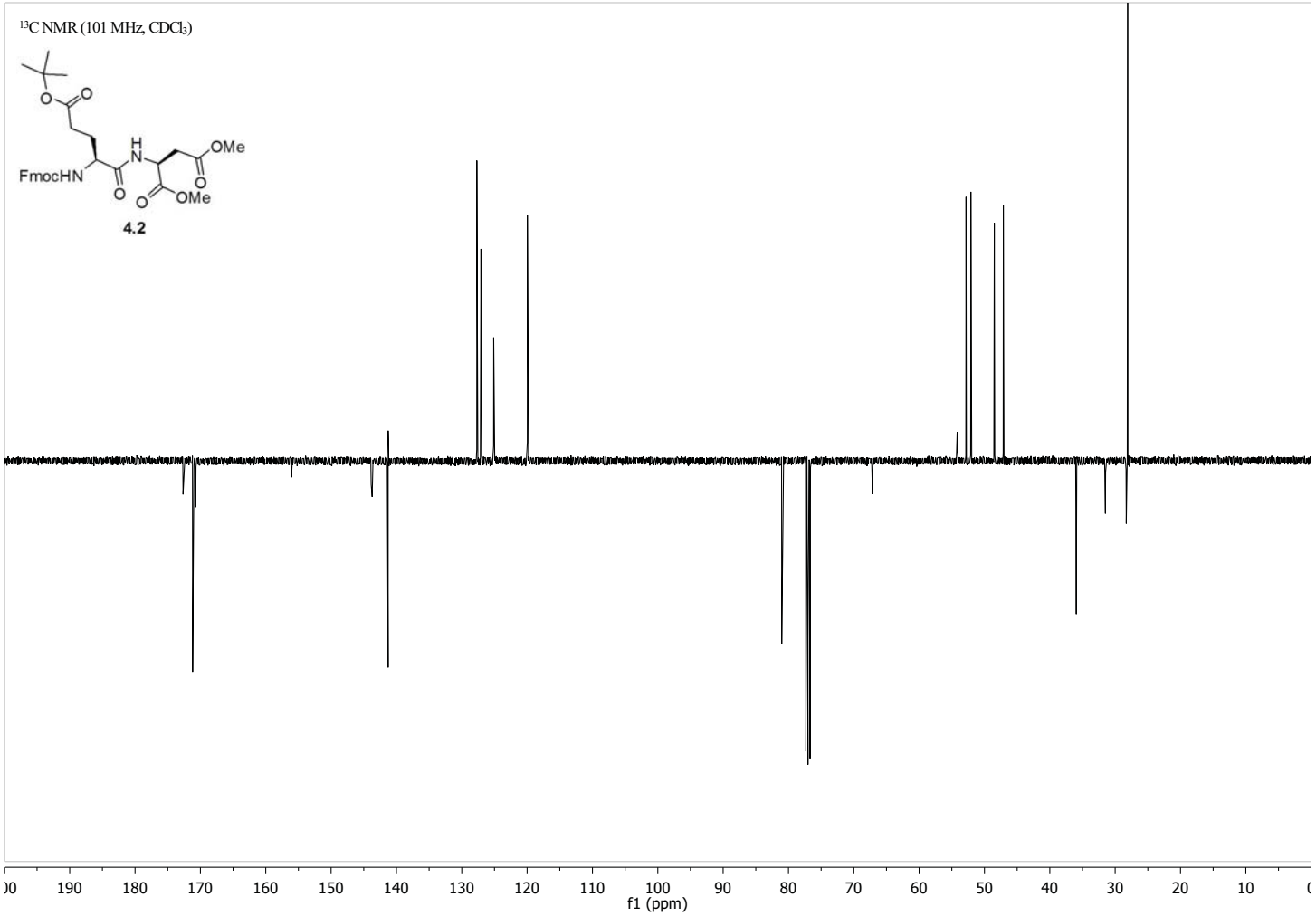
13C NMR (101 MHz, CDCl3)
FmocHN
OMe
OMe
4.2
190
180
170
160
150
140
130
120
110
100
90
80
70
60
50
40
30
20
10
f1 (ppm)

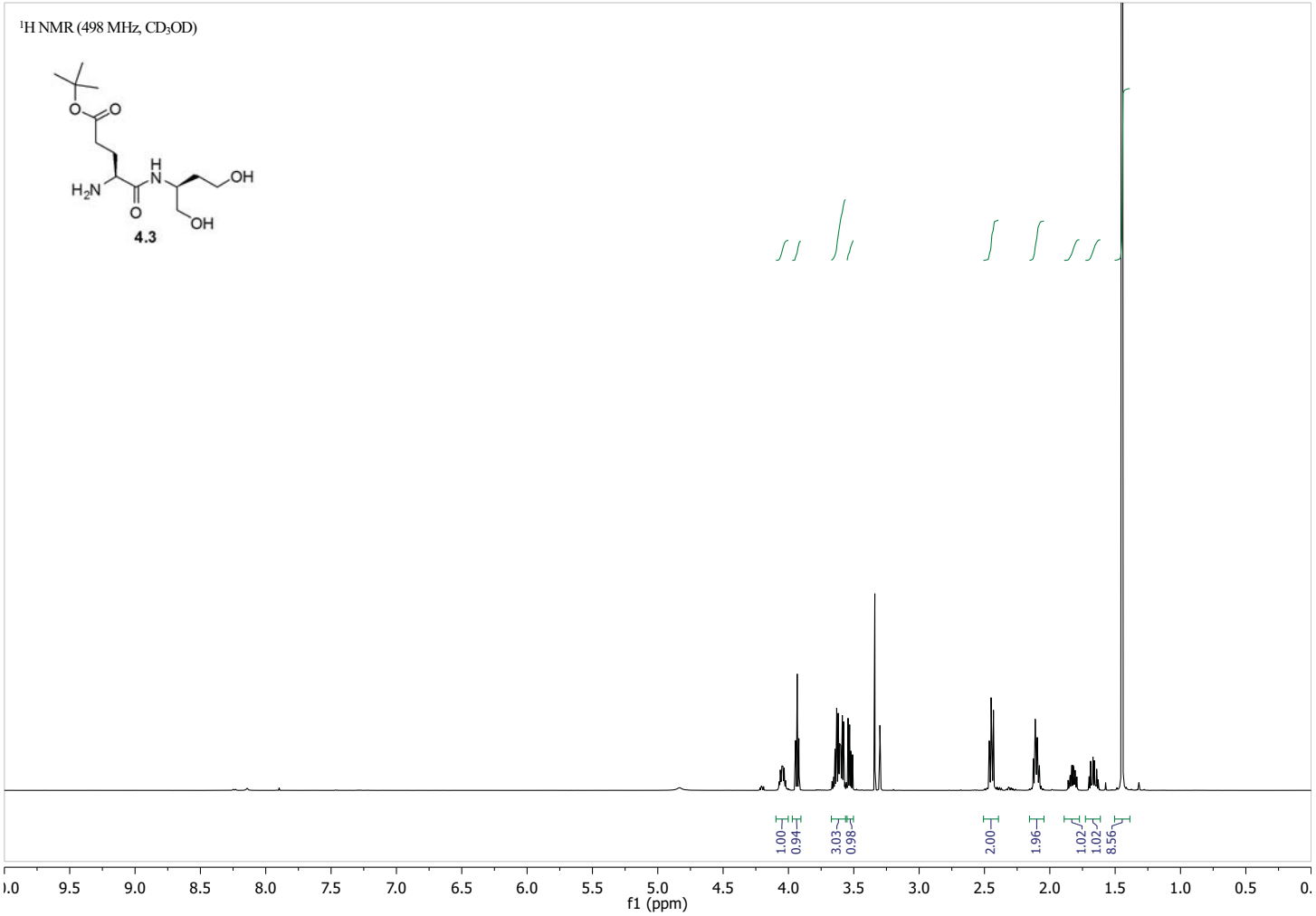
^{1}H NMR (498 MHz, CD_3OD)
4.3
1.00
0.94
3.03
0.98
2.00
1.96
1.02
1.02
8.56
f1 (ppm)

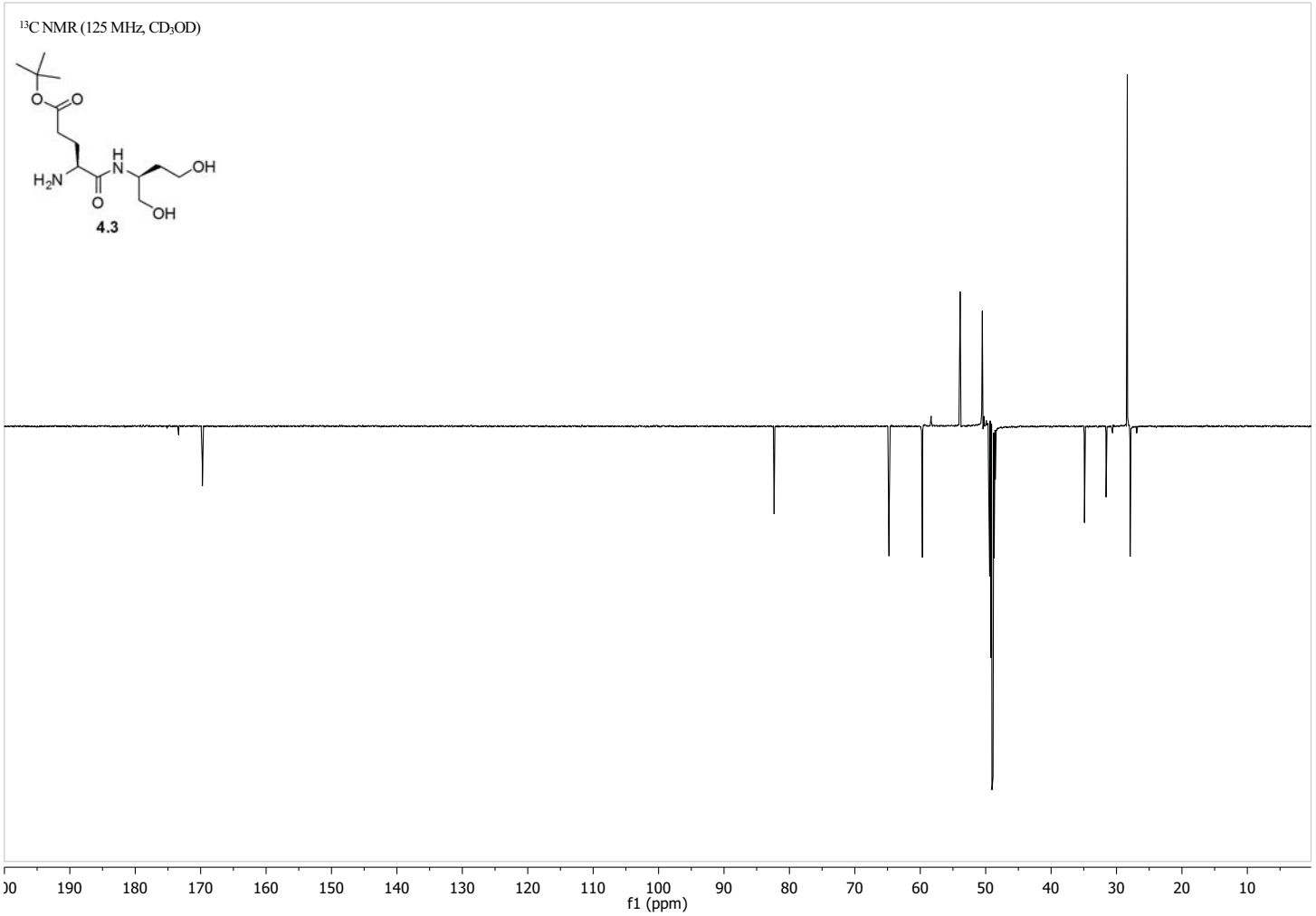
13C NMR (125 MHz, CD3OD)
4.3
f1 (ppm)

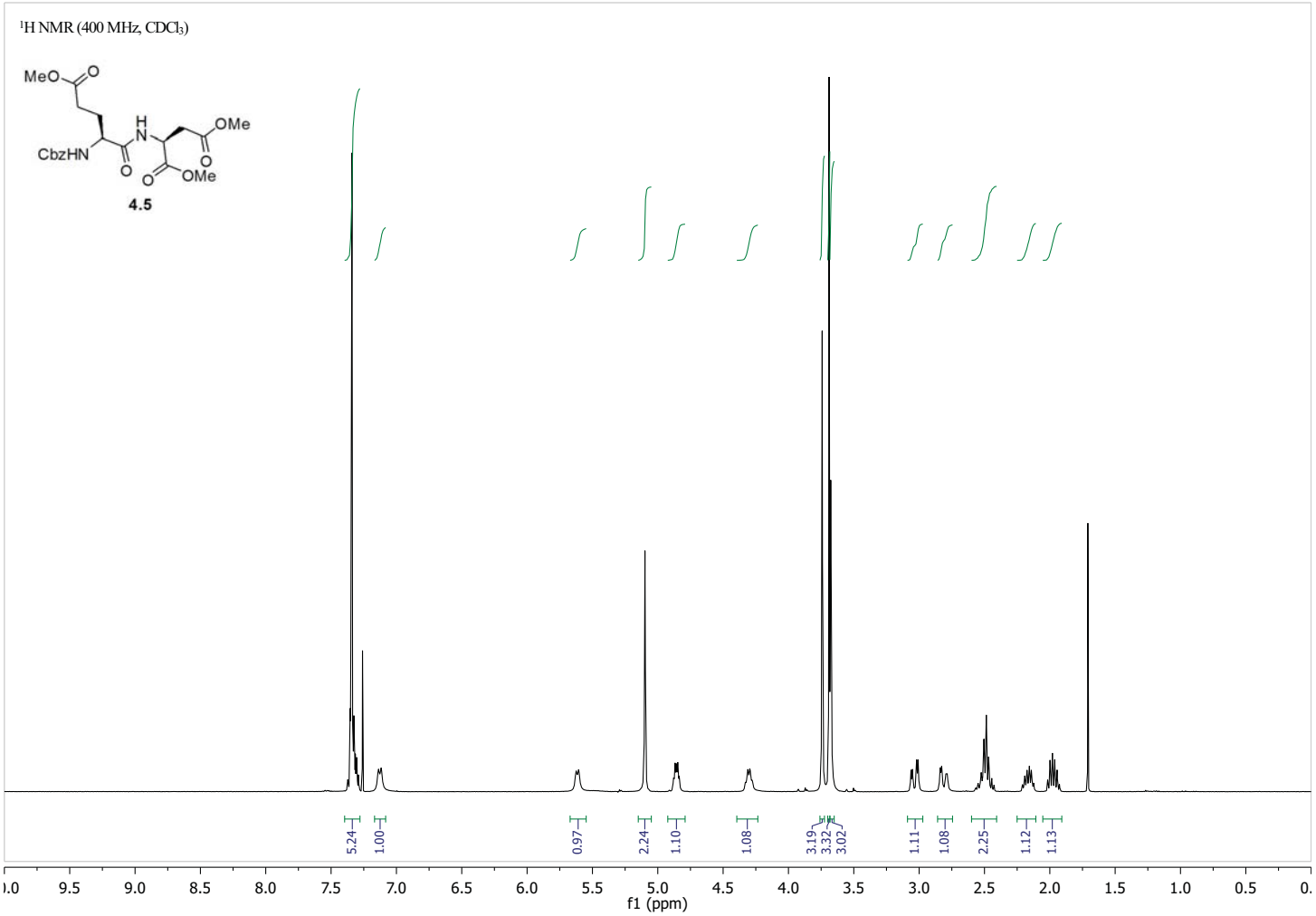
^{1}H NMR (400 MHz, $CDCl_3$)
MeO
O
H
N
OMe
CbzHN
O
O
O
OMe
4.5
5.24
1.00
0.97
2.24
1.10
1.08
3.19
3.32
3.02
1.11
1.08
2.25
1.12
1.13
9.5
9.0
8.5
8.0
7.5
7.0
6.5
6.0
5.5
5.0
4.5
4.0
3.5
3.0
2.5
2.0
1.5
1.0
0.5
f1 (ppm)

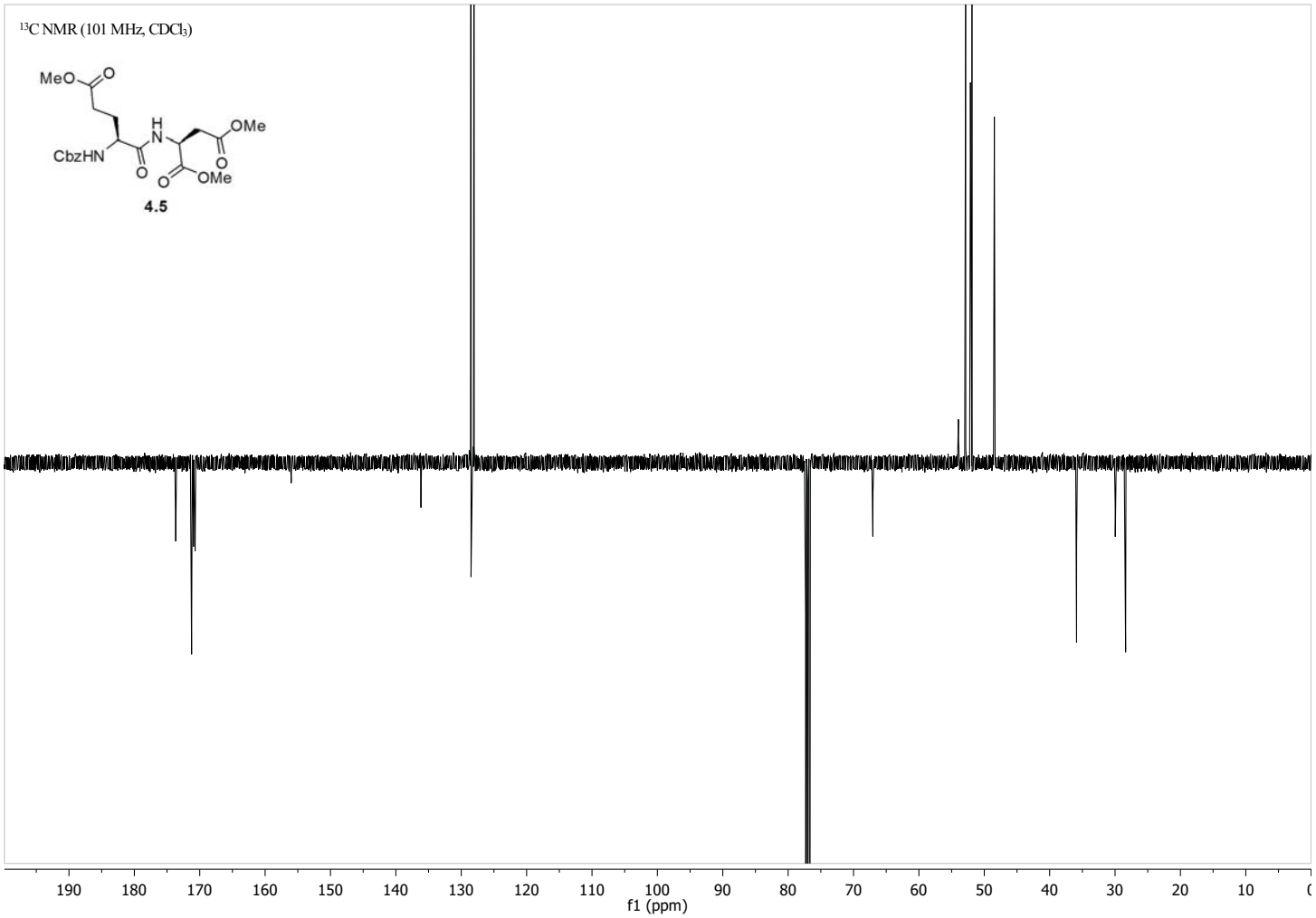
^{13}C NMR (101 MHz, $CDCl_3$)
MeO
O
H
N
OMe
CbzHN
O
O
O
OMe
4.5
190
180
170
160
150
140
130
120
110
100
90
80
70
60
50
40
30
20
10
f1 (ppm)

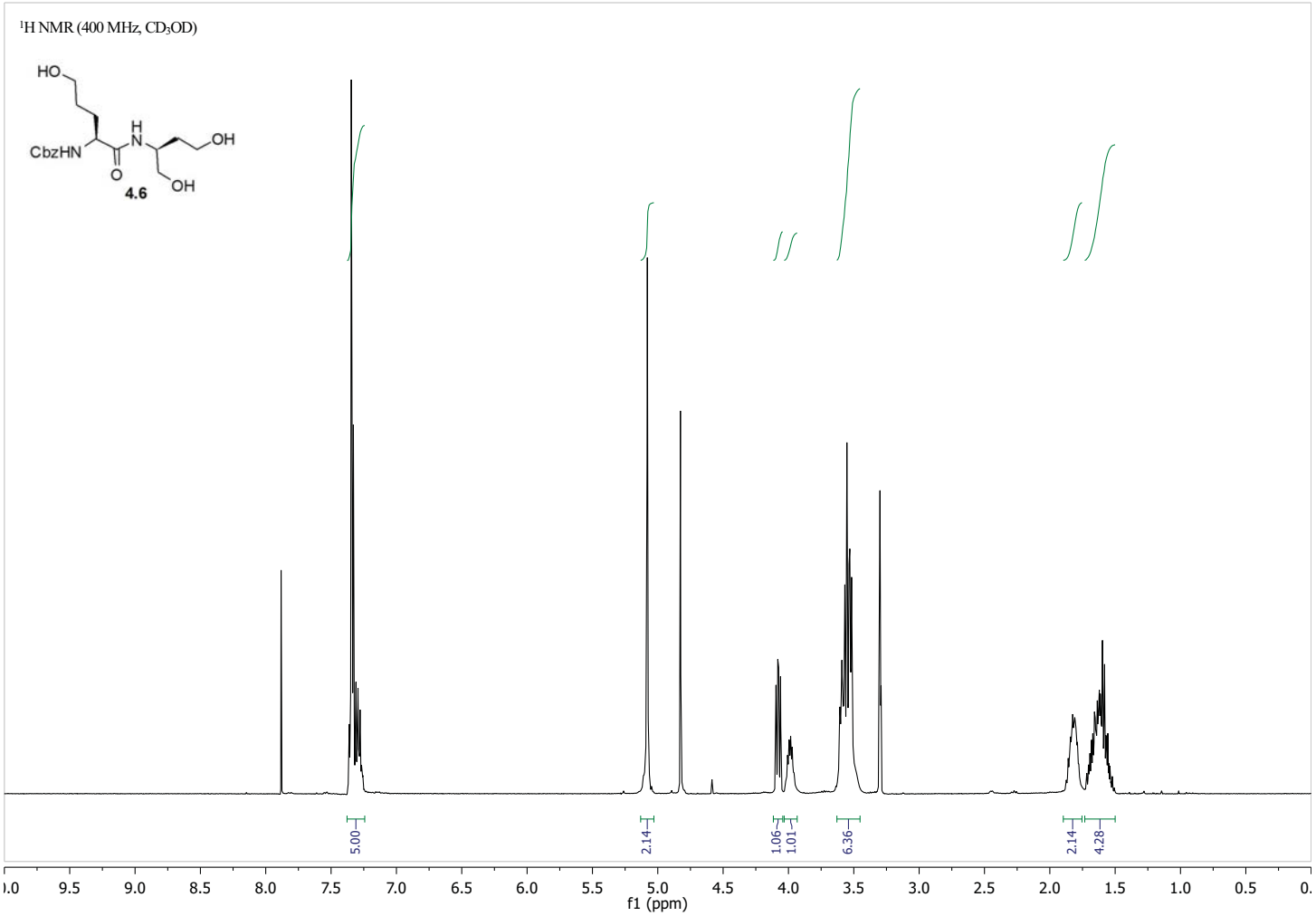
^{1}H NMR (400 MHz, CD_3OD)
HO
CbzHN
H
N
O
OH
OH
4.6
5.00
2.14
1.06
1.01
6.36
2.14
4.28
f1 (ppm)

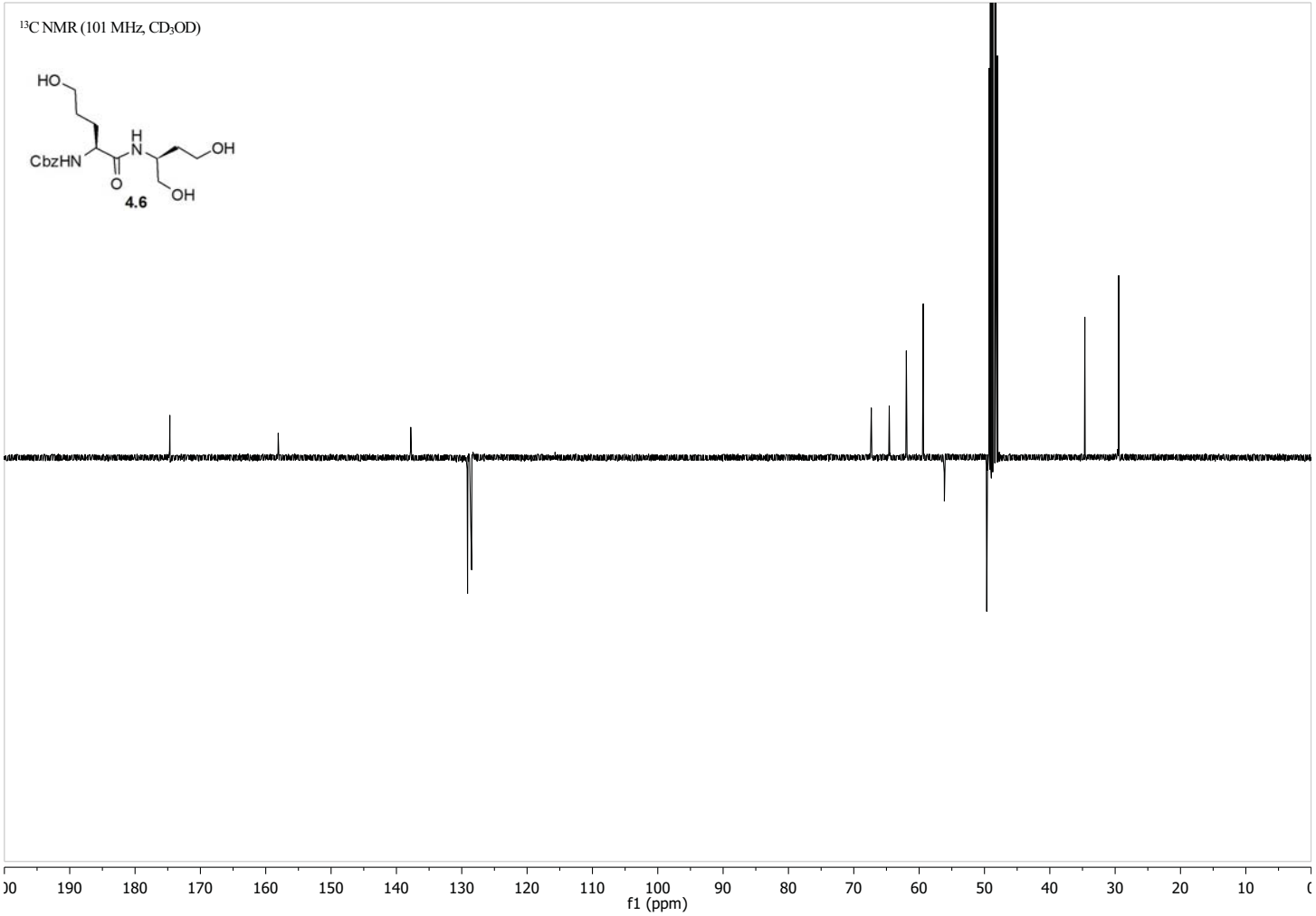
^{13}C NMR (101 MHz, CD_3OD)
HO
CbzHN
H
N
O
OH
OH
4.6
190
180
170
160
150
140
130
120
110
100
90
80
70
60
50
40
30
20
10
f1 (ppm)

^{1}H NMR (498 MHz, $CDCl_3$)

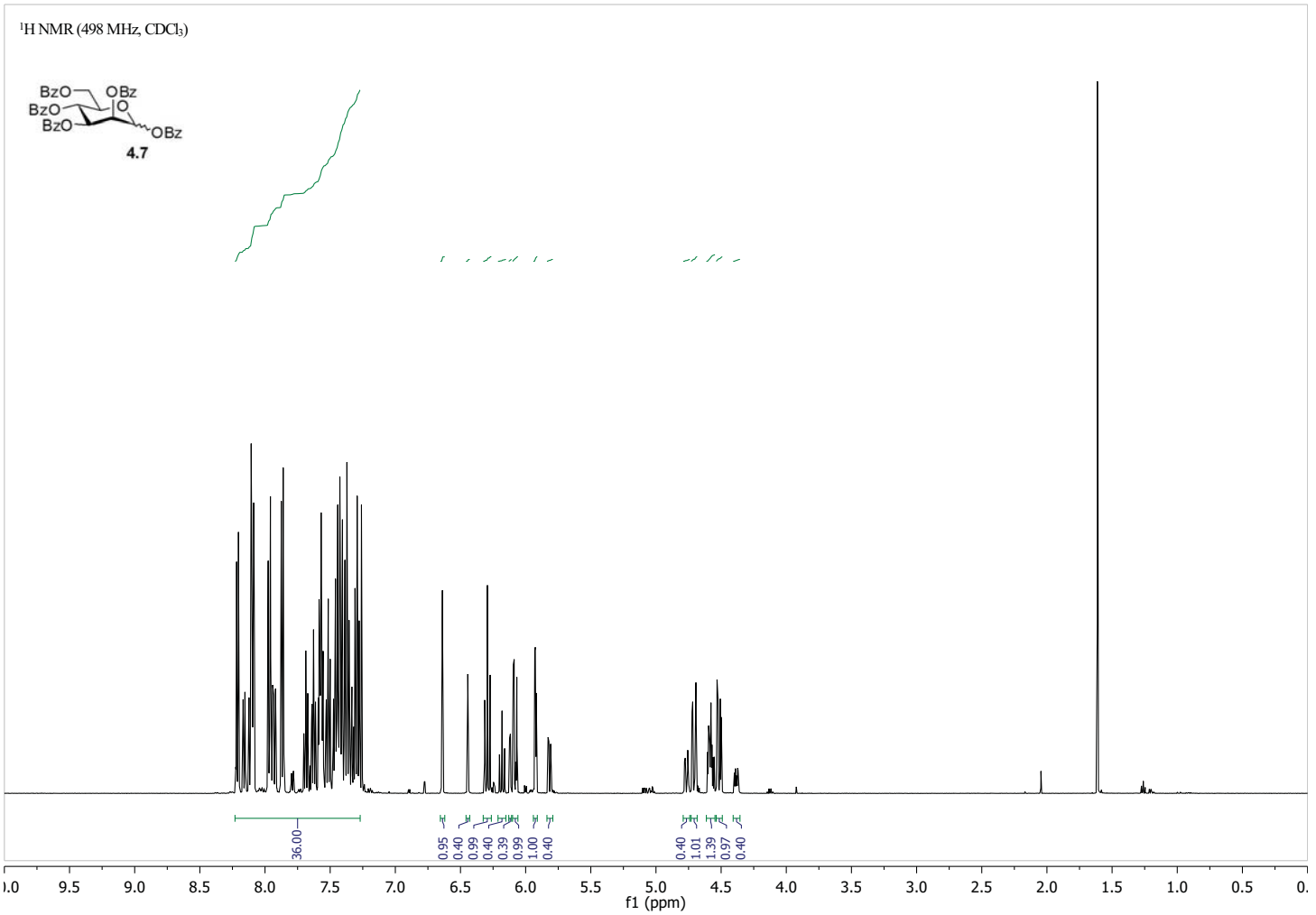

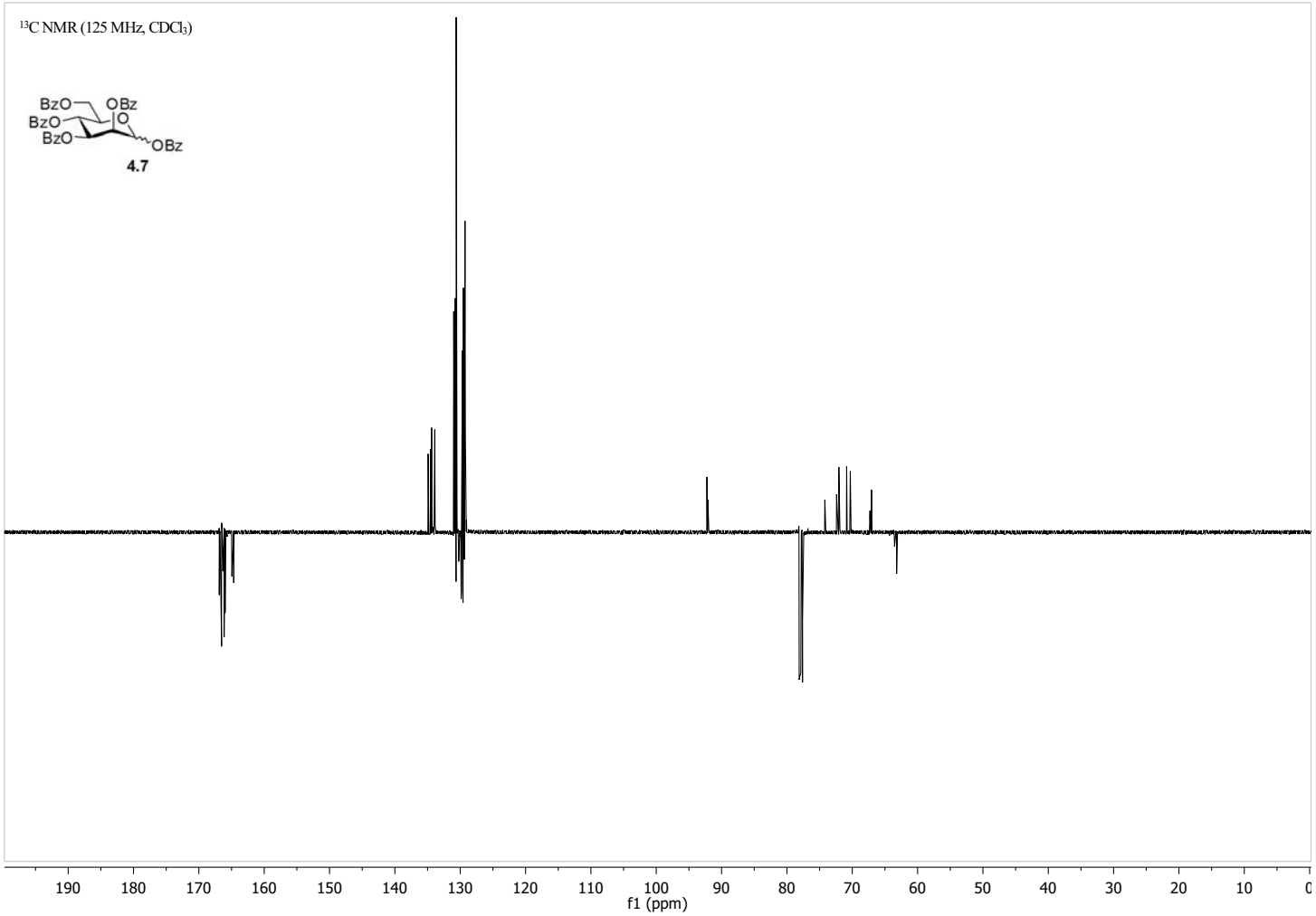
13C NMR (125 MHz, CDCl3)
BzO
OBz
BzO
O
BzO
OBz
4.7
190
180
170
160
150
140
130
120
110
100
90
80
70
60
50
40
30
20
10
f1 (ppm)

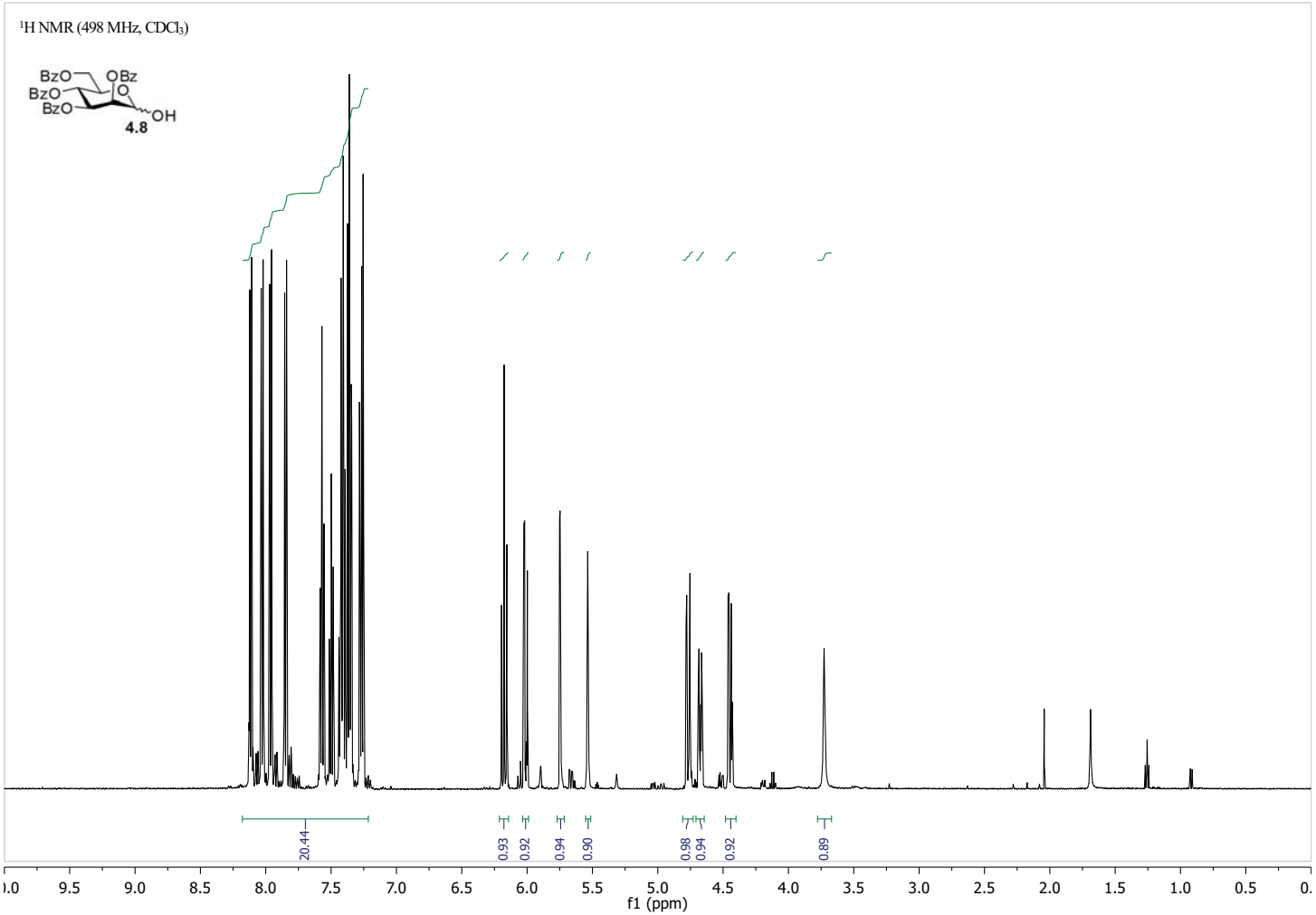
^{1}H NMR (498 MHz, $CDCl_3$)
BzO
OBz
BzO
O
BzO
OH
4.8
20.44
0.93
0.92
0.94
0.90
0.98
0.94
0.92
0.89
f1 (ppm)

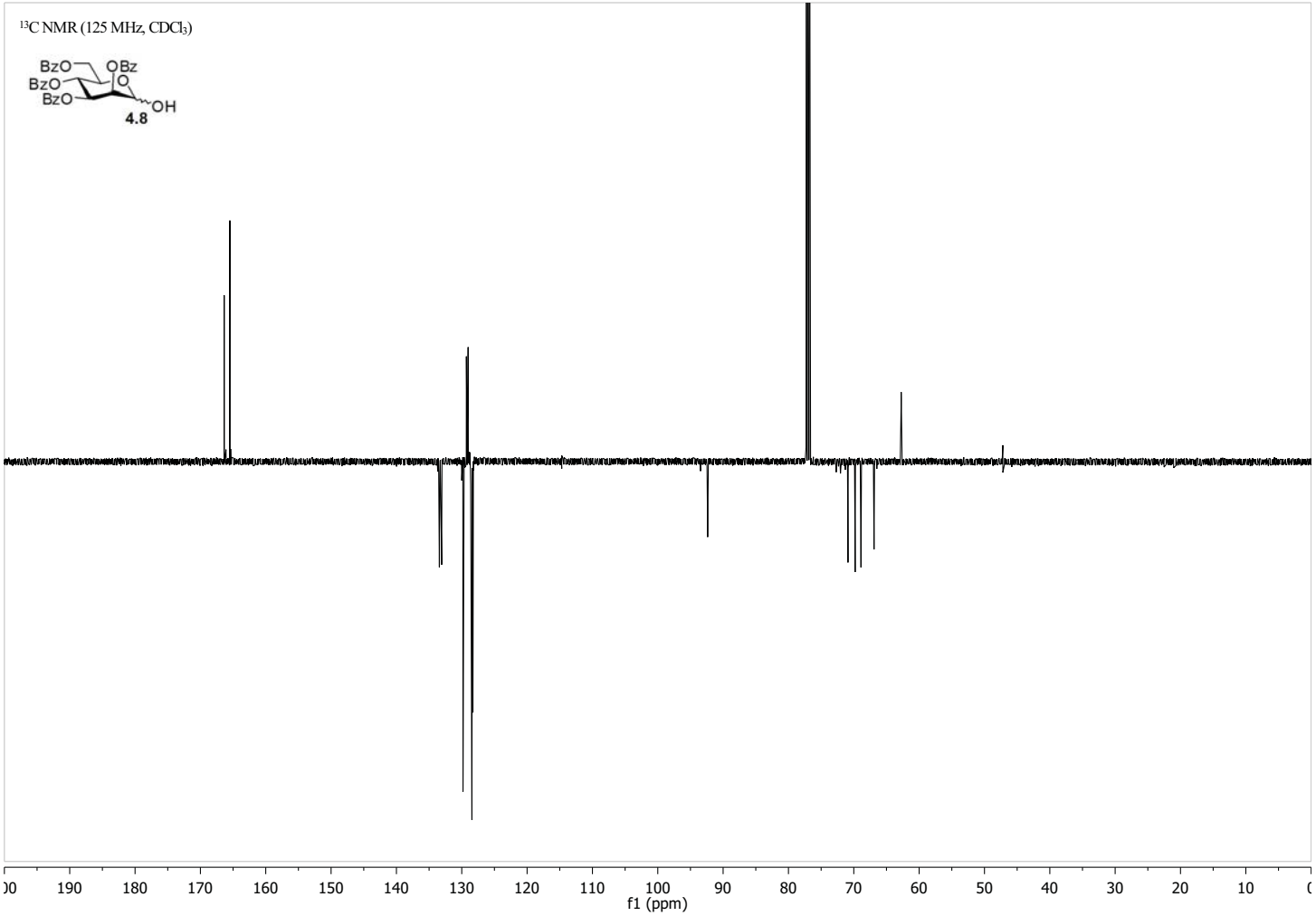
13C NMR (125 MHz, CDCl3)
BzO
OBz
BzO
O
BzO
OH
4.8
190
180
170
160
150
140
130
120
110
100
90
80
70
60
50
40
30
20
10
f1 (ppm)

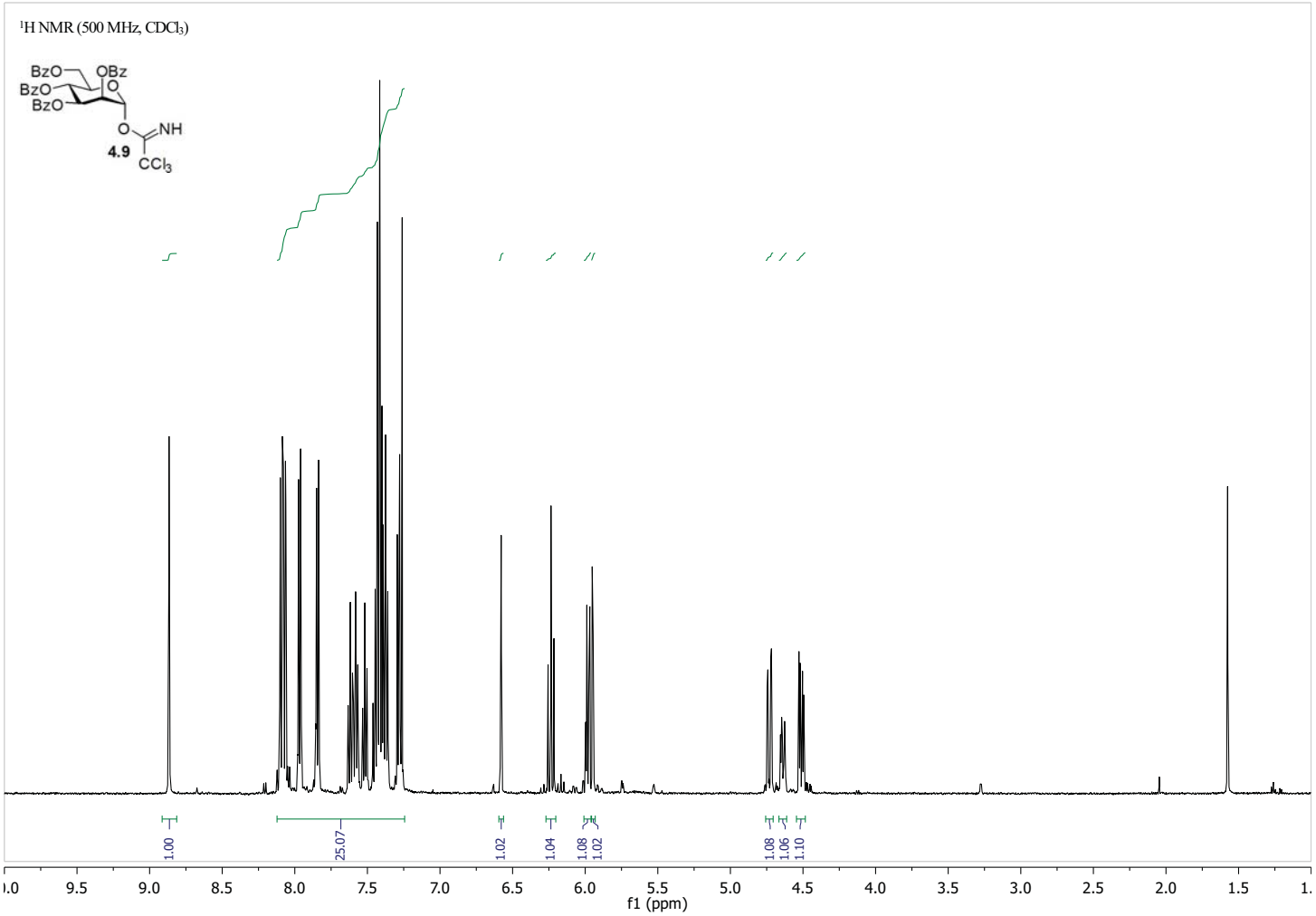
^{1}H NMR (500 MHz, $CDCl_3$)
BzO
OBz
BzO
O
BzO
O
NH
4.9
CCl_3
1.00
25.07
1.02
1.04
1.08
1.02
1.08
1.06
1.10
9.5
9.0
8.5
8.0
7.5
7.0
6.5
6.0
5.5
5.0
4.5
4.0
3.5
3.0
2.5
2.0
1.5
f1 (ppm)

^{1}H NMR (498 MHz, $CDCl_3$)

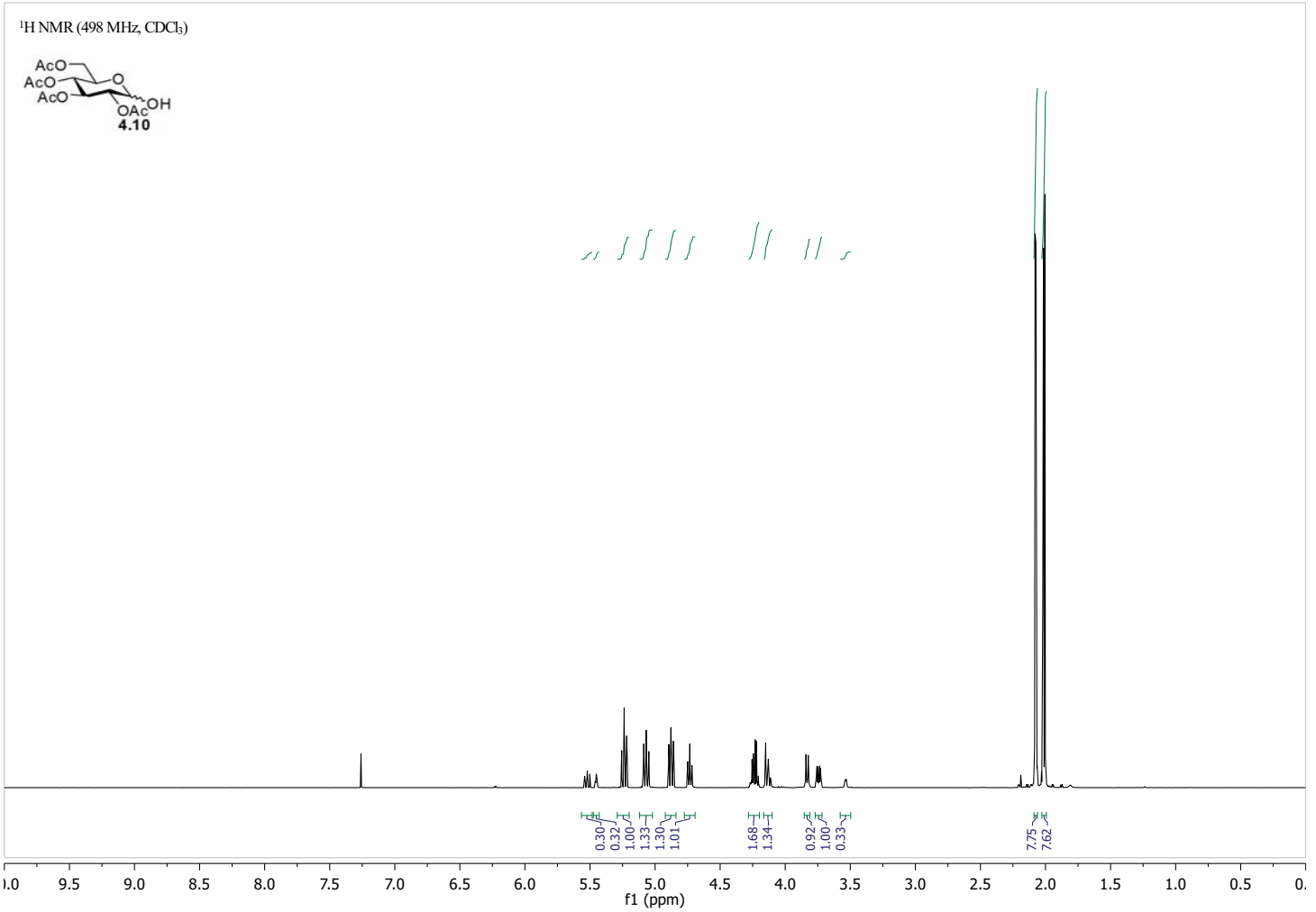

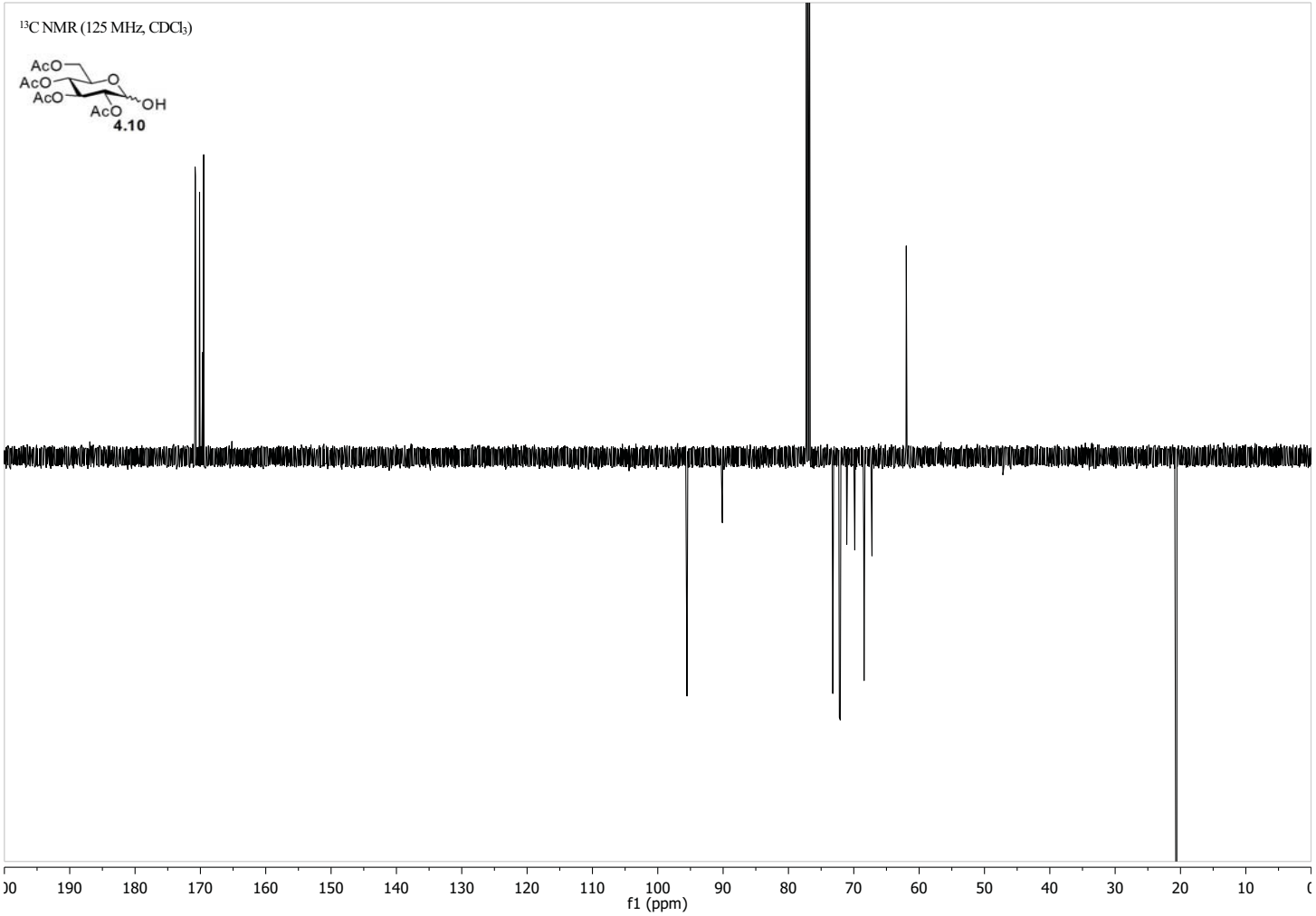
13C NMR (125 MHz, CDCl3)
AcO
AcO
AcO
AcO
OH
4.10
190
180
170
160
150
140
130
120
110
100
90
80
70
60
50
40
30
20
10
f1 (ppm)

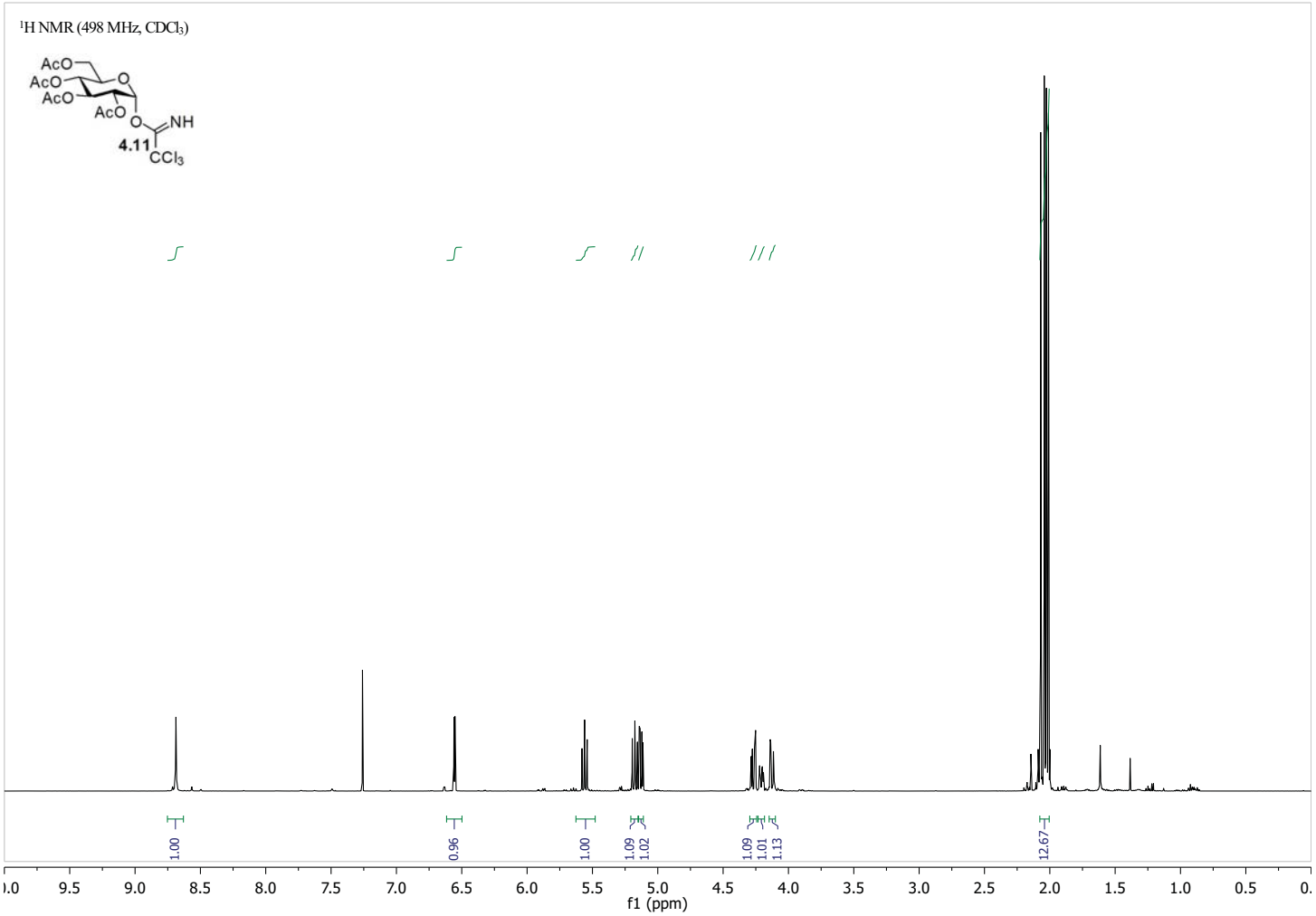
^{1}H NMR (498 MHz, $CDCl_3$)
AcO
AcO
AcO
AcO
O
NH
4.11
CCl_3
1.00
0.96
1.00
1.09
1.02
1.09
1.01
1.13
12.67
f1 (ppm)

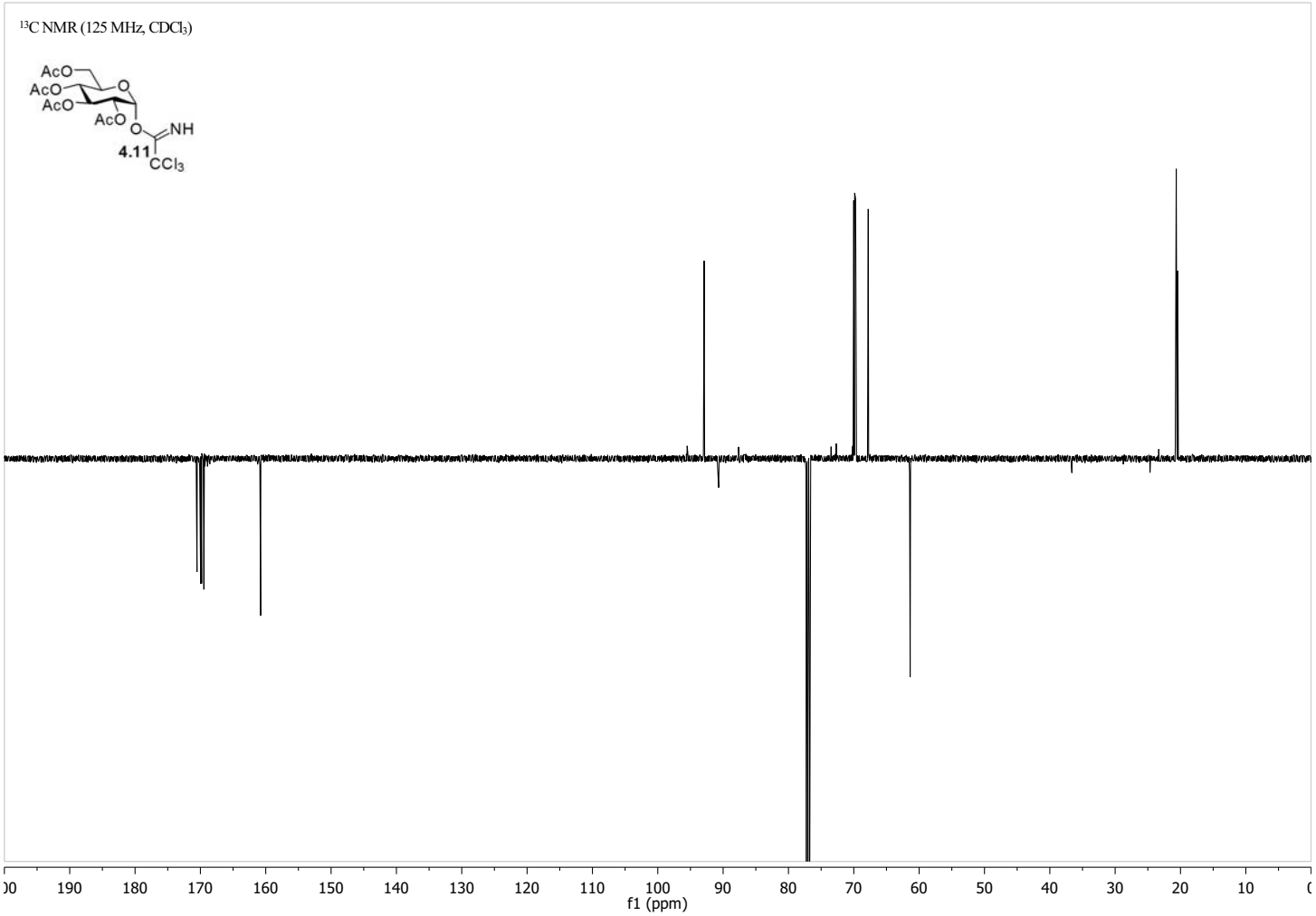
13C NMR (125 MHz, CDCl3)
AcO
AcO
AcO
AcO
O
NH
4.11
CCl3
190
180
170
160
150
140
130
120
110
100
90
80
70
60
50
40
30
20
10
f1 (ppm)

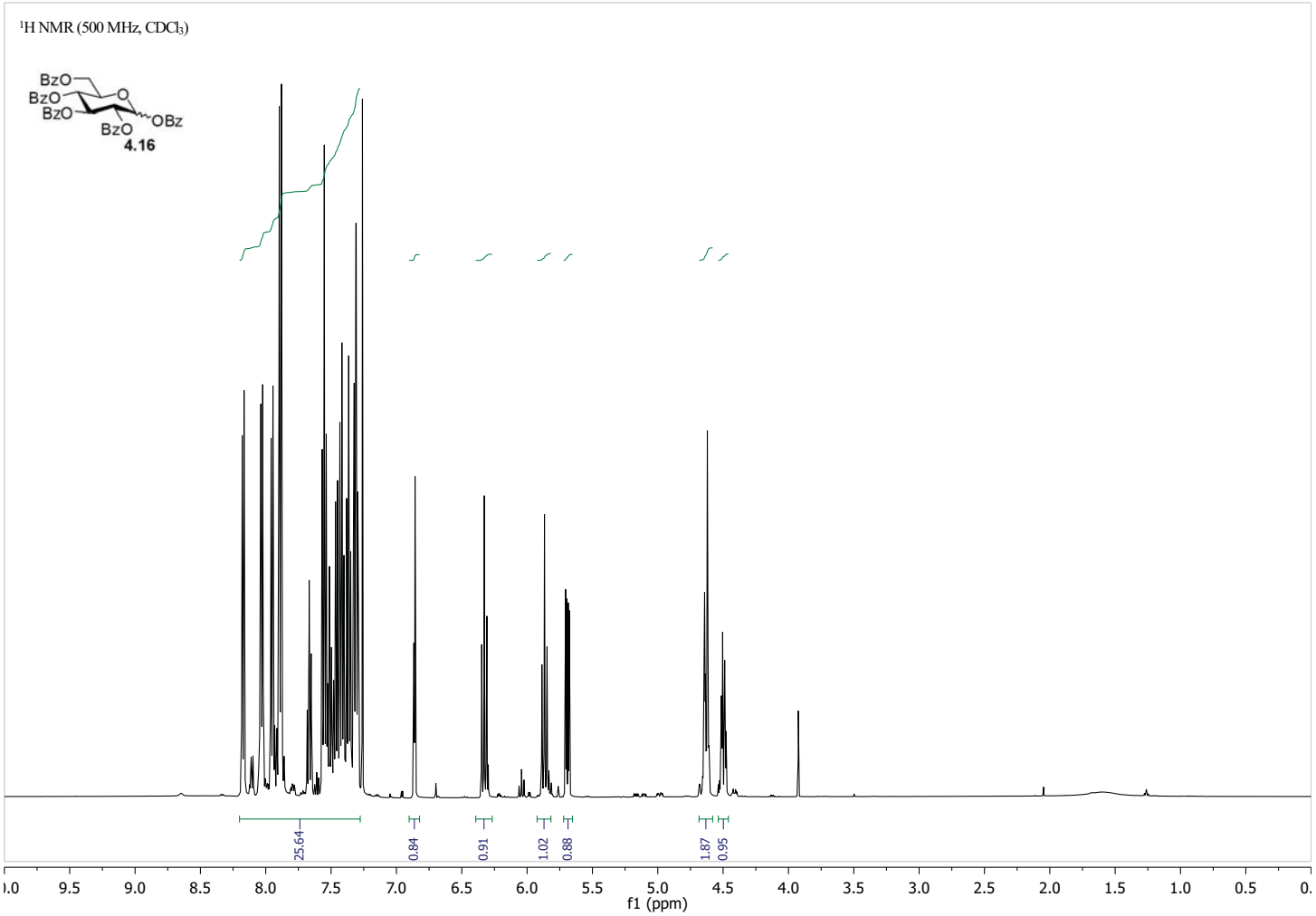
^{1}H NMR (500 MHz, CDCl$_3$)
BzO
BzO
BzO
O
OBz
BzO
4.16
25.64
0.84
0.91
1.02
0.88
1.87
0.95
f1 (ppm)

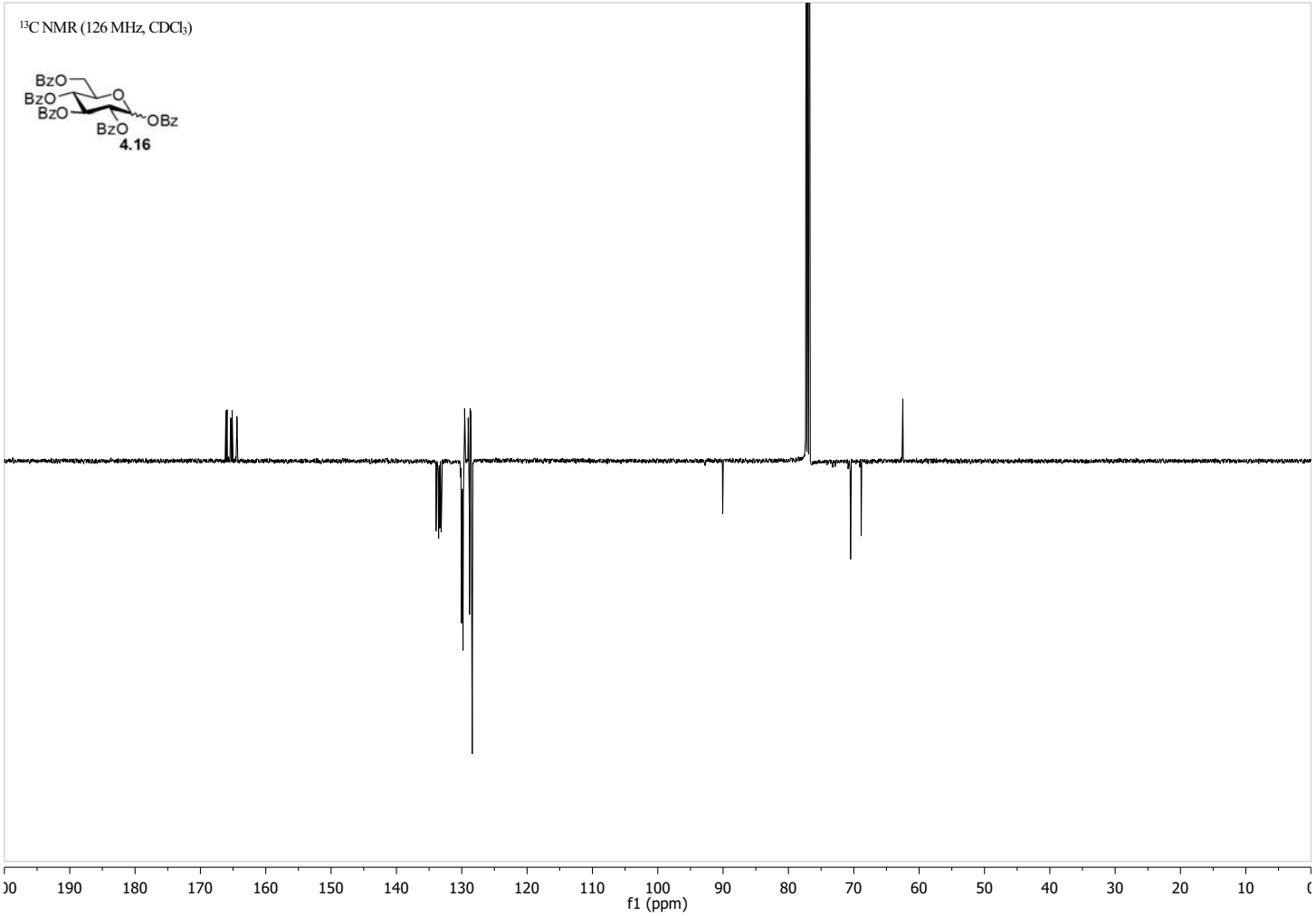
13C NMR (126 MHz, CDCl3)
BzO
BzO
BzO
BzO
OBz
4.16
190
180
170
160
150
140
130
120
110
100
90
80
70
60
50
40
30
20
10
f1 (ppm)

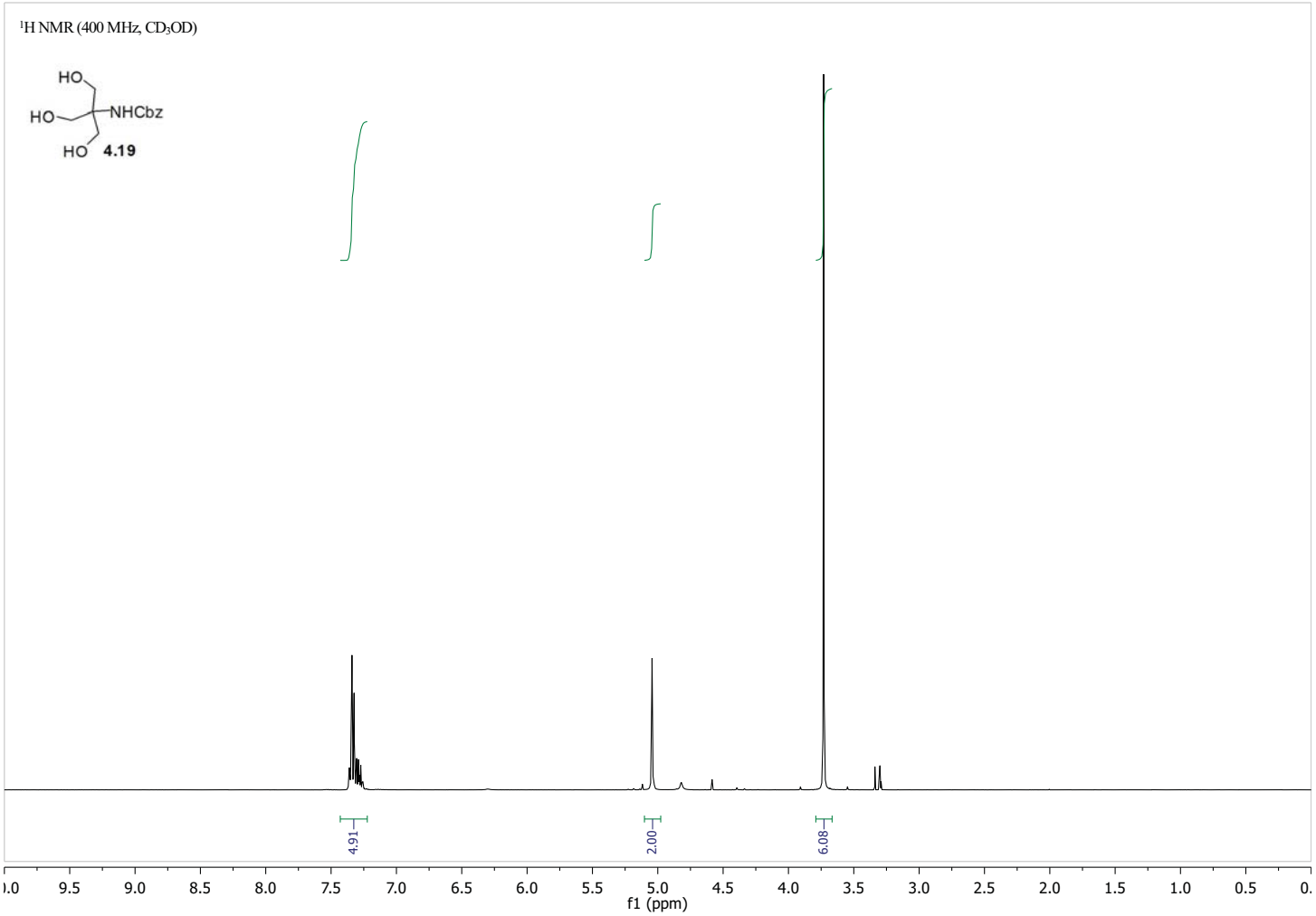
^{1}H NMR (400 MHz, CD_3OD)
HO
HO
NHCbz
HO
4.19
4.91
2.00
6.08
9.5
9.0
8.5
8.0
7.5
7.0
6.5
6.0
5.5
5.0
4.5
4.0
3.5
3.0
2.5
2.0
1.5
1.0
0.5
f1 (ppm)

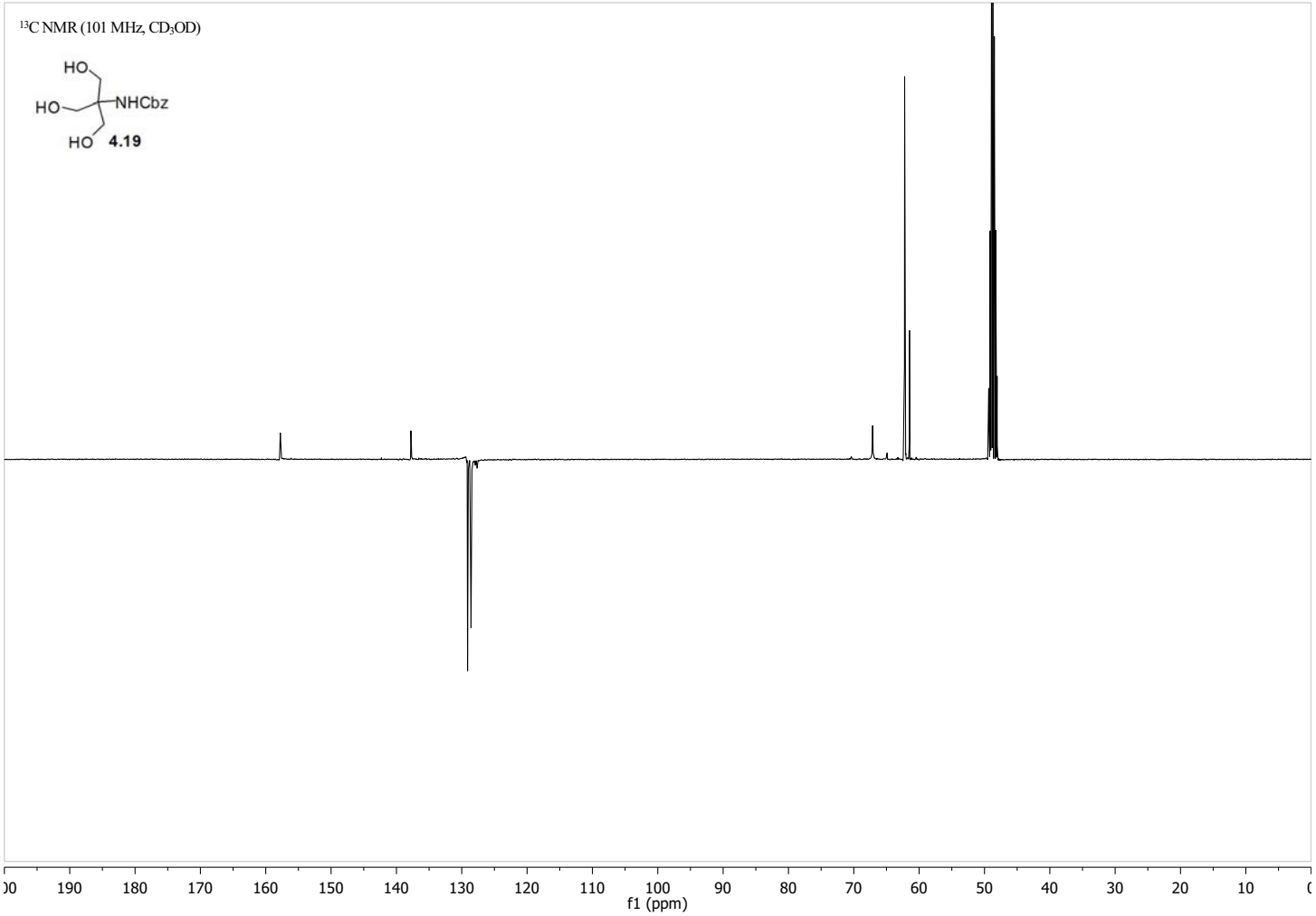
13C NMR (101 MHz, CD3OD)
HO
HO
NHCbz
HO
4.19
190
180
170
160
150
140
130
120
110
100
90
80
70
60
50
40
30
20
10
f1 (ppm)

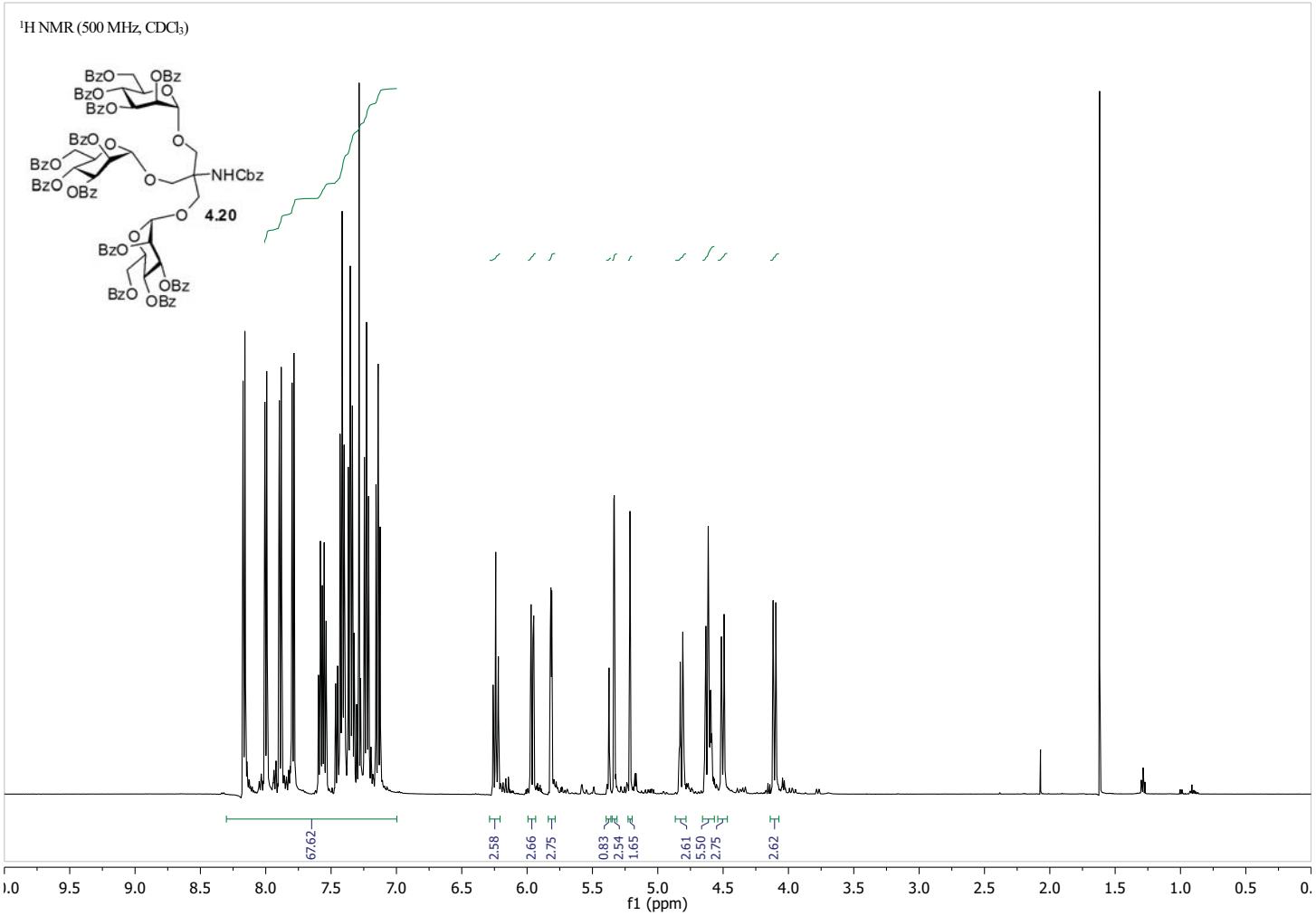
^{1}H NMR (500 MHz, $CDCl_3$)
BzO
OBz
NHCbz
4.20
67.62
2.58
2.66
2.75
0.83
2.54
1.65
2.61
5.50
2.75
2.62
f1 (ppm)

^{13}C NMR (126 MHz, $CDCl_3$)

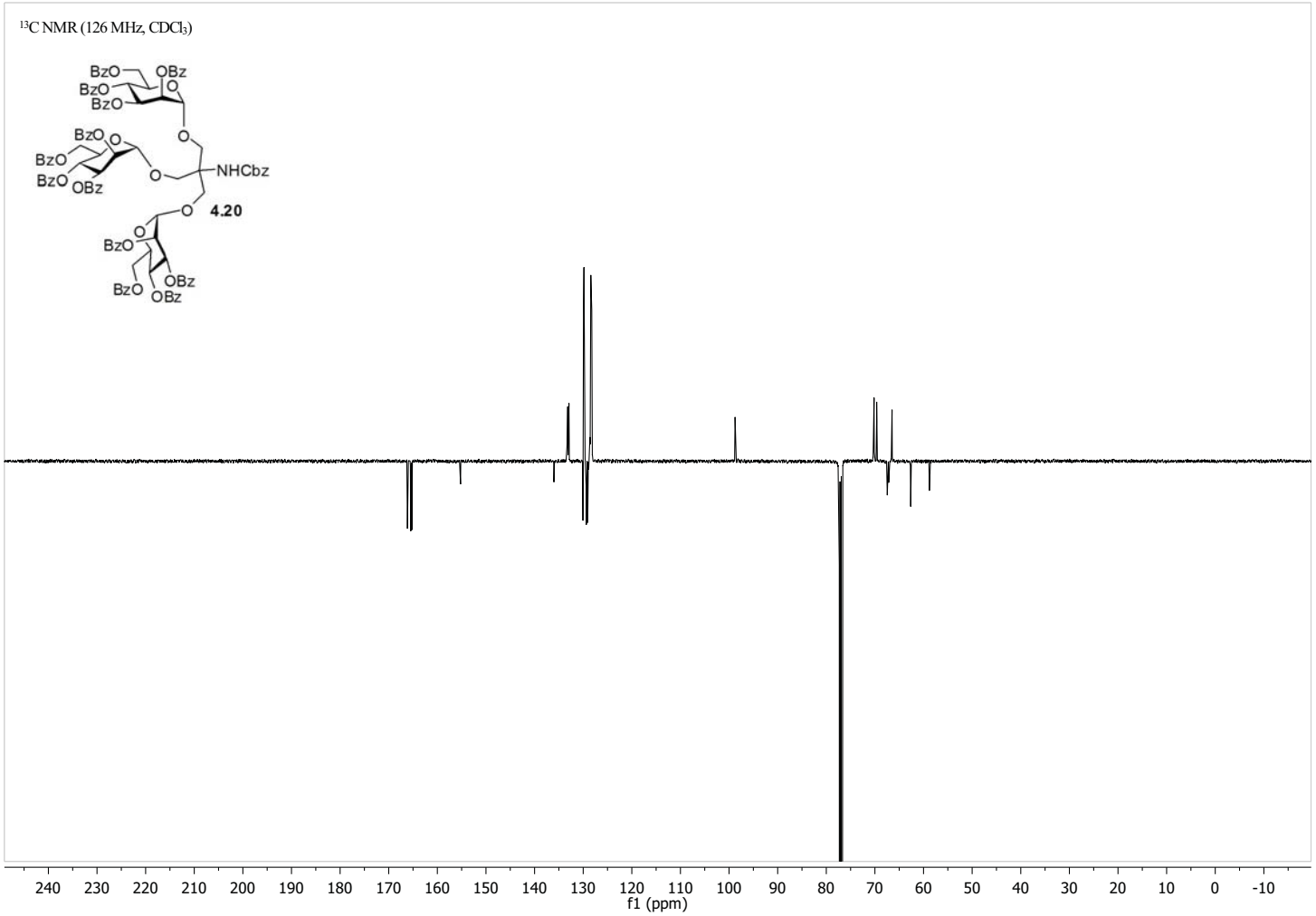

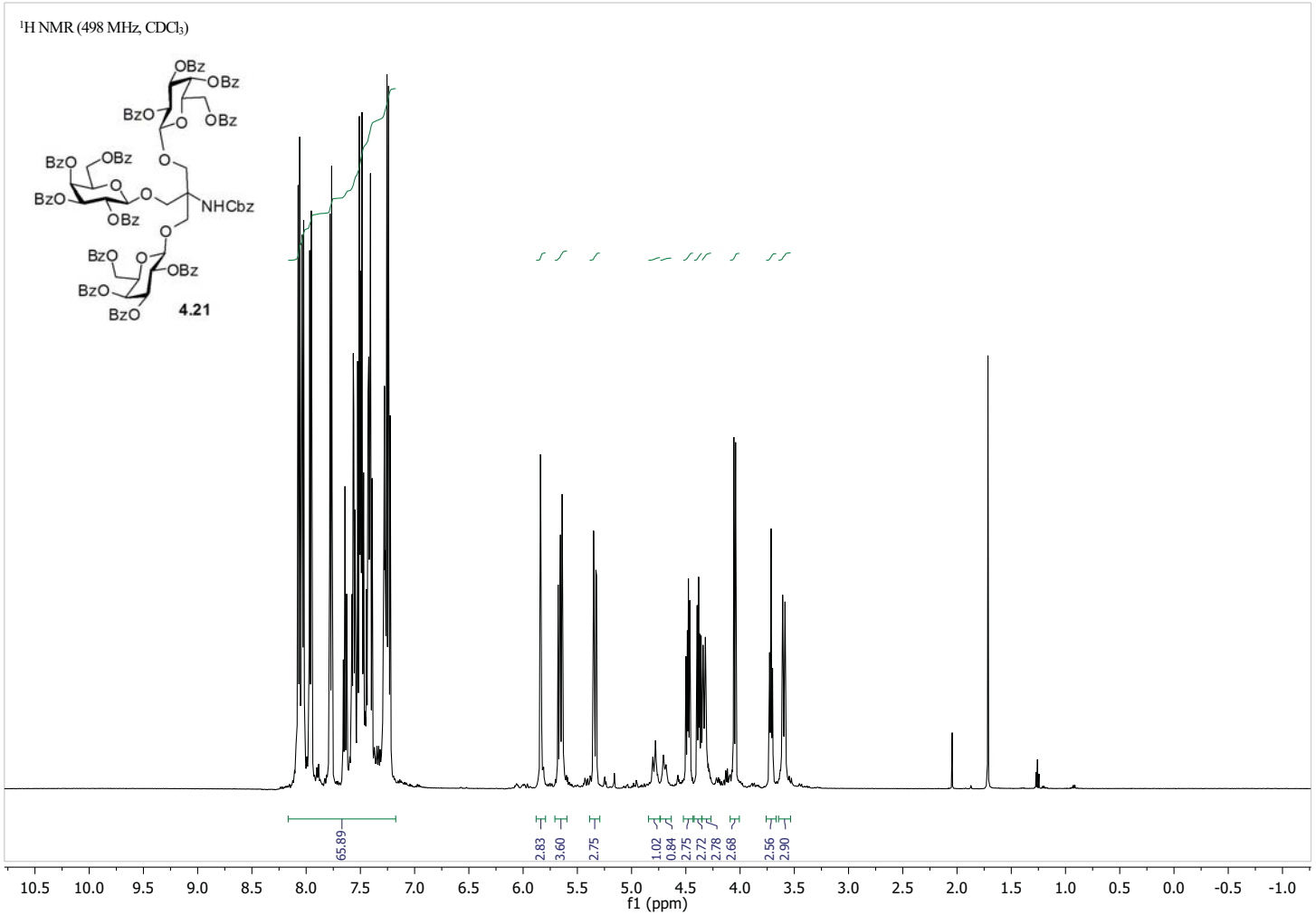
^{1}H NMR (498 MHz, $CDCl_3$)
OBz
OBz
BzO
OBz
BzO
OBz
O
BzO
O
NHCbz
OBz
O
BzO
O
OBz
BzO
BzO
4.21
65.89
2.83
3.60
2.75
1.02
0.84
2.75
2.72
2.78
2.68
2.56
2.90
10.5 10.0 9.5 9.0 8.5 8.0 7.5 7.0 6.5 6.0 5.5 5.0 4.5 4.0 3.5 3.0 2.5 2.0 1.5 1.0 0.5 0.0 -0.5 -1.0
f1 (ppm)

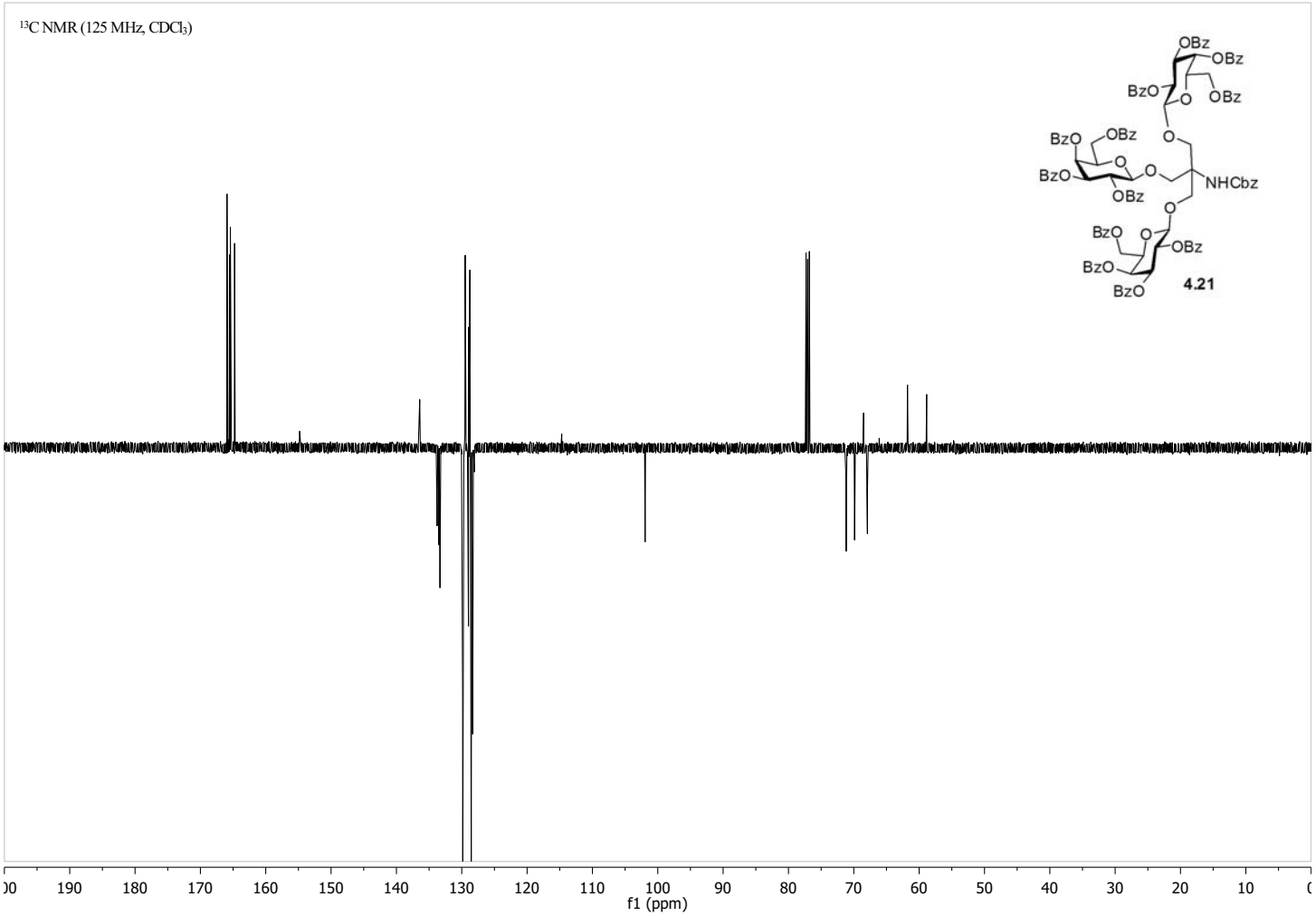
13C NMR (125 MHz, CDCl3)
OBz
OBz
BzO
OBz
BzO
OBz
O
O
O
NHCbz
BzO
OBz
BzO
O
OBz
BzO
BzO
4.21
190
180
170
160
150
140
130
120
110
100
90
80
70
60
50
40
30
20
10
f1 (ppm)

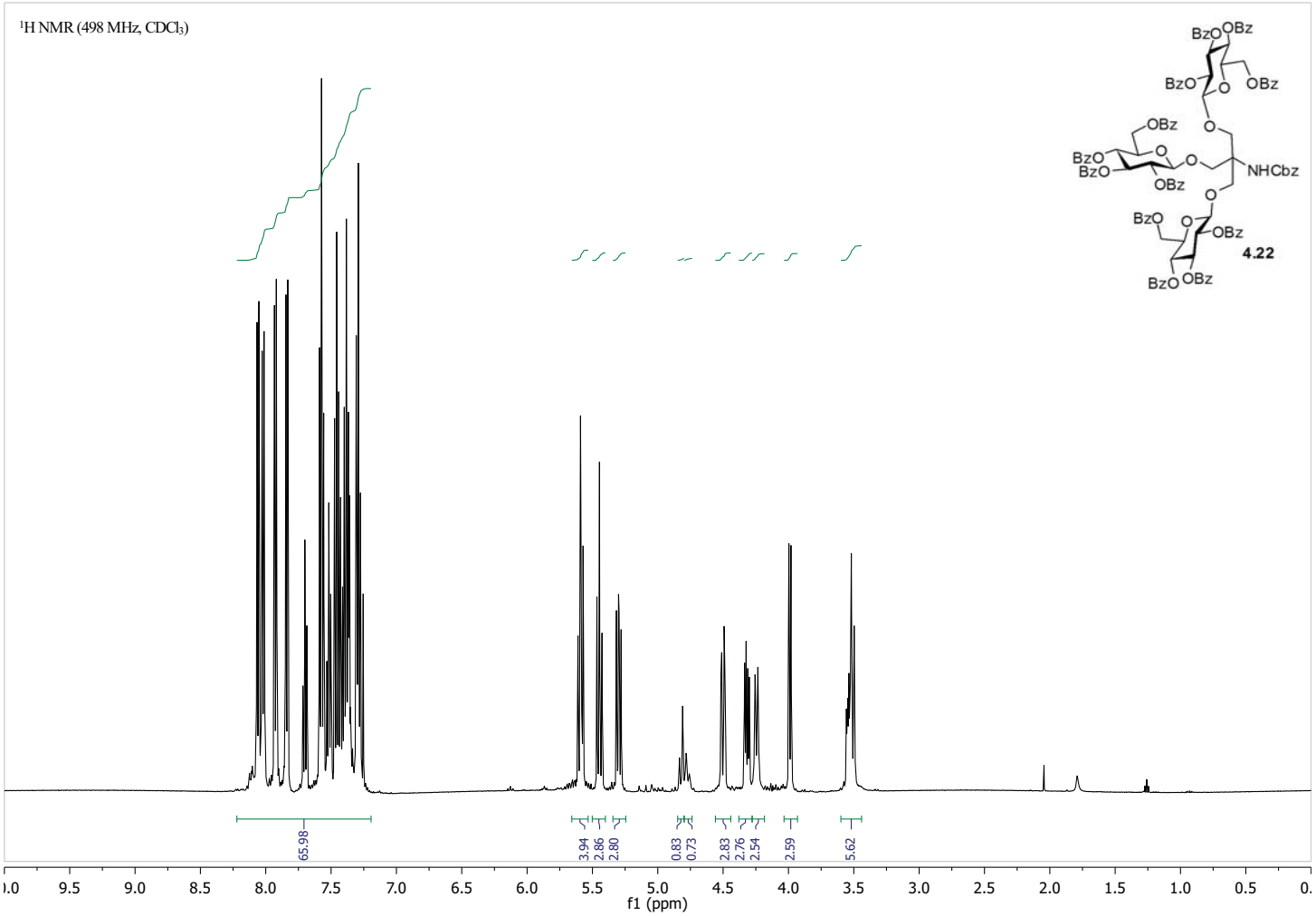
^{1}H NMR (498 MHz, $CDCl_3$)
BzO
OBz
NHCbz
4.22
65.98
3.94
2.86
2.80
0.83
0.73
2.83
2.76
2.54
2.59
5.62
f1 (ppm)

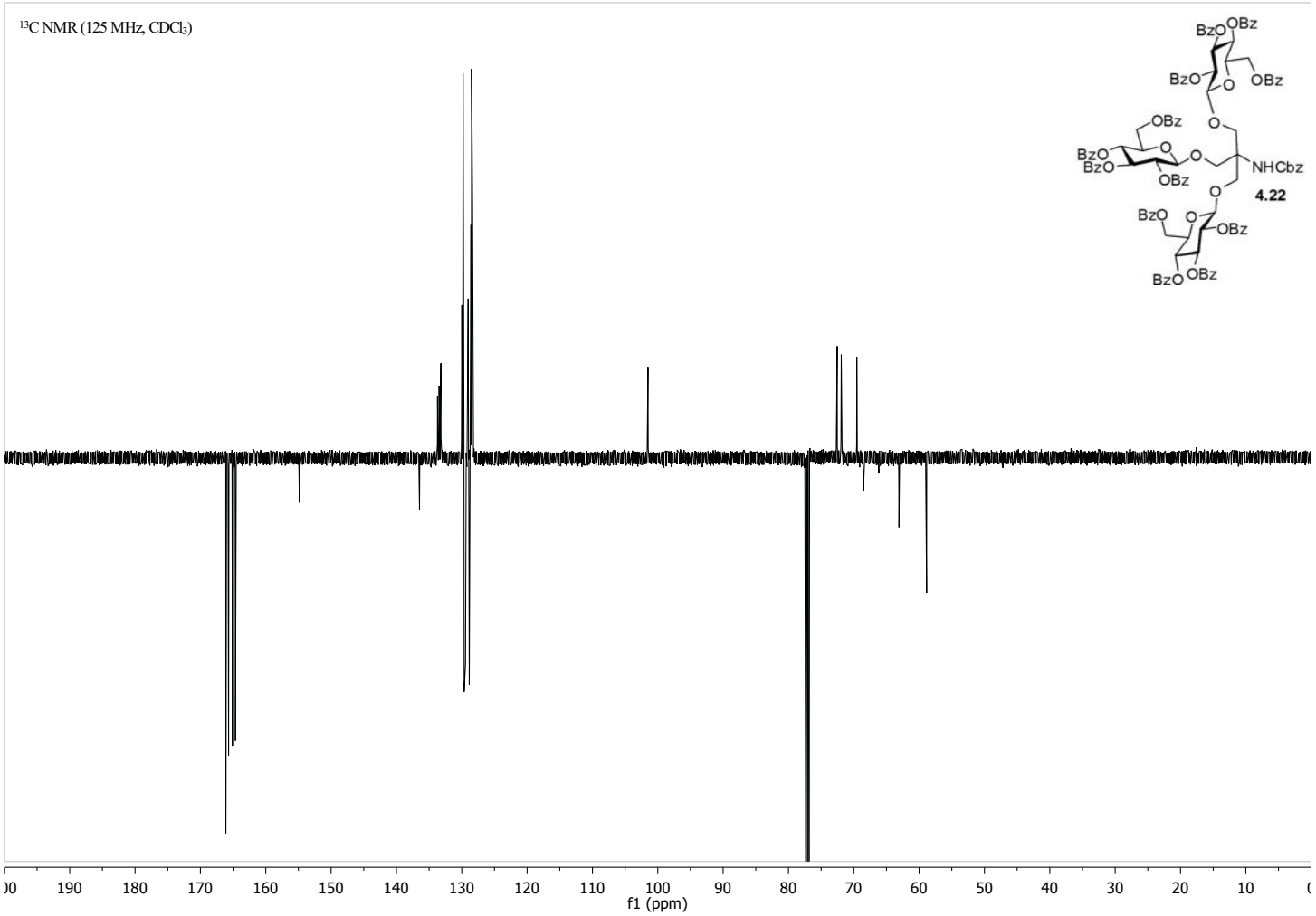
13C NMR (125 MHz, CDCl3)
BzO
OBz
NHCbz
4.22
f1 (ppm)

^{1}H NMR (498 MHz, D_2O)

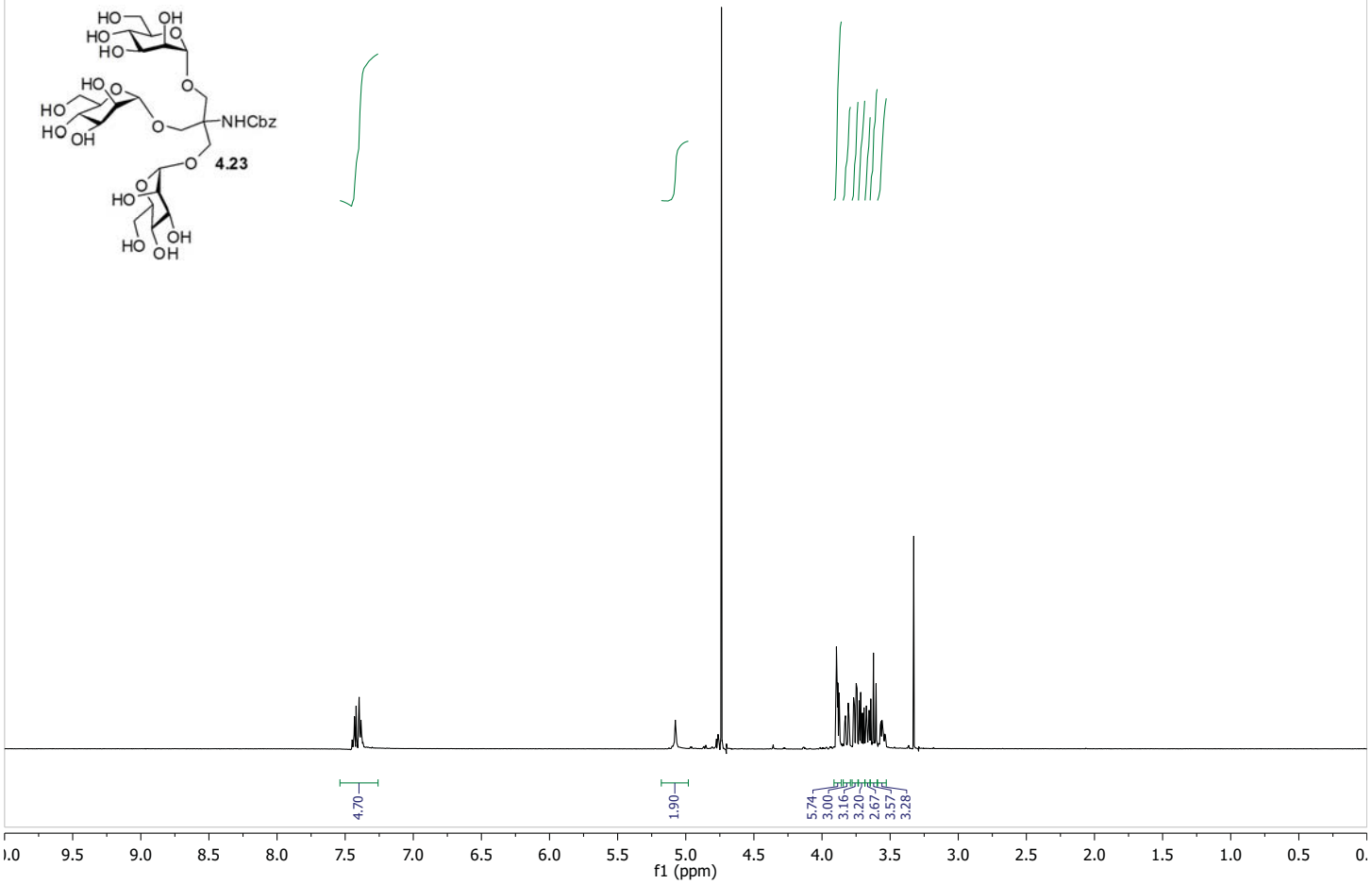

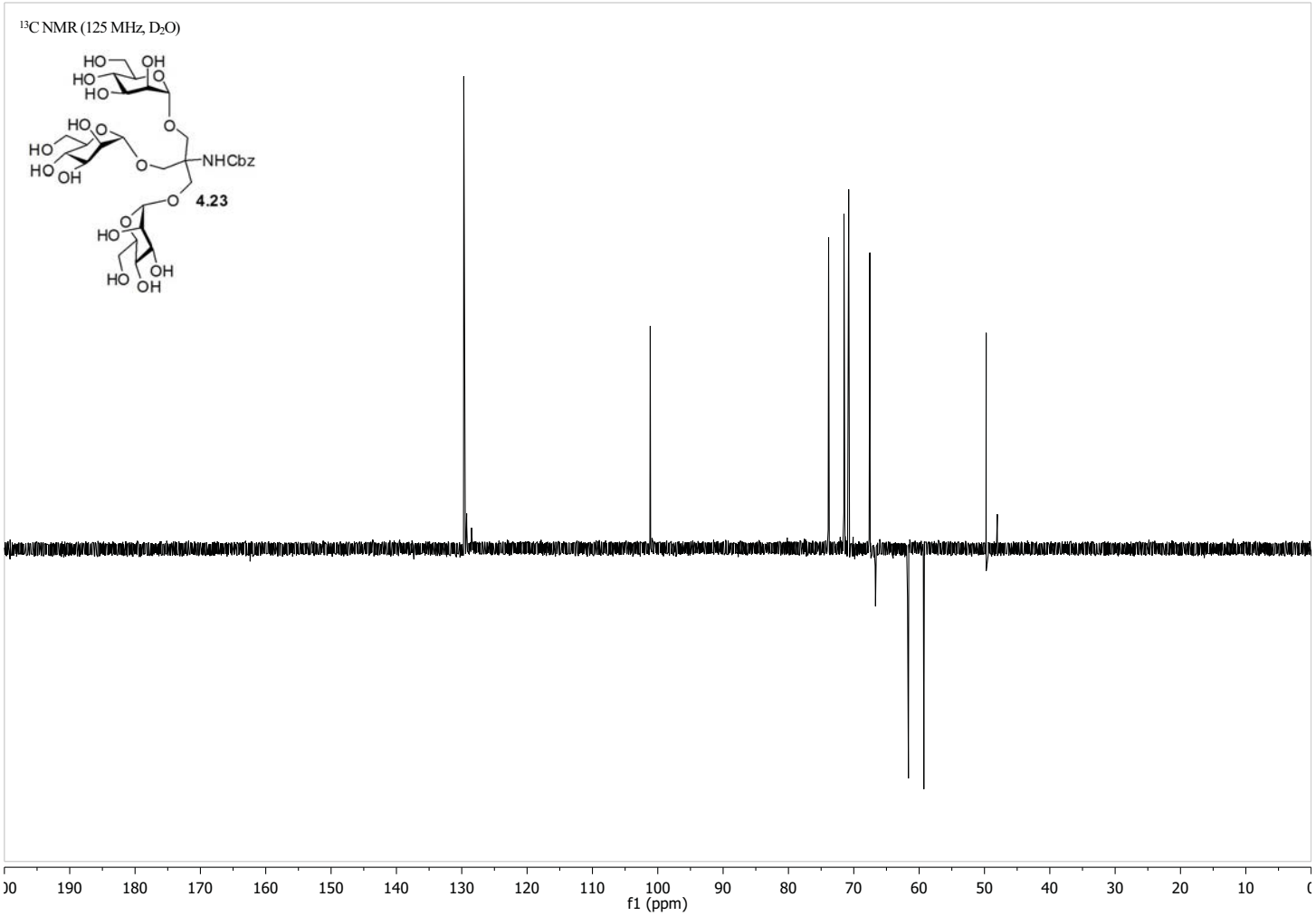
13C NMR (125 MHz, D2O)
NHCbz
4.23
f1 (ppm)

^{1}H NMR (498 MHz, D_2O)

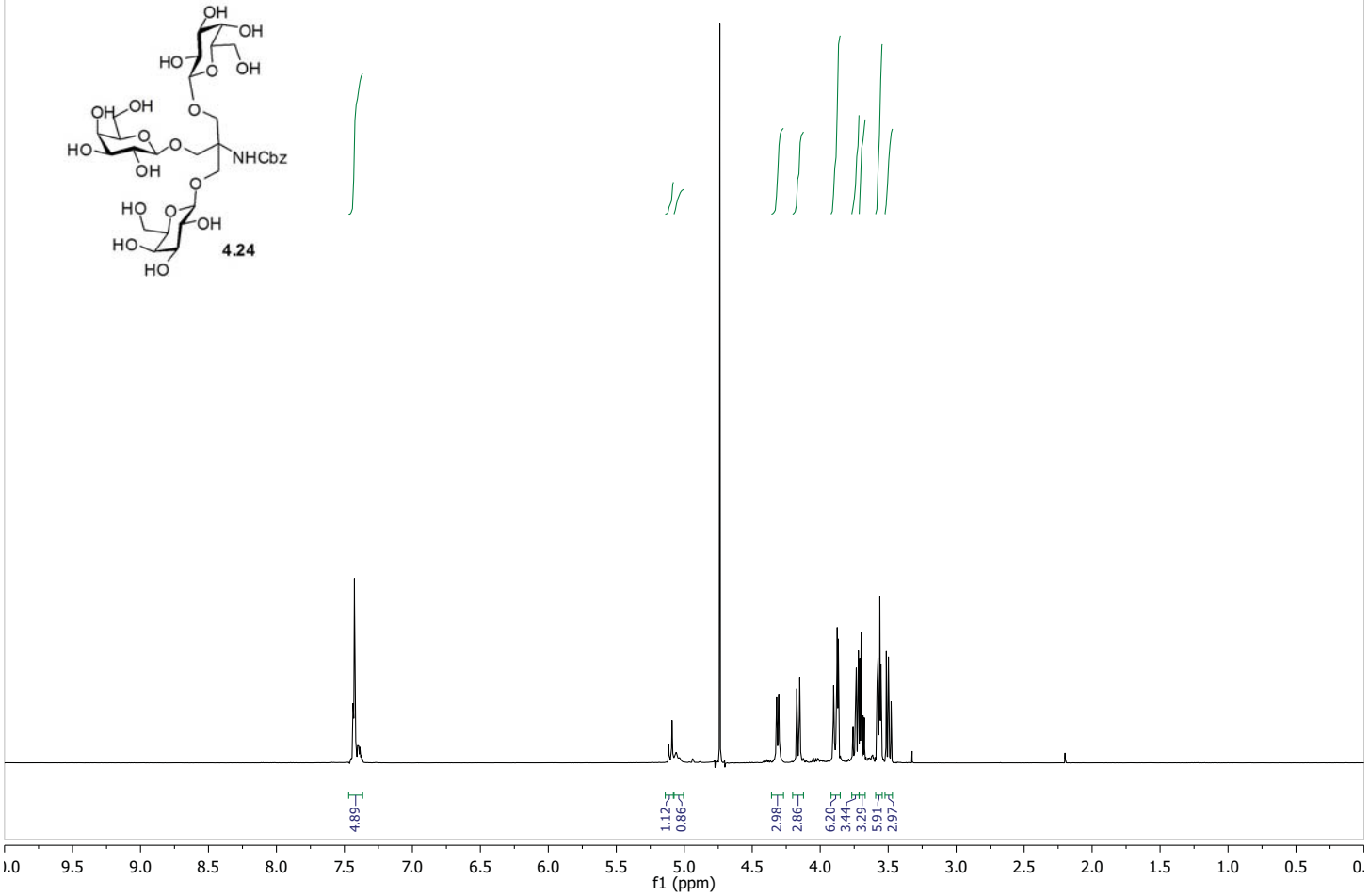

^{13}C NMR (125 MHz, D_2O)

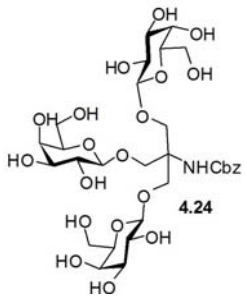

^{1}H NMR (498 MHz, D_2O)

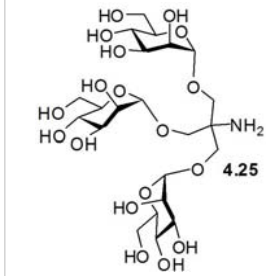

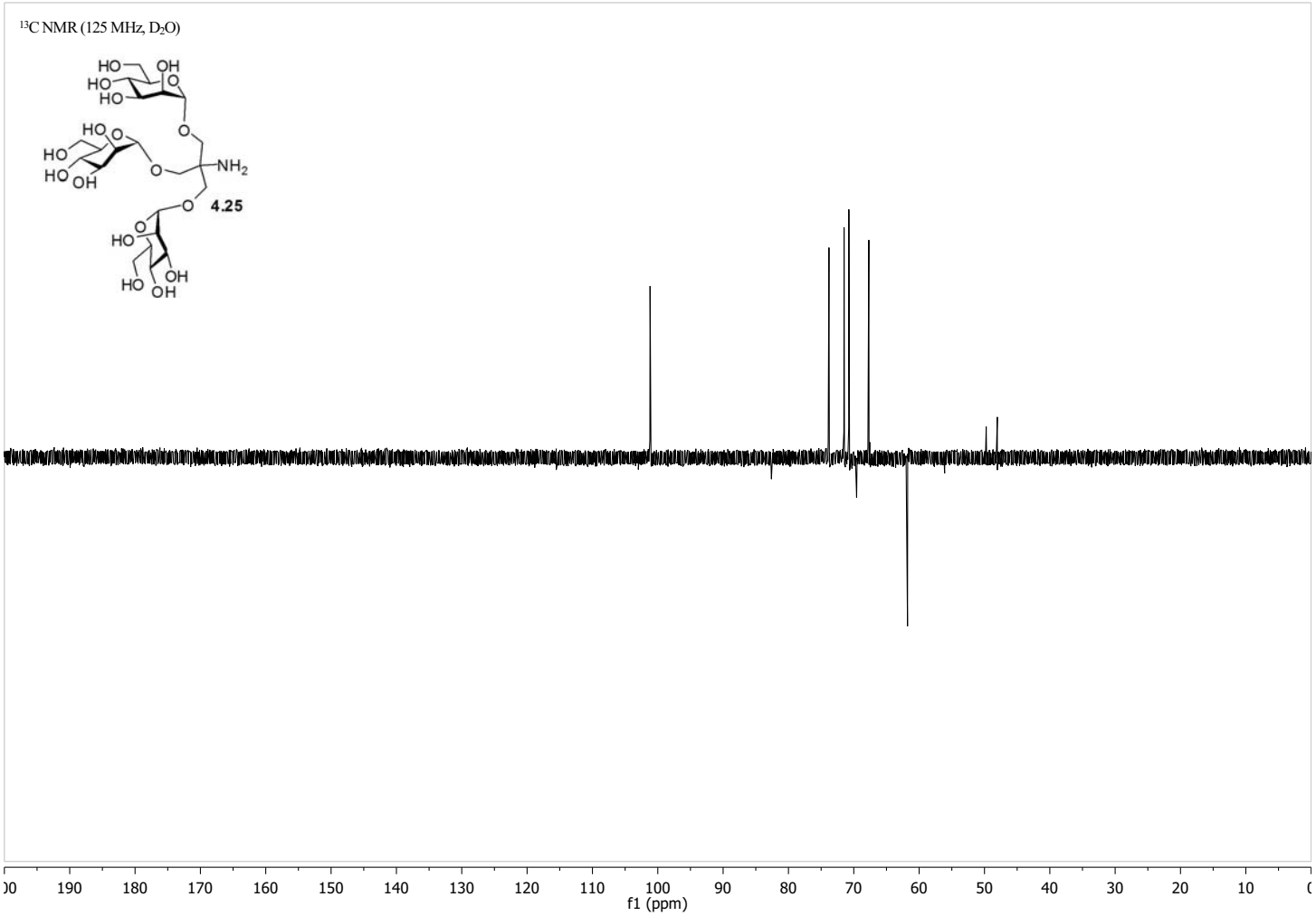
13C NMR (125 MHz, D2O)
4.25
f1 (ppm)

^{1}H NMR (498 MHz, D_2O)

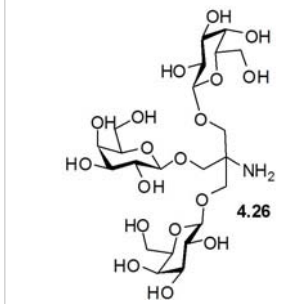

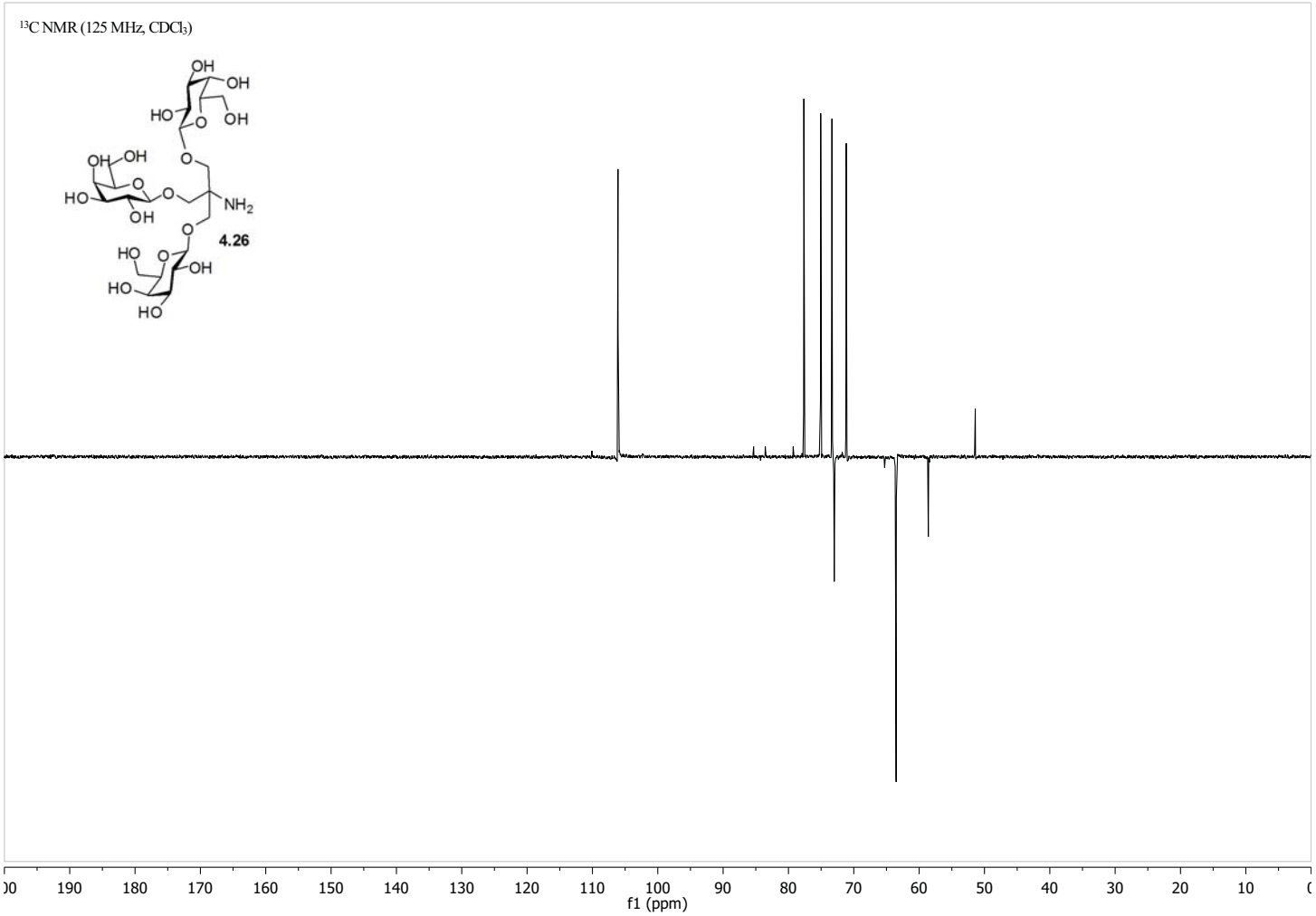
^{13}C NMR (125 MHz, $CDCl_3$)
4.26
f1 (ppm)

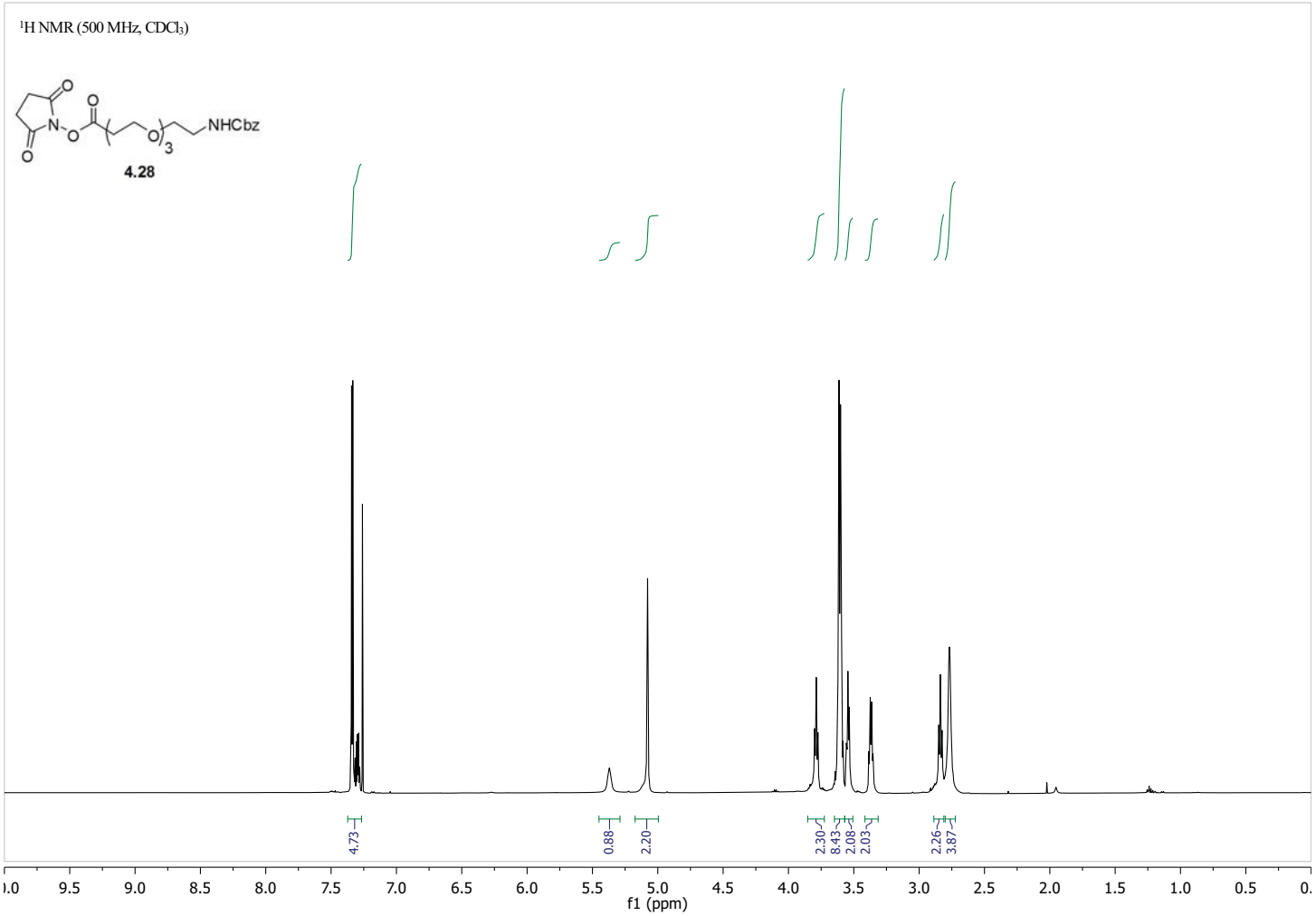
^{1}H NMR (500 MHz, $CDCl_3$)
NHCbz
4.28
4.73
0.88
2.20
2.30
8.43
2.08
2.03
2.26
3.87
f1 (ppm)

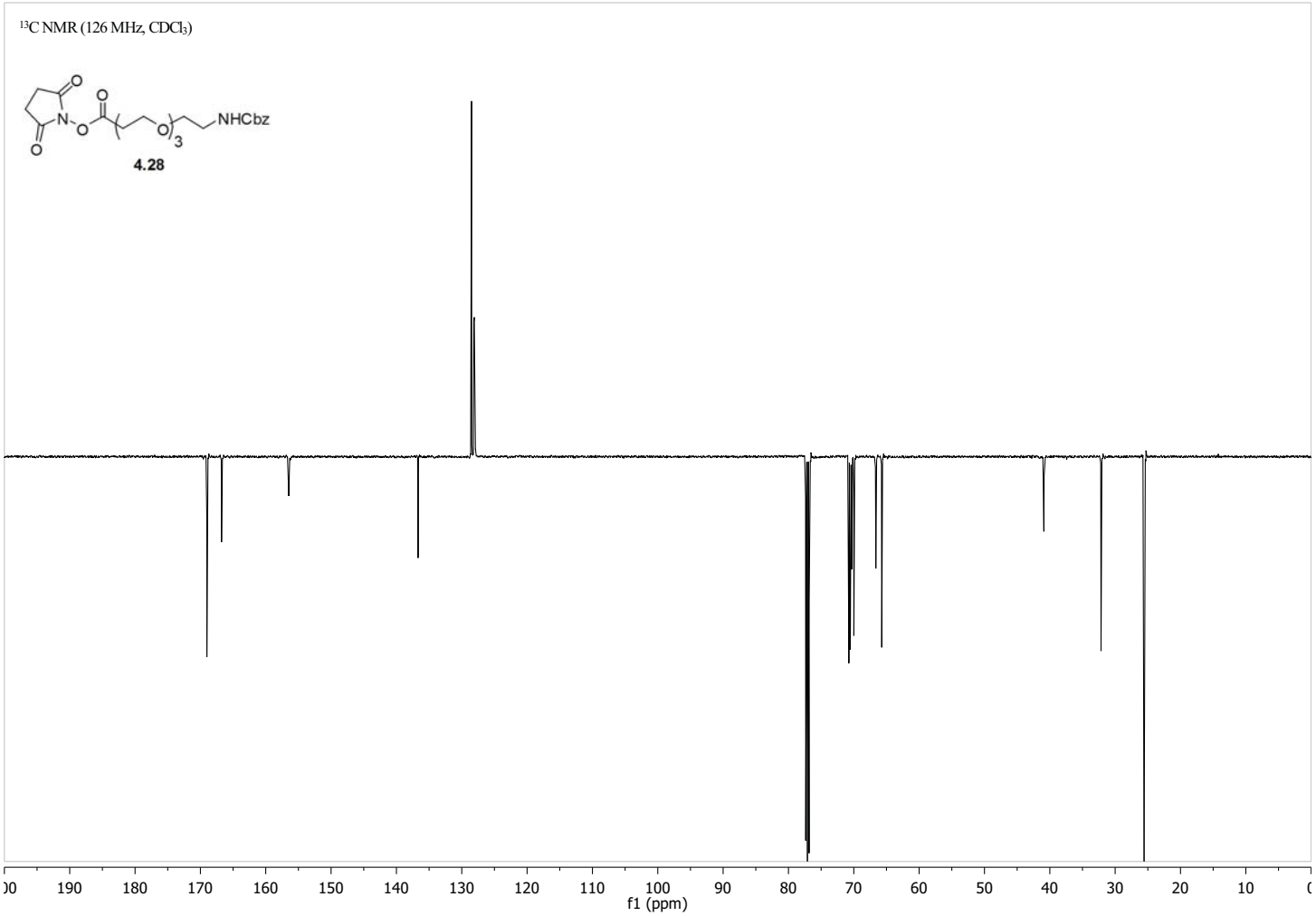
13C NMR (126 MHz, CDCl3)
NHCbz
4.28
f1 (ppm)

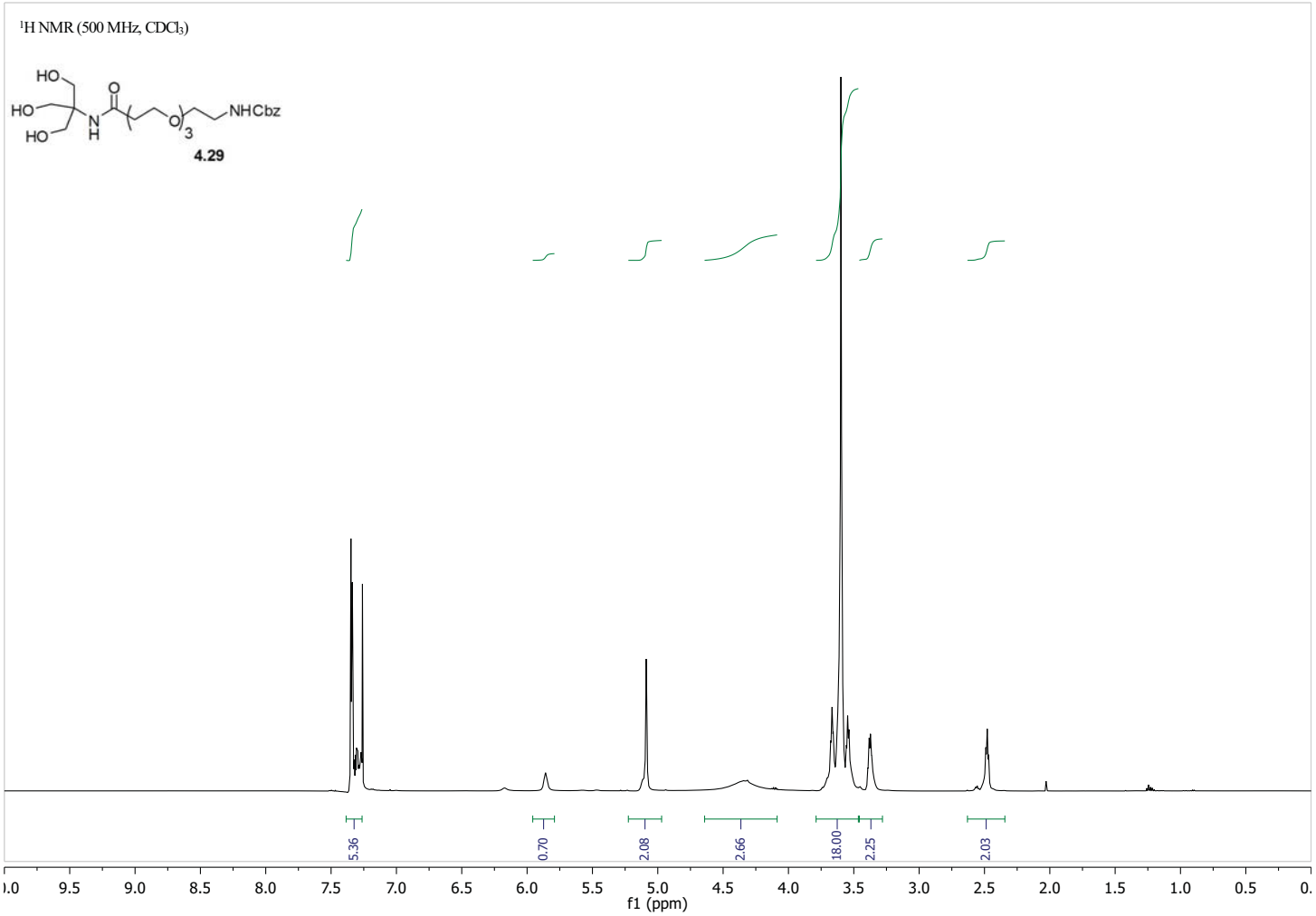
1H NMR (500 MHz, CDCl3)
HO
HO
HO
N
H
O
O
3
NHCbz
4.29
5.36
0.70
2.08
2.66
18.00
2.25
2.03
f1 (ppm)

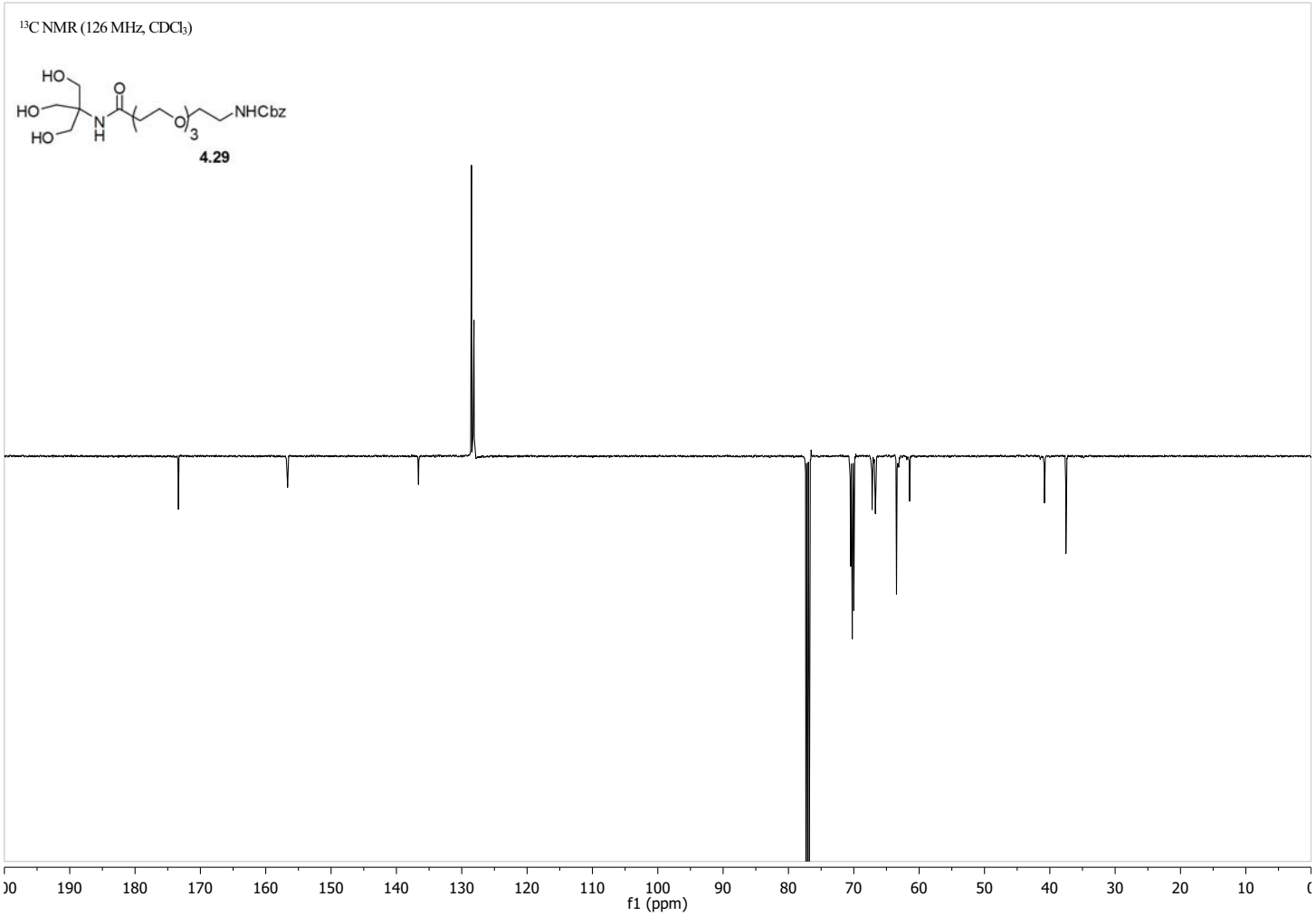
13C NMR (126 MHz, CDCl3)
HO
HO
HO
N
H
O
O
3
NHCbz
4.29
190
180
170
160
150
140
130
120
110
100
90
80
70
60
50
40
30
20
10
f1 (ppm)

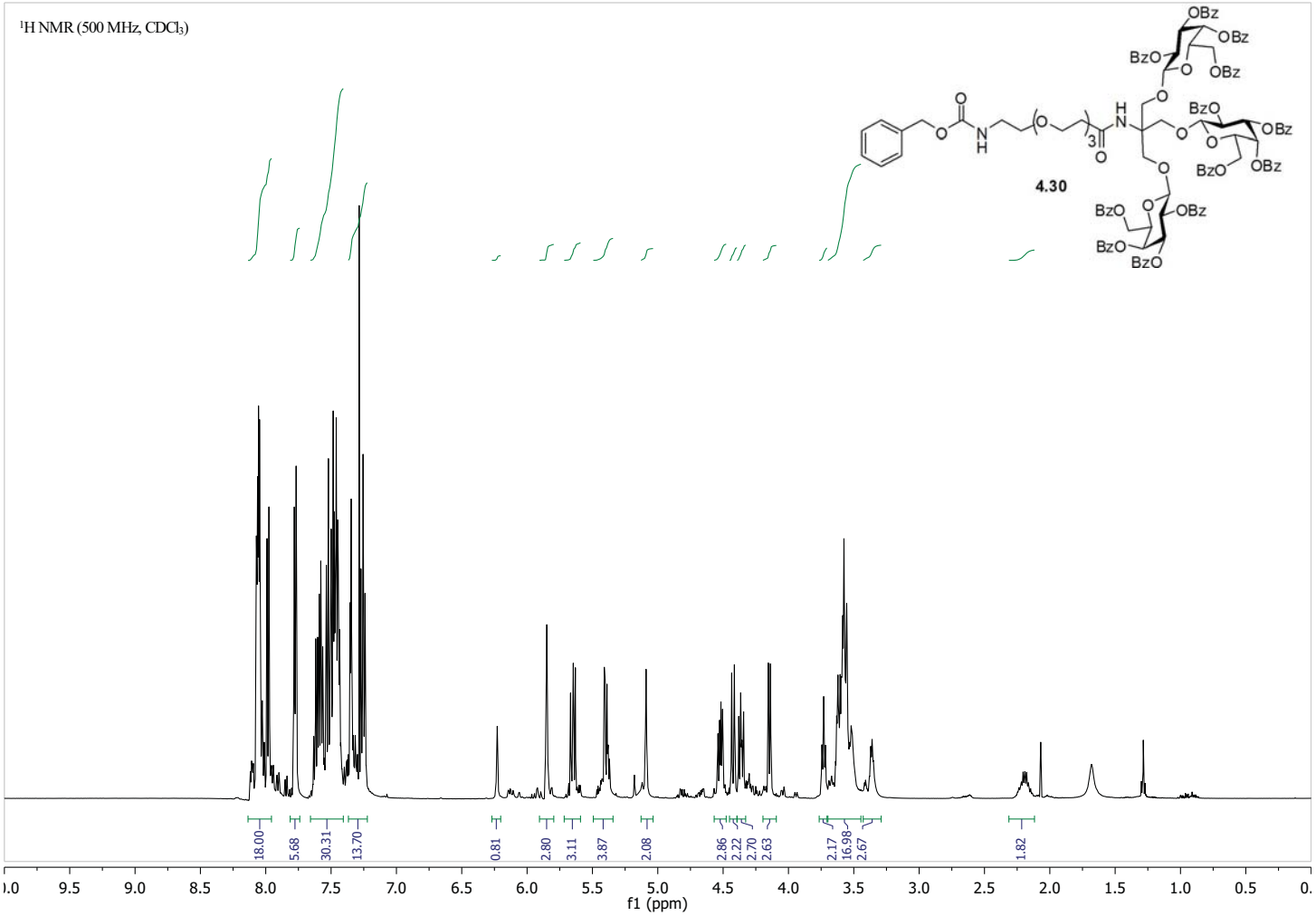
^{1}H NMR (500 MHz, CDCl$_3$)
4.30
18.00
5.68
30.31
13.70
0.81
2.80
3.11
3.87
2.08
2.86
2.22
2.70
2.63
2.17
16.98
2.67
1.82
f1 (ppm)

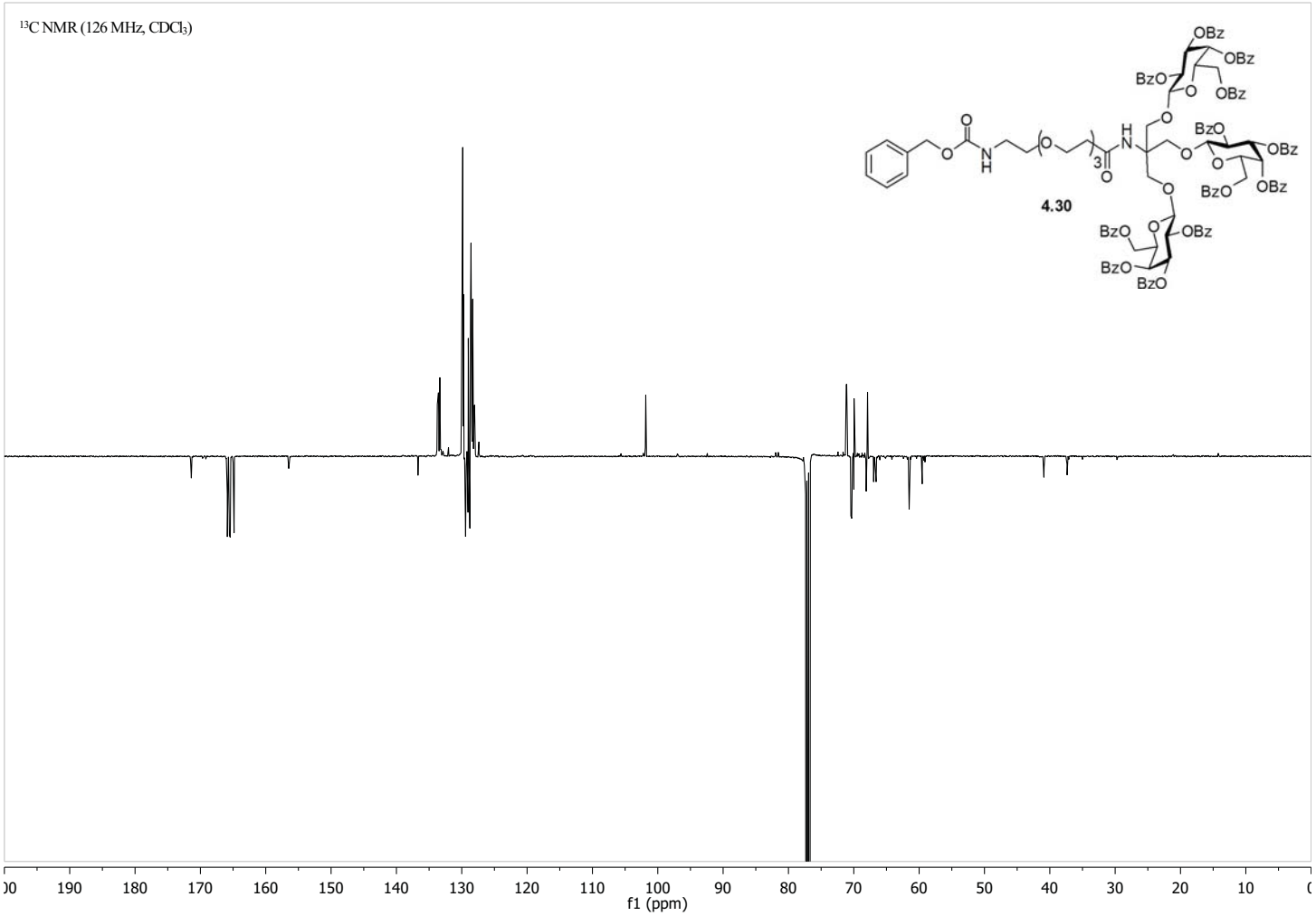
^{13}C NMR (126 MHz, $CDCl_3$)
4.30
f1 (ppm)

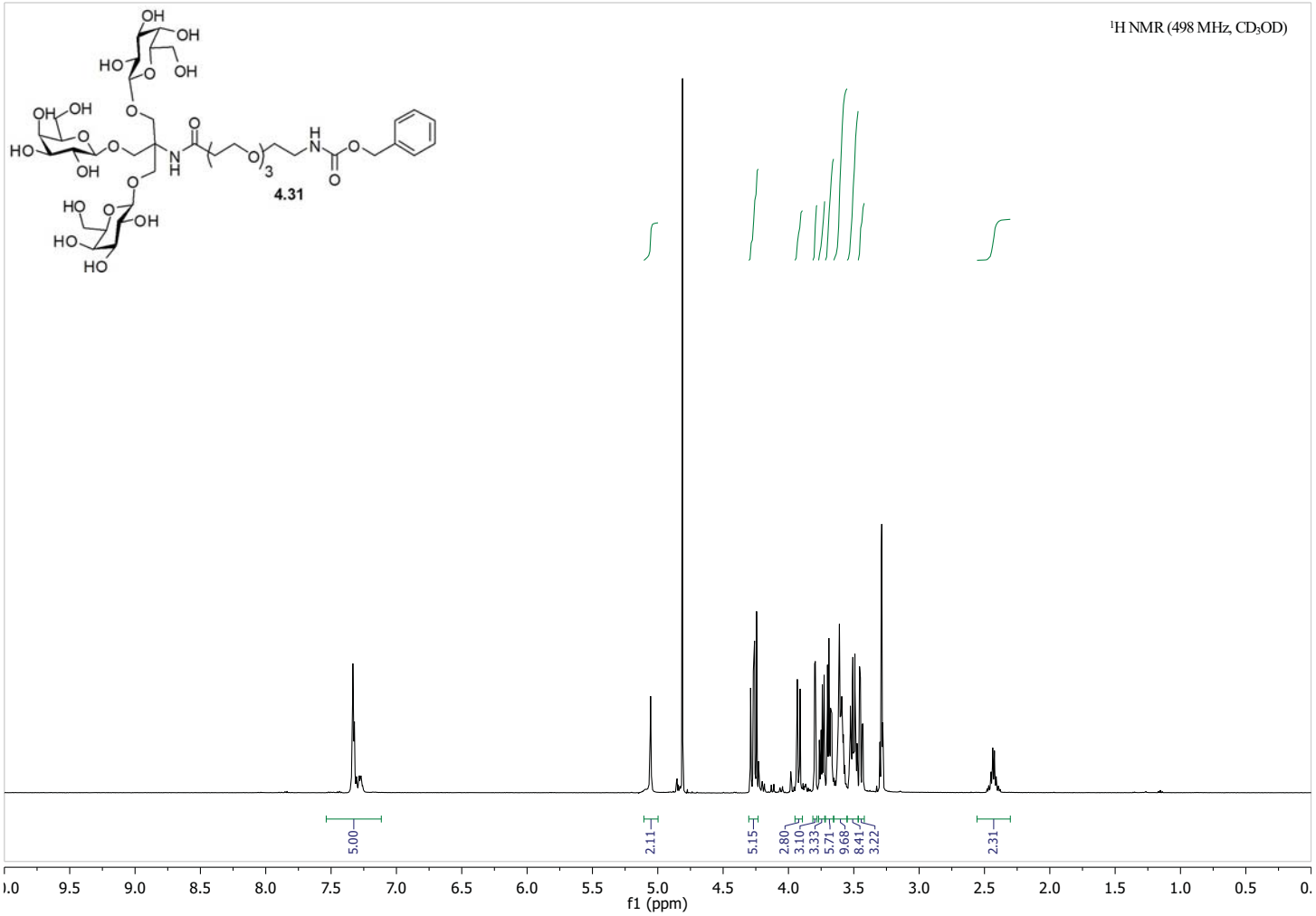
^{1}H NMR (498 MHz, CD_3OD)
4.31
5.00
2.11
5.15
2.80
3.10
3.33
5.71
9.68
8.41
3.22
2.31
f1 (ppm)

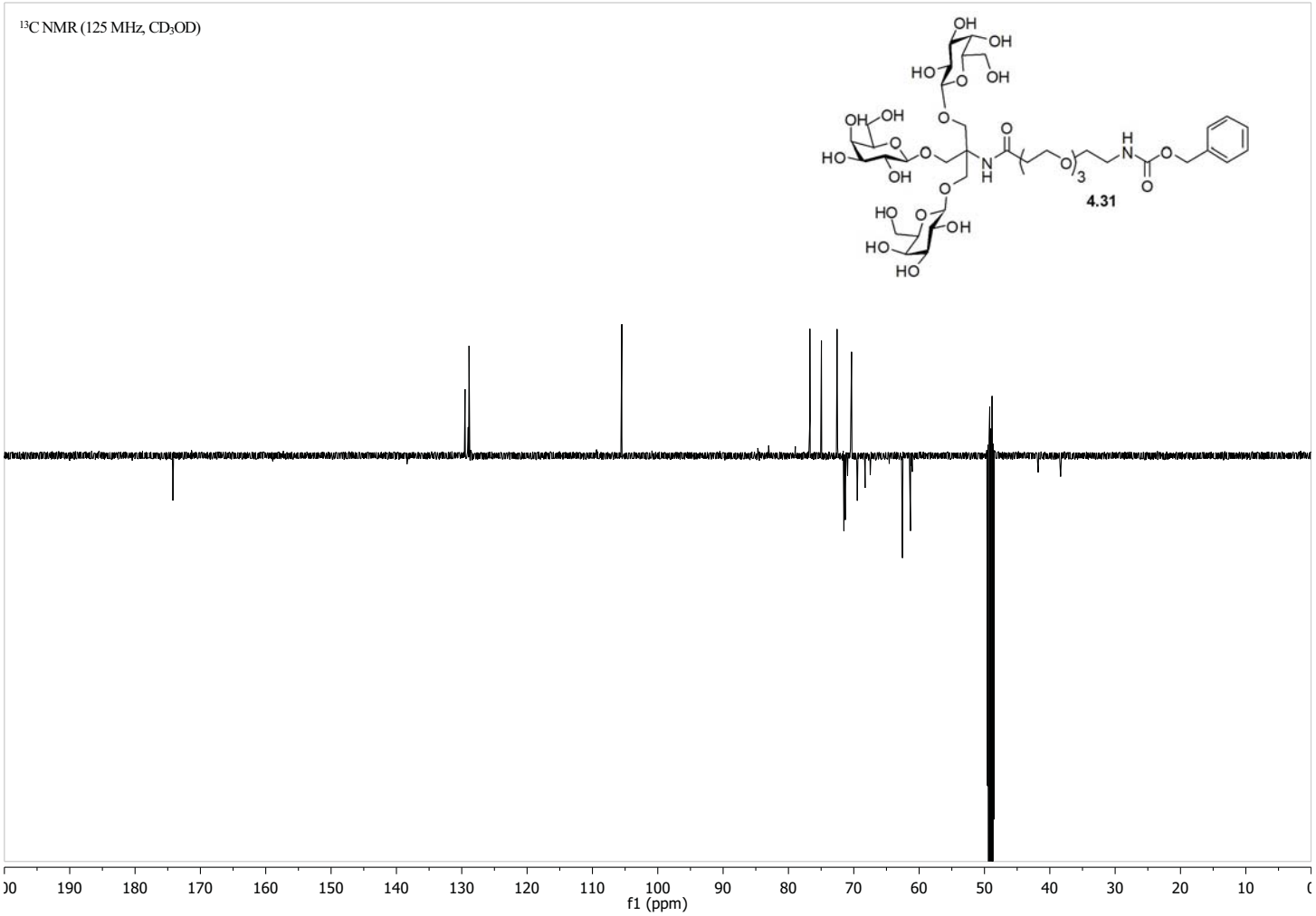
13C NMR (125 MHz, CD3OD)
4.31
f1 (ppm)

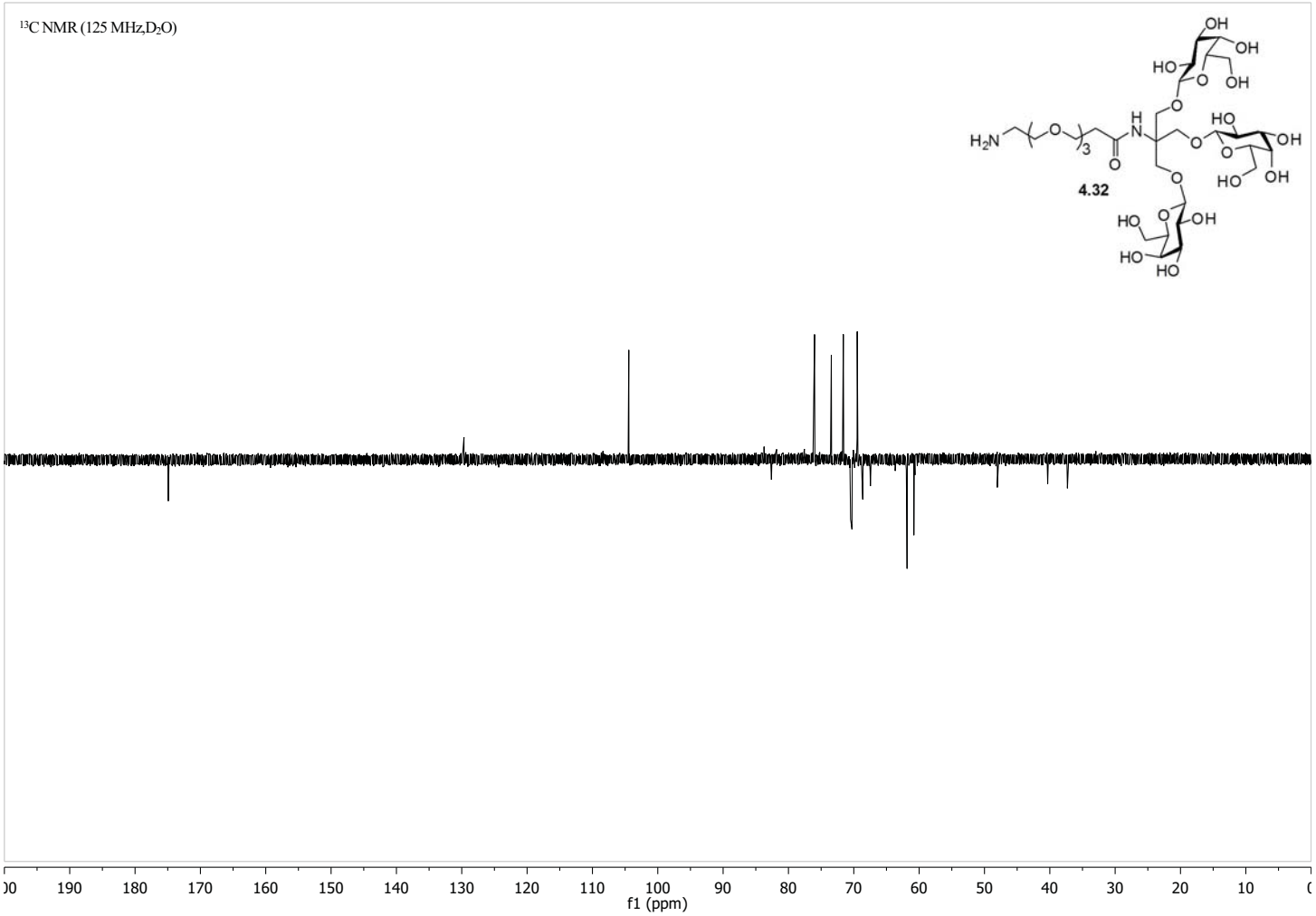
13C NMR (125 MHz,D2O)
4.32
f1 (ppm)

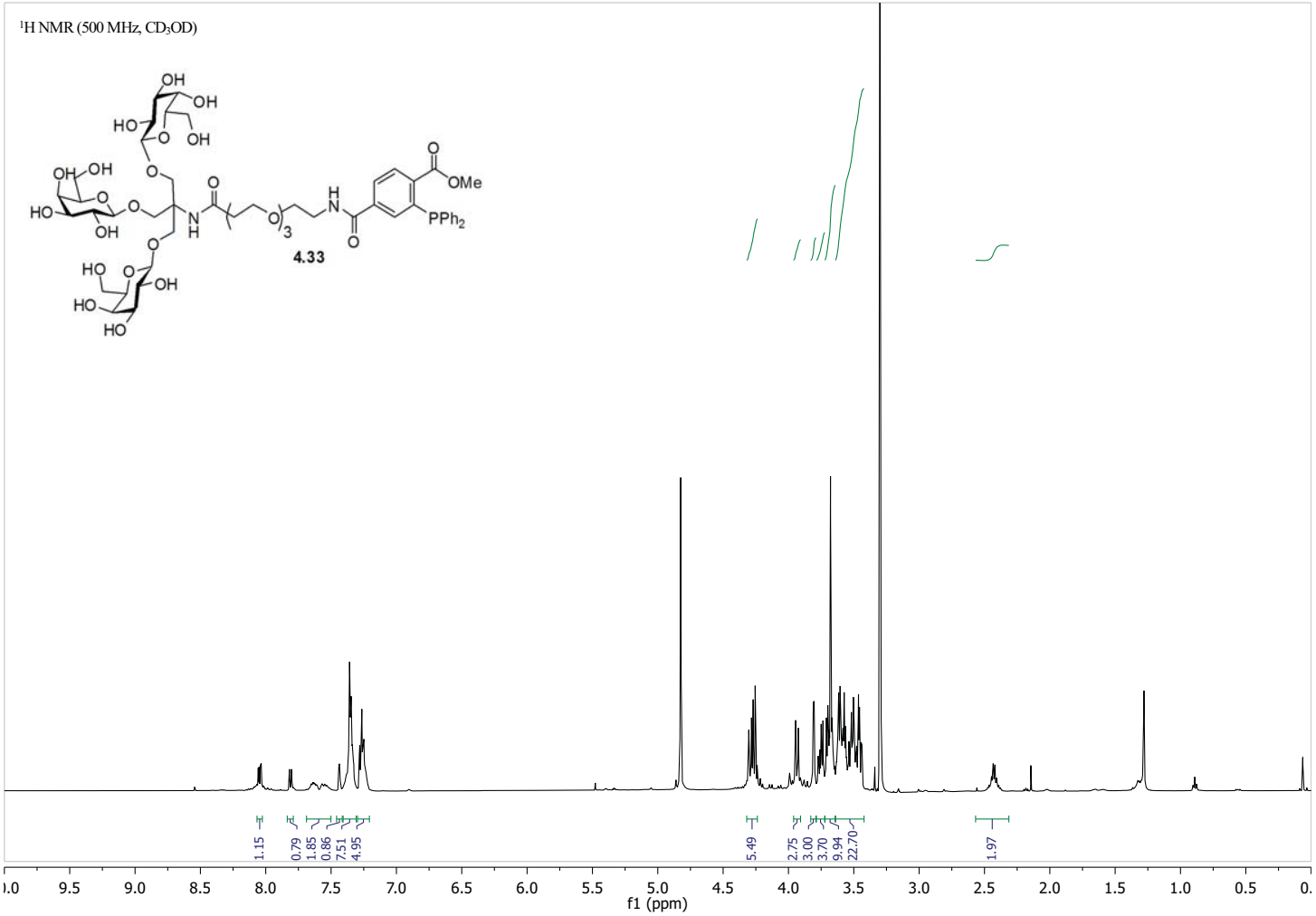
1H NMR (500 MHz, CD3OD)
4.33
1.15
0.79
1.85
0.86
7.51
4.95
5.49
2.75
3.00
3.70
9.94
22.70
1.97
f1 (ppm)

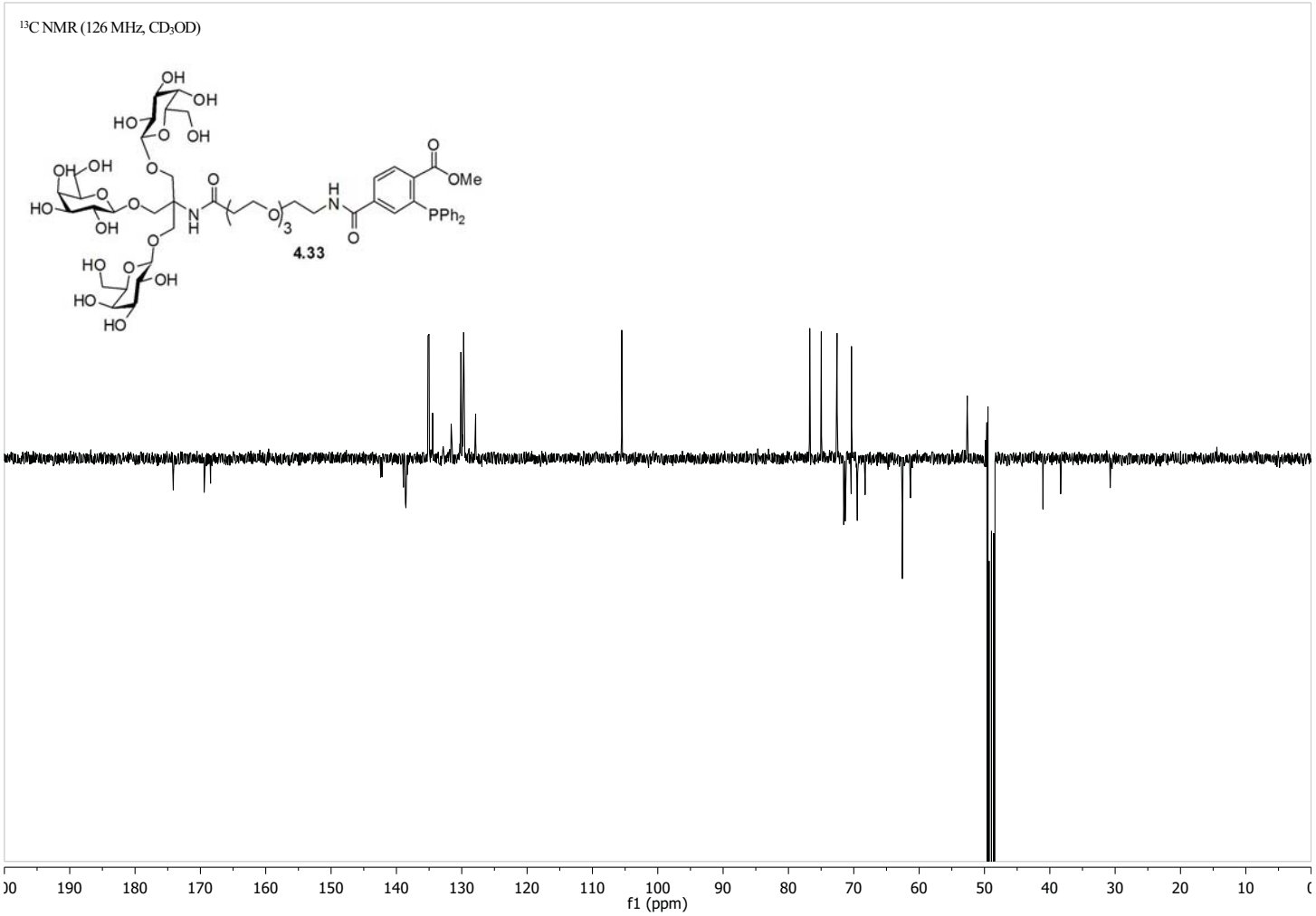
13C NMR (126 MHz, CD3OD)
4.33
f1 (ppm)

^{31}P NMR (162 MHz, CD_3OD)